UNIVERSIDADE DE SÃO PAULO
FACULDADE DE ODONTOLOGIA DE BAURU

TALITA MENDES OLIVEIRA VENTURA

Proteomic analysis of the acquired enamel pellicle and saliva in patients with head and neck cancer to submitted radiotherapy

Análise proteômica da película adquirida do esmalte e saliva em pacientes com câncer de cabeça e pescoço submetidos à radioterapia

BAURU
2021

TALITA MENDES OLIVEIRA VENTURA

Proteomic analysis of the acquired enamel pellicle and saliva in patients with head and neck cancer to submitted radiotherapy

Análise proteômica da película adquirida do esmalte e saliva em pacientes com câncer de cabeça e pescoço submetidos à radioterapia

Thesis presented to the Bauru School of Dentistry of the University of São Paulo to obtain the degree of Doctor in Science in the Applied Dental Sciences Program, Oral Biology, Stomatology, Radiology and Imaging concentration area.

Supervisor: Prof. Drª Marília Afonso Rabelo Buzalaf

Co-supervisor: Prof. Dr. Paulo Sérgio da Silva Santos

Tese apresentada à Faculdade de Odontologia de Bauru da Universidade de São Paulo para obtenção do título de Doutor em Ciências no Programa de Ciências Odontológicas Aplicadas, área de concentração Biologia Ora, Estomatologia, Radiologia e Imaginologia.

Orientadora: Prof. Drª Marília Afonso Rabelo Buzalaf

Coorientador: Prof. Dr. Paulo Sérgio da Silva Santos

Versão Corrigida

BAURU

2021

Ventura, Talita Mendes Oliveira

Proteomic analysis of the acquired enamel pellicle and saliva in patients with head and neck cancer to submitted radiotherapy / Talita Mendes Oliveira Ventura – Bauru, 2021.

346 p. : il. ; 31cm.

Tese (Doutorado) – Faculdade de Odontologia de Bauru. Universidade de São Paulo

Orientadora: Prof. Drª Marília Afonso Rabelo Buzalaf

Nota: A versão original desta tese encontra-se disponível no Serviço de Biblioteca e Documentação da Faculdade de Odontologia de Bauru – FOB/USP.

Comitê de Ética da FOB-USP
Protocolo nº: 61484116.0.0000.5417
Data: 08/02/2017

ERRATA

Universidade de São Paulo
Faculdade de Odontologia de Bauru

Assistência Técnica Acadêmica
Serviço de Pós-Graduação

FOLHA DE APROVAÇÃO

Tese apresentada e defendida por
TALITA MENDES OLIVEIRA VENTURA
e aprovada pela Comissão Julgadora
em 21 de maio de 2021.

Prof. Dr. **JONAS DE ALMEIDA RODRIGUES**
UFRGS

Prof.ª Dr.ª **ANURADHA PRAKKI**
UofT

Prof.ª Dr.ª **VANESSA SOARES LARA**
FOB-USP

Prof.ª Dr.ª **MARILIA AFONSO RABELO BUZALAF**
Presidente da Banca
FOB - USP

Profª. Drª. **Izabel Regina Fischer Rubira de Bullen**
Presidente da Comissão de Pós-Graduação

Al. Dr. Octávio Pinheiro Brisolla, 9-75 – Bauru-SP – CEP 17012-901 – C.P. 73
e-mail: posgrad@fob.usp.br – Fone/Fax (0xx14) 3235-8223
http://www.fob.usp.br

DEDICATÓRIA

A Deus,

Que sempre está ao meu lado, me dando forças e sabedoria para enfrentar os obstáculos da vida. Tua és o meu refúgio, minha luz, meu maior amor. Em Ti, eu encontro amparo e amor incondicional. Obrigada por guiar meus caminhos e me conduzir todas as vezes que me senti perdida em meus caminhos. Tu és meu tudo, o Senhor da minha vida e da minha história.

"Nenhum mal te atingirá, nenhum flagelo chegará à tua tenda, porque aos seus anjos ele mandou que te guardem em todos os teus caminhos. Eles te sustentarão em suas mãos, para que não tropeces em alguma pedra."

Salmo 90: 10-12.

Aos meus amados pais ***Orí e Germana,***

Em tudo na minha vida eu vejo vocês. Meus pais queridos, me sinto tão abençoada e privilegiada por ter vocês como pais. Sempre lutaram com todas as forças possíveis e impossíveis para que dessem oportunidades e estudos para nós. Além disso, vocês são o maior exemplo de força, fé e amor. Vocês são o meu alicerce e meu porto seguro. A vocês dedico esta tese e minha eterna gratidão.

Ao meu querido irmão ***João Vítor,***

Que é meu incentivador, conselheiro e amigo. Obrigada por ser este irmão tão querido, meu amor por você é imensurável.

Ao meu marido ***Caío,***

Por além de marido, ser o meu melhor amigo e o meu maior incentivador. Pelo amor sincero e por me apoiar. Por ser meu porto seguro e por não medir esforços para me fazer feliz. Por sempre estar por perto, por me aproximar de Deus, por ser minha calmaria em meio a tempestade. Pelo carinho, amor, respeito e por tornar os meus sonhos também os seus. Pelo amor e dedicação de sempre.

Aos ***voluntários desta pesquisa,***

Que me mostraram que apesar das diversidades e obstáculos que podem surguir pelo caminho, a vida é um presente que nos é dado todos os dias.

AGRADECIMENTOS ESPECIAIS

A minha querida e amada orientadora **Profa. Dra. Marília Afonso Rabelo Buzalaf,** Professora, só de começar a escrever eu já me emociono. Neste momento passa um filme na minha cabeça, pois já vivemos tantos momentos desde o mestrado. Já são 10 anos de FOB/USP no laboratório de bioquímica, desde a iniciação cientifica. Eu sou tão grata a Deus por ter colocado a senhora em minha vida. Eu sempre digo que todos os alunos de pós-graduação um dia tinham que ser orientados pela senhora. Que privilégio, meu Deus! Conviver com a senhora é ver o amor pela pesquisa enraizado em seu coração, que isto acaba sendo transmitido para nós. Uma vez um aluno em um seminário me disse que eu tinha traços da senhora em apresentar aula e ao falar, e que eu só poderia ser sua aluna. Naquele momento, no meio do seminário, meus olhos encheram de lágrimas, porquê é exatamente o que eu sinto, e eu até ouso dizer isto. Sinto que uma parte da senhora está em mim, pois o conhecimento e o carinho que a senhora transmite para os seus alunos trasnbordam do seu coração e isto só pode ser divino. Obrigada professora, por tantas oportunidades que a senhora me proporciona profissionalmente. Por acreditar em mim, quando muitos duvidaram (até mesmo eu). Me deu oportunidades e me proporcionou momentos que eu jamais pensei que um dia poderia alcançar. Obrigada por me confiar trabalhos incríveis e lindos que eu faço com a maior dedicação e amor do mundo, assim como a senhora nos ensina. Obrigada por nossa troca, como professora e aluna, mas também no âmbito pessoal. Eu digo para todos que se um dia Deus me permitir ser professora, quero ser assim, amável exatamente como a senhora é. Apesar da grande profissional que és, do seu currículo invejável por todos, pesquisadora extremamente diferenciada e inteligente, a humildade é a que se destaca. E claro, sem contar a beleza que é só um detalhe em meio a tantas

qualidades especiais que a senhora possui. A senhora é extremamente humilde e acessível, sempre de portas abertas para receber seus alunos. Mesmo em meio dessa pandemia, a senhora sempre me atende prontamente com todos os e-mails, telefonemas e mensagens. A senhora é a mulher maravilha, professora, só pode ser! Mas na verdade, eu prefiro acreditar que és mesmo um anjo que veio no mundo fazer a diferença na vida de tantas pessoas, seja com seus alunos, sejam com tantas pessoas que são beneficiadas com os resultados de suas pesquisas, sejam com as pessoas que tem a sorte de poder conviver com a senhora ou até mesmo com sua família, porque além de tudo a senhora é uma grande mãe e esposa. Eu me insipiro muito na senhora! Que orgulho poder dizer que sou tua aluna e que pude aprender tanto com a melhor. Obrigada por me ensinar com o coração.

Saiba que sempre estarei aqui, professora. Não importa quanto tempo passe, a senhora sempre estará comigo, pois seus ensinamentos estão gravados em mim e em meu coração. Que Nossa Senhora te guarde e te abençoe imensamente! Tê-la como orientadora é um presente de Deus. Sua humildade e simplicidade me encanta e a torna merecedora de tudo o que a senhora representa. Obrigada por tudo, sempre! Amo a senhora de todo meu coração, obrigada por ser essa pessoa incrível.

"O que importa não é o que você tem na vida,

mas quem você tem na vida."

William Shakespeares

AGRADECIMENTOS

A Deus,

Por durante esta jornada do doutorado, mas também em todos os meus caminhos, sempre colocar pessoas maravilhosas em minha vida. Por me proporcionar nascer em uma família linda, cheia de amor, carinho, união e fé. Por me sustentar nos momentos em que achei que não teria mais forças. Por me proteger e enviar seus anjos para estar de prontidão. Sinto sua presença em minha vida a cada segundo, através de milagres diários. Obrigada por ser esse Deus de perto!

"Te amar por quem não te ama, te adorar por quem não te adora, esperar por quem não espera em Ti. E pelos que não crêem, eu estou aqui."
Anjos de Resgate.

A Jesus,

Por ser o meu Rei e Salvador, por dar sua própria vida por mim. Por não me abandonar mesmo quando me sinto distante. Tu és Jesus, o meu rei e meu tudo. Obrigada pelo seu amor que nos constrange, nada é maior que isto. Obrigada por ter morrido na cruz para nos salvar e para que tivéssemos vida. Louvado seja, Senhor!

É tanto amor, que o Senhor ainda nos deu a sua mãe para amarmos.

"Te chamam de Deus e de Senhor. Te chamam de Rei, de Salvador. E eu me atrevo a Te chamar de meu Amor."
Colo de Deus.

A Nossa Senhora,

Minha mãezinha querida, o que seria de mim sem a senhora? Obrigada por ser meu refúgio e pelo amor incondicional. Sinto sua presença no meu coração e na minha alma. Obrigada por me levantar em todos os momentos deste doutorado e da minha vida. Obrigada Mãe, por sempre me atender prontamente quando eu te chamo e rogo a Ti. Por nunca me deixar sozinha, por me livrar de todas as coisas que possam me tirar da presença de Deus. Por muitas vezes me consolar em tantas viagens de madrugada a Bauru, por me dar paz quando estava em uma pandemia longe dos meus, por ser minha intercessora fiel. Não tenha nada que eu te peça que a senhora não tenha me ajudado a realizar. Eu te amo Maria, meu coração é todo seu e eu sou toda sua. *"Totus tuus, Marie."*

Aos meus queridos pais **Ori e Germana,**

Obrigada por me darem a vida. Por terem lutado por mim. A vocês que sempre estiveram do meu lado me incentivando, e a cada alegria ou derrota estiveram do meu lado, sempre. Por me ensinarem a ser fiel a Deus, que sempre me enchem de força e coragem para enfrentar os desafios da vida. Além de pais, são meus melhores amigos e intercessores. Por todas as orações e terços para que todos os meus projetos sejam abençoados. Que me mostraram que não tenha nada que eu não consiga alcançar e realizar, mesmo quando tudo parece distante e inatingível, porém com princípios e colocando Deus a frente de tudo. Obrigada meus amores, por muitas vezes que guardaram suas dores para cuidar das minhas, que choram pela minha ausência desde adolescente, mas me ensinaram a enfrentar o mundo. Por me proporcionarem algo que ninguém jamais poderá tirar de mim: o estudo. A vocês que sacrificaram os seus sonhos para realizar os meus. Obrigada por me ensinarem a ter esperança e a lutar pelo o que almejo. Obrigada por me fazer crescer em um lar cheio de amor, carinho e tantos princípios. Meus Deus, como sou abençoada por ter vocês. Eu agradeço a Deus por ter me dado a alegria de ter os melhores pais do mundo. Vocês são o meu maior exemplo. Amo vocês incondicionalmente, com toda a força do meu coração.

Ao meu querido irmão **João Vitor,**

Obrigada por ser meu parceiro, um amigo que sei que sempre poderei contar em todos os percursos da minha vida. Apesar da correria do dia a dia, sabemos que sempre estaremos aqui um pelo outro, unidos pelo coração e pela alma. Você está sempre comigo em minhas orações e no meu coração. Eu tenho um orgulho imenso de ser sua irmã, por sua guarra, perseverança, fé inabalável, profissional impecável, por ter esse coração lindo e caridoso (um dos maiores que já conheci), agora pai de uma princesa linda, nossa Lorena, que foi o maior presente para nossa família. Te amo de todo meu coração, minha admiração por você só aumenta. Você é meu pedacinho!

Ao meu marido **Caio,**

Meu amor, eu sou tão grata por ter você em minha vida. Meu incentivador, que torce por mim com todas as forças. Que enxuga minhas lágrimas, que me faz rir por qualquer bobagem, por me tirar risos fáceis só por estarmos juntos. Parece clichê, mas você é um presente na minha vida, um carinho de Deus e Maria.

Me lembro do dia que nos conhecemos, com uma grande amizade. Você estava comigo no momento mais difícil, quando minha vozinha se foi. E dali, nasceu então um amor que eu não conhecia, puro, calmo, amor divino dos céus. Deus já tinha sonhado com nosso amor, antes mesmo dos nossos olhares se cruzarem. Obrigada amor, por me fazer experimentar o amor divino através do nosso. Você, que me incentivou para realizar um dos meus maiores sonhos, aguentou firme a distância durante 6 meses, em meio a uma pandemia, ficamos sozinhos, mas nunca tive tanta certeza do quanto unidos nós estávamos, apesar das milhas e milhas de distância. Me apoiou, chorou comigo, riu, se alegrou pelas minhas conquistas, fez dos meus sonhos também os seus. Obrigada por segurar a minha mão e nunca ter soltado. Obrigada pelo carinho especial, por ter me dado o meu maior presente como eu sempre digo: o Tobias (rsrs), que chegou enchendo nossa vida de alegria e muitos "lambeijos", com ele a alegria é na certa, nosso anjinho. Porém, sei que Deus tem planos imensos para nós. Nossa família está só começando, obrigada por sonhar os planos mais malucos comigo e além disso, lutar para realizar. Te amo meu amor, você é uma pessoa muito especial, inteligente, justo, carinhoso, um coração lindo, fé inabalável, nossa são tantas qualidades, mas que nenhuma supera a sua maior: humildade e amor por Jesus. Obrigada por viver esta vida comigo. Obrigada por ser meu amor e por cuidar de mim! Dividir a vida com você é tudo que sempre sonhei. Te amo da forma mais pura e linda que se possa amar.

A minha amada e querida vó **Altamira** (*in memorian*),

Vó, a saudade que sinto da senhora chega a doer. Mas dizem que a saudade é uma lembrança boa daquilo que ficou. A senhora sempre foi o maior exemplo que eu já vi de força, garra e alegria de viver. Obrigada por tudo, pois sempre esteve ao meu lado, ensinando, me incentivando. Brava que só ela, mas acolhedora e com um amor por todos nós que jamais existiu. A senhora sempre estará no meu coração e na minha alma. Sua alegria que sempre teve de viver me faz querer ser diferente e melhor todos os dias. Te amo minha amada vó, eu sei que o céu é seu lugar.

A minha querida cunhada **Natália**,

Ná, eu só tenho que agradecer a Deus por ter colocado você em nossa família. Obrigada pelas ligações de horas, pelos conselhos, risadas e momentos de descontração. Obrigada por ter dado à vida ao nosso maior presente, nossa doce Lorena. Por vocês terem me escolhido, na maior missão da minha vida, ser madrinha da nossa boneca. Saiba que eu sempre estarei aqui para tudo que precisar, sempre. Obrigada por cuidar do meu irmão com tanto amor e carinho, por ter nos escolhido como família. Agradeço a Deus todos os dias por ter você em nossa vida. Te amo!

Ao meu amorzinho, sobrinha e afilhada **Lorena,**

Minha princesa, você chegou abalando os nossos corações e enchendo a nossa vida de alegria. Obrigada por existir, por nos trazer tanto amor e felicidade com este seu sorriso doce e olhar carinhoso. A titia ama você, com um amor que eu jamais pensei em sentir um dia. Um amor puro, incondicional e sem medidas. Estarei sempre aqui por você, conte comigo por toda a vida. Que seus dias sejam cheio de luz, assim como você é. Amo você, meu amor.

À minha amada e segunda família, meus sogros **Izilda, Marcos** e minha cunhada querida **Gabriela,**

Eu amo tanto vocês que parece que eu já era desta família desde quando nasci. Vocês são tão especiais pra mim, me sinto uma verdadeira filha. Obrigada por tanto amor, carinho, cuidado, pelas orações, força e incentivo que sempre me deram. Obrigada por todos os momentos em família, momentos de descontração, e que me fazem ter forças para lutar todos os dias. Eu sou muita grata a Deus por chamar vocês

de família, pelo presente que é o Caio, que educaram tão bem para ser um grande homem. Eu amo vocês com toda a força do meu coração.

A toda a minha amada e querida **Família,**

Obrigada pelo carinho de todos os meus primos, tios, tias que sempre se orgulharam de mim e desta forma me fizeram sentir capaz de ir além e buscar meus sonhos. Espero poder ainda dividir com vocês muitas alegrias e muitas conquistas de todos nós. Obrigada pelo amor e carinho! Eu amo cada um de uma forma muito especial.

As minhas amadas amigas e meu quinteto inabalável, **Bianca Muniz, Kamila Cardoso, Luana Antonelli** e **Mariane Dias.**

Meus amores, quem acreditaria se eu contasse que nossa amizade tem mais de 20 anos? (rsrs) Talvez isto entregaria nossas idades? Mas na verdade é que eu não me lembro da minha vida sem vocês. Desde pequenas, a panela de pressão, ninguém entra e ninguém sai, o quinteto. Amigas, eu sei que pode passar anos e anos, e nossa amizade sempre estará aqui inabalável. Somos irmãs, nascidas de mães diferentes (Uffa, que sorte a delas rsrs). Amigas foi com vocês que eu aprendi o que é lealdade, humildade, força e que beleza vai muito além de um rostinho bonito. Beleza vem de dentro, de um coração lindo e cheio de amor, como o de vocês. Obrigada por estarem presentes em todos os momentos da minha vida, nas alegrias, tristezas, nos conselhos, nos momentos de descontração. Vocês são os meus orgulhos, torço e vibro tanto com as realizações de vocês. Quem diria que chegaríamos tão longe, vocês são valentes, me ensinam só com o olhar. Eu rezo para que nossos filhos um dia tenham amigos assim como nós, pois o que temos só pode ser carinho de Deus para nossa vida, têm que ser! Obrigada por me fazerem experimentar o amor divino através da nossa amizade. Amo vocês e estarei sempre aqui, meus amores.

A minha querida amiga e companheira **Cláudia,**

Amiga meu amor, você é tão especial para mim e eu amo tanto você. Você sempre foi muito mais que uma amiga, foi também minha família, você é minha irmã. Nossa amizade é um presente! Obrigada por tudo que faz e sempre fez por mim. Eu nunca vou esquecer de todos os momentos que passamos quando morávamos juntas, e que mesmo depois disto, você sempre deixou as portas da sua casa abertas para mim, porém mais do que isto, foi as portas do seu coração. Obrigada meu amor, por tantos conselhos, por tanto carinho e amor que teve comigo durante minhas viagens incansáveis durante o doutorado. Pela caminha arrumada, pelo bolinho no café da manhã, eu nunca vou esquecer amiga. Você é um anjo e ter você como amiga, é uma benção dos céus. Obrigada por eu poder dividir minha vida com você. Te amo de todo meu coração!

A minha querida amiga e irmã de alma **Mariane Dias,**

Amiga meu amô, você é minha melhor amiga desde pequenininhas. Obrigada por tudo que você representa para mim, por ser meu refúgio e porto seguro. Que mesmo distantes sempre estaremos conectadas pelo coração. Não nascemos da mesma mãe humana, mas compartilhamos a mesma mãe divina: Nossa Senhora, que é o nosso amor maior. Amiga, obrigada por todas as vezes que guardou suas lágrimas para enxugar as minhas, por estar presente em todos os momentos da minha vida, com seus conselhos, os quais eu sigo todos eles. Você me encoraja a ser melhor, me faz acreditar que eu posso conquistar tudo, você me incentiva, me mostra os caminhos, você é luz na minha vida. Como pode isto? Mesmo longe estar tão presente. Você está em mim amiga, em cada falar, posicionamento, eu vejo você em mim ou talvez eu esteja em você, já não dá mais para distinguir. Você é meu presente da vida, meu presente dos céus. Quando nascemos, Deus disse: “Ah, essas serão irmãs”, e isto com apenas 12 dias de diferença de nascimento. Eu te admiro amiga, pelo seu coração, na mulher incrível que você se tornou, eu me espelho em você. Obrigada por me ensinar a amar de uma forma diferente, obrigada por esta amizade divina, sem cobranças e só amor. Amo você com toda a força do meu coração. Eu sempre estarei aqui, para tudo e para todo o sempre.

As minhas amadas e queridas amigas, maravilhosas: **Mariane Dias, Bianca Muniz, Kamila Cardoso, Luana Antonelli, Amanda Oliveira, Priscila Longas, Cláudia Zanini, Angélica Tsnoda, Geisa Dias** e **Cidinha,**

Amigas, a amizade de vocês me fortacele. Obrigada por vocês existirem e por trazer tanto amor e paz para minha vida. Amo cada uma de vocês de uma forma muito especial.

Aos meus queridos **colegas e amigos do Laboratório de Bioquímica,**

Aline Dionízio, Isabela Tomazini, Beatriz Souza, Tatiana Martini, Luiza Cassiano, Daiana Moreli, João Paulo Domezi, Adriana Matos, Flávia Amadeu, David Dezidério, Maria Aparecida, Juliana Pires, Juliana Trevizol, Mileni Fernandez, Cíntia Souza, Priscila Salomão, Polliana Scaffa, Senda Charone, Flávia Levy, Flávia Iano, Heloisa Pereira, Cristiane Baldini, Juliana Sanches, Thamirys Carvalho, Tamara Araujo, Samanta Moraes, Natara Dias, João Vitor Frazão, Carlos Gironda, Lethycia Almeida e em especial aos meus queridos, Vinícius Taioqui, Éven Taira, Aline Braga Adriano Pessoa, Ana Lígia Pagnan, Vanessa Fakhoury, Cíntia Tokuhara, Mariana Santesso, Gabriela Neubern e Mariana Sanches, que compartilharam comigo momentos muito especiais que vão além das bancadas do laboratório (eu sempre com o meu pezinho na cultura rsrs). Obrigada pela parceria e por tantos momentos que vivemos juntos no laboratório, por compartilharem suas vidas e seus conhecimentos acadêmicos e laboratoriais comigo. Por cada experimento, cada troca, disciplina, torcidas para os experimentos um do outro e por tantos momentos de descontração. Encontrar cada um de vocês nesta caminhado foi essencial e muito importante, pois tudo se tornou mais leve! Minha família Bioquímica, levarei vocês em meu coração por onde eu for.

A minha querida e amada amiga **Cíntia Tokuhara,**

Ci, que alegria poder te chamar de amiga. Uma amizade que foi construída com muito amor, respeito, admiração e carinho. Você é um presente que a pós-graduação me deu. Te admiro e me inspiro muito em você. Obrigada pela parceria de sempre, pela troca que temos, por tantos ensinamentos e momentos de descontração em meio aos experimentos. Obrigada por me ajudar a crescer profissionalmente e como pessoa. Você é um exemplo, com um coração imenso e lindo. Nossa amizade é um presente, que eu guardo e zelo com todo amor e carinho. Obrigada por existir e por toda a ajuda! Saiba que sempre poderá contar comigo. Amo você!

A minha querida amiga **Even Taira,**

Éven, obrigada por você existir. Por toda ajuda na realização do meu doutorado. Permanecemos juntas e unidas desde o mestrado, trabalhando juntas e podendo contar sempre uma com a outra. Obrigada por me ajudar nas coletas desta pesquisa e por todo carinho que sempre teve comigo. Estarei sempre aqui para quando precisar. Amo você!

A minha aluna de iniciação científica e que se tornou uma grande amiga **Nathalia Ribeiro,**

Ná, meus olhos já se enchem de lágrimas ao relembrar tudo que vivemos nesta pesquisa. Você foi essencial para que tudo pudesse ter sido realizado. Você foi meu braço direito e esquerdo também. Eu tenho um orgulho imenso de você. Que profissional incrível você se tornou, poder ver seu crescimento desde o curso técnico, ao qual tive a honra de ser sua professora, é realmente incrível. Acompanhar você na graduação quando você se tornou minha aluna me fez enxergar ainda mais o quanto de potencial você tem. Não importa o lugar, eu sei que onde você estiver será uma grande biomédica. Eu via toda semana sua paixão ser renovada, em cada clínica, sua atenção e carinho com nossos pacientes, sempre muito centrada, séria e cheia de vontade de trabalhar. Sem você tudo teria sido muito mais difícil, obrigada por tudo, obrigada por tanto. Hoje você está formada, levantando voos mais altos e eu me sinto muito orgulhosa por ter feito parte da sua vida. Parabéns por ser tão especial, que aluna impecável você foi. Saiba que sempre poderá contar comigo, nossa parceria foi tão grande que hoje podemos nos chamar de amigas. Amo você, Na! Você é um presente.

A minha querida **Aline Leite,**

Line, que susto que você nos deu. Não é que você foi para não voltar?! Você deixou saudades e muito conhecimento compartilhado. Meu Deus, como eu aprendi com você! Aprendi a ser forte, a não desanimar com os obstáculos da vida, me mostrou que para realizar os nossos sonhos é só querermos, sem contar o conhecimento cientifico que é só mais um detalhe em meio a tantas coisas que você me ensinou. Nunca esquecerei nossos momentos no laboratório de proteoma, o tanto que você me ensinou, as vezes com amor e as vezes com esse seu jeitinho Aline de ser, rsrs. Mas na verdade, para mim você foi um anjo que Deus colocou no meu caminho, que me ajudou em tantos protocolos, trocas de experiências e momentos de descontração. Eu levarei você em meu coração, pois seus ensinamentos estão em mim. Obrigada por tanto carinho e respeito comigo. Que Deus possa abençoar seus caminhos e te levar a ensinar tantas outras pessoas. Sucesso para você, Li! Você mora no meu coração.

A minha querida e amada amiga **Aline Braga,**

Amiga, você foi um dos meus maiores presentes da pós-graduação. É incrível a conexão que temos e acima de tudo o amor e carinho que sentimos uma pela outra. Eu agradeço a Deus todos os dias por ter colocado você nos meus caminhos, você foi meu anjo da guarda durante o doutorado. Amiga, eu nunca vou esquecer tudo que você fez por mim, por abrir as portas da sua casa para me receber durante todas as semanas de viagens a Bauru, sempre tão carinhosa comigo. Obrigada por compartilhar sua casa, sua vida e seu coração através da nossa amizade! Obrigada pelas viagens e por tanto momentos especiais que vivemos juntas. Me sinto abençoada por ter você na minha vida. Obrigada Li, saiba que sempre estarei aqui para quando precisar. Sua amizade me fortalece e me dá forças a continuar. Obrigada por todos os conselhos e ajuda! Peço a Deus que abençoe todos os seus caminhos e que você seja sempre feliz. Te amo de todo meu coração, minha querida amiga!

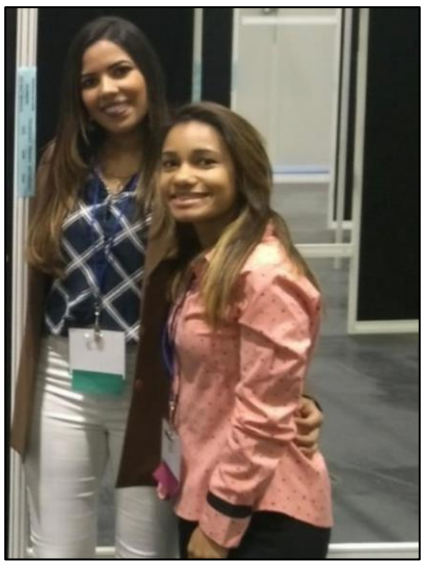

Ao meu querido e amado amigo **Vinícius Pelá,**

Vívis, eu nem tenho palavras para descrecer tudo que constríumos na nossa amizade. Você foi minha família durante a BEPE, meu amigo e irmão. Obrigada por estar ao meu lando quando realizei o meu sonho de fazer o doutorado fora, seja com os conselhos ou com o incentivo que sempre me deu. Sua amizade traz alegria para os meus dias e uma luz, que só pode ser dos ceús. Obrigada por sua amizade e por tanto momentos especiais. Obrigada pela parceria nas viagens (você é nosso fotógrafo oficial, rsrs). Obrigada amigo, por ter sido minha família em momentos que, infelizmente, eles não podiam estar por perto fisicamente. Enfrentamos uma pandemia juntos, do outro lado do mundo e hoje eu vejo que sem você eu não teria conseguido suportar. Vivemos a experiência mais incrível da nossa vida profissional e pessoal, e que benção poder dizer que estávamos juntos. Que Deus te abençoe sempre e que sua vida seja repleta de alegrias. Torço sempre por você. Amo você, meu querido amigo!

As técnicas e especialistas do Laboratório de Bioquímica, **Larissa e Thelma**,

Muito obrigada queridas Thel e Lari, vocês que sempre foram tão carinhosas comigo, pelo respeito e parceria de sempre. Obrigada por todo conhecimento compartilhado, atenção e presteza. Sempre dispostas a me ajudar em qualquer questão. Obrigada por compartilharem seus conhecimentos durante todos esses anos no laboratório e suas vidas. Eu levarei cada ensinamento comigo, pois me fizeram crescer profissionalmente. Tenho um carinho imenso por cada uma de vocês. Muito obrigada, por tudo!

Aos meus queridos professores da Disciplina de Bioquímica, **Profa. Dra. Ana Carolina Magalhães** e **Prof. Dr. Rodrigo Cardoso de Oliveira**,

Queridos professores, sou muito grata a vocês por todo conhecimento compartilhado. Agradeço por sempre estarem disponíveis a nos ajudar, pelos conselhos e por toda a troca que sempre tivemos. Obrigada pelo respeito e pelas parcerias. Eu nunca esquecerei tantos conselhos que nos davam durante as

disciplinas, vocês me fizeram crescer como profissional e levarei todos os seus ensinamentos por toda a minha vida.

A **Universidade Paulista – UNIP**, todos os funcionários e meus ex-professores que me ajudarem a me tornar a profissional que sou e em especial,

A **Profa. Dra. Patrícia Carvalho Garcia**, a **Profa. Dra. Michele Janegitz Acorci Valerio**, a **Bióloga Tatiane Andrea Lionete,** a **Biomédica Lívia Ferreira dos Santos** e a funcionária **Helen Thiago**. Serei eternamente grata por todos os ensinamentos compartilhados desde a graduação, por ter a honra de viver uma experiência única de lecionar nessa grande instituição, que me fez crescer na minha vida profissional e pessoal. Além disso, agradeço de uma forma muito carinhosa ao meu querido e eterno **Prof. Dr. Renato Massaharu Hassunuma.** Professor, eu serei eternamente grata ao senhor por todas as oportunidades que me deu durante a vida acadêmica através do seu brilhantismo em ensinar, mas também as que me deu durante a minha pós-graduação. Por me convidar a participar de projetos tão importantes e especiais como na publicação dos livros digitais, bancas de eventos e tantos outros momentos. O senhor é uma inspiração para mim, ver o seu amor em ensinar, o amor em suas aulas impecáveis, me incentiva a querer lutar e buscar a ser sempre uma profissional melhor. Muito obrigada, professor! Estarei sempre aqui para quando precisar.

A todos os meus **colegas e professores da pós-graduação**, por toda as disciplinas que fizemos juntos, por todo apoio e por compartilharem seus ensinamentos e suas experiências acadêmicas.

As secretárias do departamento **Dalva** e **Teresa**,

Minhas queridas Dalva e Teresa, muito obrigada por toda atenção que sempre dedicaram a nós alunos. Sempre me atenderam prontamente todas as vezes que precisei, retirando dúvidas e ajudando a solucionar questões burocráticas. Obrigada por toda sua atenção e presteza de sempre. Tenho um grande carinho por vocês.

As secretárias da Pós-graduação **Fátima** (*in memorian*), **Leila, Letícia, Vera e Maristela**,

Obrigada por toda atenção em responder todas as dúvidas, pela disposição de responder a e-mails tão prontamente, telefonemas e ajudar com assuntos relacionados à documentação, prazos e relatórios. Muito obrigada pela presteza de sempre!

A todos os funcionários do Centro de Pesquisa da FOB/USP, **Anderson, Luciana, Marcelo, Poliane** e **Sueli,**

Vocês me acolheram de forma única no CPC. Obrigada por sempre me ajudarem com prontuários, materiais, atendimento aos pacientes e pelos momentos de descontração. Conhecer e trabalhar com vocês durante o meu doutorado foi muito especial. Muito obrigada por tudo!

Aos meu amados e queridos **voluntários** desta pesquisa,

É uma pena, mas que devido a ética não podemos revelar o nome de vocês, mas seus nomes estão gravados em meu coração. Vocês foram extremamente fundamentais para que este trabalho fosse realizado. Que ingênua, eu que pensei que poderia ensinar algo, na verdade vocês me ensinaram tudo. Cada dia de clínica e coleta eu saia desolada, tentando entender o porquê de tudo. Porém, mesmo com o câncer que tirava tudo de vocês: fala, sono, gosto, vontade de se alimentar, autoestima, força, mas não tirava a alegria de viver. Obrigada por me ensinaram tanto, por tanto carinho que eu recebia em cada coleta, em cada olhar e sorriso por simplesmente uma conversa. Sem vocês esta pesquisa não seria possível de jeito nenhum. Obrigada por terem dado o melhor, principalmente àqueles que infelizmente não sobreviveram, mas deixaram vivos os sorrisos de vocês em minha vida. Não sei mais como estão hoje, mas tenham certeza que estarão sempre em minhas orações. Gratidão é tudo que eu tenho para falar para vocês. Muito obrigada!

Ao meu coorientador **Prof. Dr. Paulo Sérgio da Silva Santos,**

Professor, obrigada por poder nos ajudar a tornar esta pesquisa possível. Abriu as portas do Centro de Pesquisa Clínica para nós, onde se tornou a minha segunda casa. A cada clínica minha admiração e respeito pelo senhor aumentava. Que grande professor, profissional e pessoa que o senhor é. Obrigada por compartilhar seus

conhecimentos comigo e por me ajudar a crescer profissionalmente, sou muito grata ao senhor. Conte comigo sempre que precisar!

A colaboradora desta pesquisa **Profa. Dra. Cássia Maria Fisher Rubira,**

Professora querida, obrigada por nos ajudar nesta pesquisa. Lembro todos as vezes que me surgia uma dúvida, por ser um “mundo novo” trabalhar com os pacientes com câncer, e a senhora prontamente me atendia em sua sala para me tirar dúvidas, me mostrando artigos e referências para estudar e me emprestando livros. A senhora é incrível e sou muito grata por poder ter compartilhado minha pesquisa de doutorado com uma professora tão querida. Tenho uma grande admiração e respeito pela senhora! Estarei sempre aqui para quando precisar.

Ao **Prof. Dr. Jonas de Almeida Rodrigues,**

Lembro-me quando a Profa. Marília me disse sobre um projeto para desenvolvermos juntos em Bento Golçalves sobre película adquirida e provadores de vinho. Quando eu cheguei o senhor (digo senhor, pelo grande respeito que tenho), me recebeu com tanto carinho, professor. Nunca vou esquecer! Apesar de ser este professor tão importante com tamanho conhecimento, inteligência e grandes méritos, o senhor é tão acessível e humilde. Obrigada por de alguma forma, me fazer sentir parte do grupo Rodrigues et al. também. Obrigada por poder aprender tanto com vocês. As meninas, Bethânia, Natália e Nicole, foram um presente na minha vida, todos vocês são muito queridos. Serei eternamente grata por todo conhecimento e por me ajudar a crescer profissionalmente. Conte sempre comigo, professor!

Ao meu supervisor no exterior **Prof. Dr. Adrian Lussi,**

Professor Lussi, muito obrigada por me aceitar em seu laboratório e grupo de pesquisa. Obrigada por ajudar a tornar o meu sonho de fazer meu doutorado no exterior possível. Obrigada por sua disponibilidade e atenção de sempre. O senhor sempre muito atencioso nos e-mails e sempre pronto a ajudar. Thank you very much!

Ao meu supervisor no exterior **Prof. Dr. Thiago Saads Carvalho,**

Thiago, (era assim que ele gostava de ser chamado e não professor), eu tenho uma gratidão imensa por você. Obrigada por tantos ensinamentos compartilhados, por me ajudar em cada momento da minha BEPE. Sempre me atendeu prontamente em sua sala para retirar dúvidas sobre o projeto, me escutava com tamanho respeito e carinho. Obrigada por me apresentar sua família linda, que durante a BEPE passamos momentos incríveis que jamais esquecerei. Obrigada por me dar total suporte durante a pandemia e fazer me sentir que não estava sozinha. Tenho uma grande admiração por você e um carinho imenso pela Elayne e a Soso! Contem sempre comigo. Obrigada por tornar meus dias na Suiça mais leves e alegres, apesar da distância da família. Obrigada pela ajuda incondicional nos experimentos, mas também por todas as questões relacionadas a estar em um país diferente (e olha que não foram poucas, rsrs). Obrigada, Thiago! Conte sempre comigo.

Aos meus queridos **Tommy Baumman** e **Samira,**

Sou muito grata a vocês por todo apoio que sempre me deram. **Sami**, você sempre tão querida comigo, pelas conversas, momentos de descontração, ajuda nos experimentos e em discutir resultados. Obrigada por tantos momentos especiais e por todo ensinamento compartilhado. **Tommy,** sinto uma admiração tão grande por você. Um pesquisador extremamente inteligente e quando você começava a discutir os resultados todos paravam, pois assistir o seu brilhantismo na pesquisa é incrível. Muito obrigada pela ajuda em meu projeto, por querer sempre torná-lo melhor, por me ajudar a discutir os resultados e dúvidas que surgiam. Obrigada por estar com sua porta sempre aberta para nos receber. Thank you very much, Tommy. You are amazing and an inspiration for me.

A secretário do departamento **Daniela** e aos técnicos do laboratório da Universidade de Berna-Suiça**, Michel, Samuel, Brigitte, Barbara** e **Izabel,**

Obrigada por serem tão receptivos com a minha chegada. Por serem sempre prestativos e por me ajudarem em toda a minha pesquisa. Sempre com muito respeito e carinho! Dizem que os Suiços são frios, mas vocês foram tão carinhosos comigo que eu comecei a duvidar desta teoria. Obrigada por cada momento de descontração, ensinamentos e compartilhamento de experiências de vida. Sou grata a cada um de vocês e levo cada um com muito carinho em meu coração. Em especial agradeço a **Barbara** e ao **Samuel,** que me ajudaram grandemente no desenvolvimento do meu projeto de pesquisa realizado durante a BEPE, pela troca e compartilhamento de ensinamentos. Obrigada pelos seus: “Salut, Talita!”, que vinha recheado de algeria e que sempre mudava meus dias todas as manhãs com tamanho carinho. Thak you very much for everthing! Bester Dank! Merci genau!

A **Faculdade de Odontologia de Bauru- FOB/USP**, na pessoa do diretor **Prof. Dr. Carlos Ferreira dos Santos**,

É uma honra poder realizar a pós-graduação em nível de Mestrado e Doutorado nesta grande instituição, que nos dá total suporte e estrutura indiscutível. Obrigada FOB-USP por tudo que me proporcionou até hoje. É um orgulho imensurável dizer que sou FOB/USP e fazer minha pós-graduação nesta respeitada e incrível instituição.

A todos os **funcionários em geral da FOB-USP** que colaboraram de forma direta ou indiretamente no desenvolvimento deste trabalho, que contribuíram para que a minha trajetória pelo doutorado fosse ainda mais feliz.

A **Coordenação de Aperfeiçoamento de Pessoal de Nível Superior (CAPES) Código Financeiro 001** e a **Fundação de Amparo à Pesquisa do Estado de São Paulo (FAPESP),** pela concessão da minha bolsa de Doutorado no país **(Processo n°: 2017/05031-2)** e bolsa de estágio e pesquisa no exterior **(Processo n°: 2019/16815-0**; **BEPE FAPESP).** Todo este apoio financeiro foi extretamente importante para o meu crescimento profissional e pessoal. Devido a concessão das bolsas, eu pude me dedicar fielmente e integralmente as minhas atividades do doutorado, bem como em participação de congressos nacionais e internacionais que foram essenciais para o meu crescimento nesta minha jornada acadêmica.

"E tudo quanto fizerdes fazeío de todo o coração."

Colossenses 3:23

Don't be afraid

to dream.

"Bom mesmo é ir à luta com determinação,

abraçar a vida e viver com paixão,

perder com classe e vencer com ousadia,

porque o mundo pertence a quem se atreve,

e a vida é muito para ser insignificante."

Charles Chaplin.

ABSTRACT

Proteomic analysis of the acquired enamel pellicle and saliva in patients with head and neck cancer to submitted radiotherapy

Salivary glands are affected during radiotherapy in the head and neck region, leading to reduction in salivary flow and changing saliva composition. In this thesis, comprising 6 articles, we evaluated changes in the proteomic profile of the acquired enamel pellicle (AEP) and saliva in patients with head and neck cancer (HNC) submitted to radiotherapy, to search for prognosis biomarkers. In the first two articles the protocols for standardization of proteomic analysis of saliva and collection of AEP are described. In articles 3, 4 and 5, HNC patients had their AEP and saliva (unstimulated and stimulated saliva) collected before (BRT), during (2-5 weeks; DRT) and after (3-4 months; ART) radiotherapy. Saliva and AEP were also collected from healthy patients (control; C). Proteins were extracted and processed for label-free proteomics. Salivary flows were also evaluated. In total, 1,055 proteins were identified in the unstimulated saliva, among which 47 were common to all groups, while 86, 86, 286 and 395 were exclusively found in C, BRT, DRT and ART, respectively. Remarkably, alpha-enolase was increased 35-fold DRT compared with BRT, while proline-rich proteins (PRPs) were decreased. ART there was a 16-fold increase in *scaffold attachment factor-B1* and a 3-fold decrease in alpha-enolase and cystatins. When compared with C, salivary proteins of BRT patients showed increases in cystatin-C, lysozyme C, histatin-1 and PRPs (article 3). Significant differences were observed between stimulated and unstimulated salivary flows for C and BRT ($p>0.001$), but not for DRT and ART. Proteins involved with apoptosis and antibacterial function were decreased in stimulated saliva in comparison to unstimulated saliva DRT and ART (article 4). In the AEP, statherin was increased more than 9-fold and hemoglobins were increased more than 5-fold DRT compared to BRT, while lactotransferrin, PRPs cystatins, neutrophil defensins and histatin-1 were decreased. ART, lactotransferrin and isoforms of histones were increased, while statherin and alpha-amylase were decreased. MOAP-1 was exclusively found ART compared to BRT. When compared to Control, AEP of patients BRT showed an increase in proteins related to the perception of bitter taste, mucin-7 and alpha-amylases, while cystatin-S

was decreased (article 5). In article 6, we evaluated the protective effect AEP formed *in vitro* for different times on enamel, as well as its engineering with statherin peptide (StatpSpS), against initial erosion. AEP provided almost instant protection, with formation times as short as 1 min protecting the native enamel against erosion, and longer formation times did not improve the protection. StatpSpS by itself provided similar protection as the AEP. In conclusion, both HNC and radiotherapy remarkably alter the proteome of saliva and AEP. The unstimulated salivary flow is the best alternative to search for biomarkers. Monitoring alpha-enolase levels in unstimulated saliva DRT and MOAP-1 in AEP ART might be possible strategies to predict the efficacy of radiotherapy. Our results provide important information for designing more effective dental products for these patients and contribute for a better understanding of the progressive changes in salivary proteins induced by radiotherapy and the protective roles of the AEP proteins DRT.

Keywords: Proteomics. Acquired Pellicle. Enamel. Saliva. Head and neck cancer. Radiotherapy.

RESUMO

As glândulas salivares são afetadas durante a radioterapia na região da cabeça e pescoço, levando à redução do fluxo salivar e alterando a composição da saliva. Nesta tese, composta de 6 artigos, avaliamos as alterações no perfil proteômico da película adquirida do esmalte (PAE) e da saliva em pacientes com câncer de cabeça e pescoço (CCP) submetidos à radioterapia, em busca de biomarcadores prognósticos. Nos primeiros 2 artigos, os protocolos para padronização da análise proteômica da saliva e coleta da PAE são descritos. Nos artigos 3, 4 e 5, pacientes com CCP tiveram suas PAEs e salivas coletados antes (BRT), durante (2-5 semanas; DRT) e após (3-4 meses; ART) radioterapia. As salivas e PAEs também foram coletadas de pacientes saudáveis (controle; C). As proteínas foram extraídas e processadas para proteômica. Os fluxos salivares também foram avaliados. No total, 1.055 proteínas foram identificadas na saliva não-estimulada, sendo 47 comuns a todos os grupos, enquanto 86, 86, 286 e 395 foram encontradas exclusivamente C, BRT, DRT e ART, respectivamente. Notavelmente, alfa-enolase foi aumentada 35X DRT em comparação com BRT, enquanto proteínas ricas em prolina (PRPs) diminuíram. ART houve aumento de 16X da *scaffold attachment factor-B1* e diminuição de 3X da alfa-enolase e cistatinas. Em comparação ao C, nos pacientes BRT houve aumento de cistatina-C, lisozima C, histatina-1 e PRPs na saliva (artigo 3). Diferenças significativas foram observadas entre fluxos salivares estimulados e não-estimulados para C e BRT ($p>0,001$), mas não para DRT e ART. Proteínas envolvidas com apoptose e resistência antibacteriana foram diminuídas na saliva estimulada comparada com a não-estimulada DRT e ART (artigo 4). Na PAE, *Statherin* aumentou mais de 9X e hemoglobinas aumentaram mais de 5X DRT comparado com BRT, enquanto lactotransferrina, proteínas ricas em prolina, cistatinas, neutrófilo-defensinas e histatina-1 diminuíram. ART, lactotransferrina e histonas aumentaram, porém *Statherin* e alfa-amilases diminuíram. MOAP-1 foi encontrada exclusivamente ART comparada com BRT. Quando comparado ao Controle, PAE dos pacientes BRT apresentou aumento das proteínas relacionadas à percepção do sabor amargo, mucina-7 e alfa-amilases, enquanto cistatina-S diminuiu (artigo 5). No artigo 6, avaliou-se o efeito protetor da PAE formada *in vitro* no esmalte por diferentes tempos, bem como sua engenharia com peptídeo da estaterina (StatpSpS), contra erosão

inicial. A PAE protegeu quase instantaneamente esmalte natural contra a erosão, mesmo com tempos de formação tão curtos quanto 1 min. Tempos de formação mais longos não aumentaram a proteção. O StatpSpS sozinho conferiu proteção similar àquela da PAE. Em conclusão, tanto o CCP quanto a radioterapia alteram profundamente o proteoma da saliva e da PAE. O fluxo salivar não-estimulado é a melhor alternativa na busca por biomarcadores. Monitorar níveis de alfa-enolase na saliva não-estimulada DRT e MOAP-1 na PAE ART podem ser estratégias possíveis para predizer a eficácia da radioterapia. Nossos resultados fornecem importantes informações para o desenvolvimento de produtos odontológicos mais eficazes para estes pacientes e contribuem para um melhor entendimento do papel protetor da PAE e das alterações progressivas que ocorrem nas proteínas salivares em consequência da radioterapia.

Palavras-chave: Proteômica. Película Adquirida. Esmalte Dentário. Saliva. Câncer de cabeça e pescoço. Radioterapia.

TABLE OF CONTENTS

1 - Introduction

**“Ninguém é tão grande que não possa aprender,
nem tão pequeno que não possa ensinar.”**

Esopo

1 INTRODUCTION

Cancer is a major global public health problem, causing high rates of morbidity and mortality worldwide (Dandekar, Tuljapurkar et al. 2017). This is due to the growth and aging of the population and the prevalence of risky behaviors, such as tobacco and alcohol consumption, poor eating habits and changing reproductive patterns. According to GLOBOCAN, in 2018 there were 18.1 million new cancer cases and 9.6 million cancer-related deaths (Bray, Ferlay et al. 2018, Ferlay, Colombet et al. 2019). In the United States, cancer is the second most common cause of death, just behind the incidence of heart disease (Wang, Kaczor-Urbanowicz et al. 2017). Despite the differences between the types of cancer, they all share the same changes in cell physiology that lead to the formation of tumors (Wang, Kaczor-Urbanowicz et al. 2017).

Head and Neck Cancer (HNC) refers to a group of biologically similar cancers that originate in a variety of locations. Among them are the oral cavity (including lip, tongue, jaw, floor of the mouth, buccal mucosa, gingiva, retromolar triangle and hard palate), the nasal cavity and paranasal sinuses, pharynx (nasopharynx, oropharynx and hypopharynx), larynx, thyroid, trachea and salivary glands (Leemans, Braakhuis et al. 2011, Safdari, Khalili et al. 2014). Therefore, the term HNC represents malignant neoplasms of the upper aerodigestive tract, which includes the oral cavity, pharynx and larynx. The location of the disease imposes on the patient and family members intense physical, social and psychological suffering, in view of the changes caused in the individual's basic functions, such as food, breathing and speech (Cruz, Ferreira et al. 2016).

It is generally assumed that, over the past two decades, there has been a significant improvement in the quality of life of cancer patients, mainly due to the use of advanced surgical and radiotherapy techniques, as well as organ preservation protocols. However, there has been no increase in five-year survival rates in recent decades, mainly due to the frequent development of metastases, locoregional recurrences and second primary tumors (Leemans, Braakhuis et al. 2011).

HNC affects the quality of life both in diagnosis and during treatment, including functional, emotional, social and physical impacts (de Oliveira, Dos Santos et al. 2017). The treatment of HNC varies according to its histological type, location and clinical

stage. The main treatment options are surgery, radiation and chemotherapy. It is known that these treatments have functional, aesthetic and emotional consequences that directly influence the quality of life of these patients (de Oliveira, Dos Santos et al. 2017).

Squamous cell carcinoma of the head and neck is the fifth most common cancer and the sixth most common cause of cancer deaths globally. Most patients with this type of cancer have advanced disease, which can occur locally or as a metastatic disease (Soulieres, Faivre et al. 2017). In 2018, HNC was considered the seventh most common cancer worldwide with 890,000 new cases and 450,000 deaths (Bray, Ferlay et al. 2018). It is usually associated with the continued use of tobacco and alcohol (Kawakita and Matsuo 2017), but it also associated with human papillomavirus (HPV) infections (Rettig and D'Souza 2015, Chow 2020).

Radiotherapy is the therapeutic modality adopted for the treatment of HNC, being the most important non-surgical treatment for this disease. However, radiotherapy in the head and neck is related to some adverse effects, such as mucositis, hyposalivation, xerostomia, alteration of taste, dental caries and radiodermatitis, which can trigger a negative impact on the quality of life of these patients (Cruz, Ferreira et al. 2016). Of the 45% -50% of cancer patients who have a chance of cure, 70% receive radiotherapy as a treatment modality (Van De Wiele, Signore et al. 2001). However, when radiotherapy is applied to the head and neck, depending on factors such as irradiation dose, treatment time, treatment volume, dose of distribution and the concomitant use of other therapies, it can produce reversible and irreversible changes in tissues, that can also occur in healthy tissues located in areas adjacent to the tumor mass (Peterson and D'Ambrosio 1992). The deleterious effects caused by radiotherapy considered in this region are those that occur in the salivary glands, bones, teeth, mucous membranes of the mouth, muscles and joints that combine the loss of cells and the damage in local vascularization (Mira, Fullerton et al. 1982, Makkonen 1988). This is the case of the major salivary glands, which are usually present in the irradiated field, suffering the consequences of radiotherapy in the head and neck region and leading patients to severe conditions of hyposalivation and xerostomia.

Xerostomia is the deleterious effect that first affects the patient, and is also the most common, leading the patient to experience difficulties in eating, as the bolus does not form properly due to dry mouth; speaking, because the patient needs to drink fluids

for that; sleeping, because the mouth is dry and the mucous membranes are collapsed, which makes the patient wake up at night to drink water (O'Connell 2000). The atrophy that occurs in the acini, caused not only by hyperfractionated but also by conventional radiotherapy (a daily application of irradiation), leads to a decrease in salivary flow (Dorr and Hendry 2001, Mateos, Setoain et al. 2001, Warde, O'Sullivan et al. 2002) and leads to the loss of saliva functions, leaving the oral environment unprotected and prone to secondary infections, in addition to making the saliva sparse, thick and sticky (Mandel 1987).

The decrease in unstimulated salivary flow is constant in head and neck radiotherapy, when larger salivary glands are present in the irradiated area (Guebur., A. et al. 2004). Among patients irradiated in the head and neck region, xerostomia is one of the most frequent complaints (Guchelaar, Vermes et al. 1997). Studies have shown that 80% of irradiated patients complain of xerostomia (Chencharick and Mossman 1983). However, the relationship between individual perception of dry mouth (xerostomia) and the real values of salivary flows has not yet been fully defined. (Logemann, Smith et al. 2001). In some situations, there is a correlation between reduced salivary flow (hyposalivation) and a complaint of dry mouth (Pow, McMillan et al. 2003). However, in many cases there is no association between xerostomia and the findings of dysfunction of the salivary glands, that is, patients without changes in the salivary flow may complain of dryness in the mouth. Patients with xerostomia complain of oral discomfort, loss of taste, difficulties in speech and swallowing (Davies, Broadley et al. 2002). Saliva also suffers qualitative changes resulting from radiotherapy, such as decreased amylase activity, buffering capacity and pH, with consequent acidification. There are also changes in the various electrolytes such as calcium, potassium, sodium and phosphate (Silverman 1999, Pow, McMillan et al. 2003). Thus, patients who have been irradiated are more susceptible to periodontal disease, rampant cavities, fungal and bacterial oral infections. (Hancock, Epstein et al. 2003) and even dental erosion, since changes occur such as acidification of saliva (Lajer, Buchwald et al. 2009).

Another major consequence is cavities caused by radiation. Even individuals who have had no carious activity for some time can develop radiation cavities when undergoing radiation therapy (Silverman 1999). The main factor for such injuries to develop is the decrease in the amount of saliva, as well as qualitative changes

(Epstein, Chin et al. 1998). In addition, radiation has a direct effect on teeth, making them more susceptible to demineralization (Silverman 1999).

According to a study in laboratory animals, the effect of the dose of radiation still seems inconclusive. A simple dose of 250cGy is enough to cause significant changes in the physiology of these animals' salivary glands (Nagler, Baum et al. 1998), whereas a dose of 4000cGy induces irreversible damage to secretory cells (Vissink, Panders et al. 1988). Hyposalivation is one of the most frequent sequelae and is defined as a clinical condition characterized by a qualitative and quantitative reduction in salivary flow. Hyposalivation occurs when radiotherapy is applied to the salivary glands, especially if the parotid is included, as it is the most radiosensitive among the glands (Rudat, Meyer et al. 2000, Antonadou, Pepelassi et al. 2002).

Saliva plays a key role in lubrication, chewing, swallowing and digestion. It protects the integrity of oral tissues, and also provides biomarkers for local and systemic diseases. Saliva is a biological fluid composed of more than 99% water and less than 1% proteins, electrolytes and other low molecular weight components. It originates mainly from three pairs of major salivary glands (the parotid, submandibular and sublingual glands), as well as from 300 to 400 minor salivary glands present in the oral cavity (Wang, Kaczor-Urbanowicz et al. 2017). Therefore, saliva contains more than 2,000 proteins and peptides that are involved in a multitude of different biological functions in the oral cavity (Wang, Kaczor-Urbanowicz et al. 2017). Currently, mass spectrometry (MS) is the basic technology for the identification of these salivary proteins, and the proteomic analysis of saliva has distinct advantages in relation to blood, especially for low abundance proteins (Winck, Prado Ribeiro et al. 2015, Wang, Kaczor-Urbanowicz et al. 2017).

Saliva still plays a great role in the formation of the acquired pellicle, which starts forming just a few seconds after the enamel is exposed to saliva, with a rapid increase in its thickness, reaching about 10-20 nm in the first minutes, which remains stable for about 30 minutes (Hannig 1999). The acquired enamel pellicle (AEP) is an organic layer, bacterial-free, that is formed in vivo as a result of the selective adsorption of salivary proteins to the surface of tooth enamel (Dawes, Jenkins et al. 1963). Its formation is a dynamic process, influenced by several factors, such as circadian cycle, composition of the oral microbiota, proteolytic capacity of the oral environment and physical-chemical properties of the dental surfaces (Lendenmann, Grogan et al. 2000), as well as location in the oral cavity (Ventura, Cassiano et al. 2017).

The main components identified in AEP are proteins and glycoproteins, but carbohydrates, neutral lipids, phospholipids and glycolipids are also found (Hannig and Joiner 2006, Siqueira, Custodio et al. 2012). Each protein plays a special role in the pellicle and is of great importance for understanding the role of this organic film (Hannig and Joiner 2006, Vitorino, Calheiros-Lobo et al. 2007, Buzalaf, Hannas et al. 2012, Siqueira, Custodio et al. 2012). AEP proteins come mainly from glandular secretions, such as from the larger glands, as well as from the smaller glands, but they also originate from the crevicular fluid, oral mucosa and microorganisms. However, saliva is the biggest contributor to the protein composition of AEP (Hannig, Fiebiger et al. 2004).

In the formation of the AEP, initially, selective adhesion of precursor proteins, with a high affinity for hydroxyapatite, occurs. These proteins interact electrostatically with the enamel surface (Hay 1973). In the second stage of the pellicle formation, called the maturation stage, there is a rapid increase in its thickness (100-1000 nm), which together with the presence of globular structures, suggests the involvement of protein aggregates, more than individual proteins, in their development (Hannig and Balz 2001). The formation and maturation of the pellicle can also be influenced by extrinsic factors, such as tooth whitening products, abrasive dentifrices and ingestion of acidic foods and drinks (Hara and Zero 2010). Due to its composition, AEP forms a protective interface between the surface of the tooth and the oral cavity, reducing friction and abrasion. AEP also acts as a semipermeable barrier, which modulates the processes of mineralization/demineralization, modulating mineral precipitation and adherence of microorganisms to the tooth surface (Hannig and Joiner 2006, Hara and Zero 2010, Buzalaf, Hannas et al. 2012, Vukosavljevic, Custodio et al. 2014).

Due to its intimate contact with the tooth surface, AEP is of great value for maintaining dental integrity (HANNIG; JOINER, 2006; SIQUEIRA et al., 2007). Because of this, AEP is considered of great biological importance and clinical interest (Armstrong, 1968). Therefore, knowledge about the formation, composition and function of the AEP can clarify the process of adsorption of salivary proteins on the tooth surface, as well as the processes of demineralization/remineralization, bacterial adhesion and antimicrobial activity. With the development of sensitive proteomic analysis techniques in the recent years, it has been possible to characterize organic material such as proteins and peptides in the AEP (SIQUEIRA et al., 2007).

Proteomics studies have brought a breakthrough in understanding the protein composition of the AEP, as well as the impact of different proteins found in the pellicle in the prevention of dental caries and dental erosion (Vitorino, Calheiros-Lobo et al. 2007, Siqueira and Oppenheim 2009, Lee, Zimmerman et al. 2013, Zimmerman, Custodio et al. 2013, Vukosavljevic, Custodio et al. 2014, Vukosavljevic, Hutter et al. 2014, Delecrode, Siqueira et al. 2015). So, the knowledge of the composition of the PAE undoubtedly gained prominence when proteomic techniques started to be used for its elucidation, instead of the enzymatic or immunological techniques, which were previously employed (Siqueira, Custodio et al. 2012). This is due to the high sensitivity of proteomic techniques, and the fact that they allow many proteins to be identified at the same time, as well as to analyze their respective interactions and processes that are involved.

Using LC-ESI-MS/MS (liquid chromatography coupled to electrospray ionization with tandem mass spectrometry), to date, there are in the literature proteomic studies evaluating the composition of the pellicle formed *in vivo* on the enamel of deciduous and permanent teeth (Siqueira, Zhang et al. 2007, Siqueira and Oppenheim 2009, Zimmerman, Custodio et al. 2013) and two studies have investigated which proteins remain in the acquired pellicle formed on dentin *in situ* (Delecrode, Siqueira et al. 2015) or in the enamel *in vivo* (Delecrode, Siqueira et al. 2015) after exposure to citric and lactic acids, simulating erosive or cariogenic challenges, respectively. It was observed that mucins (Delecrode, Siqueira et al. 2015) and cystatins (Delecrode, Siqueira et al. 2015), when adsorbed on AEP, are resistant to acid removal in dentin and enamel, respectively. More recent studies investigated the difference in the protein profile of the AEP formed in the different dental arches (Ventura, Cassiano et al. 2017), the AEP proteome after exposure to different types of milk (Cassiano, Ventura et al. 2018) and after the application of gels containing epigallocatechin gallate (EGCG) (de Souza, da Silva Ventura et al. 2017). Interestingly, after erosive challenges with hydrochloric acid, statherin remained in the AEP formed for 3 min and 120 min (Taira, Ventura et al. 2018). Moreover, hemoglobin is increased in the AEP of patients with gastroesophageal reflux with a lower grade of erosive tooth wear (Martini, Rios et al. 2019) and AEP engineering with sugarcane-derived cystatin (CaneCPI-5), statherin-derived peptide (StN15) and hemoglobin increases acid-resistant proteins, which reduces initial erosion (Carvalho, Araujo et al. 2020).

In recent years, many efforts have been directed towards the development of new strategies for detection, diagnosis, treatment and the search for quality of life for patients with HNC. However, many of these patients are subjected to high doses of radiotherapy in extensive radiation fields, which include the oral cavity, maxilla, mandible and salivary glands. Radiotherapy, despite having the advantage of preserving the structure of tissues, causes numerous adverse reactions that manifest in the oral cavity (Specht 2002). Oral complications resulting from radiotherapy result in high morbidity and decreased quality of life, and vary in intensity, classified as mild, moderate and severe (Murad AM 1996). These adverse reactions can occur in an acute phase (during or in the weeks immediately following treatment) or in a chronic phase (months or years after radiotherapy). The severity of acute oral complications will depend on the degree of inclusion of these structures in the irradiation field (Specht 2002).

As mentioned above, the major salivary glands are usually present in the irradiated field, suffering the consequences of radiotherapy in the head and neck region and leading patients to severe conditions of hyposalivation and xerostomia. Therefore, since salivary glands are the main contributors to the protein composition of the AEP, profound changes in the proteome of this integument are expected in patients undergoing head and neck radiotherapy. To the best of our knowledge, there are no previous studies that evaluated the changes in the protein profile on saliva and AEP in patients before, during and after radiotherapy. This knowledge may help to define the best preventive and therapeutic strategies to increase the quality of life of these patients, as well as to identify possible prognostic biomarkers.

In this thesis, we evaluated changes in the proteomic profile of the acquired enamel pellicle (AEP) and saliva in patients with head and neck cancer (HNC) submitted to radiotherapy, to search for prognosis biomarkers. The thesis comprises 6 articles, with the following aims:

- Article 1: The aim was to standardize a protocol for extraction of salivary proteins for further proteomic analysis.
- Article 2: The aim was to develop an *in vitro* AEP formation protocol comparing different collection solutions for *shotgun* proteomic analysis.
- Article 3: The aim was to evaluate the proteomic profile of unstimulated saliva from cancer patients, diagnosed with HNC and submitted to treatment by radiotherapy.

- Article 4: The aim was to quantitatively compare the proteomic profile of stimulated and unstimulated saliva in patients with HNC treated with radiotherapy.
- Article 5: The aim was to evaluate the proteomic profile in the AEP *in vivo* in HNC patients treated with radiotherapy.
- Article 6: The aims to evaluate the protective effect of the AEP formed *in vitro* for different times, as well as its engineering with Statherin peptide (StatpSpS), against initial dental erosion.

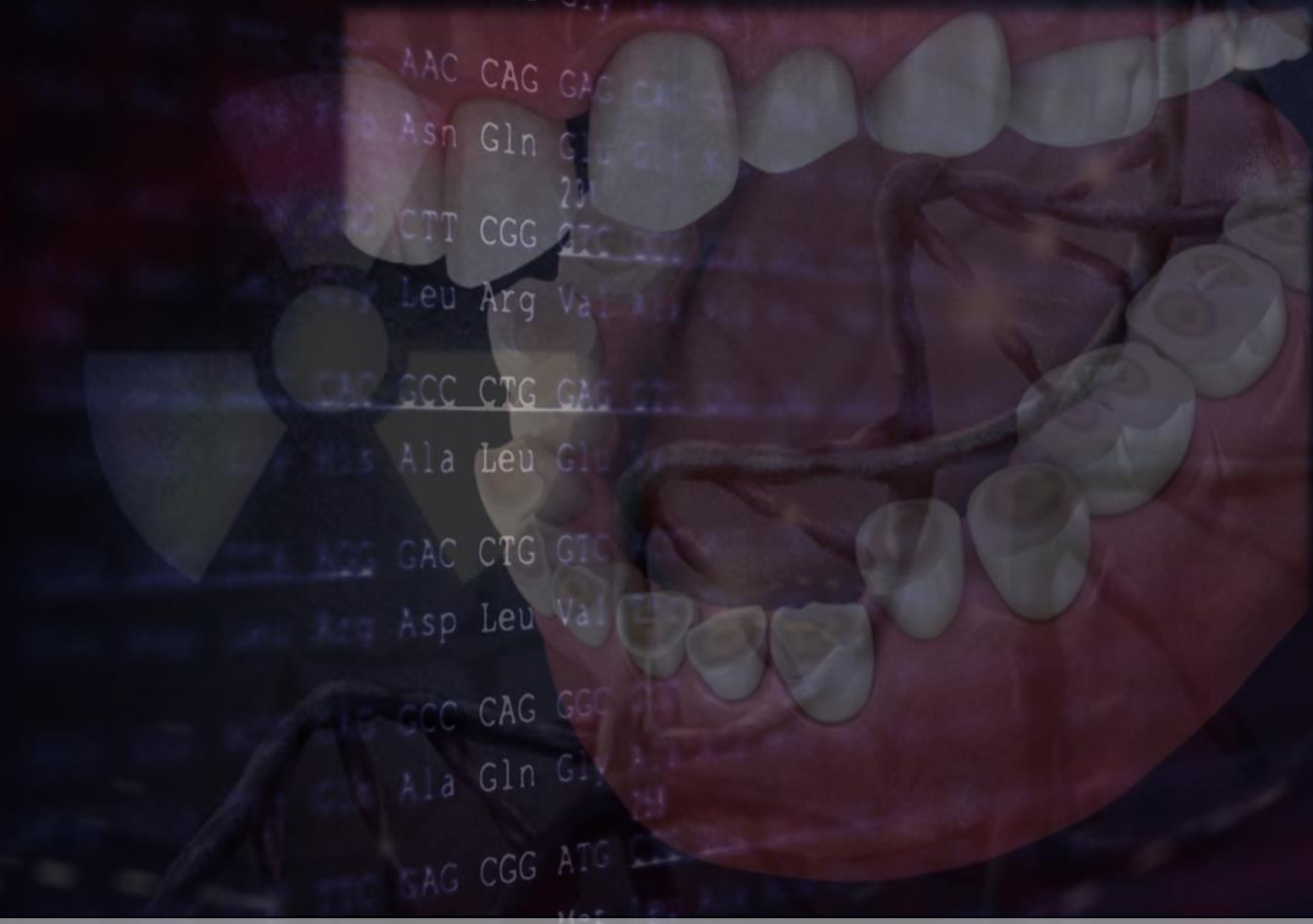

2- Articles

“Grandes realizações são possíveis quando se dá importância aos pequenos começos.”

Lao-Tsé

2.1 ARTICLE 1

Article formatted and published according to Journal of Applied Oral Science

DOI: 10.1590/1678-7757-2017-0561

Standardization of a protocol for shotgun proteomic analysis of saliva

Talita Mendes da Silva VENTURA (ORCID ID: 0000-0003-2101-1350), Nathalia Regina RIBEIRO (ORCID ID: 0000-0002-6086-6303), Aline Salgado DIONIZIO (ORCID ID: 0000-0002-8687-0124), Isabela Tomazini SABINO (ORCID ID: 0000-000107596-7855), Marília Afonso Rabelo BUZALAF (ORCID ID: 0000-0002-5985-3951)

Universidade de São Paulo, Faculdade de Odontologia de Bauru, Departamento de Ciências Biológicas, Bauru, São Paulo, Brasil.

Corresponding address:
Marília Afonso Rabelo Buzalaf
Departamento de Ciências Biológicas – Faculdade de Odontologia de Bauru – Universidade de São Paulo
Al. Octávio Pinheiro Brisolla, 9-75 - Bauru-SP – CEP 17012-901 – Brasil
Tel. + 55 14 32358346/Fax + 55 14 32271486 - e-mail: mbuzalaf@fob.usp.br

Submitted: November 14, 2017
Modification: December 22, 2017
Accepted: January 12, 2018

ABSTRACT

Saliva contains numerous proteins and peptides, each of them carries a number of biological functions that are very important in maintaining the health of the oral cavity and also yield information about both local and systemic diseases. Currently the proteomic analysis is the basis for large scale identification of these proteins and discovery of new biomarkers of distinct diseases. **Objective:** This study compared methodologies for extraction of salivary proteins for proteomic analysis. **Material and Methods:** Saliva samples were collected from 10 healthy volunteers. In the first test, it was evaluated the necessity of using an albumin and IgG depletion column, employing pooled samples from the 10 volunteers. In the second test, analysis of the pooled samples was compared with individual analysis of one sample. Salivary proteins were extracted and processed for analysis by LC-ESI-MS/MS. **Results:** In the first test, only 35 proteins were identified when the albumin and IgG depletion column was used, while 248 proteins were identified when the column was not used. In the second test, the pooled sample allowed identification of 212 proteins, such as carbonic anhydrase 6, cystatins isoforms, histatin 1 and 3, lysozyme C, mucin-7, protein S100-A8 and A9, statherin, while individual analysis allowed the identification of 239 proteins, among which are carbonic anhydrase 6, isoforms of cystatin, histatin-1 and -3, lactotransferrin, lyzozyme C, mucin-7, protein S100-A8 and A9, serotransferrin and statherin. **Conclusions:** The standardization of the protocol for salivary proteomic analysis was satisfactory, since the identification detected typical salivary proteins other proteins were also identified, which allowed the identification of a greater number of proteins. The results indicate that it is not necessary to use the column for depletion of albumin and IgG and that it is possible to perform individual analysis of saliva samples.

Keywords: Methods. Proteomics. Standardization. Saliva.

INTRODUCTION

Saliva is a biological fluid composed of more than 99% water and less than 1% protein, electrolytes and other low molecular weight components. It originates mainly from three pairs of major salivary glands (parotid, submandibular and sublingual glands), as well as from 300 to 400 minor salivary glands present in the oral cavity. Saliva plays a key role in lubrication, chewing, swallowing and digestion. It protects the integrity of oral tissues, and also provides biomarkers for local and systemic diseases[17]. Therefore, saliva contains more than 2000 proteins and peptides that are involved in an infinity of different biological functions in the oral cavity[17]. Saliva still plays a large role in the formation of the acquired pellicle, which begins only a few seconds after exposure of the enamel to saliva[5].

Human saliva is a biological fluid with enormous diagnostic potential. Because saliva can be non-invasively collected, it provides an attractive alternative for blood, serum or plasma[13]

In the saliva human were identified 1166 proteins and high portions of these proteins were found in serum. Currently, progress in salivary diagnostics has demonstrated that these contents can be very informative for the detection of oral diseases and systematic[20].

Proteomics, a new field of research centered on the identification, quantitation, and characterization of proteins and their interplay, is based to a large extent on the robustness, sensitivity, speed, and throughput of mass spectrometric procedures[6]. Currently, mass spectrometry (MS) is the basic technology for large-scale identification of these salivary proteins, and proteomic analysis of saliva has distinct advantages in relation to blood, especially for proteins of low abundance[17,18]. One of the main challenges in proteomic analysis is the fact that highly abundant proteins can impair the identification of low abundance proteins, considering the dynamic range of the equipment. In the case of saliva, albumin and IgG are very abundant and some authors have recommended using columns for depletion of these proteins during the extraction procedure[7,8] the saliva contains numerous proteins and peptides, each of them carries several significant biological functions. These proteins are not only important in maintaining the health of the oral cavity but also may yield information about both local and systemic disease. Functions of the saliva are not only restricted to processing food for digestion. Saliva contains a large number of proteins, which play important roles in the regulation of the immune defense, endocrine system and maintenance of mucosal tissue and dental health[1].

Saliva may contain locally expressed proteins and other substances that can be used as indicators of diseases that called biomarkers, can be closely related to an individual's health condition and can change greatly when diseases afflict. In general, most studies view saliva wrongly as a homogeneous body fluid. It is also not stable but constantly in change and the

composition is affected among other things by sampling methodology, environment, periodicity, oral hygiene, psychological status and general health[6,13,20].

Considering the importance of saliva in the homeostasis of the oral cavity, as well as its great potential as a diagnostic fluid, the aim of the present study was to standardize a protocol for extraction of salivary proteins for further proteomic analysis. In the first test, we evaluated the need of using an albumin and immunoglobulin G (IgG) column to deplete these proteins during protein extraction. In the second test, we compared analysis of samples pooled from 10 volunteers in relation to individual analysis.

MATERIAL AND METHODS

Ethical aspects and human subjects

The protocol of this study was submitted and approved by the Ethics Committee in Research with Human Beings of the Bauru School of Dentistry - FOB/USP (CAAE No. 61484116.0.0000.5417). Based on previous *in vivo* study[18], ten participants with good general and oral health took part of the study. Inclusion criteria were: nonsmokers with good general and oral health, stimulated salivary flow >1 mL/min and non-stimulated salivary flow <0.25 mL / min, with salivary pH>6.0.

Saliva collection

The volunteers were asked to rest for 15 minutes before collecting saliva, sitting upright. They were asked not to speak or eat before beginning to collect saliva. First, they rinsed their mouths with 5 mL of drinking deionized water and then they were asked to swallow saliva for 5 minutes. After this period, the volunteers spit out all the saliva that was put together in the mouth in a plastic tube immersed in ice for 10 minutes (non-stimulated flow). The saliva samples were immediately centrifuged at 14,000 g for 15 minutes at 4°C to remove all debris, such as insoluble material, cell debris and food debris. The supernatant from each sample was collected and frozen at -80°C until analysis. These procedures based on previous studies[6,18].

Preparation of the saliva samples

The experiments were performed into two phases. The first test was done to evaluate whether or not the albumin & IgG Depletion SpinTrap column (GE Healthcare®, Buckinghamshire, UK) should be used. The second test was performed after the results of the

first to compare analysis of salivary samples pooled from all the 10 volunteers with analysis of an individual sample from one selected volunteer.

For the first test, 100 µl of saliva from each volunteer was taken and transferred to 10 new tubes. For the second test, 100 µl of each saliva sample was also taken and transferred to 10 new tubes to constitute the pool, while 1 ml of saliva was taken from only one of the volunteers (randomly selected) for individual analysis.

Proteins from the saliva samples were extracted using an equal volume of a solution containing 6 M urea, 2 thiourea in 50 mM NH_4HCO_3 pH 7.8. The samples were vortexed at 4°C for 10 minutes, sonicated for 5 minutes and centrifuged at 14,000 g at 4°C for 10 minutes. This step was repeated once more. It is noteworthy that for the first test (with or without the use of the albumin and IgG depletion column), 100 µl of the extraction solution was added to each Eppendorf tube. For the second test (pool X individual analysis), 100 µl of the extraction solution were added in each Eppendorf tube (for the samples that will be pooled later on), while for the individual sample, 1 ml of the extraction solution was added. In all the cases, an equal volume of saliva sample and extraction solution was used. For the pooled samples, after the extraction procedure, the content of the 10 tubes was placed in one tube, constituting the pool for further analysis.

After extraction, for the first test, the pooled sample was loaded into the albumin & IgG depletion columns, according to the manufacturer´s instructions Albumin & IgG Depletion SpinTrap column (GE Healthcare®, Buckinghamshire, UK). This column was not used in the second test.

The samples were then concentrated to 150 µl using a Falcon Amicon tubes (Merck Millipore®, Tullagreen, County Cork, IRL). After concentration, the samples were reduced with 5 mM dithiothreitol (DTT) for 40 minutes at 37°C, alkylated with 10 mM iodoacetamide (IAA) for 30 minutes in the dark. After this procedure, 100 µl of 50 mM NH_4HCO_3 were added and the samples were digested with 2% (w/w) trypsin (Promega®, Madison, USA) for 14 hours at 37°C. After this period, 10 µl of 5% formic acid was added to stop the trypsin reaction, then the samples were purified and desalted using the C18 Spin columns (Thermo Scientific®, Rockford, Illinois, USA) and a 1 ul aliquot of each sample from the tests was withdrawn for protein quantification by the Bradford method (Bio-Rad®, Hercules, Califórnia, USA)[16]. The samples were resuspended in the solution containing 3% acetonitrile and 0.1% formic acid to be submitted to nano Liquid Chromatagraphy Electron Spray Ionization Tandem Mass Spectrometry - LC-ESI-MS/MS (Waters, Manchester, New Hampshire, UK).

Shotgun label-free quantitative proteomic analysis

Peptides identification was performed on a nanoACQUITY UPLC-Xevo QTof MS system (Waters, Manchester, New Hampshire, UK). The nanoACQUITY UPLC was equipped with nanoACQUITY HSS T3, analytical reverse phase column (75 µm X 150 mm, 1.8 µm particle size (Waters, Manchester, New Hampshire, UK). The column was equilibrated with mobile phase A (0.1% formic acid in water). Then, the peptides were separated with a linear gradient of 7-85% mobile phase B (0.1% formic acid in ACN) for 70 min at a flow rate of 0.35 µL/min. The column temperature was maintained at 55°C. The Xevo G2 Q-TOF mass spectrometer was operated in positive nanoelectrospray ion mode and data were collected using the MSE method in elevated energy (19-45 V), which allows data acquisition of both precursor and fragment ions, in one injection. Source conditions used included capillary voltage, 2.5 kV; sample cone, 30 V; extraction cone, 5.0 V and source temperature, 80øC. Data acquisition occurred over 70 min and the scan range was 50–2000 Da. The lockspray, used to ensure accuracy and reproducibility, was run with a [Glu1] fibrinopeptide solution (1 pmol/µL) at a flow rate of 1 µL/min, as a reference ion in positive mode at m/z 785.8427. ProteinLynx Global Server (PLGS) version 3.0 was used to process and search the LC-MSE continuum data. Proteins were identified with the embedded ion accounting algorithm in the software and a search of the Homo sapiens database (reviewed only, UniProtKB/Swiss-Prot) downloaded on September 2015 from UniProtKB (http://www.uniprot.org/). The use of the human database excludes the identification of bacterial proteins that could be present in the saliva.

RESULTS

In the first test, when the albumin and IgG depletion column was used, the total amount of protein recovered from the pooled samples after extraction was 8 µg, while only 35 salivary proteins were identified. Among them are proteins typically found in saliva, such as alpha-amylase 1 and 2B, isoforms of cystatin, isoforms of hemoglobin and mucin-7, among others (Table 1). When the depletion column was not used, the amount of protein recovered was much higher (48.0 µg) and 248 proteins were identified, among them many typical components of saliva such as alpha-amylase 1 and 2B, many isoforms of cystatin, carbonic anhydrase 6, lactotransferrin, lysozyme C, mucin-7, proline-rich protein 4, protein S100-A9, serotranferrin, statherin, several isoforms of hemoglobin, among others (Table 2).

In the second test, for comparison of analysis of pooled X individual sample, the depletion column was not employed. For the pooled sample, the amount of protein recovered after extraction was 54.02 µg, which allowed the identification of 212 proteins, including alpha-

amylase 1 and 2B, carbonic anhydrase 6, isoforms of cystatin (B, C, D, S, AS, SN), histatin 1 and 3, lysozyme C, mucin-7, protein S100 -A8 and A9, statherin, several isoforms of hemoglobin, among others (Table 3). In the analysis of the individual sample, 25.13 µg of total protein were obtained and 239 proteins were identified, among which are alpha-amylase 1 and 2B, alpha-enolase, carbonic anhydrase 6, many isoforms of cystatin (B, C-D, S, SA, SN), histatin -1 and 3, Ig alpha-2 chain C region, Ig a chain C region, lactotransferrin, lyzozyme C, mucin-7, protein S100-8 and A9, serotransferrin, statherin, among other proteins (Table 4).

DISCUSSION

This study aimed to standardize a protocol for proteomic analysis of saliva that is sensitive, easy to perform and of low cost, to be used in future experiments involving quantitative shotgun proteomics. The first issue to be solved was related to the necessity of depletion of highly abundant proteins in saliva, such as albumin and IgG[8,14] that could mask and make difficult the identification of low abundance biomarkers. Krief and collaborators[7] (2011), evaluated whether depletion of salivary amylase, albumin and IgGs could improve the ability to visualize proteins in two-dimensional gel electrophoresis (2-DE) in oral fluids. They observed a total of 36 new spots after depletion and 58 spots showed more than twofold increase intensity after depletion[7]. Therefore, we hypothesized that this better identification profile could occur not only in two-dimensional electrophoresis gel (2-DE), but also in shotgun proteomics, when albumin and IgG were depleted. Thus, in the first test we performed, we compared the use or not of the albumin and IgG depletion column after the extraction process of the salivary proteins. For this, we used a pool of ten saliva samples. When the column was used, only 35 proteins were identified (Table 1). This figure increased to 248 when the column was not employed (Table 2). We believe that this occurred because when using the albumin and IgG depletion column, there was also the depletion of other proteins, since using the column increases one more process in the methodology and also, that many proteins could bind to albumin and IgGs, thus being depleted together. It is also noteworthy that among the identified proteins, in both situations, are proteins typically found in saliva. However, when the depletion column was employed, classical salivary proteins such as 14-3-3 proteins, histatins, statherin, lactoperoxidade, lactotransferrin, lysozyme C, neutrophil defensins, protein S-100 A9, serotransferrin and some isoforms of cystatin were not identified. Thus, contrarily to which was observed in gel-based proteomics[7], in shotgun proteomics the use of albumin and IgG depletion column impaired protein identification according to our workflow. Some studies, however, report advantages in using depletion columns when more than workflow is employed [14]. However, this increases the time and cost of the analysis.

After performing the first test, in the subsequent test, we compared analysis of pooled samples (from ten individuals) *versus* individual analysis, without using the depletion column. In the individual analysis 239 proteins were identified (Table 4), while 212 proteins were identified in the pooled sample (Table 3). One-hundred and twenty-three proteins were common to both groups (data not shown) and among them are most of the proteins typically found in saliva. The proteins exclusively found in the individual sample or in the pooled sample are proteins not typically reported in saliva, which might be related to individual variation. It should be noted that especially in quantitative shotgun proteomics the analysis of individual samples is important, to allow confident comparison among the groups under study.

Generally, the methodologies used in proteomics are classified into two main categories: the bottom-up, which is also called shotgun proteomics or top-down proteomics. Both methodologies have advantages and limitations and their employment depends on the treatment given to the sample[9]. The shotgun proteomics is characterized by analyzing samples after proteolytic digestion in peptides, which is typically performed with trypsin[2,9], while the top-down proteome of a sample involves analysis of intact proteins[9]. In shotgun proteomics, proteins from a complex mixture are digested and the resulting peptides are analyzed by mass spectrometry. One of the advantages of this strategy is to investigate a large number of proteins regardless of their size. The limitations are related to incomplete coverage of the protein sequence, loss of post-translational modifications and degradation as a result of proteolytic digestion[4,9]. The top-down proteomics differs from the shotgun as it explores intact proteins by injecting the proteins into the mass spectrometer without performing digestion, minimizing any change in the sample and allowing a better characterization of post-translational modifications, especially those related to naturally occurring cleavages and alternative splicing[3], avoiding interference problems based on peptides and allowing deducing the primary structure of the protein[4,9]. However, this technique is considered bounded by the collision energy required in protein fragmentation that is insufficient for proteins greater than 50 KDa and its application is restricted to the analysis of purified proteins[4,9,11]. In addition, top-down proteomics method requires the use of one or more forms of separation prior to mass spectrometry analysis[12]. Moreover, the top-down platforms are intrinsically limited by the sample treatments required for use in mass spectrometry, involving the use of acids such as formic and trifluoroacetic acid[9,12,19], which inevitably exclude proteins that are insoluble in acidic solutions. In addition, intact high molecular weight proteins and heterogeneous glycosylated proteins are not accessible, in their naturally occurring form, even to the best level of the mass spectrometry[2].

In previous studies it was demonstrated that the top-down platforms cannot achieve the same coverage of shotgun platforms for different reasons, such as: i) the intact protein must be soluble in the acid solution compatible with an ESI-MS analysis; (ii) the protein should

not be heterogenous (glycosylated isoforms), because in this case the intact protein mass cannot be deduced by the ESI spectrum; (iii) protein dimensions have to be limited because MS-MS fragmentation spectra are too complex to be interpreted[3,15]. However, the top-down strategy may reveal the richness of the isoform and the diversity of post-translational modifications, which in the shotgun proteomics strategy may result in the relevant loss of this molecular information[2,3]. Thus, shotgun proteomics may exhibit this deficiency to the human saliva proteome, where many proteins such as basic PRPs and acids are not very susceptible to the action of proteolytic enzymes and reveal very similar sequences. Therefore, many fragments cannot be related to a specific original protein. However, the shotgun platforms showed the best performance in terms of number of components detected, because the sensitivity of mass spectrometry is sufficient to reveal thousands of peptides in a single analysis. In this way, shotgun proteomics covers the largest variety of detectable components, regardless of their mass, because the proteolytic digestion of large proteins almost always generates peptides that can disclose the presence of the protein in a complex mixture. Due to these reasons, the number of salivary components currently detectable by shotgun proteomics approaches is more than five times greater than the number of components detected by any other platform[2,10]. Thus, in the present study we employed shotgun proteomics.

Based on the results found in the two tests, the protocol for salivary shotgun proteomic analysis was satisfactory, since it allowed the identification of a good number of proteins, including those typically found in saliva. Moreover, it is easy to perform and cheaper than methods previously described, since it does not require the use of depletion columns. Furthermore, it allows individual analysis of the samples, which is very important in quantitative proteomics. Thus, this protocol could be used in future studies involving shotgun proteomic analysis of saliva.

Acknowledgements

The authors thank FAPESP for the concession of a scholarship to the first author (Proc. 2017/05031-2).

REFERENCES

1. Camisasca DR, da Rós Goncalves L, Soares MR, Sandim V, Nogueira FC, Garcia CH, et al. A proteomic approach to compare saliva from individuals with and without oral leukoplakia. J Proteomics. 2017;151:43-52.

2- Castagnola M, Cabras T, Iavarone F, Vincenzoni F, Vitali A, Pisano E, et al. Top-down platform for deciphering the human salivary proteome. J Matern Fetal Neonatal Med. 2012;25(Suppl 5):27-43.

3- Castagnola M, Scarano E, Passali GC, Messana I, Cabras T, Iavarone F, et al. Salivary biomarkers and proteomics: future diagnostic and clinical utilities. Acta Otorhinolaryngol Ital. 2017;37(2):94-101.

4- Catherman AD, Skinner OS, Kelleher NL. Top Down proteomics: facts and perspectives. Biochem Biophys Res Commun. 2014;445(4):683-93.

5- Hannig M. Ultrastructural investigation of pellicle morphogenesis at two different intraoral sites during a 24-h period. Clin Oral Investig. 1999;3(2):88-95.

6- Jasim H, Olausson P, Hedenberg-Magnusson B, Ernberg M, Ghafouri B. The proteomic profile of whole and glandular saliva in healthy pain-free subjects. Sci Rep. 2016;6:39073.

7- Krief G, Deutsch O, Gariba S, Zaks B, Aframian DJ, Palmon A. Improved visualization of low abundance oral fluid proteins after triple depletion of alpha amylase, albumin and IgG. Oral Dis. 2011;17(1):45-52.

8- Krief G, Deutsch O, Zaks B, Wong DT, Aframian DJ, Palmon A. Comparison of diverse affinity based high-abundance protein depletion strategies for improved bio-marker discovery in oral fluids. J Proteomics. 2012;75(13):4165-75.

9- Manconi B, Liori B, Cabras T, Iavarone F, Manni A, Messana I, et al. Top-down HPLC-ESI-MS proteomic analysis of saliva of edentulous subjects evidenced high levels of cystatin A, cystatin B and SPRR3. Arch Oral Biol. 2017;77:68-74.

10- Messana I, Cabras T, Iavarone F, Vincenzoni F, Urbani A, Castagnola M. Unraveling the different proteomic platforms. J Sep Sci. 2013;36(1):128-39.

11- Nesatyy VJ, Suter MJ. Analysis of environmental stress response on the proteome level. Mass Spectrom Rev. 2008;27(6):556-74.

12- Peng Y, Chen X, Sato T, Rankin SA, Tsuji RF, Ge Y. Purification and high-resolution top-down mass spectrometric characterization of human salivary alpha-amylase. Anal Chem. 2012;84(7):3339-46.

13- Schweigel H, Wicht M, Schwendicke F. Salivary and pellicle proteome: a datamining analysis. Sci Rep. 2016;6:38882.

14- Sivadasan P, Gupta MK, Sathe GJ, Balakrishnan L, Palit P, Gowda H, et al. Human salivary proteome - a resource of potential biomarkers for oral cancer. J Proteomics. 2015;127(Pt A):89-95.

15- Tipton JD, Tran JC, Catherman AD, Ahlf DR, Durbin KR, Kelleher NL. Analysis of intact protein isoforms by mass spectrometry. J Biol Chem. 2011;286(29):25451-8.

16- Ventura TM, Cassiano LP, Souza e Silva CM, Taira EA, Leite AL, Rios D, et al. The proteomic profile of the acquired enamel pellicle according to its location in the dental arches. Arch Oral Biol. 2017;79:20-9.

17- Wang X, Kaczor-Urbanowicz KE, Wong DT. Salivary biomarkers in cancer detection. Med Oncol. 2017;34(1):7.

18- Winck FV, Prado Ribeiro AC, Ramos Domingues R, Ling LY, Riaño-Pachón DM, Rivera C, et al. Insights into immune responses in oral cancer through proteomic analysis of saliva and salivary extracellular vesicles. Sci Rep. 2015;5:16305.

19- Wu S, Brown JN, Tolić N, Meng D, Liu X, Zhang H, et al. Quantitative analysis of human salivary gland-derived intact proteome using top-down mass spectrometry. Proteomics. 2014;14(10):1211-22.

20- Xiao H, Wong DT. Proteomic analysis of microvesicles in human saliva by gel electrophoresis with liquid chromatography-mass spectrometry. Anal Chim Acta. 2012;723:61-7.

Tables:

Table 1. Salivary proteins identified when the albumin and IgG depletion column was used.

Table 2. Salivary proteins identified when the albumin and IgG depletion column was not used.

Table 3. Proteins of the saliva identified in the *pool* analysis.

Table 4. Proteins of the saliva identified in only in the individual analysis.

Table 1- Salivary proteins identified when the albumin and IgG depletion column was used

Accession number	Protein name	score	Cover (%)
P04745	Alpha-amylase 1	7589.70	54.99
P19961	Alpha-amylase 2B	6833.20	47.75
P04280	Basic salivary proline-rich protein 1	488.14	43.88
P02812	Basic salivary proline-rich protein 2	3642.44	45.67
P49407	Beta-arrestin-1	158.66	9.09
P01036	Cystatin-S	1465.11	31.91
P09228	Cystatin-AS	516.59	24.11
P01037	Cystatin-SN	1378.19	21.28
Q9UGM3	Deleted in malignant brain tumors 1 protein	98.93	2.11
P14867	Gamma-aminobutyric acid receptor subunit alpha-1	92.53	7.46
G3V1N2	HCG1745306_ isoform CRA_a	456.20	22.73
P69905	Hemoglobin subunit alpha	1306.87	28.17
P68871	Hemoglobin subunit beta	1659.66	66.67
P02042	Hemoglobin subunit delta	497.84	25.17
A0A0G2JMB2	Ig alpha-2 chain C region (Fragment)	559.94	16.76
P01876	Immunoglobulin heavy constant alpha 1	912.82	30.59
P01877	Immunoglobulin heavy constant alpha 2	345.30	20.00
P01591	Immunoglobulin J chain	1363.63	36.48
P01834	Immunoglobulin kappa constant	333.71	51.40
P0CG04	Immunoglobulin lambda constant 1	136.40	14.15
P0DOY2	Immunoglobulin lambda constant 2	165.46	23.58
P0DOY3	Immunoglobulin lambda constant 3	153.74	23.58
P0CF74	Immunoglobulin lambda constant 6	136.40	14.15
B9A064	Immunoglobulin lambda-like polypeptide 5	136.40	7.01
P31025	Lipocalin-1	1181.01	26.70
Q8TAX7	Mucin-7	95.21	3.71
P04746	Pancreatic alpha-amylase	6723.99	41.49
P01833	Polymeric immunoglobulin receptor	305.15	15.58
P12273	Prolactin-inducible protein	1027.80	40.41
A0A0A0MT31	Proline-rich protein 4	8108.76	72.29
Q5VSP4	Putative lipocalin 1-like protein 1	958.48	6.79
P02810	Salivary acidic proline-rich phosphoprotein 1/2	8108.76	72.29
P02814	Submaxillary gland androgen-regulated protein 3B	2090.48	65.82
A0A087WZY1	Uncharacterized protein	7158.08	16.60
Q96DA0	Zymogen granule protein 16 homolog B	721.70	41.83

able 2- Salivary proteins identified when the albumin and IgG depletion column was not used

Accession number	Protein name	*score*	Cover (%)
Q15118	[Pyruvate dehydrogenase (acetyl-transferring)] kinase isozyme 1_ mitochondrial	89.50	8.26
P31946	14-3-3 protein beta/alpha	166.37	3.25
P62258	14-3-3 protein epsilon	177.85	3.14
Q04917	14-3-3 protein eta	166.37	3.25
P61981	14-3-3 protein gamma	166.37	3.24
P31947	14-3-3 protein sigma	166.37	3.23
P27348	14-3-3 protein theta	195.23	12.65
P63104	14-3-3 protein zeta/delta	166.37	3.27
Q6ZVK8	8-oxo-dGDP phosphatase NUDT18	138.11	19.50
E5KP25	A/G-specific adenine DNA glycosylase	242.24	5.28
P68032	Actin_ alpha cardiac muscle 1	10751.18	40.05
P68133	Actin_ alpha skeletal muscle	10681.87	33.95
P62736	Actin_ aortic smooth muscle	10396.48	37.14
P60709	Actin_ cytoplasmic 1	18715.02	66.67
P63261	Actin_ cytoplasmic 2	18715.02	66.67
P63267	Actin_ gamma-enteric smooth muscle	10327.17	31.12

Q6P461	Acyl-coenzyme A synthetase ACSM6_ mitochondrial	399.16	13.33
Q9UIF7	Adenine DNA glycosylase	242.24	5.31
Q9Y6U3	Adseverin	51.66	5.17
C9JKR2	Albumin_ isoform CRA_k	25004.47	77.94
P02763	Alpha-1-acid glycoprotein 1	259.49	7.46
P01009	Alpha-1-antitrypsin	114.17	14.59
P01023	Alpha-2-macroglobulin	195.37	14.25
P04745	Alpha-amylase 1	125762.3	77.69
P19961	Alpha-amylase 2B	85518.55	67.91
Q69YU3	Ankyrin repeat domain-containing protein 34A	213.80	23.19
Q5T3N1	Annexin (Fragment)	419.03	34.31
P04083	Annexin A1	454.28	33.53
P03973	Antileukoproteinase	822.96	40.15
Q16671	Anti-Muellerian hormone type-2 receptor	646.30	18.32
P02647	Apolipoprotein A-I	436.68	32.58
B1APP8	ATP-dependent 6-phosphofructokinase_ platelet type	156.72	21.29
O14965	Aurora kinase A	187.17	8.93
P04280	Basic salivary proline-rich protein 1	13742.73	44.39
P02812	Basic salivary proline-rich protein 2	36329.24	69.23
Q6W2J9	BCL-6 corepressor	171.50	2.34
P61769	Beta-2-microglobulin	7681.87	54.62
Q562R1	Beta-actin-like protein 2	1631.58	17.02
Q96DR5	BPI fold-containing family A member 2	4054.46	40.56
Q8TDL5	BPI fold-containing family B member 1	238.42	27.27
Q8N4F0	BPI fold-containing family B member 2	4941.71	32.97
Q8N4G4	CA6 protein	236.85	4.47
P23280	Carbonic anhydrase 6	1927.33	43.83
P07339	Cathepsin D	153.05	17.96
H0YDT2	Cathepsin W (Fragment)	152.45	12.32
A0A087X2B6	Cell cycle and apoptosis regulator protein 2	186.22	13.60
O60308	Centrosomal protein of 104 kDa	36.50	3.35
O94986	Centrosomal protein of 152 kDa	24.18	5.03
O75153	Clustered mitochondria protein homolog	864.26	9.93
P35606	Coatomer subunit beta'	186.05	6.73
G3V1A4	Cofilin 1 (Non-muscle)_ isoform CRA_a	613.65	18.79
P23528	Cofilin-1	613.65	16.87
Q8TD31	Coiled-coil alpha-helical rod protein 1	47.65	2.43
Q9P0B6	Coiled-coil domain-containing protein 167	170.32	15.46
P01024	Complement C3	181.96	9.32
Q2VPA4	Complement component receptor 1-like protein	148.59	7.21
P04080	Cystatin-B	3144.06	55.10
P01034	Cystatin-C	1547.12	31.51
P28325	Cystatin-D	535.37	47.89
P01036	Cystatin-S	41046.83	73.76
P09228	Cystatin-SA	21107.61	53.90
P01037	Cystatin-SN	40764.24	68.09
P54108	Cysteine-rich secretory protein 3	371.45	26.94
Q9UGM3	Deleted in malignant brain tumors 1 protein	274.04	6.80
Q8IYB7	DIS3-like exonuclease 2	192.96	5.42
Q9NVU0	DNA-directed RNA polymerase III subunit RPC5	187.74	4.66
Q1HG43	Dual oxidase maturation factor 1	248.89	13.12
O95714	E3 ubiquitin-protein ligase HERC2	190.34	5.05
Q8NG27	E3 ubiquitin-protein ligase Praja-1	680.83	14.31
P43897	Elongation factor Ts_ mitochondrial	129.02	9.23
Q0PNE2	Elongator complex protein 6	63.64	13.53
V9HW75	Epididymis secretory protein Li 109	337.33	22.86
P02675	Fibrinogen beta chain	420.77	40.73
P02679	Fibrinogen gamma chain	453.82	22.52

Q0PRL4	Forkhead box P2 variant 3	142.49	10.19
Q8N6B5	Forkhead box P2_ isoform CRA_d (Fragment)	142.49	11.84
O15409	Forkhead box protein P2	199.65	12.45
O95872	G patch domain and ankyrin repeat-containing protein 1	268.32	17.70
P19526	Galactoside 2-alpha-L-fucosyltransferase 1	174.70	13.42
P48058	Glutamate receptor 4	50.22	2.55
P04406	Glyceraldehyde-3-phosphate dehydrogenase	190.90	16.72
P00738	Haptoglobin	349.21	24.88
G3V1N2	HCG1745306_ isoform CRA_a	22783.57	58.18
P69905	Hemoglobin subunit alpha	27452.86	59.15
P68871	Hemoglobin subunit beta	49667.26	95.24
P02042	Hemoglobin subunit delta	9498.60	33.33
P02100	Hemoglobin subunit epsilon	1940.46	6.80
P69891	Hemoglobin subunit gamma-1	1940.46	6.80
P69892	Hemoglobin subunit gamma-2	1940.46	6.80
P02790	Hemopexin	460.96	22.51
P15515	Histatin-1	32092.25	36.84
P15516	Histatin-3	7558.25	13.73
P57058	Hormonally up-regulated neu tumor-associated kinase	218.10	3.50
Q9BS19	HPX protein	352.10	21.65
A0A0G2JMB2	Ig alpha-2 chain C region (Fragment)	22147.53	68.24
A0A0A0MS07	Ig gamma-1 chain C region (Fragment)	1490.66	45.76
A0A087WYJ9	Ig mu chain C region	2129.91	40.71
P04220	Ig mu heavy chain disease protein	1800.88	31.97
P01876	Immunoglobulin heavy constant alpha 1	25196.43	61.19
P01877	Immunoglobulin heavy constant alpha 2	18459.82	64.12
P01857	Immunoglobulin heavy constant gamma 1	3671.28	50.91
P01859	Immunoglobulin heavy constant gamma 2	729.35	38.34
P01860	Immunoglobulin heavy constant gamma 3	487.81	24.93
P01861	Immunoglobulin heavy constant gamma 4	599.47	20.18
P01871	Immunoglobulin heavy constant mu	2171.72	47.68
A0A075B7F0	Immunoglobulin heavy variable 3/OR16-10 (non-functional) (Fragment)	378.41	9.48
S4R460	Immunoglobulin heavy variable 3/OR16-9 (non-functional)	5403.28	31.25
P01762	Immunoglobulin heavy variable 3-11	378.41	9.40
P01766	Immunoglobulin heavy variable 3-13	378.41	9.48
A0A0C4DH32	Immunoglobulin heavy variable 3-20 (Fragment)	378.41	9.40
A0A0B4J1V1	Immunoglobulin heavy variable 3-21	378.41	9.40
A0A0B4J1X8	Immunoglobulin heavy variable 3-43	378.41	9.32
P01763	Immunoglobulin heavy variable 3-48	378.41	9.40
P01780	Immunoglobulin heavy variable 3-7	401.30	17.09
P01782	Immunoglobulin heavy variable 3-9	378.41	9.32
P01591	Immunoglobulin J chain	18415.28	42.14
P01834	Immunoglobulin kappa constant	16816.83	85.98
P0CG04	Immunoglobulin lambda constant 1	9338.45	77.36
P0DOY2	Immunoglobulin lambda constant 2	13921.14	77.36
P0DOY3	Immunoglobulin lambda constant 3	13921.14	77.36
P0CF74	Immunoglobulin lambda constant 6	13267.04	50.94
A0M8Q6	Immunoglobulin lambda constant 7	10499.89	36.79
B9A064	Immunoglobulin lambda-like polypeptide 5	9338.45	38.32
P08069	Insulin-like growth factor 1 receptor	32.75	5.63
P06870	Kallikrein-1	227.71	10.31
Q9Y5K2	Kallikrein-4	304.56	17.72
P13645	Keratin_ type I cytoskeletal 10	297.80	2.05
Q99456	Keratin_ type I cytoskeletal 12	421.18	14.17
P13646	Keratin_ type I cytoskeletal 13	4810.33	46.94
P02533	Keratin_ type I cytoskeletal 14	158.42	4.24
P19012	Keratin_ type I cytoskeletal 15	1164.86	14.25

P08779	Keratin_ type I cytoskeletal 16	158.42	4.23
Q04695	Keratin_ type I cytoskeletal 17	143.47	2.08
P08727	Keratin_ type I cytoskeletal 19	529.84	6.75
P35908	Keratin_ type II cytoskeletal 2 epidermal	300.25	22.07
Q01546	Keratin_ type II cytoskeletal 2 oral	165.14	12.07
P19013	Keratin_ type II cytoskeletal 4	876.71	42.13
P13647	Keratin_ type II cytoskeletal 5	489.99	7.97
P02538	Keratin_ type II cytoskeletal 6A	794.78	31.56
P04259	Keratin_ type II cytoskeletal 6B	765.88	28.01
P48668	Keratin_ type II cytoskeletal 6C	765.88	28.01
O95678	Keratin_ type II cytoskeletal 75	190.38	3.81
Q5XKE5	Keratin_ type II cytoskeletal 79	190.38	3.93
O14777	Kinetochore protein NDC80 homolog	410.89	9.03
P22079	Lactoperoxidase	1724.32	34.13
P02788	Lactotransferrin	382.65	32.11
Q9C099	Leucine-rich repeat and coiled-coil domain-containing protein 1	270.77	9.98
Q9NPC1	Leukotriene B4 receptor 2	209.15	4.37
P31025	Lipocalin-1	19334.38	57.95
P28330	Long-chain specific acyl-CoA dehydrogenase_ mitochondrial	137.44	9.07
Q8IYD9	Lung adenoma susceptibility protein 2	141.09	9.14
P61626	Lysozyme C	10190.75	70.27
Q14680	Maternal embryonic leucine zipper kinase	208.24	8.14
P42679	Megakaryocyte-associated tyrosine-protein kinase	156.39	10.85
P01033	Metalloproteinase inhibitor 1	858.61	44.44
Q2QL34	Mpv17-like protein	240.73	11.73
Q8TAX7	Mucin-7	11686.20	15.65
Q8NCY6	Myb/SANT-like DNA-binding domain-containing protein 4	176.81	11.30
P24158	Myeloblastin	175.85	4.69
Q8NCE2	Myotubularin-related protein 14	342.16	19.38
Q9NYA4	Myotubularin-related protein 4	234.57	15.82
F8WCT3	NEDD8-conjugating enzyme UBE2F	167.98	37.18
P59665	Neutrophil defensin 1	1037.46	17.02
P59666	Neutrophil defensin 3	1037.46	17.02
O00221	NF-kappa-B inhibitor epsilon	176.16	6.80
Q2L696	Nucb2 splice variant	337.33	24.62
Q14980	Nuclear mitotic apparatus protein 1	278.08	4.96
Q9Y618	Nuclear receptor corepressor 2	44.62	3.33
A0A087WSV8	Nucleobindin 2_ isoform CRA_b	337.33	22.86
P80303	Nucleobindin-2	337.33	22.86
O75414	Nucleoside diphosphate kinase 6	140.72	14.52
C9JQB1	Nucleoside diphosphate kinase	140.72	19.15
Q9GZK3	Olfactory receptor 2B2	166.49	19.33
Q5SZR7	Ornithine decarboxylase antizyme 3	300.95	18.55
Q7RTY7	Ovochymase-1	190.59	10.05
P04746	Pancreatic alpha-amylase	79860.79	59.10
P13796	Plastin-2	364.90	18.02
P13797	Plastin-3	259.13	4.29
P01833	Polymeric immunoglobulin receptor	10715.77	41.62
Q6S8J3	POTE ankyrin domain family member E	7556.27	11.07
A5A3E0	POTE ankyrin domain family member F	7557.11	13.67
P0CG38	POTE ankyrin domain family member I	6915.24	6.79
P0CG39	POTE ankyrin domain family member J	2868.60	5.97
P51531	Probable global transcription activator SNF2L2	158.85	2.01
Q53EL6	Programmed cell death protein 4	138.40	8.74
P12273	Prolactin-inducible protein	31682.10	76.71
Q16378	Proline-rich protein 4	312.60	21.64
H0Y4B9	Propionyl-CoA carboxylase alpha chain_ mitochondrial (Fragment)	231.31	20.90
P07602	Prosaposin	205.84	9.35

D6RDZ2	Protein FAM193B (Fragment)	266.86	35.56
Q14320	Protein FAM50A	176.55	10.62
Q5VT40	Protein FAM78B	141.80	10.73
Q8N7I0	Protein GVQW1	164.91	17.95
Q6P5S2	Protein LEG1 homolog	1162.24	29.09
Q8ND56	Protein LSM14 homolog A	270.50	9.50
Q8WYL5	Protein phosphatase Slingshot homolog 1	322.72	3.91
Q5THK1	Protein PRR14L	367.74	10.13
P06702	Protein S100-A9	571.65	39.47
Q96EA4	Protein Spindly	138.75	2.64
Q58EX7	Puratrophin-1	166.93	2.60
Q9BYX7	Putative beta-actin-like protein 3	1002.92	10.67
Q5VSP4	Putative lipocalin 1-like protein 1	3906.17	11.11
A8K554	Putative protein ZNF815	163.67	26.15
Q96GD0	Pyridoxal phosphate phosphatase	92.62	11.15
H3BR70	Pyruvate kinase	336.60	18.03
P14618	Pyruvate kinase PKM	336.60	12.43
Q15276	Rab GTPase-binding effector protein 1	349.01	8.24
H3BPI9	Receptor protein serine/threonine kinase (Fragment)	641.71	47.67
P02810	Salivary acidic proline-rich phosphoprotein 1/2	40463.03	26.51
Q14674	Separin	32.80	4.39
Q9BZL6	Serine/threonine-protein kinase D2	165.21	3.87
B4DTS2	Serine/threonine-protein kinase	165.21	3.83
J3QLP4	Serine/threonine-protein kinase RIO3 (Fragment)	335.03	50.56
G3V5U8	Serine/threonine-protein phosphatase 2A regulatory subunit B'' subunit gamma	157.81	24.53
P02787	Serotransferrin	5631.55	44.41
P02768	Serum albumin	65771.62	81.28
P40763	Signal transducer and activator of transcription 3	43.20	6.10
Q9UBC9	Small proline-rich protein 3	424.01	65.09
A1L4H1	Soluble scavenger receptor cysteine-rich domain-containing protein SSC5D	62.36	2.67
P02808	Statherin	52769.28	53.23
P02814	Submaxillary gland androgen-regulated protein 3B	52053.05	65.82
Q9UMS6	Synaptopodin-2	184.00	1.83
G5E9B5	TCF3 (E2A) fusion partner (In childhood Leukemia)_ isoform CRA_b	165.61	19.67
Q8WW35	Tctex1 domain-containing protein 2	188.69	14.08
Q7Z6L1	Tectonin beta-propeller repeat-containing protein 1	350.11	12.62
Q9UKR8	Tetraspanin-16	313.97	27.35
P20061	Transcobalamin-1	230.38	20.32
A6H8Y1	Transcription factor TFIIIB component B'' homolog	167.29	2.82
O95359	Transforming acidic coiled-coil-containing protein 2	372.27	6.41
P55072	Transitional endoplasmic reticulum ATPase	236.03	10.92
P29401	Transketolase	133.40	13.80
Q8NDV7	Trinucleotide repeat-containing gene 6A protein	180.44	3.98
K7EQY5	Tyrosine-protein kinase	156.39	10.87
Q86TW2	Uncharacterized aarF domain-containing protein kinase 1	174.76	10.57
H3BMD7	Uncharacterized protein (Fragment)	240.73	19.49
A0A087WZK3	Uncharacterized protein (Fragment)	469.24	43.09
A0A087WZY1	Uncharacterized protein	40463.03	16.60
A0A087WUV0	Uncharacterized protein	464.85	8.62
E7ESA3	Uncharacterized protein	188.69	18.87
Q9HB07	UPF0160 protein MYG1_ mitochondrial	435.46	12.23
Q9NY84	Vascular non-inflammatory molecule 3	540.71	10.58
Q14508	WAP four-disulfide core domain protein 2	1637.99	33.87
E9PDB0	WD repeat-containing protein 49	424.40	5.02
Q86UP3	Zinc finger homeobox protein 4	205.12	3.06
Q5FWF6	Zinc finger protein 789	138.52	9.41

Q17R98	Zinc finger protein 827	296.41	2.87
P25311	Zinc-alpha-2-glycoprotein	5026.17	55.03
Q96DA0	Zymogen granule protein 16 homolog B	47333.93	56.73

Table 3- Proteins of the saliva identified in the *pool* analysis

Accession number	**Protein name**	***score***	**Cover(%)**
P16885	1-phosphatidylinositol 4_5-bisphosphate phosphodiesterase gamma-2	314.78	4.51
P68032	Actin_ alpha cardiac muscle 1	6085.31	31.30
P68133	Actin_ alpha skeletal muscle	6085.31	31.30
P62736	Actin_ aortic smooth muscle	4676.94	28.38
P60709	Actin_ cytoplasmic 1	17496	67.20
P63261	Actin_ cytoplasmic 2	17496	67.20
P63267	Actin_ gamma-enteric smooth muscle	4676.94	28.46
Q01518	Adenylyl cyclase-associated protein 1	440.27	26.11
C9JKR2	Albumin_ isoform CRA_k	26466.72	74.82
P01009	Alpha-1-antitrypsin	2252.60	22.97
P01023	Alpha-2-macroglobulin	665.70	22.86
P04745	Alpha-amylase 1	153591.90	78.86
P19961	Alpha-amylase 2B	110753.50	58.51
P06733	Alpha-enolase	1637.76	33.87
Q01484	Ankyrin-2	52.62	2.75
P03973	Antileukoproteinase	701.53	28.03
P63010	AP-2 complex subunit beta	338.39	2.35
P02647	Apolipoprotein A-I	612.31	39.70
P02652	Apolipoprotein A-II	886.78	69.00
Q5FYB0	Arylsulfatase J	389.18	10.35
Q8IYB8	ATP-dependent RNA helicase SUPV3L1_ mitochondrial	235.17	6.23
P04280	Basic salivary proline-rich protein 1	3925.20	58.67
P02812	Basic salivary proline-rich protein 2	73554.97	69.47
P61769	Beta-2-microglobulin	3725.17	48.74
Q562R1	Beta-actin-like protein 2	1532.83	13.30
P13929	Beta-enolase	264.78	13.36
Q96DR5	BPI fold-containing family A member 2	4561.18	58.23
Q8N4F0	BPI fold-containing family B member 2	6508.75	30.79
A0A087WXK1	BRCA1-A complex subunit Abraxas (Fragment)	332.77	16.93
Q8N4G4	CA6 protein	419.28	4.47
O75638	Cancer/testis antigen 2	716.39	19.05
P23280	Carbonic anhydrase 6	15792.21	62.01
P00450	Ceruloplasmin	71.04	8.45
E9PM92	Chromosome 11 open reading frame 58	258.69	15.29
P01024	Complement C3	833.42	21.17
P51160	Cone cGMP-specific 3'_5'-cyclic phosphodiesterase subunit alpha'	232.14	11.07
H3BRY3	Coronin	502.10	22.11
P31146	Coronin-1A	502.10	24.95
Q92772	Cyclin-dependent kinase-like 2	457.97	11.97
P04080	Cystatin-B	2288.27	45.92
P01034	Cystatin-C	3131.85	51.37
P28325	Cystatin-D	3348.32	61.97
P01036	Cystatin-S	34860.66	73.76
P09228	Cystatin-SA	24277.69	67.38
P01037	Cystatin-SN	23133.23	70.21
P54108	Cysteine-rich secretory protein 3	284.38	21.63
P32320	Cytidine deaminase	1245.08	66.44
Q9UGM3	Deleted in malignant brain tumors 1 protein	306.82	4.97
Q13609	Deoxyribonuclease gamma	411.37	15.74
A0A0A0MT68	Deoxyribonuclease	411.37	16.67

P27487	Dipeptidyl peptidase 4	73.31	4.83
O60216	Double-strand-break repair protein rad21 homolog	322.95	19.02
R4GN68	Dual-specificity mitogen-activated protein kinase kinase 4	780.16	97.56
V9HW75	Epididymis secretory protein Li 109	954.67	25.48
B1AK53	Espin	277.28	4.80
Q01469	Fatty acid-binding protein_ epidermal	475.76	30.37
Q8NCQ5	F-box only protein 15	465.73	3.73
P02679	Fibrinogen gamma chain	372.17	21.63
Q08380	Galectin-3-binding protein	237.96	18.97
P06744	Glucose-6-phosphate isomerase	222.14	22.04
E7ETY7	Glutathione peroxidase	341.42	22.78
P09211	Glutathione S-transferase P	519.29	25.71
P04406	Glyceraldehyde-3-phosphate dehydrogenase	407.39	11.64
Q8IWJ2	GRIP and coiled-coil domain-containing protein 2	718.24	4.81
P00738	Haptoglobin	960.32	41.87
G3V1N2	HCG1745306_ isoform CRA_a	11936.33	57.27
P69905	Hemoglobin subunit alpha	13598.42	54.93
P68871	Hemoglobin subunit beta	18402.54	89.80
P02042	Hemoglobin subunit delta	5838.89	63.95
P02100	Hemoglobin subunit epsilon	3895.00	6.80
P69891	Hemoglobin subunit gamma-1	3895.00	6.80
P69892	Hemoglobin subunit gamma-2	3895.00	6.80
P15515	Histatin-1	16204.54	36.84
P15516	Histatin-3	2631.50	13.73
Q16695	Histone H3.1t	524.06	23.53
Q05469	Hormone-sensitive lipase	43.68	5.30
Q4G0P3	Hydrocephalus-inducing protein homolog	15.21	1.93
A0A0G2JMB2	Ig alpha-2 chain C region (Fragment)	43004.29	79.12
A0A0A0MS07	Ig gamma-1 chain C region (Fragment)	2528.80	42.37
A0A087WYJ9	Ig mu chain C region	4012.85	48.67
P04220	Ig mu heavy chain disease protein	3190.64	37.85
P01876	Immunoglobulin heavy constant alpha 1	38140.46	73.65
P01877	Immunoglobulin heavy constant alpha 2	32255.84	65.29
P01857	Immunoglobulin heavy constant gamma 1	4336.06	47.88
P01859	Immunoglobulin heavy constant gamma 2	1181.17	37.42
P01860	Immunoglobulin heavy constant gamma 3	1276.14	14.59
P01861	Immunoglobulin heavy constant gamma 4	1489.84	38.23
P01871	Immunoglobulin heavy constant mu	4017.99	50.33
A0A075B7F0	Immunoglobulin heavy variable 3/OR16-10 (non-functional) (Fragment)	299.80	9.48
A0A075B7B8	Immunoglobulin heavy variable 3/OR16-12 (non-functional) (Fragment)	242.49	9.40
A0A075B7E8	Immunoglobulin heavy variable 3/OR16-13 (non-functional) (Fragment)	242.49	9.40
S4R460	Immunoglobulin heavy variable 3/OR16-9 (non-functional)	5489.71	31.25
P01762	Immunoglobulin heavy variable 3-11	299.80	9.40
P01766	Immunoglobulin heavy variable 3-13	299.80	9.48
A0A0C4DH32	Immunoglobulin heavy variable 3-20 (Fragment)	299.80	9.40
A0A0B4J1V1	Immunoglobulin heavy variable 3-21	299.80	9.40
P01764	Immunoglobulin heavy variable 3-23	242.49	12.82
P01768	Immunoglobulin heavy variable 3-30	242.49	31.62
P01772	Immunoglobulin heavy variable 3-33	242.49	31.62
A0A0B4J1X8	Immunoglobulin heavy variable 3-43	299.80	9.32
P01763	Immunoglobulin heavy variable 3-48	299.80	9.40
P01767	Immunoglobulin heavy variable 3-53	242.49	12.93
A0A0C4DH42	Immunoglobulin heavy variable 3-66	242.49	12.93
P01780	Immunoglobulin heavy variable 3-7	299.80	9.40
A0A0B4J1X5	Immunoglobulin heavy variable 3-74	242.49	9.40
P01782	Immunoglobulin heavy variable 3-9	299.80	9.32

P01591	Immunoglobulin J chain	20006.96	49.06
P01834	Immunoglobulin kappa constant	28856.88	82.24
A0A0C4DH90	Immunoglobulin kappa variable 3/OR2-268 (non-functional) (Fragment)	362.90	7.76
P04433	Immunoglobulin kappa variable 3-11	1198.54	26.09
P01624	Immunoglobulin kappa variable 3-15	362.90	7.83
A0A075B6H7	Immunoglobulin kappa variable 3-7 (non-functional) (Fragment)	362.90	7.76
A0A0A0MRZ8	Immunoglobulin kappa variable 3D-11	1198.54	26.09
A0A0C4DH55	Immunoglobulin kappa variable 3D-7	362.90	7.56
P06312	Immunoglobulin kappa variable 4-1	250.98	19.83
P0CG04	Immunoglobulin lambda constant 1	40610.55	77.36
P0DOY2	Immunoglobulin lambda constant 2	44714.51	93.40
P0DOY3	Immunoglobulin lambda constant 3	44714.51	93.40
P0CF74	Immunoglobulin lambda constant 6	23147.62	50.94
A0M8Q6	Immunoglobulin lambda constant 7	19435.36	36.79
P01715	Immunoglobulin lambda variable 3-1	344.58	38.26
B9A064	Immunoglobulin lambda-like polypeptide 5	40610.55	38.32
Q9BQU0	Inhibitory NK receptor	242.62	11.21
Q9NVH2	Integrator complex subunit 7	267.39	4.26
Q01638	Interleukin-1 receptor-like 1	304.24	7.01
H0YNL8	Iron-responsive element-binding protein 2	377.91	29.09
A0A0G2JPA6	Killer cell immunoglobulin-like receptor 3DL2	242.62	11.64
P22079	Lactoperoxidase	2259.91	35.11
P02788	Lactotransferrin	862.74	28.59
A6NMS7	Leucine-rich repeat-containing protein 37A	263.12	1.71
A6NM11	Leucine-rich repeat-containing protein 37A2	252.18	1.71
O60309	Leucine-rich repeat-containing protein 37A3	276.06	4.53
P31025	Lipocalin-1	14925.97	53.98
Q86W92	Liprin-beta-1	292.75	10.29
P00338	L-lactate dehydrogenase A chain	196.57	21.69
Q9BY66	Lysine-specific demethylase 5D	307.10	8.58
P61626	Lysozyme C	15283.53	66.89
P14174	Macrophage migration inhibitory factor	616.56	47.83
C9JF79	Malate dehydrogenase (Fragment)	263.72	11.71
P40925	Malate dehydrogenase_ cytoplasmic	653.55	11.38
Q5HYA8	Meckelin	241.84	1.61
Q9Y4B5	Microtubule cross-linking factor 1	26.23	1.52
Q8TAX7	Mucin-7	13700.40	9.28
U3KPS2	Myeloblastin	554.69	17.67
P24158	Myeloblastin	631.43	28.52
Q9NYA4	Myotubularin-related protein 4	315.44	7.11
P59665	Neutrophil defensin 1	1789.52	25.53
P59666	Neutrophil defensin 3	1789.52	25.53
Q9BYH8	NF-kappa-B inhibitor zeta	371.15	4.32
Q2L696	Nucb2 splice variant	663.95	25.13
A0A087WSV8	Nucleobindin 2_ isoform CRA_b	954.67	25.48
P80303	Nucleobindin-2	954.67	25.48
P04746	Pancreatic alpha-amylase	88276.59	55.97
P42338	Phosphatidylinositol 4_5-bisphosphate 3-kinase catalytic subunit beta isoform	561.79	6.26
A0A0A0MRF9	Phosphoinositide phospholipase C	313.90	4.55
P13796	Plastin-2	283.93	25.04
Q86YL7	Podoplanin	866.94	34.57
P11940	Polyadenylate-binding protein 1	582.59	10.69
E7ERJ7	Polyadenylate-binding protein	582.59	11.26
Q8NDX5	Polyhomeotic-like protein 3	348.42	3.05
P01833	Polymeric immunoglobulin receptor	12791.93	57.98
Q8TCS8	Polyribonucleotide nucleotidyltransferase 1_ mitochondrial	32.49	3.19

Q6S8J3	POTE ankyrin domain family member E	4118.47	13.86
A5A3E0	POTE ankyrin domain family member F	4040.70	11.72
P0CG38	POTE ankyrin domain family member I	3413.22	4.74
P0CG39	POTE ankyrin domain family member J	2796.68	3.85
Q8TED1	Probable glutathione peroxidase 8	341.42	17.22
Q8IZM9	Probable sodium-coupled neutral amino acid transporter 6	426.92	6.80
K7EJ44	Profilin	470.78	37.50
P07737	Profilin-1	910.82	49.29
P12273	Prolactin-inducible protein	30448.27	76.71
A0A0A0MT31	Proline-rich protein 4	23475.68	72.29
P07602	Prosaposin	510.46	39.12
Q5W0V3	Protein FAM160B1	862.81	23.66
Q6P5S2	Protein LEG1 homolog	6592.09	36.97
Q9H7Z3	Protein NRDE2 homolog	45.79	1.20
P05109	Protein S100-A8	3184.30	23.66
P06702	Protein S100-A9	1737.55	77.19
O14795	Protein unc-13 homolog B	59.05	1.19
H3BQ60	Puratrophin-1 (Fragment)	266.79	50.00
Q9BYX7	Putative beta-actin-like protein 3	2063.16	10.67
Q5VSP4	Putative lipocalin 1-like protein 1	3097.31	11.11
P52566	Rho GDP-dissociation inhibitor 2	1026.87	30.35
P35913	Rod cGMP-specific 3'_5'-cyclic phosphodiesterase subunit beta	374.14	8.08
P02810	Salivary acidic proline-rich phosphoprotein 1/2	4566.91	72.29
P02787	Serotransferrin	4566.92	48.42
P02768	Serum albumin	63281.61	75.04
O00193	Small acidic protein	258.69	13.11
P02808	Statherin	41653.6	48.39
P02814	Submaxillary gland androgen-regulated protein 3B	20898.6	65.82
Q9UH99	SUN domain-containing protein 2	70.82	1.67
A0A075B6V5	T cell receptor alpha variable 36/delta variable 7 (Fragment)	278.89	24.78
Q7Z6L1	Tectonin beta-propeller repeat-containing protein 1	384.23	7.12
F2Z350	Testis-expressed protein 29	447.37	32.14
Q7Z4L5	Tetratricopeptide repeat protein 21B	78.57	4.56
P20061	Transcobalamin-1	378.51	22.86
P29401	Transketolase	676.10	30.98
Q6ZMR5	Transmembrane protease serine 11A	281.15	11.16
P02766	Transthyretin	438.46	44.22
P60174	Triosephosphate isomerase	651.56	36.36
O43818	U3 small nucleolar RNA-interacting protein 2	297.84	16.00
A0A0J9YY99	Uncharacterized protein (Fragment)	242.49	12.82
H7C2Y3	Uncharacterized protein C2orf80 (Fragment)	318.87	16.41
H0Y8H3	Uncharacterized protein C3orf67 (Fragment)	590.54	74.68
A0A087WZY1	Uncharacterized protein	22581.8	16.60
A0A0G2JMZ2	Uncharacterized protein	252.18	1.71
A0A0G2JRT3	Uncharacterized protein	252.18	1.77
P02774	Vitamin D-binding protein	245.21	21.52
Q14508	WAP four-disulfide core domain protein 2	935.99	33.87
Q9UDV6	Zinc finger protein 212	424.39	16.97
P25311	Zinc-alpha-2-glycoprotein	2292.60	31.54
Q96DA0	Zymogen granule protein 16 homolog B	46355.09	58.17

Table 4- Proteins of the saliva identified in only in the individual analysis

Accession number	**Protein name**	***score***	**Cover(%)**
P31947	14-3-3 protein sigma	297.17	24.60
O00231	26S proteasome non-ATPase regulatory subunit 11	453.07	10.66
P68032	Actin_ alpha cardiac muscle 1	7799.84	26.53

P68133	Actin_ alpha skeletal muscle	7799.84	26.53
P62736	Actin_ aortic smooth muscle	7555.95	23.61
P60709	Actin_ cytoplasmic 1	17763.84	65.60
P63261	Actin_ cytoplasmic 2	17763.84	65.60
P63267	Actin_ gamma-enteric smooth muscle	7555.95	23.67
Q0VD77	ADAMTS-like protein 5	410.00	32.06
P00813	Adenosine deaminase	350.67	12.67
O60503	Adenylate cyclase type 9	471.53	5.69
Q99996	A-kinase anchor protein 9	34.16	3.58
C9JKR2	Albumin_ isoform CRA_k	29220.48	74.82
P01009	Alpha-1-antitrypsin	413.67	11.24
P01023	Alpha-2-macroglobulin	445.71	15.33
A8K2U0	Alpha-2-macroglobulin-like protein 1	148.51	10.32
P04745	Alpha-amylase 1	97076.24	78.86
P19961	Alpha-amylase 2B	77429.32	62.82
P06733	Alpha-enolase	1439.59	49.08
Q8N6M6	Aminopeptidase O	261.58	10.13
Q01484	Ankyrin-2	39.24	4.22
P02652	Apolipoprotein A-II	941.64	47.00
Q14562	ATP-dependent RNA helicase DHX8	365.21	7.38
Q8IYB8	ATP-dependent RNA helicase SUPV3L1_ mitochondrial	331.22	7.00
P04280	Basic salivary proline-rich protein 1	8867.97	44.39
P02812	Basic salivary proline-rich protein 2	54196.77	69.71
I3L192	Basigin (Fragment)	185.70	16.88
P61769	Beta-2-microglobulin	2754.07	54.62
Q562R1	Beta-actin-like protein 2	1943.05	10.90
P13929	Beta-enolase	131.58	7.60
O95342	Bile salt export pump	495.58	8.18
Q96DR5	BPI fold-containing family A member 2	6426.16	43.37
Q8N4F0	BPI fold-containing family B member 2	6613.00	37.99
Q9NQY0	Bridging integrator 3	398.03	11.46
Q8N4G4	CA6 protein	294.75	4.47
O75808	Calpain-15	215.66	3.68
P23280	Carbonic anhydrase 6	9824.04	57.47
Q0P665	CCDC88C protein	188.41	0.00
Q8N163	Cell cycle and apoptosis regulator protein 2	573.49	11.05
O14647	Chromodomain-helicase-DNA-binding protein 2	250.16	2.84
H0Y7A8	Chromosome 9 open reading frame 3 (Fragment)	236.18	19.31
P35606	Coatomer subunit beta'	189.71	2.21
A2ABG0	Complement C2 (Fragment)	409.38	20.25
P01024	Complement C3	526.68	24.53
Q53SF7	Cordon-bleu protein-like 1	168.78	4.32
P04080	Cystatin-B	1041.42	70.41
P01034	Cystatin-C	3437.76	51.37
P28325	Cystatin-D	2141.16	75.35
P01036	Cystatin-S	28189.63	76.60
P09228	Cystatin-SA	13641.19	67.38
P01037	Cystatin-SN	28293.31	70.21
P54108	Cysteine-rich secretory protein 3	373.11	34.29
Q8NF50	Dedicator of cytokinesis protein 8	351.74	5.72
Q9UGM3	Deleted in malignant brain tumors 1 protein	285.95	7.05
Q5TBH6	Dihydroxyacetone phosphate acyltransferase (Fragment)	182.78	23.42
P28340	DNA polymerase delta catalytic subunit	269.07	5.15
M0R2B7	DNA polymerase	269.07	5.03
Q5T4S7	E3 ubiquitin-protein ligase UBR4	22.83	2.70
Q92838	Ectodysplasin-A	258.64	15.86
Q8N3D4	EH domain-binding protein 1-like protein 1	260.45	4.33
Q6P179	Endoplasmic reticulum aminopeptidase 2	522.88	7.92

Q7L775	EPM2A-interacting protein 1	277.97	2.80
Q9H501	ESF1 homolog	205.30	12.22
A0A1B0GUN9	Espin	59.79	6.02
Q8IXL6	Extracellular serine/threonine protein kinase FAM20C	322.36	5.48
Q01469	Fatty acid-binding protein_ epidermal	444.20	32.59
Q9BZK7	F-box-like/WD repeat-containing protein TBL1XR1	376.57	15.18
P02675	Fibrinogen beta chain	187.44	13.03
P15328	Folate receptor alpha	400.38	35.80
Q8NHY3	GAS2-like protein 2	287.31	6.14
P06396	Gelsolin	427.99	17.77
O14893	Gem-associated protein 2	443.14	31.07
P53611	Geranylgeranyl transferase type-2 subunit beta	470.85	16.92
P06744	Glucose-6-phosphate isomerase	787.26	28.49
P04406	Glyceraldehyde-3-phosphate dehydrogenase	793.86	39.40
O95427	GPI ethanolamine phosphate transferase 1	233.92	7.73
Q8IWJ2	GRIP and coiled-coil domain-containing protein 2	22.31	1.25
P00738	Haptoglobin	1233.11	55.42
P00739	Haptoglobin-related protein	281.28	15.52
G3V1N2	HCG1745306_ isoform CRA_a	15851.36	94.55
E7BWR8	HCG2043595_ isoform CRA_a	252.74	7.76
P69905	Hemoglobin subunit alpha	16443.62	83.80
P68871	Hemoglobin subunit beta	22740.65	95.24
P02042	Hemoglobin subunit delta	5150.58	39.46
P02100	Hemoglobin subunit epsilon	2097.61	6.80
P69891	Hemoglobin subunit gamma-1	2097.61	6.80
P69892	Hemoglobin subunit gamma-2	2097.61	6.80
P15515	Histatin-1	5208.41	36.84
P15516	Histatin-3	4795.66	13.73
E9PRF4	Histone-lysine N-methyltransferase (Fragment)	316.72	3.89
Q15047	Histone-lysine N-methyltransferase SETDB1	316.72	3.80
P47902	Homeobox protein CDX-1	196.38	26.04
P31270	Homeobox protein Hox-A11	264.91	14.38
P09630	Homeobox protein Hox-C6	93.47	4.68
Q4G0P3	Hydrocephalus-inducing protein homolog	264.63	2.46
A0A0G2JMB2	Ig alpha-2 chain C region (Fragment)	48303.27	79.12
A0A0A0MS07	Ig gamma-1 chain C region (Fragment)	3209.86	45.76
A0A087WYJ9	Ig mu chain C region	3019.36	54.87
P04220	Ig mu heavy chain disease protein	2170.36	39.90
P01876	Immunoglobulin heavy constant alpha 1	40927.72	84.42
P01877	Immunoglobulin heavy constant alpha 2	28394.92	68.53
P01857	Immunoglobulin heavy constant gamma 1	5891.82	50.91
P01859	Immunoglobulin heavy constant gamma 2	1360.10	31.29
P01860	Immunoglobulin heavy constant gamma 3	1756.61	30.24
P01861	Immunoglobulin heavy constant gamma 4	1509.92	30.89
P01871	Immunoglobulin heavy constant mu	3019.36	54.75
A0A075B7D0	Immunoglobulin heavy variable 1/OR15-1 (non-functional) (Fragment)	252.28	10.26
A0A075B7F0	Immunoglobulin heavy variable 3/OR16-10 (non-functional) (Fragment)	3426.81	13.79
S4R460	Immunoglobulin heavy variable 3/OR16-9 (non-functional)	8502.51	36.46
P01762	Immunoglobulin heavy variable 3-11	3426.81	23.08
P01766	Immunoglobulin heavy variable 3-13	3426.81	13.79
A0A0C4DH32	Immunoglobulin heavy variable 3-20 (Fragment)	3426.81	13.68
A0A0B4J1V1	Immunoglobulin heavy variable 3-21	3426.81	23.08
A0A0B4J1X8	Immunoglobulin heavy variable 3-43	3426.81	13.56
P01763	Immunoglobulin heavy variable 3-48	3426.81	23.08
P01780	Immunoglobulin heavy variable 3-7	3426.81	23.08
P01782	Immunoglobulin heavy variable 3-9	3426.81	13.56

A0A0B4J1U7	Immunoglobulin heavy variable 6-1	294.24	5.79
P01591	Immunoglobulin J chain	21280.25	68.55
P01834	Immunoglobulin kappa constant	37053.21	85.98
P04433	Immunoglobulin kappa variable 3-11	1303.48	26.09
P01619	Immunoglobulin kappa variable 3-20	868.06	7.76
A0A0A0MRZ8	Immunoglobulin kappa variable 3D-11	1303.48	26.09
P06312	Immunoglobulin kappa variable 4-1	423.92	19.83
P0CG04	Immunoglobulin lambda constant 1	33910.90	77.36
P0DOY2	Immunoglobulin lambda constant 2	40674.07	77.36
P0DOY3	Immunoglobulin lambda constant 3	40674.07	77.36
P0CF74	Immunoglobulin lambda constant 6	30147.40	50.94
A0M8Q6	Immunoglobulin lambda constant 7	22557.57	36.79
B9A064	Immunoglobulin lambda-like polypeptide 5	33910.9	38.32
P06870	Kallikrein-1	196.20	10.31
P43626	Killer cell immunoglobulin-like receptor 2DL1	252.74	7.76
A0A0G2JNJ6	Killer cell immunoglobulin-like receptor 2DS1	325.76	16.62
Q9HAQ2	Kinesin-like protein KIF9	158.59	4.43
B4DZK5	Kinesin-like protein	133.37	10.51
Q6H2H3	KIR2DL1	252.74	7.76
P22079	Lactoperoxidase	1577.03	41.43
P02788	Lactotransferrin	1069.99	35.21
Q6PKG0	La-related protein 1	139.16	6.20
P09960	Leukotriene A-4 hydrolase	225.55	19.31
P31025	Lipocalin-1	8361.36	51.14
P00338	L-lactate dehydrogenase A chain	986.52	20.78
Q9BYZ2	L-lactate dehydrogenase A-like 6B	323.86	8.66
Q9BY66	Lysine-specific demethylase 5D	59.78	0.78
P61626	Lysozyme C	9288.56	54.05
P14174	Macrophage migration inhibitory factor	254.18	55.65
P14780	Matrix metalloproteinase-9	225.62	15.13
Q96JG8	Melanoma-associated antigen D4	150.96	6.07
P01033	Metalloproteinase inhibitor 1	445.25	29.95
Q96GX9	Methylthioribulose-1-phosphate dehydratase	198.99	23.14
O15021	Microtubule-associated serine/threonine-protein kinase 4	168.04	3.43
O43283	Mitogen-activated protein kinase kinase kinase 13	533.35	8.70
Q8TAX7	Mucin-7	10429.01	15.65
Q8NI22	Multiple coagulation factor deficiency protein 2	260.43	23.97
O75970	Multiple PDZ domain protein	43.13	2.32
P24158	Myeloblastin	341.23	17.19
P59665	Neutrophil defensin 1	2353.04	15.96
P59666	Neutrophil defensin 3	2353.04	15.96
P04746	Pancreatic alpha-amylase	64829.77	60.27
Q08752	Peptidyl-prolyl cis-trans isomerase D	470.08	17.57
P13796	Plastin-2	531.41	28.87
P01833	Polymeric immunoglobulin receptor	16305.42	45.42
Q6S8J3	POTE ankyrin domain family member E	3659.07	9.49
A5A3E0	POTE ankyrin domain family member F	3575.10	10.14
P0CG38	POTE ankyrin domain family member I	2591.40	5.67
P0CG39	POTE ankyrin domain family member J	1362.79	4.82
P17844	Probable ATP-dependent RNA helicase DDX5	220.36	4.89
I3L3D5	Profilin (Fragment)	1209.81	10.91
P07737	Profilin-1	1209.81	20.71
P12273	Prolactin-inducible protein	22984.41	89.04
A0A0A0MT31	Proline-rich protein 4	52615.69	72.29
P07602	Prosaposin	316.92	22.52
Q9P219	Protein Daple	206.07	0.69
P49354	Protein farnesyltransferase/geranylgeranyltransferase type-1 subunit alpha	1184.15	17.41

Q6P5S2	Protein LEG1 homolog	7928.19	40.00
Q9H7Z3	Protein NRDE2 homolog	339.41	6.79
Q8WYL5	Protein phosphatase Slingshot homolog 1	286.92	2.38
O43663	Protein regulator of cytokinesis 1	83.55	7.42
P05109	Protein S100-A8	1391.46	31.18
P06702	Protein S100-A9	2043.00	78.07
Q9NQW1	Protein transport protein Sec31B	442.02	7.63
Q92954	Proteoglycan 4	188.50	2.78
Q96MK3	Pseudokinase FAM20A	287.95	8.50
Q9BYX7	Putative beta-actin-like protein 3	1353.87	29.07
Q5VSP4	Putative lipocalin 1-like protein 1	3095.80	11.11
Q5JXB2	Putative ubiquitin-conjugating enzyme E2 N-like	341.70	32.03
A4QN01	Putative uncharacterized protein encoded by LINC01553	191.02	19.53
Q15276	Rab GTPase-binding effector protein 1	211.79	8.58
Q9Y2J0	Rabphilin-3A	47.85	7.93
Q14699	Raftlin	796.05	17.30
G3XAJ6	Raft-linking protein_ isoform CRA_c	779.81	13.84
P52565	Rho GDP-dissociation inhibitor 1	251.72	19.61
Q8IXT5	RNA-binding protein 12B	263.79	6.39
K4DI92	RWD domain containing 4A	636.75	30.48
Q6NW29	RWD domain-containing protein 4	636.75	30.32
P02810	Salivary acidic proline-rich phosphoprotein 1/2	52615.69	72.29
Q9BZL6	Serine/threonine-protein kinase D2	403.28	9.68
B4DTS2	Serine/threonine-protein kinase	401.26	9.57
P02787	Serotransferrin	4390.41	39.26
P02768	Serum albumin	64055.35	79.80
P02808	Statherin	25654.54	48.39
P02814	Submaxillary gland androgen-regulated protein 3B	50678.11	65.82
P00441	Superoxide dismutase [Cu-Zn]	1005.47	45.45
H0YN01	Talin-2	197.30	34.55
Q92609	TBC1 domain family member 5	344.39	5.16
Q7Z6L1	Tectonin beta-propeller repeat-containing protein 1	62.51	2.49
Q6N022	Teneurin-4	64.41	4.15
P10599	Thioredoxin	300.36	32.38
Q96J01	THO complex subunit 3	335.46	20.51
Q5JTD0	Tight junction-associated protein 1	432.54	3.95
P37837	Transaldolase	676.70	23.74
P20061	Transcobalamin-1	670.49	33.26
A6H8Y1	Transcription factor TFIIIB component B" homolog	67.01	6.17
P29401	Transketolase	1109.18	29.05
Q9C0B7	Transport and Golgi organization protein 6 homolog	101.09	8.78
P60174	Triosephosphate isomerase	582.07	15.73
P07437	Tubulin beta chain	251.86	5.86
Q13885	Tubulin beta-2A chain	268.91	5.84
Q9BVA1	Tubulin beta-2B chain	251.86	5.84
P04350	Tubulin beta-4A chain	242.62	5.86
P68371	Tubulin beta-4B chain	242.62	5.84
H3BLT7	Tubulin monoglycylase TTLL3 (Fragment)	205.55	1.15
Q9NVE5	Ubiquitin carboxyl-terminal hydrolase 40	49.55	6.15
Q70EL2	Ubiquitin carboxyl-terminal hydrolase 45	709.84	12.04
D6RC01	Ubiquitinyl hydrolase 1	685.20	10.14
B4DSH7	UDP-galactose translocator	296.27	22.16
H7C2Y3	Uncharacterized protein C2orf80 (Fragment)	203.05	50.78
Q9H1L0	Uncharacterized protein MIR1-1HG	440.61	32.48
A0A087WZY1	Uncharacterized protein	50162.86	16.60
J3QRI8	UPF0183 protein C16orf70 (Fragment)	350.13	32.65
Q13488	V-type proton ATPase 116 kDa subunit a isoform 3	105.99	9.40
Q14508	WAP four-disulfide core domain protein 2	2122.26	33.87

Q9NXC5	WD repeat-containing protein mio	208.07	1.94
Q9BUG6	Zinc finger and SCAN domain-containing protein 5A	97.41	13.71
Q8N8U3	Zinc finger CCHC domain-containing protein 5	189.02	7.79
Q9H0M4	Zinc finger CW-type PWWP domain protein 1	242.57	7.10
Q9NWS9	Zinc finger protein 446	77.75	7.56
P25311	Zinc-alpha-2-glycoprotein	1420.80	28.19
Q96DA0	Zymogen granule protein 16 homolog B	32673.11	56.73

2.2 ARTICLE 2

Article formatted and published according to Journal of Applied Oral Science

DOI: 10.1590/1678-7757-2020-0189

Optimizing the formation of the acquired enamel pellicle *in vitro* for proteomic analysis

Vinícius Taioqui PELÁ[1+] (ORCID ID: 0000-0001-7933-4422, Talita Mendes Oliveira VENTURA[2+] (ORCID ID: 0000-0003-2101-1350), Marília Afonso Rabelo BUZALAF[2*] (ORCID ID: 0000-0002-5985-3951)

[1]Universidade Federal de São Carlos, Departamento de Genética e Evolução, São Carlos, SP, Brasil.
[2]Universidade de São Paulo, Faculdade de Odontologia de Bauru, Departamento de Ciências Biológicas, Bauru, São Paulo, Brasil.

Corresponding address:
Marília Afonso Rabelo Buzalaf
Departamento de Ciências Biológicas – Faculdade de Odontologia de Bauru – Universidade de São Paulo
Al. Octávio Pinheiro Brisolla, 9-75 - Bauru-SP – CEP 17012-901 – Brasil
Tel. + 55 14 32358346/Fax + 55 14 32271486 - e-mail: mbuzalaf@fob.usp.br

Submitted: March 24, 2020
Modification: May 14, 2020
Accepted: June, 18, 2020

[+]The authors contributed equally to the study

ABSTRACT

Saliva is the major contributor for the protein composition of the acquired enamel pellicle (AEP), a bacteria-free organic layer formed by the selective adsorption of salivary proteins on the surface of the enamel. However, the amount of proteins that can be recovered is even smaller under *in vitro* condition, due to the absence of continuous salivary flow. **Objective:** This study developed an *in vitro* AEP protocol for proteomics analysis using a new formation technique with different collection solutions. **Methodology:** 432 bovine enamel specimens were prepared (4x4 mm) and divided into four groups (n=108). Unstimulated saliva was provided by nine subjects. The new AEP formation technique was based on saliva resupply by a new one every 30 min within 120 minutes at 37ºC under agitation. AEP was collected using an electrode filter paper soaked in the collection solutions according with the group: 1) 3% citric acid (CA); 2) 0.5% sodium dodecyl sulfate (SDS); 3) CA followed by SDS (CA+SDS); 4) SDS followed by CA (SDS+CA). The pellicles collected were processed for analysis through LC-ESI-MS/MS technique. **Results:** A total of 55 proteins were identified. The total numbers of proteins identified in each group were 40, 21, 28 and 41 for the groups CA, SDS, CA+SDS and SDS+CA, respectively. Twenty-three typical AEP proteins were identified in all groups, but Mucin was only found in CA and CA+SDS, while three types of PRP were not found in the SDS group. Moreover, a typical enamel protein, Enamelin, was identified in the CA+SDS group only. **Conclusion:** The new technique of the *in vitro* AEP formation through saliva replacement was essential for a higher number of the proteins identified. In addition, considering practicality, quantity and quality of identified proteins, citric acid seems to be the best solution to be used for collection of AEP proteins.

Keywords: Pellicle. Enamel. Saliva. Proteomics. Methods.

INTRODUCTION

Saliva is formed mainly by the secretion of salivary glands. This fluid is essential for the homeostasis of the oral cavity, since it cleans, lubricates and protects the oral tissues, as well as acting as a buffering agent and source of calcium and phosphate ions for remineralization of the teeth.[1] Moreover, saliva is the major contributor for the protein composition of the acquired enamel pellicle (AEP), a bacteria-free organic layer formed by the selective adsorption of salivary proteins on the surface of the enamel,[2] but containing also carbohydrates, neutral lipids, phospholipids and glycolipids.[3-5] These organic components grant important functions to the AEP that acts as a diffusion barrier, reducing the direct contact of the acids with the tooth surface, slowing down tooth dissolution.[1,6,7]

The ability of the AEP to protect the enamel surface against acids is due mainly to its protein composition, especially by the proteins present in the basal layer. These remain in the AEP after exposure to acids[8] and are currently objects of great interest, since they might protect against dental caries and erosion. In the last few years, proteomic approaches have been used to identify these proteins[9-12] so that they can be added to dental products which, when applied, could modify the composition of the AEP, increasing its protective potential against acids.[13]

One of the main difficulties faced in the studies involving proteomic analysis of the AEP is the small amount of proteins that can be obtained, which can impair analysis, both in *in vitro*, *in situ* and *in vivo*. The amount of proteins that can be recovered is even smaller under *in vitro* condition, due to the absence of continuous salivary flow. Moreover, in the *in vivo* studies available so far, AEP samples collected from 8-10 volunteers are pooled in order to obtain enough proteins to be analyzed by mass spectrometry,[10-12,14-18] which does not allow proper assessment of the biological variation of the samples. In these *in vivo* studies, the collection of the AEP samples is done with filter paper soaked in 3% citric acid.

Recently, the proteome of the acquired pellicle formed *in situ* on ceramic specimens and collected by incubation in Tris-HCl buffer containing Triton X-100 followed by ultrasonication in RIPA buffer was analyzed from individual volunteers, with high inter-individual and inter-day consistency.[19] However, the protocol of collection of the AEP employed by Delius 2017[19] is not viable to be employed *in vivo*, since Triton X-100 is toxic and sonication is not possible. In addition, 0.5% dodecyl sodium sulphate (SDS) has been employed for the collection of AEP samples for analysis of individual proteins by immunoblotting,[20] but SDS was not tested for collection of AEP samples for proteomic analyses yet.

Thus, the aim of this study was to develop an *in vitro* AEP formation protocol comparing different collection solutions for shotgun proteomic analysis. The solutions tested (3% citric acid and 0.5% SDS, alone or in combination) were chosen based on their potential to be employed under *in vivo* conditions, which would allow individual analysis and better assessment of biological variation among the volunteers in future studies.

METHODOLOGY

Ethical aspects and subjects

This study was approved by the local Ethics Committees (Human and Animal, protocols 86772718.0.0000.5417 and 007/2018, respectively) of Bauru School of Dentistry, University of São Paulo, SP, Brazil).

Nine young adult subjects of both genders took part in the study, after signing an informed consent document. The exclusion criteria for the volunteers were: presence of caries lesions, use of medication that could change the salivary flow, gingivitis, smoking habit, periodontitis, low salivary flow (unstimulated and stimulated flows should be greater than 0.1 and 1.0 mL/minute, respectively).

The volunteers received a kit containing a toothbrush, toothpaste and floss for oral hygiene standardization. In the morning (to avoid circadian effects),[21] after oral hygiene (2 hours), unstimulated saliva was collected from each volunteer in tubes, kept in ice. Saliva samples were immediately centrifuged (4.500 xg at 4°C, 15 min). The supernatants were collected, pooled and added to a 1:100 protease inhibitor (phenylmethane sulfonyl fluoride - PMSF, N-Ethyhlmaleimide - NEM and Phenantroline).[9] Saliva supernatants were stored at -80ºC, until use.

Preparation of bovine specimens

Bovine incisors underwent a process of screening and cleaning (removal of soft tissue) before preparation. Each tooth was glued on an acrylic plate with thermoactive dental plaster (Kerr Corporation, Orange, CA, EUA) for the separation of the root and coronary portions. The crowns were cut using a precision cutting machine (ISOMET Low Speed Saw Buehler Ltd., Lake Bluff, IL, EUA), with two diamond discs (double-sided XL 12205 ‘high concentration’, 102 × 12.7 × 0.3 mm3; Extec Diamont Wafering Blade, Enfield, CT, USA) separated by a 4-mm thick spacer, in order to obtain 4 × 4 × 2 mm enamel specimens.

Study groups

A total of 432 standardized bovine enamel specimens were obtained and divided into four groups (n=108/group), according to the solution used to collect the AEP, as follows: 1) 3% citric acid (CA)16; 2) 0.5% sodium lauryl sulfate (SDS)20; 3) CA followed by SDS (CA+SDS); 4) SDS followed by CA (SDS+CA).

Formation of AEP *in vitro*

For the formation of the AEP, the specimens were placed in 96-well microplates in which 250 µL of saliva were added. The AEP was then allowed to form for 120 min. For the constant control of the temperature and agitation, a ThermoMixer® (Eppendorf ThermoMixer® C, Hamburg, Germany) was used at 37°C, under agitation. The mainly particularity in this study was the new methodology adopted regarding the resupply of saliva. For this, during the AEP formation (120 min), saliva was exchanged three times (every 30 min). This way, the previous saliva was removed and a new sample was immediately added (250 µL).

Collection of the AEP

After the formation of AEP, the specimens were immediately withdrawn from saliva and washed with a small spray of deionized water for three seconds and air dried. The AEP was collected using an electrode filter paper 5 × 10 mm (Electrode Wick, Bio-Rad, Hercules, CA, USA) soaked in the collection solutions according with the respective group. The excess of the acid was removed with absorbent paper. For CA+SDS and SDS+CA groups, one filter paper was used for the first solution and a new filter paper was used for the second one. One filter paper was used for 6 specimens only and then resupplied by a new one.

For AEP collection, each paper soaked with their respective solution was rubbed (no pressure) on the enamel surface, with the aid of tweezers.[16] The filter papers used to collect AEP from the specimens of the same group were placed in 2 mL tubes and stored at -80°C. The experiment was repeated for additional 2 consecutive days.

Shotgun proteomics analysis by NanoLC-ESI-MS/MS

The methods were exactly as described elsewhere.[17] The papers with the samples were cut into small pieces with the aid of sterile scissors and tweezers. The filter papers containing the AEP collected from 3 different days (triplicate collection) for each of the groups

were pooled to obtain enough amount of AEP proteins to be submitted to the proteomic analysis.

The peptides identification was performed on a nanoACQUITY UPLC-Xevo QTof MS system (Waters, Manchester, UK). In addition, ProteinLynx Global Server (PLGS) version 3.0 was used to process and search the continuum LC-MSE data. Samples from each group were analyzed in triplicate (technical triplicates). Proteins were searched for on the Homo sapiens proteome database (reviewed only, UniProtKB/Swiss-Prot) downloaded on April 2017 from UniProtKB (http://www.uniprot.org/).[17]

Finally, the identified proteins were classified and assigned by biological function,[18, 22] origin and molecular interaction (http://www.uniprot.org/) (Table S1).

RESULTS

The total amount of AEP proteins recovered was very similar for all the groups, ranging between 26 and 33 µg. A total of 55 proteins were identified (Figure 1), among which are 20 proteins typically found in the AEP, such as two isoforms of Alpha-amylase, two isoforms of Basic salivary proline-rich protein, three isoforms of Cystatin, five isoforms of Hemoglobin, Lysozyme, Mucin-7, Pancreatic alpha-amylase, Proline-rich protein 4, Protein S100-A9, Salivary acidic proline-rich phosphoprotein ½, Statherin and Submaxillary gland androgen-regulated protein 3B (Table S1). The total numbers of proteins identified in each group were 40, 21, 28 and 41 for CA, SDS, CA+SDS and SDS+CA, respectively. Among them, 15, 14, 14 and 9 are proteins typically found in the AEP (Table 1). Additionally, the proteins found exclusively in one of the groups was 8, 0, 5 e 4 for the groups CA, SDS, CA+SDS and SDS+CA, respectively (Table 1; Figure 1).

Fifteen proteins were identified in all groups (Figure 1), most of them being proteins typically described in the AEP, such as Pancreatic alpha-amylase, Submaxillary gland androgen-regulated protein 3B, Immunoglobulin heavy constant alpha 1, Immunoglobulin heavy constant alpha 2, two isoforms of Alpha-amylase, three isoforms of Cystatin, Lysozyme C and Statherin (Table S1).

Remarkably, Mucin-7 was only identified in the CA and CA+SDS groups, while Protein S100-A9 was only found in the CA and SDS+CA groups. On the other hand, isoforms of Hemoglobin were only detected in the SDS and SDS+CA groups. Moreover, a typical enamel protein, Enamelin, was identified in the CA+SDS group only. Furthermore, 3 types of PRP were not found in the SDS group (Table S1).

DISCUSSION

The proteomic analysis of AEP formed *in vitro* is an important tool in pre-clinical studies since it allows preliminary evaluation of preventive agents for dental caries and dental erosion. In addition, in *in vitro* studies it is possible to recover the enamel specimens over which the AEP is formed to be submitted to distinct tests, which is not feasible *in vivo*. However, to date there is only one study where the proteomic profile of the AEP formed *in vitro* was evaluated.[25] In this sense, our main aim was to develop an *in vitro* protocol of the AEP formation using different solutions previously described in the literature to collect AEP proteins for shotgun proteomic analysis.

The main reason for such scarcity of studies is the small amount of proteins that can be recovered from the *in vitro* formed AEP, whereas that in *in vivo* condition the AEP is formed under continuous salivary flow, which is not present *in vitro*. In order to overcome this, in this study we resupplied the saliva in which the specimens were immersed every 30 min during the two-hour period of AEP formation. This procedure was successful for an *in vitro* study, since it allowed recovery of approximately 30 µg of proteins that is enough for proper proteomic analysis. In contrast, pilot studies performed for the definition of this protocol with the absence of saliva exchange demonstrated the failure in the recovery proteins of the AEP (data not shown). Despite the fact that saliva was resupplied every 30 to increase the total amount of recovered proteins, it is possible that the solution used to collect the AEP proteins may also influence the amount of recovered proteins.

To date, most of the studies available in the literature employ 3% citric acid for collected of the acquired pellicle.[9-11,14-18,23-25] However, in these studies, the proteins collected from 8-10 volunteers are pooled in order to obtain enough amount of proteins to be analyzed by mass spectrometry, i.e., it is not possible to perform individual analysis. More recently, the pellicle proteins formed on ceramic specimens *in situ* were eluted by incubation in TRIS-HCl buffer containing SDS, followed by ultrasonication in RIPA-buffer. This procedure allowed analysis of individual samples with high inter-individual and inter-day consistency.[19] However, it cannot be done *in vivo*, due to the necessity of sonication and to the toxicity of the detergents employed. SDS has been employed to collection AEP proteins *in vivo* in order to perform immunoblotting analysis.[20] Since SDS is biocompatible and can be used to collected AEP proteins *in*

vivo, in the present study we evaluated both 3% citric acid and 0.5% SDS, alone or in combination, in order to develop a method of collection of AEP proteins that results in large amount of proteins and can be employed in different protocols (*in vitro*, *in situ* and *in vivo*).

The obtained results indicate that the amount of proteins (ranging between 26 and 33 µg) recovered when these solutions were used was satisfactory, especially considering an *in vitro* study. Moreover, among the 55 proteins identified in all groups, 15 are common to all of them, most of which are classical players of the AEP. It could be expected that the combinations CA + SDS or SDS + CA could increase the total number of identified proteins, in comparison to CA or SDS only, since the acid and the detergent could be expected to remove different proteins of the AEP. However, this was not the case, since the total number of identified proteins were 40, 21, 28 and 41 for CA, SDS, CA + SDS and SDS + CA groups, respectively. It is also important to consider the quality of the identified proteins. Mucin included among the pellicle precursors[25] and associated with lubrication[3] and protection against erosive challenges[26] was only identified in the CA and CA + SDS groups. This means that the use of SDS first might not remove this protein. Moreover, Enamelin, a typical enamel protein, was identified only in the CA + SDS group, indicating that this combination might remove a layer of enamel.

Thus, the results obtained indicate that the new technique develop by resupply of saliva for the AEP formation in the present study was essential for a higher number of the proteins identified by proteomics analysis. In addition, 3% citric acid is, among the tested solutions, the best one to remove AEP proteins for shotgun proteomic analysis. The amounts and quality of proteins recovered when 3% citric acid was used is satisfactory, especially considering the *in vitro* protocol of this study. Moreover, the amount of proteins recovered when CA was used (around 30 µg) might be enough to allow proteomic analysis of biological triplicates, since not assessing the biological variability is currently the major shortcoming of the proteomic studies of the AEP. It would be desirable to compare the proteomic profile of AEPs formed *in vitro, in situ* and *in vivo*, so that the results of *in vitro* and *in situ* studies can be extrapolated to the clinical condition.

ACKNOWLEDGMENTS

The authors thank FAPESP for the scholarships to the first (2017/04857-4) and second (2017/05031-2) authors. This study was financed in part by the Coordenação de Aperfeiçoamento de Pessoal de Nível Superior - Brasil (CAPES) - Finance Code 001.

Authors' contributions

Pelá, Vinícius Taioqui: Conceptualization (Equal); Data curation (Equal); Formal analysis (Equal); Funding acquisition (Equal); Investigation (Equal); Methodology (Equal); Project administration (Equal); Resources (Equal); Software (Equal); Supervision (Equal); Validation (Equal); Visualization (Equal); Writing-original draft (Equal); Writing-review & editing (Equal). **Ventura, Talita Mendes Oliveira:** Conceptualization (Equal); Data curation (Equal); Formal analysis (Equal); Funding acquisition (Equal); Investigation (Equal); Methodology (Equal); Project administration (Equal); Resources (Equal); Software (Equal); Supervision (Equal); Validation (Equal); Visualization (Equal); Writing-original draft (Equal); Writing-review & editing (Equal). **Buzalaf, Marília Afonso Rabelo:** Conceptualization (Equal); Data curation (Supporting); Formal analysis (Supporting); Funding acquisition (Equal); Investigation (Equal); Methodology (Supporting); Project administration (Equal); Resources (Equal); Software (Equal); Supervision (Equal); Validation (Equal); Visualization (Equal); Writing-original draft (Equal); Writing-review & editing (Equal).

REFERENCES

1- Buzalaf MA, Hannas AR, Kato MT. Saliva and dental erosion. J Appl Oral Sci. 2012;20(5):493-502. doi: 10.1590/s1678-77572012000500001

2- Dawes C, Jenkins GN, Tonge CH. The nomenclature of the integuments of the enamel surface of the teeth. Br Dent J. 1963;65-8.

3- Hannig M, Joiner A. The structure, function and properties of the acquired pellicle. Monogr Oral Sci. 2006;19:29-64. doi: 10.1159/000090585

4- Siqueira WL, Custodio W, McDonald EE. New insights into the composition and functions of the acquired enamel pellicle. J Dent Res. 2012;91(12):1110-8. doi: 10.1177/0022034512462578

5- Slomiany BL, Murty VL, Zdebska E, Slomiany A, Gwozdzinski K, Mandel ID. Tooth surface-pellicle lipids and their role in the protection of dental enamel against lactic-acid diffusion in man. Arch Oral Biol. 1986;31(3):187-91. doi: 10.1016/0003-9969(86)90126-3

6- Vukosavljevic D, Custodio W, Buzalaf MA, Hara AT, Siqueira WL. Acquired pellicle as a modulator for dental erosion. Arch Oral Biol. 2014;59(6):631-8. doi: 10.1016/j.archoralbio.2014.02.002

7- Hannig M, Fiebiger M, Guntzer M, Dobert A, Zimehl R, Nekrashevych Y. Protective effect of the in situ formed short-term salivary pellicle. Arch Oral Biol. 2004;49(11):903-10. doi: 10.1016/j.archoralbio.2004.05.008

8- Hannig C, Berndt D, Hoth-Hannig W, Hannig M. The effect of acidic beverages on the ultrastructure of the acquired pellicle--an in situ study. Arch Oral Biol. 2009;54(6):518-26. doi: 10.1016/j. archoralbio.2009.02.009

9- Delecrode TR, Siqueira WL, Zaidan FC, Bellini MR, Leite AL, Xiao Y, et al. Exposure to acids changes the proteomic of acquired dentine pellicle. J Dent. 2015;43(5):583-8. doi: 10.1016/j.jdent.2015.02.001

10- Delecrode TR, Siqueira WL, Zaidan FC, Bellini MR, Moffa EB, Mussi MC, et al. Identification of acid-resistant proteins in acquired enamel pellicle. J Dent. 2015;43(12):1470-5. doi: 10.1016/j. jdent.2015.10.009

11- Taira EA, Ventura TM, Cassiano LP, Silva CM, Martini T, Leite AL, et al. Changes in the proteomic profile of acquired enamel pellicles as a function of their time of formation and hydrochloric acid exposure. Caries Res. 2018;52(5):367-77. doi: 10.1159/000486969 12- Martini T, Rios D, Cassiano LP, Silva CM, Taira EA, Ventura TM, et al. Proteomics of acquired pellicle in gastroesophageal reflux disease patients with or without erosive tooth wear. J Dent. 2019;81:64-9. doi: 10.1016/j.jdent.2018.12.007

13- Santiago AC, Khan ZN, Miguel MC, Gironda CC, Soares-Costa A, Pela VT, et al. A new sugarcane cystatin strongly binds to dental enamel and reduces erosion. J Dent Res. 2017;96(9):1051-7. doi: 10.1177/0022034517712981

14- Cassiano LP, Ventura TM, Silva CM, Leite AL, Magalhaes AC, Pessan JP, et al. Protein profile of the acquired enamel pellicle after rinsing with whole milk, fat-free milk, and water: an in vivo study. Caries Res. 2018;52(4):288-96. doi: 10.1159/000485390

15- Lee YH, Zimmerman JN, Custodio W, Xiao Y, Basiri T, HatibovicKofman S, et al. Proteomic evaluation of acquired enamel pellicle during in vivo formation. PloS One. 2013;8(7):e67919. doi: 10.1371/ journal.pone.0067919

16- Siqueira WL, Zhang W, Helmerhorst EJ, Gygi SP, Oppenheim FG. Identification of protein components in in vivo human acquired enamel pellicle using LC-ESI-MS/MS. J Proteome Res. 2007;6(6):2152-60. doi: 10.1021/pr060580k

17- Ventura TM, Cassiano LP, Souza ES, Taira EA, Leite AL, Rios D, et al. The proteomic profile of the acquired enamel pellicle according to its location in the dental arches. Arch Oral Biol. 2017;79:20-9. doi: 10.1016/j.archoralbio.2017.03.001

18- Zimmerman JN, Custodio W, Hatibovic-Kofman S, Lee YH, Xiao Y, Siqueira WL. Proteome and peptidome of human acquired enamel pellicle on deciduous teeth. Int J Mol Sci. 2013;14(1):920-34. doi: 10.3390/ijms14010920

19- Delius J, Trautmann S, Medard G, Kuster B, Hannig M, Hofmann T. Label-free quantitative proteome analysis of the surface-bound salivary pellicle. Colloids Surf B Biointerfaces. 2017;152:68-76. doi: 10.1016/j.colsurfb.2017.01.005

20- Mutahar M, O'Toole S, Carpenter G, Bartlett D, Andiappan M, Moazzez R. Reduced statherin in acquired enamel pellicle on eroded teeth compared to healthy teeth in the same subjects: an in-vivo study. PloS One. 2017;12(8):e0183660. eCollection 2017. doi: 10.1371/ journal.pone.0183660.

21- Dawes C, Ong BY. Circadian rhythms in the concentrations of protein and the main electrolytes in human unstimulated parotid saliva. Arch Oral Biol. 1973;18(10):1233-42. doi: 10.1016/0003-9969(73)90035-6

22- Rison SC, Hodgman TC, Thornton JM. Comparison of functional annotation schemes for genomes. Funct Integr Genomics. 2000;1(1):56- 69. doi: 10.1007/s101420000005

23- Siqueira WL, Bakkal M, Xiao Y, Sutton JN, Mendes FM. Quantitative proteomic analysis of the effect of fluoride on the acquired enamel pellicle. PloS One. 2012;7(8):e42204. doi: 10.1371/journal. pone.0042204

24- Souza ES, Silva Ventura TM, Pau L, Silva LC, Lima Leite A, Buzalaf MA. Effect of gels containing chlorhexidine or epigallocatechin-3-gallate on the protein composition of the acquired enamel pellicle. Arch Oral Biol. 2017;82:92-8. doi: 10.1016/j.archoralbio.2017.05.024

25- Siqueira WL, Custodio W, McDonald EE. New insights into the composition and functions of the acquired enamel pellicle. J Dent Res. 2012;91(12):1110-8. doi: 10.1177/0022034512462578

26- Jordao MC, Ionta FQ, Bergantin BT, Oliveira GC, Moretto MJ, Honorio HM, et al. The effect of mucin in artificial saliva on erosive rehardening and demineralization. Caries Res. 2017;51(2):136-40. doi: 10.1159/000454817

Figure legend

Figure 1. Venn Diagram with the numbers of the exclusive proteins from each group and the proteins common to 2 or more group.

Supplementary data

Table S1. Classification of proteins from the acquired pellicle collected *in vitro* from represented in each group.

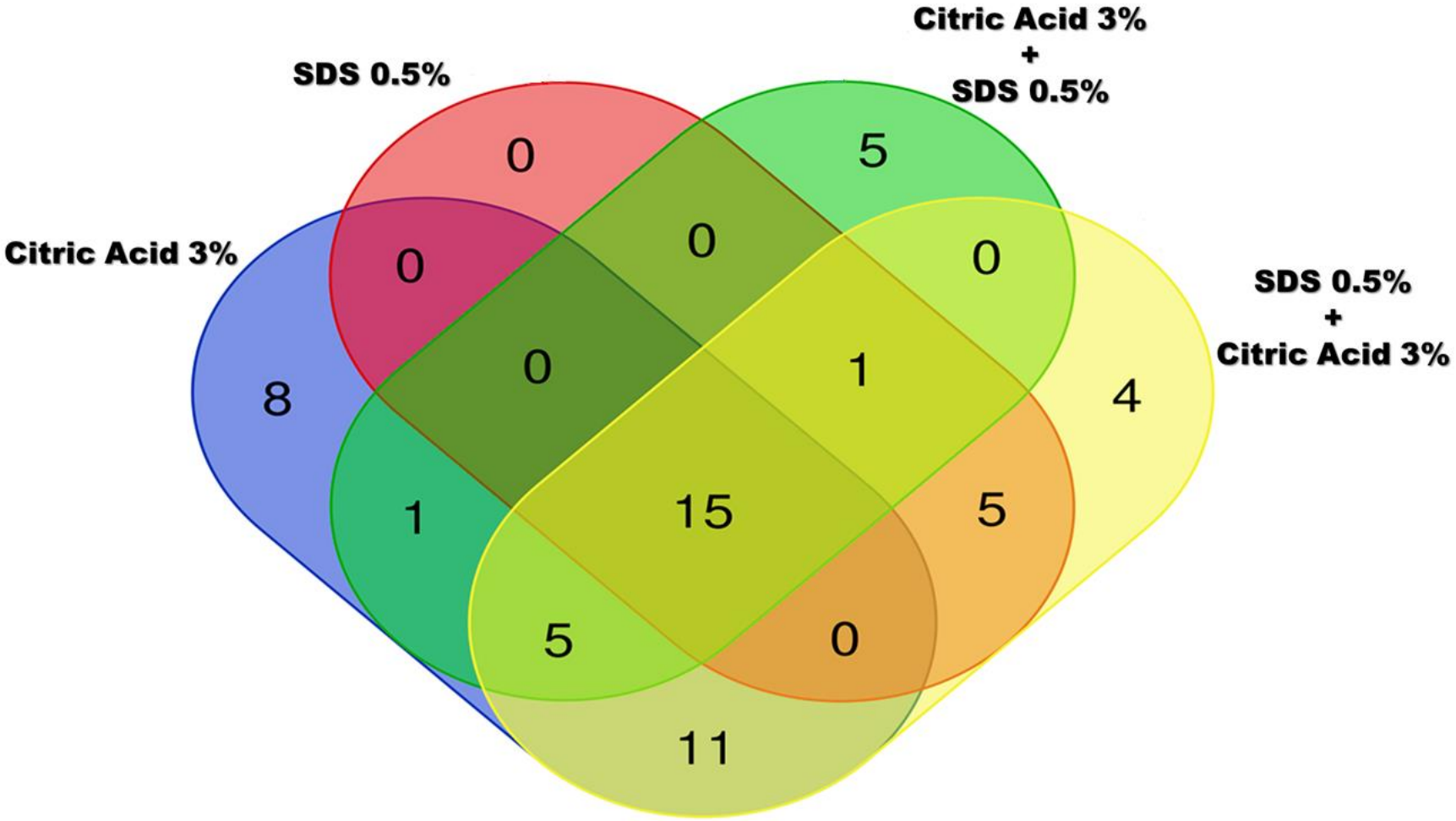
Citric Acid 3%
+
SDS 0.5%
SDS 0.5%
Citric Acid 3%
SDS 0.5%
+
Citric Acid 3%
0
5
0
0
0
0
1
8
4
1
15
5
5
0
11

Table 1. Proteins identified in the acquired enamel pellicle formed *in vitro* on enamel specimens and collected using different solutions.

Group	Accession number	Protein Name	Score
CA	P68032	Actin_ alpha cardiac muscle 1	65.6055
	P68133	Actin_ alpha skeletal muscle	65.6055
	P62736	Actin_ aortic smooth muscle	65.6055
	P60709	Actin_ cytoplasmic 1	65.6055
	P63261	Actin_ cytoplasmic 2	65.6055
	P63267	Actin_ gamma-enteric smooth muscle	65.6055
	P04745	**Alpha-amylase 1**	452.4455
	P19961	**Alpha-amylase 2B**	579.3912
	G5E9X6	**Basic salivary proline-rich protein 1**	155.8623
	P02812	**Basic salivary proline-rich protein 2**	155.8623
	Q562R1	Beta-actin-like protein 2	78.1257
	Q96RL1*	BRCA1-A complex subunit RAP80	47.3122
	P38398*	Breast cancer type 1 susceptibility protein	85.8217
	P23280	Carbonic anhydrase 6	144.9005
	Q9BXL7*	Caspase recruitment domain-containing protein 11	60.8839
	P01036	**Cystatin-S**	2640.733
	P09228	**Cystatin-SA**	451.4857
	P01037	**Cystatin-SN**	2646.624
	Q9UGM3	Deleted in malignant brain tumors 1 protein	86.0094
	P01876	Immunoglobulin heavy constant alpha 1	866.7542
	P01877	Immunoglobulin heavy constant alpha 2	806.5165
	P31025	Lipocalin-1	623.5907
	P61626	**Lysozyme C**	268.2844
	Q8TAX7	**Mucin-7**	417.1399
	C9JTN7*	Nucleolysin TIA-1 isoform p40	92.8821
	P04746	**Pancreatic alpha-amylase**	1996.417
	Q6S8J3	POTE ankyrin domain family member E	65.6055
	A5A3E0	POTE ankyrin domain family member F	65.6055
	A0A0A0MT31	**Proline-rich protein 4**	420.9096
	P06702	**Protein S100-A9**	711.9667
	Q9BYX7	Putative beta-actin-like protein 3	65.6055
	Q5VSP4	Putative lipocalin 1-like protein 1	204.5444
	P02810	**Salivary acidic proline-rich phosphoprotein 1/2**	420.9096
	Q8NBW4*	Sodium-coupled neutral amino acid transporter 9	255.0823
	Q86WA9*	Sodium-independent sulfate anion transporter	262.1345
	P02808	**Statherin**	54090.52
	P02814	**Submaxillary gland androgen-regulated protein 3B**	3959.276
	P17987*	T-complex protein 1 subunit alpha	59.5312
	A0A087WZY1	Uncharacterized protein	420.9096
	P25311*	Zinc-alpha-2-glycoprotein	496.7979
SDS	P04745	**Alpha-amylase 1**	274.6967
	P19961	**Alpha-amylase 2B**	274.6967
	Q8N4G4	CA6 protein	76.7328
	P23280	Carbonic anhydrase 6	301.6657

	P01036	**Cystatin-S**	293.6917
	P09228	**Cystatin-SA**	216.0704
	P01037	**Cystatin-SN**	274.2227
	Q9UGM3	Deleted in malignant brain tumors 1 protein	56.2783
	P68871	**Hemoglobin subunit beta**	293.9594
	P02042	**Hemoglobin subunit delta**	293.9594
	P02100	**Hemoglobin subunit epsilon**	293.9594
	P69891	**Hemoglobin subunit gamma-1**	293.9594
	P69892	**Hemoglobin subunit gamma-2**	293.9594
	P01876	**Immunoglobulin heavy constant alpha 1**	290.1472
	P01877	**Immunoglobulin heavy constant alpha 2**	9.2098
	P31025	Lipocalin-1	1070.104
	P61626	**Lysozyme C**	731.9259
	P04746	**Pancreatic alpha-amylase**	36.6661
	Q5VSP4	Putative lipocalin 1-like protein 1	1070.104
	P02808	**Statherin**	20250.94
	P02814	**Submaxillary gland androgen-regulated protein 3B**	1497.902
CA+SDS	P04745	**Alpha-amylase 1**	181.0646
	P19961	**Alpha-amylase 2B**	166.898
	G5E9X6	**Basic salivary proline-rich protein 1**	552.4909
	P02812	**Basic salivary proline-rich protein 2**	552.4909
	Q8N4G4	CA6 protein	67.728
	Q8N4G4	CA6 protein	47.9429
	P23280	Carbonic anhydrase 6	728.2514
	P08603*	Complement factor H	38.0628
	Q03591*	Complement factor H-related protein 1	38.0628
	P01036	**Cystatin-S**	1556.063
	P09228	**Cystatin-SA**	1013.174
	P01037	**Cystatin-SN**	205.9523
	Q9UGM3	Deleted in malignant brain tumors 1 protein	118.9028
	O75928*	E3 SUMO-protein ligase PIAS2	24.2121
	Q9NRM1*	Enamelin	15.9628
	P01876	Immunoglobulin heavy constant alpha 1	154.7424
	P01877	Immunoglobulin heavy constant alpha 2	79.6826
	Q8WYH8*	Inhibitor of growth protein 5	95.4649
	P31025	Lipocalin-1	1275.895
	P61626	**Lysozyme C**	1199.526
	Q8TAX7	**Mucin-7**	93.5897
	P04746	**Pancreatic alpha-amylase**	166.898
	A0A0A0MT31	**Proline-rich protein 4**	325.6618
	Q5VSP4	Putative lipocalin 1-like protein 1	1275.895
	P02810	**Salivary acidic proline-rich phosphoprotein 1/2**	325.6618
	P02808	**Statherin**	32088.14
	P02814	**Submaxillary gland androgen-regulated protein 3B**	1053.619
	A0A087WZY1	Uncharacterized protein	325.6618
SDS+CA	P68032	Actin_ alpha cardiac muscle 1	145.4612
	P68133	Actin_ alpha skeletal muscle	145.4612

	P62736	Actin_ aortic smooth muscle	145.4612
	P60709	Actin_ cytoplasmic 1	145.4612
	P63261	Actin_ cytoplasmic 2	145.4612
	P63267	Actin_ gamma-enteric smooth muscle	145.4612
	P04745	**Alpha-amylase 1**	3352.857
	P19961	**Alpha-amylase 2B**	3008.341
	G5E9X6	**Basic salivary proline-rich protein 1**	174.755
	P02812	**Basic salivary proline-rich protein 2**	174.755
	Q562R1	Beta-actin-like protein 2	72.3325
	Q8N4G4	CA6 protein	48.5939
	P23280	Carbonic anhydrase 6	836.3896
	P01036	**Cystatin-S**	1501.204
	P09228	**Cystatin-SA**	657.3894
	P01037	**Cystatin-SN**	1529.473
	Q9UGM3	Deleted in malignant brain tumors 1 protein	233.5314
	P68871	**Hemoglobin subunit beta**	761.2395
	P02042	**Hemoglobin subunit delta**	761.2395
	P02100	**Hemoglobin subunit epsilon**	761.2395
	P69891	**Hemoglobin subunit gamma-1**	761.2395
	P69892	**Hemoglobin subunit gamma-2**	761.2395
	P01876	**Immunoglobulin heavy constant alpha 1**	621.9611
	P01877	**Immunoglobulin heavy constant alpha 2**	182.5975
	P01591*	Immunoglobulin J chain	946.0537
	Q9H1B7*	Interferon regulatory factor 2-binding protein-like	9.3029
	P31025	Lipocalin-1	1312.528
	P61626	**Lysozyme C**	4389.076
	P04746	**Pancreatic alpha-amylase**	3061.443
	Q6S8J3	POTE ankyrin domain family member E	117.0785
	A5A3E0	POTE ankyrin domain family member F	117.0785
	P0CG38*	POTE ankyrin domain family member I	69.466
	P0CG39*	POTE ankyrin domain family member J	69.466
	A0A0A0MT31	**Proline-rich protein 4**	368.7032
	P06702	**Protein S100-A9**	132.0728
	Q9BYX7	Putative beta-actin-like protein 3	47.6124
	Q5VSP4	Putative lipocalin 1-like protein 1	1295.604
	P02810	**Salivary acidic proline-rich phosphoprotein 1/2**	368.7032
	P02808	**Statherin**	32670.96
	P02814	**Submaxillary gland androgen-regulated protein 3B**	1295.599
	A0A087WZY1	Uncharacterized protein	368.7032

* Proteins exclusively identified in each group. Proteins highlighted in bold are typical of the acquired enamel pellicle. The groups are: 3% citric acid (CA), 0,5% sodium dodecyl sulfate (SDS), 3% citric acid plus 0,5% sodium dodecyl sulfate (CA+SDS) and 0,5% Sodium dodecyl sulfate plus 3% citric acid (SDS+CA).

Table S1. Classification of proteins from the acquired pellicle collected *in vitro* represented in each group.

Accession number	Protein Name	*Score*	CA	SLS	CA + SLS	SLS + CA
P68032	Actin_ alpha cardiac muscle 1 (d, m, n, q, u, w)	65.6055	X			x
P68133	Actin_ alpha skeletal muscle (b, d, m, n, q, u, w)	65.6055	X			x
P62736	Actin_ aortic smooth muscle (b, d, m, n, q, u)	65.6055	X			x
P60709	Actin_ cytoplasmic 1 (b, m, n, q, u, w)	65.6055	X			x
P63261	Actin_ cytoplasmic 2 (a, d, g, j, n, q, u, w)	65.6055	X			x
P63267	Actin_ gamma-enteric smooth muscle (b, m, n, q, u, w)	65.6055	X			x
P04745	Alpha-amylase 1 (a, g, o, u)	452.4455	X	x	x	x
P19961	Alpha-amylase 2B (a, g, o, u)	579.3912	X	x	x	x
G5E9X6	Basic salivary proline-rich protein 1 (b, l, o, u)	155.8623	X		x	x
P02812	Basic salivary proline-rich protein 2 (b, l, o, u)	155.8623	X		x	x
Q562R1	Beta-actin-like protein 2 (b, m, n, u, w)	78.1257	X			x
Q96RL1	BRCA1-A complex subunit RAP80 (d, m, p, u)	47.3122	X			
P38398	Breast cancer type 1 susceptibility protein (b, e, m, n, p, u)	85.8217	X			
Q8N4G4	CA6 protein (a,m,t,u)	76.7328		x	x	x
P23280	Carbonic anhydrase 6 (a, g, o, u)	301.6657	X	x	x	x
Q9BXL7	Caspase recruitment domain-containing protein 11(c, e, m, n, s, w)	60.8839	X			
P08603	Complement factor H (b, m, o, u)	38.0628			x	
Q03591	Complement factor H-related protein 1 (a, m, o, w)	38.0628			x	
P01036	Cystatin-S (a, b, g, o, u)	2640.733	X	x	x	x
P09228	Cystatin-SA (a, b, g, o, u)	451.4857	x	x	x	x
P01037	Cystatin-SN (a, b, g, o, u)	2646.624	x	x	x	x
Q9UGM3	Deleted in malignant brain tumors 1 protein (f, m, n, o, v, w)	86.0094	x	x	x	x
O75928	E3 SUMO-protein ligase PIAS2 (e, m, p, u)	24.2121			x	
Q9NRM1	Enamelin (b, d, m, o, w)	15.9628			x	
P68871	Hemoglobin subunit beta (b, c, m, n, o, u, w)	293.9594		x		x
P02042	Hemoglobin subunit delta (b, c, m, n, o, u, w)	293.9594		x		x
P02100	Hemoglobin subunit epsilon (b, c, m, n, u)	293.9594		x		x
P69891	Hemoglobin subunit gamma-1(b, c, h, n, o, u, w)	293.9594		x		x
P69892	Hemoglobin subunit gamma-2 (b, c, m, n, u)	293.9594		x		x
P01876	Immunoglobulin heavy constant alpha 1 (b, e, i, j, o, u)	866.7542	x	x	x	x
P01877	Immunoglobulin heavy constant alpha 2 (b, e, i, j, o, u)	806.5165	x	x	x	x
P01591	Immunoglobulin J chain (a, b, m, o, w)	946.0537				x
Q8WYH8	Inhibitor of growth protein 5 (b, m, p, u)	95.4649			x	
Q9H1B7	Interferon regulatory factor 2-binding protein-like (b, m, p, u)	9.3029				x

P31025	Lipocalin-1 (a, b, m, o, w)	623.5907	x	x	x	x
P61626	Lysozyme C (a, b, g, i, j, o, u, w)	268.2844	x	x	x	x
Q8TAX7	Mucin-7 (b, i, k, o, u)	417.1399	x		x	
C9JTN7	Nucleolysin TIA-1 isoform p40 (b,m,n,x)	92.8821	x			
P04746	Pancreatic alpha-amylase (a, g, o, u)	1996.417	x	x	x	x
Q6S8J3	POTE ankyrin domain family member E (b, m, o, u)	65.6055	x			x
A5A3E0	POTE ankyrin domain family member F (b, m, o, u)	65.6055	x			x
P0CG38	POTE ankyrin domain family member I (b, m, o, u)	69.466				x
P0CG39	POTE ankyrin domain family member J (b, m, o, u)	69.466				x
A0A0A0MT31	Proline-rich protein 4 (b, l, p, u)	420.9096	x		x	x
P06702	Protein S100-A9 (a, b, g, i, j, n, o, q, s, u, w)	711.9667	x			x
Q9BYX7	Putative beta-actin-like protein 3 (a, m, n, q, u, w)	65.6055	x			x
Q5VSP4	Putative lipocalin 1-like protein 1 (b, m, o, x)	204.5444	x	x	x	x
P02810	Salivary acidic proline-rich phosphoprotein 1/2 (b, d, h, l, o, u, v)	420.9096	x		x	x
Q8NBW4	Sodium-coupled neutral amino acid transporter 9 (f, m, r, u, w)	255.0823	x			
Q86WA9	Sodium-independent sulfate anion transporter (c, m, s, u)	262.1345	x			
P02808	Statherin (b, e, i, l, o, u)	54090.52	x	x	x	x
P02814	Submaxillary gland androgen-regulated protein 3B (a, g, o, u, w)	3959.276	x	x	x	x
P17987	T-complex protein 1 subunit alpha (e, m, n, w)	59.5312	x			
A0A087WZY1	Uncharacterized protein (m, t, x)	420.9096	x		x	x
P25311	Zinc-alpha-2-glycoprotein (a, b, g, o, u, w)	496.7979	x			

Classification of proteins according to: General Function: a) metabolism; b) biological process; c) transport; d) structure and structural organization; e) information pathways; f) miscellanea; Function in AP: g) metabolism; h) tissue regeneration; i) antimicrobial; j) immune response; k) lubrication; l) biomineralization; m) unknown biological function; Origin: n) cytoplasm origin; o) extracellular origin; p) nucleus origin; q) cytoskeleton origin; r) intracellular origin; s) membrane origin; t) unknown protein origin; Interaction: u) protein/protein interaction; v) calcium/phosphate binding; w) other molecular interaction; x) unknown molecular interaction. The groups are: 3% citric acid (CA), 0,5% sodium lauryl sulfate (SLS), 3% citric acid plus 0,5% sodium lauryl sulfate (CA+SLS) and 0,5% Sodium lauryl sulfate plus 3% citric acid (SLS+CA).

2.3 ARTICLE 3

Article formatted and published according to Clinical Oral Investigations

DOI: 10.1007/s00784-021-03995-5

Radiotherapy changes the salivary proteome in head and neck cancer patients: evaluation before, during and after treatment

Talita Mendes Oliveira Ventura[1], Nathalia Regina Ribeiro[1], Even Akemi Taira[1], Aline de Lima Leite[1], Aline Dionizio[1], Cássia Maria Fischer Rubira[2], Paulo Sérgio da Silva Santos[2], Marília Afonso Rabelo Buzalaf [1*]

[1]Department of Biological Sciences, Stomatology and Oral Biology – Discipline of Biochemistry, Bauru School of Dentistry, University of São Paulo, Bauru, SP, Brazil. Al. Octávio Pinheiro Brisolla, 9-75, Bauru, SP, 17012-90, Brazil.

[2]Department of Surgery, Stomatology, Pathology and Radiology – Discipline of Radiology and Stomatology, Bauru School of Dentistry, University of São Paulo, SP, Brazil. Al. Octávio Pinheiro Brisolla, 9-75, Bauru, SP, 17012-90, Brazil.

***Corresponding Author:** Marília Afonso Rabelo Buzalaf - Department of Biological Sciences, Bauru Dental School, University of São Paulo. Al. Octávio Pinheiro Brisolla, 9-75 Bauru-SP, 17012-901 Brazil. Tel. + 55 14 32358346; Fax + 55 14 32271486; E-mail: mbuzalaf@fob.usp.br

to whom reprint requests must be sent)

Received: 3 September 2020

Accepted: 17 May 2021

Published: 29 May 2021

Graphical Abstract

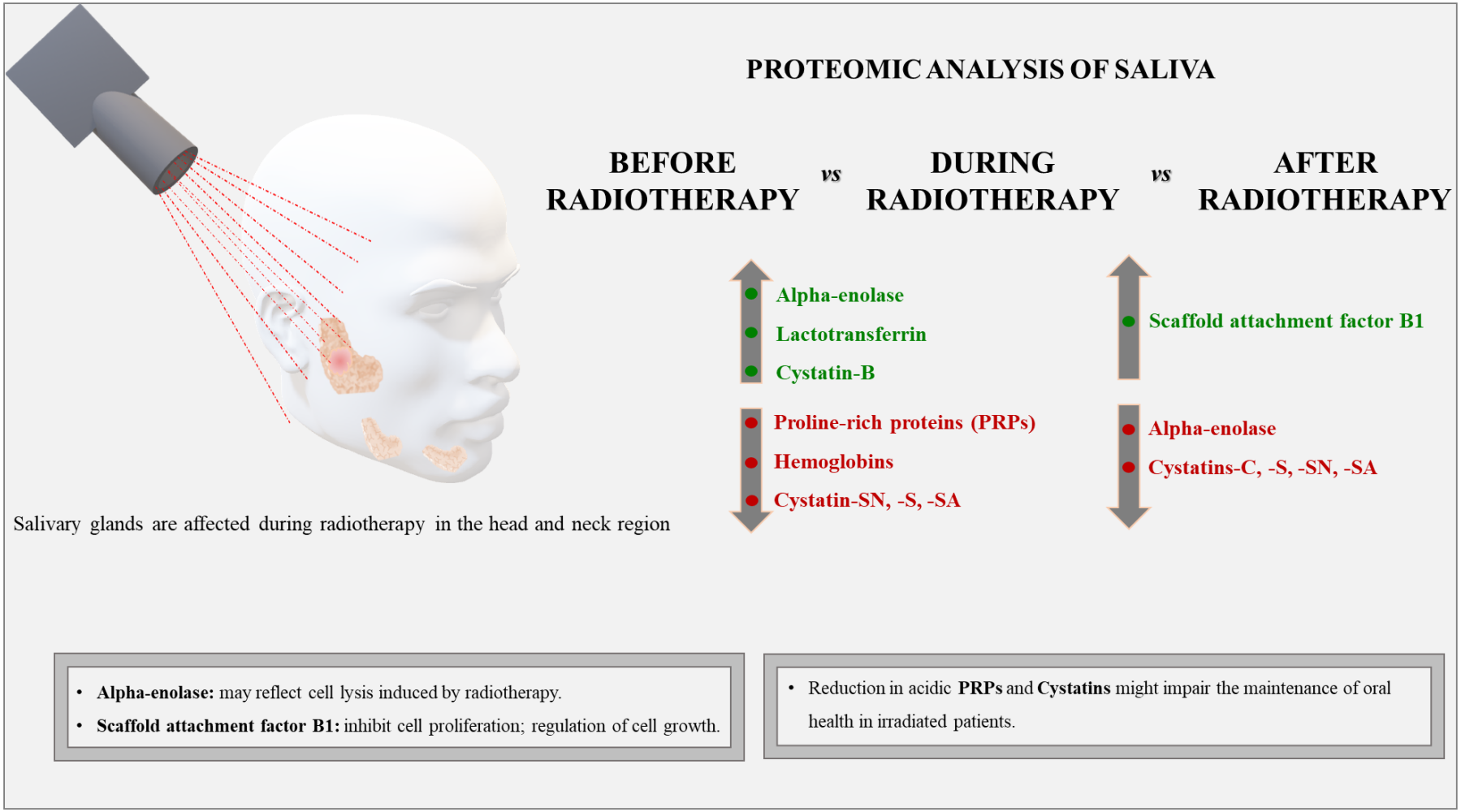

Abstract

Objectives: Salivary glands are affected during radiotherapy in the head and neck region, leading to a reduction in salivary flow and changes its composition. Besides negatively affecting the oral soft tissues, this can also lead to dental impairment. Thus, we evaluated the effect of radiotherapy in the proteomic profile of the saliva in patients with head-and-neck-cancer (HNC). **Materials and methods:** HNC patients had their saliva collected before (BRT), during (2-5 weeks; DRT) and after (3-4 months; ART) radiotherapy. Saliva was also collected from healthy volunteers (control; C). Samples were processed for proteomic analysis. **Results:** In total 1.055 proteins were identified, among which 46 were common to all groups, while 86, 86, 286 and 395 were exclusively found in C, BRT, DRT and ART, respectively. Remarkably, alpha-enolase was increased 35-fold DRT compared with BRT, while proline-rich proteins were decreased. ART there was a 16-fold increase in scaffold attachment factor-B1 and a 3-fold decrease in alpha-enolase and several cystatins. When compared with C, salivary proteins of BRT patients showed increases cystatin-C, lysozyme C, histatin-1 and proline-rich proteins. **Conclusion/Clinical revelance:** Both HNC and radiotherapy remarkably change the salivary protein composition. Altogether, our results, for the first time, suggest investigating alpha-enolase levels in saliva DRT in future studies as a possible biomarker and strategy to predict the efficiency of the treatment. Moreover, our data provide important insights for designing dental products that are more effective for these patients and contribute to a better understanding of the progressive changes in salivary proteins induced by radiotherapy.

Keywords: saliva, proteomics, head and neck cancer, radiotherapy, biomarkes, dental caries.

INTRODUCTION

Head and neck cancer (HNC) refers to a class of biologically equivalent cancers that originate from various locations. Among the sites are the oral cavity, which includes the tongue, mouth floor, mucosa, gingiva, lip, maxilla, hard palate and retromolar trigone, besides nasal cavity and paranasal sinuses, larynx and pharynx (hypopharynx, nasopharynx and oropharynx), thyroid, trachea and salivary gland [1,2]. Therefore, the term HNC represents malignant neoplasms of the upper aerodigestive tract, which includes the oral cavity, pharynx and larynx. The location of the disease causes great social, physical and psychological suffering on the patient and family members, considering changes in the basic functions of the individual, such as feeding, breathing and speech [3]. Considered the fifth most frequent cancer and the sixth most common etiology of cancer deaths in the world, squamous cell carcinoma of the head and neck can occur as metastatic disease or locally and most patients have advanced disease [4].

Radiotherapy is a widely used treatment that aims to destroy neoplastic cells so that there is a reduction or disappearance of the malignant neoplasm. However, it can produce important changes in the quality of life of these patients during and after treatment [5]. The deleterious effects caused by the radiotherapy considered in this region are those that occur in the salivary glands, bones, teeth, mucous membranes of the mouth, muscles and joints that combine the loss of cells and the damage in the local vascularization [6,7]. This is the case of the larger salivary glands, which are usually present in the irradiated field, suffering the consequences of radiotherapy in the head and neck region and leading patients to severe cases of hyposalivation and xerostomia. Studies have shown that 80% of irradiated patients complain of xerostomia [8].

Many attempts directed to the development of new treatment, detection and diagnosis strategies, aiming at increasing the quality of life of patients with HNC have been carried out in recent years. However, many of these patients are submitted to high doses of radiotherapy in extensive radiation fields, which will include the buccal cavity, maxilla, mandible and salivary glands. Radiotherapy, despite having the advantage of preserving tissue structure, leads to innumerable adverse reactions manifested in the oral cavity [9]. Oral complications resulting from radiotherapy result in high morbidity and decrease in quality of life, vary in intensity, and are generally classified as mild, moderate and severe [10,11]. Adverse effects can occur in two phases: during treatment or in the weeks to follow (called the acute phase) and months or years after treatment (called the chronic phase). However, the grade of inclusion of the structures in the irradiation field is what will lead to the severity of oral complications [9,11].

Therefore, since the salivary glands are present in the irradiated field, profound changes in the proteome of saliva are expected in patients undergoing head and neck radiotherapy. The knowledge of these alterations can help to better design preventive and therapeutic strategies for the patients, as well as to identify biomarkers. For this reason, the objective of this study was to evaluate the proteomic profile of unstimulated saliva from cancer patients, diagnosed with CCP and submitted to treatment by radiotherapy. This proteomic profile was evaluated before, during and after the radiotherapy, in order to verify the proteomic changes in the unstimulated saliva, as well as to analyze the mechanisms involved in these alterations in comparison to the control volunteers.

MATERIALS AND METHODS

Ethical aspects and patients

The collection of the saliva started after approval by the local Institutional Ethics Committee (No. 61484116.0.0000.5417), Bauru School of Dentistry, University of São Paulo and signature of informed consent. The study was carried out in accordance with the Declaration of Helsinki.

Unstimulated saliva was collected from nine patients with HNC, who were submitted to radiotherapy treatment (33-36 sessions, irradiation dose of 187cGy [12]) and who attended the Clinical Research Center of Bauru School of Dentistry. All patients were ex-smokers. More information about the conditions of the patients is available in table 1. The saliva was collected in three different periods, as follows: before radiotherapy (BRT); during radiotherapy (DRT; between weeks 2 and 5); after radiotherapy (ART; 3 to 4 months after radiotherapy). Nine volunteers with good oral and general health, non-smokers, with no caries, gingivitis, periodontitis or other oral conditions that could alter the composition of the oral fluids, as well as those who were not using drugs, drugs or tobacco, were included as controls. Volunteers presenting risk factors for erosive tooth wear, such as excessive consumption of carbonated beverages, acidic food and drinks, swimming activities or gastric disorders such as gastroesophageal reflux and bulimia, were excluded (Control group; C) [13].

Patients with HNC were aged between 34 and 72 years, from both genders (7 male and 2 female). Healthy volunteers were paired by age and gender with HNC patients. Total sample size (n=18; 9 patients with HNC and 9 healthy volunteers) was based on previous *in vivo* similar studies involving proteomic analysis of saliva [14-18].

Saliva collection

The saliva collection was carried out in the morning, so that circadian cycle influences did not occur [19]. The collection of unstimulated saliva was performed strictly as previously described [15]. Patients spat out all saliva formed in ice-immersed tubes during the 10 min period. After collection, the saliva was centrifuged at 4.500 xg for 15 min at 4 °C to remove possible debris such as insoluble material, cells and food debris. The supernatant from each saliva sample was removed and frozen at -80 °C until the proteomics analysis. These procedures were based also on other previous studies [17,15,14].

Preparation of the saliva samples for proteomic analysis

The protocol previously standardized by our group was followed [15]. However, in the present study, the analyses were done in biological triplicates, after pooling samples from 3 volunteers for each group. Briefly, the tubes containing the supernatants collected from the unstimulated saliva were defrosted immersed in ice. A pool of each group was performed in triplicate, containing 333.33 μL of saliva from each volunteer, which was transfered to new tubes. Therefore, each 3 saliva samples (from 3 different individuals) were pooled in order to obtain 3 samples with 1000 μL of saliva for each group tested (BRT, DRT, ART and C). The proteins from the saliva samples were extracted using a volume similar to the samples (1:1). Then 1000 μL of an extraction solution containing 6 M urea, 2 M thiourea in 50 mM NH_4HCO_3 at pH 7.8 was added in the samples. Samples were vortexed for 10 min at 4 °C, sonicated for 5 min and centrifuged at 20.817 xg for 10 min at 4 ° C. These extraction procedures were repeated one more time. After extraction, 50 mM NH_4HCO_3 (1.5 X sample volume) was added, in order to reduce the concentration of urea and thiourea and avoid interference in the digestion. The samples were concentrated with Amicon tubes (Amicon Ultra-15 Centrifugal Filter Units - Merck Millipore®, Tullagreen, County Cork, Ireland) and centrifuged at 4.500 xg at 4 °C to a volume of approximately 150 μL. The total protein quantification was performed by Bradford method (Bio-Rad Bradford Assays, Hercules, California, USA) and the samples were then reduced (5 mM dithiothreitol, Bio Rad Laboratories, Canada) and alkylated (10 mM iodoacetamide, GE Healthcare, Little Chalfont, Buckinghamshire UK). In sequence, 100 μL of 50 mM NH_4HCO_3 pH 7.8 were added and then digestion was carried out for 14 h at 37 °C by the addition of 2% (w/w) trypsin (Thermo Scientific Pierce Trypsin Protease, Rockford, lL, USA). Digestion was stopped by the addition of 5% formic acid solution. Samples were

desalted and purified using C18 spin columns (Thermo Scientific, Rockford, Illinois, USA). A 1-μL aliquot of each sample was removed for protein quantification by the Bradford method (Bio-Rad Bradford Assays, Hercules, Califórnia, USA). Samples were then resuspended in 3% acetonitrile and 0.1% formic acid for nanoLC-ESI-MS/MS.

Acquisition nanoLC-ESI-MS/MS

Data acquisition was performed by Xevo G2-S mass spectrometer coupled to the nanoACQUITY UPLC (booth from Waters, Manchester, UK) controlled by MassLynx v.4.1 (Waters, Manchester, UK). Data collection was in data independent acquisition mode (LC-MSE), and the mass range from 50 to 200 m/z, that system was used for the peptide analysis, exactly as previously described [13,15]. All samples were analyzed in technical triplicate, thus totaling 9 analyses for each group. The software ProteinLynx Global Server (PLGS) version 3.0 (Waters, Manchester, UK) was used to process and search for continuous LC-MSE data. The proteins were identified using the software's ion counting algorithm, and a search was performed on the Homo sapiens database (revised only, UniProtKB/Swiss-Prot) downloaded in October 2019 from UniProtKB (http: //www.uniprot .org).

Shotgun Label-free quantitative proteomic analysis

Protein Lynx Global Service software (PLGS, v 3.0, Waters, Manchester, UK) was used for analyzing nine raw MS files from each group for the label-free quantitative analysis. In the quantitative analysis, the proteins identified with a confidence score higher than 95% were included. The identical peptides from each triplicate by sample were pooled according to mass accuracy (<10 ppm) and the retention time tolerance <0.25 min, using the clustering software included in the PLGS. The difference in expression between the groups was analyzed by *t* test ($p < 0.05$) [20,13]. The following relevant comparisons were performed: DRT x BRT; ART x BRT; ART x DRT; BRT x C; DRT x C; ART x C.

Bioinformatics analysis

Initially, the reviewed and unreviewed proteins were analyzed by their accession number by UNIPROT, and reverse proteins, repetead proteins and repeated fragments were excluded. For bioinformatics analysis, the gene ontology was evaluated according to the

ClueGo® pluggins of the Cytoscape® 3.7.2 Software. The functional distribution of proteins identified with differential expression in the period DRT vs BRT was selected. Protein categories was based on Gene Ontology (GO) annotation of the broad Biological Process, Molecular Function, Immune System Process and Cell Component. Terms of significance (Kappa = 0.04) and distribution were according to the percentage of the number of associated genes. The number of access of the proteins was provided by UNIPROT.

Statistical analysis

The software InStat version 3.0 for Windows (GraphPad Software Inc., La Jolla, CA, USA) was used. Data regarding unstimulated salivary flow of CCP patients passed normality after logarithmic transformation and were analyzed by repeated-measures ANOVA and Tukey´s test ($p<0.05$).

RESULTS

Table 1 shows the characterization of the patients regarding gender, age, type of cancer, lifestyle and their conditions.

The mean (±SD) unstimulated salivary flow was 0.49±0.29, 0.17±0.24, 0.06±0.1 and 0.89±0.40 mL/min for BRT, DRT, ART and control, respectively. After logarithmic transformation, repeated-measures ANOVA revealed significant differences among the groups ($F=22.06$, $p<0.0001$). Unstimulated salivary flow reduced significantly DRT when compared with BRT and ART compared with DRT (Figure 1).

A total of 1.055 proteins were identified in the saliva considering the 4 groups. Among them, 46 were identified in all the groups, including Alpha-amylase 1 and 2B, Basic salivary proline-rich protein 1 and 2, BPI fold-containing family member 1 and 2, Carbonic anhydrase 6, Cystatin-C, -S, -SA and -SN, 6 isoforms of Immunoglobulins, Lysozyme, Lysozyme C, Mucin-7, Profilin-1, Prolactin-inducible protein, Proline-rich protein 4, Salivary acidic proline-rich phosphoprotein ½, Serum albumin and Submaxillary gland androgen-regulated protein 3B, among others (Figure 2, Table 2).

On the other hand, 86 proteins were only identified in the C group and 86 proteins were exclusively identified before radiotherapy (BRT group). In irradiated HNC patients, 286 proteins were identified only during radiotherapy (DRT group), including A disintergin and metalloproteinase with thrombospodin motifs 1 and 12, Alipoprotein L1 and L4, among others,

while 395 proteins were identified only after radiotherapy (ART group), including A disintegrin and metalloproteinase with thrombospodin motifs 9, Alipoprotein A-IV, Carbonic anhydrase 1, T-lymphoma invasion and metastasis-inducing protein 1, Vitamin D-binding protein, among others (Figure 2, Table 3).

Regarding the quantitative analysis, 20 and 18 proteins were increased and decreased, respectively, DRT in comparison with BRT. Radiotherapy decreased the following proteins: Alpha-amylase 1 and 2B, Pancreatic alpha-amylase, 3 isoforms of Cystatin (Cystatin-SN, Cystatin-S and Cystatin-SA), Submaxillary gland androgen-regulated protein 3B, Basic salivary proline-rich protein 1 and 2, Proline-rich protein 4 and Salivary acidic proline-rich phosphopotein ½. However, Lactotransferrin, Immunoglobulin heavy constant apha 1 and 2, Cystatin-B, and BPI fold-containing family B member 2 and Alpha-enolase (35-fold increase) were increased DRT (Table 4).

After radiotherapy (ART), 14 proteins were increased such as Scaffold attachment factor B1, BPI fold-containing family B member 2 and 2 isoforms of Albumin (Albumin_isoform CRA_K and Serum albumin) and another 11 were decreased: Alpha-amylase 1 and 2B, Alpha-enolase, 4 isoforms of Cystatin (Cystatin-C, Cystatin-S, Cystatin-SN, Cystatin-SA) and Collagen alpha-1(XII) chain compared with DRT (Table 4).

For the comparison ART vs. BRT, 38 proteins were decreased in the first, such as 5 isoforms of Immunoglobulins, Alipoprotein A-I, 7 isoforms of Hemoglobin (gamma-1 and 2, delta, epsilon, beta, alpha and HCG1745306_isoforms CRA_a), Prolactin-inducible protein, Alpha-amylase 1 and 2B, Submaxillary gland androgen-regulated protein 3B, Cystatin-C, Cystatin-SN, Cystatin-SA, Cystatin-S, Proline-rich protein 4, Salivary acidic proline-rich phodphoprotein ½, Basic salivary proline-rich protein 1 and 2, while 29 proteins were increased in the first. Among the increased proteins are Protein FAM160B1, Cystatin-B, Lactotransferrin, Alpha-enolase, Beta-enolase, BPI fold containing family member 1 and 2, Mucin-7, Profilin-1, Serotransferrin and Carbonic anhydrase 6 (Table 4).

In addition, each treatment period of HNC patients was compared with the control group. Therefore, in the BRT vs. C comparison, 28 and 23 proteins were increased and decreased, respectively, in the first. Among the decreased proteins are Cystatin-SA, Cystatin-SN, Lysozyme, BPI fold-containing family A and B member 1 and 2, Statherin and 2 isoforms of Proline-rich protein (Proline-rich protein 4 and Salivary acidic proline-rich phosphoprotein ½), while Vitamin D 25-hydroxylase, Cystatin-C, Lysozyme C, Histatin-1, 3 isoform of Proline-rich protein, Alpha-amylase 1 and 2B, 2 isoforms of Albumin (Albumin_isoform

CRA_K and Serum albumin), Cystatin-D and 5 isoforms of Immunoglobulins were increased in the HNC patients before radiotherapy compared healthy controls (Table 4).

For the DRT vs. C comparison, 13 and 17 proteins were increased and decreased, respectively, in the first. Eight isoforms of Actin protein and 2 isoforms of Albumin (Serum albumin and Albumin_isoform CRA_K) were increased DRT in patients with HNC compared to healthy controls, while 5 isoforms of Proline-rich protein, Cystatin-SN, Cystatin-S, Prolactin-inducible protein, Pancreatic alpha-amylase, Alpha-amylase 2B, BPI fold-containing family B member 2 were decreased (Table 4).

Finally, for the comparison ART vs. C, 13 proteins were decreased, such as Alpha-amylase 1 and 2B, Pancreatic alpha-amylase, 5 isoforms of Proline-rich protein, Cystatin-SN and Cystatin-S, while 10 proteins, including Albumin_isofrom CRA_K and Serum ambumin were increased in the first (Table 4).

DISCUSSION

Among the cancer patients that have possibilities of cure (45-50%), nearly 70% receive radiotherapy, which is the most employed non-surgical treatment for cancer patients [21]. In the case of patients with HNC, the salivary glands are highly affected since they are present in the irradiated field, leading to irreversible salivary gland hypofunction [5]. Saliva has several functions that are essential to the homeostasis of the oral cavity and most of these functions are played by proteins [22]. Therefore, profound alterations in the proteomic profile of saliva are expected during and after radiotherapy, which could impact in the quality of life of HNC patients. To the best of our knowledge, this is the first study to report the protein changes in the saliva of HNC patients along radiotherapy. For this purpose, unstimulated saliva was collected from the same HNC patients before, during and after radiotherapy, as well as from healthy donors.

There was a remarkable reduction in the salivary flow DRT (2-5 weeks of treatment), of around 65% compared with BRT, which was reduced to around 10% of BRT values ART (3-4 months after radiotherapy). This is consistent with the literature [23,24]. The mechanism underlying salivary hypofunction after radiotherapy is not precisely known so far, despite the loss of acinar cells and disturbance in water secretion mediated by muscarinic receptors have been proposed [25]. In the present study, we found remarkably higher numbers of unique proteins in the DRT and ART groups (286 and 395 proteins, respectively) that presented the lower salivary flows (means of 0.17 and 0.06 mL/min, respectively). One possible explanation

for these expressive numbers of unique proteins could be the dramatic decrease in salivary flow induced by radiotherapy, thus increasing the protein concentration in saliva. However, the total amounts of proteins found in the conditions BRT, DRT and ART were very similar in our study (data not shown). In fact, the literature is contradictory regarding the protein concentration in saliva in function of irradiation. Some studies report an increase in total protein concentration [26-28], while another one did not find changes in this parameter during radiotherapy [29]. It should be noted that in all the above-mentioned studies stimulated saliva was collected, mostly from the parotid gland, while in the present study we collected whole unstimulated saliva, which makes it difficult the direct comparison of the results. The analysis of Table 3 shows that nearly all unique proteins found DRT and ART are intracellular proteins that most likely originate from the oral mucosa and are not secreted by the salivary glands. This might happen as a consequence of mucosal ulceration since the oral mucosa becomes dry and atrophic due to the poor lubrication in the function of the reduced salivary flow [30].

Regarding the proteins differentially expressed in HNC patients BRT when compared with control volunteers, we could see an increase, in the first, in several proteins that are typically described in saliva, such as isoforms of cystatins, lysozyme, alpha -amylases and isoforms of PRPs. These increases were expressive and could be attributed to alterations provoked by the cancer itself. Based on our results, we found that the unstimulated saliva proteome of patients with HNC is significantly different from healthy controls, since only 69 proteins were identified in common between these groups. These findings corroborate a previous study, in which the saliva proteome was evaluated in patients with oral squamous cell carcinoma (OSCC) and in healthy patients. Through the SELDI-TOF analysis, 74 mass peaks were identified, with a significantly different intensity in the saliva of patients with OSCC compared to controls and only 22 of these peaks were characterized in common for differential expression. [31].

In addition, among the proteins identified, Matrin-3 was identified exclusively BRT. Matrin-3 suppresses tumorigenicity, induces cell death by apoptosis and inhibits the migration and invasion of basal-type in breast cancer cells [32]. Yang et al, 2020 strongly suggested that Matrin-3 also offers the possibility to predict the aggressiveness and metastatic potential of breast cancer and the patient's survival. Therefore, perhaps this protein identified in the HNC can play an important role as a prognostic biomarker for this type of cancer as well, which should be evaluated in future studies. The profile of the proteome is of great relevance in understanding the pathogenic mechanisms of the disease, since proteins are the final products

of genetic information and the final effectors of many cellular functions, identifying reliable markers and providing important clues for more targeted therapy [31].

Remarkable changes in the differential protein expression were found upon radiotherapy. DRT, proteins with well-known functions in saliva, such as Alpha-amylase 1 and 2B, Cystatins SN, S and SA, as well as several isoforms of Proline-rich proteins (PRPs, with decrease greater than 2-fold), both basic and acidic, were reduced in comparison with BRT (Table 4). The decrease in acidic PRPs is consistent with previous findings [31]. The balance among the different acidic PRPs in the saliva is closely related to microbial adhesion to the tooth structure [32]. Thus, a reduction in acidic PRPs might impair the maintenance of oral health in irradiated patients.

On the other hand, Lactotransferrin was increased more than 7-fold DRT compared with BRT. These findings are consistent with previous reports of increased lactotransferrin levels in saliva not only during [28], but also 3 to 6 months after radiotherapy [33]. Lactotransferrin, an important multifunctional iron-binding protein, is well-known for its antimicrobial activity, which includes both bacteriostasis due to its ability to sequester free iron, inhibiting the microbial growth, as well as direct bactericidal properties that lead to lipopolysaccharide release from the bacterial outer membrane (UNIPROT). The increase is beneficial to irradiated patients since lactotransferrin has a radioprotective effect on salivary glands [34]. This is related to its action on cell proliferation and cell-cycle progression, affecting acinar cell structure and function after irradiation, suggesting that supplementation with this protein is as a good alternative to prevent irradiation effects in salivary glands [35].

Another protein with important functions in saliva and cancer progression that was more than 3-fold increased DRT compared with BRT was Cystatin-B. Cystatins are reversible inhibitors of cysteine peptidases [36], which during carcinogenesis were found in the tumor microenvironment and they are related to proliferation, metastasis and invasion of tumor cells through the degradation of the extracellular matrix, cell suppression, extracellular interactions, in addition to the promotion of angiogenesis [37]. Moreover, cystatin-B has an antibacterial function [38] and is increased in the acquired enamel pellicle under erosive and cariogenic challenges [39]. Thus, the increase of cystatin-B in saliva may not only be an indicator of the success of radiotherapy to fight the tumor, but also may have a protective effect against dental caries and erosion.

Another protein that was increased DRT compared with BRT was D (2) dopamine receptor (D2R; 6-fold increase). This receptor is coupled to protein G and its activation inhibits adenylate cyclase-mediated cAMP production [40]. It has been shown that D2R signaling

contributes to the proliferation and maintenance of some cancer cells [41]. Its increase DRT might be related to cell lysis (both of acinar cells and mucosal cells) DRT, which is in-line with the increase in 7 isoforms of actin, as well as with damage to the cytoskeleton, which was the most affected process DRT (Fig. 3). The same rationale could be applied for Alpha-enolase (ENO-1) that presented the highest increased in the present study DRT compared with BRT (36-fold). Besides its well-known classical action in the glycolytic pathway, this enzyme is now included among the "moonlighting" proteins, i.e., it has important functions in several cellular processes not related to its classical function in glycolysis [42,43]. It is reported that cell-surface enolase acts as a receptor for plasminogen that is activated upon binding to alpha-enolase [44], increasing cancer cell invasion and metastasis [45]. Thus, the high increase in alpha-enolase DRT compared with before reflects cell lysis induced by radiotherapy. It is important to highlight that ART alpha-enolase levels decreased nearly 3-fold in comparison with DRT. In addition, DRT, Scaffold attachment factor B1, a protein related to the reduction in cell proliferation was increased more than 16-fold in comparison with DRT, indicating the beneficial effects of the therapy. It is also important to note that alpha-enolase was not found in the saliva of control volunteers. These results suggest that monitoring alpha-enolase levels DRT might be a good indicative of the efficacy of the treatment, since high levels of this enzyme might indicate efficient cell lysis.

CONCLUSION

In conclusion, our data contribute to a better understanding of the progressive changes in salivary proteins induced by radiotherapy. We observed that during and after radiotherapy there is a substantial increase in cellular proteins in saliva, not commonly reported in healthy people. This is a consequence of cell lysis induced by radiotherapy in HNC patients. Proteins typically secreted in saliva by salivary glands present minor changes. It would be interesting to evaluate the impact of these radiotherapy-induced changes in salivary proteins on the proteomic changes of the acquired enamel pellicle since this integument confers important protection to the tooth structure. This knowledge could guide the development of oral products to benefit HNC patients submitted to radiotherapy. Moreover, our results suggest that monitoring alpha-enolase levels in saliva during radiotherapy could be a possible strategy to predict the efficiency of the treatment, which should be evaluated in further studies.

ACKNOWLEDGEMENTS

The authors are grateful especialy the trial participants and their families, and the staff of the Clinical Research Center of the FOB/USP. The authors are gratefull to Mrs. Larissa Tercilia Grizzo for technical support with proteomic analysis. The authors thank FAPESP for financial support and for the concession of a scholarship to the first (Proc. FAPESP 2017/05031-2) and second (Proc. FAPESP 2018/17860-6) authors. This study was financed in part by the Coordenação de Aperfeiçoamento de Pessoal de Nível Superior - Brazil (CAPES) - Finance Code 001.

COMPLICANCE WITH ETHICAL STANDARDS

Conflits of Interest

The authors declare no conflict of interest.

Ethical Aproval

The collection of the samples started after approval by the local Institutional Ethics Committee (No. 61484116.0.0000.5417), Bauru School of Dentistry, University of São Paulo and signature of informed consent. The study was performed in accordance with the Declaration of Helsinki.

REFERENCES

1. Safdari Y, Khalili M, Farajnia S, Asgharzadeh M, Yazdani Y, Sadeghi M (2014) Recent advances in head and neck squamous cell carcinoma--a review. Clin Biochem. 47 (13-14):1195-1202. doi:10.1016/j.clinbiochem.2014.05.06610.1016/j.clinbiochem.2014.05.066
2. Leemans CR, Braakhuis BJ, Brakenhoff RH (2011) The molecular biology of head and neck cancer. Nat Rev Cancer. 11 (1):9-22. doi:10.1038/nrc298210.1038/nrc2982
3. Cruz FO, Ferreira EB, Vasques CI, Mata LR, Reis PE (2016) Validation of an educative manual for patients with head and neck cancer submitted to radiation therapy. Rev Lat Am Enfermagem. 24. doi:10.1590/1518-8345.0949.270610.1590/1518-8345.0949.2706
4. Soulieres D, Faivre S, Mesia R, Remenar E, Li SH, Karpenko A, Dechaphunkul A, Ochsenreither S, Kiss LA, Lin JC, Nagarkar R, Tamas L, Kim SB, Erfan J, Alyasova A, Kasper S, Barone C, Turri S, Chakravartty A, Chol M, Aimone P, Hirawat S, Licitra L (2017) Buparlisib and paclitaxel in patients with platinum-pretreated recurrent or metastatic squamous cell carcinoma of the head and neck (BERIL-1): a randomised, double-blind, placebo-controlled phase 2 trial. Lancet Oncol. doi:10.1016/S1470-2045(17)30064-510.1016/S1470-2045(17)30064-5
5. Zago SD (2006) The radiotherapy effect on the quality of life of patients with head and neck cancer. Revista Brasileira de Cancerologia. 52(4):323-329
6. Mira JG, Fullerton GD, Wescott WB (1982) Correlation between initial salivary flow rate and radiation dose in the production of xerostomia. Acta Radiol Oncol. 21 (3):151-154
7. Makkonen T (1988) Studies on oral complications of head and neck cancer radiotherapy. Proc Finn Dent Soc. 84 Suppl 4-5:1-111
8. Chencharick JD, Mossman KL (1983) Nutritional consequences of the radiotherapy of head and neck cancer. Cancer. 51 (5):811-815. doi:10.1002/1097-0142(19830301)51:5<811::aid-cncr2820510511>3.0.co;2-m10.1002/1097-0142(19830301)51:5<811::aid-cncr2820510511>3.0.co;2-m
9. Specht L (2002) Oral complications in the head and neck radiation patient. Introduction and scope of the problem. Support Care Cancer. 10 (1):36-39
10. Murad AM KA (1996) Oncologia: bases clínicas do tratamento. Rio de Janeiro: Guanabara Koogan;. 1.ed

11. Jham BC, da Silva Freire AR (2006) Oral complications of radiotherapy in the head and neck. Braz J Otorhinolaryngol. 72 (5):704-708. doi:10.1016/s1808-8694(15)31029-610.1016/s1808-8694(15)31029-6
12. Shyh-An Yeh MD (2010) Radiotherapy for Head and Neck Cancer. Seminars in Plastic Surgery. 24(2):127-136
13. Ventura T, Cassiano LPS, Souza ESCM, Taira EA, Leite AL, Rios D, Buzalaf MAR (2017) The proteomic profile of the acquired enamel pellicle according to its location in the dental arches. Arch Oral Biol. 79:20-29. doi:10.1016/j.archoralbio.2017.03.00110.1016/j.archoralbio.2017.03.001
14. Winck FV, Prado Ribeiro AC, Ramos Domingues R, Ling LY, Riano-Pachon DM, Rivera C, Brandao TB, Gouvea AF, Santos-Silva AR, Coletta RD, Paes Leme AF (2015) Insights into immune responses in oral cancer through proteomic analysis of saliva and salivary extracellular vesicles. Sci Rep. 5:16305. doi:10.1038/srep1630510.1038/srep16305
15. Ventura T, Ribeiro NR, Dionizio AS, Sabino IT, Buzalaf MAR (2018) Standardization of a protocol for shotgun proteomic analysis of saliva. J Appl Oral Sci. 26:e20170561. doi:10.1590/1678-7757-2017-056110.1590/1678-7757-2017-0561
16. Delmonico L, Bravo M, Silvestre RT, Ornellas MH, De Azevedo CM, Alves G (2016) Proteomic profile of saliva and plasma from women with impalpable breast lesions. Oncol Lett. 12 (3):2145-2152. doi:10.3892/ol.2016.482810.3892/ol.2016.4828
17. Jasim H, Olausson P, Hedenberg-Magnusson B, Ernberg M, Ghafouri B (2016) The proteomic profile of whole and glandular saliva in healthy pain-free subjects. Sci Rep. 6:39073. doi:10.1038/srep3907310.1038/srep39073
18. Penteado CAS, Batista TBD, Chaiben CL, Bonacin BG, Ventura TMO, Dionizio A, Couto Souza PH, Buzalaf MAR, Azevedo-Alanis LR (2020) Salivary protein candidates for biomarkers of oral disorders in alcohol and tobacco dependents. Oral Dis. doi:10.1111/odi.1333710.1111/odi.13337
19. Dawes C (1972) Circadian rhythms in human salivary flow rate and composition. J Physiol. 220 (3):529-545
20. Taira EA, Ventura TMS, Cassiano LPS, Silva CMS, Martini T, Leite AL, Rios D, Magalhaes AC, Buzalaf MAR (2018) Changes in the Proteomic Profile of Acquired Enamel Pellicles as a Function of Their Time of Formation and Hydrochloric Acid Exposure. Caries Res. 52 (5):367-377. doi:10.1159/00048696910.1159/000486969
21. Van De Wiele C, Signore A, Scopinaro F, Waterhouse R, Dierckx RA, Imitt (2001) Imaging tumour hypoxia: where are we? Nucl Med Commun. 22 (9):945-947
22. Buzalaf MA, Hannas AR, Kato MT (2012) Saliva and dental erosion. J Appl Oral Sci. 20 (5):493-502. doi:10.1590/s1678-77572012000500001
23. Shannon IL, Starcke EN, Wescott WB (1977) Effect of Radiotherapy on Whole Saliva Flow. J Dent Res. 56 (6):693-693. doi: 10.1177/00220345770560062201Doi 10.1177/00220345770560062201
24. Dirix P, Nuyts S, Van den Bogaert W (2006) Radiation-induced xerostomia in patients with head and neck cancer: a literature review. Cancer. 107 (11):2525-2534. doi:10.1002/cncr.2230210.1002/cncr.22302
25. Vissink A, Mitchell JB, Baum BJ, Limesand KH, Jensen SB, Fox PC, Elting LS, Langendijk JA, Coppes RP, Reyland ME (2010) Clinical management of salivary gland hypofunction and xerostomia in head-and-neck cancer patients: successes and barriers. Int J Radiat Oncol Biol Phys. 78 (4):983-991. doi: 10.1016/j.ijrobp.2010.06.05210.1016/j.ijrobp.2010.06.052
26. Cowman RA, Baron SS, Glassman AH, Davis ME, Strosberg AM (1983) Changes in Protein-Composition of Saliva from Radiation-Induced Xerostomia Patients and Its Effect on Growth of Oral Streptococci. Journal of dental research. 62 (3):336-340. doi: 10.1177/00220345830620030601Doi 10.1177/00220345830620030601
27. Funegard U, Franzen L, Ericson T, Henriksson R (1994) Parotid-Saliva Composition during and after Irradiation of Head and Neck-Cancer. Oral Oncol. 30b (4):230-233. doi: 10.1016/0964-1955(94)90002-7Doi 10.1016/0964-1955(94)90002-7
28. Makkonen TA, Tenovuo J, Vilja P, Heimdahl A (1986) Changes in the Protein-Composition of Whole Saliva during Radiotherapy in Patients with Oral or Pharyngeal Cancer. Oral Surg Oral Med O. 62 (3):270-275. doi: 10.1016/0030-4220(86)90007-1Doi 10.1016/0030-4220(86)90007-1

29. Anderson MW, Izutsu KT, Rice JC (1981) Parotid-Gland Patho-Physiology after Mixed Gamma and Neutron-Irradiation of Cancer-Patients. Oral Surg Oral Med O. 52 (5):495-500. doi:Doi 10.1016/0030-4220(81)90361-3Doi 10.1016/0030-4220(81)90361-3
30. Vissink A, Jansma J, Spijkervet FKL, Burlage FR, Coppes RP (2003) Oral sequelae of head and neck radiotherapy. Crit Rev Oral Biol M. 14 (3):199-212. doi: 10.1177/154411130301400305Doi 10.1177/154411130301400305
31. Gallo C, Ciavarella D, Santarelli A, Ranieri E, Colella G, Lo Muzio L, Lo Russo L (2016) Potential Salivary Proteomic Markers of Oral Squamous Cell Carcinoma. Cancer Genomics Proteomics. 13 (1):55-61
32. Yang J, Lee SJ, Kwon Y, Ma L, Kim J (2020) Tumor suppressive function of Matrin 3 in the basal-like breast cancer. Biol Res. 53 (1):42. doi:10.1186/s40659-020-00310-610.1186/s40659-020-00310-6
33. Hannig M, Dounis E, Henning T, Apitz N, Stosser L (2006) Does irradiation affect the protein composition of saliva? Clin Oral Investig. 10 (1):61-65. doi:10.1007/s00784-005-0026-z10.1007/s00784-005-0026-z
34. Stenudd C, Nordlund A, Ryberg M, Johansson I, Kallestal C, Stromberg N (2001) The association of bacterial adhesion with dental caries. J Dent Res. 80 (11):2005-2010. doi:10.1177/00220345010800111101 10.1177/00220345010800111101
35. Richards TM, Hurley T, Grove L, Harrington KJ, Carpenter GH, Proctor GB, Nutting CM (2017) The effect of parotid gland-sparing intensity-modulated radiotherapy on salivary composition, flow rate and xerostomia measures. Oral Dis. 23 (7):990-1000. doi:10.1111/odi.1268610.1111/odi.12686
36. Nishimura Y, Homma-Takeda S, Kim HS, Kakuta I (2014) Radioprotection of mice by lactoferrin against irradiation with sublethal X-rays. J Radiat Res. 55 (2):277-282. doi:10.1093/jrr/rrt11710.1093/jrr/rrt117
37. Sakai M, Matsushita T, Hoshino R, Ono H, Ikai K, Sakai T (2017) Identification of the protective mechanisms of Lactoferrin in the irradiated salivary gland. Sci Rep. 7 (1):9753. doi:10.1038/s41598-017-10351-910.1038/s41598-017-10351-9
38. Bobek LA, Levine MJ (1992) Cystatins - Inhibitors of Cysteine Proteinases. Crit Rev Oral Biol M. 3 (4):307-332. doi: 10.1177/10454411920030040101Doi 10.1177/10454411920030040101
39. Petushkova AI, Savvateeva LV, Korolev DO, Zamyatnin AA (2019) Cysteine Cathepsins: Potential Applications in Diagnostics and Therapy of Malignant Tumors. Biochemistry-Moscow+. 84 (7):746-761. doi:10.1134/S000629791907006x10.1134/S000629791907006x
40. Xiao PP, Hu YH, Sun L (2010) Scophthalmus maximus cystatin B enhances head kidney macrophage-mediated bacterial killing. Dev Comp Immunol. 34 (12):1237-1241. doi: 10.1016/j.dci.2010.07.00810.1016/j.dci.2010.07.008
41. Delecrode TR, Siqueira WL, Zaidan FC, Bellini MR, Moffa EB, Mussi MC, Xiao Y, Buzalaf MA (2015) Identification of acid-resistant proteins in acquired enamel pellicle. Journal of dentistry. 43 (12):1470-1475. doi: 10.1016/j.jdent.2015.10.00910.1016/j.jdent.2015.10.009
42. Missale C, Nash SR, Robinson SW, Jaber M, Caron MG (1998) Dopamine receptors: From structure to function. Physiol Rev. 78 (1):189-225
43. Sachlos E, Risueno RM, Laronde S, Shapovalova Z, Lee JH, Russell J, Malig M, McNicol JD, Fiebig-Comyn A, Graham M, Levadoux-Martin M, Lee JB, Giacomelli AO, Hassell JA, Fischer-Russell D, Trus MR, Foley R, Leber B, Xenocostas A, Brown ED, Collins TJ, Bhatia M (2012) Identification of Drugs Including a Dopamine Receptor Antagonist that Selectively Target Cancer Stem Cells. Cell. 149 (6):1284-1297. doi: 10.1016/j.cell.2012.03.04910.1016/j.cell.2012.03.049
44. Kim JW, Dang CV (2005) Multifaceted roles of glycolytic enzymes. Trends Biochem Sci. 30 (3):142-150. doi: 10.1016/j.tibs.2005.01.00510.1016/j.tibs.2005.01.005
45. Jung DW, Kim WH, Williams DR (2014) Chemical genetics and its application to moonlighting in glycolytic enzymes. Biochem Soc T. 42:1756-1761. doi:10.1042/Bst2014020110.1042/Bst20140201
46. Miles LA, Dahlberg CM, Plescia J, Felez J, Kato K, Plow EF (1991) Role of Cell-Surface Lysines in Plasminogen Binding to Cells - Identification of Alpha-Enolase as a Candidate Plasminogen Receptor. Biochemistry-Us. 30 (6):1682-1691. doi: 10.1021/bi00220a034DOI 10.1021/bi00220a034
47. Dano K, Behrendt N, Hoyer-Hansen G, Johnsen M, Lund LR, Ploug M, Romer J (2005) Plasminogen activation and cancer. Thromb Haemostasis. 93 (4):676-681. doi:10.1160/Th05-01-005410.1160/Th05-01-0054

FIGURE LEGENDS

Fig 1. Mean of log unstimulated salivary flow in cancer patients before (BRT), during (DRT) or after (ART) radiotherapy. Distinct letters denote significant differences among the groups. Repeated-measures ANOVA and Tukey´s test ($p<0.05$). n=9**.**

Fig 2. Venn diagram showing the relation of the proteins identified in common among the groups, as well as the number of proteins exclusively found in one of the groups. Among them 1,055 proteins identified, 86, 86, 286 and 395 were identified only in the control group, in cancer patients before (BRT), during (DRT) or after (ART) radiotherapy, while 46 proteins were common to all groups.

Fig 3. Graphs of the functional distribution of proteins identified with differential expression in the period DRT vs BRT. Protein categories based on Gene Ontology (GO) annotation of the broad Biological Process, Molecular Function, Immune System Process and Cell Component. Terms of significance (Kappa = 0.04) and distribution according to the percentage of the number of associated genes. The number of access to proteins was provided by UNIPROT. The gene ontology was evaluated according to the ClueGo® pluggins of the software Cytoscape® 3.7.2.

Table 1. Characterization of the patients with HNC regarding gender, age, type of cancer, lifestyle and their conditions.

Patients	Gender	Age	Ex-smoker and Ex-drinkers	Type of cancer	Oral hygiene	Radiotherapy Sessions	Surgery	Mucositis/ Phase	Laser Therapy
1 - Nº 0479	male	49	Yes	Oropharynx Carcinoma and Tongue Base	Patient with good oral hygiene without focus of infection	33 sessions	No	Yes Grade I and II	Yes
2- Nº 0490	male	72	Yes	Occult grade III Squamous Cell Carcinoma, with cervical metastasis	*Patient with some dental restorations to do before radiotherapy	33 sessions	Yes, 2 months and 20 days before radiotherapy	Yes Grade II	Yes
3- Nº 0495	male	65	Yes	Tongue Squamous Cell Carcinoma – left side	*Patient with some restorations to do and dental caries before radiotherapy	33 sessions	Yes, 3 months and 11 days before radiotherapy	Yes Grade II and III	Yes
4- Nº 0541	female	34	Yes	Tongue Squamous Cell Carcinoma – left side	Patient with good oral hygiene without focus of infection	35 sessions	Yes, after radiotherapy	Yes Grade II	Yes
5- Nº 0553	male	58	Yes	Tongue base Squamous Cell Carcinoma	Patient with good oral hygiene without focus of infection	35 sessions	No	Yes Grade II and III	Yes
6- N° 0570	male	44	Yes	Esophagus Squamous Cell Carcinoma and Amygdala (relapse)	*Patient had dental caries in several teeth	36 sessions	Yes, 3 months and 27 days	Yes Grade II	Yes

					and chronic periodontitis		before radiotherapy		
7- Nº 0644	male	52	Yes	Retromolar Trigone (Jaw) Squamous Cell Carcinoma	*Patient had two dental extractions before radiotherapy	33 sessions	Yes, 2 months and 24 days before radiotherapy	Yes Grade III	Yes
8- N° 0667	male	55	Yes	Tongue Base - left side	*Patient had dental calculus and dental caries before radiotherapy	35 sessions	No	Yes Grade II and III	Yes
9- Nº 0635	female	67	Yes	Hypopharyngeal Squamous Cell Carcinoma	*Patient had some dental caries before radiotherapy	35 sessions	No	Yes Grade II	Yes

*Patients were treated at the Clinical Research Center of the Bauru Dental School before starting radiotherapy.

Table 2. Proteins identified in common in the unstimulated saliva in all groups: Control, BRT, DRT and ART.

°Accession number	Protein name	*PLGS* Score
P68032	Actin_ alpha cardiac muscle 1	1822
P68133	Actin_ alpha skeletal muscle	1822
P62736	Actin_ aortic smooth muscle	1822
P60709	Actin_ cytoplasmic 1	3917
P63261	Actin_ cytoplasmic 2	3917
P63267	Actin_ gamma-enteric smooth muscle	1822
C9JKR2	Albumin_ isoform CRA_k	4089
P04745	Alpha-amylase 1	40491
P19961	Alpha-amylase 2B	32796
P04280	Basic salivary proline-rich protein 1	11098
P02812	Basic salivary proline-rich protein 2	13300
Q562R1	Beta-actin-like protein 2	870
Q8TDL5	BPI fold-containing family B member 1	310
Q8N4F0	BPI fold-containing family B member 2	1057
P23280	Carbonic anhydrase 6	1175
P01034	Cystatin-C	1874
P01036	Cystatin-S	11830
P09228	Cystatin-SA	6668
P01037	Cystatin-SN	5608
P01876	Immunoglobulin heavy constant alpha 1	6416
P01877	Immunoglobulin heavy constant alpha 2	4993
S4R460	Immunoglobulin heavy variable 3/OR16-9 (non-functional)	1623
P01591	Immunoglobulin J chain	3631
P01834	Immunoglobulin kappa constant	2293
P0CG04	Immunoglobulin lambda constant 1	7427
P31025	Lipocalin-1	5611
F8VV32	Lysozyme	1202
P61626	Lysozyme C	857
Q8TAX7	Mucin-7	597
P04746	Pancreatic alpha-amylase	26183
P01833	Polymeric immunoglobulin receptor	1562
Q6S8J3	POTE ankyrin domain family member E	1199
A5A3E0	POTE ankyrin domain family member F	1199
P0CG38	POTE ankyrin domain family member I	626
P07737	Profilin-1	682
P12273	Prolactin-inducible protein	5504
A0A0A0MT31	Proline-rich protein 4	23729
Q5W0V3	Protein FAM160B1	717
Q9BYX7	Putative beta-actin-like protein 3	2302
Q5VSP4	Putative lipocalin 1-like protein 1	1428
P02810	Salivary acidic proline-rich phosphoprotein 1/2	23729

P02768	Serum albumin	6056
Q8WXA9	Splicing regulatory glutamine/lysine-rich protein 1	329
P02814	Submaxillary gland androgen-regulated protein 3B	11077
A0A087WZY1	Uncharacterized protein	14156
Q96DA0	Zymogen granule protein 16 homolog B	4692

° Identification is based on protein ID from UniProt protein database. reviewed only (http://www.uniprot.org/).

Table 3. Proteins identified in the unstimulated saliva of head and neck cancer patients exclusively before radiotherapy (BRT), during radiotherapy (DRT) or after radiotherapy (ART). Proteins exclusive in the unstimulated saliva of control patients were also identified for comparison.

Access number	Protein name	PLGS Score	Unique
Q8TE99	2-phosphoxylose phosphatase 1	364	Control*
P42765	3-ketoacyl-CoA thiolase_ mitochondrial	363	Control
Q9H2P0	Activity-dependent neuroprotector homeobox protein	112	Control
O00116	Alkyldihydroxyacetonephosphate synthase_ peroxisomal	141	Control
E9PKC5	AMP deaminase	381	Control
Q01432	AMP deaminase 3	385	Control
H7C3N6	Anoctamin (Fragment)	278	Control
A0A087WW05	Aspartyl/asparaginyl beta-hydroxylase (Fragment)	1009	Control
Q5TC12	ATP synthase mitochondrial F1 complex assembly factor 1	416	Control
Q01813	ATP-dependent 6-phosphofructokinase_ platelet type	295	Control
Q9NRL2	Bromodomain adjacent to zinc finger domain protein 1A	453	Control
O00478	Butyrophilin subfamily 3 member A3	647	Control
P19022	Cadherin-2	660	Control
P43235	Cathepsin K	153	Control
B4DRP8	cDNA FLJ54872_ highly similar to Zinc finger protein 461	759	Control
P56749	Claudin-12	643	Control
Q9NRD9	Dual oxidase 1	308	Control
H0YAC4	Exosome RNA helicase MTR4 (Fragment)	799	Control
Q9BRP7	Ferredoxin-fold anticodon-binding domain-containing protein 1	227	Control
Q0PRL4	Forkhead box P2 variant 3	302	Control
Q8N6B5	Forkhead box P2_ isoform CRA_d (Fragment)	302	Control
P98177	Forkhead box protein O4	274	Control
O15409	Forkhead box protein P2	359	Control
Q6ZNW5	GDP-D-glucose phosphorylase 1	719	Control
Q9NZD1	G-protein coupled receptor family C group 5 member D	490	Control
C9JVX5	HCG1651889_ isoform CRA_d (Fragment)	519	Control
G3V201	HCG1985539_ isoform CRA_e	346	Control
K7ERT9	Hsp70-binding protein 1 (Fragment)	335	Control
P01714	Immunoglobulin lambda variable 3-19	331	Control
O95050	Indolethylamine N-methyltransferase	360	Control
H3BSR8	INMT-MINDY4 readthrough (NMD candidate) (Fragment)	330	Control
Q8N201	Integrator complex subunit 1	588	Control

P20592	Interferon-induced GTP-binding protein Mx2	1186	Control
P42702	Leukemia inhibitory factor receptor	292	Control
P18428	Lipopolysaccharide-binding protein	329	Control
Q13296	Mammaglobin-A	430	Control
Q8TCB7	Methyltransferase-like protein 6	298	Control
Q9H1A3	Methyltransferase-like protein 9	188	Control
O43684	Mitotic checkpoint protein BUB3	438	Control
Q9P1T7	MyoD family inhibitor domain-containing protein	420	Control
Q9BYH8	NF-kappa-B inhibitor zeta	263	Control
B3KNX7	Non-specific serine/threonine protein kinase	406	Control
E9PNR1	Oxysterol-binding protein-related protein 9 (Fragment)	289	Control
D6RC77	Phosphoacetylglucosamine mutase (Fragment)	350	Control
Q7Z3K3	Pogo transposable element with ZNF domain	357	Control
Q9P0L9	Polycystic kidney disease 2-like 1 protein	138	Control
H0YAT0	Probable C-mannosyltransferase DPY19L4 (Fragment)	361	Control
C9JH25	Proline-rich transmembrane protein 4	534	Control
Q8IVL5	Prolyl 3-hydroxylase 2	185	Control
O15460	Prolyl 4-hydroxylase subunit alpha-2	755	Control
Q92824	Proprotein convertase subtilisin/kexin type 5	443	Control
P49354	Protein farnesyltransferase/geranylgeranyltransferase type-1 subunit alpha	582	Control
Q9BWQ6	Protein YIPF2	226	Control
Q96QU1	Protocadherin-15	305	Control
Q7Z2F6	Putative protein ZNF720	355	Control
A6NKP2	Putative short-chain dehydrogenase/reductase family 42E member 2	97	Control
Q13153	Serine/threonine-protein kinase PAK 1	406	Control
Q9NY27	Serine/threonine-protein phosphatase 4 regulatory subunit 2	517	Control
Q9Y345	Sodium- and chloride-dependent glycine transporter 2	198	Control
Q9NY46	Sodium channel protein type 3 subunit alpha	85	Control
P23975	Sodium-dependent noradrenaline transporter	332	Control
X6R3N0	Solute carrier family 27 (Fatty acid transporter)_ member 3_ isoform CRA_d	364	Control
Q5K4L6	Solute carrier family 27 member 3	364	Control
Q96R06	Sperm-associated antigen 5	418	Control
Q9H4L7	SWI/SNF-related matrix-associated actin-dependent regulator of chromatin subfamily A containing DEAD/H box 1	704	Control
F8WCE4	Synaptogyrin-1	319	Control
C9JA29	Syndetin (Fragment)	308	Control
Q9Y2K9	Syntaxin-binding protein 5-like	367	Control
O60784	Target of Myb protein 1	419	Control
E7EWG2	TNFAIP3-interacting protein 1 (Fragment)	537	Control
Q6UW50	TOM1	409	Control
Q9Y296	Trafficking protein particle complex subunit 4	404	Control
F8VRN7	Transmembrane protein 116	898	Control
H3BRE9	Transporter	332	Control
M0QZD8	Uncharacterized protein	410	Control
A0A286YET3	Uncharacterized protein	719	Control

M0R1J3	Uncharacterized protein (Fragment)	403	Control
H3BUV5	Uncharacterized protein (Fragment)	435	Control
H0Y8H3	Uncharacterized protein C3orf67 (Fragment)	516	Control
Q8N3P4	Vacuolar protein sorting-associated protein 8 homolog	372	Control
A0A0A0MRV3	WD repeat domain 8_ isoform CRA_c	120	Control
Q96KV7	WD repeat-containing protein 90	353	Control
Q9P2S5	WD repeat-containing protein WRAP73	130	Control
G3V577	X-linked retinitis pigmentosa GTPase regulator-interacting protein 1 (Fragment)	366	Control
Q8TBC5	Zinc finger and SCAN domain-containing protein 18	124	Control
Q8TAF7	Zinc finger protein 461	759	Control
Q86XE5	4-hydroxy-2-oxoglutarate aldolase_ mitochondrial	502	BRT*
Q6VMQ6	Activating transcription factor 7-interacting protein 1	478	BRT
Q8IUX7	Adipocyte enhancer-binding protein 1	354	BRT
Q9H4A4	Aminopeptidase B	328	BRT
P51693	Amyloid-like protein 1	210	BRT
K7ENE0	Ankyrin repeat domain-containing protein 27	346	BRT
C9JP59	Ankyrin repeat_ SAM and basic leucine zipper domain-containing protein 1 (Fragment)	1159	BRT
Q8NFD5	AT-rich interactive domain-containing protein 1B	95	BRT
D6R9B7	Axonemal dynein light chain domain-containing protein 1 (Fragment)	744	BRT
Q9NQY0	Bridging integrator 3	880	BRT
E7EMB3	Calmodulin-2	533	BRT
P48509	CD151 antigen	283	BRT
E9PMT5	CD3 delta	588	BRT
B7Z4G8	cDNA FLJ56046_ highly similar to Amyloid-like protein 1 (APLP)(APLP-1)	210	BRT
Q4KMG0	Cell adhesion molecule-related/down-regulated by oncogenes	472	BRT
A0A2R8Y7X1	Chromodomain-helicase-DNA-binding protein 4 (Fragment)	382	BRT
H3BRY3	Coronin	476	BRT
P31146	Coronin-1A	520	BRT
Q8NDL9	Cytosolic carboxypeptidase-like protein 5	358	BRT
Q9H4C3	E3 ubiquitin-protein ligase Mdm2	390	BRT
Q8NFF5	FAD synthase	216	BRT
H0YIY4	Gephyrin (Fragment)	455	BRT
A0A1C7CYW1	Glycogen debranching enzyme	241	BRT
P16260	Graves disease carrier protein	411	BRT
Q9BXW7	Haloacid dehalogenase-like hydrolase domain-containing 5	297	BRT
Q09028	Histone-binding protein RBBP4	524	BRT
P01871	Immunoglobulin heavy constant mu	416	BRT
Q9NVH2	Integrator complex subunit 7	443	BRT
P13598	Intercellular adhesion molecule 2	232	BRT
Q9P2K6	Kelch-like protein 42	258	BRT
Q9HCC9	Lateral signaling target protein 2 homolog	576	BRT
Q6GTX8	Leukocyte-associated immunoglobulin-like receptor 1	611	BRT
O75145	Liprin-alpha-3	130	BRT
P38571	Lysosomal acid lipase/cholesteryl ester hydrolase	183	BRT

Q86VI4	Lysosomal-associated transmembrane protein 4B	365	BRT
P43243	Matrin-3	515	BRT
A0A0D9SF86	Membrane-associated guanylate kinase_ WW and PDZ domain-containing protein 2 (Fragment)	529	BRT
H7C4V5	Metabotropic glutamate receptor 8 (Fragment)	337	BRT
O75121	Microfibrillar-associated protein 3-like	221	BRT
Q9Y2H9	Microtubule-associated serine/threonine-protein kinase 1	246	BRT
Q9NZJ7	Mitochondrial carrier homolog 1	315	BRT
Q9NYZ2	Mitoferrin-1	556	BRT
Q86WG5	Myotubularin-related protein 13	207	BRT
P03897	NADH-ubiquinone oxidoreductase chain 3	390	BRT
Q6ZS30	Neurobeachin-like protein 1	293	BRT
Q99574	Neuroserpin	277	BRT
H7C1V7	N-glycosylase/DNA lyase (Fragment)	394	BRT
Q9UKX7	Nuclear pore complex protein Nup50	348	BRT
H3BPW6	Obscurin (Fragment)	378	BRT
Q9UMX2	Ornithine decarboxylase antizyme 3	631	BRT
Q06710	Paired box protein Pax-8	316	BRT
P42356	Phosphatidylinositol 4-kinase alpha	200	BRT
E9PSF8	Phosphatidylinositol 4-phosphate 5-kinase type-1 alpha	480	BRT
Q9UJ90	Potassium voltage-gated channel subfamily E regulatory beta subunit 5	325	BRT
Q16557	Pregnancy-specific beta-1-glycoprotein 3	457	BRT
A1A519	Protein FAM170A	302	BRT
Q6P5S2	Protein LEG1 homolog	1304	BRT
B5MCF8	Protein Mpv17	427	BRT
Q5JR12	Protein phosphatase 1J	258	BRT
A4QPH2	Putative phosphatidylinositol 4-kinase alpha-like protein P2	162	BRT
Q9HBR0	Putative sodium-coupled neutral amino acid transporter 10	350	BRT
Q14D33	Receptor-transporting protein 5	2899	BRT
A1L4H1	Soluble scavenger receptor cysteine-rich domain-containing protein SSC5D	386	BRT
E5RJM7	Solute carrier family 45 member 4 (Fragment)	497	BRT
Q5T0L3	Spermatogenesis-associated protein 46	638	BRT
Q86VE3	Spermidine/spermine N(1)-acetyltransferase-like protein 1	519	BRT
Q12770	Sterol regulatory element-binding protein cleavage-activating protein	506	BRT
O14994	Synapsin-3	305	BRT
P18827	Syndecan-1	305	BRT
A0A087WT01	T cell receptor alpha variable 27	393	BRT
G3V1T3	TAP binding protein-like_ isoform CRA_c	595	BRT
Q9BX59	Tapasin-related protein	497	BRT
Q8NDV7	Trinucleotide repeat-containing gene 6A protein	272	BRT
A0A2R8Y670	Tuberin (Fragment)	908	BRT
Q03169	Tumor necrosis factor alpha-induced protein 2	376	BRT
Q16890	Tumor protein D53	304	BRT
K7EJK4	Uncharacterized protein (Fragment)	1200	BRT
Q9H1L0	Uncharacterized protein MIR1-1HG	387	BRT

H0YCW7	von Willebrand factor A domain-containing protein 3B (Fragment)	618	BRT
A6NK53	Zinc finger protein 233	391	BRT
O94892	Zinc finger protein 432	806	BRT
Q6P3V2	Zinc finger protein 585A	1200	BRT
Q86XU0	Zinc finger protein 677	494	BRT
Q9H7X3	Zinc finger protein 696	298	BRT
Q9Y6R6	Zinc finger protein 780B	560	BRT
A8MQ14	Zinc finger protein 850	391	BRT
Q15029	116 kDa U5 small nuclear ribonucleoprotein component	143	DRT*
Q9H9V9	2-oxoglutarate and iron-dependent oxygenase JMJD4	121	DRT
H0YFS2	4F2 cell-surface antigen heavy chain (Fragment)	326	DRT
Q00013	55 kDa erythrocyte membrane protein	199	DRT
Q16875	6-phosphofructo-2-kinase/fructose-2_6-bisphosphatase 3	320	DRT
Q9UHI8	A disintegrin and metalloproteinase with thrombospondin motifs 1	416	DRT
P58397	A disintegrin and metalloproteinase with thrombospondin motifs 12	231	DRT
Q01518	Adenylyl cyclase-associated protein 1	310	DRT
Q9NZ52	ADP-ribosylation factor-binding protein GGA3	214	DRT
O43572	A-kinase anchor protein 10_ mitochondrial	371	DRT
Q11128	Alpha-(1_3)-fucosyltransferase 5	115	DRT
P51993	Alpha-(1_3)-fucosyltransferase 6	115	DRT
P12814	Alpha-actinin-1	805	DRT
O43707	Alpha-actinin-4	195	DRT
Q8IY63	Angiomotin-like protein 1	260	DRT
F8WB76	Ankyrin repeat domain-containing protein 54 (Fragment)	134	DRT
P03973	Antileukoproteinase	601	DRT
F8WB77	Apolipoprotein L1	875	DRT
Q9BPW4	Apolipoprotein L4	185	DRT
O15033	Apoptosis-resistant E3 ubiquitin protein ligase 1	327	DRT
Q9ULH1	Arf-GAP with SH3 domain_ ANK repeat and PH domain-containing protein 1	183	DRT
O00571	ATP-dependent RNA helicase DDX3X	162	DRT
O15523	ATP-dependent RNA helicase DDX3Y	189	DRT
H0Y488	AT-rich interactive domain-containing protein 1A	136	DRT
A6NKF2	AT-rich interactive domain-containing protein 3C	115	DRT
J3QRN2	Beta-2-glycoprotein 1 (Fragment)	414	DRT
Q96IK1	Biorientation of chromosomes in cell division protein 1	190	DRT
P80723	Brain acid soluble protein 1	173	DRT
Q14681	BTB/POZ domain-containing protein KCTD2	160	DRT
Q4G0X4	BTB/POZ domain-containing protein KCTD21	106	DRT
Q96EU7	C1GALT1-specific chaperone 1	171	DRT
O75309	Cadherin-16	115	DRT
Q9NZU7	Calcium-binding protein 1	243	DRT
Q9NPB3	Calcium-binding protein 2	122	DRT
Q9ULU8	Calcium-dependent secretion activator 1	353	DRT
Q6MZZ7	Calpain-13	188	DRT

Q9UBL0	cAMP-regulated phosphoprotein 21	505	DRT
Q92523	Carnitine O-palmitoyltransferase 1_ muscle isoform	228	DRT
P78368	Casein kinase I isoform gamma-2	138	DRT
Q9Y6M4	Casein kinase I isoform gamma-3	138	DRT
A6H8Y7	CCDC73 protein	306	DRT
Q99795	Cell surface A33 antigen	150	DRT
Q8N8E3	Centrosomal protein of 112 kDa	348	DRT
O94986	Centrosomal protein of 152 kDa	234	DRT
Q8TEP8	Centrosomal protein of 192 kDa	119	DRT
H0Y900	Centrosomal protein of 63 kDa (Fragment)	147	DRT
E9PIK0	Centrosome-associated protein 350 (Fragment)	157	DRT
P00450	Ceruloplasmin	150	DRT
Q8IYW2	Cilia- and flagella-associated protein 46	178	DRT
Q9P2M7	Cingulin	196	DRT
Q9P2I0	Cleavage and polyadenylation specificity factor subunit 2	161	DRT
G9CGD6	CNK3/IPCEF1 fusion protein	331	DRT
A0A0B4J1Z0	COBL-like 1_ isoform CRA_a	179	DRT
Q6ZRK6	Coiled-coil domain-containing protein 73	319	DRT
Q9UMD9	Collagen alpha-1(XVII) chain	504	DRT
Q6UXH8	Collagen and calcium-binding EGF domain-containing protein 1	456	DRT
Q9BXJ2	Complement C1q tumor necrosis factor-related protein 7	253	DRT
A0A0D9SG04	Cordon-bleu protein-like 1	179	DRT
B7ZLQ8	CPEB4 protein	233	DRT
Q6UUV7	CREB-regulated transcription coactivator 3	578	DRT
Q7Z408	CUB and sushi domain-containing protein 2	207	DRT
Q5TAH7	CUB and Sushi multiple domains 2_ isoform CRA_c	191	DRT
Q7Z5Q1	Cytoplasmic polyadenylation element-binding protein 2	240	DRT
Q8NE35	Cytoplasmic polyadenylation element-binding protein 3	213	DRT
Q17RY0	Cytoplasmic polyadenylation element-binding protein 4	233	DRT
Q5M775	Cytospin-B	653	DRT
P07585	Decorin	351	DRT
A0A2R8YD85	Dedicator of cytokinesis protein 10	81	DRT
A0A075B7B1	Desmuslin_ isoform CRA_a	96	DRT
Q7L591	Docking protein 3	100	DRT
Q9NYC9	Dynein heavy chain 9_ axonemal	342	DRT
O95714	E3 ubiquitin-protein ligase HERC2	341	DRT
A0RZB6	Endoplasmic reticulum chaperone SIL1 (Fragment)	622	DRT
Q6P2E9	Enhancer of mRNA-decapping protein 4	98	DRT
P98073	Enteropeptidase	253	DRT
P54764	Ephrin type-A receptor 4	179	DRT
P62508	Estrogen-related receptor gamma	340	DRT
Q6ZN32	ETS translocation variant 3-like protein	148	DRT
C9JF49	Exportin-1 (Fragment)	255	DRT
P55060	Exportin-2	94	DRT
O43592	Exportin-T	275	DRT
Q08945	FACT complex subunit SSRP1	235	DRT

Q92945	Far upstream element-binding protein 2	141	DRT
P14324	Farnesyl pyrophosphate synthase	315	DRT
Q96IV6	Fatty acid hydroxylase domain-containing protein 2	566	DRT
Q4VXH1	F-box/WD repeat-containing protein 2 (Fragment)	153	DRT
Q96NE9	FERM domain-containing protein 6	159	DRT
A0A0G2JJI2	G patch domain and ankyrin repeat-containing protein 1 (Fragment)	314	DRT
P21217	Galactoside 3(4)-L-fucosyltransferase	115	DRT
A0A1B0GU82	Gamma-aminobutyric acid receptor subunit alpha-1	277	DRT
O95749	Geranylgeranyl pyrophosphate synthase	443	DRT
Q86X53	Glutamate-rich protein 1	346	DRT
Q86W71	GOLGA4 protein	316	DRT
Q9C091	GREB1-like protein	282	DRT
H7C010	GRIP and coiled-coil domain-containing protein 2 (Fragment)	194	DRT
Q6IX74	Growth arrest and DNA damage-inducible protein GADD45 beta (Fragment)	398	DRT
O43903	Growth arrest-specific protein 2	227	DRT
A0A2R8YGL0	Hamartin (Fragment)	333	DRT
Q9H6D7	HAUS augmin-like complex subunit 4	211	DRT
A0A0A6YYF2	HCG1811249_ isoform CRA_e	191	DRT
A0A0A0MTS5	HCG1811249_ isoform CRA_f	191	DRT
G3V3R4	HCG1983504_ isoform CRA_c	156	DRT
G3V2N6	HCG1983504_ isoform CRA_d	156	DRT
G3V2R8	HCG1983504_ isoform CRA_e	156	DRT
Q6AI08	HEAT repeat-containing protein 6	439	DRT
G3V2J8	Heat shock protein HSP 90-alpha (Fragment)	183	DRT
A0A024R4E5	High density lipoprotein binding protein (Vigilin)_ isoform CRA_a	343	DRT
Q7Z353	Highly divergent homeobox	116	DRT
P42357	Histidine ammonia-lyase	245	DRT
J3KPH8	Histone deacetylase	411	DRT
Q8WUI4	Histone deacetylase 7	411	DRT
H0Y9L4	Histone-lysine N-methyltransferase NSD2 (Fragment)	220	DRT
A0A140T9Z3	HLA class II histocompatibility antigen_ DO beta chain (Fragment)	271	DRT
O60479	Homeobox protein DLX-3	286	DRT
O00410	Importin-5	178	DRT
B7WPL9	Inositol hexakisphosphate and diphosphoinositol-pentakisphosphate kinase	457	DRT
Q6PFW1	Inositol hexakisphosphate and diphosphoinositol-pentakisphosphate kinase 1	457	DRT
P08514	Integrin alpha-IIb	88	DRT
Q8WWN9	Interactor protein for cytohesin exchange factors 1	331	DRT
Q8NAC3	Interleukin-17 receptor C	195	DRT
Q9NZM3	Intersectin-2	233	DRT
H0YNL8	Iron-responsive element-binding protein 2	206	DRT
Q99456	Keratin_ type I cytoskeletal 12	220	DRT
Q02241	Kinesin-like protein KIF23	91	DRT
O00139	Kinesin-like protein KIF2A	164	DRT

H0YN41	Kinetochore scaffold 1	204	DRT
E9PHC9	Krueppel-like factor 7	466	DRT
Q16787	Laminin subunit alpha-3	203	DRT
H0YBR8	La-related protein 1 (Fragment)	444	DRT
O75387	Large neutral amino acids transporter small subunit 3	313	DRT
O75112	LIM domain-binding protein 3	372	DRT
H3BQT4	Lipase maturation factor 1 (Fragment)	186	DRT
E9PP16	Liprin-beta-2	233	DRT
P33241	Lymphocyte-specific protein 1	194	DRT
O15550	Lysine-specific demethylase 6A	149	DRT
Q6ZMT4	Lysine-specific demethylase 7A	67	DRT
O43451	Maltase-glucoamylase_ intestinal	321	DRT
Q9UM22	Mammalian ependymin-related protein 1	510	DRT
Q9H8J5	MANSC domain-containing protein 1	203	DRT
C9JGN2	Mediator of RNA polymerase II transcription subunit 15 (Fragment)	240	DRT
A2RUB1	Meiosis-specific coiled-coil domain-containing protein MEIOC	111	DRT
C9JK50	Melanoma-associated antigen 4 (Fragment)	116	DRT
E7EVA0	Microtubule-associated protein	325	DRT
Q3SY69	Mitochondrial 10-formyltetrahydrofolate dehydrogenase	141	DRT
Q8IVH8	Mitogen-activated protein kinase kinase kinase kinase 3	156	DRT
Q96T76	MMS19 nucleotide excision repair protein homolog	155	DRT
Q96HT8	MORF4 family-associated protein 1-like 1	178	DRT
P30304	M-phase inducer phosphatase 1	202	DRT
Q96T58	Msx2-interacting protein	106	DRT
P02686	Myelin basic protein	276	DRT
P12882	Myosin-1	246	DRT
Q9UKX3	Myosin-13	241	DRT
Q9UKX2	Myosin-2	256	DRT
Q9Y623	Myosin-4	240	DRT
O00308	NEDD4-like E3 ubiquitin-protein ligase WWP2	246	DRT
Q5QGS0	Neurite extension and migration factor	143	DRT
O94856	Neurofascin	172	DRT
P30990	Neurotensin/neuromedin N	182	DRT
P80188	Neutrophil gelatinase-associated lipocalin	184	DRT
Q86UT6	NLR family member X1	225	DRT
Q8TAT6	Nuclear protein localization protein 4 homolog	834	DRT
Q5SRE5	Nucleoporin NUP188 homolog	278	DRT
P0DN81	Olfactory receptor 13C7	140	DRT
Q8IXM7	Outer dense fiber protein 3-like protein 1	215	DRT
H0YCU5	Phosphofurin acidic cluster sorting protein 1 (Fragment)	229	DRT
Q8NEL9	Phospholipase DDHD1	219	DRT
P20020	Plasma membrane calcium-transporting ATPase 1	114	DRT
Q9H4M7	Pleckstrin homology domain-containing family A member 4	285	DRT
P11465	Pregnancy-specific beta-1-glycoprotein 2	235	DRT
H0Y8P7	Pre-mRNA 3'-end-processing factor FIP1 (Fragment)	119	DRT
Q15034	Probable E3 ubiquitin-protein ligase HERC3	446	DRT

K7EJ44	Profilin	176	DRT
K7EJN8	Proline-rich protein 22 (Fragment)	655	DRT
E9PMZ2	Protein arginine N-methyltransferase 1 (Fragment)	573	DRT
A0A1W2PQ30	Protein Aster-B	277	DRT
P58658	Protein eva-1 homolog C	219	DRT
Q92833	Protein Jumonji	82	DRT
Q8N3A8	Protein mono-ADP-ribosyltransferase PARP8	512	DRT
Q9Y6F6	Protein MRVI1	205	DRT
Q86WI3	Protein NLRC5	127	DRT
Q86U86	Protein polybromo-1	241	DRT
Q5JSZ9	Protein PRRC2B (Fragment)	179	DRT
Q9BVV6	Protein TALPID3	182	DRT
Q9NQW1	Protein transport protein Sec31B	418	DRT
Q93096	Protein tyrosine phosphatase type IVA 1	167	DRT
Q9Y5F7	Protocadherin gamma-C4	225	DRT
Q8N9H6	Putative uncharacterized protein C8orf31	195	DRT
Q15929	Putative zinc finger protein 56	599	DRT
Q2TAK8	PWWP domain-containing DNA repair factor 3A	199	DRT
Q9Y3Y4	Pygopus homolog 1	294	DRT
Q2PPJ7	Ral GTPase-activating protein subunit alpha-2	321	DRT
J3QLV2	Receptor tyrosine-protein kinase erbB-2 (Fragment)	711	DRT
P10586	Receptor-type tyrosine-protein phosphatase F	173	DRT
P28827	Receptor-type tyrosine-protein phosphatase mu	247	DRT
Q15256	Receptor-type tyrosine-protein phosphatase R	358	DRT
Q96P16	Regulation of nuclear pre-mRNA domain-containing protein 1A	634	DRT
P28749	Retinoblastoma-like protein 1	219	DRT
Q5T5U3	Rho GTPase-activating protein 21	239	DRT
Q15434	RNA-binding motif_ single-stranded-interacting protein 2	167	DRT
Q9UKM9	RNA-binding protein Raly	242	DRT
H7C357	Run domain Beclin-1-interacting and cysteine-rich domain-containing protein (Fragment)	147	DRT
Q9UL12	Sarcosine dehydrogenase_ mitochondrial	323	DRT
Q7Z7L1	Schlafen family member 11	258	DRT
P13521	Secretogranin-2	342	DRT
Q5T5U6	Selenide_ water dikinase 1 (Fragment)	421	DRT
Q96I15	Selenocysteine lyase	525	DRT
Q92854	Semaphorin-4D	197	DRT
Q9P0U3	Sentrin-specific protease 1	147	DRT
Q14674	Separin	255	DRT
E7EPG2	Septin-5 (Fragment)	159	DRT
Q8IYP2	Serine protease 58	150	DRT
E5RHP4	Serine/threonine-protein phosphatase (Fragment)	268	DRT
P67775	Serine/threonine-protein phosphatase 2A catalytic subunit alpha isoform	268	DRT
P62714	Serine/threonine-protein phosphatase 2A catalytic subunit beta isoform	268	DRT
Q8N8A2	Serine/threonine-protein phosphatase 6 regulatory ankyrin repeat subunit B	130	DRT

H7C0U8	Serrate RNA effector molecule homolog (Fragment)	219	DRT
Q9UHB9	Signal recognition particle subunit SRP68	253	DRT
Q5JXA9	Signal-regulatory protein beta-2	171	DRT
A0A2R8YCJ5	Small integral membrane protein 41	222	DRT
H9KVA1	Solute carrier family 22 member 17	203	DRT
A0A1B0GVP8	Solute carrier family 26 member 10 (Fragment)	273	DRT
Q9UMY4	Sorting nexin-12	165	DRT
Q96JI7	Spatacsin	153	DRT
G5EA09	Syndecan binding protein (Syntenin)_ isoform CRA_a	229	DRT
O15061	Synemin	107	DRT
A0A0B4J271	T cell receptor alpha variable 12-3	223	DRT
A0A0J9YWI7	Taste receptor type 2	154	DRT
P59541	Taste receptor type 2 member 30	154	DRT
A0A087WXG5	TBC1 domain family member 17	200	DRT
Q9NUY8	TBC1 domain family member 23	266	DRT
Q9P273	Teneurin-3	232	DRT
Q5TAX3	Terminal uridylyltransferase 4	158	DRT
Q96FV3	Tetraspanin-17	179	DRT
P37173	TGF-beta receptor type-2	146	DRT
Q86W42	THO complex subunit 6 homolog	181	DRT
Q9P031	Thyroid transcription factor 1-associated protein 26	170	DRT
E9PMZ8	T-lymphoma invasion and metastasis-inducing protein 2 (Fragment)	108	DRT
F6SA91	TNF receptor-associated factor	207	DRT
Q9BUZ4	TNF receptor-associated factor 4	207	DRT
Q8WXI9	Transcriptional repressor p66-beta	318	DRT
O94759	Transient receptor potential cation channel subfamily M member 2	236	DRT
Q9HBA0	Transient receptor potential cation channel subfamily V member 4	112	DRT
P55072	Transitional endoplasmic reticulum ATPase	214	DRT
Q86WS5	Transmembrane protease serine 12	170	DRT
P07437	Tubulin beta chain	201	DRT
Q13885	Tubulin beta-2A chain	201	DRT
Q9BVA1	Tubulin beta-2B chain	201	DRT
Q13509	Tubulin beta-3 chain	201	DRT
Q12923	Tyrosine-protein phosphatase non-receptor type 13	196	DRT
Q70CQ3	Ubiquitin carboxyl-terminal hydrolase 30	210	DRT
Q9H9J4	Ubiquitin carboxyl-terminal hydrolase 42	172	DRT
Q9H0E7	Ubiquitin carboxyl-terminal hydrolase 44	311	DRT
O14562	Ubiquitin domain-containing protein UBFD1	194	DRT
D6RJB3	Ubiquitin-conjugating enzyme E2 D3	717	DRT
Q9BZL1	Ubiquitin-like protein 5	732	DRT
F8VRI7	Ubiquitinyl hydrolase 1	279	DRT
P78381	UDP-galactose translocator	285	DRT
A0A0B4J269	Uncharacterized protein	201	DRT
H7C4K7	Uncharacterized protein (Fragment)	274	DRT

O15063	Uncharacterized protein KIAA0355	262	DRT
K7EP79	Uncharacterized serine/threonine-protein kinase SBK3 (Fragment)	124	DRT
Q8WVF2	Unique cartilage matrix-associated protein	204	DRT
Q14CZ0	UPF0472 protein C16orf72	201	DRT
Q96RL7	Vacuolar protein sorting-associated protein 13A	196	DRT
Q5THJ4	Vacuolar protein sorting-associated protein 13D	160	DRT
Q00341	Vigilin	343	DRT
P08670	Vimentin	210	DRT
P01282	VIP peptides	449	DRT
Q8IZU2	WD repeat-containing protein 17	123	DRT
O95388	WNT1-inducible-signaling pathway protein 1	282	DRT
M0R1Y0	Zinc finger and SCAN domain-containing protein 30	277	DRT
A0A0D9SF71	Zinc finger E-box-binding homeobox 2	577	DRT
P17023	Zinc finger protein 19	155	DRT
K7EL19	Zinc finger protein 235 (Fragment)	122	DRT
Q9HBT8	Zinc finger protein 286A	256	DRT
Q06732	Zinc finger protein 33B	224	DRT
M0R0R1	Zinc finger protein 415 (Fragment)	226	DRT
Q9BX82	Zinc finger protein 471	176	DRT
Q3MIS6	Zinc finger protein 528	181	DRT
Q96ND8	Zinc finger protein 583	183	DRT
Q6ZNG1	Zinc finger protein 600	184	DRT
Q2M218	Zinc finger protein 630	532	DRT
Q3SXZ3	Zinc finger protein 718	872	DRT
B4E159	Zinc finger protein 721	872	DRT
B4DXR9	Zinc finger protein 732	872	DRT
Q6ZN06	Zinc finger protein 813	163	DRT
P31946	14-3-3 protein beta/alpha	310	ART*
Q04917	14-3-3 protein eta	310	ART
P61981	14-3-3 protein gamma	310	ART
P27348	14-3-3 protein theta	335	ART
P63104	14-3-3 protein zeta/delta	687	ART
Q15147	1-phosphatidylinositol 4_5-bisphosphate phosphodiesterase beta-4	533	ART
P82664	28S ribosomal protein S10_ mitochondrial	340	ART
P52209	6-phosphogluconate dehydrogenase_ decarboxylating	318	ART
Q9P2N4	A disintegrin and metalloproteinase with thrombospondin motifs 9	266	ART
Q13085	Acetyl-CoA carboxylase 1	144	ART
Q16515	Acid-sensing ion channel 2	114	ART
Q08AH3	Acyl-coenzyme A synthetase ACSM2A_ mitochondrial	412	ART
Q68CK6	Acyl-coenzyme A synthetase ACSM2B_ mitochondrial	311	ART
Q76L82	Additional sex combs like 1 (Drosophila)_ isoform CRA_d	243	ART
Q5TCS8	Adenylate kinase 9	746	ART
Q9Y3D8	Adenylate kinase isoenzyme 6	597	ART
O94910	Adhesion G protein-coupled receptor L1	141	ART

Q02952	A-kinase anchor protein 12	111	ART
Q12802	A-kinase anchor protein 13	282	ART
Q9BTE6	Alanyl-tRNA editing protein Aarsd1	229	ART
O60218	Aldo-keto reductase family 1 member B10	252	ART
P02763	Alpha-1-acid glycoprotein 1	412	ART
P01011	Alpha-1-antichymotrypsin	254	ART
P01009	Alpha-1-antitrypsin	186	ART
H0Y9H2	Alpha-adducin (Fragment)	333	ART
H7C5V0	Alpha-sarcoglycan (Fragment)	271	ART
P12821	Angiotensin-converting enzyme	148	ART
Q8IWZ3	Ankyrin repeat and KH domain-containing protein 1	129	ART
Q5JPF3	Ankyrin repeat domain-containing protein 36C	110	ART
Q12955	Ankyrin-3	116	ART
P06727	Apolipoprotein A-IV	108	ART
G3V3T3	Apoptotic chromatin condensation inducer in the nucleus (Fragment)	110	ART
P16050	Arachidonate 15-lipoxygenase	250	ART
H7C264	Arf-GAP with dual PH domain-containing protein 1 (Fragment)	128	ART
Q8NEN0	Armadillo repeat-containing protein 2	120	ART
O00327	Aryl hydrocarbon receptor nuclear translocator-like protein 1	205	ART
Q498B9	ASXL1 protein	214	ART
Q8NHQ9	ATP-dependent RNA helicase DDX55	117	ART
P41182	B-cell lymphoma 6 protein	179	ART
O00587	Beta-1_3-N-acetylglucosaminyltransferase manic fringe	185	ART
P35612	Beta-adducin	225	ART
P07686	Beta-hexosaminidase subunit beta	81	ART
A0A0A0MR97	Bromodomain adjacent to zinc finger domain protein 2B	62	ART
B7ZM11	C2orf73 protein	286	ART
P27482	Calmodulin-like protein 3	915	ART
P20807	Calpain-3	155	ART
Q9Y4C5	Carbohydrate sulfotransferase 2	155	ART
P00915	Carbonic anhydrase 1	1501	ART
A5YKK6	CCR4-NOT transcription complex subunit 1	174	ART
B4DYW9	cDNA FLJ61485_ highly similar to Zinc finger protein 215	212	ART
G5EA36	Cell division cycle 27_ isoform CRA_c	434	ART
P30260	Cell division cycle protein 27 homolog	434	ART
P49454	Centromere protein F	124	ART
A0A0U1RRI6	Centromere protein V-like protein 3	154	ART
Q02224	Centromere-associated protein E	52	ART
Q5SW79	Centrosomal protein of 170 kDa	218	ART
Q9BV73	Centrosome-associated protein CEP250	43	ART
O00408	cGMP-dependent 3'_5'-cyclic phosphodiesterase	197	ART
P51797	Chloride transport protein 6	159	ART
Q9HC52	Chromobox protein homolog 8	161	ART
E9PQA1	Chromosome 11 open reading frame 58	220	ART
O60271	C-Jun-amino-terminal kinase-interacting protein 4	79	ART
Q16630	Cleavage and polyadenylation specificity factor subunit 6	161	ART

P10909	Clusterin	154	ART
Q9UJ98	Cohesin subunit SA-3	219	ART
Q5VVM6	Coiled-coil domain-containing protein 30	84	ART
Q96ER9	Coiled-coil domain-containing protein 51	229	ART
H7BY33	Coiled-coil domain-containing protein 88B	84	ART
P12111	Collagen alpha-3(VI) chain	241	ART
P01024	Complement C3	497	ART
P17927	Complement receptor type 1	84	ART
Q14028	Cyclic nucleotide-gated cation channel beta-1	112	ART
Q00536	Cyclin-dependent kinase 16	219	ART
Q00537	Cyclin-dependent kinase 17	108	ART
Q07002	Cyclin-dependent kinase 18	153	ART
Q14204	Cytoplasmic dynein 1 heavy chain 1	113	ART
O75891	Cytosolic 10-formyltetrahydrofolate dehydrogenase	420	ART
Q9UGM3	Deleted in malignant brain tumors 1 protein	294	ART
Q8NG44	Delta 3+6/2 progesterone receptor	104	ART
Q8NG42	Delta 6/2 progesterone receptor	104	ART
Q6IQ26	DENN domain-containing protein 5A	187	ART
B4E1G1	Derlin	143	ART
Q9BUN8	Derlin-1	205	ART
Q02487	Desmocollin-2	206	ART
P32926	Desmoglein-3	215	ART
A0A0B4J2C2	Discs_ large (Drosophila) homolog-associated protein 4_ isoform CRA_b	277	ART
Q9Y2H0	Disks large-associated protein 4	277	ART
P54098	DNA polymerase subunit gamma-1	266	ART
O75771	DNA repair protein RAD51 homolog 4	918	ART
Q9UBZ9	DNA repair protein REV1	121	ART
P49736	DNA replication licensing factor MCM2	704	ART
K7EMH3	DNA-directed RNA polymerase_ mitochondrial (Fragment)	109	ART
O75190	DnaJ homolog subfamily B member 6	314	ART
O75165	DnaJ homolog subfamily C member 13	146	ART
E9PEI6	DPCR1	105	ART
Q6P0N6	DST protein	64	ART
Q96M86	Dynein heavy chain domain-containing protein 1	192	ART
P11532	Dystrophin	180	ART
H0Y339	E3 ubiquitin-protein ligase COP1 (Fragment)	205	ART
Q7Z6Z7	E3 ubiquitin-protein ligase HUWE1	150	ART
Q8IUD6	E3 ubiquitin-protein ligase RNF135	227	ART
Q53HC9	EARP and GARP complex-interacting protein 1	234	ART
Q05BV3	Echinoderm microtubule-associated protein-like 5	723	ART
Q8NDI1	EH domain-binding protein 1	242	ART
Q5T6L9	Endoplasmic reticulum membrane-associated RNA degradation protein	417	ART
Q9H6T0	Epithelial splicing regulatory protein 2	185	ART
I6L9I8	EPN3 protein	147	ART
Q9H201	Epsin-3	179	ART

Q14152	Eukaryotic translation initiation factor 3 subunit A	100	ART
Q0VAP4	FANCA protein	152	ART
O15360	Fanconi anemia group A protein	158	ART
P23142	Fibulin-1	320	ART
G5E965	Forkhead box P1_ isoform CRA_f	342	ART
A0A3B3IRS5	Forkhead box P1_ isoform CRA_g	342	ART
Q9H334	Forkhead box protein P1	351	ART
J3KPS3	Fructose-bisphosphate aldolase	382	ART
P04075	Fructose-bisphosphate aldolase A	382	ART
P09972	Fructose-bisphosphate aldolase C	64	ART
M0R108	Galectin-16	409	ART
P47929	Galectin-7	156	ART
Q86XP6	Gastrokine-2	302	ART
A0A2U3TZV9	Girdin	80	ART
Q6IA69	Glutamine-dependent NAD(+) synthetase	477	ART
B5MC36	Glutathione hydrolase 1 proenzyme	189	ART
Q14390	Glutathione hydrolase light chain 2	189	ART
P48637	Glutathione synthetase	207	ART
Q08378	Golgin subfamily A member 3	186	ART
Q86VD9	GPI mannosyltransferase 4	440	ART
P49685	G-protein coupled receptor 15	171	ART
G5E9S6	HCG1994835	473	ART
Q7Z2R1	HCG19985_ isoform CRA_b	462	ART
K7EN88	HCG2039718_ isoform CRA_g	873	ART
G3XAL8	HCG21296_ isoform CRA_a	233	ART
O00165	HCLS1-associated protein X-1	166	ART
Q53T59	HCLS1-binding protein 3	169	ART
K7ENF6	Heat shock 70 kDa protein 12A (Fragment)	190	ART
P11142	Heat shock cognate 71 kDa protein	241	ART
Q03014	Hematopoietically-expressed homeobox protein HHEX	171	ART
P35680	Hepatocyte nuclear factor 1-beta	166	ART
A5PLL3	Histone acetyltransferase	252	ART
Q92794	Histone acetyltransferase KAT6A	253	ART
Q8WYB5	Histone acetyltransferase KAT6B	463	ART
Q9UBN7	Histone deacetylase 6	264	ART
Q03164	Histone-lysine N-methyltransferase 2A	172	ART
Q8NEZ4	Histone-lysine N-methyltransferase 2C	246	ART
Q9H9B1	Histone-lysine N-methyltransferase EHMT1	134	ART
Q92800	Histone-lysine N-methyltransferase EZH1	159	ART
O96028	Histone-lysine N-methyltransferase NSD2	176	ART
E0YMJ8	HNF1 beta A splice variant 3	166	ART
P57058	Hormonally up-regulated neu tumor-associated kinase	91	ART
Q4G0P3	Hydrocephalus-inducing protein homolog	325	ART
P01859	Immunoglobulin heavy constant gamma 2	971	ART
P01861	Immunoglobulin heavy constant gamma 4	707	ART
Q8TDY8	Immunoglobulin superfamily DCC subclass member 4	122	ART

Q8NBJ7	Inactive C-alpha-formylglycine-generating enzyme 2	272	ART
A0A3B3IU04	Inositol 1_4_5-trisphosphate receptor type 1	371	ART
Q14571	Inositol 1_4_5-trisphosphate receptor type 2	342	ART
Q9UKX5	Integrin alpha-11	122	ART
A0A087X131	Integrin alpha-X	323	ART
J3QQL2	Integrin beta (Fragment)	112	ART
P16144	Integrin beta-4	124	ART
P18510	Interleukin-1 receptor antagonist protein	118	ART
Q96CU4	Intraflagellar transport protein 56	214	ART
P06870	Kallikrein-1	226	ART
O95198	Kelch-like protein 2	146	ART
Q2M2I5	Keratin_ type I cytoskeletal 24	190	ART
P04264	Keratin_ type II cytoskeletal 1	81	ART
Q01546	Keratin_ type II cytoskeletal 2 oral	122	ART
Q8IUB9	Keratin-associated protein 19-1	358	ART
Q5T011	KICSTOR complex protein SZT2	128	ART
Q6UWL6	Kin of IRRE-like protein 2	98	ART
Q4R9M9	Kinesin family member 1Bbeta isoform II	233	ART
Q07866	Kinesin light chain 1	143	ART
O60333	Kinesin-like protein KIF1B	233	ART
Q96Q89	Kinesin-like protein KIF20B	490	ART
Q7Z4S6	Kinesin-like protein KIF21A	113	ART
Q8NBT2	Kinetochore protein Spc24	169	ART
Q6PIL6	Kv channel-interacting protein 4	263	ART
Q8NBH2	Kyphoscoliosis peptidase	538	ART
B4DGA7	Kyphoscoliosis peptidase	442	ART
Q9UNP4	Lactosylceramide alpha-2_3-sialyltransferase	338	ART
O00515	Ladinin-1	168	ART
Q96JM4	Leucine-rich repeat and IQ domain-containing protein 1	177	ART
Q8TE12	LIM homeobox transcription factor 1-alpha	64	ART
Q8IVV2	Lipoxygenase homology domain-containing protein 1	231	ART
O95274	Ly6/PLAUR domain-containing protein 3	207	ART
Q9UJU2	Lymphoid enhancer-binding factor 1	178	ART
Q8N5G2	Macoilin	141	ART
Q8NFP4	MAM domain-containing glycosylphosphatidylinositol anchor protein 1	108	ART
C9JQX2	Mannosyltransferase	440	ART
Q86YW9	Mediator of RNA polymerase II transcription subunit 12-like protein	287	ART
Q8N4V1	Membrane magnesium transporter 1	204	ART
H7C4S7	Membrane-associated guanylate kinase_ WW and PDZ domain-containing protein 1 (Fragment)	359	ART
Q14831	Metabotropic glutamate receptor 7	232	ART
E5RJR3	Methionine adenosyltransferase 2 subunit beta	1414	ART
O75030	Microphthalmia-associated transcription factor	466	ART
Q9Y584	Mitochondrial import inner membrane translocase subunit Tim22	590	ART

O43615	Mitochondrial import inner membrane translocase subunit TIM44	283	ART
O43683	Mitotic checkpoint serine/threonine-protein kinase BUB1	88	ART
O15427	Monocarboxylate transporter 4	137	ART
A0A1B0GV46	Mucin-like protein 3	108	ART
Q9H8L6	Multimerin-2	367	ART
O75970	Multiple PDZ domain protein	505	ART
E9PPE2	Myb/SANT-like DNA-binding domain-containing protein 2	303	ART
A0A3B3ITT2	Myelin transcription factor 1-like protein	421	ART
P05164	Myeloperoxidase	181	ART
Q9NZM1	Myoferlin	57	ART
P10916	Myosin regulatory light chain 2_ ventricular/cardiac muscle isoform	172	ART
Q7Z406	Myosin-14	298	ART
M0R0W4	NACHT_ LRR and PYD domains-containing protein 5 (Fragment)	284	ART
Q6IQ20	N-acyl-phosphatidylethanolamine-hydrolyzing phospholipase D	220	ART
F8W029	Nascent polypeptide-associated complex subunit alpha	510	ART
O14513	Nck-associated protein 5	197	ART
O75161	Nephrocystin-4	167	ART
E9PNX2	Neuronal acetylcholine receptor subunit alpha-10	114	ART
P59665	Neutrophil defensin 1	950	ART
P59666	Neutrophil defensin 3	950	ART
P29597	Non-receptor tyrosine-protein kinase TYK2	317	ART
Q7Z6G3	N-terminal EF-hand calcium-binding protein 2	299	ART
D6RH30	Nuclear factor NF-kappa-B p105 subunit (Fragment)	99	ART
J3QL49	Nuclear pore complex protein Nup85 (Fragment)	735	ART
P52948	Nuclear pore complex protein Nup98-Nup96	334	ART
J3QKP0	Nuclear receptor corepressor 1 (Fragment)	111	ART
Q86WB0	Nuclear-interacting partner of ALK	397	ART
C9JTN7	Nucleolysin TIA-1 isoform p40	372	ART
Q01085	Nucleolysin TIAR	372	ART
Q9NWT1	p21-activated protein kinase-interacting protein 1	158	ART
H0Y2Y4	Palmitoyltransferase (Fragment)	341	ART
P49023	Paxillin	91	ART
Q96A99	Pentraxin-4	115	ART
Q15154	Pericentriolar material 1 protein	90	ART
Q9UIL8	PHD finger protein 11	132	ART
P00439	Phenylalanine-4-hydroxylase	297	ART
A0A0J9YVR0	Phosphatase and actin regulator (Fragment)	112	ART
Q8IZ21	Phosphatase and actin regulator 4	132	ART
Q9NTJ5	Phosphatidylinositide phosphatase SAC1	135	ART
P42338	Phosphatidylinositol 4_5-bisphosphate 3-kinase catalytic subunit beta isoform	197	ART
E9PEF1	Phosphodiesterase	191	ART
P00558	Phosphoglycerate kinase 1	195	ART
P07205	Phosphoglycerate kinase 2	249	ART
O14939	Phospholipase D2	259	ART

E7EVM7	Piezo-type mechanosensitive ion channel component	158	ART
Q9H5I5	Piezo-type mechanosensitive ion channel component 2	176	ART
Q6IQ23	Pleckstrin homology domain-containing family A member 7	123	ART
D6RH25	Plexin-D1	234	ART
Q3YAB7	Potassium channel interacting protein 4	263	ART
P0CG39	POTE ankyrin domain family member J	372	ART
Q6UN15	Pre-mRNA 3'-end-processing factor FIP1	108	ART
Q9UMS4	Pre-mRNA-processing factor 19	148	ART
Q6P2Q9	Pre-mRNA-processing-splicing factor 8	340	ART
Q9Y4D8	Probable E3 ubiquitin-protein ligase HECTD4	142	ART
Q15751	Probable E3 ubiquitin-protein ligase HERC1	168	ART
Q5GLZ8	Probable E3 ubiquitin-protein ligase HERC4	150	ART
P06401	Progesterone receptor	104	ART
Q14005	Pro-interleukin-16	82	ART
P56975	Pro-neuregulin-3_ membrane-bound isoform	102	ART
O75081	Protein CBFA2T3	1058	ART
A8MVW0	Protein FAM171A2	125	ART
Q658Y4	Protein FAM91A1	167	ART
I3L2A7	Protein moonraker (Fragment)	370	ART
Q9Y6V0	Protein piccolo	254	ART
Q9Y520	Protein PRRC2C	307	ART
Q9Y2M2	Protein SSUH2 homolog	183	ART
E5RGR9	Protein YIPF5 (Fragment)	719	ART
Q7Z7L7	Protein zer-1 homolog	236	ART
Q86YA3	Protein ZGRF1	253	ART
Q08188	Protein-glutamine gamma-glutamyltransferase E	161	ART
Q9Y5I1	Protocadherin alpha-11	201	ART
Q9Y5F1	Protocadherin beta-12	933	ART
P35247	Pulmonary surfactant-associated protein D	174	ART
Q8IXJ9	Putative Polycomb group protein ASXL1	251	ART
P0CL83	Putative STAG3-like protein 1	217	ART
P0CL84	Putative STAG3-like protein 2	217	ART
Q5JXB2	Putative ubiquitin-conjugating enzyme E2 N-like	721	ART
Q9NSJ1	Putative zinc finger protein 355P	268	ART
H3BQ34	Pyruvate kinase	3666	ART
P14618	Pyruvate kinase PKM	3760	ART
K7ENJ9	Rab GTPase-binding effector protein 1 (Fragment)	294	ART
Q5T1S4	Rab9 effector protein with kelch motifs	127	ART
Q9Y4G8	Rap guanine nucleotide exchange factor 2	174	ART
Q8TEU7	Rap guanine nucleotide exchange factor 6	217	ART
Q15283	Ras GTPase-activating protein 2	452	ART
Q504U0	Renal cancer differentiation gene 1 protein	539	ART
Q6ZW31	Rho GTPase-activating protein SYDE1	234	ART
Q9BQY4	Rhox homeobox family member 2	357	ART
J3QQZ2	RNA binding protein fox-1 homolog	203	ART
F5H5U2	RNA helicase	117	ART

K7EJX6	RNA-binding protein fox-1 homolog 3 (Fragment)	203	ART
Q96LT9	RNA-binding region-containing protein 3	260	ART
H7C4J7	Roundabout homolog 2 (Fragment)	726	ART
Q15413	Ryanodine receptor 3	182	ART
P0DP57	Secreted Ly-6/uPAR domain-containing protein 2	836	ART
O14640	Segment polarity protein dishevelled homolog DVL-1	108	ART
Q9NQ38	Serine protease inhibitor Kazal-type 5	207	ART
Q13243	Serine/arginine-rich splicing factor 5	309	ART
Q9Y2H1	Serine/threonine-protein kinase 38-like	313	ART
Q13535	Serine/threonine-protein kinase ATR	306	ART
Q9Y3F4	Serine-threonine kinase receptor-associated protein	157	ART
P29508	Serpin B3	293	ART
Q6IA17	Single Ig IL-1-related receptor	154	ART
Q8ND83	SLAIN motif-containing protein 1	184	ART
O00193	Small acidic protein	220	ART
Q8NBW4	Sodium-coupled neutral amino acid transporter 9	504	ART
Q6ICL7	Solute carrier family 35 member E4	113	ART
O94875	Sorbin and SH3 domain-containing protein 2	638	ART
G5E9Y6	Spermatogenesis associated 4_ isoform CRA_a	161	ART
Q8NEY3	Spermatogenesis-associated protein 4	222	ART
Q9Y657	Spindlin-1	213	ART
Q5JUX0	Spindlin-3	213	ART
A0A1W2PR54	Spindlin-3	213	ART
G3V0H1	SRY (Sex determining region Y)-box 5_ isoform CRA_f	133	ART
P0CL85	STAG3-like protein 3	217	ART
Q15772	Striated muscle preferentially expressed protein kinase	140	ART
A6NHR9	Structural maintenance of chromosomes flexible hinge domain-containing protein 1	223	ART
E9PD53	Structural maintenance of chromosomes protein	161	ART
Q9NTJ3	Structural maintenance of chromosomes protein 4	163	ART
Q6ZRP7	Sulfhydryl oxidase 2	268	ART
O94901	SUN domain-containing protein 1	217	ART
P00441	Superoxide dismutase [Cu-Zn]	900	ART
C9JFZ1	Synaptojanin-1	143	ART
Q86SS6	Synaptotagmin-9	303	ART
Q9HCH5	Synaptotagmin-like protein 2	228	ART
Q9NX95	Syntabulin	303	ART
A0A075B6T7	T cell receptor alpha variable 6	153	ART
Q9Y4G6	Talin-2	148	ART
E2GH26	T-cell factor-4 variant L	144	ART
C6ZRJ7	TCF7L2 isoform pFC8A_TCF7L2_A3_ex1-12_13_13a	144	ART
C6ZRJ6	TCF7L2 isoform pFC8A_TCF7L2_D5_ex3_4a-11_12_13a_14	144	ART
C6ZRK5	TCF7L2 isoform pFC8A_TCF7L2_ex1-11-13-14	144	ART
Q5VVR7	TCF7L2 isoform pFC8A_TCF7L2_H7_ex1-11-13-13b	144	ART
Q9UIF3	Tektin-2	157	ART
Q86US8	Telomerase-binding protein EST1A	386	ART
Q9BXU2	Testis-expressed protein 13B	220	ART

Q96N46	Tetratricopeptide repeat protein 14	133	ART
Q8NDW8	Tetratricopeptide repeat protein 21A	104	ART
Q8NI27	THO complex subunit 2	122	ART
Q6ZMP0	Thrombospondin type-1 domain-containing protein 4	515	ART
H0YLT6	Tight junction protein ZO-1 (Fragment)	194	ART
Q13009	T-lymphoma invasion and metastasis-inducing protein 1	96	ART
Q12888	TP53-binding protein 1	78	ART
Q92844	TRAF family member-associated NF-kappa-B activator	189	ART
Q15560	Transcription elongation factor A protein 2	159	ART
P36402	Transcription factor 7	144	ART
B7WNT5	Transcription factor 7 (T-cell specific_ HMG-box)_ isoform CRA_c	144	ART
Q9HCS4	Transcription factor 7-like 1	245	ART
Q9NQB0	Transcription factor 7-like 2	144	ART
P35711	Transcription factor SOX-5	133	ART
A6H8Y1	Transcription factor TFIIIB component B" homolog	97	ART
Q7Z410	Transmembrane protease serine 9	68	ART
Q7Z2Z1	Treslin	120	ART
Q9H2D6	TRIO and F-actin-binding protein	105	ART
P60174	Triosephosphate isomerase	306	ART
Q9C040	Tripartite motif-containing protein 2	152	ART
E7EWD5	TSC22 domain family protein 3	146	ART
Q02223	Tumor necrosis factor receptor superfamily member 17	142	ART
E9PM19	Tyrosine-protein kinase	311	ART
Q8IYU4	Ubiquilin-like protein	140	ART
Q9Y4E8	Ubiquitin carboxyl-terminal hydrolase 15	211	ART
Q9NVE5	Ubiquitin carboxyl-terminal hydrolase 40	294	ART
H7C2L6	UDP-N-acetylglucosamine--dolichyl-phosphate N-acetylglucosaminephosphotransferase (Fragment)	261	ART
A0JNW5	UHRF1-binding protein 1-like	304	ART
E7EVH7	Uncharacterized protein	143	ART
E9PCH4	Uncharacterized protein	212	ART
S4R2X8	Uncharacterized protein (Fragment)	401	ART
K7EQU8	Uncharacterized protein (Fragment)	832	ART
K7EIL6	Uncharacterized protein (Fragment)	867	ART
Q8N5S3	Uncharacterized protein C2orf73	299	ART
Q86XI8	Uncharacterized protein ZSWIM9	95	ART
Q9UBC5	Unconventional myosin-Ia	186	ART
Q9Y4I1	Unconventional myosin-Va	150	ART
Q9ULV0	Unconventional myosin-Vb	149	ART
Q9NQX4	Unconventional myosin-Vc	171	ART
P22415	Upstream stimulatory factor 1	272	ART
P11684	Uteroglobin	714	ART
P19320	Vascular cell adhesion protein 1	90	ART
O60504	Vinexin	255	ART
P02774	Vitamin D-binding protein	447	ART
Q6UXI7	Vitrin	327	ART

Q7Z3J2	VPS35 endosomal protein sorting factor-like	109	ART
O43516	WAS/WASL-interacting protein family member 1	334	ART
Q8IWG1	WD repeat-containing protein 63	203	ART
Q5VTH9	WD repeat-containing protein 78	272	ART
Q96KN7	X-linked retinitis pigmentosa GTPase regulator-interacting protein 1	181	ART
C9J6P4	Zinc finger CCCH-type antiviral protein 1	277	ART
Q9UBW7	Zinc finger MYM-type protein 2	195	ART
E9PSE6	Zinc finger protein 195 (Fragment)	219	ART
Q9UL58	Zinc finger protein 215	228	ART
O75437	Zinc finger protein 254	471	ART
Q96JL9	Zinc finger protein 333	735	ART
M0R230	Zinc finger protein 417	412	ART
Q96JC4	Zinc finger protein 479	210	ART
Q8NB42	Zinc finger protein 527	188	ART
O15090	Zinc finger protein 536	120	ART
Q14966	Zinc finger protein 638	414	ART
Q0P6G1	ZNF527 protein	188	ART

*Indicates unique proteins in alphabetical order.

Table 4. Relative quantification of proteins identified in the unstimulated saliva from patients with head and neck cancer in different periods of treatment with radiotherapy and control group. Control; Before Radiotherapy (BRT); During Radiotherapy (DRT); After Radiotherapy (ART).

°Accession number	Protein name	PLGS score	+Ratio DRT:BRT	*P*
P06733	**Alpha-enolase**	**183**	**35.87**	**<0.01**
P02788	**Lactotransferrin**	**268**	**7.32**	**<0.01**
F8VUV1	**D(2) dopamine receptor**	**153**	**6.75**	**0.03**
Q5T200	**Zinc finger CCCH domain-containing protein 13**	**234**	**5.93**	**0.02**
P04080	**Cystatin-B**	**437**	**3.78**	**0.01**
P62736	**Actin_ aortic smooth muscle**	**900**	**3.74**	**<0.01**
P63267	**Actin_ gamma-enteric smooth muscle**	**900**	**3.63**	**<0.01**
P68133	**Actin_ alpha skeletal muscle**	**900**	**3.56**	**<0.01**
A5A3E0	**POTE ankyrin domain family member F**	**733**	**3.56**	**<0.01**
Q562R1	**Beta-actin-like protein 2**	**342**	**3.49**	**<0.01**
P68032	**Actin_ alpha cardiac muscle 1**	**900**	**3.46**	**<0.01**
P60709	**Actin_ cytoplasmic 1**	**2588**	**3.39**	**<0.01**
P63261	**Actin_ cytoplasmic 2**	**2588**	**3.39**	**<0.01**
Q6S8J3	**POTE ankyrin domain family member E**	**746**	**3.35**	**<0.01**
P0CG38	**POTE ankyrin domain family member I**	**568**	**3.35**	**0.02**
Q9BYX7	**Putative beta-actin-like protein 3**	**2302**	**2.66**	**<0.01**
Q03112	Histone-lysine N-methyltransferase MECOM	422	1.92	<0.01
P01877	Immunoglobulin heavy constant alpha 2	4993	1.88	<0.01
P01876	Immunoglobulin heavy constant alpha 1	6416	1.82	<0.01
Q8N4F0	BPI fold-containing family B member 2	1052	1.65	0.04
P04745	Alpha-amylase 1	26013	0.79	<0.01

P04746	Pancreatic alpha-amylase	19253	0.79	<0.01
P01037	Cystatin-SN	7696	0.69	<0.01
P19961	Alpha-amylase 2B	20507	0.68	<0.01
P31025	Lipocalin-1	5611	0.50	**0.03**
Q5VSP4	**Putative lipocalin 1-like protein 1**	**1428**	**0.48**	**0.01**
P02814	**Submaxillary gland androgen-regulated protein 3B**	**11077**	**0.36**	**<0.01**
P01036	**Cystatin-S**	**11830**	**0.23**	**<0.01**
P02812	**Basic salivary proline-rich protein 2**	**13300**	**0.19**	**<0.01**
A0A0A0MT31	**Proline-rich protein 4**	**17610**	**0.18**	**<0.01**
P04280	**Basic salivary proline-rich protein 1**	**11098**	**0.18**	**<0.01**
P09228	**Cystatin-SA**	**6668**	**0.18**	**<0.01**
P02810	**Salivary acidic proline-rich phosphoprotein 1/2**	**17610**	**0.18**	**<0.01**
A0A087WZY1	**Uncharacterized protein**	**11462**	**0.17**	**<0.01**
P68871	**Hemoglobin subunit beta**	**347**	**0.07**	**<0.01**
G3V1N2	**HCG1745306_ isoform CRA_a**	**4936**	**0.06**	**<0.01**
P69905	**Hemoglobin subunit alpha**	**8233**	**0.06**	**<0.01**
H7C555	**Cadherin-related family member 3 (Fragment)**	**272**	**0.04**	**<0.01**
°Accession number	**Protein name**	**PLGS score**	**⁺Ratio ART:BRT**	***P***
Q5W0V3	**Protein FAM160B1**	**204**	**8.50**	**<0.01**
Q8WXA9	**Splicing regulatory glutamine/lysine-rich protein 1**	**242**	**7.32**	**<0.01**
P04080	**Cystatin-B**	**437**	**3.82**	**<0.01**
P02788	**Lactotransferrin**	**268**	**3.71**	**<0.01**
P13929	**Beta-enolase**	**124**	**3.13**	**<0.01**
Q8N4F0	**BPI fold-containing family B member 2**	**1052**	**2.97**	**<0.01**
P06733	**Alpha-enolase**	**183**	**2.61**	**<0.01**
Q96DA0	**Zymogen granule protein 16 homolog B**	**508**	**2.61**	**<0.01**
Q8TAX7	**Mucin-7**	**430**	**2.56**	**<0.01**
Q8TDL5	**BPI fold-containing family B member 1**	**336**	**2.29**	**0.03**
P0CG38	**POTE ankyrin domain family member I**	**568**	**2.23**	**<0.01**
P01857	**Immunoglobulin heavy constant gamma 1**	**239**	**2.18**	**<0.01**
Q99470	**Stromal cell-derived factor 2**	**244**	**2.18**	**<0.01**
P07737	**Profilin-1**	**682**	**2.12**	**0.01**
Q562R1	Beta-actin-like protein 2	342	1.84	<0.01
P25311	Zinc-alpha-2-glycoprotein	858	1.77	<0.01
P63261	Actin_ cytoplasmic 2	2588	1.75	<0.01
P68133	Actin_ alpha skeletal muscle	900	1.73	<0.01
P60709	Actin_ cytoplasmic 1	2588	1.73	<0.01
P68032	Actin_ alpha cardiac muscle 1	900	1.72	<0.01
P62736	Actin_ aortic smooth muscle	900	1.70	<0.01
Q9BZW7	Testis-specific gene 10 protein	187	1.70	<0.01
P63267	Actin_ gamma-enteric smooth muscle	900	1.67	<0.01
A5A3E0	POTE ankyrin domain family member F	733	1.46	<0.01
Q6S8J3	POTE ankyrin domain family member E	746	1.43	<0.01
P01877	Immunoglobulin heavy constant alpha 2	4993	1.42	<0.01

P02787	Serotransferrin	412	1.35	<0.01
P23280	Carbonic anhydrase 6	1175	1.28	<0.01
Q03112	Histone-lysine N-methyltransferase MECOM	422	0.84	<0.01
P01591	Immunoglobulin J chain	3631	0.79	<0.01
P12273	Prolactin-inducible protein	5504	0.69	0.04
S4R460	Immunoglobulin heavy variable 3/OR16-9 (non-functional)	1623	0.66	0.04
P0CF74	Immunoglobulin lambda constant 6	553	0.66	0.03
P01876	Immunoglobulin heavy constant alpha 1	6416	0.59	<0.01
P02647	Apolipoprotein A-I	596	0.55	0.02
P01833	Polymeric immunoglobulin receptor	1595	0.53	<0.01
Q9H972	Uncharacterized protein C14orf93	1167	0.50	**<0.01**
E5RG79	**Zinc finger homeobox protein 4 (Fragment)**	**380**	**0.40**	**0.03**
P69891	**Hemoglobin subunit gamma-1**	**347**	**0.38**	**0.01**
P02042	**Hemoglobin subunit delta**	**347**	**0.38**	**<0.01**
P02100	**Hemoglobin subunit epsilon**	**347**	**0.37**	**<0.01**
P69892	**Hemoglobin subunit gamma-2**	**347**	**0.37**	**<0.01**
A0A2R8Y7X9	**GLOBIN domain-containing protein**	**347**	**0.36**	**<0.01**
P04746	**Pancreatic alpha-amylase**	**19253**	**0.36**	**<0.01**
P68871	**Hemoglobin subunit beta**	**347**	**0.35**	**<0.01**
P61769	**Beta-2-microglobulin**	**791**	**0.35**	**<0.01**
P04745	**Alpha-amylase 1**	**26013**	**0.34**	**<0.01**
P01834	**Immunoglobulin kappa constant**	**2293**	**0.28**	**<0.01**
Q5VSP4	**Putative lipocalin 1-like protein 1**	**1428**	**0.24**	**<0.01**
Q13332	**Receptor-type tyrosine-protein phosphatase S**	**517**	**0.21**	**0.01**
Q8NHS7	**PTPRS protein**	**517**	**0.21**	**<0.01**
P02814	**Submaxillary gland androgen-regulated protein 3B**	**11077**	**0.20**	**<0.01**
P31025	**Lipocalin-1**	**5611**	**0.19**	**<0.01**
P01034	**Cystatin-C**	**567**	**0.12**	**<0.01**
P46821	**Microtubule-associated protein 1B**	**324**	**0.08**	**<0.01**
P01037	**Cystatin-SN**	**7696**	**0.08**	**<0.01**
A0A0A0MT31	**Proline-rich protein 4**	**17610**	**0.07**	**<0.01**
P02810	**Salivary acidic proline-rich phosphoprotein 1/2**	**17610**	**0.07**	**<0.01**
A0A087WZY1	**Uncharacterized protein**	**11462**	**0.07**	**<0.01**
P09228	**Cystatin-SA**	**6668**	**0.05**	**<0.01**
P19961	**Alpha-amylase 2B**	**20507**	**0.05**	**<0.01**
P01036	**Cystatin-S**	**11830**	**0.04**	**<0.01**
P69905	**Hemoglobin subunit alpha**	**8233**	**0.02**	**<0.01**
P02812	**Basic salivary proline-rich protein 2**	**13300**	**0.02**	**<0.01**
P04280	**Basic salivary proline-rich protein 1**	**11098**	**0.02**	**<0.01**
G3V1N2	**HCG1745306_ isoform CRA_a**	**4936**	**0.02**	**<0.01**
°Accession number	**Protein name**	**PLGS score**	**⁺Ratio ART:DRT**	***P***
Q15424	**Scaffold attachment factor B1**	**183**	**16.44**	**<0.01**
Q9BZW7	**Testis-specific gene 10 protein**	**113**	**4.71**	**0.03**
O15021	**Microtubule-associated serine/threonine-protein kinase 4**	**216**	**3.46**	**0.04**

P19013	**Keratin_ type II cytoskeletal 4**	**759**	**2.86**	**0.01**
Q03112	**Histone-lysine N-methyltransferase MECOM**	**364**	**2.72**	**<0.01**
P04259	**Keratin_ type II cytoskeletal 6B**	**427**	**2.48**	**<0.01**
P35908	**Keratin_ type II cytoskeletal 2 epidermal**	**262**	**2.44**	**0.02**
P13647	**Keratin_ type II cytoskeletal 5**	**228**	**2.44**	**0.02**
P02538	**Keratin_ type II cytoskeletal 6A**	**470**	**2.41**	**<0.01**
P48668	**Keratin_ type II cytoskeletal 6C**	**470**	**2.20**	**<0.01**
Q8N4F0	BPI fold-containing family B member 2	1086	1.99	<0.01
P13646	Keratin_ type I cytoskeletal 13	296	1.77	<0.01
C9JKR2	Albumin_ isoform CRA_k	2144	1.17	0.04
P02768	Serum albumin	2424	1.14	**0.02**
P19961	Alpha-amylase 2B	746	0.70	<0.01
P04746	**Pancreatic alpha-amylase**	**714**	**0.45**	**<0.01**
P04745	**Alpha-amylase 1**	**1059**	**0.43**	**<0.01**
Q9BYX7	**Putative beta-actin-like protein 3**	**328**	**0.41**	**0.01**
P01034	**Cystatin-C**	**540**	**0.37**	**0.02**
P19012	**Keratin_ type I cytoskeletal 15**	**268**	**0.36**	**0.01**
P06733	**Alpha-enolase**	**437**	**0.34**	**<0.01**
P01036	**Cystatin-S**	**2991**	**0.28**	**<0.01**
P01037	**Cystatin-SN**	**1561**	**0.28**	**<0.01**
P09228	**Cystatin-SA**	**1001**	**0.21**	**<0.01**
Q99715	**Collagen alpha-1(XII) chain**	**105**	**0.05**	**<0.01**

°Accession number	**Protein name**	**PLGS score**	**⁺Ratio BRT:Control**	***p***
Q6VVX0	**Vitamin D 25-hydroxylase**	**194**	**26.58**	**<0.01**
Q5VSP4	**Putative lipocalin 1-like protein 1**	**241**	**13.46**	**0.02**
P32418	**Sodium/calcium exchanger 1**	**476**	**12.43**	**<0.01**
P31025	**Lipocalin-1**	**381**	**12.30**	**<0.01**
P01034	**Cystatin-C**	**1874**	**8.50**	**<0.01**
P61626	**Lysozyme C**	**857**	**6.75**	**<0.01**
P15515	**Histatin-1**	**1163**	**5.16**	**<0.01**
P02814	**Submaxillary gland androgen-regulated protein 3B**	**8894**	**4.85**	**<0.01**
Q99973	**Telomerase protein component 1**	**860**	**2.77**	**0.01**
P04745	**Alpha-amylase 1**	**40491**	**2.46**	**<0.01**
P02812	**Basic salivary proline-rich protein 2**	**4204**	**2.46**	**<0.01**
P04746	**Pancreatic alpha-amylase**	**26183**	**2.41**	**<0.01**
P19961	**Alpha-amylase 2B**	**32796**	**2.32**	**<0.01**
S4R460	**Immunoglobulin heavy variable 3/OR16-9 (non-functional)**	**535**	**2.32**	**<0.01**
P04280	**Basic salivary proline-rich protein 1**	**2904**	**2.23**	**<0.01**
H7C555	**Cadherin-related family member 3 (Fragment)**	**138**	**2.10**	**<0.01**
Q8WXA9	Splicing regulatory glutamine/lysine-rich protein 1	329	1.99	0.04
C9JKR2	Albumin_ isoform CRA_k	3204	1.86	<0.01
P28325	Cystatin-D	5841	1.82	<0.01
P0CG38	POTE ankyrin domain family member I	626	1.77	<0.01
P61769	Beta-2-microglobulin	286	1.70	<0.01

A0M8Q6	Immunoglobulin lambda constant 7	902	1.55	0.02
P01036	Cystatin-S	6209	1.52	<0.01
P0DOY2	Immunoglobulin lambda constant 2	7642	1.48	0.04
P02768	Serum albumin	6056	1.45	<0.01
P01591	Immunoglobulin J chain	2335	1.40	<0.01
P0CG04	Immunoglobulin lambda constant 1	7427	1.25	0.04
P01833	Polymeric immunoglobulin receptor	1562	1.22	<0.01
P09228	Cystatin-SA	2577	0.97	<0.01
P01834	Immunoglobulin kappa constant	1733	0.87	0.03
A0A0A0MT31	Proline-rich protein 4	23729	0.77	<0.01
P02810	Salivary acidic proline-rich phosphoprotein 1/2	23729	0.76	<0.01
A0A087WZY1	Uncharacterized protein	14156	0.76	<0.01
P02808	Statherin	24107	0.75	<0.01
Q562R1	Beta-actin-like protein 2	870	0.68	<0.01
P12273	Prolactin-inducible protein	5127	0.68	<0.01
Q6S8J3	POTE ankyrin domain family member E	1199	0.64	<0.01
A5A3E0	POTE ankyrin domain family member F	1199	0.64	<0.01
Q8N4F0	BPI fold-containing family B member 2	1057	0.62	<0.01
P01877	Immunoglobulin heavy constant alpha 2	4989	0.60	<0.01
P63261	Actin_ cytoplasmic 2	3917	0.55	<0.01
P60709	Actin_ cytoplasmic 1	3917	0.54	<0.01
Q8TDL5	BPI fold-containing family B member 1	310	0.54	0.02
Q96DR5	**BPI fold-containing family A member 2**	**925**	**0.48**	**<0.01**
P07737	**Profilin-1**	**331**	**0.48**	**<0.01**
Q6ZTU2	**Putative EP400-like protein**	**371**	**0.45**	**0.01**
P01876	**Immunoglobulin heavy constant alpha 1**	**5728**	**0.45**	**<0.01**
F8VV32	**Lysozyme**	**712**	**0.34**	**<0.01**
P01037	**Cystatin-SN**	**5608**	**0.32**	**<0.01**
Q5W0V3	**Protein FAM160B1**	**717**	**0.06**	**<0.01**

°Accession number	Protein name	PLGS score	+Ratio DRT:Control	*P*
Q562R1	**Beta-actin-like protein 2**	**870**	**3.42**	**<0.01**
P63267	**Actin_ gamma-enteric smooth muscle**	**1822**	**2.83**	**<0.01**
P68032	**Actin_ alpha cardiac muscle 1**	**1822**	**2.75**	**<0.01**
P68133	**Actin_ alpha skeletal muscle**	**1822**	**2.75**	**<0.01**
P62736	**Actin_ aortic smooth muscle**	**1822**	**2.69**	**<0.01**
Q6S8J3	**POTE ankyrin domain family member E**	**1199**	**2.46**	**<0.01**
A5A3E0	**POTE ankyrin domain family member F**	**1199**	**2.44**	**0.01**
Q9BYX7	**Putative beta-actin-like protein 3**	**602**	**2.27**	**0.03**
P60709	**Actin_ cytoplasmic 1**	**3917**	**2.10**	**<0.01**
P63261	**Actin_ cytoplasmic 2**	**3917**	**2.05**	**<0.01**
C9JKR2	Albumin_ isoform CRA_k	3204	1.82	<0.01
P02768	Serum albumin	6056	1.72	<0.01
P01877	Immunoglobulin heavy constant alpha 2	4989	1.36	<0.01
P04746	Pancreatic alpha-amylase	26183	0.82	<0.01
P19961	Alpha-amylase 2B	32796	0.78	<0.01

Q8N4F0	BPI fold-containing family B member 2	1057	0.57	0.01
P01833	**Polymeric immunoglobulin receptor**	**1562**	**0.50**	**<0.01**
P01037	**Cystatin-SN**	**5608**	**0.49**	**<0.01**
P01036	**Cystatin-S**	**6209**	**0.47**	**<0.01**
P04280	**Basic salivary proline-rich protein 1**	**2904**	**0.45**	**<0.01**
P02812	**Basic salivary proline-rich protein 2**	**4204**	**0.44**	**<0.01**
P12273	**Prolactin-inducible protein**	**5127**	**0.43**	**0.01**
Q96DA0	**Zymogen granule protein 16 homolog B**	**4692**	**0.40**	**<0.01**
P0CG04	**Immunoglobulin lambda constant 1**	**7427**	**0.28**	**0.03**
A0A0A0MT31	**Proline-rich protein 4**	**23729**	**0.20**	**<0.01**
A0A087WZY1	**Uncharacterized protein**	**14156**	**0.17**	**<0.01**
I3L228	**Sphingomyelin phosphodiesterase 3 (Fragment)**	**501**	**0.13**	**<0.01**
P02814	**Submaxillary gland androgen-regulated protein 3B**	**8894**	**0.11**	**<0.01**
P02810	**Salivary acidic proline-rich phosphoprotein 1/2**	**23729**	**0.07**	**<0.01**
H7C555	**Cadherin-related family member 3 (Fragment)**	**138**	**0.04**	**<0.01**
°Accession number	**Protein name**	**PLGS score**	**+Ratio ART:Control**	***P***
P0CG38	**POTE ankyrin domain family member I**	**626**	**4.53**	**0.02**
P68133	**Actin_ alpha skeletal muscle**	**1822**	**3.00**	**<0.01**
Q562R1	**Beta-actin-like protein 2**	**870**	**2.97**	**<0.01**
P68032	**Actin_ alpha cardiac muscle 1**	**1822**	**2.89**	**<0.01**
P63267	**Actin_ gamma-enteric smooth muscle**	**1822**	**2.86**	**<0.01**
P62736	**Actin_ aortic smooth muscle**	**1822**	**2.64**	**<0.01**
C9JKR2	**Albumin_ isoform CRA_k**	**3204**	**2.56**	**<0.01**
P02768	**Serum albumin**	**6056**	**2.05**	**<0.01**
P60709	Actin_ cytoplasmic 1	3917	1.75	<0.01
P63261	Actin_ cytoplasmic 2	3917	1.75	0.01
P01833	Polymeric immunoglobulin receptor	1562	0.54	<0.01
P04745	**Alpha-amylase 1**	**40491**	**0.37**	**<0.01**
P19961	**Alpha-amylase 2B**	**32796**	**0.36**	**<0.01**
P04746	**Pancreatic alpha-amylase**	**26183**	**0.34**	**<0.01**
P12273	**Prolactin-inducible protein**	**5127**	**0.33**	**0.01**
P02814	**Submaxillary gland androgen-regulated protein 3B**	**8894**	**0.28**	**<0.01**
P04280	**Basic salivary proline-rich protein 1**	**2904**	**0.18**	**<0.01**
P02812	**Basic salivary proline-rich protein 2**	**4204**	**0.18**	**<0.01**
P01037	**Cystatin-SN**	**5608**	**0.08**	**<0.01**
P01036	**Cystatin-S**	**6209**	**0.08**	**<0.01**
A0A087WZY1	**Uncharacterized protein**	**14156**	**0.06**	**0.01**
A0A0A0MT31	**Proline-rich protein 4**	**23729**	**0.04**	**<0.01**
P02810	**Salivary acidic proline-rich phosphoprotein 1/2**	**23729**	**0.04**	**<0.01**

Differential expression among the groups was expressed as $p<0.05$. Proteins highlighted in bold are increased or decreased more than 2-fold.

Abbreviations: BRT, before radiotherapy; DRT, during radiotherapy; ART, after radiotherapy; C, control group.

°Identification is based on protein ID from UniProt protein database. reviewed only (http://www.uniprot.org/).

+Proteins with expression significantly altered are organized according to the ratio.

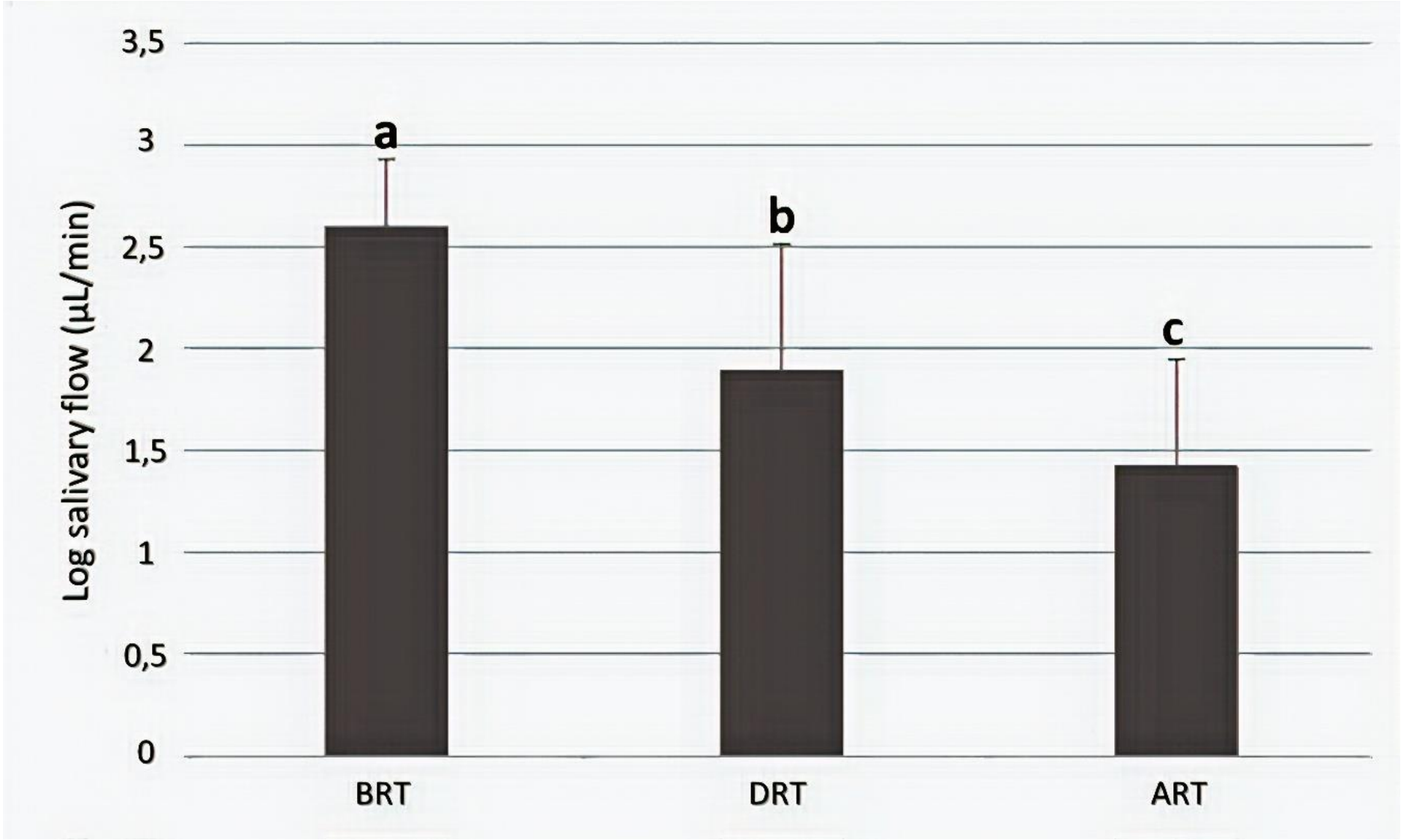
3,5
3
2,5
2
1,5
1
0,5
0
Log salivary flow (µL/min)
a
b
c
BRT
DRT
ART

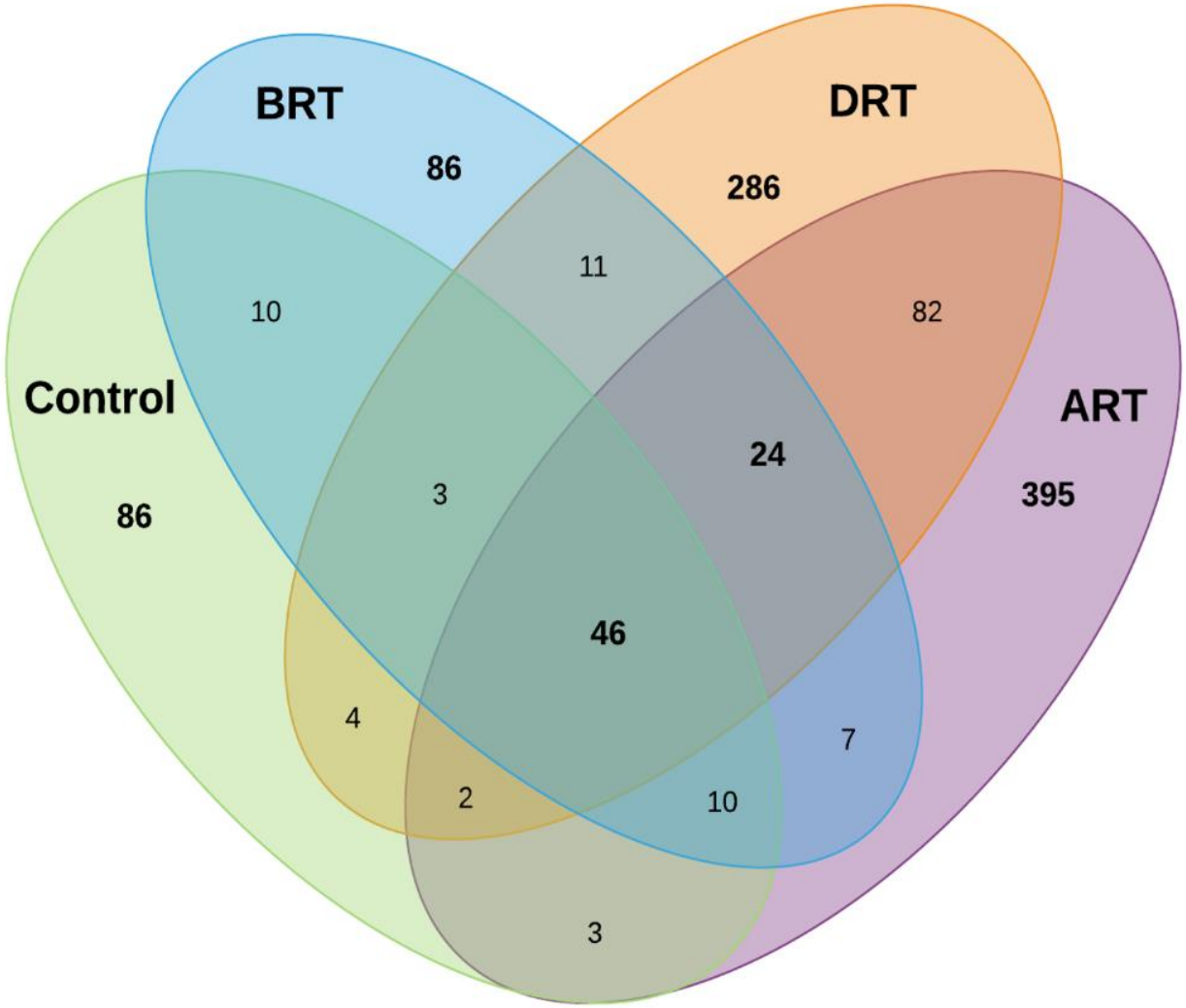
BRT
86
DRT
286
Control
86
ART
395
10
11
82
3
24
46
4
7
2
10
3

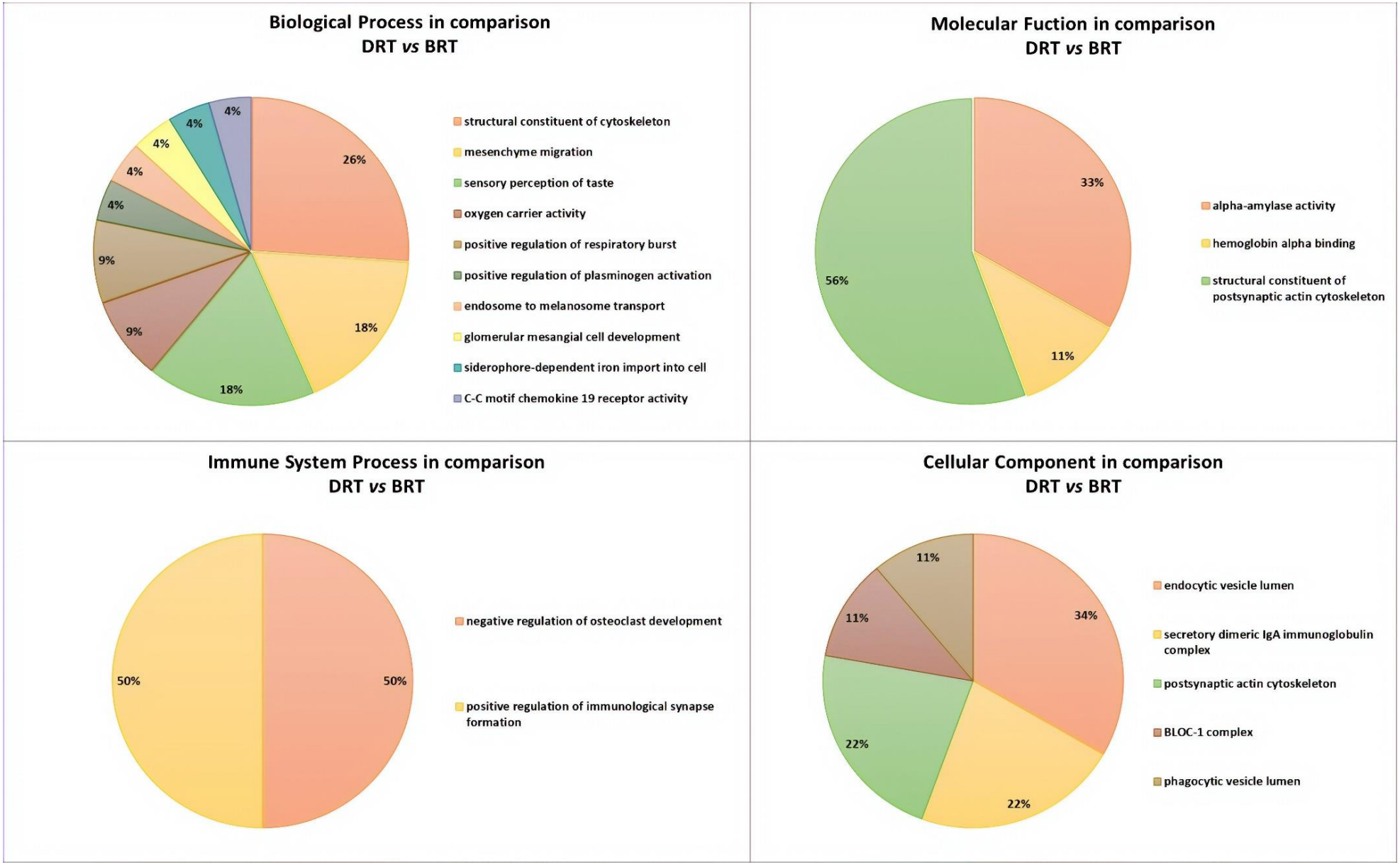
Biological Process in comparison
DRT vs BRT
26%
18%
18%
9%
9%
4%
4%
4%
4%
4%
structural constituent of cytoskeleton
mesenchyme migration
sensory perception of taste
oxygen carrier activity
positive regulation of respiratory burst
positive regulation of plasminogen activation
endosome to melanosome transport
glomerular mesangial cell development
siderophore-dependent iron import into cell
C-C motif chemokine 19 receptor activity
Molecular Fuction in comparison
DRT vs BRT
33%
11%
56%
alpha-amylase activity
hemoglobin alpha binding
structural constituent of postsynaptic actin cytoskeleton
Immune System Process in comparison
DRT vs BRT
50%
50%
negative regulation of osteoclast development
positive regulation of immunological synapse formation
Cellular Component in comparison
DRT vs BRT
34%
22%
22%
11%
11%
endocytic vesicle lumen
secretory dimeric IgA immunoglobulin complex
postsynaptic actin cytoskeleton
BLOC-1 complex
phagocytic vesicle lumen

Supplementary material

Table S1. Proteins identified in the unstimulated saliva of head and neck cancer patients in all groups. Control, before radiotherapy (BRT), during radiotherapy (DRT) and after radiotherapy (ART).

Access number	Protein name	*PLGS Score*	Control	BRT	DRT	ART
Q15029	116 kDa U5 small nuclear ribonucleoprotein component	143	-	-	Yes	-
P31946	14-3-3 protein beta/alpha	310	-	-	-	Yes
P62258	14-3-3 protein epsilon	357	-	-	Yes	Yes
Q04917	14-3-3 protein eta	310	-	-	-	Yes
P61981	14-3-3 protein gamma	310	-	-	-	Yes
P31947	14-3-3 protein sigma	731	-	-	Yes	Yes
P27348	14-3-3 protein theta	335	-	-	-	Yes
P63104	14-3-3 protein zeta/delta	687	-	-	-	Yes
Q15147	1-phosphatidylinositol 4_5-bisphosphate phosphodiesterase beta-4	533	-	-	-	Yes
P82664	28S ribosomal protein S10_ mitochondrial	340	-	-	-	Yes
Q9H9V9	2-oxoglutarate and iron-dependent oxygenase JMJD4	121	-	-	Yes	-
Q8TE99	2-phosphoxylose phosphatase 1	364	Yes	-	-	-
P42765	3-ketoacyl-CoA thiolase_ mitochondrial	363	Yes	-	-	-
H0YFS2	4F2 cell-surface antigen heavy chain (Fragment)	326	-	-	Yes	-
Q86XE5	4-hydroxy-2-oxoglutarate aldolase_ mitochondrial	502	-	Yes	-	-
Q00013	55 kDa erythrocyte membrane protein	199	-	-	Yes	-
Q16875	6-phosphofructo-2-kinase/fructose-2_6-bisphosphatase 3	320	-	-	Yes	-
P52209	6-phosphogluconate dehydrogenase_ decarboxylating	318	-	-	-	Yes
Q9UHI8	A disintegrin and metalloproteinase with thrombospondin motifs 1	416	-	-	Yes	-
P58397	A disintegrin and metalloproteinase with thrombospondin motifs 12	231	-	-	Yes	-
Q9P2N4	A disintegrin and metalloproteinase with thrombospondin motifs 9	266	-	-	-	Yes
Q13085	Acetyl-CoA carboxylase 1	144	-	-	-	Yes
O00763	Acetyl-CoA carboxylase 2	291	-	Yes	-	Yes
Q16515	Acid-sensing ion channel 2	114	-	-	-	Yes
P68032	Actin_ alpha cardiac muscle 1	1822	Yes	Yes	Yes	Yes
P68133	Actin_ alpha skeletal muscle	1822	Yes	Yes	Yes	Yes
P62736	Actin_ aortic smooth muscle	1822	Yes	Yes	Yes	Yes
P60709	Actin_ cytoplasmic 1	3917	Yes	Yes	Yes	Yes
P63261	Actin_ cytoplasmic 2	3917	Yes	Yes	Yes	Yes
P63267	Actin_ gamma-enteric smooth muscle	1822	Yes	Yes	Yes	Yes

Q6VMQ6	Activating transcription factor 7-interacting protein 1	478	-	Yes	-	-
Q9H2P0	Activity-dependent neuroprotector homeobox protein	112	Yes	-	-	-
Q08AH3	Acyl-coenzyme A synthetase ACSM2A_ mitochondrial	412	-	-	-	Yes
Q68CK6	Acyl-coenzyme A synthetase ACSM2B_ mitochondrial	311	-	-	-	Yes
Q76L82	Additional sex combs like 1 (Drosophila)_ isoform CRA_d	243	-	-	-	Yes
Q5TCS8	Adenylate kinase 9	746	-	-	-	Yes
Q9Y3D8	Adenylate kinase isoenzyme 6	597	-	-	-	Yes
Q01518	Adenylyl cyclase-associated protein 1	310	-	-	Yes	-
O94910	Adhesion G protein-coupled receptor L1	141	-	-	-	Yes
Q8IUX7	Adipocyte enhancer-binding protein 1	354	-	Yes	-	-
Q9NZ52	ADP-ribosylation factor-binding protein GGA3	214	-	-	Yes	-
O43572	A-kinase anchor protein 10_ mitochondrial	371	-	-	Yes	-
Q02952	A-kinase anchor protein 12	111	-	-	-	Yes
Q12802	A-kinase anchor protein 13	282	-	-	-	Yes
Q9BTE6	Alanyl-tRNA editing protein Aarsd1	229	-	-	-	Yes
C9JKR2	Albumin_ isoform CRA_k	4089	Yes	Yes	Yes	Yes
O60218	Aldo-keto reductase family 1 member B10	252	-	-	-	Yes
O00116	Alkyldihydroxyacetonephosphate synthase_ peroxisomal	141	Yes	-	-	-
Q11128	Alpha-(1_3)-fucosyltransferase 5	115	-	-	Yes	-
P51993	Alpha-(1_3)-fucosyltransferase 6	115	-	-	Yes	-
P02763	Alpha-1-acid glycoprotein 1	412	-	-	-	Yes
P01011	Alpha-1-antichymotrypsin	254	-	-	-	Yes
P01009	Alpha-1-antitrypsin	186	-	-	-	Yes
P01023	Alpha-2-macroglobulin	158	-	Yes	-	Yes
P12814	Alpha-actinin-1	805	-	-	Yes	-
O43707	Alpha-actinin-4	195	-	-	Yes	-
H0Y9H2	Alpha-adducin (Fragment)	333	-	-	-	Yes
P04745	Alpha-amylase 1	40491	Yes	Yes	Yes	Yes
P19961	Alpha-amylase 2B	32796	Yes	Yes	Yes	Yes
P06733	Alpha-enolase	183		Yes	Yes	Yes
H7C5V0	Alpha-sarcoglycan (Fragment)	271	-	-	-	Yes
Q9H4A4	Aminopeptidase B	328	-	Yes	-	-
E9PKC5	AMP deaminase	381	Yes	-	-	-
Q01432	AMP deaminase 3	385	Yes	-	-	-
P51693	Amyloid-like protein 1	210	-	Yes	-	-
Q8IY63	Angiomotin-like protein 1	260	-	-	Yes	-
P12821	Angiotensin-converting enzyme	148	-	-	-	Yes
Q8IWZ3	Ankyrin repeat and KH domain-containing protein 1	129	-	-	-	Yes
K7ENE0	Ankyrin repeat domain-containing protein 27	346	-	Yes	-	-

Q5JPF3	Ankyrin repeat domain-containing protein 36C	110	-	-	-	Yes
F8WB76	Ankyrin repeat domain-containing protein 54 (Fragment)	134	-	-	Yes	-
C9JP59	Ankyrin repeat_ SAM and basic leucine zipper domain-containing protein 1 (Fragment)	1159	-	Yes	-	-
Q12955	Ankyrin-3	116	-	-	-	Yes
E5RK69	Annexin	123	-	-	Yes	Yes
P04083	Annexin A1	1713	-	-	Yes	Yes
P08133	Annexin A6	287	-	-	Yes	Yes
H7C3N6	Anoctamin (Fragment)	278	Yes	-	-	-
P03973	Antileukoproteinase	601	-	-	Yes	-
P02647	Apolipoprotein A-I	862	-	Yes	Yes	Yes
P06727	Apolipoprotein A-IV	108	-	-	-	Yes
F8WB77	Apolipoprotein L1	875	-	-	Yes	-
Q9BPW4	Apolipoprotein L4	185	-	-	Yes	-
O15033	Apoptosis-resistant E3 ubiquitin protein ligase 1	327			Yes	
G3V3T3	Apoptotic chromatin condensation inducer in the nucleus (Fragment)	110	-	-	-	Yes
P16050	Arachidonate 15-lipoxygenase	250	-	-	-	Yes
H7C264	Arf-GAP with dual PH domain-containing protein 1 (Fragment)	128	-	-	-	Yes
Q9ULH1	Arf-GAP with SH3 domain_ ANK repeat and PH domain-containing protein 1	183	-	-	Yes	-
Q9P2R6	Arginine-glutamic acid dipeptide repeats protein	1025	-	-	Yes	Yes
Q8NEN0	Armadillo repeat-containing protein 2	120	-	-	-	Yes
O00327	Aryl hydrocarbon receptor nuclear translocator-like protein 1	205	-	-	-	Yes
A0A087WW05	Aspartyl/asparaginyl beta-hydroxylase (Fragment)	1009	Yes	-	-	-
Q498B9	ASXL1 protein	214	-	-	-	Yes
Q5TC12	ATP synthase mitochondrial F1 complex assembly factor 1	416	Yes	-	-	-
Q01813	ATP-dependent 6-phosphofructokinase_ platelet type	295	Yes	-	-	-
O94762	ATP-dependent DNA helicase Q5	447	Yes	-	-	Yes
O00571	ATP-dependent RNA helicase DDX3X	162	-	-	Yes	-
O15523	ATP-dependent RNA helicase DDX3Y	189	-	-	Yes	-
Q9BQ39	ATP-dependent RNA helicase DDX50	218	-	-	Yes	Yes
Q8NHQ9	ATP-dependent RNA helicase DDX55	117	-	-	-	Yes
Q8IYB8	ATP-dependent RNA helicase SUPV3L1_ mitochondrial	248	-	-	Yes	Yes
H0Y488	AT-rich interactive domain-containing protein 1A	136	-	-	Yes	-
Q8NFD5	AT-rich interactive domain-containing protein 1B	95	-	Yes	-	-
A6NKF2	AT-rich interactive domain-containing protein 3C	115	-	-	Yes	-
Q8WXE1	ATR-interacting protein	247	-	-	Yes	Yes

D6R9B7	Axonemal dynein light chain domain-containing protein 1 (Fragment)	744	-	Yes	-	-
Q9Y2J2	Band 4.1-like protein 3	482	-	-	Yes	Yes
P04280	Basic salivary proline-rich protein 1	11098	Yes	Yes	Yes	Yes
P02812	Basic salivary proline-rich protein 2	13300	Yes	Yes	Yes	Yes
P41182	B-cell lymphoma 6 protein	179	-	-	-	Yes
O00587	Beta-1_3-N-acetylglucosaminyltransferase manic fringe	185	-	-	-	Yes
J3QRN2	Beta-2-glycoprotein 1 (Fragment)	414	-	-	Yes	-
P61769	Beta-2-microglobulin	791	Yes	Yes	-	Yes
Q562R1	Beta-actin-like protein 2	870	Yes	Yes	Yes	Yes
P35612	Beta-adducin	225	-	-	-	Yes
P13929	Beta-enolase	124	-	Yes	Yes	Yes
P07686	Beta-hexosaminidase subunit beta	81	-	-	-	Yes
Q96IK1	Biorientation of chromosomes in cell division protein 1	190	-	-	Yes	-
Q96DR5	BPI fold-containing family A member 2	925	Yes	Yes	-	-
Q8TDL5	BPI fold-containing family B member 1	310	Yes	Yes	Yes	Yes
Q8N4F0	BPI fold-containing family B member 2	1057	Yes	Yes	Yes	Yes
P80723	Brain acid soluble protein 1	173	-	-	Yes	-
Q9NQY0	Bridging integrator 3	880	-	Yes	-	-
Q9NRL2	Bromodomain adjacent to zinc finger domain protein 1A	453	Yes	-	-	-
A0A0A0MR97	Bromodomain adjacent to zinc finger domain protein 2B	62	-	-	-	Yes
Q14681	BTB/POZ domain-containing protein KCTD2	160	-	-	Yes	-
Q4G0X4	BTB/POZ domain-containing protein KCTD21	106	-	-	Yes	-
O00478	Butyrophilin subfamily 3 member A3	647	Yes	-	-	-
Q96EU7	C1GALT1-specific chaperone 1	171	-	-	Yes	-
B7ZM11	C2orf73 protein	286	-	-	-	Yes
O75309	Cadherin-16	115	-	-	Yes	-
P19022	Cadherin-2	660	Yes	-	-	-
H7C555	Cadherin-related family member 3 (Fragment)	272	Yes	Yes	Yes	-
Q9NZU7	Calcium-binding protein 1	243	-	-	Yes	-
Q9NPB3	Calcium-binding protein 2	122	-	-	Yes	-
Q9ULU8	Calcium-dependent secretion activator 1	353	-	-	Yes	-
E7EMB3	Calmodulin-2	533	-	Yes	-	-
P27482	Calmodulin-like protein 3	915	-	-	-	Yes
Q6MZZ7	Calpain-13	188	-	-	Yes	-
P20807	Calpain-3	155	-	-	-	Yes
Q9UBL0	cAMP-regulated phosphoprotein 21	505	-	-	Yes	-
Q6ZU35	Cancer-related regulator of actin dynamics	762	-	-	Yes	Yes
Q9Y4C5	Carbohydrate sulfotransferase 2	155	-	-	-	Yes
P00915	Carbonic anhydrase 1	1501	-	-	-	Yes

P23280	Carbonic anhydrase 6	1175	Yes	Yes	Yes	Yes
Q92523	Carnitine O-palmitoyltransferase 1_ muscle isoform	228	-	-	Yes	-
P78368	Casein kinase I isoform gamma-2	138	-	-	Yes	-
Q9Y6M4	Casein kinase I isoform gamma-3	138	-	-	Yes	-
P43235	Cathepsin K	153	Yes	-	-	-
A6H8Y7	CCDC73 protein	306	-	-	Yes	-
A5YKK6	CCR4-NOT transcription complex subunit 1	174	-	-	-	Yes
P48509	CD151 antigen	283	-	Yes	-	-
E9PMT5	CD3 delta	588	-	Yes	-	-
P16070	CD44 antigen	448	Yes	Yes	-	Yes
B4DRP8	cDNA FLJ54872_ highly similar to Zinc finger protein 461	759	Yes	-	-	-
B7Z4G8	cDNA FLJ56046_ highly similar to Amyloid-like protein 1 (APLP)(APLP-1)	210	-	Yes	-	-
B4DYW9	cDNA FLJ61485_ highly similar to Zinc finger protein 215	212	-	-	-	Yes
Q4KMG0	Cell adhesion molecule-related/down-regulated by oncogenes	472	-	Yes	-	-
G5EA36	Cell division cycle 27_ isoform CRA_c	434	-	-	-	Yes
P30260	Cell division cycle protein 27 homolog	434	-	-	-	Yes
Q99795	Cell surface A33 antigen	150	-	-	Yes	-
P49454	Centromere protein F	124	-	-	-	Yes
A0A0U1RRI6	Centromere protein V-like protein 3	154	-	-	-	Yes
Q02224	Centromere-associated protein E	52	-	-	-	Yes
Q8N8E3	Centrosomal protein of 112 kDa	348	-	-	Yes	-
O94986	Centrosomal protein of 152 kDa	234	-	-	Yes	-
Q5SW79	Centrosomal protein of 170 kDa	218	-	-	-	Yes
Q8TEP8	Centrosomal protein of 192 kDa	119	-	-	Yes	-
H0Y900	Centrosomal protein of 63 kDa (Fragment)	147	-	-	Yes	-
E9PIK0	Centrosome-associated protein 350 (Fragment)	157	-	-	Yes	-
Q9BV73	Centrosome-associated protein CEP250	43	-	-	-	Yes
P00450	Ceruloplasmin	150	-	-	Yes	-
O00408	cGMP-dependent 3'_5'-cyclic phosphodiesterase	197	-	-	-	Yes
P51797	Chloride transport protein 6	159	-	-	-	Yes
Q9HC52	Chromobox protein homolog 8	161	-	-	-	Yes
A0A2R8Y7X1	Chromodomain-helicase-DNA-binding protein 4 (Fragment)	382	-	Yes	-	-
Q9HCK8	Chromodomain-helicase-DNA-binding protein 8	205	-	-	Yes	Yes
E9PQA1	Chromosome 11 open reading frame 58	220	-	-	-	Yes
F8VXK5	Chromosome 12 open reading frame 75	1155	-	Yes	-	Yes
Q8IYW2	Cilia- and flagella-associated protein 46	178	-	-	Yes	-
Q9P2M7	Cingulin	196	-	-	Yes	-
J3KPP4	Cisplatin resistance-associated overexpressed protein_ isoform CRA_b	206	-	Yes	Yes	-

O60271	C-Jun-amino-terminal kinase-interacting protein 4	79	-	-	-	Yes
P56749	Claudin-12	643	Yes	-	-	-
Q9P2I0	Cleavage and polyadenylation specificity factor subunit 2	161	-	-	Yes	-
Q16630	Cleavage and polyadenylation specificity factor subunit 6	161	-	-	-	Yes
P10909	Clusterin	154	-	-	-	Yes
G9CGD6	CNK3/IPCEF1 fusion protein	331	-	-	Yes	-
A0A0B4J1Z0	COBL-like 1_ isoform CRA_a	179	-	-	Yes	-
Q9UJ98	Cohesin subunit SA-3	219	-	-	-	Yes
Q5VVM6	Coiled-coil domain-containing protein 30	84	-	-	-	Yes
Q96ER9	Coiled-coil domain-containing protein 51	229	-	-	-	Yes
Q6ZRK6	Coiled-coil domain-containing protein 73	319	-	-	Yes	-
H7BY33	Coiled-coil domain-containing protein 88B	84	-	-	-	Yes
Q6ZUT6	Coiled-coil domain-containing protein 9B	355	-	Yes	-	Yes
Q99715	Collagen alpha-1(XII) chain	105	-	-	Yes	Yes
Q9UMD9	Collagen alpha-1(XVII) chain	504	-	-	Yes	-
P12111	Collagen alpha-3(VI) chain	241	-	-	-	Yes
Q6UXH8	Collagen and calcium-binding EGF domain-containing protein 1	456	-	-	Yes	-
Q9BXJ2	Complement C1q tumor necrosis factor-related protein 7	253	-	-	Yes	-
P01024	Complement C3	497	-	-	-	Yes
P17927	Complement receptor type 1	84	-	-	-	Yes
A0A0D9SG04	Cordon-bleu protein-like 1	179	-	-	Yes	-
Q9UBG3	Cornulin	182	-	-	Yes	Yes
H3BRY3	Coronin	476	-	Yes	-	-
P31146	Coronin-1A	520	-	Yes	-	-
B7ZLQ8	CPEB4 protein	233	-	-	Yes	-
Q6UUV7	CREB-regulated transcription coactivator 3	578	-	-	Yes	-
Q7Z408	CUB and sushi domain-containing protein 2	207	-	-	Yes	-
Q5TAH7	CUB and Sushi multiple domains 2_ isoform CRA_c	191	-	-	Yes	-
C9J4L5	Cyclic AMP-responsive element-binding protein 1 (Fragment)	792	Yes	Yes	-	-
Q14028	Cyclic nucleotide-gated cation channel beta-1	112	-	-	-	Yes
Q00536	Cyclin-dependent kinase 16	219	-	-	-	Yes
Q00537	Cyclin-dependent kinase 17	108	-	-	-	Yes
Q07002	Cyclin-dependent kinase 18	153	-	-	-	Yes
P04080	Cystatin-B	636	-	Yes	Yes	Yes
P01034	Cystatin-C	1874	Yes	Yes	Yes	Yes
P28325	Cystatin-D	5841	Yes	Yes	-	-
P01036	Cystatin-S	11830	Yes	Yes	Yes	Yes

P09228	Cystatin-SA	6668	Yes	Yes	Yes	Yes
P01037	Cystatin-SN	5608	Yes	Yes	Yes	Yes
Q14204	Cytoplasmic dynein 1 heavy chain 1	113	-	-	-	Yes
Q7Z5Q1	Cytoplasmic polyadenylation element-binding protein 2	240	-	-	Yes	-
Q8NE35	Cytoplasmic polyadenylation element-binding protein 3	213	-	-	Yes	-
Q17RY0	Cytoplasmic polyadenylation element-binding protein 4	233	-	-	Yes	-
O75891	Cytosolic 10-formyltetrahydrofolate dehydrogenase	420	-	-	-	Yes
Q8NDL9	Cytosolic carboxypeptidase-like protein 5	358	-	Yes	-	-
Q5M775	Cytospin-B	653	-	-	Yes	-
F8VUV1	D(2) dopamine receptor	153	-	Yes	Yes	-
P07585	Decorin	351	-	-	Yes	-
A0A2R8YD85	Dedicator of cytokinesis protein 10	81	-	-	Yes	-
Q9UGM3	Deleted in malignant brain tumors 1 protein	294	-	-	-	Yes
Q8NG44	Delta 3+6/2 progesterone receptor	104	-	-	-	Yes
Q8NG42	Delta 6/2 progesterone receptor	104	-	-	-	Yes
Q9ULE3	DENN domain-containing protein 2A	296	-	-	Yes	Yes
Q6IQ26	DENN domain-containing protein 5A	187	-	-	-	Yes
B4E1G1	Derlin	143	-	-	-	Yes
Q9BUN8	Derlin-1	205	-	-	-	Yes
Q02487	Desmocollin-2	206	-	-	-	Yes
P32926	Desmoglein-3	215	-	-	-	Yes
A0A075B7B1	Desmuslin_ isoform CRA_a	96	-	-	Yes	-
A0A0B4J2C2	Discs_ large (Drosophila) homolog-associated protein 4_ isoform CRA_b	277	-	-	-	Yes
Q9Y2H0	Disks large-associated protein 4	277	-	-	-	Yes
P54098	DNA polymerase subunit gamma-1	266	-	-	-	Yes
O75771	DNA repair protein RAD51 homolog 4	918	-	-	-	Yes
Q9UBZ9	DNA repair protein REV1	121	-	-	-	Yes
P49736	DNA replication licensing factor MCM2	704	-	-	-	Yes
K7EMH3	DNA-directed RNA polymerase_ mitochondrial (Fragment)	109	-	-	-	Yes
O75190	DnaJ homolog subfamily B member 6	314	-	-	-	Yes
O75165	DnaJ homolog subfamily C member 13	146	-	-	-	Yes
Q7L591	Docking protein 3	100	-	-	Yes	-
E5RI01	Double-strand-break repair protein rad21 homolog	468	-	Yes	Yes	-
E9PEI6	DPCR1	105	-	-	-	Yes
Q6P0N6	DST protein	64	-	-	-	Yes
Q9NRD9	Dual oxidase 1	308	Yes	-	-	-
Q9NYC9	Dynein heavy chain 9_ axonemal	342	-	-	Yes	-
Q96M86	Dynein heavy chain domain-containing protein 1	192	-	-	-	Yes
P11532	Dystrophin	180	-	-	-	Yes

H0Y339	E3 ubiquitin-protein ligase COP1 (Fragment)	205	-	-	-	Yes
O95714	E3 ubiquitin-protein ligase HERC2	341	-	-	Yes	-
Q7Z6Z7	E3 ubiquitin-protein ligase HUWE1	150	-	-	-	Yes
Q9H4C3	E3 ubiquitin-protein ligase Mdm2	390	-	Yes	-	-
Q8IUD6	E3 ubiquitin-protein ligase RNF135	227	-	-	-	Yes
Q53HC9	EARP and GARP complex-interacting protein 1	234	-	-	-	Yes
Q05BV3	Echinoderm microtubule-associated protein-like 5	723	-	-	-	Yes
Q8NDI1	EH domain-binding protein 1	242	-	-	-	Yes
A0RZB6	Endoplasmic reticulum chaperone SIL1 (Fragment)	622	-	-	Yes	-
Q5T6L9	Endoplasmic reticulum membrane-associated RNA degradation protein	417	-	-	-	Yes
P14138	Endothelin-3	454	-	Yes	Yes	-
Q6P2E9	Enhancer of mRNA-decapping protein 4	98	-	-	Yes	-
P98073	Enteropeptidase	253	-	-	Yes	-
P54764	Ephrin type-A receptor 4	179	-	-	Yes	-
Q9H6T0	Epithelial splicing regulatory protein 2	185	-	-	-	Yes
I6L9I8	EPN3 protein	147	-	-	-	Yes
Q9H201	Epsin-3	179	-	-	-	Yes
P62508	Estrogen-related receptor gamma	340	-	-	Yes	-
Q6ZN32	ETS translocation variant 3-like protein	148	-	-	Yes	-
Q14152	Eukaryotic translation initiation factor 3 subunit A	100	-	-	-	Yes
H0YAC4	Exosome RNA helicase MTR4 (Fragment)	799	Yes	-	-	-
C9JF49	Exportin-1 (Fragment)	255	-	-	Yes	-
P55060	Exportin-2	94	-	-	Yes	-
O43592	Exportin-T	275	-	-	Yes	-
Q08945	FACT complex subunit SSRP1	235	-	-	Yes	-
Q8NFF5	FAD synthase	216	-	Yes	-	-
Q0VAP4	FANCA protein	152	-	-	-	Yes
O15360	Fanconi anemia group A protein	158	-	-	-	Yes
Q92945	Far upstream element-binding protein 2	141	-	-	Yes	-
P14324	Farnesyl pyrophosphate synthase	315	-	-	Yes	-
Q96IV6	Fatty acid hydroxylase domain-containing protein 2	566	-	-	Yes	-
Q4VXH1	F-box/WD repeat-containing protein 2 (Fragment)	153	-	-	Yes	-
Q96NE9	FERM domain-containing protein 6	159	-	-	Yes	-
Q9BRP7	Ferredoxin-fold anticodon-binding domain-containing protein 1	227	Yes	-	-	-
P23142	Fibulin-1	320	-	-	-	Yes
G5E965	Forkhead box P1_ isoform CRA_f	342	-	-	-	Yes
A0A3B3IRS5	Forkhead box P1_ isoform CRA_g	342	-	-	-	Yes
Q0PRL4	Forkhead box P2 variant 3	302	Yes	-	-	-
Q8N6B5	Forkhead box P2_ isoform CRA_d (Fragment)	302	Yes	-	-	-

P98177	Forkhead box protein O4	274	Yes	-	-	-
Q9H334	Forkhead box protein P1	351	-	-	-	Yes
O15409	Forkhead box protein P2	359	Yes	-	-	-
J3KPS3	Fructose-bisphosphate aldolase	382	-	-	-	Yes
P04075	Fructose-bisphosphate aldolase A	382	-	-	-	Yes
P09972	Fructose-bisphosphate aldolase C	64	-	-	-	Yes
A0A0G2JJI2	G patch domain and ankyrin repeat-containing protein 1 (Fragment)	314	-	-	Yes	-
P21217	Galactoside 3(4)-L-fucosyltransferase	115	-	-	Yes	-
M0R108	Galectin-16	409	-	-	-	Yes
P47929	Galectin-7	156	-	-	-	Yes
A0A1B0GU82	Gamma-aminobutyric acid receptor subunit alpha-1	277	-	-	Yes	-
P09104	Gamma-enolase	401	-	Yes	Yes	Yes
Q86XP6	Gastrokine-2	302	-	-	-	Yes
Q6ZNW5	GDP-D-glucose phosphorylase 1	719	Yes	-	-	-
Q14687	Genetic suppressor element 1	162	Yes	-	Yes	Yes
H0YIY4	Gephyrin (Fragment)	455	-	Yes	-	-
O95749	Geranylgeranyl pyrophosphate synthase	443	-	-	Yes	-
A0A2U3TZV9	Girdin	80	-	-	-	Yes
A0A2R8Y7X9	GLOBIN domain-containing protein	2599	-	Yes	Yes	Yes
P06744	Glucose-6-phosphate isomerase	167	Yes	-	-	Yes
Q86X53	Glutamate-rich protein 1	346	-	-	Yes	-
Q6IA69	Glutamine-dependent NAD(+) synthetase	477	-	-	-	Yes
B5MC36	Glutathione hydrolase 1 proenzyme	189	-	-	-	Yes
Q14390	Glutathione hydrolase light chain 2	189	-	-	-	Yes
P09211	Glutathione S-transferase P	1240	-	-	Yes	Yes
P48637	Glutathione synthetase	207	-	-	-	Yes
P04406	Glyceraldehyde-3-phosphate dehydrogenase	2661	-	-	Yes	Yes
A0A1C7CYW1	Glycogen debranching enzyme	241	-	Yes	-	-
Q86W71	GOLGA4 protein	316	-	-	Yes	-
Q08378	Golgin subfamily A member 3	186	-	-	-	Yes
Q13439	Golgin subfamily A member 4	375	-	-	Yes	Yes
Q86VD9	GPI mannosyltransferase 4	440	-	-	-	Yes
P49685	G-protein coupled receptor 15	171	-	-	-	Yes
Q9NZD1	G-protein coupled receptor family C group 5 member D	490	Yes	-	-	-
P16260	Graves disease carrier protein	411	-	Yes	-	-
Q9C091	GREB1-like protein	282	-	-	Yes	-
H7C010	GRIP and coiled-coil domain-containing protein 2 (Fragment)	194	-	-	Yes	-
Q6IX74	Growth arrest and DNA damage-inducible protein GADD45 beta (Fragment)	398	-	-	Yes	-
O43903	Growth arrest-specific protein 2	227	-	-	Yes	-
Q9BXW7	Haloacid dehalogenase-like hydrolase domain-containing 5	297	-	Yes	-	-

A0A2R8YGL0	Hamartin (Fragment)	333	-	-	Yes	-
P00738	Haptoglobin	313	-	Yes	Yes	Yes
Q9H6D7	HAUS augmin-like complex subunit 4	211	-	-	Yes	-
C9JVX5	HCG1651889_ isoform CRA_d (Fragment)	519	Yes	-	-	-
G3V1N2	HCG1745306_ isoform CRA_a	4936	-	Yes	Yes	Yes
A0A0A6YYF2	HCG1811249_ isoform CRA_e	191	-	-	Yes	-
A0A0A0MTS5	HCG1811249_ isoform CRA_f	191	-	-	Yes	-
G3V3R4	HCG1983504_ isoform CRA_c	156	-	-	Yes	-
G3V2N6	HCG1983504_ isoform CRA_d	156	-	-	Yes	-
G3V2R8	HCG1983504_ isoform CRA_e	156	-	-	Yes	-
G3V201	HCG1985539_ isoform CRA_e	346	Yes	-	-	-
G5E9S6	HCG1994835	473	-	-	-	Yes
Q7Z2R1	HCG19985_ isoform CRA_b	462	-	-	-	Yes
K7EN88	HCG2039718_ isoform CRA_g	873	-	-	-	Yes
G3XAL8	HCG21296_ isoform CRA_a	233	-	-	-	Yes
O00165	HCLS1-associated protein X-1	166	-	-	-	Yes
Q53T59	HCLS1-binding protein 3	169	-	-	-	Yes
Q6AI08	HEAT repeat-containing protein 6	439	-	-	Yes	-
K7ENF6	Heat shock 70 kDa protein 12A (Fragment)	190	-	-	-	Yes
P11142	Heat shock cognate 71 kDa protein	241	-	-	-	Yes
P04792	Heat shock protein beta-1	3768	-	-	Yes	Yes
G3V2J8	Heat shock protein HSP 90-alpha (Fragment)	183	-	-	Yes	-
Q03014	Hematopoietically-expressed homeobox protein HHEX	171	-	-	-	Yes
P69905	Hemoglobin subunit alpha	8233	-	Yes	Yes	Yes
P68871	Hemoglobin subunit beta	1435	-	Yes	Yes	Yes
P02042	Hemoglobin subunit delta	1031	-	Yes	Yes	Yes
P02100	Hemoglobin subunit epsilon	1031	-	Yes	Yes	Yes
P69891	Hemoglobin subunit gamma-1	1031	-	Yes	Yes	Yes
P69892	Hemoglobin subunit gamma-2	1031	-	Yes	Yes	Yes
P35680	Hepatocyte nuclear factor 1-beta	166	-	-	-	Yes
A0A024R4E5	High density lipoprotein binding protein (Vigilin)_ isoform CRA_a	343	-	-	Yes	-
Q7Z353	Highly divergent homeobox	116	-	-	Yes	-
P15515	Histatin-1	1163	Yes	Yes	-	-
P42357	Histidine ammonia-lyase	245	-	-	Yes	-
A5PLL3	Histone acetyltransferase	252	-	-	-	Yes
Q92794	Histone acetyltransferase KAT6A	253	-	-	-	Yes
Q8WYB5	Histone acetyltransferase KAT6B	463	-	-	-	Yes
J3KPH8	Histone deacetylase	411	-	-	Yes	-
Q9UBN7	Histone deacetylase 6	264	-	-	-	Yes
Q8WUI4	Histone deacetylase 7	411	-	-	Yes	-
U3KQK0	Histone H2B	369	-	-	Yes	Yes
Q96A08	Histone H2B type 1-A	299	-	-	Yes	Yes

P33778	Histone H2B type 1-B	369	-	-	Yes	Yes
P62807	Histone H2B type 1-C/E/F/G/I	369	-	-	Yes	Yes
P58876	Histone H2B type 1-D	369	-	-	Yes	Yes
Q93079	Histone H2B type 1-H	369	-	-	Yes	Yes
P06899	Histone H2B type 1-J	369	-	-	Yes	Yes
O60814	Histone H2B type 1-K	369	-	-	Yes	Yes
Q99880	Histone H2B type 1-L	369	-	-	Yes	Yes
Q99879	Histone H2B type 1-M	369	-	-	Yes	Yes
Q99877	Histone H2B type 1-N	369	-	-	Yes	Yes
P23527	Histone H2B type 1-O	369	-	-	Yes	Yes
Q16778	Histone H2B type 2-E	369	-	-	Yes	Yes
Q5QNW6	Histone H2B type 2-F	369	-	-	Yes	Yes
Q8N257	Histone H2B type 3-B	369	-	-	Yes	Yes
P57053	Histone H2B type F-S	369	-	-	Yes	Yes
Q09028	Histone-binding protein RBBP4	524	-	Yes	-	-
Q03164	Histone-lysine N-methyltransferase 2A	172	-	-	-	Yes
Q8NEZ4	Histone-lysine N-methyltransferase 2C	246	-	-	-	Yes
Q9H9B1	Histone-lysine N-methyltransferase EHMT1	134	-	-	-	Yes
Q92800	Histone-lysine N-methyltransferase EZH1	159	-	-	-	Yes
Q03112	Histone-lysine N-methyltransferase MECOM	364	-	-	Yes	Yes
O96028	Histone-lysine N-methyltransferase NSD2	176	-	-	-	Yes
H0Y9L4	Histone-lysine N-methyltransferase NSD2 (Fragment)	220	-	-	Yes	-
A0A140T9Z3	HLA class II histocompatibility antigen_ DO beta chain (Fragment)	271	-	-	Yes	-
E0YMJ8	HNF1 beta A splice variant 3	166	-	-	-	Yes
O60479	Homeobox protein DLX-3	286	-	-	Yes	-
P57058	Hormonally up-regulated neu tumor-associated kinase	91	-	-	-	Yes
K7ERT9	Hsp70-binding protein 1 (Fragment)	335	Yes	-	-	-
Q4G0P3	Hydrocephalus-inducing protein homolog	325	-	-	-	Yes
P01876	Immunoglobulin heavy constant alpha 1	6416	Yes	Yes	Yes	Yes
P01877	Immunoglobulin heavy constant alpha 2	4993	Yes	Yes	Yes	Yes
P01857	Immunoglobulin heavy constant gamma 1	431	-	Yes	Yes	Yes
P01859	Immunoglobulin heavy constant gamma 2	971	-	-	-	Yes
P01860	Immunoglobulin heavy constant gamma 3	134	-	-	Yes	Yes
P01861	Immunoglobulin heavy constant gamma 4	707	-	-	-	Yes
P01871	Immunoglobulin heavy constant mu	416	-	Yes	-	-
S4R460	Immunoglobulin heavy variable 3/OR16-9 (non-functional)	1623	Yes	Yes	Yes	Yes
P01591	Immunoglobulin J chain	3631	Yes	Yes	Yes	Yes
P01834	Immunoglobulin kappa constant	2293	Yes	Yes	Yes	Yes

P0CG04	Immunoglobulin lambda constant 1	7427	Yes	Yes	Yes	Yes
P0DOY2	Immunoglobulin lambda constant 2	2980	Yes	Yes	-	Yes
P0DOY3	Immunoglobulin lambda constant 3	2980	Yes	Yes	-	Yes
P0CF74	Immunoglobulin lambda constant 6	4054	Yes	Yes	-	Yes
A0M8Q6	Immunoglobulin lambda constant 7	902	Yes	Yes	-	Yes
P01714	Immunoglobulin lambda variable 3-19	331	Yes	-	-	-
B9A064	Immunoglobulin lambda-like polypeptide 5	7427	Yes	Yes	-	Yes
Q8TDY8	Immunoglobulin superfamily DCC subclass member 4	122	-	-	-	Yes
O00410	Importin-5	178	-	-	Yes	-
Q8NBJ7	Inactive C-alpha-formylglycine-generating enzyme 2	272	-	-	-	Yes
O95050	Indolethylamine N-methyltransferase	360	Yes	-	-	-
H3BSR8	INMT-MINDY4 readthrough (NMD candidate) (Fragment)	330	Yes	-	-	-
A0A3B3IU04	Inositol 1_4_5-trisphosphate receptor type 1	371	-	-	-	Yes
Q14571	Inositol 1_4_5-trisphosphate receptor type 2	342	-	-	-	Yes
B7WPL9	Inositol hexakisphosphate and diphosphoinositol-pentakisphosphate kinase	457	-	-	Yes	-
Q6PFW1	Inositol hexakisphosphate and diphosphoinositol-pentakisphosphate kinase 1	457	-	-	Yes	-
Q8N201	Integrator complex subunit 1	588	Yes	-	-	-
Q9NVH2	Integrator complex subunit 7	443	-	Yes	-	-
Q9UKX5	Integrin alpha-11	122	-	-	-	Yes
P08514	Integrin alpha-IIb	88	-	-	Yes	-
A0A087X131	Integrin alpha-X	323	-	-	-	Yes
J3QQL2	Integrin beta (Fragment)	112	-	-	-	Yes
P16144	Integrin beta-4	124	-	-	-	Yes
Q8WWN9	Interactor protein for cytohesin exchange factors 1	331	-	-	Yes	-
P13598	Intercellular adhesion molecule 2	232	-	Yes	-	-
P20592	Interferon-induced GTP-binding protein Mx2	1186	Yes	-	-	-
P18510	Interleukin-1 receptor antagonist protein	118	-	-	-	Yes
Q8NAC3	Interleukin-17 receptor C	195	-	-	Yes	-
Q9NZM3	Intersectin-2	233	-	-	Yes	-
Q96CU4	Intraflagellar transport protein 56	214	-	-	-	Yes
H0YNL8	Iron-responsive element-binding protein 2	206	-	-	Yes	-
P06870	Kallikrein-1	226	-	-	-	Yes
O95198	Kelch-like protein 2	146	-	-	-	Yes
Q9P2K6	Kelch-like protein 42	258	-	Yes	-	-
P13645	Keratin_ type I cytoskeletal 10	172	-	-	Yes	Yes
Q99456	Keratin_ type I cytoskeletal 12	220	-	-	Yes	-
P13646	Keratin_ type I cytoskeletal 13	296	-	-	Yes	Yes

P02533	Keratin_ type I cytoskeletal 14	241	-	-	Yes	Yes
P19012	Keratin_ type I cytoskeletal 15	268	-	-	Yes	Yes
P08779	Keratin_ type I cytoskeletal 16	220	-	-	Yes	Yes
Q04695	Keratin_ type I cytoskeletal 17	200	-	-	Yes	Yes
P08727	Keratin_ type I cytoskeletal 19	207	-	-	Yes	Yes
Q2M2I5	Keratin_ type I cytoskeletal 24	190	-	-	-	Yes
P04264	Keratin_ type II cytoskeletal 1	81	-	-	-	Yes
P35908	Keratin_ type II cytoskeletal 2 epidermal	285	-	-	Yes	Yes
Q01546	Keratin_ type II cytoskeletal 2 oral	122	-	-	-	Yes
P19013	Keratin_ type II cytoskeletal 4	759	-	-	Yes	Yes
P13647	Keratin_ type II cytoskeletal 5	338	-	-	Yes	Yes
P02538	Keratin_ type II cytoskeletal 6A	470	-	-	Yes	Yes
P04259	Keratin_ type II cytoskeletal 6B	427	-	-	Yes	Yes
P48668	Keratin_ type II cytoskeletal 6C	470	-	-	Yes	Yes
Q86Y46	Keratin_ type II cytoskeletal 73	487	-	-	Yes	Yes
O95678	Keratin_ type II cytoskeletal 75	228	-	-	Yes	Yes
Q5XKE5	Keratin_ type II cytoskeletal 79	259	-	-	Yes	Yes
Q8IUB9	Keratin-associated protein 19-1	358	-	-	-	Yes
Q5T011	KICSTOR complex protein SZT2	128	-	-	-	Yes
Q6UWL6	Kin of IRRE-like protein 2	98	-	-	-	Yes
Q4R9M9	Kinesin family member 1Bbeta isoform II	233	-	-	-	Yes
Q07866	Kinesin light chain 1	143	-	-	-	Yes
O60333	Kinesin-like protein KIF1B	233	-	-	-	Yes
Q96Q89	Kinesin-like protein KIF20B	490	-	-	-	Yes
Q7Z4S6	Kinesin-like protein KIF21A	113	-	-	-	Yes
Q02241	Kinesin-like protein KIF23	91	-	-	Yes	-
O00139	Kinesin-like protein KIF2A	164	-	-	Yes	-
Q8NBT2	Kinetochore protein Spc24	169	-	-	-	Yes
H0YN41	Kinetochore scaffold 1	204	-	-	Yes	-
E9PHC9	Krueppel-like factor 7	466	-	-	Yes	-
Q6PIL6	Kv channel-interacting protein 4	263	-	-	-	Yes
Q8NBH2	Kyphoscoliosis peptidase	538	-	-	-	Yes
B4DGA7	Kyphoscoliosis peptidase	442	-	-	-	Yes
P22079	Lactoperoxidase	453	Yes	Yes	-	Yes
Q9UNP4	Lactosylceramide alpha-2_3-sialyltransferase	338	-	-	-	Yes
P02788	Lactotransferrin	268	-	Yes	Yes	Yes
O00515	Ladinin-1	168	-	-	-	Yes
Q16787	Laminin subunit alpha-3	203	-	-	Yes	-
H0YBR8	La-related protein 1 (Fragment)	444	-	-	Yes	-
O75387	Large neutral amino acids transporter small subunit 3	313	-	-	Yes	-
Q9HCC9	Lateral signaling target protein 2 homolog	576	-	Yes	-	-
Q96JM4	Leucine-rich repeat and IQ domain-containing protein 1	177	-	-	-	Yes

P42702	Leukemia inhibitory factor receptor	292	Yes	-	-	-
Q6GTX8	Leukocyte-associated immunoglobulin-like receptor 1	611	-	Yes	-	-
O75112	LIM domain-binding protein 3	372	-	-	Yes	-
Q8TE12	LIM homeobox transcription factor 1-alpha	64	-	-	-	Yes
H3BQT4	Lipase maturation factor 1 (Fragment)	186	-	-	Yes	-
P31025	Lipocalin-1	5611	Yes	Yes	Yes	Yes
P18428	Lipopolysaccharide-binding protein	329	Yes	-	-	-
P50851	Lipopolysaccharide-responsive and beige-like anchor protein	304	-	Yes	Yes	-
Q8IVV2	Lipoxygenase homology domain-containing protein 1	231	-	-	-	Yes
O75145	Liprin-alpha-3	130	-	Yes	-	-
E9PP16	Liprin-beta-2	233	-	-	Yes	-
O95232	Luc7-like protein 3	206	-	Yes	Yes	-
O95274	Ly6/PLAUR domain-containing protein 3	207	-	-	-	Yes
P33241	Lymphocyte-specific protein 1	194	-	-	Yes	-
Q9UJU2	Lymphoid enhancer-binding factor 1	178	-	-	-	Yes
Q9UGL1	Lysine-specific demethylase 5B	803	-	Yes	Yes	-
Q9BY66	Lysine-specific demethylase 5D	113	-	Yes	Yes	-
O15550	Lysine-specific demethylase 6A	149	-	-	Yes	-
Q6ZMT4	Lysine-specific demethylase 7A	67	-	-	Yes	-
P38571	Lysosomal acid lipase/cholesteryl ester hydrolase	183	-	Yes	-	-
Q86VI4	Lysosomal-associated transmembrane protein 4B	365	-	Yes	-	-
F8VV32	Lysozyme	1202	Yes	Yes	Yes	Yes
P61626	Lysozyme C	857	Yes	Yes	Yes	Yes
Q8N5G2	Macoilin	141	-	-	-	Yes
O43451	Maltase-glucoamylase_ intestinal	321	-	-	Yes	-
Q8NFP4	MAM domain-containing glycosylphosphatidylinositol anchor protein 1	108	-	-	-	Yes
Q13296	Mammaglobin-A	430	Yes	-	-	-
Q9UM22	Mammalian ependymin-related protein 1	510	-	-	Yes	-
C9JQX2	Mannosyltransferase	440	-	-	-	Yes
Q9H8J5	MANSC domain-containing protein 1	203	-	-	Yes	-
P43243	Matrin-3	515	-	Yes	-	-
Q86YW9	Mediator of RNA polymerase II transcription subunit 12-like protein	287	-	-	-	Yes
C9JGN2	Mediator of RNA polymerase II transcription subunit 15 (Fragment)	240	-	-	Yes	-
A2RUB1	Meiosis-specific coiled-coil domain-containing protein MEIOC	111	-	-	Yes	-
C9JK50	Melanoma-associated antigen 4 (Fragment)	116	-	-	Yes	-
Q8N4V1	Membrane magnesium transporter 1	204	-	-	-	Yes

H7C4S7	Membrane-associated guanylate kinase_ WW and PDZ domain-containing protein 1 (Fragment)	359	-	-	-	Yes
A0A0D9SF86	Membrane-associated guanylate kinase_ WW and PDZ domain-containing protein 2 (Fragment)	529	-	Yes	-	-
Q14831	Metabotropic glutamate receptor 7	232	-	-	-	Yes
H7C4V5	Metabotropic glutamate receptor 8 (Fragment)	337	-	Yes	-	-
E5RJR3	Methionine adenosyltransferase 2 subunit beta	1414	-	-	-	Yes
Q8TCB7	Methyltransferase-like protein 6	298	Yes	-	-	-
Q9H1A3	Methyltransferase-like protein 9	188	Yes	-	-	-
O75121	Microfibrillar-associated protein 3-like	221	-	Yes	-	-
O75030	Microphthalmia-associated transcription factor	466	-	-	-	Yes
E7EVA0	Microtubule-associated protein	325	-	-	Yes	-
P46821	Microtubule-associated protein 1B	324	-	Yes	Yes	Yes
P27816	Microtubule-associated protein 4	487	Yes	-	Yes	-
Q9Y2H9	Microtubule-associated serine/threonine-protein kinase 1	246	-	Yes	-	-
O15021	Microtubule-associated serine/threonine-protein kinase 4	216	-	-	Yes	Yes
Q3SY69	Mitochondrial 10-formyltetrahydrofolate dehydrogenase	141	-	-	Yes	-
Q9NZJ7	Mitochondrial carrier homolog 1	315	-	Yes	-	-
Q9Y584	Mitochondrial import inner membrane translocase subunit Tim22	590	-	-	-	Yes
O43615	Mitochondrial import inner membrane translocase subunit TIM44	283	-	-	-	Yes
Q9NYZ2	Mitoferrin-1	556	-	Yes	-	-
Q8IVH8	Mitogen-activated protein kinase kinase kinase kinase 3	156	-	-	Yes	-
O43684	Mitotic checkpoint protein BUB3	438	Yes	-	-	-
O43683	Mitotic checkpoint serine/threonine-protein kinase BUB1	88	-	-	-	Yes
Q96T76	MMS19 nucleotide excision repair protein homolog	155	-	-	Yes	-
O15427	Monocarboxylate transporter 4	137	-	-	-	Yes
Q96HT8	MORF4 family-associated protein 1-like 1	178	-	-	Yes	-
P30304	M-phase inducer phosphatase 1	202	-	-	Yes	-
Q96T58	Msx2-interacting protein	106	-	-	Yes	-
Q8TAX7	Mucin-7	597	Yes	Yes	Yes	Yes
A0A1B0GV46	Mucin-like protein 3	108	-	-	-	Yes
Q9H8L6	Multimerin-2	367	-	-	-	Yes
O75970	Multiple PDZ domain protein	505	-	-	-	Yes
E9PPE2	Myb/SANT-like DNA-binding domain-containing protein 2	303	-	-	-	Yes
P02686	Myelin basic protein	276	-	-	Yes	-
Q9Y2G1	Myelin regulatory factor	131	-	-	Yes	Yes
A0A3B3ITT2	Myelin transcription factor 1-like protein	421	-	-	-	Yes

P05164	Myeloperoxidase	181	-	-	-	Yes
Q9P1T7	MyoD family inhibitor domain-containing protein	420	Yes	-	-	-
Q9NZM1	Myoferlin	57	-	-	-	Yes
Q5VU43	Myomegalin	292	-	-	Yes	Yes
P10916	Myosin regulatory light chain 2_ ventricular/cardiac muscle isoform	172	-	-	-	Yes
P12882	Myosin-1	246	-	-	Yes	-
Q9UKX3	Myosin-13	241	-	-	Yes	-
Q7Z406	Myosin-14	298	-	-	-	Yes
Q9UKX2	Myosin-2	256	-	-	Yes	-
Q9Y623	Myosin-4	240	-	-	Yes	-
Q86WG5	Myotubularin-related protein 13	207	-	Yes	-	-
M0R0W4	NACHT_ LRR and PYD domains-containing protein 5 (Fragment)	284	-	-	-	Yes
Q6IQ20	N-acyl-phosphatidylethanolamine-hydrolyzing phospholipase D	220	-	-	-	Yes
P03897	NADH-ubiquinone oxidoreductase chain 3	390	-	Yes	-	-
F8W029	Nascent polypeptide-associated complex subunit alpha	510	-	-	-	Yes
O14513	Nck-associated protein 5	197	-	-	-	Yes
O00308	NEDD4-like E3 ubiquitin-protein ligase WWP2	246	-	-	Yes	-
P18615	Negative elongation factor E	344	-	Yes	Yes	Yes
O75161	Nephrocystin-4	167	-	-	-	Yes
O00533	Neural cell adhesion molecule L1-like protein	213	-	-	Yes	Yes
Q5QGS0	Neurite extension and migration factor	143	-	-	Yes	-
Q6ZS30	Neurobeachin-like protein 1	293	-	Yes	-	-
O94856	Neurofascin	172	-	-	Yes	-
E9PNX2	Neuronal acetylcholine receptor subunit alpha-10	114	-	-	-	Yes
Q99574	Neuroserpin	277	-	Yes	-	-
P30990	Neurotensin/neuromedin N	182	-	-	Yes	-
P59665	Neutrophil defensin 1	950	-	-	-	Yes
P59666	Neutrophil defensin 3	950	-	-	-	Yes
P80188	Neutrophil gelatinase-associated lipocalin	184	-	-	Yes	-
Q9BYH8	NF-kappa-B inhibitor zeta	263	Yes	-	-	-
H7C1V7	N-glycosylase/DNA lyase (Fragment)	394	-	Yes	-	-
Q86UT6	NLR family member X1	225	-	-	Yes	-
P29597	Non-receptor tyrosine-protein kinase TYK2	317	-	-	-	Yes
B3KNX7	Non-specific serine/threonine protein kinase	406	Yes	-	-	-
Q7Z6G3	N-terminal EF-hand calcium-binding protein 2	299	-	-	-	Yes
D6RH30	Nuclear factor NF-kappa-B p105 subunit (Fragment)	99	-	-	-	Yes
Q9UKX7	Nuclear pore complex protein Nup50	348	-	Yes	-	-

J3QL49	Nuclear pore complex protein Nup85 (Fragment)	735	-	-	-	Yes
P52948	Nuclear pore complex protein Nup98-Nup96	334	-	-	-	Yes
Q8TAT6	Nuclear protein localization protein 4 homolog	834	-	-	Yes	-
J3QKP0	Nuclear receptor corepressor 1 (Fragment)	111	-	-	-	Yes
Q9Y618	Nuclear receptor corepressor 2	206	-	-	Yes	Yes
Q86WB0	Nuclear-interacting partner of ALK	397	-	-	-	Yes
C9JTN7	Nucleolysin TIA-1 isoform p40	372	-	-	-	Yes
Q01085	Nucleolysin TIAR	372	-	-	-	Yes
Q5SRE5	Nucleoporin NUP188 homolog	278	-	-	Yes	-
H3BPW6	Obscurin (Fragment)	378	-	Yes	-	-
P0DN81	Olfactory receptor 13C7	140	-	-	Yes	-
Q9UMX2	Ornithine decarboxylase antizyme 3	631	-	Yes	-	-
Q8IXM7	Outer dense fiber protein 3-like protein 1	215	-	-	Yes	-
E9PNR1	Oxysterol-binding protein-related protein 9 (Fragment)	289	Yes	-	-	-
Q9NWT1	p21-activated protein kinase-interacting protein 1	158	-	-	-	Yes
Q06710	Paired box protein Pax-8	316	-	Yes	-	-
H0Y2Y4	Palmitoyltransferase (Fragment)	341	-	-	-	Yes
P04746	Pancreatic alpha-amylase	26183	Yes	Yes	Yes	Yes
P49023	Paxillin	91	-	-	-	Yes
Q96A99	Pentraxin-4	115	-	-	-	Yes
Q15154	Pericentriolar material 1 protein	90	-	-	-	Yes
Q9UIL8	PHD finger protein 11	132	-	-	-	Yes
P00439	Phenylalanine-4-hydroxylase	297	-	-	-	Yes
A0A0J9YVR0	Phosphatase and actin regulator (Fragment)	112	-	-	-	Yes
Q8IZ21	Phosphatase and actin regulator 4	132	-	-	-	Yes
Q9NTJ5	Phosphatidylinositide phosphatase SAC1	135	-	-	-	Yes
P42338	Phosphatidylinositol 4_5-bisphosphate 3-kinase catalytic subunit beta isoform	197	-	-	-	Yes
P42356	Phosphatidylinositol 4-kinase alpha	200	-	Yes	-	-
E9PSF8	Phosphatidylinositol 4-phosphate 5-kinase type-1 alpha	480	-	Yes	-	-
D6RC77	Phosphoacetylglucosamine mutase (Fragment)	350	Yes	-	-	-
E9PEF1	Phosphodiesterase	191	-	-	-	Yes
H0YCU5	Phosphofurin acidic cluster sorting protein 1 (Fragment)	229	-	-	Yes	-
P00558	Phosphoglycerate kinase 1	195	-	-	-	Yes
P07205	Phosphoglycerate kinase 2	249	-	-	-	Yes
O14939	Phospholipase D2	259	-	-	-	Yes
Q8NEL9	Phospholipase DDHD1	219	-	-	Yes	-
E7EVM7	Piezo-type mechanosensitive ion channel component	158	-	-	-	Yes
Q9H5I5	Piezo-type mechanosensitive ion channel component 2	176	-	-	-	Yes

P20020	Plasma membrane calcium-transporting ATPase 1	114	-	-	Yes	-
Q9H4M7	Pleckstrin homology domain-containing family A member 4	285	-	-	Yes	-
Q6IQ23	Pleckstrin homology domain-containing family A member 7	123	-	-	-	Yes
D6RH25	Plexin-D1	234	-	-	-	Yes
Q7Z3K3	Pogo transposable element with ZNF domain	357	Yes	-	-	-
Q9P0L9	Polycystic kidney disease 2-like 1 protein	138	Yes	-	-	-
P01833	Polymeric immunoglobulin receptor	1562	Yes	Yes	Yes	Yes
Q3YAB7	Potassium channel interacting protein 4	263	-	-	-	Yes
Q9UJ90	Potassium voltage-gated channel subfamily E regulatory beta subunit 5	325	-	Yes	-	-
Q6S8J3	POTE ankyrin domain family member E	1199	Yes	Yes	Yes	Yes
A5A3E0	POTE ankyrin domain family member F	1199	Yes	Yes	Yes	Yes
P0CG38	POTE ankyrin domain family member I	626	Yes	Yes	Yes	Yes
P0CG39	POTE ankyrin domain family member J	372	-	-	-	Yes
P11465	Pregnancy-specific beta-1-glycoprotein 2	235	-	-	Yes	-
Q16557	Pregnancy-specific beta-1-glycoprotein 3	457	-	Yes	-	-
Q6UN15	Pre-mRNA 3'-end-processing factor FIP1	108	-	-	-	Yes
H0Y8P7	Pre-mRNA 3'-end-processing factor FIP1 (Fragment)	119	-	-	Yes	-
Q9UMS4	Pre-mRNA-processing factor 19	148	-	-	-	Yes
Q6P2Q9	Pre-mRNA-processing-splicing factor 8	340	-	-	-	Yes
H0YAT0	Probable C-mannosyltransferase DPY19L4 (Fragment)	361	Yes	-	-	-
Q9Y4D8	Probable E3 ubiquitin-protein ligase HECTD4	142	-	-	-	Yes
Q15751	Probable E3 ubiquitin-protein ligase HERC1	168	-	-	-	Yes
Q15034	Probable E3 ubiquitin-protein ligase HERC3	446	-	-	Yes	-
Q5GLZ8	Probable E3 ubiquitin-protein ligase HERC4	150	-	-	-	Yes
K7EJ44	Profilin	176	-	-	Yes	-
P07737	Profilin-1	682	Yes	Yes	Yes	Yes
P06401	Progesterone receptor	104	-	-	-	Yes
Q14005	Pro-interleukin-16	82	-	-	-	Yes
P12273	Prolactin-inducible protein	5504	Yes	Yes	Yes	Yes
K7EJN8	Proline-rich protein 22 (Fragment)	655	-	-	Yes	-
A0A0A0MT31	Proline-rich protein 4	23729	Yes	Yes	Yes	Yes
C9JH25	Proline-rich transmembrane protein 4	534	Yes	-	-	-
Q8IVL5	Prolyl 3-hydroxylase 2	185	Yes	-	-	-
O15460	Prolyl 4-hydroxylase subunit alpha-2	755	Yes	-	-	-
Q12884	Prolyl endopeptidase FAP	201	-	-	Yes	Yes
P56975	Pro-neuregulin-3_ membrane-bound isoform	102	-	-	-	Yes
Q92824	Proprotein convertase subtilisin/kexin type 5	443	Yes	-	-	-

E9PMZ2	Protein arginine N-methyltransferase 1 (Fragment)	573	-	-	Yes	-
A0A1W2PQ30	Protein Aster-B	277	-	-	Yes	-
O75081	Protein CBFA2T3	1058	-	-	-	Yes
P58658	Protein eva-1 homolog C	219	-	-	Yes	-
Q5W0V3	Protein FAM160B1	717	Yes	Yes	Yes	Yes
A1A519	Protein FAM170A	302	-	Yes	-	-
A8MVW0	Protein FAM171A2	125	-	-	-	Yes
Q658Y4	Protein FAM91A1	167	-	-	-	Yes
Q68CZ1	Protein fantom	358	-	Yes	Yes	-
P49354	Protein farnesyltransferase/geranylgeranyltransferase type-1 subunit alpha	582	Yes	-	-	-
Q92833	Protein Jumonji	82	-	-	Yes	-
Q6P5S2	Protein LEG1 homolog	1304	-	Yes	-	-
Q8N3A8	Protein mono-ADP-ribosyltransferase PARP8	512	-	-	Yes	-
I3L2A7	Protein moonraker (Fragment)	370	-	-	-	Yes
B5MCF8	Protein Mpv17	427	-	Yes	-	-
Q9Y6F6	Protein MRVI1	205	-	-	Yes	-
Q86WI3	Protein NLRC5	127	-	-	Yes	-
O14974	Protein phosphatase 1 regulatory subunit 12A	357	-	-	Yes	Yes
Q5JR12	Protein phosphatase 1J	258	-	Yes	-	-
Q9Y6V0	Protein piccolo	254	-	-	-	Yes
Q86U86	Protein polybromo-1	241	-	-	Yes	-
Q5THK1	Protein PRR14L	239	-	-	Yes	Yes
Q5JSZ9	Protein PRRC2B (Fragment)	179	-	-	Yes	-
Q9Y520	Protein PRRC2C	307	-	-	-	Yes
Q13123	Protein Red	115	-	Yes	-	Yes
P06702	Protein S100-A9	564	Yes	-	Yes	Yes
Q9Y2M2	Protein SSUH2 homolog	183	-	-	-	Yes
Q9BVV6	Protein TALPID3	182	-	-	Yes	-
Q9NQW1	Protein transport protein Sec31B	418	-	-	Yes	-
Q93096	Protein tyrosine phosphatase type IVA 1	167	-	-	Yes	-
K7EQH3	Protein YIPF (Fragment)	226	Yes	-	-	Yes
Q9BWQ6	Protein YIPF2	226	Yes	-	-	-
E5RGR9	Protein YIPF5 (Fragment)	719	-	-	-	Yes
Q7Z7L7	Protein zer-1 homolog	236	-	-	-	Yes
Q86YA3	Protein ZGRF1	253	-	-	-	Yes
Q08188	Protein-glutamine gamma-glutamyltransferase E	161	-	-	-	Yes
Q9Y5I1	Protocadherin alpha-11	201	-	-	-	Yes
Q9Y5F1	Protocadherin beta-12	933	-	-	-	Yes
Q14517	Protocadherin Fat 1	202	-	-	Yes	Yes
Q9Y5F7	Protocadherin gamma-C4	225	-	-	Yes	-
Q96QU1	Protocadherin-15	305	Yes	-	-	-

Q8NHS7	PTPRS protein	517	-	Yes	-	Yes
P35247	Pulmonary surfactant-associated protein D	174	-	-	-	Yes
Q9BYX7	Putative beta-actin-like protein 3	2302	Yes	Yes	Yes	Yes
Q6ZTU2	Putative EP400-like protein	312	Yes	Yes	-	Yes
Q58FF6	Putative heat shock protein HSP 90-beta 4	170	-	-	Yes	Yes
Q5VSP4	Putative lipocalin 1-like protein 1	1428	Yes	Yes	Yes	Yes
A4QPH2	Putative phosphatidylinositol 4-kinase alpha-like protein P2	162	-	Yes	-	-
Q8IXJ9	Putative Polycomb group protein ASXL1	251	-	-	-	Yes
Q7Z2F6	Putative protein ZNF720	355	Yes	-	-	-
A6NKP2	Putative short-chain dehydrogenase/reductase family 42E member 2	97	Yes	-	-	-
Q9HBR0	Putative sodium-coupled neutral amino acid transporter 10	350	-	Yes	-	-
P0CL83	Putative STAG3-like protein 1	217	-	-	-	Yes
P0CL84	Putative STAG3-like protein 2	217	-	-	-	Yes
Q5JXB2	Putative ubiquitin-conjugating enzyme E2 N-like	721	-	-	-	Yes
Q8N9H6	Putative uncharacterized protein C8orf31	195	-	-	Yes	-
Q9NSJ1	Putative zinc finger protein 355P	268	-	-	-	Yes
Q15929	Putative zinc finger protein 56	599	-	-	Yes	-
Q2TAK8	PWWP domain-containing DNA repair factor 3A	199	-	-	Yes	-
Q9Y3Y4	Pygopus homolog 1	294	-	-	Yes	-
H3BQ34	Pyruvate kinase	3666	-	-	-	Yes
P14618	Pyruvate kinase PKM	3760	-	-	-	Yes
Q15276	Rab GTPase-binding effector protein 1	192	-	-	Yes	Yes
K7ENJ9	Rab GTPase-binding effector protein 1 (Fragment)	294	-	-	-	Yes
Q5T1S4	Rab9 effector protein with kelch motifs	127	-	-	-	Yes
Q2PPJ7	Ral GTPase-activating protein subunit alpha-2	321	-	-	Yes	-
Q9Y4G8	Rap guanine nucleotide exchange factor 2	174	-	-	-	Yes
Q8TEU7	Rap guanine nucleotide exchange factor 6	217	-	-	-	Yes
Q15283	Ras GTPase-activating protein 2	452	-	-	-	Yes
J3QLV2	Receptor tyrosine-protein kinase erbB-2 (Fragment)	711	-	-	Yes	-
Q14D33	Receptor-transporting protein 5	2899	-	Yes	-	-
P10586	Receptor-type tyrosine-protein phosphatase F	173	-	-	Yes	-
P28827	Receptor-type tyrosine-protein phosphatase mu	247	-	-	Yes	-
Q15256	Receptor-type tyrosine-protein phosphatase R	358	-	-	Yes	-
Q13332	Receptor-type tyrosine-protein phosphatase S	517	-	Yes	Yes	Yes
Q96P16	Regulation of nuclear pre-mRNA domain-containing protein 1A	634	-	-	Yes	-

Q504U0	Renal cancer differentiation gene 1 protein	539	-	-	-	Yes
P28749	Retinoblastoma-like protein 1	219	-	-	Yes	-
Q5T5U3	Rho GTPase-activating protein 21	239	-	-	Yes	-
Q9P2N2	Rho GTPase-activating protein 28	848	-	Yes	Yes	-
Q6ZW31	Rho GTPase-activating protein SYDE1	234	-	-	-	Yes
O94989	Rho guanine nucleotide exchange factor 15	370	-	Yes	Yes	-
Q9BQY4	Rhox homeobox family member 2	357	-	-	-	Yes
J3QQZ2	RNA binding protein fox-1 homolog	203	-	-	-	Yes
F5H5U2	RNA helicase	117	-	-	-	Yes
Q15434	RNA-binding motif_ single-stranded-interacting protein 2	167	-	-	Yes	-
P49756	RNA-binding protein 25	283	Yes	-	Yes	Yes
K7EJX6	RNA-binding protein fox-1 homolog 3 (Fragment)	203	-	-	-	Yes
Q9UKM9	RNA-binding protein Raly	242	-	-	Yes	-
Q96LT9	RNA-binding region-containing protein 3	260	-	-	-	Yes
H7C4J7	Roundabout homolog 2 (Fragment)	726	-	-	-	Yes
H7C357	Run domain Beclin-1-interacting and cysteine-rich domain-containing protein (Fragment)	147	-	-	Yes	-
Q15413	Ryanodine receptor 3	182	-	-	-	Yes
Q9BY12	S phase cyclin A-associated protein in the endoplasmic reticulum	309	-	-	Yes	Yes
A0A096LPE2	SAA2-SAA4 readthrough	319	-	-	Yes	Yes
P02810	Salivary acidic proline-rich phosphoprotein 1/2	23729	Yes	Yes	Yes	Yes
Q9UL12	Sarcosine dehydrogenase_ mitochondrial	323	-	-	Yes	-
Q15424	Scaffold attachment factor B1	358	-	-	Yes	Yes
Q7Z7L1	Schlafen family member 11	258	-	-	Yes	-
P0DP57	Secreted Ly-6/uPAR domain-containing protein 2	836	-	-	-	Yes
P13521	Secretogranin-2	342	-	-	Yes	-
O14640	Segment polarity protein dishevelled homolog DVL-1	108	-	-	-	Yes
Q5T5U6	Selenide_ water dikinase 1 (Fragment)	421	-	-	Yes	-
Q96I15	Selenocysteine lyase	525	-	-	Yes	-
Q92854	Semaphorin-4D	197	-	-	Yes	-
Q9P0U3	Sentrin-specific protease 1	147	-	-	Yes	-
Q14674	Separin	255	-	-	Yes	-
E7EPG2	Septin-5 (Fragment)	159	-	-	Yes	-
Q8IYP2	Serine protease 58	150	-	-	Yes	-
Q9NQ38	Serine protease inhibitor Kazal-type 5	207	-	-	-	Yes
Q13243	Serine/arginine-rich splicing factor 5	309	-	-	-	Yes
Q9Y2H1	Serine/threonine-protein kinase 38-like	313	-	-	-	Yes
Q13535	Serine/threonine-protein kinase ATR	306	-	-	-	Yes
Q13153	Serine/threonine-protein kinase PAK 1	406	Yes	-	-	-
Q96Q15	Serine/threonine-protein kinase SMG1	393	Yes	-	Yes	-

E5RHP4	Serine/threonine-protein phosphatase (Fragment)	268	-	-	Yes	-
P67775	Serine/threonine-protein phosphatase 2A catalytic subunit alpha isoform	268	-	-	Yes	-
P62714	Serine/threonine-protein phosphatase 2A catalytic subunit beta isoform	268	-	-	Yes	-
Q9NY27	Serine/threonine-protein phosphatase 4 regulatory subunit 2	517	Yes	-		-
Q8N8A2	Serine/threonine-protein phosphatase 6 regulatory ankyrin repeat subunit B	130	-	-	Yes	-
Q9Y3F4	Serine-threonine kinase receptor-associated protein	157	-	-	-	Yes
P02787	Serotransferrin	412	-	Yes	Yes	Yes
P29508	Serpin B3	293	-	-	-	Yes
H7C0U8	Serrate RNA effector molecule homolog (Fragment)	219	-	-	Yes	-
P02768	Serum albumin	6056	Yes	Yes	Yes	Yes
G3V1D9	Serum amyloid A protein	319	-	-	Yes	Yes
P0DJI8	Serum amyloid A-1 protein	457	-	-	Yes	Yes
P0DJI9	Serum amyloid A-2 protein	368	-	-	Yes	Yes
Q9UHB9	Signal recognition particle subunit SRP68	253	-	-	Yes	-
Q5JXA9	Signal-regulatory protein beta-2	171	-	-	Yes	-
Q6IA17	Single Ig IL-1-related receptor	154	-	-	-	Yes
Q8ND83	SLAIN motif-containing protein 1	184	-	-	-	Yes
O00193	Small acidic protein	220	-	-	-	Yes
A0A2R8YCJ5	Small integral membrane protein 41	222	-	-	Yes	-
Q9Y345	Sodium- and chloride-dependent glycine transporter 2	198	Yes	-	-	-
Q9NY46	Sodium channel protein type 3 subunit alpha	85	Yes	-	-	-
P32418	Sodium/calcium exchanger 1	476	Yes	Yes	-	-
Q8NBW4	Sodium-coupled neutral amino acid transporter 9	504	-	-	-	Yes
P23975	Sodium-dependent noradrenaline transporter	332	Yes	-	-	-
A1L4H1	Soluble scavenger receptor cysteine-rich domain-containing protein SSC5D	386	-	Yes	-	-
H9KVA1	Solute carrier family 22 member 17	203	-	-	Yes	-
A0A1B0GVP8	Solute carrier family 26 member 10 (Fragment)	273	-	-	Yes	-
X6R3N0	Solute carrier family 27 (Fatty acid transporter)_ member 3_ isoform CRA_d	364	Yes	-	-	-
Q5K4L6	Solute carrier family 27 member 3	364	Yes	-	-	-
Q6ICL7	Solute carrier family 35 member E4	113	-	-	-	Yes
E5RJM7	Solute carrier family 45 member 4 (Fragment)	497	-	Yes	-	-
O94875	Sorbin and SH3 domain-containing protein 2	638	-	-	-	Yes
Q9UMY4	Sorting nexin-12	165	-	-	Yes	-
Q96JI7	Spatacsin	153	-	-	Yes	-
Q96R06	Sperm-associated antigen 5	418	Yes	-	-	-

G5E9Y6	Spermatogenesis associated 4_ isoform CRA_a	161	-	-	-	Yes
Q8NEY3	Spermatogenesis-associated protein 4	222	-	-	-	Yes
Q5T0L3	Spermatogenesis-associated protein 46	638	-	Yes	-	-
Q86VE3	Spermidine/spermine N(1)-acetyltransferase-like protein 1	519	-	Yes	-	-
I3L228	Sphingomyelin phosphodiesterase 3 (Fragment)	501	Yes	-	Yes	-
Q9Y657	Spindlin-1	213	-	-	-	Yes
Q5JUX0	Spindlin-3	213	-	-	-	Yes
A0A1W2PR54	Spindlin-3	213	-	-	-	Yes
Q8WXA9	Splicing regulatory glutamine/lysine-rich protein 1	329	Yes	Yes	Yes	Yes
G3V0H1	SRY (Sex determining region Y)-box 5_ isoform CRA_f	133	-	-	-	Yes
P0CL85	STAG3-like protein 3	217	-	-	-	Yes
P02808	Statherin	24107	Yes	Yes	-	-
Q12770	Sterol regulatory element-binding protein cleavage-activating protein	506	-	Yes	-	-
Q15772	Striated muscle preferentially expressed protein kinase	140	-	-	-	Yes
Q99470	Stromal cell-derived factor 2	451	-	Yes	Yes	Yes
A6NHR9	Structural maintenance of chromosomes flexible hinge domain-containing protein 1	223	-	-	-	Yes
E9PD53	Structural maintenance of chromosomes protein	161	-	-	-	Yes
Q9NTJ3	Structural maintenance of chromosomes protein 4	163	-	-	-	Yes
P02814	Submaxillary gland androgen-regulated protein 3B	11077	Yes	Yes	Yes	Yes
Q6ZRP7	Sulfhydryl oxidase 2	268	-	-	-	Yes
O94901	SUN domain-containing protein 1	217	-	-	-	Yes
P00441	Superoxide dismutase [Cu-Zn]	900	-	-	-	Yes
Q9H4L7	SWI/SNF-related matrix-associated actin-dependent regulator of chromatin subfamily A containing DEAD/H box 1	704	Yes	-	-	-
O14994	Synapsin-3	305	-	Yes	-	-
F8WCE4	Synaptogyrin-1	319	Yes	-	-	-
C9JFZ1	Synaptojanin-1	143	-	-	-	Yes
Q86SS6	Synaptotagmin-9	303	-	-	-	Yes
Q9HCH5	Synaptotagmin-like protein 2	228	-	-	-	Yes
G5EA09	Syndecan binding protein (Syntenin)_ isoform CRA_a	229	-	-	Yes	-
P18827	Syndecan-1	305	-	Yes	-	-
C9JA29	Syndetin (Fragment)	308	Yes	-	-	-
O15061	Synemin	107	-	-	Yes	-
Q9NX95	Syntabulin	303	-	-	-	Yes
Q9Y2K9	Syntaxin-binding protein 5-like	367	Yes	-	-	-
A0A0B4J271	T cell receptor alpha variable 12-3	223	-	-	Yes	-
A0A087WT01	T cell receptor alpha variable 27	393	-	Yes	-	-

A0A075B6T7	T cell receptor alpha variable 6	153	-	-	-	Yes
Q9Y4G6	Talin-2	148	-	-	-	Yes
G3V1T3	TAP binding protein-like_ isoform CRA_c	595	-	Yes	-	-
Q9BX59	Tapasin-related protein	497	-	Yes	-	-
O60784	Target of Myb protein 1	419	Yes	-	-	-
A0A0J9YWI7	Taste receptor type 2	154	-	-	Yes	-
P59541	Taste receptor type 2 member 30	154	-	-	Yes	-
A0A087WXG5	TBC1 domain family member 17	200	-	-	Yes	-
Q9NUY8	TBC1 domain family member 23	266	-	-	Yes	-
E2GH26	T-cell factor-4 variant L	144	-	-	-	Yes
C6ZRJ7	TCF7L2 isoform pFC8A_TCF7L2_A3_ex1-12_13_13a	144	-	-	-	Yes
C6ZRJ6	TCF7L2 isoform pFC8A_TCF7L2_D5_ex3_4a-11_12_13a_14	144	-	-	-	Yes
C6ZRK5	TCF7L2 isoform pFC8A_TCF7L2_ex1-11-13-14	144	-	-	-	Yes
Q5VVR7	TCF7L2 isoform pFC8A_TCF7L2_H7_ex1-11-13-13b	144	-	-	-	Yes
Q9UIF3	Tektin-2	157	-	-	-	Yes
Q99973	Telomerase protein component 1	860	Yes	Yes	-	-
Q86US8	Telomerase-binding protein EST1A	386	-	-	-	Yes
Q9P273	Teneurin-3	232	-	-	Yes	-
Q5TAX3	Terminal uridylyltransferase 4	158	-	-	Yes	-
Q9BXU2	Testis-expressed protein 13B	220	-	-	-	Yes
Q9BZW7	Testis-specific gene 10 protein	187	-	Yes	Yes	Yes
A6NNI4	Tetraspanin	863	Yes	Yes	Yes	-
Q96FV3	Tetraspanin-17	179	-	-	Yes	-
Q96N46	Tetratricopeptide repeat protein 14	133	-	-	-	Yes
Q8NDW8	Tetratricopeptide repeat protein 21A	104	-	-	-	Yes
P37173	TGF-beta receptor type-2	146	-	-	Yes	-
Q8NI27	THO complex subunit 2	122	-	-	-	Yes
Q86W42	THO complex subunit 6 homolog	181	-	-	Yes	-
Q6ZMP0	Thrombospondin type-1 domain-containing protein 4	515	-	-	-	Yes
Q9P031	Thyroid transcription factor 1-associated protein 26	170	-	-	Yes	-
H0YLT6	Tight junction protein ZO-1 (Fragment)	194	-	-	-	Yes
Q13009	T-lymphoma invasion and metastasis-inducing protein 1	96	-	-	-	Yes
E9PMZ8	T-lymphoma invasion and metastasis-inducing protein 2 (Fragment)	108	-	-	Yes	-
F6SA91	TNF receptor-associated factor	207	-	-	Yes	-
Q9BUZ4	TNF receptor-associated factor 4	207	-	-	Yes	-
E7EWG2	TNFAIP3-interacting protein 1 (Fragment)	537	Yes	-	-	-
Q6UW50	TOM1	409	Yes	-	-	-
Q12888	TP53-binding protein 1	78	-	-	-	Yes

Q92844	TRAF family member-associated NF-kappa-B activator	189	-	-	-	Yes
Q9Y296	Trafficking protein particle complex subunit 4	404	Yes	-	-	-
Q15560	Transcription elongation factor A protein 2	159	-	-	-	Yes
P36402	Transcription factor 7	144	-	-	-	Yes
B7WNT5	Transcription factor 7 (T-cell specific_ HMG-box)_ isoform CRA_c	144	-	-	-	Yes
Q9HCS4	Transcription factor 7-like 1	245	-	-	-	Yes
Q9NQB0	Transcription factor 7-like 2	144	-	-	-	Yes
P35711	Transcription factor SOX-5	133	-	-	-	Yes
A6H8Y1	Transcription factor TFIIIB component B" homolog	97	-	-	-	Yes
Q8WXI9	Transcriptional repressor p66-beta	318	-	-	Yes	-
O94759	Transient receptor potential cation channel subfamily M member 2	236	-	-	Yes	-
Q9HBA0	Transient receptor potential cation channel subfamily V member 4	112	-	-	Yes	-
P55072	Transitional endoplasmic reticulum ATPase	214	-	-	Yes	-
P29401	Transketolase	243	-	-	Yes	Yes
Q86WS5	Transmembrane protease serine 12	170	-	-	Yes	-
Q7Z410	Transmembrane protease serine 9	68	-	-	-	Yes
F8VRN7	Transmembrane protein 116	898	Yes	-	-	-
H3BRE9	Transporter	332	Yes	-	-	-
Q7Z2Z1	Treslin	120	-	-	-	Yes
Q8NDV7	Trinucleotide repeat-containing gene 6A protein	272	-	Yes	-	-
Q9H2D6	TRIO and F-actin-binding protein	105	-	-	-	Yes
P60174	Triosephosphate isomerase	306	-	-	-	Yes
Q9C040	Tripartite motif-containing protein 2	152	-	-	-	Yes
E7EWD5	TSC22 domain family protein 3	146	-	-	-	Yes
A0A2R8Y670	Tuberin (Fragment)	908	-	Yes	-	-
P07437	Tubulin beta chain	201	-	-	Yes	-
Q13885	Tubulin beta-2A chain	201	-	-	Yes	-
Q9BVA1	Tubulin beta-2B chain	201	-	-	Yes	-
Q13509	Tubulin beta-3 chain	201	-	-	Yes	-
Q03169	Tumor necrosis factor alpha-induced protein 2	376	-	Yes	-	-
Q02223	Tumor necrosis factor receptor superfamily member 17	142	-	-	-	Yes
Q16890	Tumor protein D53	304	-	Yes	-	-
E9PM19	Tyrosine-protein kinase	311	-	-	-	Yes
Q12923	Tyrosine-protein phosphatase non-receptor type 13	196	-	-	Yes	-
Q8IYU4	Ubiquilin-like protein	140	-	-	-	Yes
Q9Y4E8	Ubiquitin carboxyl-terminal hydrolase 15	211	-	-	-	Yes
Q70CQ3	Ubiquitin carboxyl-terminal hydrolase 30	210	-	-	Yes	-
Q70CQ2	Ubiquitin carboxyl-terminal hydrolase 34	351	Yes	-	Yes	-

Q9NVE5	Ubiquitin carboxyl-terminal hydrolase 40	294	-	-	-	Yes
Q9H9J4	Ubiquitin carboxyl-terminal hydrolase 42	172	-	-	Yes	-
Q9H0E7	Ubiquitin carboxyl-terminal hydrolase 44	311	-	-	Yes	-
O14562	Ubiquitin domain-containing protein UBFD1	194	-	-	Yes	-
D6RJB3	Ubiquitin-conjugating enzyme E2 D3	717	-	-	Yes	-
Q9BZL1	Ubiquitin-like protein 5	732	-	-	Yes	-
F8VRI7	Ubiquitinyl hydrolase 1	279	-	-	Yes	-
P78381	UDP-galactose translocator	285	-	-	Yes	-
H7C2L6	UDP-N-acetylglucosamine--dolichyl-phosphate N-acetylglucosaminephosphotransferase (Fragment)	261	-	-	-	Yes
A0JNW5	UHRF1-binding protein 1-like	304	-	-	-	Yes
M0QZD8	Uncharacterized protein	410	Yes	-	-	-
A0A286YET3	Uncharacterized protein	719	Yes	-	-	-
A0A087WZY1	Uncharacterized protein	14156	Yes	Yes	Yes	Yes
A0A0B4J269	Uncharacterized protein	201	-	-	Yes	-
E7EVH7	Uncharacterized protein	143	-	-	-	Yes
E9PCH4	Uncharacterized protein	212	-	-	-	Yes
K7EJK4	Uncharacterized protein (Fragment)	1200	-	Yes	-	-
M0R1J3	Uncharacterized protein (Fragment)	403	Yes	-	-	-
H3BUV5	Uncharacterized protein (Fragment)	435	Yes	-	-	-
H7C4K7	Uncharacterized protein (Fragment)	274	-	-	Yes	-
K7ERI5	Uncharacterized protein (Fragment)	989	-	-	Yes	Yes
S4R2X8	Uncharacterized protein (Fragment)	401	-	-	-	Yes
K7EQU8	Uncharacterized protein (Fragment)	832	-	-	-	Yes
K7EIL6	Uncharacterized protein (Fragment)	867	-	-	-	Yes
Q9H972	Uncharacterized protein C14orf93	1167	-	Yes	Yes	Yes
A8MV24	Uncharacterized protein C17orf98	179	-	-	Yes	Yes
Q8N5S3	Uncharacterized protein C2orf73	299	-	-	-	Yes
H0Y8H3	Uncharacterized protein C3orf67 (Fragment)	516	Yes	-	-	-
O15063	Uncharacterized protein KIAA0355	262	-	-	Yes	-
A0A2R8Y6P1	Uncharacterized protein KIAA1211 (Fragment)	751	-	-	Yes	Yes
Q9H1L0	Uncharacterized protein MIR1-1HG	387	-	Yes	-	-
Q86XI8	Uncharacterized protein ZSWIM9	95	-	-	-	Yes
K7EP79	Uncharacterized serine/threonine-protein kinase SBK3 (Fragment)	124	-	-	Yes	-
Q9UBC5	Unconventional myosin-Ia	186	-	-	-	Yes
Q9Y4I1	Unconventional myosin-Va	150	-	-	-	Yes
Q9ULV0	Unconventional myosin-Vb	149	-	-	-	Yes
Q9NQX4	Unconventional myosin-Vc	171	-	-	-	Yes
Q8WVF2	Unique cartilage matrix-associated protein	204	-	-	Yes	-
Q14CZ0	UPF0472 protein C16orf72	201	-	-	Yes	-
P22415	Upstream stimulatory factor 1	272	-	-	-	Yes

P11684	Uteroglobin	714	-	-	-	Yes
A0A0A0MSM3	Utrophin (Fragment)	516	-	-	Yes	Yes
Q96RL7	Vacuolar protein sorting-associated protein 13A	196	-	-	Yes	-
Q5THJ4	Vacuolar protein sorting-associated protein 13D	160	-	-	Yes	-
Q8N3P4	Vacuolar protein sorting-associated protein 8 homolog	372	Yes	-	-	-
P19320	Vascular cell adhesion protein 1	90	-	-	-	Yes
M0R3C3	Very-long-chain enoyl-CoA reductase	183	-	-	Yes	Yes
Q00341	Vigilin	343	-	-	Yes	-
P08670	Vimentin	210	-	-	Yes	-
O60504	Vinexin	255	-	-	-	Yes
P01282	VIP peptides	449	-	-	Yes	-
Q6VVX0	Vitamin D 25-hydroxylase	194	Yes	Yes	-	-
P02774	Vitamin D-binding protein	447	-	-	-	Yes
Q6UXI7	Vitrin	327	-	-	-	Yes
Q8IZS8	Voltage-dependent calcium channel subunit alpha-2/delta-3	391	Yes	Yes	-	-
H0YCW7	von Willebrand factor A domain-containing protein 3B (Fragment)	618	-	Yes	-	-
Q7Z3J2	VPS35 endosomal protein sorting factor-like	109	-	-	-	Yes
Q14508	WAP four-disulfide core domain protein 2	982	-	Yes	Yes	Yes
O43516	WAS/WASL-interacting protein family member 1	334	-	-	-	Yes
A0A0A0MRV3	WD repeat domain 8_ isoform CRA_c	120	Yes	-	-	-
Q8IZU2	WD repeat-containing protein 17	123	-	-	Yes	-
Q8IWG1	WD repeat-containing protein 63	203	-	-	-	Yes
Q5VTH9	WD repeat-containing protein 78	272	-	-	-	Yes
Q96KV7	WD repeat-containing protein 90	353	Yes	-	-	-
Q9P2S5	WD repeat-containing protein WRAP73	130	Yes	-	-	-
O95388	WNT1-inducible-signaling pathway protein 1	282	-	-	Yes	-
Q96KN7	X-linked retinitis pigmentosa GTPase regulator-interacting protein 1	181	-	-	-	Yes
G3V577	X-linked retinitis pigmentosa GTPase regulator-interacting protein 1 (Fragment)	366	Yes	-	-	-
Q8TBC5	Zinc finger and SCAN domain-containing protein 18	124	Yes	-	-	-
M0R1Y0	Zinc finger and SCAN domain-containing protein 30	277	-	-	Yes	-
Q5T200	Zinc finger CCCH domain-containing protein 13	234	Yes	Yes	Yes	-
C9J6P4	Zinc finger CCCH-type antiviral protein 1	277	-	-	-	Yes
A0A0D9SF71	Zinc finger E-box-binding homeobox 2	577	-	-	Yes	-
E5RG79	Zinc finger homeobox protein 4 (Fragment)	428	Yes	Yes	-	Yes
Q9UBW7	Zinc finger MYM-type protein 2	195	-	-	-	Yes
Q9UJU3	Zinc finger protein 112	478	-	-	Yes	Yes

Q15928	Zinc finger protein 141	872	-	-	Yes	Yes
D6RIY0	Zinc finger protein 141 (Clone pHZ-44)_ isoform CRA_c	872	-	-	Yes	Yes
P17023	Zinc finger protein 19	155	-	-	Yes	-
E9PSE6	Zinc finger protein 195 (Fragment)	219	-	-	-	Yes
Q9UL58	Zinc finger protein 215	228	-	-	-	Yes
A6NK53	Zinc finger protein 233	391	-	Yes	-	-
K7EL19	Zinc finger protein 235 (Fragment)	122	-	-	Yes	-
O75437	Zinc finger protein 254	471	-	-	-	Yes
Q9HBT8	Zinc finger protein 286A	256	-	-	Yes	-
Q96JL9	Zinc finger protein 333	735	-	-	-	Yes
Q06732	Zinc finger protein 33B	224	-	-	Yes	-
M0R0R1	Zinc finger protein 415 (Fragment)	226	-	-	Yes	-
M0R230	Zinc finger protein 417	412	-	-	-	Yes
O94892	Zinc finger protein 432	806	-	Yes	-	-
Q8N7K0	Zinc finger protein 433	302	-	-	Yes	Yes
Q8TAF7	Zinc finger protein 461	759	Yes	-	-	-
Q9BX82	Zinc finger protein 471	176	-	-	Yes	-
Q96JC4	Zinc finger protein 479	210	-	-	-	Yes
Q8TB69	Zinc finger protein 519	906	-	-	Yes	Yes
Q8NB42	Zinc finger protein 527	188	-	-	-	Yes
Q3MIS6	Zinc finger protein 528	181	-	-	Yes	-
O15090	Zinc finger protein 536	120	-	-	-	Yes
Q96ND8	Zinc finger protein 583	183	-	-	Yes	-
Q6P3V2	Zinc finger protein 585A	1200	-	Yes	-	-
Q8IYB9	Zinc finger protein 595	887	-	-	Yes	Yes
Q6ZNG1	Zinc finger protein 600	184	-	-	Yes	-
Q2M218	Zinc finger protein 630	532	-	-	Yes	-
Q14966	Zinc finger protein 638	414	-	-	-	Yes
Q86XU0	Zinc finger protein 677	494	-	Yes	-	-
Q9H7X3	Zinc finger protein 696	298	-	Yes	-	-
Q3SXZ3	Zinc finger protein 718	872	-	-	Yes	-
B4E159	Zinc finger protein 721	872	-	-	Yes	-
B4DXR9	Zinc finger protein 732	872	-	-	Yes	-
Q9Y6R6	Zinc finger protein 780B	560	-	Yes	-	-
Q6ZN06	Zinc finger protein 813	163	-	-	Yes	-
A8MQ14	Zinc finger protein 850	391	-	Yes	-	-
P25311	Zinc-alpha-2-glycoprotein	858	-	Yes	-	Yes
Q0P6G1	ZNF527 protein	188	-	-	-	Yes
Q96DA0	Zymogen granule protein 16 homolog B	4692	Yes	Yes	Yes	Yes

2.4 ARTICLE 4

Article formatted and published according to Oral Oncology

DOI: 10.1016/j.oraloncology.2021.105315

Title: Is there difference in the comparative and quantitative salivary proteome between stimulated and unstimulated saliva in head and neck cancer patients treated by radiotherapy?

Talita Mendes Oliveira Ventura[a], Paulo Sérgio da Silva Santos[b], Nathalia Regina Ribeiro[a], Aline de Lima Leite[a], Even Akemi Taira[a], Aline Dionizio[a], Cássia Maria Fischer Rubira[b], Marília Afonso Rabelo Buzalaf [a*]

[a]Department of Biological Sciences, Bauru School of Dentistry, University of São Paulo, Bauru, SP, Brazil. Al. Octávio Pinheiro Brisolla, 9-75, Bauru, SP, 17012-90, Brazil.

[b]Department of Surgery, Stomatology, Pathology and Radiology, Bauru School of Dentistry, University of São Paulo, SP, Brazil. Al. Octávio Pinheiro Brisolla, 9-75, Bauru, SP, 17012-90, Brazil.

***Corresponding Author:** Marília Afonso Rabelo Buzalaf - Department of Biological Sciences, Bauru School of Dentistry, University of São Paulo. Al. Octávio Pinheiro Brisolla, 9-75 Bauru-SP, 17012-901 Brazil. Tel. + 55 14 32358346; Fax + 55 14 32271486; E-mail: mbuzalaf@fob.usp.br

(to whom reprint requests must be sent)

Received: 6 April 2021
Received in revised from 12 April 2021
Accepted: 20 April 2021
Available online: 10 May 2021

Graphical Abstract

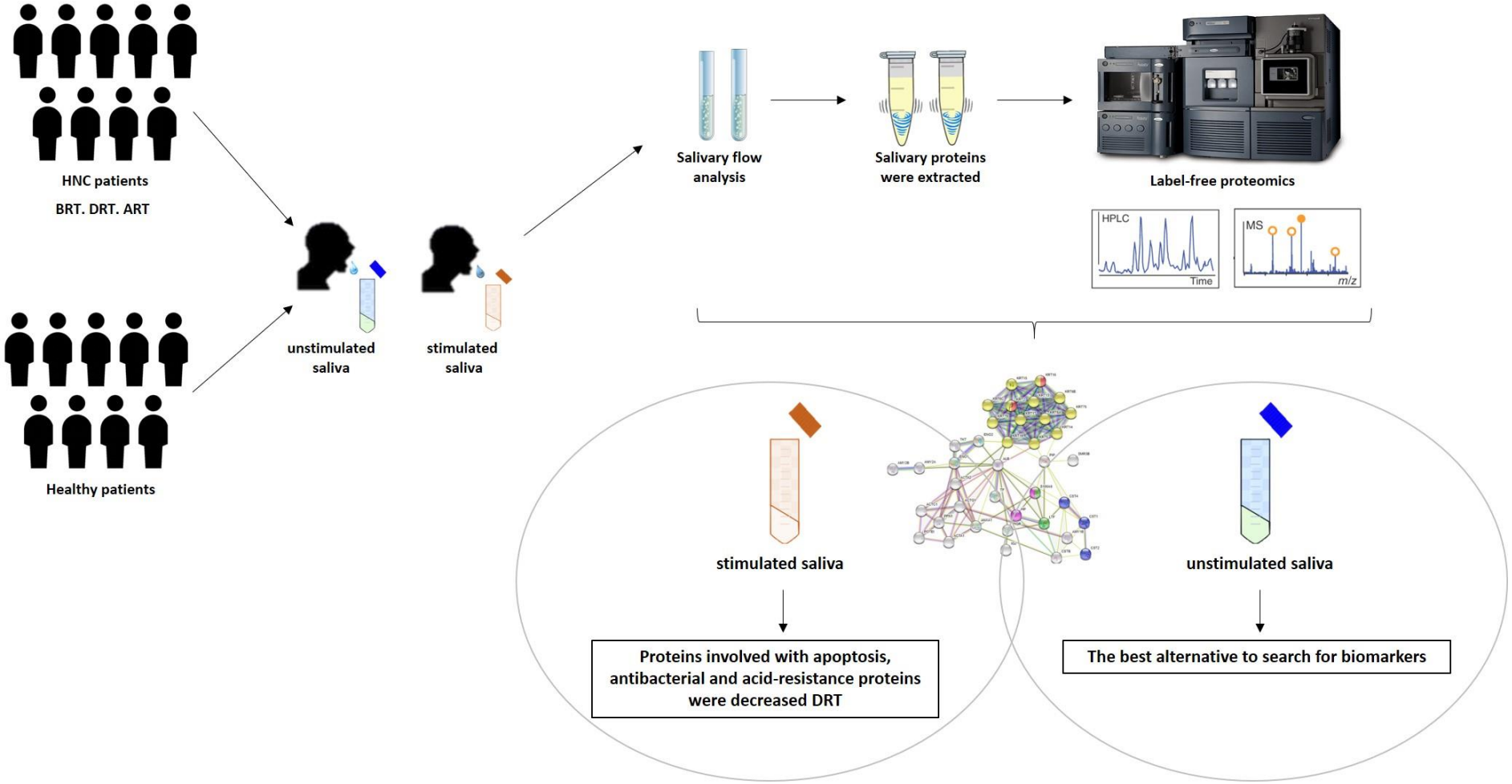

Abstract

Stimulation of saliva production is an alternative to improve the quality of life of patients treated by radiotherapy. However, there is no information about changes in the salivary proteome of stimulated and unstimulated saliva in these patients. Objectives: Thus, we evaluated the difference in the proteomic profile of stimulated and unstimulated saliva in patients with head and neck cancer (HNC) treated by radiotherapy. Methods: Stimulated and unstimulated saliva were collected from 9 patients with HNC before (BRT), during (DRT; 2-5 weeks) and after (ART; 3-4 months) treatment. Healthy patients paired by age and gender also had their saliva collected (C; control group). The stimulated and unstimulated salivary flow were evaluated ($p<0.05$). Salivary proteins were extracted and processed for shotgun proteomic analysis. Results: Significant differences were observed between stimulated and unstimulated salivary flows for C and BRT ($p>0.001$), but not for DRT and ART. Proteins involved with apoptosis, antibacterial and acid-resistance were decreased in stimulated saliva in comparison to unstimulated saliva DRT and ART. Isoforms of keratins were not identified in control and BRT. Conclusion: there is a marked difference in the protein profile of stimulated and unstimulated salivary flows in HNC patients treated by radiotherapy. In addition, saliva stimulation in patients with HNC decreases important proteins involved with dental protection. The unstimulated salivary flow seems to be the best alternative to search for biomarkers. Our results contribute in an unprecedented way to understand the changes in the salivary proteome of different flows in HNC patients undergoing radiotherapy treatment.

Keywords: stimulated saliva, unstimulated saliva, proteomic analysis, head and neck cancer, radiotherapy.

Introduction

Saliva plays a key role in oral health, presenting important functions such as antimicrobial action, lubrication and maintenance of mucous membranes, digestion, taste, phonation, buffering capacity, dental remineralization, besides being extremely important for the formation of the acquired enamel pellicle [1, 2]. Saliva is secreted by the three major salivary glands and the minor salivary glands that are found throughout the mucosa of the upper aerodigestive tract [3]. Therefore, any factor that may interfere with the homeostasis of saliva production and composition can directly affect these functions and, consequently, oral health.

In patients diagnosed with head and neck cancer (HNC), radiotherapy is the form of treatment adopted [4]. HNC most commonly presents as squamous cell carcinoma emanating from the lining of the mucosa of the upper aerodigestive tract that includes the oral cavity, oropharynx, hypopharynx and larynx [5]. However, HNC can also include salivary glands, thyroid gland, paranasal sinuses and periorbital structures. [6]. In 2018, HNC was considered the seventh most common cancer worldwide with 890,000 new cases and 450,000 deaths [7]. It is usually associated with the continued use of tobacco and alcohol [5], but also by human papillomavirus (HPV) infections [8, 9].

Among the treatments for HNC, radiotherapy is considered one of the main and most important treatments [4]. The main objective of radiotherapy is to achieve local control of the tumor, minimizing damage to critical organs [6]. However, radiotherapy in the head and neck region leads to serious damage to adjacent tissues, such as the salivary glands [6]. When the salivary glands are in the irradiated field, irreversible damage to the salivary glands occurs in 63-93% of patients [10]. Damage to the salivary glands typically manifests as a reduction in the secretion of saliva, which can generate dry mouth sensation (xerostomia), oral discomfort, altered taste, oral mucositis, difficulty in speaking, swallowing and chewing [10], and increased risk of dental demineralization and dental caries. [11]. In general, hyposalivation and xerostomia cause a substantial reduction in the quality of life of these patients. [10, 12]

Once patients develop hyposalivation, stimulatory agents can be used to increase residual salivary function. This provides a wide range of interventions for hypofunction of the salivary gland [13]. For patients who present some degree of residual salivary gland parenchyma, stimulation of salivary gland function may be appropriate [12]. This stimulation can be performed through medications [14] or through chewing gums that can activate the salivary reflex [15]. In addition, the topical application of salivary substitutes may offer some benefit, as they can provide a moisture-retaining coating on the oral mucosa and consequent

stimulation [12, 16]. Therefore, the main concerns are in relation to the evaluation of symptoms and strategies that aim to prevent potential oral and dental complications.

In this sense, there are no data on quantitative and comparative protein changes in stimulated and unstimulated saliva from patients with HNC who receive radiotherapy treatment. Thus, the aim of this study was to quantitatively compare the proteomic profile of stimulated and unstimulated saliva in patients with HNC treated with radiotherapy.

The null hypothesis tested was: there is no quantitative and qualitative difference in the *in vivo* proteome of stimulated and unstimulated saliva from patients with HNC treated by radiotherapy, before, during or after treatment.

Material and Methods

Ethical aspects

This study was submitted to the local Institutional Ethics Committee (No. 61484116.0.0000.5417). Stimulated and unstimulated saliva were collected after approval and signing the informed consent form. The study was carried out in accordance with the Declaration of Helsinki.

Patients information

Nine patients with HNC who attended the Clinical Research Center of Bauru School of Dentistry and who were treated with Linear Accelerator Radiotherapy (33-36 sessions, irradiation dose of 187cGy [17]) had their stimulated and unstimulated saliva collected. Patients with HNC were ex-smokers/ex-drinkers. Patients who presented problems such as dental restorations, dental caries, periodontitis or needed tooth extraction were treated before starting radiotherapy.

HNC patients were aged between 34 and 72 years, from both genders (7 male and 2 female). Stimulated and unstimulated saliva were colleted before radiotherapy (BRT); during radiotherapy (DRT; between weeks 2 and 5) and after radiotherapy (ART; 3 to 4 months after radiotherapy). Among the affected sites were Oropharynx Carcinoma and Tongue Base; Occult grade III Squamous Cell Carcinoma with cervical metastasis; Tongue Squamous Cell Carcinoma; Esophagus Squamous Cell Carcinoma and Amygdala; Retromolar Trigone (Jaw) Squamous Cell Carcinoma and Hypopharyngeal Squamous Cell Carcinoma. In addition, all

patients presented mucositis during treatment (4 patients with grade II, 3 patients with grades II and III, 1 patient with grade III and 1 patient with grade I and II) (Table 1). Therefore, all patients had to undergo laser therapy and analgesic/anti-inflammatory therapy during treatment. Healthy volunteers were paired by age (±5 years) and gender with HNC patients.

Nine health patients with good oral and general health, non-smokers, with no caries, gingivitis, periodontitis or other oral conditions that could alter the composition of the oral fluids, as well as those who were not using drugs, drugs or tobacco, were included as controls. Patients presenting risk factors for erosive tooth wear, such as excessive consumption of carbonated beverages, acidic food and drinks, swimming activities or gastric disorders such as gastroesophageal reflux and bulimia, were excluded (Control group; C) [18].

The sample size was calculated with MSstats [19] using data from our previous experiment [20], considering $\alpha = 0.05$ and $1-\beta = 0.8$. The effect size (difference in protein abundance) was considered as 1.5. The estimated number of samples was 3/group. We included 9 volunteers in each group, in order to constitute 3 pools (biological triplicates).

Saliva collection

Unstimulated and stimulated salivary flow of all patients who participated in the study was measured before the beginning of each collection period.

In order to avoid interference from the circadian cycle, saliva was collected in the morning [21]. The collection of stimulated and unstimulated saliva was performed strictly as previously described [22, 23]. Patients rinsed their mouths with 5 mL of deionized water before collection. For the collection of unstimulated saliva, the patients spat out all the saliva formed in tubes immersed in ice for 10 minutes. For the collection of stimulated saliva, the patients chewed a Parafilm® (5 cm) and all the saliva formed by the stimulation was spat out in tubes immersed in ice. After collection, samples were centrifuged at 4,500 x g for 15 min at 4 °C to remove possible debris such as insoluble material, cells and food debris. The supernatant from each sample was collected and frozen at -80 ° C until proteomics analysis. These procedures were based also on previous studies [22-24].

Shotgun Label-free quantitative proteomic analysis

Stimulated and unstimulated saliva proteins from patients with HNC and healthy patients were extracted and prepared in biological triplicate. For this, a pool of each group was

performed in triplicate, containing 333.33 μL of saliva from each patient, which was transfered to new tubes. Therefore, each 3 saliva samples (from 3 different patients) were pooled to obtain 3 samples containing 1000 μL of saliva for each group tested. The proteins from the saliva samples were extracted using extraction solution containing 6 M Urea, 2 M Thiourea in 50 mM Ammonium Bicarbonate, pH 7.8, in a volume similar to the samples (1:1). The procedures for the preparation of saliva samples and shotgun proteomic analysis were standardized by our group and were performed exactly as described by Ventura, et al 2018. [23].

Data acquisition was performed by Xevo G2-S mass spectrometer coupled to the nanoACQUITY UPLC (booth from Waters, Manchester, UK) controlled by MassLynx v.4.1 (Waters, Manchester, UK). Data collection was in data independent acquisition mode (LC-MSE), and the mass range from 50 to 200 m/z, that system was used for the peptide analysis, exactly as previously described [18, 23]. All samples were analyzed in technical triplicate, thus totaling 9 analyses for each group. The software ProteinLynx Global Server (*PLGS*) version 3.0 (Waters, Manchester, UK) was used to process and search for continuous LC-MSE data. The proteins were identified using the software's ion counting algorithm, and a search was performed on the Homo sapiens database (revised only, UniProtKB/Swiss-Prot) downloaded in October 2019 from UniProtKB (http: //www.uniprot .org).

For the label-free quantitative analysis, Protein Lynx Global Service software (PLGS, v 3.0, Waters, Manchester, UK) was used for analyzing nine raw MS files from each group. In the quantitative analysis, the proteins identified with a confidence score higher than 95% were included. The identical peptides from each triplicate by sample were pooled according to mass accuracy (<10 ppm) and the retention time tolerance <0.25 min, using the clustering software included in the *PLGS*. The difference in expression between the groups was analyzed by *t* test ($p<0.05$). The following relevant comparisons were performed: BRT Stimulated Saliva *vs* Unstimulated Saliva; DRT Stimulated Saliva *vs* Unstimulated Saliva; ART Stimulated Saliva *vs* Unstimulated Saliva; Control Stimulated Saliva *vs* Unstimulated Saliva.

Bioinformatics analysis

Reviewed and unreviewed proteins were analyzed by their access number by UNIPROT, and repetead proteins, reverse proteins and repeated fragments were excluded. Gene ontology was evaluated according to the ClueGo® pluggins of the Cytoscape® 3.8.2 Software. The functional distribution of proteins identified with differential expression in the different comparison was done. Protein categories was based on Gene Ontology (GO)

annotation of the broad Biological Process and Immune System Process. Terms of significance (Kappa = 0.04) and distribution were according to the percentage of the number of associated genes. The number of access of the proteins was provided by UNIPROT.

Statistical analysis

The software GraphPad Prism version 5.0 for Windows (GraphPad Software Inc., La Jolla, CA, USA), was used for salivary flow analysis. Data were checked for normality (Kolmogorov-Smirnov test) and homogeneity (Bartlett's test). Data referring to stimulated and unstimulated saliva BRT and Control passed the normality test and were analyzed with parametric *t* test($p<0.05$). Data regarding stimulated and unstimulated saliva DRT and ART did not pass the normality test and were analyzed by non-parametric *Mann Whitney* test ($p<0.05$).

Results

The total mean amount of protein recovered (µg), the mean (±SD), median and interquartile range (IQR) from stimulated and unstimulated salivary flow (mL/min) for BRT, DRT, ART and control are shown in Table 2.

Comparing the stimulated and unstimulated salivary flows, for the Control and BRT groups, the stimulated salivary flow was significantly higher than the unstimulated one ($p <0.05$). On the other hand, no significant difference was observed for the DRT and ART groups (Table 2).

For the quantitative proteomics analysis, in the comparison BRT Stimulated saliva vs Unstimulated saliva, the total number of proteins identified were 154 and 196, respectively, among which 65 proteins were common to both groups (Fig 1A). Eighty-nine proteins were identified exclusively in stimulated saliva, while 131 proteins were uniquely identified unstimulated saliva (Table S1). Regarding the differentially expressed proteins, 2 and 51 proteins were increased and decreased, respectively, in the stimulated saliva in comparison to the unstimulated one, BRT. Among the down-regulated proteins are: *Submaxillary gland androgen-regulated protein 3B*, 5 isoforms of actin, *Histatin-1*, 5 isoforms of immunoglobulins, *GLOBIN domain-containing protein, Cell adhesion molecule-related/down-regulated by oncogenes, Hemoglobin subunit gamma-1, Cystatin-SN, Mitoferrin-1, Hemoglobin subunit delta, Hemoglobin subunit epsilon, Salivary acidic proline-rich phosphoprotein ½* (decreased 2-fold), Cystatin-B (decreased 2-fold), *Protein fantom, Alpha-amylase 1* and *2B, Proline-rich*

protein 4 (nearly decreased 3-fold), 2 isofromfs of albumin (*Albumin_ isoform CRA_k* and *Serum albumin*), *Histone-lysine N-methyltransferase MECOM, Statherin* (decreased 4-fold), *Carbonic anhydrase 6, Endothelin-3, BPI fold-containing family B member 2, Cystatin-C* (nearly decreased 6-fold), *Cystatin-S* (decrease more than 6-fold), *Cystatin-SA* (nearly decrease 8-fold), *HCG1745306_ isoform CRA_a, Hemoglobin subunit alpha* (decreased 8-fold), *Hemoglobin subunit beta* (decreased 9-fold), *Prolactin-inducible protein* (decreased 9-fold), *Lipocalin-1, Putative lipocalin 1-like protein 1, Basic salivary proline-rich protein 1* (nearly decrease 20-fold), *Basic salivary proline-rich protein 2* (decreased 50-fold) and *Vitamin D 25-hydroxylase* (decreased 100-fold). Among the up-regulated protein in the stimulated saliva BRT are *POTE ankyrin domain family member I* and *Stromal cell-derived factor 2* (Table S1).

Fig. 2 show the functional analysis according to the biological process and immune system process, respectively, by Gene Ontology (GO) with the most significant term, for the comparison between Stimulated saliva vs Unstimulated saliva BRT. Among them, we would like to emphasize vitamin D3 25-hydroxylase activity (2.11%), negative regulation of bone mineralization (2.1%) and negative regulation of T cell apoptotic process (2.1%) (Fig. 2). The categories with the highest percentages of genes in the immune system process were polymeric immunoglobulin receptor activity (11.1%), antibacterial humoral response (33.3%) and antimicrobial humoral response (55.6%) (Fig. 2).

When we compared DRT Stimulated saliva vs Unstimulated saliva, the total number of proteins identified were 319 and 454, respectively, with 74 proteins common to both groups (Fig 1B). Among them, 245 proteins were identified exclusively in the Stimulated saliva, while 380 proteins were uniquely identified in the Unstimulated saliva (Table S2). In the differentially expressed proteins, 11 and 40 proteins were increased and decreased, respectively, in the Stimulated saliva DRT. Among the down-regulated proteins are *Immunoglobulin J chain, Submaxillary gland androgen-regulated protein 3B,* 10 isoformfs of Keratin (decreased more than 2-fold), 2 isoforms of albumin (*Serum albumin* and *Albumin_ isoform CRA_k*), *Prolactin-inducible protein, Lactotransferrin, Cystatin-B* (5-fold decrease), *Protein S100-A9* (decreased more than 6-fold), *Cystatin-S* (14-fold decrease), 3 isoforms of amylase, *Cystatin-SN* (decrease more tha 16-fold), *Histone-lysine N-methyltransferase MECOM, Cystatin-SA* (decrease more than 16-fold), *Immunoglobulin heavy constant alpha 2 (*decreased more than 20-fold), *Immunoglobulin kappa constant* (decreased 25-fold), *Immunoglobulin heavy constant alpha 1* (decreased 25-fold) and *Alpha-(1_3)-fucosyltransferase 6* with an expressive decrease more than 100-fold in the stimulated saliva DRT. Among the up-regulated proteins are 4 isoforms of actin, *Haptoglobin, Serotransferrin,* 2 isoforms of Keratin, *Profilin* (increased more than 2-

fold) and *Splicing regulatory glutamine/lysine-rich protein 1* (increased more than 7-fold) (Table S2).

Fig 3 show the functional analysis according to the biological processed and immune system processes, respectively, by Gene Ontology (GO) with the most significant term, for the comparison between Stimulated saliva vs Unstimulated saliva DRT. Among them, we would like to emphasize protein localization to bicellular tight junction (2.0%), negative regulation of T cell apoptotic process (2.0%), mesenchyme migration (5.9%) and cornification (25.5%) (Fig. 3). The categories with the highest percentages of genes in the immune system process were polymeric immunoglobulin receptor activity (7.7%), negative regulation of T-helper 2 cell differentiation (7.7%), negative regulation of macrophage chemotaxis (7.7%), antimicrobial humoral immune response mediated by antimicrobial peptide (23.1%) and antimicrobial humoral response (53.8%) (Fig. 3).

For the comparison ART Stimulated saliva vs Unstimulated saliva, the total number of proteins identified were 321 and 548, respectively, with 92 proteins common to both groups (Fig 1C). Among them, 229 proteins were identified exclusively in the Stimulated saliva, while 456 proteins were uniquely identified in the Unstimulated saliva (Table S3). In the differentially expressed proteins, 12 and 53 proteins were increased and decreased, respectively, in the Stimulated saliva ART. Among the down-regulated proteins are *Lysozyme C, BPI fold-containing family B member 2, Salivary acidic proline-rich phosphoprotein ½, Proline-rich protein 4, Histone-lysine N-methyltransferase MECOM, Hemoglobin subunit alpha, Cystatin-SN, -B, -S* (decreased more than 2-fold), 8 isoforms of Immunoglobulins (decreased more than 2-fold), *Lactotransferrin* (decreased 3-fold), *Prolactin-inducible protein* (decreased 4-fold), 2 isoforms of albumin, *14-3-3 protein sigma* (decreased 7-fold), *Neural cell adhesion molecule L1-like protein* (decreased more than 12-fold) and *Probable E3 ubiquitin-protein ligase HERC1* (decreased 50-fold). Among the up-regulated proteins in the Stimulated saliva ART are *Alpha-amylase 1, Immunoglobulin kappa constant, Basic salivary proline-rich protein 2, Myelin regulatory factor, Cystatin-SA* (increased 3-fold), *Talin-2, Angiotensin-converting enzyme* (increased more than 4-fold) and *Acetyl-CoA carboxylase 2* (increased more than 32-fold) (Table S3).

Fig. 4 show the functional analysis according to the biological process and immune system process, respectively, by Gene Ontology (GO) with the most significant term, for the comparison between Stimulated saliva vs Unstimulated saliva ART. Among them, the categories with the most affected percentages of genes in the biological process were antimicrobial humoral response (7.7%), monosaccharide biosynthetic process (7.7%), Fc-

gamma receptor signaling pathway involved in phagocytosis (8.8%), negative regulation of endopeptidase activity (11%), humoral immune response (15.4%) and retina homeostasis (18.7%) (Fig. 4). The categories with the percentages of genes in the immune system process were polymeric immunoglobulin receptor activity (6.2%), antimicrobial humoral response (43.8%) and Fc-gamma receptor signaling pathway involved in phagocytosis (50.0%) (Fig. 4).

For the comparison of the Control group Stimulated saliva vs Unstimulated saliva, the total numbers of proteins identified were 190 and 168, respectively, with 59 proteins common to both groups (Fig 1D). Among them, 131 proteins were identified exclusively in the Stimulated saliva, while 109 proteins were identified exclusively in the Unstimulated saliva (Table S4). In the quantitative analysis, 7 and 8 proteins were increased and decreased, respectively, in the Stimulated saliva from the Control group. Among the down-regulated proteins are *Basic salivary proline-rich protein 1* and *2, Submaxillary gland androgen-regulated protein 3B,* 3 isoforms of immunoglobulins, *Zymogen granule protein 16 homolog B* and *Statherin* (decreased nearly 4-fold). However, 2 isoforms of albumin (*Serum albumin* and *Albumin_ isoform CRA_k*), *Cystatin-SA, Alpha-amylase 1* and *2B,* and *Histatin-1* (increased nearly 3-fold) were up-regulated in stimulated saliva when compared to unstimulated saliva (Table S4).

Fig. 5 shows the functional analysis according to the biological process by Gene Ontologies (GO) with the most significant term, for the comparison between Control Stimulated saliva vs Unstimulated saliva. Among them, the categories with the percentages of genes were maintenance of mitochondrion location (16.7%), negative regulation of bone mineralization (16.7%), detection of chemical stimulus involved in sensory perception of bitter taste (33.3%) and positive regulation of respiratory burst (33.3%).

Discussion

The reduction in salivary flow during radiotherapy treatment in patients with HNC is well known. Due to the radiation received in the head and neck region, organs such as the salivary glands can be affected, causing irreversible tissue damage in some situations [25]. Due to the reduction in the salivary flow, the quality of life of these patients is reduced, since saliva is an important fluid for the homeostasis of the oral cavity [1], besides being considered an important source of biomarkers [3,26]. Because its collection is non invasive, its processing is

considered simpler (but accurate) and does not cause discomfort to the patient, as in blood collection, for example, this fluid has great biological and clinical interest.

This is the first study to compare quantitatively the protein profile of stimulated and unstimulated salivary flows of cancer patients treated with radiotherapy. As we observed in our results, although the objective was not to compare the flows of the different groups, but to compare the stimulated and unstimulated salivary within the same group, it was normal range (>1 mL/min and >0.4 mL/min for stimulated and unstimulated flows, respectively) [27-29], despite having a tendency of reduction when compared to the salivary flow values of healthy patients (Table 2). However, when the patients undergo radiotherapy (DRT), the difference between stimulated and unstimulated salivary flows is not significant, which also occurs 3–4 months after radiotherapy treatment (ART) (Table 2). Thus, our data show that the reduction in salivary flow during and after radiotherapy occurs both in stimulated and unstimulated salivary flows. For this reason, therapeutic alternatives to increase salivary flow are prescribed to these patients, to stimulate salivary flow [29].

When we performed comparative and quantitative analyses of stimulated and unstimulated salivary flows during and after treatment, in the proteomic analysis important proteins were differently expressed. Thus, null hypothesis was rejected. Firstly, in relation to the control group, it was possible to verify that acid-resistant proteins such as PRPs and *Statherin* (almost 4-fold decrease) (UNIPROT) were decreased in stimulated saliva when compared to unstimulated saliva. In addition, immunoglobulins and *Lysozyme C* were identified exclusively in unstimulated saliva. *Lysozyme C* has mainly bacteriolytic function in tissues and body fluids and are associated with the monocyte-macrophage system, increasing the activity of immunoagents (UNIPROT). On the other hand, proteins such as amylases, albumin, *Cystatin-SA* and *Histatin-1* were increased in the stimulated salivary flow in healthy patients. Histatins have several functions such as buffering, modulation of mineral formation, as well as potent antifungal and antibacterial activities [30]. In addition, hemoglobins and *Cystatin-B*, which are considered acid-resistant proteins, were identified exclusively in the stimulated saliva in the control group. Hemoglobin is increased in the acquired enamel pellicle (AEP) and in saliva of patients suffering from gastroesophageal reflux who have a lower degree of erosive tooth wear [31,32]. Also, C*ystatin-B* is a reversible inhibitor of strong binding of intracellular thiol proteinase. Participates in inhibitory activity of cysteine-type endopeptidase (UNIPROT), is present in many tissues, including squamous mucous epithelia, and has also been identified in extracellular fluids, such as urine in patients with bladder cancer [33]. *Cystatin-B* and PRPs have been reported to be components of the cornified cell envelope of epidermal keratinocytes,

a layer of isodipeptide-crosslinked proteins and disulfide bonds. In addition, the identification of *Cystatin-B* and *-S* proteins, which are mainly of intracellular origin and represent the main constituents of the envelope of cornified cells may be an indication of inflammation of the mucosal epithelia [34].

BRT, *Matrin-3* was identified exclusively in the unstimulated salivary flow. *Matrin-3* provides the possibility to predict the aggressiveness of breast cancer. Also, *Matrin-3* suppresses tumorigenicity, induces cell death by apoptosis and inhibits the migration and invasion of basal-type in breast cancer cells [36]. Thus, perhaps *Matrin-3* can play an important role as a prognostic biomarker in the HNC, which should be evaluated in future studies.

When different salivary flows were compared DRT, *Lactotrasnferrin, Prolactin-inducible protein, Protein S100-A9,* as well as isoforms of amylases, keratins, albumins, cystatins, PRPs and immunoglobulins were decreased in stimulated salivary flow compared to unstimulated one. Regarding the unique proteins identified, *A disintegrin and metalloproteinase with thrombospondin motifs 12, A disintegrin and metalloproteinase with thrombospondin motifs 1, Apoptosis-resistant E3 ubiquitin protein ligase,* 14-3-3 proteins and histones that are involved in processes of apoptosis (UNIPROT) and hemoglobins, immunoglobulins, *Lyzosyme C* and *Mucin-7,* were identified exclusively in the unstimulated salivary flow DRT. Among the exclusive proteins, *Mucin-7* works as a protection in the humoral antimicrobial immune response, promoting the elimination of bacteria in the oral cavity and assisting in chewing, speech and swallowing (UNIPROT) [36].

When comparing ART salivary flows, important proteins that are involved with apoptotic processes were identified exclusively in unstimulated saliva, such as *Calpain-3, Clusterin, Complement C3* and *Lymphoid enhancer-binding factor* 1 (UNIPROT). In addition to 6 isoforms of the 14-3-3 protein that is involved with deacetylation of histones [37], *A disintegrin and metalloproteinase with thrombospondin motifs 9* that is involved with angiogenesis [38], 5 isoforms of hemoglobins, *Cystatin-C* and *Mucin-7.*

On the other hand, *Mucin-20* was identified exclusively in the stimulated saliva ART. *Mucin-20* is a transmembrane glycoprotein secreted by the epithelium and is largely overexpressed in epithelial tumor cells. In addition, *Mucin-20* is considered a molecular biomarker for the prognosis of some epithelial tumors and squamous cell carcinoma of the esophagus in patients who received neoadjuvant chemotherapy followed by surgery [39]. However, important proteins that are directly linked with the homeostasis of oral health and are involved in the formation of the AEP [2] were reduced in the stimulated salivary flow when

compared to the unstimulated salivary flow ART (Table S3). Among these are*:* hemoglobin, cystatins, albumins, several immunoglobulins, PSPs, *Lysozyme C* and *Lactotransferrin*.

It is worth mentioning that in the different periods (BRT, DRT and ART), isoforms of amylases, albumins, immunoglobulins, proline-rich proteins, cistatinas, which have important functions in the oral cavity, were decreased in the stimulated salivary flow when compared to the unstimulated salivary one. On the other hand, Profilin that regulates the dynamics and polymerization of microtubules, being able to coordinate actin polymer systems and appears to be related to essential biochemical and cellular cytoskeletal roles that go wrong in cancer [40] was identified increased in the stimulated saliva DRT in comparison with unstimulated saliva and exclusively in the stimulated saliva ART.

Among the proteins identified in the proteomic analysis, isoforms of keratin caught our attention. In the different comparisons of salivary flows for the control group (healthy patients) and before radiotherapy (BRT), this protein was not identified. However, when the stimulated and unstimulated salivas of the group DRT were quantitatively compared, two isoforms of the keratin protein (*Keratin_ type II cytoskeletal 6A* and *6B*) were increased in the stimulated salivary flow, but 11 isoforms were decreased. In addition, 4 keratin isoforms (*Keratin_type I cytoskeletal 10* and *-12, Keratin_type II cytoskeletal 4* and *-73*) were identified exclusively in unstimulated saliva DRT. After the treatment (ART), 19 isoforms of keratin were identified exclusively in the unstimulated salivary flow and no isoform was identified in the stimulated salivary flow. Thus, the isoforms identified only in these groups can be related to the radiotherapy treatment. Due to this, we constructed interaction networks for these proteins using the String tool (Fig 6). In the network, it was possible to observe that these proteins have protein-protein interactions and are related to cornification processes. The cornification process is involved with programmed cell death that occurs in the epidermis, morphologically and biochemically unlike apoptosis processes. This leads to the formation of corneocytes, that is, dead keratinocytes that are necessary for the function of the cornified skin layer (mechanical resistance, elasticity, water repellency and structural stability) [41]. In addition, this process was also observed in the functional analysis of the most affected processes in the DRT group with 25.5% (Fig. 3).

Thus, we raise the hypothesis that the unstimulated salivary flow might be the most appropriate fluid when it is intended to identify possible biomarkers in saliva. We cannot forget to mention that, although the two isoforms of the keratin protein are increased in the stimulated salivary flow DRT, the *Keratin_ type II cytoskeletal 6A* is also involved with wound healing and repair processes (UNIPROT). Thus, we believe that the increase in this protein may be

related to the laser therapy treatments to which these patients were submitted, since episodes of mucositis are frequent due to radiation.

Considering that unstimulated saliva might have a better potential as a source for biomarkers, isoforms of histones that are involved with processes of DNA methylation, the main epigenetic mechanisms to memory and cellular identity, influencing the cellular microenvironment [42], were identified exclusively in unstimulated salivary flows during (19 isoforms) and after (24 isoforms) radiotherapy (Tables S2; S3). The identification and increase of histones ART have already been reported in the acquired enamel pellicle in patients with HNC [43]. Only one isoform of histone was identified in both groups: *Histone-lysine N-methyltransferase MECOM* that is involved with the regulation of the cell cycle and apoptotic process (UNIPROT). However, this protein was reduced in the stimulated salivary flow when compared to the unstimulated salivary flow, which provides additional support to our hypothesis that unstimulated salivary flow might be a better source of tumor and apoptotic markers.

Taken together, our data suggest that future studies involving the search for biomarkers, should use unstimulated saliva. In addition, stimulating salivary flow in cancer patients undergoing radiotherapy seems to reduce proteins involved with antibacterial and acid-resistant protection. On the other hand, however, we cannot forget to mention the importance of saliva in lubricating and increasing the quality of life of these patients. A limitation of the present study was that we did not compare the different salivary flows in the different treatment periods, since this is the aim of an undergoing study.

Conclusion

In conclusion, there is a marked difference in the protein profile of stimulated and unstimulated salivary flows of patients with HNC treated by radiotherapy. This difference was observed before, during and after treatment, as well as in healthy patients. The unstimulated salivary flow seems to be the best alternative to search for biomarkers. In addition, saliva stimulation in patients with HNC decreases important proteins that participate in the oral health homeostasis, with antibacterial and acid-resistant properties. Finally, our results contribute in an unprecedented way to understand the changes in the salivary proteome of different flows in cancer patients undergoing radiotherapy treatment, thus being able to be used for future studies for the development of dental products more directed to this group of patients to improve their

quality of life, since flow stimulation is encouraged during radiotherapy. In addition, we suggest the use of unstimulated saliva for future studies that search for salivary biomarkers.

Declaration of Competing Interest

The authors declare that they have no known competing financial interests or personal relationships that could have appeared to influence the work reported in this paper.

Acknowledgements

The authors thank FAPESP for financial support and for the concession of a scholarship to the first (Proc. FAPESP 2017/05031-2) and third (Proc. FAPESP 2018/17860-6) authors. This study was financed in part by the Coordenação de Aperfeiçoamento de Pessoal de Nível Superior - Brazil (CAPES) - Finance Code 001. The funders had no role in study design, data collection and analysis, decision to publish or preparation of the manuscript. All authors gave their final approval and agree to be accountable for all aspects of the work. The authors are grateful especially the trial participants, their families and the staff of the Clinical Research Center at Bauru School of Dentistry. The authors are grateful to Mrs. Larissa Tercilia Grizzo for technical support with proteomic analysis.

Funding

This work was financially supported by FAPESP (Proc. 2017/05031-2 and Proc. 2018/17860-6). This work was financed in part by CAPES – Finance Code 001. The Funding sources had no involvement in the study design, in the collection, analysis and interpretation of data, in the writing of the report and in the decision to submit the article for publication.

Author's Contributions

Ventura TMO, Buzalaf MAR, Santos PSS and Rubira CMF conceived and designed the study. Ventura TMO, Ribeiro NR, Taira EA and Dionizio A acquired the data. Ventura TMO, Leite AL and Buzalaf MAR quality control of data. Ventura TMO, Ribeiro NR and Buzalaf MAR data analysis and interpretation. Ventura TMO and Buzalaf MAR statistical analysis. Ventura TMO and Buzalaf MAR drafted the manuscript. Ventura TMO, Leite AL, Santos PSS and Buzalaf MAR manuscript editing. Buzalaf MAR, Santos PSS and Rubira CMF supervised the study.

All authors have revised and agreed with the final version of the manuscript.

References

[1] Buzalaf MAR, Hannas AR, Kato MT. Saliva and dental erosion. J Appl Oral Sci 2012;20:493–502.
[2] Vukosavljevic D, Custodio W, Buzalaf MAR, Hara AT, Siqueira WL. Acquired pellicle as a modulator for dental erosion. Arch Oral Biol 2014;59:631–8.
[3] Wang X, Kaczor-Urbanowicz KE, Wong DT. Salivary biomarkers in cancer detection. Med Oncol 2017;34:7.
[4] Semrau R. The Role of Radiotherapy in the Definitive and Postoperative Treatment of Advanced Head and Neck Cancer. Oncol Res Treat 2017;40:347–52.
[5] Kawakita D, Matsuo K. Alcohol and head and neck cancer. Cancer Metastasis Rev 2017;36:425–34.
[6] Yeh SA. Radiotherapy for head and neck cancer. Semin Plast Surg 2010;24:127–36.
[7] Bray F, Ferlay J, Soerjomataram I, Siegel RL, Torre LA, Jemal A. Global cancer statistics 2018: GLOBOCAN estimates of incidence and mortality worldwide for 36 cancers in 185 countries. CA Cancer J Clin 2018;68:394–424.
[8] Chow LQM. Head and Neck Cancer. N Engl J Med 2020;382:60–72.
[9] Rettig EM, D'Souza G. Epidemiology of head and neck cancer. Surg Oncol Clin N Am 2015;24:379–96.
[10] Rogers SN, Ahad SA, Murphy AP. A structured review and theme analysis of papers published on 'quality of life' in head and neck cancer: 2000–2005. Oral Oncol 2007;43:843–68.
[11] Deng J, Jackson L, Epstein JB, Migliorati CA, Murphy BA. Dental demineralization and caries in patients with head and neck cancer. Oral Oncol 2015;51:824–31.
[12] Mercadante V, Al Hamad A, Lodi G, Porter S, Fedele S. Interventions for the management of radiotherapy-induced xerostomia and hyposalivation: A systematic review and meta-analysis. Oral Oncol 2017;66:64–74.
[13] Plemons JM, Al-Hashimi I, Marek CL. American Dental Association Council on Scientific A. Managing xerostomia and salivary gland hypofunction: executive summary of a report from the American Dental Association Council on Scientific Affairs. J Am Dent Assoc 2014;145:867–73.
[14] Brimhall J, Jhaveri MA, Yepes JF. Efficacy of cevimeline vs. pilocarpine in the secretion of saliva: a pilot study. Spec Care Dentist 2013;33:123–7.
[15] Furness S, Worthington HV, Bryan G, Birchenough S, McMillan R. Interventions for the management of dry mouth: topical therapies. Cochrane Db Syst Rev 2011.
[16] Dost F, Farah CS. Stimulating the discussion on saliva substitutes: a clinical perspective. Aust Dent J 2013;58:11–7.
[17] Shyh-An Yeh MD. Radiotherapy for Head and Neck Cancer. Semin Plast Surg 2010; 24(2):127–36.
[18] Ventura T, Cassiano LPS, Souza ESCM, Taira EA, Leite AL, Rios D, et al. The proteomic profile of the acquired enamel pellicle according to its location in the dental arches. Arch Oral Biol 2017;79:20–9.
[19] Choi M, Chang CY, Clough T, Broudy D, Killeen T, MacLean B, et al. MSstats: an R package for statistical analysis of quantitative mass spectrometry-based proteomic experiments. Bioinformatics 2014;30:2524–6.
[20] Batista TBD, Chaiben CL, Penteado CAS, Nascimento JMC, Ventura TMO, Dionizio A, et al. Salivary proteome characterization of alcohol and tobacco dependents. Drug Alcohol Depend 2019;204:107510.
[21] Dawes C. Circadian rhythms in human salivary flow rate and composition. J Physiol 1972;220:529–45.

[22] Jasim H, Olausson P, Hedenberg-Magnusson B, Ernberg M, Ghafouri B. The proteomic profile of whole and glandular saliva in healthy pain-free subjects. Sci Rep 2016;6:39073.
[23] Ventura T, Ribeiro NR, Dionizio AS, Sabino IT, Buzalaf MAR. Standardization of a protocol for shotgun proteomic analysis of saliva. J Appl Oral Sci 2018;26: e20170561.
[24] Winck FV, Prado Ribeiro AC, Ramos Domingues R, Ling LY, Riano-Pachon DM, Rivera C, et al. Insights into immune responses in oral cancer through proteomic analysis of saliva and salivary extracellular vesicles. Sci Rep 2015;5:16305.
[25] Jasmer KJ, Gilman KE, Munoz Forti K, Weisman GA, Limesand KH. Radiation- Induced Salivary Gland Dysfunction: Mechanisms, Therapeutics and Future Directions. J Clin Med 2020;9.
[26] Buzalaf MAR, Ortiz AC, Carvalho TS, Fideles SOM, Araujo TT, Moraes SM, et al. Saliva as a diagnostic tool for dental caries, periodontal disease and cancer: is there a need for more biomarkers? Expert Rev Mol Diagn 2020;20:543–55.
[27] Dawes C. Physiological factors affecting salivary flow rate, oral sugar clearance, and the sensation of dry mouth in man. J Dent Res. 1987;66 Spec No:648–53.
[28] Dawes C. How much saliva is enough for avoidance of xerostomia? Caries Res 2004;38:236–40.
[29] Paim ED, Berbert MCB, Zanella VG, Martins VB, Macagnan FE. Effects of transcutaneous electrical nerve stimulation on the salivary flow of patients with hyposalivation induced by radiotherapy in the head and neck region-A randomised clinical trial. J Oral Rehabil 2019;46:1142–50.
[30] Siqueira WL, Lee YH, Xiao YZ, Held K, Wong W. Identification and characterization of histatin 1 salivary complexes by using mass spectrometry. Proteomics 2012;12: 3426–35.
[31] Martini T, Rios D, Cassiano LPS, Silva CMS, Taira EA, Ventura TMS, et al. Proteomics of acquired pellicle in gastroesophageal reflux disease patients with or without erosive tooth wear. J Dent 2019;81:64–9.
[32] Martini T, Rios D, Dionizio A, Cassiano LP, Pela VT, Silva CMS, et al. Salivary hemoglobin protects against erosive tooth wear in gastric reflux patients. Caries Res 2020;54:466–74.
[33] Feldman AS, Banyard J, Wu CL, McDougal WS, Zetter BR. Cystatin B as a tissue and urinary biomarker of bladder cancer recurrence and disease progression. Clin Cancer Res 2009;15:1024–31.
[34] Manconi B, Liori B, Cabras T, Iavarone F, Manni A, Messana I, et al. Top-down HPLC-ESI-MS proteomic analysis of saliva of edentulous subjects evidenced high levels of cystatin A, cystatin B and SPRR3. Arch Oral Biol 2017;77:68–74.
[35] Yang J, Lee SJ, Kwon Y, Ma L, Kim J. Tumor suppressive function of Matrin 3 in the basal-like breast cancer. Biol Res 2020;53:42.
[36] Crosara KTB, Zuanazzi D, Moffa EB, Xiao Y, Machado M, Siqueira WL. Revealing the Amylase Interactome in Whole Saliva Using Proteomic Approaches. Biomed Res Int 2018;2018:6346954.
[37] Jain N, Janning P, Neumann H. 14-3-3 protein Bmh1 triggers short-range compaction of mitotic chromosomes by recruiting sirtuin deacetylase Hst2. J Biol Chem 2020.
[38] Tokuhara CK, Santesso MR, Oliveira GSN, Ventura T, Doyama JT, Zambuzzi WF, et al. Updating the role of matrix metalloproteinases in mineralized tissue and related diseases. J Appl Oral Sci 2019;27:e20180596.
[39] Wang H, Shen LY, Lin Y, Shi Q, Yang YB, Chen KN. The expression and prognostic significance of Mucin 13 and Mucin 20 in esophageal squamous cell carcinoma. J Cancer Res Ther 2015;11:C74–9.
[40] Pimm ML, Hotaling J, Henty-Ridilla JL. Profilin choreographs actin and microtubules in cells and cancer. Int Rev Cell Mol Biol 2020;355:155–204.

[41] Eckhart L, Lippens S, Tschachler E, Declercq W. Cell death by cornification. Biochim Biophys Acta 2013;1833:3471–80.
[42] Blancafort P, Jin J, Frye S. Writing and rewriting the epigenetic code of cancer cells: from engineered proteins to small molecules. Mol Pharmacol 2013;83: 563–76.
[43] Ventura TMO, Ribeiro NR, Taira EA, de Souza ESCM, Rubira CMF, da Silva Santos PS, et al. Radiotherapy changes acquired enamel pellicle proteome in head and neck cancer patients. J Dent 2021:103642.

Figure legends

Fig 1. Venn diagram showing the relation of the proteins identified in common among the groups, as well as the number of proteins exclusively found in one of the groups in each comparison.

Fig 2. Graphs of the functional distribution of proteins identified with differential expression in the stimulated saliva vs unstimulated saliva BRT. Protein categories based on Gene Ontology (GO) annotation of the broad Biological Process and Immune System Process. Terms of significance (Kappa = 0.04) and distribution according to the percentage of the number of associated genes. The number of access to proteins was provided by UNIPROT. The gene ontology was evaluated according to the ClueGo® pluggins of the software Cytoscape® 3.8.2.

Fig 3. Graphs of the functional distribution of proteins identified with differential expression in the stimulated saliva vs unstimulated saliva DRT. Protein categories based on Gene Ontology (GO) annotation of the broad Biological Process and Immune System Process. Terms of significance (Kappa = 0.04) and distribution according to the percentage of the number of associated genes. The number of access to proteins was provided by UNIPROT. The gene ontology was evaluated according to the ClueGo® pluggins of the software Cytoscape® 3.8.2.

Fig 4. Graphs of the functional distribution of proteins identified with differential expression in the stimulated saliva vs unstimulated saliva ART. Protein categories based on Gene Ontology (GO) annotation of the broad Biological Process and Immune System Process. Terms of significance (Kappa = 0.04) and distribution according to the percentage of the number of associated genes. The number of access to proteins was provided by UNIPROT. The gene ontology was evaluated according to the ClueGo® pluggins of the software Cytoscape® 3.8.2.

Fig 5. Graphs of the functional distribution of proteins identified with differential expression in the stimulated saliva vs unstimulated saliva in the Control group. Protein categories based on Gene Ontology (GO) annotation of the broad Biological Process. Terms of significance (Kappa = 0.04) and distribution according to the percentage of the number of associated genes. The number of access to proteins was provided by UNIPROT. The gene ontology was evaluated according to the ClueGo® pluggins of the software Cytoscape® 3.8.2.

Fig 6. Interaction networks to establish the interaction between proteins identified with differential expression DRT in the comparison stimulated saliva vs. unstimulated saliva and unique keratin proteins idenfied in the unstimulated saliva ART. Interaction networks created by STRING® (https://string-db.org/cgi/network.pl). (A) The red color of the nodes indicates proteins that are involved with keratinocyte migration (*Keratin, type II cytoskeletal 2 epidermal and Keratin, type I cytoskeletal 16*), nodes yellow color indicates formation of the cornified envelope (all keratins), green color nodes indicates proteins involved with metal sequestration by antimicrobial proteins (*Protein S100-A9* and *Lactotransferrin*), antioxidant process (*Protein S100-A9* and *Haptoglobin*) and salivary secrection (*Cystatin-S, -SN, -SA*). (B) The red color of the nodes indicates proteins that are involved with cornification (all proteins), green color nodes indicate proteins that are involved with structural constituent of epidermis (*Keratin, type II cytoskeletal 2 epidermal, Keratin, type II cytoskeletal 1* and *Keratin, type I cytoskeletal 10*), yellow color nodes incicates proteins involved with structural constituent of cytoskeleton (*Keratin, type II cytoskeletal 5, -6A, -6B* and *2 epidermal, Keratin, type I cytoskeletal 14, -15, -16, -17* and *-19*), blue color nodes indicates proteins that are involved with keratinocyte migration (*Keratin, type II cytoskeletal 2 epidermal* and *Keratin, type I cytoskeletal 16*).

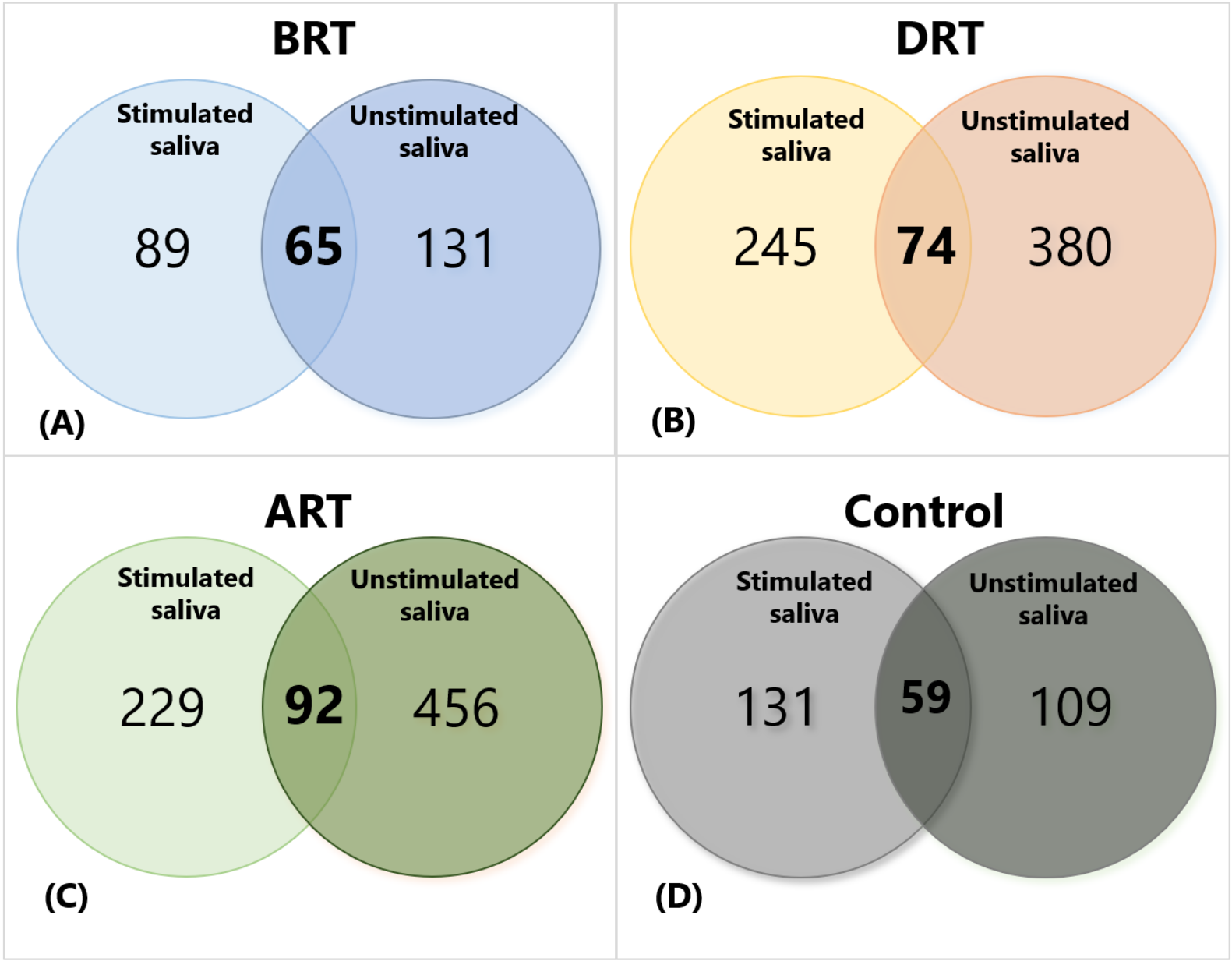
BRT
Stimulated saliva
Unstimulated saliva
89
65
131
(A)
DRT
Stimulated saliva
Unstimulated saliva
245
74
380
(B)
ART
Stimulated saliva
Unstimulated saliva
229
92
456
(C)
Control
Stimulated saliva
Unstimulated saliva
131
59
109
(D)

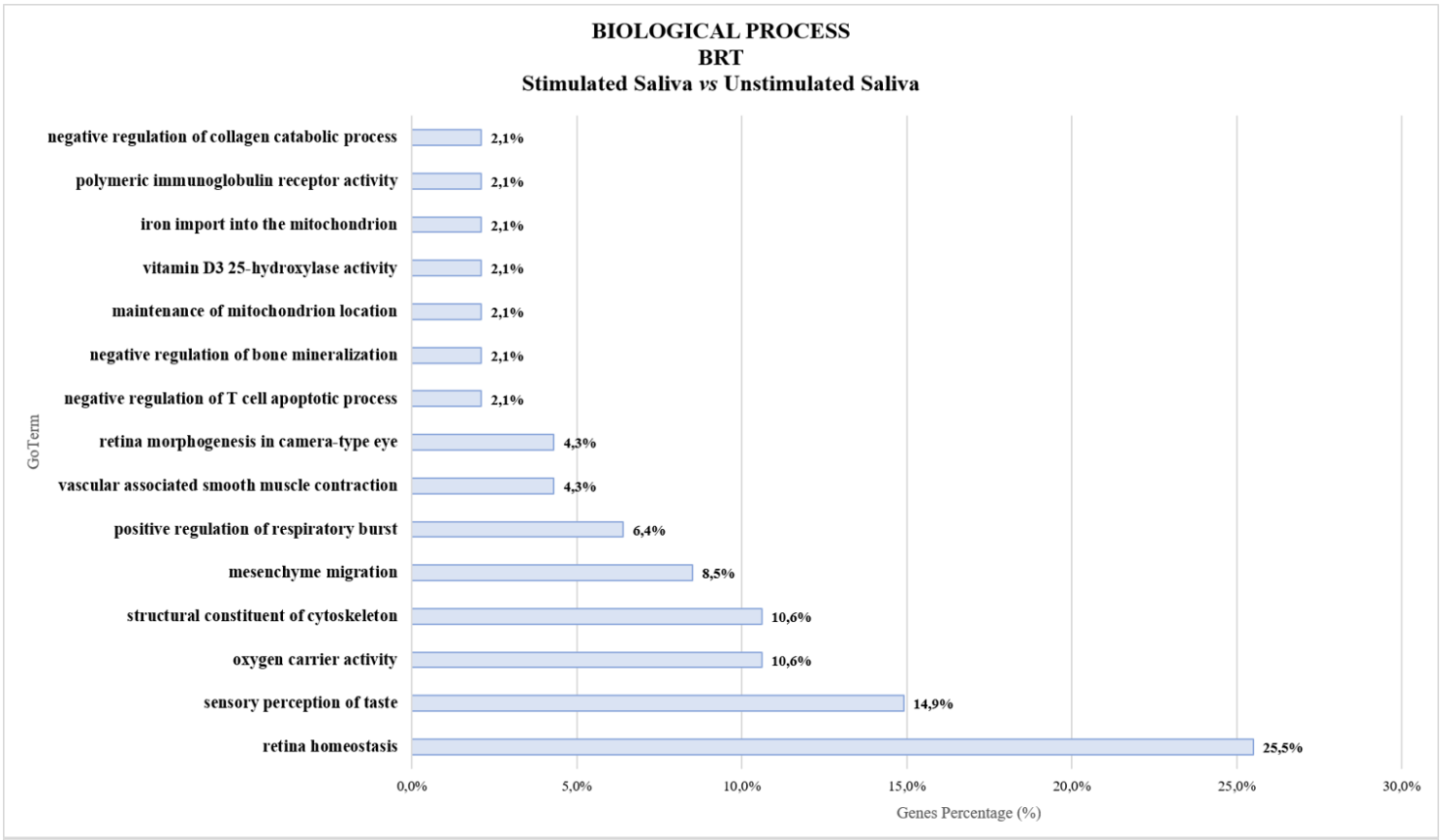
BIOLOGICAL PROCESS
BRT
Stimulated Saliva vs Unstimulated Saliva
GoTerm
negative regulation of collagen catabolic process
polymeric immunoglobulin receptor activity
iron import into the mitochondrion
vitamin D3 25-hydroxylase activity
maintenance of mitochondrion location
negative regulation of bone mineralization
negative regulation of T cell apoptotic process
retina morphogenesis in camera-type eye
vascular associated smooth muscle contraction
positive regulation of respiratory burst
mesenchyme migration
structural constituent of cytoskeleton
oxygen carrier activity
sensory perception of taste
retina homeostasis
2,1%
2,1%
2,1%
2,1%
2,1%
2,1%
2,1%
4,3%
4,3%
6,4%
8,5%
10,6%
10,6%
14,9%
25,5%
0,0%
5,0%
10,0%
15,0%
20,0%
25,0%
30,0%
Genes Percentage (%)

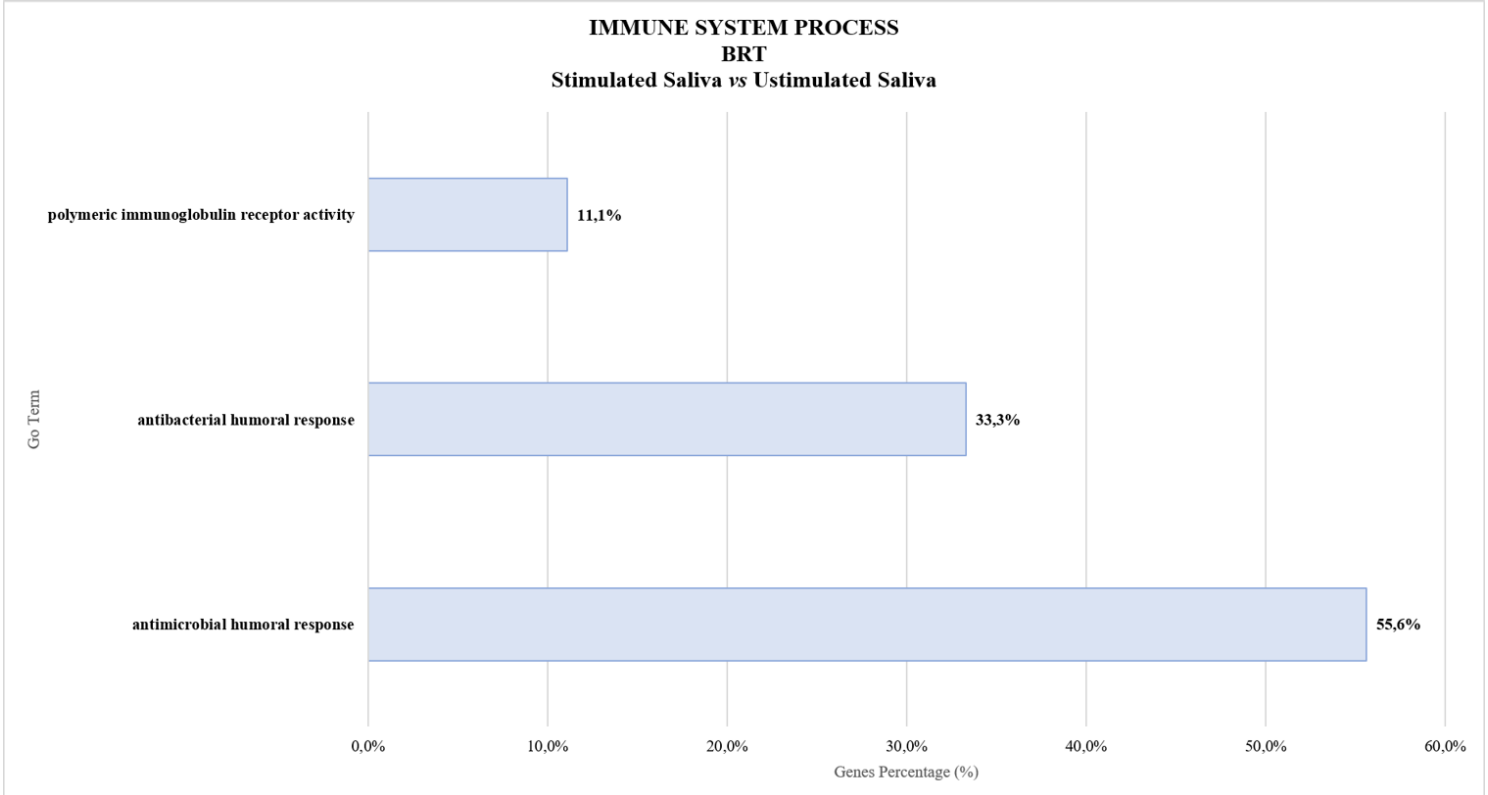
IMMUNE SYSTEM PROCESS
BRT
Stimulated Saliva vs Ustimulated Saliva
Go Term
polymeric immunoglobulin receptor activity
antibacterial humoral response
antimicrobial humoral response
11,1%
33,3%
55,6%
0,0%
10,0%
20,0%
30,0%
40,0%
50,0%
60,0%
Genes Percentage (%)

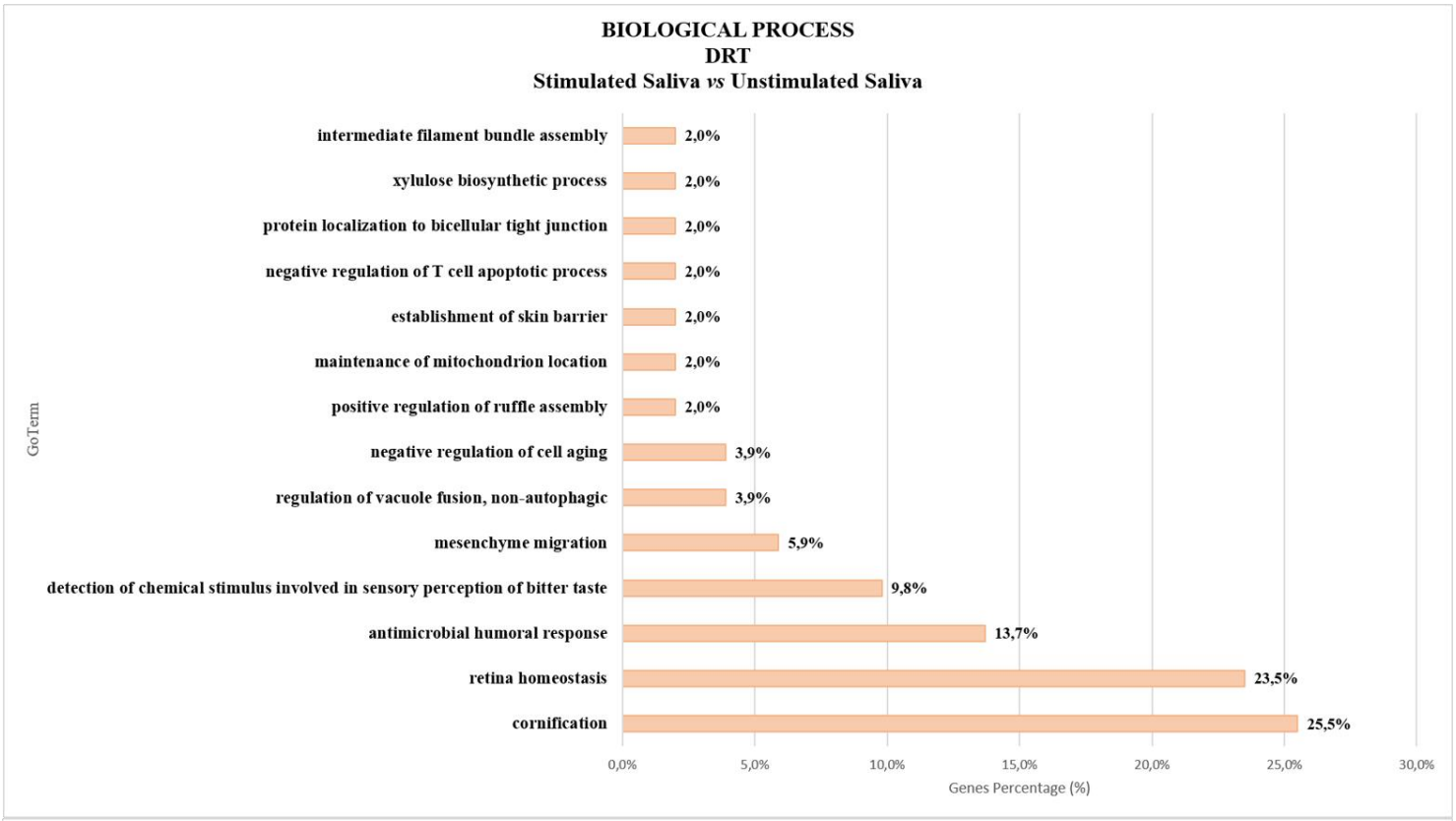
BIOLOGICAL PROCESS
DRT
Stimulated Saliva vs Unstimulated Saliva
GoTerm
intermediate filament bundle assembly
xylulose biosynthetic process
protein localization to bicellular tight junction
negative regulation of T cell apoptotic process
establishment of skin barrier
maintenance of mitochondrion location
positive regulation of ruffle assembly
negative regulation of cell aging
regulation of vacuole fusion, non-autophagic
mesenchyme migration
detection of chemical stimulus involved in sensory perception of bitter taste
antimicrobial humoral response
retina homeostasis
cornification
2,0%
2,0%
2,0%
2,0%
2,0%
2,0%
2,0%
3,9%
3,9%
5,9%
9,8%
13,7%
23,5%
25,5%
0,0% 5,0% 10,0% 15,0% 20,0% 25,0% 30,0%
Genes Percentage (%)

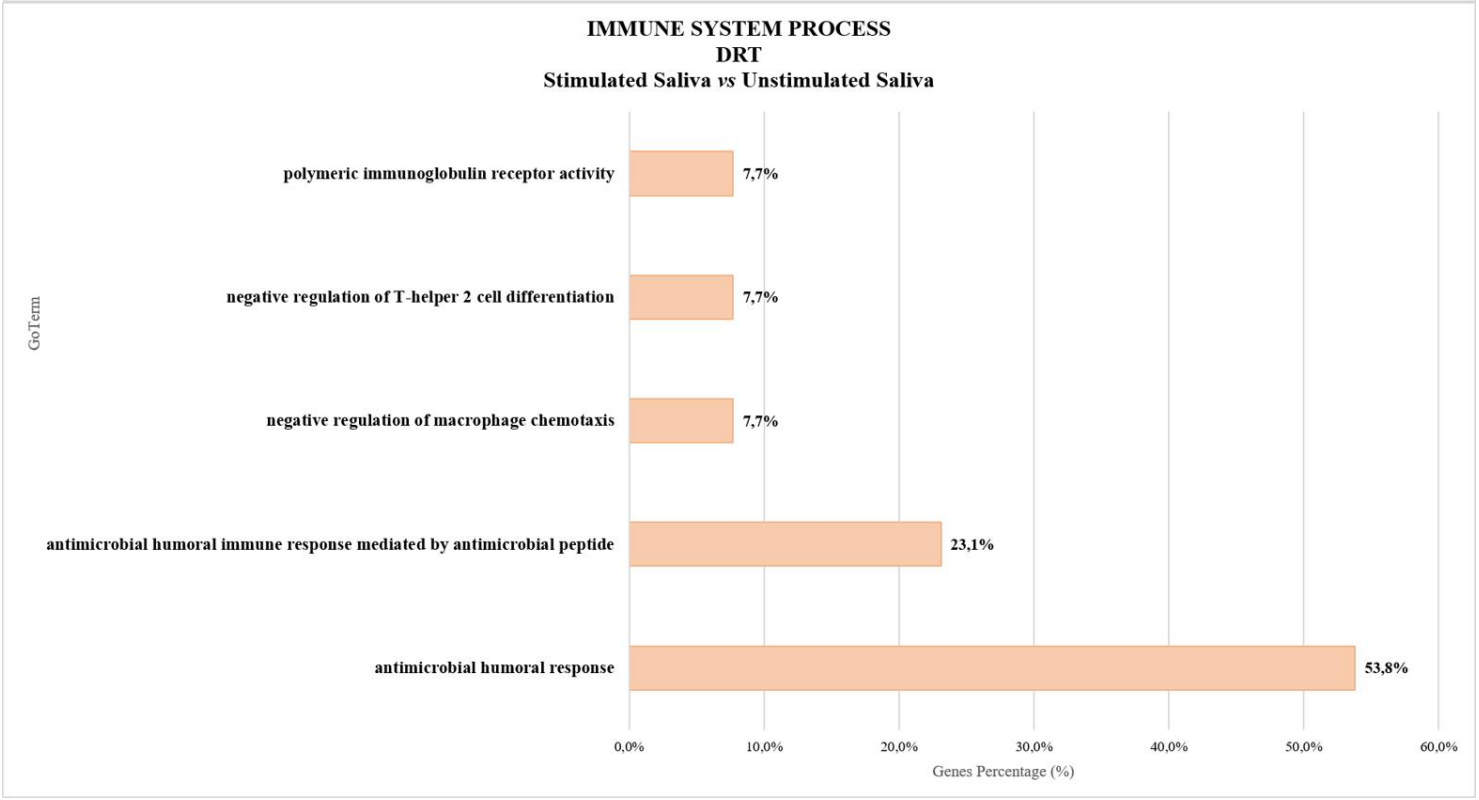
IMMUNE SYSTEM PROCESS
DRT
Stimulated Saliva vs Unstimulated Saliva
GoTerm
polymeric immunoglobulin receptor activity
negative regulation of T-helper 2 cell differentiation
negative regulation of macrophage chemotaxis
antimicrobial humoral immune response mediated by antimicrobial peptide
antimicrobial humoral response
7,7%
7,7%
7,7%
23,1%
53,8%
0,0% 10,0% 20,0% 30,0% 40,0% 50,0% 60,0%
Genes Percentage (%)

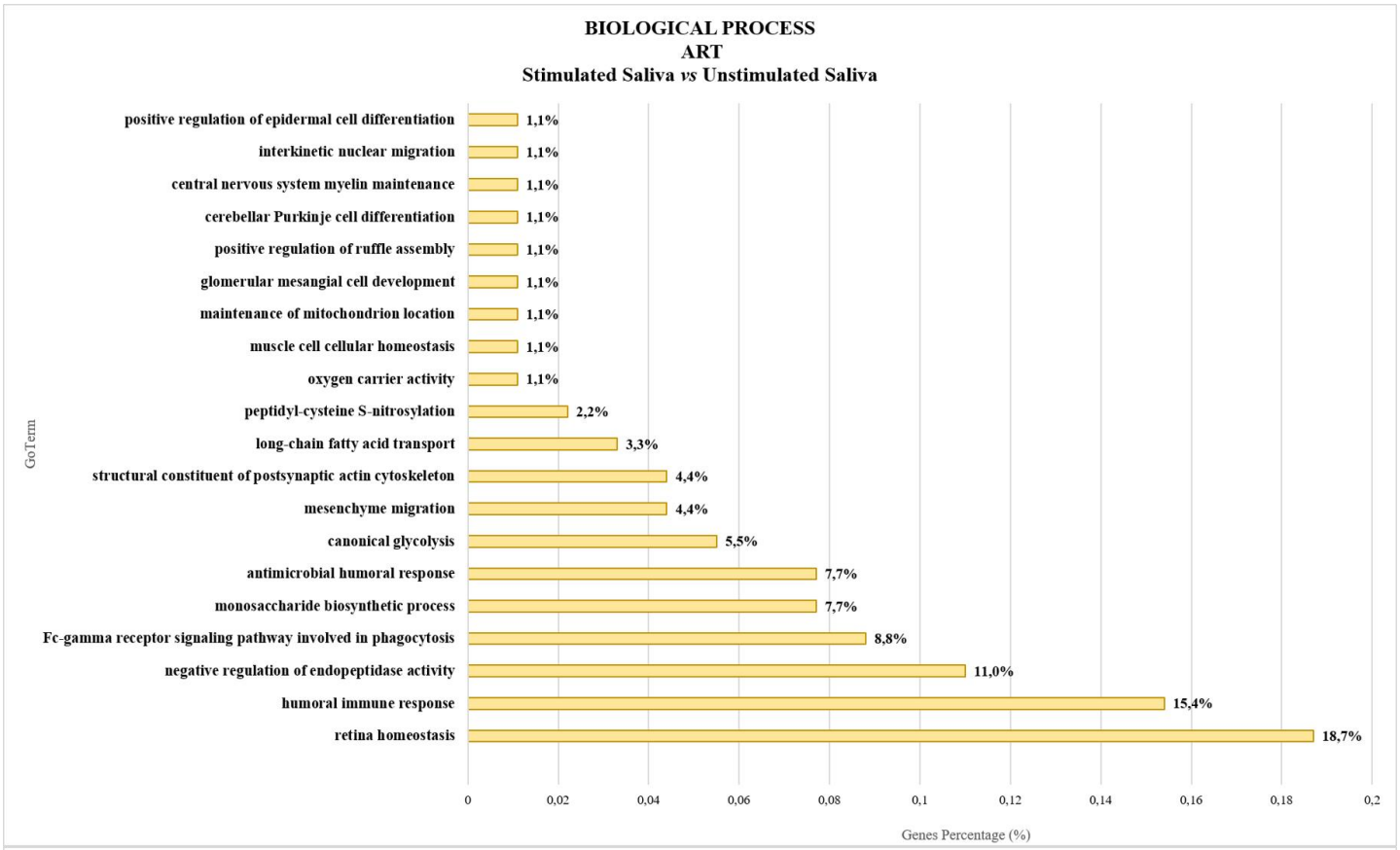
BIOLOGICAL PROCESS
ART
Stimulated Saliva vs Unstimulated Saliva
positive regulation of epidermal cell differentiation 1,1%
interkinetic nuclear migration 1,1%
central nervous system myelin maintenance 1,1%
cerebellar Purkinje cell differentiation 1,1%
positive regulation of ruffle assembly 1,1%
glomerular mesangial cell development 1,1%
maintenance of mitochondrion location 1,1%
muscle cell cellular homeostasis 1,1%
oxygen carrier activity 1,1%
peptidyl-cysteine S-nitrosylation 2,2%
long-chain fatty acid transport 3,3%
structural constituent of postsynaptic actin cytoskeleton 4,4%
mesenchyme migration 4,4%
canonical glycolysis 5,5%
antimicrobial humoral response 7,7%
monosaccharide biosynthetic process 7,7%
Fc-gamma receptor signaling pathway involved in phagocytosis 8,8%
negative regulation of endopeptidase activity 11,0%
humoral immune response 15,4%
retina homeostasis 18,7%
GoTerm
0 0,02 0,04 0,06 0,08 0,1 0,12 0,14 0,16 0,18 0,2
Genes Percentage (%)

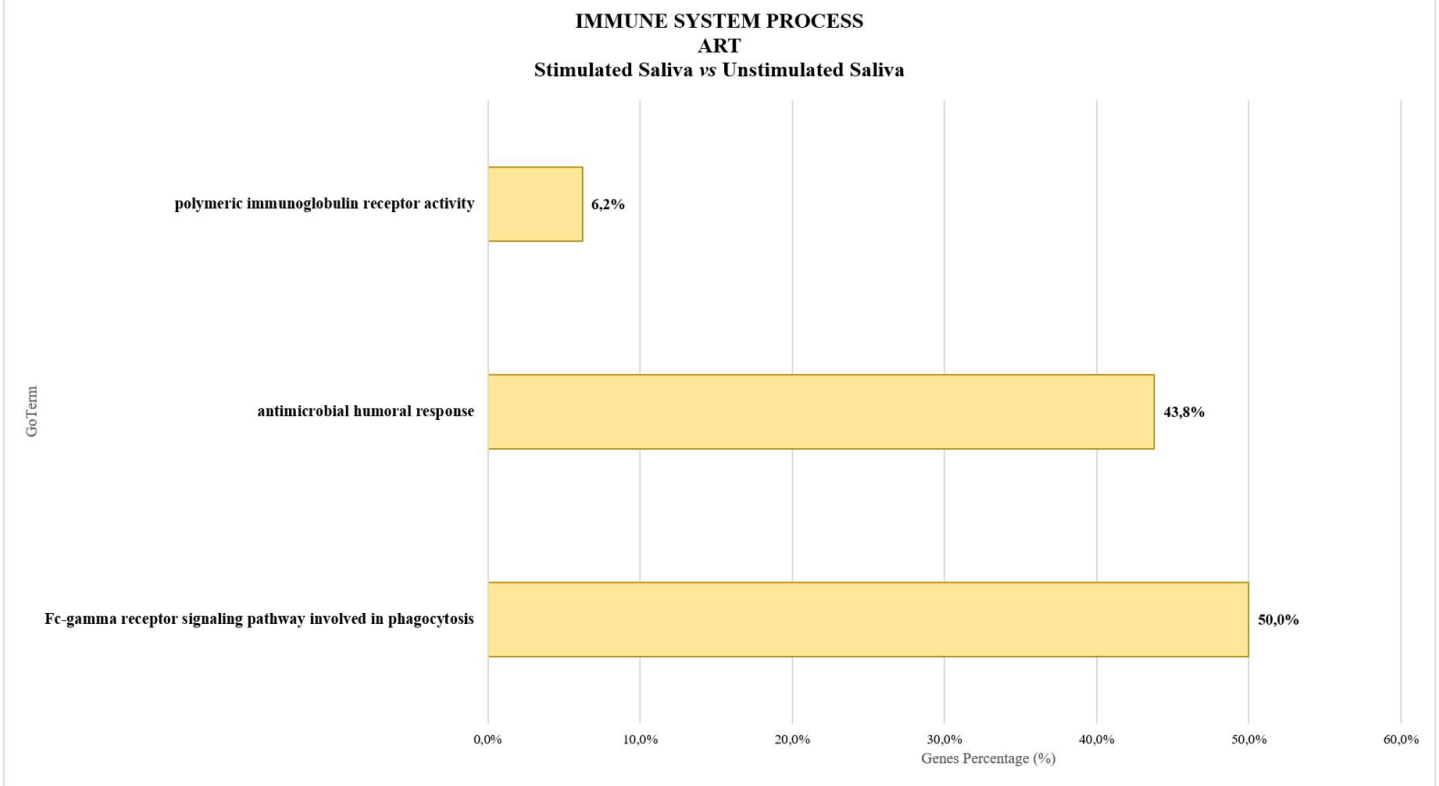
IMMUNE SYSTEM PROCESS
ART
Stimulated Saliva vs Unstimulated Saliva
polymeric immunoglobulin receptor activity 6,2%
antimicrobial humoral response 43,8%
Fc-gamma receptor signaling pathway involved in phagocytosis 50,0%
GoTerm
0,0% 10,0% 20,0% 30,0% 40,0% 50,0% 60,0%
Genes Percentage (%)

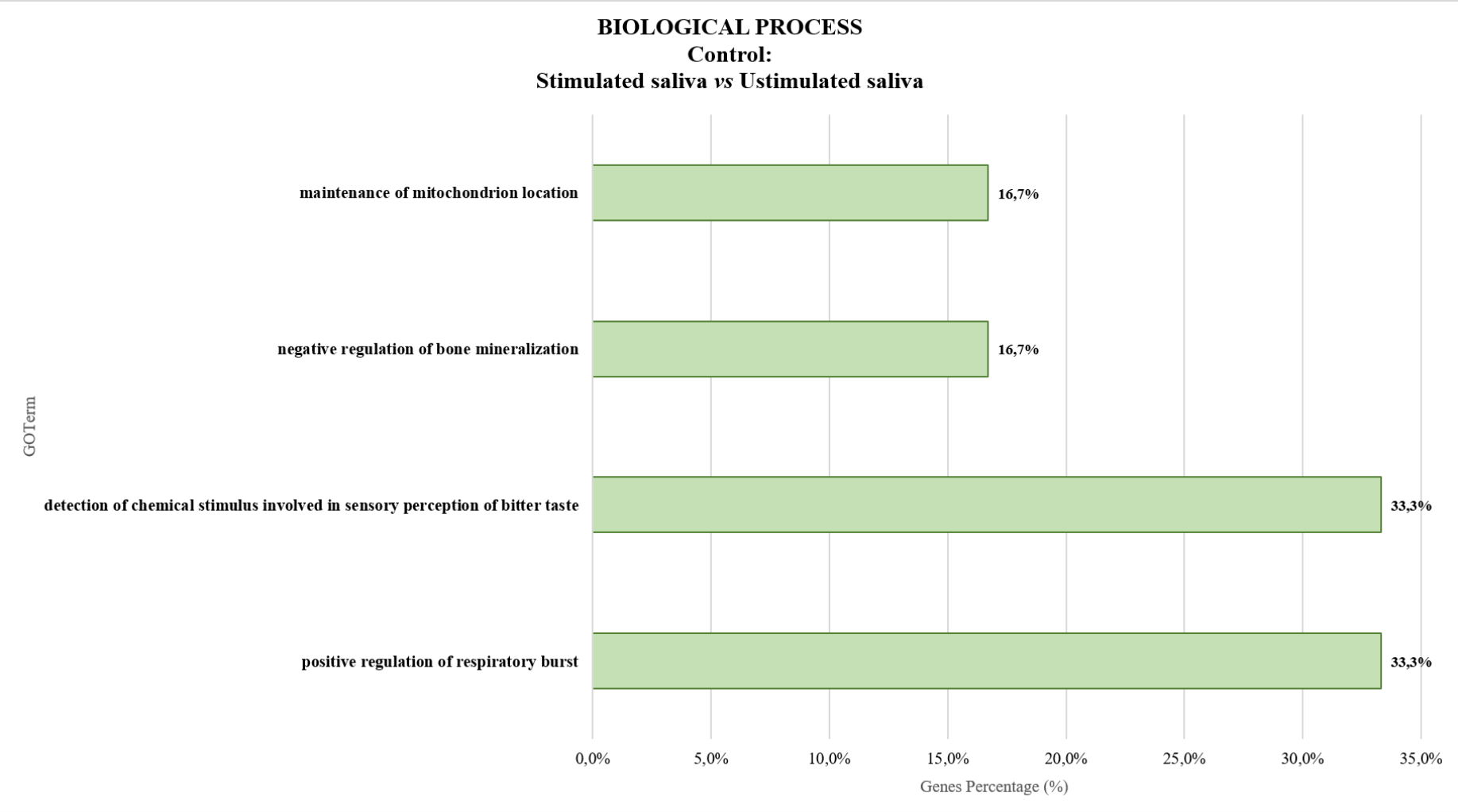
BIOLOGICAL PROCESS
Control:
Stimulated saliva *vs* Ustimulated saliva
maintenance of mitochondrion location
16,7%
negative regulation of bone mineralization
16,7%
detection of chemical stimulus involved in sensory perception of bitter taste
33,3%
positive regulation of respiratory burst
33,3%
GOTerm
0,0%
5,0%
10,0%
15,0%
20,0%
25,0%
30,0%
35,0%
Genes Percentage (%)

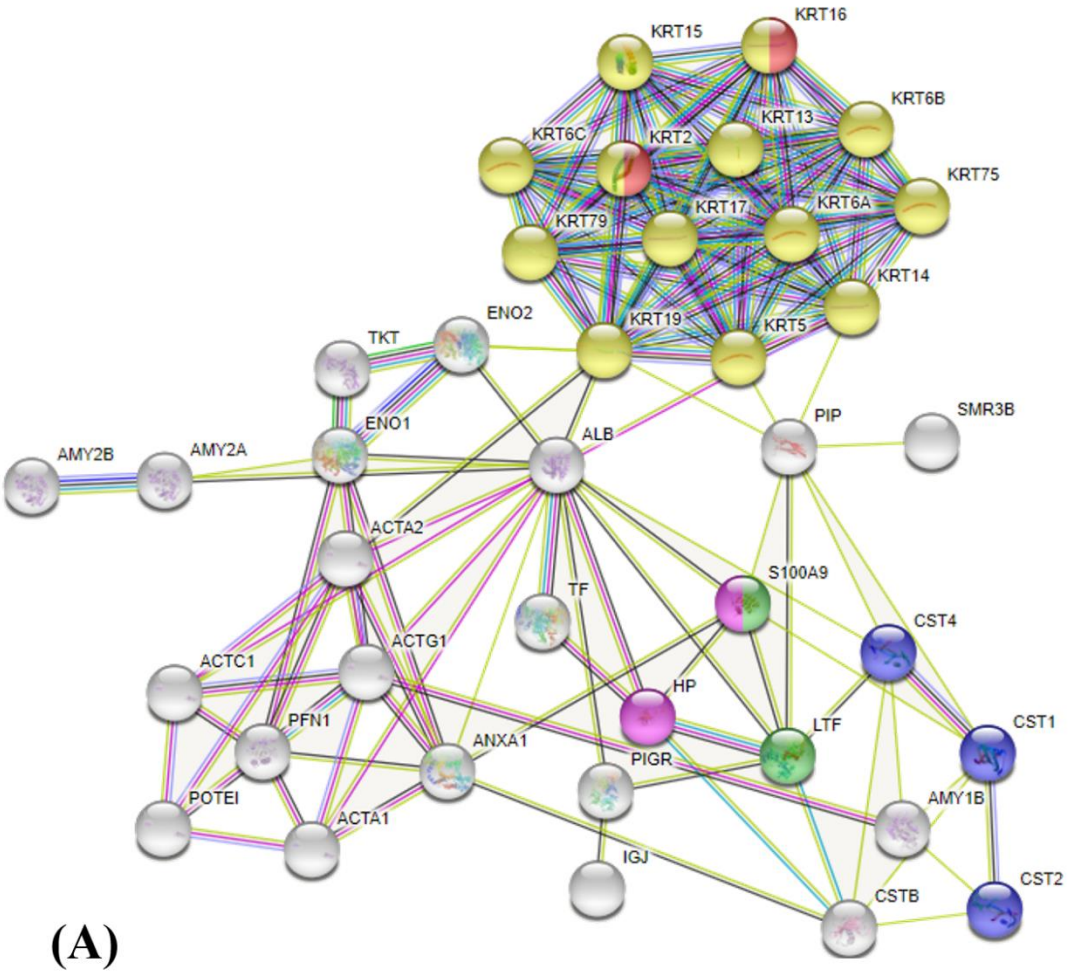
KRT16
KRT15
KRT6B
KRT13
KRT6C
KRT2
KRT75
KRT17
KRT6A
KRT79
KRT14
ENO2
KRT19
KRT5
TKT
PIP
SMR3B
ENO1
ALB
AMY2B
AMY2A
ACTA2
S100A9
TF
CST4
ACTG1
ACTC1
HP
PFN1
LTF
CST1
ANXA1
PIGR
AMY1B
POTEI
ACTA1
IGJ
CSTB
CST2
(A)

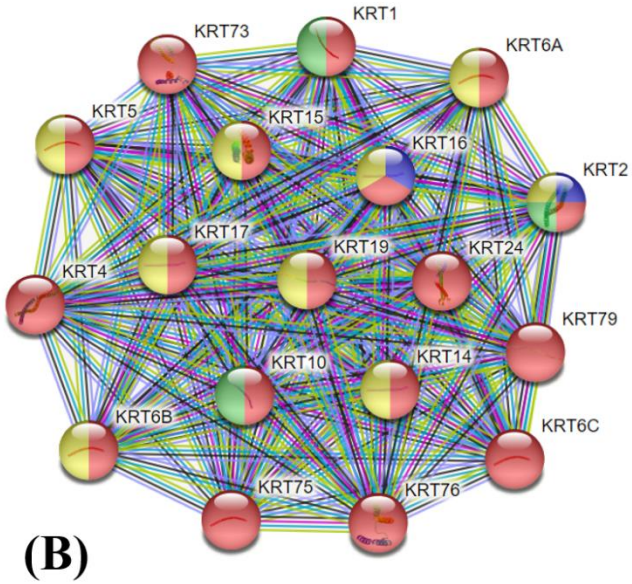
KRT1
KRT73
KRT6A
KRT5
KRT15
KRT16
KRT2
KRT17
KRT19
KRT24
KRT4
KRT79
KRT10
KRT14
KRT6B
KRT6C
KRT75
KRT76
(B)

Table 1. Patients information with HNC regarding gender, age, affected site of cancer, lifestyle and grade of mucositis.

Patients	Gender	Age	Ex-smoker and Ex-drinkers	Affected sites of cancer	Mucositis
1.	male	49	Yes	Oropharynx Carcinoma and Tongue Base	Grade I and II
*2.	male	72	Yes	Occult grade III Squamous Cell Carcinoma with cervical metastasis	Grade II
*3.	male	65	Yes	Tongue Squamous Cell Carcinoma	Grade II and III
4.	female	34	Yes	Tongue Squamous Cell Carcinoma	Grade II
5.	male	58	Yes	Tongue Squamous Cell Carcinoma	Grade II and III
*6.	male	44	Yes	Esophagus Squamous Cell Carcinoma and Amygdala	Grade II
*7.	male	52	Yes	Retromolar Trigone (Jaw) Squamous Cell Carcinoma	Grade III
*8.	male	55	Yes	Tongue Squamous Cell Carcinoma	Grade II and III
*9.	female	67	Yes	Hypopharyngeal Squamous Cell Carcinoma	Grade II

*Patients who presented problems such as dental restorations, dental caries, periodontitis or needed tooth extraction were treated before starting radiotherapy.

Table 2. Mean µg protein and Mean ± standard deviation (SD) or Median and interquartile range (IQR) for stimulated and unstimulated salivary flow from HNC patients before radiotherapy (BRT), during radiotherapy (DRT), after radiotherapy (ART) and Control (healthy patients).

Groups	Mean µg protein stimulated salivary flow	Mean µg protein unstimulated salivary flow	Stimulated salivary flow (mL/min)	Unstimulated salivary flow (mL/min)
			Mean ± SD	**Mean ± SD**
Control	113.10 µg	60.05 µg	2.29±1.27 [a]	0.89±0.40 [b]
BRT	51.96 µg	84.18 µg	1.24±0.64 [a]	0.49±0.29 [b]
			Median (IQR)	**Median (IQR)**
DRT	114.00 µg	114.07 µg	0.20 (0.06-0.30) [a]	0.10 (0.020-0.023) [a]
ART	108.95 µg	131.73 µg	0.01 (0.00-0.04) [a]	0.02 (0.01-0.08) [a]

Analyzing the salivary flow (stimulated and unstimulated), distinct lowercase letters denote significant differences ($p<0.05$) between the different salivary flows for the same group. n=9.

Supplementary Tables

Supplementary Table 1. Proteins with significantly altered expression in the stimulated saliva in comparison with Unstimulated saliva before radiotherapy (BRT) in patients with head and neck cancer.

[+]Access number	Protein name	PLGS Score	*Ratio BRT Stimulated:Unstimulated
Q99470	Stromal cell-derived factor 2	244	1.40
P0CG38	POTE ankyrin domain family member I	568	1.34
Q562R1	Beta-actin-like protein 2	342	0.80
P63267	Actin_ gamma-enteric smooth muscle	900	0.80
P02814	Submaxillary gland androgen-regulated protein 3B	11077	0.79
P68133	Actin_ alpha skeletal muscle	900	0.76
P68032	Actin_ alpha cardiac muscle 1	900	0.75
P04746	Pancreatic alpha-amylase	19253	0.69
P63261	Actin_ cytoplasmic 2	2588	0.68
P15515	Histatin-1	337	0.60
P60709	Actin_ cytoplasmic 1	2588	0.59
P01876	Immunoglobulin heavy constant alpha 1	6416	0.59
A0A2R8Y7X9	GLOBIN domain-containing protein	347	0.57
Q4KMG0	Cell adhesion molecule-related/down-regulated by oncogenes	472	0.57
P69891	Hemoglobin subunit gamma-1	347	0.55
P01037	Cystatin-SN	7696	0.52
Q9NYZ2	Mitoferrin-1	556	0.52
P02042	Hemoglobin subunit delta	347	0.51
P02100	Hemoglobin subunit epsilon	347	0.51
P62736	**Actin_ aortic smooth muscle**	**900**	**0.50**
P01877	**Immunoglobulin heavy constant alpha 2**	**4993**	**0.50**
P01833	**Polymeric immunoglobulin receptor**	**1595**	**0.46**
P02810	**Salivary acidic proline-rich phosphoprotein 1/2**	**17610**	**0.46**
Q9BYX7	**Putative beta-actin-like protein 3**	**2302**	**0.45**
P04080	**Cystatin-B**	**437**	**0.41**
Q68CZ1	**Protein fantom**	**270**	**0.38**
P04745	**Alpha-amylase 1**	**26013**	**0.36**
S4R460	**Immunoglobulin heavy variable 3/OR16-9 (non-functional)**	**1623**	**0.36**
P19961	**Alpha-amylase 2B**	**20507**	**0.36**
A0A0A0MT31	**Proline-rich protein 4**	**17610**	**0.34**
A0A087WZY1	**Uncharacterized protein**	**11462**	**0.33**
E5RG79	**Zinc finger homeobox protein 4 (Fragment)**	**380**	**0.31**
C9JKR2	**Albumin_ isoform CRA_k**	**4089**	**0.30**
Q03112	**Histone-lysine N-methyltransferase MECOM**	**422**	**0.30**
P02808	**Statherin**	**6072**	**0.25**
P23280	**Carbonic anhydrase 6**	**1175**	**0.23**
P14138	**Endothelin-3**	**454**	**0.22**

P01591	**Immunoglobulin J chain**	**3631**	**0.21**
P01834	**Immunoglobulin kappa constant**	**2293**	**0.21**
Q8N4F0	**BPI fold-containing family B member 2**	**1052**	**0.19**
P01034	**Cystatin-C**	**567**	**0.18**
P02768	**Serum albumin**	**7856**	**0.16**
P01036	**Cystatin-S**	**11830**	**0.15**
P09228	**Cystatin-SA**	**6668**	**0.13**
G3V1N2	**HCG1745306_ isoform CRA_a**	**4936**	**0.12**
P69905	**Hemoglobin subunit alpha**	**8233**	**0.12**
P68871	**Hemoglobin subunit beta**	**347**	**0.11**
P12273	**Prolactin-inducible protein**	**5504**	**0.11**
P31025	**Lipocalin-1**	**5611**	**0.07**
Q5VSP4	**Putative lipocalin 1-like protein 1**	**1428**	**0.07**
P04280	**Basic salivary proline-rich protein 1**	**11098**	**0.05**
P02812	**Basic salivary proline-rich protein 2**	**13300**	**0.02**
Q6VVX0	**Vitamin D 25-hydroxylase**	**822**	**0.01**
O96019	Actin-like protein 6A	251	˚Stimulated saliva
A0A087WZA0	Adhesion G-protein-coupled receptor G5	227	˚Stimulated saliva
Q9BTE6	Alanyl-tRNA editing protein Aarsd1	329	˚Stimulated saliva
Q8N957	Ankyrin repeat and fibronectin type-III domain-containing protein 1	132	˚Stimulated saliva
Q9UKV3	Apoptotic chromatin condensation inducer in the nucleus	391	˚Stimulated saliva
Q9P2R6	Arginine-glutamic acid dipeptide repeats protein	402	˚Stimulated saliva
Q14562	ATP-dependent RNA helicase DHX8	416	˚Stimulated saliva
Q8WXE1	ATR-interacting protein	286	˚Stimulated saliva
Q9Y2J2	Band 4.1-like protein 3	199	˚Stimulated saliva
P55286	Cadherin-8	555	˚Stimulated saliva
Q9HC52	Chromobox protein homolog 8	464	˚Stimulated saliva
F8WCC1	Chromosome transmission fidelity protein 18 homolog	125	˚Stimulated saliva
Q16630	Cleavage and polyadenylation specificity factor subunit 6	391	˚Stimulated saliva
Q5T0U0	Coiled-coil domain-containing protein 122	247	˚Stimulated saliva
Q96P44	Collagen alpha-1(XXI) chain	81	˚Stimulated saliva
P42695	Condensin-2 complex subunit D3	156	˚Stimulated saliva
J3KQV6	COP9 signalosome complex subunit 7b	821	˚Stimulated saliva
Q96HV7	CPSF3L protein	416	˚Stimulated saliva
O95476	CTD nuclear envelope phosphatase 1	524	˚Stimulated saliva
A0A0A0MQR0	Cytochrome P450_ family 4_ subfamily F_ polypeptide 2_ isoform CRA_a	258	˚Stimulated saliva
Q8IYX4	Dead end protein homolog 1	277	˚Stimulated saliva
Q2KHR2	DNA-binding protein RFX7	91	˚Stimulated saliva
P42892	Endothelin-converting enzyme 1	114	˚Stimulated saliva
Q9H6S3	Epidermal growth factor receptor kinase substrate 8-like protein 2	270	˚Stimulated saliva
Q14152	Eukaryotic translation initiation factor 3 subunit A	391	˚Stimulated saliva
Q9NRA8	Eukaryotic translation initiation factor 4E transporter	391	˚Stimulated saliva

Q9BRP7	Ferredoxin-fold anticodon-binding domain-containing protein 1	318	˚Stimulated saliva
P09211	Glutathione S-transferase P	536	˚Stimulated saliva
Q8IWJ2	GRIP and coiled-coil domain-containing protein 2	176	˚Stimulated saliva
J3KQ12	HCG2020143_ isoform CRA_b	420	˚Stimulated saliva
Q8WYH8	Inhibitor of growth protein 5	169	˚Stimulated saliva
Q6GPH6	Inositol 1_4_5-trisphosphate receptor-interacting protein-like 1	122	˚Stimulated saliva
Q5TA45	Integrator complex subunit 11	416	˚Stimulated saliva
Q86UP2	Kinectin	604	˚Stimulated saliva
Q9Y234	Lipoyltransferase 1_ mitochondrial	414	˚Stimulated saliva
A0A087WZ62	Mannosyltransferase	318	˚Stimulated saliva
Q9Y2X0	Mediator of RNA polymerase II transcription subunit 16	287	˚Stimulated saliva
E7EVA0	Microtubule-associated protein	367	˚Stimulated saliva
B5MEG9	Microtubule-associated protein 4 (Fragment)	357	˚Stimulated saliva
O43148	mRNA cap guanine-N7 methyltransferase	178	˚Stimulated saliva
P26651	mRNA decay activator protein ZFP36	255	˚Stimulated saliva
O95394	Phosphoacetylglucosamine mutase	261	˚Stimulated saliva
P78329	Phylloquinone omega-hydroxylase CYP4F2	258	˚Stimulated saliva
Q6UN15	Pre-mRNA 3'-end-processing factor FIP1	391	˚Stimulated saliva
Q5VTL8	Pre-mRNA-splicing factor 38B	391	˚Stimulated saliva
O43143	Pre-mRNA-splicing factor ATP-dependent RNA helicase DHX15	391	˚Stimulated saliva
Q86U06	Probable RNA-binding protein 23	191	˚Stimulated saliva
Q9UKY7	Protein CDV3 homolog	465	˚Stimulated saliva
Q9C073	Protein FAM117A	287	˚Stimulated saliva
J3KT97	Protein Njmu-R1 (Fragment)	338	˚Stimulated saliva
Q13522	Protein phosphatase 1 regulatory subunit 1A	160	˚Stimulated saliva
Q9Y520	Protein PRRC2C	447	˚Stimulated saliva
A0A0C4DGW5	Protein Red	391	˚Stimulated saliva
F8WED9	Protein SSUH2 homolog	146	˚Stimulated saliva
A0A0A0MRN0	PRP38 pre-mRNA processing factor 38 (Yeast) domain containing B_ isoform CRA_b	391	˚Stimulated saliva
R4GMN3	Pulmonary surfactant-associated protein A2 (Fragment)	875	˚Stimulated saliva
Q96I85	Putative uncharacterized protein C14orf144	395	˚Stimulated saliva
Q16849	Receptor-type tyrosine-protein phosphatase-like N	137	˚Stimulated saliva
A6NHM7	Rho GTPase activating protein 22_ isoform CRA_a	98	˚Stimulated saliva
Q5T5U3	Rho GTPase-activating protein 21	40	˚Stimulated saliva
Q7Z5H3	Rho GTPase-activating protein 22	98	˚Stimulated saliva
P49756	RNA-binding protein 25	404	˚Stimulated saliva
P52756	RNA-binding protein 5	143	˚Stimulated saliva
Q96G97	Seipin	420	˚Stimulated saliva
Q8IYP2	Serine protease 58	121	˚Stimulated saliva
Q15772	Striated muscle preferentially expressed protein kinase	55	˚Stimulated saliva

Q15572	TATA box-binding protein-associated factor RNA polymerase I subunit C	265	˚Stimulated saliva
Q8NI27	THO complex subunit 2	473	˚Stimulated saliva
Q6P4D7	TM6SF1 protein	522	˚Stimulated saliva
Q12888	TP53-binding protein 1	82	˚Stimulated saliva
Q8TDR0	TRAF3-interacting protein 1	391	˚Stimulated saliva
Q9BZW5	Transmembrane 6 superfamily member 1	534	˚Stimulated saliva
A0A0A0MR82	Transmembrane protease serine	101	˚Stimulated saliva
Q6ZMR5	Transmembrane protease serine 11A	101	˚Stimulated saliva
F8VP39	Transmembrane protein 116	548	˚Stimulated saliva
Q6ZMB5	Transmembrane protein 184A	278	˚Stimulated saliva
A0A0G2JIV5	TRIM40	342	˚Stimulated saliva
O14717	tRNA (cytosine(38)-C(5))-methyltransferase	341	˚Stimulated saliva
P08621	U1 small nuclear ribonucleoprotein 70 kDa	391	˚Stimulated saliva
Q9NPG3	Ubinuclein-1	172	˚Stimulated saliva
H3BRL3	Ubiquitin domain-containing protein UBFD1	150	˚Stimulated saliva
Q3KQV9	UDP-N-acetylhexosamine pyrophosphorylase-like protein 1	184	˚Stimulated saliva
Q8IYS4	Uncharacterized protein C16orf71	135	˚Stimulated saliva
Q96F83	Uncharacterized protein CLBA1	89	˚Stimulated saliva
Q8TBC5	Zinc finger and SCAN domain-containing protein 18	70	˚Stimulated saliva
H7C1I7	Zinc finger MYM-type protein 4 (Fragment)	94	˚Stimulated saliva
Q12901	Zinc finger protein 155	210	˚Stimulated saliva
Q9UK13	Zinc finger protein 221	219	˚Stimulated saliva
M0QY76	Zinc finger protein 36_ C3H type_ homolog (Mouse)_ isoform CRA_a	255	˚Stimulated saliva
Q86XE5	4-hydroxy-2-oxoglutarate aldolase_ mitochondrial	502	˚Unstimulated saliva
F5H5C3	Acetyl-CoA carboxylase 2 (Fragment)	273	˚Unstimulated saliva
Q6VMQ6	Activating transcription factor 7-interacting protein 1	478	˚Unstimulated saliva
Q8IUX7	Adipocyte enhancer-binding protein 1	354	˚Unstimulated saliva
P01023	Alpha-2-macroglobulin	71	˚Unstimulated saliva
Q9H4A4	Aminopeptidase B	328	˚Unstimulated saliva
P51693	Amyloid-like protein 1	210	˚Unstimulated saliva
K7ENE0	Ankyrin repeat domain-containing protein 27	346	˚Unstimulated saliva
C9JP59	Ankyrin repeat_ SAM and basic leucine zipper domain-containing protein 1 (Fragment)	1159	˚Unstimulated saliva
P02647	Apolipoprotein A-I	596	˚Unstimulated saliva
Q8NFD5	AT-rich interactive domain-containing protein 1B	95	˚Unstimulated saliva
D6R9B7	Axonemal dynein light chain domain-containing protein 1 (Fragment)	744	˚Unstimulated saliva
P61769	Beta-2-microglobulin	791	˚Unstimulated saliva
Q96DR5	BPI fold-containing family A member 2	252	˚Unstimulated saliva
Q8TDL5	BPI fold-containing family B member 1	336	˚Unstimulated saliva
Q9NQY0	Bridging integrator 3	880	˚Unstimulated saliva
H7C555	Cadherin-related family member 3 (Fragment)	272	˚Unstimulated saliva
E7EMB3	Calmodulin-2	533	˚Unstimulated saliva

P48509	CD151 antigen	283	°Unstimulated saliva
E9PMT5	CD3 delta	588	°Unstimulated saliva
P16070	CD44 antigen	448	°Unstimulated saliva
B7Z4G8	cDNA FLJ56046_ highly similar to Amyloid-like protein 1 (APLP)(APLP-1)	210	°Unstimulated saliva
A0A2R8Y7X1	Chromodomain-helicase-DNA-binding protein 4 (Fragment)	382	°Unstimulated saliva
F8VXK5	Chromosome 12 open reading frame 75	1155	°Unstimulated saliva
J3KPP4	Cisplatin resistance-associated overexpressed protein_ isoform CRA_b	204	°Unstimulated saliva
Q6ZUT6	Coiled-coil domain-containing protein 9B	355	°Unstimulated saliva
H3BRY3	Coronin	476	°Unstimulated saliva
P31146	Coronin-1A	520	°Unstimulated saliva
C9J4L5	Cyclic AMP-responsive element-binding protein 1 (Fragment)	344	°Unstimulated saliva
P28325	Cystatin-D	5265	°Unstimulated saliva
Q8NDL9	Cytosolic carboxypeptidase-like protein 5	358	°Unstimulated saliva
F8VUV1	D(2) dopamine receptor	153	°Unstimulated saliva
E5RI01	Double-strand-break repair protein rad21 homolog	468	°Unstimulated saliva
Q9H4C3	E3 ubiquitin-protein ligase Mdm2	390	°Unstimulated saliva
Q8NFF5	FAD synthase	216	°Unstimulated saliva
H0YIY4	Gephyrin (Fragment)	455	°Unstimulated saliva
A0A1C7CYW1	Glycogen debranching enzyme	241	°Unstimulated saliva
P16260	Graves disease carrier protein	411	°Unstimulated saliva
Q9BXW7	Haloacid dehalogenase-like hydrolase domain-containing 5	297	°Unstimulated saliva
P00738	Haptoglobin	293	°Unstimulated saliva
Q09028	Histone-binding protein RBBP4	524	°Unstimulated saliva
P01857	Immunoglobulin heavy constant gamma 1	239	°Unstimulated saliva
P01871	Immunoglobulin heavy constant mu	416	°Unstimulated saliva
P0CG04	Immunoglobulin lambda constant 1	2955	°Unstimulated saliva
P0DOY2	Immunoglobulin lambda constant 2	2980	°Unstimulated saliva
P0DOY3	Immunoglobulin lambda constant 3	2980	°Unstimulated saliva
P0CF74	Immunoglobulin lambda constant 6	553	°Unstimulated saliva
A0M8Q6	Immunoglobulin lambda constant 7	553	°Unstimulated saliva
B9A064	Immunoglobulin lambda-like polypeptide 5	2955	°Unstimulated saliva
Q9NVH2	Integrator complex subunit 7	443	°Unstimulated saliva
P13598	Intercellular adhesion molecule 2	232	°Unstimulated saliva
Q9P2K6	Kelch-like protein 42	258	°Unstimulated saliva
K7EJK4	KRAB domain-containing protein	1200	°Unstimulated saliva
P22079	Lactoperoxidase	453	°Unstimulated saliva
P02788	Lactotransferrin	268	°Unstimulated saliva
Q9HCC9	Lateral signaling target protein 2 homolog	576	°Unstimulated saliva
Q6GTX8	Leukocyte-associated immunoglobulin-like receptor 1	611	°Unstimulated saliva
P50851	Lipopolysaccharide-responsive and beige-like anchor protein	304	°Unstimulated saliva
O75145	Liprin-alpha-3	130	°Unstimulated saliva
O95232	Luc7-like protein 3	204	°Unstimulated saliva

Q9UGL1	Lysine-specific demethylase 5B	803	°Unstimulated saliva
Q9BY66	Lysine-specific demethylase 5D	113	°Unstimulated saliva
P38571	Lysosomal acid lipase/cholesteryl ester hydrolase	183	°Unstimulated saliva
Q86VI4	Lysosomal-associated transmembrane protein 4B	365	°Unstimulated saliva
P43243	Matrin-3	515	°Unstimulated saliva
A0A0D9SF86	Membrane-associated guanylate kinase_ WW and PDZ domain-containing protein 2 (Fragment)	529	°Unstimulated saliva
H7C4V5	Metabotropic glutamate receptor 8 (Fragment)	337	°Unstimulated saliva
O75121	Microfibrillar-associated protein 3-like	221	°Unstimulated saliva
P46821	Microtubule-associated protein 1B	324	°Unstimulated saliva
Q9Y2H9	Microtubule-associated serine/threonine-protein kinase 1	246	°Unstimulated saliva
Q9NZJ7	Mitochondrial carrier homolog 1	315	°Unstimulated saliva
Q8TAX7	Mucin-7	430	°Unstimulated saliva
Q86WG5	Myotubularin-related protein 13	207	°Unstimulated saliva
P03897	NADH-ubiquinone oxidoreductase chain 3	390	°Unstimulated saliva
Q6ZS30	Neurobeachin-like protein 1	293	°Unstimulated saliva
Q99574	Neuroserpin	277	°Unstimulated saliva
H7C1V7	N-glycosylase/DNA lyase (Fragment)	394	°Unstimulated saliva
Q9UKX7	Nuclear pore complex protein Nup50	348	°Unstimulated saliva
Q9UMX2	Ornithine decarboxylase antizyme 3	631	°Unstimulated saliva
Q06710	Paired box protein Pax-8	316	°Unstimulated saliva
P42356	Phosphatidylinositol 4-kinase alpha	200	°Unstimulated saliva
E9PSF8	Phosphatidylinositol 4-phosphate 5-kinase type-1 alpha	480	°Unstimulated saliva
Q9UJ90	Potassium voltage-gated channel subfamily E regulatory beta subunit 5	325	°Unstimulated saliva
Q16557	Pregnancy-specific beta-1-glycoprotein 3	457	°Unstimulated saliva
Q5W0V3	Protein FAM160B1	204	°Unstimulated saliva
A1A519	Protein FAM170A	302	°Unstimulated saliva
Q6P5S2	Protein LEG1 homolog	1304	°Unstimulated saliva
B5MCF8	Protein Mpv17	427	°Unstimulated saliva
Q5JR12	Protein phosphatase 1J	258	°Unstimulated saliva
Q8NHS7	PTPRS protein	517	°Unstimulated saliva
Q6ZTU2	Putative EP400-like protein	312	°Unstimulated saliva
A4QPH2	Putative phosphatidylinositol 4-kinase alpha-like protein P2	162	°Unstimulated saliva
Q9HBR0	Putative sodium-coupled neutral amino acid transporter 10	350	°Unstimulated saliva
Q14D33	Receptor-transporting protein 5	2899	°Unstimulated saliva
Q13332	Receptor-type tyrosine-protein phosphatase S	517	°Unstimulated saliva
Q9P2N2	Rho GTPase-activating protein 28	630	°Unstimulated saliva
O94989	Rho guanine nucleotide exchange factor 15	370	°Unstimulated saliva
P02787	Serotransferrin	412	°Unstimulated saliva
J3KNC4	Sodium- and chloride-dependent glycine transporter 2	235	°Unstimulated saliva
P32418	Sodium/calcium exchanger 1	376	°Unstimulated saliva

A1L4H1	Soluble scavenger receptor cysteine-rich domain-containing protein SSC5D	386	°Unstimulated saliva
E5RJM7	Solute carrier family 45 member 4 (Fragment)	497	°Unstimulated saliva
Q5T0L3	Spermatogenesis-associated protein 46	638	°Unstimulated saliva
Q86VE3	Spermidine/spermine N(1)-acetyltransferase-like protein 1	519	°Unstimulated saliva
Q8WXA9	Splicing regulatory glutamine/lysine-rich protein 1	242	°Unstimulated saliva
Q12770	Sterol regulatory element-binding protein cleavage-activating protein	506	°Unstimulated saliva
O14994	Synapsin-3	305	°Unstimulated saliva
P18827	Syndecan-1	305	°Unstimulated saliva
A0A087WT01	T cell receptor alpha variable 27	393	°Unstimulated saliva
G3V1T3	TAP binding protein-like_ isoform CRA_c	595	°Unstimulated saliva
Q9BX59	Tapasin-related protein	497	°Unstimulated saliva
Q9BZW7	Testis-specific gene 10 protein	187	°Unstimulated saliva
E9PMR4	Tetraspanin	283	°Unstimulated saliva
Q8NDV7	Trinucleotide repeat-containing gene 6A protein	272	°Unstimulated saliva
A0A2R8Y670	Tuberin (Fragment)	908	°Unstimulated saliva
Q03169	Tumor necrosis factor alpha-induced protein 2	376	°Unstimulated saliva
Q16890	Tumor protein D53	304	°Unstimulated saliva
Q9H972	Uncharacterized protein C14orf93	1167	°Unstimulated saliva
Q9H1L0	Uncharacterized protein MIR1-1HG	387	°Unstimulated saliva
Q8IZS8	Voltage-dependent calcium channel subunit alpha-2/delta-3	362	°Unstimulated saliva
H0YCW7	von Willebrand factor A domain-containing protein 3B (Fragment)	618	°Unstimulated saliva
Q14508	WAP four-disulfide core domain protein 2	982	°Unstimulated saliva
Q5T200	Zinc finger CCCH domain-containing protein 13	234	°Unstimulated saliva
A6NK53	Zinc finger protein 233	391	°Unstimulated saliva
O94892	Zinc finger protein 432	806	°Unstimulated saliva
Q6P3V2	Zinc finger protein 585A	1200	°Unstimulated saliva
Q86XU0	Zinc finger protein 677	494	°Unstimulated saliva
Q9H7X3	Zinc finger protein 696	298	°Unstimulated saliva
Q9Y6R6	Zinc finger protein 780B	560	°Unstimulated saliva
A8MQ14	Zinc finger protein 850	391	°Unstimulated saliva
P25311	Zinc-alpha-2-glycoprotein	858	°Unstimulated saliva

[+]Identification is based on protein ID from UniProt protein database, reviewed only (http://www.uniprot.org/).
[*]Proteins with expression significantly altered are organized according to the ratio.
°Indicates unique protein in alphabetical order.
Proteins highlighted in bold are increased or decreased more than 2-fold.

Supplementary Table 2. Proteins with significantly altered expression in the stimulated saliva in comparison with Unstimulated saliva during radiotherapy (DRT) in patients with head and neck cancer.

[+]Access number	**Protein name**	***PLGS* Score**	***Ratio DRT Stimulated:Unstimulated**
Q8WXA9	**Splicing regulatory glutamine/lysine-rich protein 1**	**325**	**7.10**

K7EJ44	**Profilin**	**176**	**2.66**
P04259	Keratin_ type II cytoskeletal 6B	427	1.99
P02538	Keratin_ type II cytoskeletal 6A	470	1.97
P02787	Serotransferrin	147	1.84
P29401	Transketolase	243	1.57
P00738	Haptoglobin	313	1.46
P63261	Actin_ cytoplasmic 2	128	1.25
P68032	Actin_ alpha cardiac muscle 1	128	1.17
P62736	Actin_ aortic smooth muscle	128	1.17
P68133	Actin_ alpha skeletal muscle	128	1.16
P09104	Gamma-enolase	401	0.55
P01591	Immunoglobulin J chain	1229	0.51
P02814	**Submaxillary gland androgen-regulated protein 3B**	**777**	**0.46**
P08779	**Keratin_ type I cytoskeletal 16**	**220**	**0.42**
P02533	**Keratin_ type I cytoskeletal 14**	**241**	**0.40**
P06733	**Alpha-enolase**	**437**	**0.39**
C9JKR2	**Albumin_ isoform CRA_k**	**2144**	**0.35**
P07737	**Profilin-1**	**390**	**0.35**
P19012	**Keratin_ type I cytoskeletal 15**	**268**	**0.27**
O95678	**Keratin_ type II cytoskeletal 75**	**228**	**0.26**
Q5XKE5	**Keratin_ type II cytoskeletal 79**	**259**	**0.26**
P35908	**Keratin_ type II cytoskeletal 2 epidermal**	**262**	**0.26**
P13647	**Keratin_ type II cytoskeletal 5**	**228**	**0.26**
P0CG38	**POTE ankyrin domain family member I**	**723**	**0.25**
Q04695	**Keratin_ type I cytoskeletal 17**	**200**	**0.24**
P12273	**Prolactin-inducible protein**	**389**	**0.23**
P02788	**Lactotransferrin**	**142**	**0.23**
P08727	**Keratin_ type I cytoskeletal 19**	**207**	**0.23**
Q9ULE3	**DENN domain-containing protein 2A**	**296**	**0.23**
P04083	**Annexin A1**	**1713**	**0.22**
P28749	**Retinoblastoma-like protein 1**	**219**	**0.22**
P01833	**Polymeric immunoglobulin receptor**	**621**	**0.20**
P02768	**Serum albumin**	**2424**	**0.20**
P04080	**Cystatin-B**	**636**	**0.20**
P06702	**Protein S100-A9**	**564**	**0.16**
P13646	**Keratin_ type I cytoskeletal 13**	**296**	**0.14**
Q86WS5	**Transmembrane protease serine 12**	**170**	**0.14**
Q8IYW2	**Cilia- and flagella-associated protein 46**	**178**	**0.11**
P01036	**Cystatin-S**	**2991**	**0.07**
P04746	**Pancreatic alpha-amylase**	**714**	**0.07**
P04745	**Alpha-amylase 1**	**1059**	**0.07**
P19961	**Alpha-amylase 2B**	**746**	**0.07**
P01037	**Cystatin-SN**	**1561**	**0.06**
Q03112	**Histone-lysine N-methyltransferase MECOM**	**364**	**0.06**
P09228	**Cystatin-SA**	**1001**	**0.06**

P01877	**Immunoglobulin heavy constant alpha 2**	**4275**	**0.05**
P01834	**Immunoglobulin kappa constant**	**803**	**0.04**
P48668	**Keratin_ type II cytoskeletal 6C**	**470**	**0.04**
P01876	**Immunoglobulin heavy constant alpha 1**	**4220**	**0.04**
P51993	**Alpha-(1_3)-fucosyltransferase 6**	**115**	**0.01**
P19174	1-phosphatidylinositol 4_5-bisphosphate phosphodiesterase gamma-1	123	°Stimulated saliva
P52209	6-phosphogluconate dehydrogenase_ decarboxylating	272	°Stimulated saliva
Q6PJH3	A kinase (PRKA) anchor protein (Yotiao) 9_ isoform CRA_c	74	°Stimulated saliva
Q13085	Acetyl-CoA carboxylase 1	247	°Stimulated saliva
Q9H568	Actin-like protein 8	103	°Stimulated saliva
Q6JQN1	Acyl-CoA dehydrogenase family member 10	146	°Stimulated saliva
O95996	Adenomatous polyposis coli protein 2	121	°Stimulated saliva
Q9UHB7	AF4/FMR2 family member 4	160	°Stimulated saliva
Q9Y4W6	AFG3-like protein 2	74	°Stimulated saliva
Q99996	A-kinase anchor protein 9	234	°Stimulated saliva
Q86XL3	Ankyrin repeat and LEM domain-containing protein 2	77	°Stimulated saliva
Q6ZW76	Ankyrin repeat and SAM domain-containing protein 3	264	°Stimulated saliva
P06727	Apolipoprotein A-IV	61	°Stimulated saliva
P04424	Argininosuccinate lyase	81	°Stimulated saliva
Q5FYB0	Arylsulfatase J	132	°Stimulated saliva
Q9NVI7	ATPase family AAA domain-containing protein 3A	111	°Stimulated saliva
Q96FC9	ATP-dependent DNA helicase DDX11	133	°Stimulated saliva
K7EJ04	AT-rich interactive domain-containing protein 3A (Fragment)	109	°Stimulated saliva
C9JD65	Autophagy-related protein 9 (Fragment)	319	°Stimulated saliva
Q7Z3C6	Autophagy-related protein 9A	319	°Stimulated saliva
O95817	BAG family molecular chaperone regulator 3	52	°Stimulated saliva
P26998	Beta-crystallin B3	136	°Stimulated saliva
Q6QNY1	Biogenesis of lysosome-related organelles complex 1 subunit 2	147	°Stimulated saliva
G3XAF7	Breast carcinoma amplified sequence 1_ isoform CRA_c	104	°Stimulated saliva
O75363	Breast carcinoma-amplified sequence 1	126	°Stimulated saliva
Q6UX41	Butyrophilin-like protein 8	430	°Stimulated saliva
E7ETZ0	Calmodulin-1	249	°Stimulated saliva
E7EMB3	Calmodulin-2	142	°Stimulated saliva
U3KQU6	Carboxypeptidase	159	°Stimulated saliva
A6NG92	CCDC144A protein	69	°Stimulated saliva
B4DFC0	cDNA FLJ59192_ highly similar to Secretion-regulating guanine nucleotide exchange factor	175	°Stimulated saliva
P49454	Centromere protein F	154	°Stimulated saliva
Q6ZU80	Centrosomal protein of 128 kDa	227	°Stimulated saliva
Q9C0D2	Centrosomal protein of 295 kDa	91	°Stimulated saliva
P51797	Chloride transport protein 6	77	°Stimulated saliva

Q14839	Chromodomain-helicase-DNA-binding protein 4	279	°Stimulated saliva
Q16630	Cleavage and polyadenylation specificity factor subunit 6	237	°Stimulated saliva
A2RUR9	Coiled-coil domain-containing protein 144A	80	°Stimulated saliva
Q6TFL3	Coiled-coil domain-containing protein 171	213	°Stimulated saliva
Q5VVM6	Coiled-coil domain-containing protein 30	92	°Stimulated saliva
Q9UFE4	Coiled-coil domain-containing protein 39	106	°Stimulated saliva
Q92793	CREB-binding protein	122	°Stimulated saliva
Q13617	Cullin-2	71	°Stimulated saliva
Q14028	Cyclic nucleotide-gated cation channel beta-1	111	°Stimulated saliva
E5RI39	Cyclin-C (Fragment)	196	°Stimulated saliva
K7EQ67	Cysteine protease (Fragment)	217	°Stimulated saliva
Q9NZV1	Cysteine-rich motor neuron 1 protein	251	°Stimulated saliva
Q9NSE2	Cytokine-inducible SH2-containing protein	228	°Stimulated saliva
P52701	DNA mismatch repair protein Msh6	248	°Stimulated saliva
H0Y5T4	DNA polymerase zeta catalytic subunit (Fragment)	83	°Stimulated saliva
B3KP42	DNA repair-scaffolding protein	233	°Stimulated saliva
P0CAP2	DNA-directed RNA polymerase II subunit GRINL1A	186	°Stimulated saliva
E9PP13	DNA-directed RNA polymerase II subunit GRINL1A_ isoforms 4/5	186	°Stimulated saliva
P61218	DNA-directed RNA polymerases I_ II_ and III subunit RPABC2	335	°Stimulated saliva
Q5W0Z5	Doublesex- and mab-3-related transcription factor 3 (Fragment)	137	°Stimulated saliva
Q63HN8	E3 ubiquitin-protein ligase RNF213	97	°Stimulated saliva
Q8NHG8	E3 ubiquitin-protein ligase ZNRF2	219	°Stimulated saliva
Q96G75	E3 ubiquitin-protein transferase RMND5B	69	°Stimulated saliva
Q96C19	EF-hand domain-containing protein D2	223	°Stimulated saliva
Q12929	Epidermal growth factor receptor kinase substrate 8	540	°Stimulated saliva
Q9BQI3	Eukaryotic translation initiation factor 2-alpha kinase 1	152	°Stimulated saliva
Q99613	Eukaryotic translation initiation factor 3 subunit C	178	°Stimulated saliva
P55010	Eukaryotic translation initiation factor 5	94	°Stimulated saliva
Q01780	Exosome component 10	74	°Stimulated saliva
K7EPQ1	Fas-binding factor 1 (Fragment)	114	°Stimulated saliva
A0AVI2	Fer-1-like protein 5	113	°Stimulated saliva
Q5T376	FERM domain containing 4A_ isoform CRA_c (Fragment)	104	°Stimulated saliva
Q9P2Q2	FERM domain-containing protein 4A	138	°Stimulated saliva
G5E965	Forkhead box P1_ isoform CRA_f	339	°Stimulated saliva
A0A3B3IRS5	Forkhead box P1_ isoform CRA_g	339	°Stimulated saliva
I3L4U8	Forkhead box protein K2 (Fragment)	432	°Stimulated saliva
Q9H334	Forkhead box protein P1	339	°Stimulated saliva
Q9NXC5	GATOR complex protein MIOS	214	°Stimulated saliva
A0A2R8Y7B1	Girdin	164	°Stimulated saliva
A0A1W2PR19	Glutathione S-transferase theta-4	133	°Stimulated saliva

O75791	GRB2-related adapter protein 2	100	°Stimulated saliva
Q8IZT8	Heparan sulfate glucosamine 3-O-sulfotransferase 5	85	°Stimulated saliva
Q7Z4V5	Hepatoma-derived growth factor-related protein 2	238	°Stimulated saliva
A5PLL3	Histone acetyltransferase	154	°Stimulated saliva
Q92794	Histone acetyltransferase KAT6A	154	°Stimulated saliva
Q8NEZ4	Histone-lysine N-methyltransferase 2C	185	°Stimulated saliva
C9JH95	Histone-lysine N-methyltransferase_ H3 lysine-79 specific (Fragment)	192	°Stimulated saliva
P31270	Homeobox protein Hox-A11	87	°Stimulated saliva
P31276	Homeobox protein Hox-C13	128	°Stimulated saliva
Q8WYH8	Inhibitor of growth protein 5	130	°Stimulated saliva
O43314	Inositol hexakisphosphate and diphosphoinositol-pentakisphosphate kinase 2	119	°Stimulated saliva
Q9H0H0	Integrator complex subunit 2	176	°Stimulated saliva
H3BSV1	Integrin alpha-L (Fragment)	140	°Stimulated saliva
Q12906	Interleukin enhancer-binding factor 3	99	°Stimulated saliva
P22301	Interleukin-10	255	°Stimulated saliva
P78413	Iroquois-class homeodomain protein IRX-4	162	°Stimulated saliva
C9J5J2	Isoamyl acetate-hydrolyzing esterase 1 homolog (Fragment)	325	°Stimulated saliva
Q96MG2	Junctional sarcoplasmic reticulum protein 1	191	°Stimulated saliva
G3XAE9	KIAA0423_ isoform CRA_a	131	°Stimulated saliva
Q6PJI1	KIF9 protein	94	°Stimulated saliva
J3QLI1	Kinase suppressor of Ras 1 (Fragment)	181	°Stimulated saliva
B4DZK5	Kinesin-like protein	94	°Stimulated saliva
Q9HAQ2	Kinesin-like protein KIF9	108	°Stimulated saliva
O14901	Krueppel-like factor 11	107	°Stimulated saliva
M0R228	KxDL motif-containing protein 1 (Fragment)	268	°Stimulated saliva
Q4G0J3	La-related protein 7	85	°Stimulated saliva
Q9H089	Large subunit GTPase 1 homolog	102	°Stimulated saliva
Q8N653	Leucine-zipper-like transcriptional regulator 1	203	°Stimulated saliva
Q8N6C8	Leukocyte immunoglobulin-like receptor subfamily A member 3	74	°Stimulated saliva
P59901	Leukocyte immunoglobulin-like receptor subfamily A member 4	87	°Stimulated saliva
Q6PI73	Leukocyte immunoglobulin-like receptor subfamily A member 6	74	°Stimulated saliva
Q8N423	Leukocyte immunoglobulin-like receptor subfamily B member 2	74	°Stimulated saliva
O75022	Leukocyte immunoglobulin-like receptor subfamily B member 3	74	°Stimulated saliva
U5XJZ2	LILRA6	74	°Stimulated saliva
H0YA17	Lipopolysaccharide-responsive and beige-like anchor protein (Fragment)	160	°Stimulated saliva
B7ZM74	LOC441476 protein	63	°Stimulated saliva
P28330	Long-chain specific acyl-CoA dehydrogenase_ mitochondrial	158	°Stimulated saliva
P01130	Low-density lipoprotein receptor	110	°Stimulated saliva
P10619	Lysosomal protective protein	161	°Stimulated saliva
P41594	Metabotropic glutamate receptor 5	69	°Stimulated saliva

E5RJR3	Methionine adenosyltransferase 2 subunit beta	139	°Stimulated saliva
Q9Y4B5	Microtubule cross-linking factor 1	188	°Stimulated saliva
O43615	Mitochondrial import inner membrane translocase subunit TIM44	192	°Stimulated saliva
O43683	Mitotic checkpoint serine/threonine-protein kinase BUB1	303	°Stimulated saliva
Q9Y6D9	Mitotic spindle assembly checkpoint protein MAD1	125	°Stimulated saliva
Q7Z406	Myosin-14	134	°Stimulated saliva
Q15599	Na(+)/H(+) exchange regulatory cofactor NHE-RF2	168	°Stimulated saliva
F8WE33	Neutral cholesterol ester hydrolase 1	132	°Stimulated saliva
Q92542	Nicastrin	221	°Stimulated saliva
Q14686	Nuclear receptor coactivator 6	118	°Stimulated saliva
Q86WB0	Nuclear-interacting partner of ALK	266	°Stimulated saliva
Q96HC4	PDZ and LIM domain protein 5	114	°Stimulated saliva
V9GY63	Phosphoinositide phospholipase C (Fragment)	115	°Stimulated saliva
E7EVM7	Piezo-type mechanosensitive ion channel component	132	°Stimulated saliva
Q9H5I5	Piezo-type mechanosensitive ion channel component 2	135	°Stimulated saliva
P13796	Plastin-2	80	°Stimulated saliva
Q9HB19	Pleckstrin homology domain-containing family A member 2	188	°Stimulated saliva
A0A3B3IST3	Pleckstrin homology domain-containing family A member 8	119	°Stimulated saliva
Q9H7P9	Pleckstrin homology domain-containing family G member 2	248	°Stimulated saliva
Q15149	Plectin	183	°Stimulated saliva
P0CG47	Polyubiquitin-B	654	°Stimulated saliva
P0CG48	Polyubiquitin-C	654	°Stimulated saliva
Q92620	Pre-mRNA-splicing factor ATP-dependent RNA helicase PRP16	266	°Stimulated saliva
Q969E8	Pre-rRNA-processing protein TSR2 homolog	194	°Stimulated saliva
Q8IY21	Probable ATP-dependent RNA helicase DDX60	89	°Stimulated saliva
Q15751	Probable E3 ubiquitin-protein ligase HERC1	79	°Stimulated saliva
P14921	Protein C-ets-1	210	°Stimulated saliva
Q96JJ7	Protein disulfide-isomerase TMX3	110	°Stimulated saliva
Q86YD7	Protein FAM90A1	80	°Stimulated saliva
A0A0B4J2F0	Protein PIGBOS1	1068	°Stimulated saliva
J3KQP8	Protein prenyltransferase alpha subunit repeat-containing protein 1 (Fragment)	500	°Stimulated saliva
P05109	Protein S100-A8	211	°Stimulated saliva
Q13796	Protein Shroom2	145	°Stimulated saliva
Q8N7X2	Protein STPG3	63	°Stimulated saliva
O14795	Protein unc-13 homolog B	93	°Stimulated saliva
A8MPP1	Putative ATP-dependent RNA helicase DDX11-like protein 8	133	°Stimulated saliva
Q92771	Putative ATP-dependent RNA helicase DDX12	133	°Stimulated saliva
Q8IYA2	Putative coiled-coil domain-containing protein 144C	79	°Stimulated saliva

Q9BZD3	Putative GRINL1B complex locus protein 2	201	°Stimulated saliva
A6NDY2	Putative protein FAM90A10P	80	°Stimulated saliva
P0C7W8	Putative protein FAM90A13P	80	°Stimulated saliva
P0C7W9	Putative protein FAM90A14P	80	°Stimulated saliva
P0C7V4	Putative protein FAM90A15P	80	°Stimulated saliva
A6NEW6	Putative protein FAM90A16P/FAM90A17P	80	°Stimulated saliva
A6NE21	Putative protein FAM90A18P/FAM90A19P	80	°Stimulated saliva
D6RGX4	Putative protein FAM90A26	80	°Stimulated saliva
A8MXJ8	Putative protein FAM90A5P	80	°Stimulated saliva
A6NKC0	Putative protein FAM90A7P	80	°Stimulated saliva
A6NJQ4	Putative protein FAM90A8P	80	°Stimulated saliva
A6NNJ1	Putative protein FAM90A9P	80	°Stimulated saliva
A4D174	Putative uncharacterized protein C7orf71	91	°Stimulated saliva
Q9H6N6	Putative uncharacterized protein MYH16	102	°Stimulated saliva
P0CG31	Putative zinc finger protein 286B	247	°Stimulated saliva
P14618	Pyruvate kinase PKM	731	°Stimulated saliva
P61018	Ras-related protein Rab-4B	139	°Stimulated saliva
P63244	Receptor of activated protein C kinase 1	201	°Stimulated saliva
P49796	Regulator of G-protein signaling 3	143	°Stimulated saliva
A5PLK6	Regulator of G-protein signaling protein-like	52	°Stimulated saliva
Q5VXC0	Regulator of G-protein-signaling 3	135	°Stimulated saliva
F8VQR0	Rho GTPase-activating protein 9 (Fragment)	105	°Stimulated saliva
K7EMB1	RING finger protein unkempt homolog	947	°Stimulated saliva
Q96E39	RNA binding motif protein_ X-linked-like-1	346	°Stimulated saliva
P38159	RNA-binding motif protein_ X chromosome	346	°Stimulated saliva
A0A1B0GUK8	RNA-binding motif protein_ X-linked-like-1 (Fragment)	279	°Stimulated saliva
Q14DU5	ROCK2 protein	62	°Stimulated saliva
Q9Y6N7	Roundabout homolog 1	364	°Stimulated saliva
Q49A90	RPS27A protein	654	°Stimulated saliva
A0A1B0GUB0	Ryanodine receptor 3 (Fragment)	83	°Stimulated saliva
Q9NWH9	SAFB-like transcription modulator	415	°Stimulated saliva
G3V1B4	Secretion regulating guanine nucleotide exchange factor_ isoform CRA_a	213	°Stimulated saliva
Q9UGK8	Secretion-regulating guanine nucleotide exchange factor	213	°Stimulated saliva
Q9HC98	Serine/threonine-protein kinase Nek6	396	°Stimulated saliva
Q86UE8	Serine/threonine-protein kinase tousled-like 2	472	°Stimulated saliva
Q9Y6X0	SET-binding protein	336	°Stimulated saliva
Q8NEM2	SHC SH2 domain-binding protein 1	124	°Stimulated saliva
Q6ZNX1	Shieldin complex subunit 3	66	°Stimulated saliva
Q8TD22	Sideroflexin-5	278	°Stimulated saliva
J3KPM9	Signal transducer and activator of transcription	202	°Stimulated saliva
P42224	Signal transducer and activator of transcription 1-alpha/beta	202	°Stimulated saliva
Q7Z6B7	SLIT-ROBO Rho GTPase-activating protein 1	152	°Stimulated saliva
O75044	SLIT-ROBO Rho GTPase-activating protein 2	143	°Stimulated saliva

P0DMP2	SLIT-ROBO Rho GTPase-activating protein 2B	143	°Stimulated saliva
P0DJJ0	SLIT-ROBO Rho GTPase-activating protein 2C	143	°Stimulated saliva
Q9Y448	Small kinetochore-associated protein	175	°Stimulated saliva
A0A1W2PPJ3	Sodium channel protein	81	°Stimulated saliva
P35498	Sodium channel protein type 1 subunit alpha	84	°Stimulated saliva
Q9UQD0	Sodium channel protein type 8 subunit alpha	86	°Stimulated saliva
F8WEK3	Solute carrier family 12 member 9	276	°Stimulated saliva
A0A1B0GTB7	Spectrin alpha chain_ non-erythrocytic 1 (Fragment)	232	°Stimulated saliva
Q96SI9	Spermatid perinuclear RNA-binding protein	62	°Stimulated saliva
Q13435	Splicing factor 3B subunit 2	234	°Stimulated saliva
Q9H040	SprT-like domain-containing protein Spartan	76	°Stimulated saliva
P78524	Suppression of tumorigenicity 5 protein	364	°Stimulated saliva
F8VRQ4	SWI/SNF-related matrix-associated actin-dependent regulator of chromatin subfamily D member 1	166	°Stimulated saliva
Q6STE5	SWI/SNF-related matrix-associated actin-dependent regulator of chromatin subfamily D member 3	71	°Stimulated saliva
G3V1T3	TAP binding protein-like_ isoform CRA_c	277	°Stimulated saliva
Q9BX59	Tapasin-related protein	277	°Stimulated saliva
Q9ULW0	Targeting protein for Xklp2	63	°Stimulated saliva
Q5I0X7	Tetratricopeptide repeat protein 32	654	°Stimulated saliva
P07202	Thyroid peroxidase	77	°Stimulated saliva
Q13009	T-lymphoma invasion and metastasis-inducing protein 1	204	°Stimulated saliva
Q9Y4F4	TOG array regulator of axonemal microtubules protein 1	136	°Stimulated saliva
Q6BEB4	Transcription factor Sp5	96	°Stimulated saliva
O00268	Transcription initiation factor TFIID subunit 4	155	°Stimulated saliva
Q9Y6A5	Transforming acidic coiled-coil-containing protein 3	149	°Stimulated saliva
Q92545	Transmembrane protein 131	137	°Stimulated saliva
E9PIS2	Transmembrane protein 135 (Fragment)	198	°Stimulated saliva
F8WF52	tRNA (cytosine(34)-C(5))-methyltransferase_ mitochondrial	275	°Stimulated saliva
Q9UJT1	Tubulin delta chain	361	°Stimulated saliva
P06241	Tyrosine-protein kinase Fyn	218	°Stimulated saliva
Q969X6	U3 small nucleolar RNA-associated protein 4 homolog	271	°Stimulated saliva
Q86UV5	Ubiquitin carboxyl-terminal hydrolase 48	129	°Stimulated saliva
P62979	Ubiquitin-40S ribosomal protein S27a	654	°Stimulated saliva
P62987	Ubiquitin-60S ribosomal protein L40	654	°Stimulated saliva
A0A2R8Y422	Ubiquitin-like domain-containing protein	654	°Stimulated saliva
A0A1W2PRG0	Uncharacterized protein	133	°Stimulated saliva
A6NGY3	Uncharacterized protein C5orf52	95	°Stimulated saliva
Q9BZX2	Uridine-cytidine kinase 2	142	°Stimulated saliva
E5RJ10	Vacuolar protein sorting-associated protein 37A	229	°Stimulated saliva
Q68DQ2	Very large A-kinase anchor protein	154	°Stimulated saliva

P02774	Vitamin D-binding protein	354	°Stimulated saliva
B5TYJ1	Voltage-dependent P/Q-type calcium channel subunit alpha	120	°Stimulated saliva
O00555	Voltage-dependent P/Q-type calcium channel subunit alpha-1A	120	°Stimulated saliva
P12955	Xaa-Pro dipeptidase	538	°Stimulated saliva
Q9UQR1	Zinc finger protein 148	150	°Stimulated saliva
Q9HCE3	Zinc finger protein 532	178	°Stimulated saliva
Q8IVC4	Zinc finger protein 584	96	°Stimulated saliva
P35789	Zinc finger protein 93	180	°Stimulated saliva
P08151	Zinc finger protein GLI1	140	°Stimulated saliva
P10075	Zinc finger protein GLI4	152	°Stimulated saliva
Q15029	116 kDa U5 small nuclear ribonucleoprotein component	143	°Unstimulated saliva
P62258	14-3-3 protein epsilon	209	°Unstimulated saliva
P31947	14-3-3 protein sigma	184	°Unstimulated saliva
Q9H9V9	2-oxoglutarate and iron-dependent oxygenase JMJD4	121	°Unstimulated saliva
H0YFS2	4F2 cell-surface antigen heavy chain (Fragment)	326	°Unstimulated saliva
Q00013	55 kDa erythrocyte membrane protein	199	°Unstimulated saliva
Q16875	6-phosphofructo-2-kinase/fructose-2_6-bisphosphatase 3	320	°Unstimulated saliva
Q9UHI8	A disintegrin and metalloproteinase with thrombospondin motifs 1	416	°Unstimulated saliva
P58397	A disintegrin and metalloproteinase with thrombospondin motifs 12	231	°Unstimulated saliva
Q9NZ52	ADP-ribosylation factor-binding protein GGA3	214	°Unstimulated saliva
O43572	A-kinase anchor protein 10_ mitochondrial	371	°Unstimulated saliva
Q11128	Alpha-(1_3)-fucosyltransferase 5	115	°Unstimulated saliva
P12814	Alpha-actinin-1	805	°Unstimulated saliva
O43707	Alpha-actinin-4	195	°Unstimulated saliva
Q8IY63	Angiomotin-like protein 1	260	°Unstimulated saliva
F8WB76	Ankyrin repeat domain-containing protein 54 (Fragment)	134	°Unstimulated saliva
E7EMC6	Annexin	115	°Unstimulated saliva
P08133	Annexin A6	287	°Unstimulated saliva
P03973	Antileukoproteinase	601	°Unstimulated saliva
P02647	Apolipoprotein A-I	352	°Unstimulated saliva
F8WB77	Apolipoprotein L1	875	°Unstimulated saliva
Q9BPW4	Apolipoprotein L4	185	°Unstimulated saliva
O15033	Apoptosis-resistant E3 ubiquitin protein ligase 1	327	°Unstimulated saliva
Q9ULH1	Arf-GAP with SH3 domain_ ANK repeat and PH domain-containing protein 1	183	°Unstimulated saliva
Q9P2R6	Arginine-glutamic acid dipeptide repeats protein	1025	°Unstimulated saliva
O00571	ATP-dependent RNA helicase DDX3X	162	°Unstimulated saliva
O15523	ATP-dependent RNA helicase DDX3Y	189	°Unstimulated saliva
Q9BQ39	ATP-dependent RNA helicase DDX50	218	°Unstimulated saliva
Q8IYB8	ATP-dependent RNA helicase SUPV3L1_ mitochondrial	248	°Unstimulated saliva

H0Y488	AT-rich interactive domain-containing protein 1A	136	°Unstimulated saliva
A6NKF2	AT-rich interactive domain-containing protein 3C	115	°Unstimulated saliva
Q8WXE1	ATR-interacting protein	247	°Unstimulated saliva
A0A0A0MRA8	Band 4.1-like protein 3	482	°Unstimulated saliva
P04280	Basic salivary proline-rich protein 1	4778	°Unstimulated saliva
P02812	Basic salivary proline-rich protein 2	4778	°Unstimulated saliva
J3QRN2	Beta-2-glycoprotein 1 (Fragment)	414	°Unstimulated saliva
Q96IK1	Biorientation of chromosomes in cell division protein 1	190	°Unstimulated saliva
Q8TDL5	BPI fold-containing family B member 1	206	°Unstimulated saliva
Q8N4F0	BPI fold-containing family B member 2	1086	°Unstimulated saliva
P80723	Brain acid soluble protein 1	173	°Unstimulated saliva
Q14681	BTB/POZ domain-containing protein KCTD2	160	°Unstimulated saliva
Q4G0X4	BTB/POZ domain-containing protein KCTD21	106	°Unstimulated saliva
Q96EU7	C1GALT1-specific chaperone 1	171	°Unstimulated saliva
O75309	Cadherin-16	115	°Unstimulated saliva
H7C555	Cadherin-related family member 3 (Fragment)	222	°Unstimulated saliva
Q9NZU7	Calcium-binding protein 1	243	°Unstimulated saliva
Q9NPB3	Calcium-binding protein 2	122	°Unstimulated saliva
Q9ULU8	Calcium-dependent secretion activator 1	353	°Unstimulated saliva
Q6MZZ7	Calpain-13	188	°Unstimulated saliva
Q9UBL0	cAMP-regulated phosphoprotein 21	505	°Unstimulated saliva
Q6ZU35	Cancer-related regulator of actin dynamics	762	°Unstimulated saliva
P23280	Carbonic anhydrase 6	6651	°Unstimulated saliva
Q92523	Carnitine O-palmitoyltransferase 1_ muscle isoform	228	°Unstimulated saliva
P78368	Casein kinase I isoform gamma-2	138	°Unstimulated saliva
Q9Y6M4	Casein kinase I isoform gamma-3	138	°Unstimulated saliva
A6H8Y7	CCDC73 protein	306	°Unstimulated saliva
Q99795	Cell surface A33 antigen	150	°Unstimulated saliva
Q8N8E3	Centrosomal protein of 112 kDa	348	°Unstimulated saliva
Q8TEP8	Centrosomal protein of 192 kDa	119	°Unstimulated saliva
H0Y900	Centrosomal protein of 63 kDa (Fragment)	147	°Unstimulated saliva
E9PIK0	Centrosome-associated protein 350 (Fragment)	157	°Unstimulated saliva
P00450	Ceruloplasmin	150	°Unstimulated saliva
A0A2R8Y808	Chromodomain-helicase-DNA-binding protein 8 (Fragment)	193	°Unstimulated saliva
Q9P2M7	Cingulin	196	°Unstimulated saliva
J3KPP4	Cisplatin resistance-associated overexpressed protein_ isoform CRA_b	206	°Unstimulated saliva
Q9P2I0	Cleavage and polyadenylation specificity factor subunit 2	161	°Unstimulated saliva
G9CGD6	CNK3/IPCEF1 fusion protein	331	°Unstimulated saliva
A0A0B4J1Z0	COBL-like 1_ isoform CRA_a	179	°Unstimulated saliva
Q6ZRK6	Coiled-coil domain-containing protein 73	319	°Unstimulated saliva
Q99715	Collagen alpha-1(XII) chain	105	°Unstimulated saliva

Q9UMD9	Collagen alpha-1(XVII) chain	504	°Unstimulated saliva
Q6UXH8	Collagen and calcium-binding EGF domain-containing protein 1	456	°Unstimulated saliva
Q9BXJ2	Complement C1q tumor necrosis factor-related protein 7	253	°Unstimulated saliva
M0R1Q1	Complement C3 (Fragment)	461	°Unstimulated saliva
A0A0D9SG04	Cordon-bleu protein-like 1	179	°Unstimulated saliva
Q9UBG3	Cornulin	182	°Unstimulated saliva
B7ZLQ8	CPEB4 protein	233	°Unstimulated saliva
Q6UUV7	CREB-regulated transcription coactivator 3	578	°Unstimulated saliva
Q5TAH7	CUB and Sushi multiple domains 2_ isoform CRA_c	191	°Unstimulated saliva
P01034	Cystatin-C	540	°Unstimulated saliva
Q7Z5Q1	Cytoplasmic polyadenylation element-binding protein 2	240	°Unstimulated saliva
Q8NE35	Cytoplasmic polyadenylation element-binding protein 3	213	°Unstimulated saliva
Q17RY0	Cytoplasmic polyadenylation element-binding protein 4	233	°Unstimulated saliva
Q5M775	Cytospin-B	653	°Unstimulated saliva
P07585	Decorin	351	°Unstimulated saliva
A0A2R8YD85	Dedicator of cytokinesis protein 10	81	°Unstimulated saliva
A0A075B7B1	Desmuslin_ isoform CRA_a	96	°Unstimulated saliva
Q7L591	Docking protein 3	100	°Unstimulated saliva
E5RI01	Double-strand-break repair protein rad21 homolog	350	°Unstimulated saliva
Q9NYC9	Dynein heavy chain 9_ axonemal	342	°Unstimulated saliva
O95714	E3 ubiquitin-protein ligase HERC2	341	°Unstimulated saliva
A0RZB6	Endoplasmic reticulum chaperone SIL1 (Fragment)	622	°Unstimulated saliva
P14138	Endothelin-3	212	°Unstimulated saliva
Q6P2E9	Enhancer of mRNA-decapping protein 4	98	°Unstimulated saliva
P98073	Enteropeptidase	253	°Unstimulated saliva
P54764	Ephrin type-A receptor 4	179	°Unstimulated saliva
P62508	Estrogen-related receptor gamma	340	°Unstimulated saliva
Q6ZN32	ETS translocation variant 3-like protein	148	°Unstimulated saliva
C9JF49	Exportin-1 (Fragment)	255	°Unstimulated saliva
P55060	Exportin-2	94	°Unstimulated saliva
O43592	Exportin-T	275	°Unstimulated saliva
Q08945	FACT complex subunit SSRP1	235	°Unstimulated saliva
Q92945	Far upstream element-binding protein 2	141	°Unstimulated saliva
P14324	Farnesyl pyrophosphate synthase	315	°Unstimulated saliva
Q96IV6	Fatty acid hydroxylase domain-containing protein 2	566	°Unstimulated saliva
Q4VXH1	F-box/WD repeat-containing protein 2 (Fragment)	153	°Unstimulated saliva
Q96NE9	FERM domain-containing protein 6	159	°Unstimulated saliva
A0A0G2JJI2	G patch domain and ankyrin repeat-containing protein 1 (Fragment)	314	°Unstimulated saliva
A0A0B4J269	G_PROTEIN_RECEP_F1_2 domain-containing protein	201	°Unstimulated saliva
P21217	Galactoside 3(4)-L-fucosyltransferase	115	°Unstimulated saliva

A0A1B0GU82	Gamma-aminobutyric acid receptor subunit alpha-1	277	°Unstimulated saliva
Q14687	Genetic suppressor element 1	85	°Unstimulated saliva
O95749	Geranylgeranyl pyrophosphate synthase	443	°Unstimulated saliva
A0A2R8Y7X9	GLOBIN domain-containing protein	1031	°Unstimulated saliva
K7ERC6	Glucose-6-phosphate isomerase (Fragment)	282	°Unstimulated saliva
Q86X53	Glutamate-rich protein 1	346	°Unstimulated saliva
P09211	Glutathione S-transferase P	1240	°Unstimulated saliva
P04406	Glyceraldehyde-3-phosphate dehydrogenase	293	°Unstimulated saliva
A0A087WTW2	Golgin subfamily A member 4	615	°Unstimulated saliva
Q9C091	GREB1-like protein	282	°Unstimulated saliva
H7C010	GRIP and coiled-coil domain-containing protein 2 (Fragment)	194	°Unstimulated saliva
Q6IX74	Growth arrest and DNA damage-inducible protein GADD45 beta (Fragment)	398	°Unstimulated saliva
O43903	Growth arrest-specific protein 2	227	°Unstimulated saliva
A0A2R8YGL0	Hamartin (Fragment)	333	°Unstimulated saliva
Q9H6D7	HAUS augmin-like complex subunit 4	211	°Unstimulated saliva
G3V1N2	HCG1745306_ isoform CRA_a	217	°Unstimulated saliva
A0A0A6YYF2	HCG1811249_ isoform CRA_e	191	°Unstimulated saliva
A0A0A0MTS5	HCG1811249_ isoform CRA_f	191	°Unstimulated saliva
G3V3R4	HCG1983504_ isoform CRA_c	156	°Unstimulated saliva
G3V2N6	HCG1983504_ isoform CRA_d	156	°Unstimulated saliva
G3V2R8	HCG1983504_ isoform CRA_e	156	°Unstimulated saliva
Q6AI08	HEAT repeat-containing protein 6	439	°Unstimulated saliva
P04792	Heat shock protein beta-1	3768	°Unstimulated saliva
G3V2J8	Heat shock protein HSP 90-alpha (Fragment)	183	°Unstimulated saliva
P69905	Hemoglobin subunit alpha	320	°Unstimulated saliva
P68871	Hemoglobin subunit beta	1435	°Unstimulated saliva
P02042	Hemoglobin subunit delta	1031	°Unstimulated saliva
P02100	Hemoglobin subunit epsilon	1031	°Unstimulated saliva
P69891	Hemoglobin subunit gamma-1	1031	°Unstimulated saliva
P69892	Hemoglobin subunit gamma-2	1031	°Unstimulated saliva
A0A024R4E5	High density lipoprotein binding protein (Vigilin)_ isoform CRA_a	343	°Unstimulated saliva
Q7Z353	Highly divergent homeobox	116	°Unstimulated saliva
P42357	Histidine ammonia-lyase	245	°Unstimulated saliva
J3KPH8	Histone deacetylase	411	°Unstimulated saliva
Q8WUI4	Histone deacetylase 7	411	°Unstimulated saliva
U3KQK0	Histone H2B	369	°Unstimulated saliva
Q96A08	Histone H2B type 1-A	299	°Unstimulated saliva
P33778	Histone H2B type 1-B	369	°Unstimulated saliva
P62807	Histone H2B type 1-C/E/F/G/I	369	°Unstimulated saliva
P58876	Histone H2B type 1-D	369	°Unstimulated saliva
Q93079	Histone H2B type 1-H	369	°Unstimulated saliva
P06899	Histone H2B type 1-J	369	°Unstimulated saliva
O60814	Histone H2B type 1-K	369	°Unstimulated saliva
Q99880	Histone H2B type 1-L	369	°Unstimulated saliva

Q99879	Histone H2B type 1-M	369	°Unstimulated saliva
Q99877	Histone H2B type 1-N	369	°Unstimulated saliva
P23527	Histone H2B type 1-O	369	°Unstimulated saliva
Q16778	Histone H2B type 2-E	369	°Unstimulated saliva
Q5QNW6	Histone H2B type 2-F	369	°Unstimulated saliva
Q8N257	Histone H2B type 3-B	369	°Unstimulated saliva
P57053	Histone H2B type F-S	369	°Unstimulated saliva
H0Y9L4	Histone-lysine N-methyltransferase NSD2 (Fragment)	220	°Unstimulated saliva
A0A140T9Z3	HLA class II histocompatibility antigen_ DO beta chain (Fragment)	271	°Unstimulated saliva
O60479	Homeobox protein DLX-3	286	°Unstimulated saliva
J3KTP9	Hydrocephalus-inducing protein homolog (Fragment)	155	°Unstimulated saliva
P01857	Immunoglobulin heavy constant gamma 1	431	°Unstimulated saliva
P01860	Immunoglobulin heavy constant gamma 3	134	°Unstimulated saliva
P0CG04	Immunoglobulin lambda constant 1	249	°Unstimulated saliva
A0M8Q6	Immunoglobulin lambda constant 7	233	°Unstimulated saliva
O00410	Importin-5	178	°Unstimulated saliva
B7WPL9	Inositol hexakisphosphate and diphosphoinositol-pentakisphosphate kinase	457	°Unstimulated saliva
Q6PFW1	Inositol hexakisphosphate and diphosphoinositol-pentakisphosphate kinase 1	457	°Unstimulated saliva
P08514	Integrin alpha-IIb	88	°Unstimulated saliva
Q8WWN9	Interactor protein for cytohesin exchange factors 1	331	°Unstimulated saliva
Q8NAC3	Interleukin-17 receptor C	195	°Unstimulated saliva
Q9NZM3	Intersectin-2	233	°Unstimulated saliva
H0YNL8	Iron-responsive element-binding protein 2	206	°Unstimulated saliva
P13645	Keratin_ type I cytoskeletal 10	172	°Unstimulated saliva
Q99456	Keratin_ type I cytoskeletal 12	220	°Unstimulated saliva
P19013	Keratin_ type II cytoskeletal 4	759	°Unstimulated saliva
Q86Y46	Keratin_ type II cytoskeletal 73	487	°Unstimulated saliva
Q02241	Kinesin-like protein KIF23	91	°Unstimulated saliva
O00139	Kinesin-like protein KIF2A	164	°Unstimulated saliva
H0YN41	Kinetochore scaffold 1	204	°Unstimulated saliva
K7ERI5	KRAB domain-containing protein	219	°Unstimulated saliva
E9PHC9	Krueppel-like factor 7	466	°Unstimulated saliva
Q16787	Laminin subunit alpha-3	203	°Unstimulated saliva
H0YBR8	La-related protein 1 (Fragment)	444	°Unstimulated saliva
O75387	Large neutral amino acids transporter small subunit 3	313	°Unstimulated saliva
O75112	LIM domain-binding protein 3	372	°Unstimulated saliva
H3BQT4	Lipase maturation factor 1 (Fragment)	186	°Unstimulated saliva
P31025	Lipocalin-1	221	°Unstimulated saliva
E9PP16	Liprin-beta-2	233	°Unstimulated saliva
O95232	Luc7-like protein 3	206	°Unstimulated saliva
P33241	Lymphocyte-specific protein 1	194	°Unstimulated saliva
Q9UGL1	Lysine-specific demethylase 5B	155	°Unstimulated saliva

Q9BY66	Lysine-specific demethylase 5D	65	°Unstimulated saliva
O15550	Lysine-specific demethylase 6A	149	°Unstimulated saliva
Q6ZMT4	Lysine-specific demethylase 7A	67	°Unstimulated saliva
F8VV32	Lysozyme	380	°Unstimulated saliva
P61626	Lysozyme C	387	°Unstimulated saliva
O43451	Maltase-glucoamylase_ intestinal	321	°Unstimulated saliva
Q9UM22	Mammalian ependymin-related protein 1	510	°Unstimulated saliva
Q9H8J5	MANSC domain-containing protein 1	203	°Unstimulated saliva
C9JGN2	Mediator of RNA polymerase II transcription subunit 15 (Fragment)	240	°Unstimulated saliva
A2RUB1	Meiosis-specific coiled-coil domain-containing protein MEIOC	111	°Unstimulated saliva
C9JK50	Melanoma-associated antigen 4 (Fragment)	116	°Unstimulated saliva
E7EVA0	Microtubule-associated protein	325	°Unstimulated saliva
P46821	Microtubule-associated protein 1B	278	°Unstimulated saliva
P27816	Microtubule-associated protein 4	336	°Unstimulated saliva
Q3SY69	Mitochondrial 10-formyltetrahydrofolate dehydrogenase	141	°Unstimulated saliva
Q8IVH8	Mitogen-activated protein kinase kinase kinase kinase 3	156	°Unstimulated saliva
Q96T76	MMS19 nucleotide excision repair protein homolog	155	°Unstimulated saliva
Q96HT8	MORF4 family-associated protein 1-like 1	178	°Unstimulated saliva
P30304	M-phase inducer phosphatase 1	202	°Unstimulated saliva
Q96T58	Msx2-interacting protein	106	°Unstimulated saliva
Q8TAX7	Mucin-7	597	°Unstimulated saliva
P02686	Myelin basic protein	276	°Unstimulated saliva
Q9Y2G1	Myelin regulatory factor	124	°Unstimulated saliva
P12882	Myosin-1	246	°Unstimulated saliva
Q9UKX3	Myosin-13	241	°Unstimulated saliva
Q9UKX2	Myosin-2	256	°Unstimulated saliva
Q9Y623	Myosin-4	240	°Unstimulated saliva
O00308	NEDD4-like E3 ubiquitin-protein ligase WWP2	246	°Unstimulated saliva
E9PD43	Negative elongation factor E (Fragment)	206	°Unstimulated saliva
Q5QGS0	Neurite extension and migration factor	143	°Unstimulated saliva
O94856	Neurofascin	172	°Unstimulated saliva
P30990	Neurotensin/neuromedin N	182	°Unstimulated saliva
Q86UT6	NLR family member X1	225	°Unstimulated saliva
Q8TAT6	Nuclear protein localization protein 4 homolog	834	°Unstimulated saliva
H7C184	Nuclear receptor corepressor 2 (Fragment)	96	°Unstimulated saliva
Q5SRE5	Nucleoporin NUP188 homolog	278	°Unstimulated saliva
P0DN81	Olfactory receptor 13C7	140	°Unstimulated saliva
Q8IXM7	Outer dense fiber protein 3-like protein 1	215	°Unstimulated saliva
H0YCU5	Phosphofurin acidic cluster sorting protein 1 (Fragment)	229	°Unstimulated saliva
Q8NEL9	Phospholipase DDHD1	219	°Unstimulated saliva
P20020	Plasma membrane calcium-transporting ATPase 1	114	°Unstimulated saliva

Q9H4M7	Pleckstrin homology domain-containing family A member 4	285	°Unstimulated saliva
P11465	Pregnancy-specific beta-1-glycoprotein 2	235	°Unstimulated saliva
H0Y8P7	Pre-mRNA 3'-end-processing factor FIP1 (Fragment)	119	°Unstimulated saliva
J3KPF0	Probable E3 ubiquitin-protein ligase HECTD4	195	°Unstimulated saliva
K7EJN8	Proline-rich protein 22 (Fragment)	655	°Unstimulated saliva
Q12884	Prolyl endopeptidase FAP	201	°Unstimulated saliva
E9PMZ2	Protein arginine N-methyltransferase 1 (Fragment)	573	°Unstimulated saliva
A0A1W2PQ30	Protein Aster-B	277	°Unstimulated saliva
P58658	Protein eva-1 homolog C	219	°Unstimulated saliva
Q5W0V3	Protein FAM160B1	325	°Unstimulated saliva
Q68CZ1	Protein fantom	358	°Unstimulated saliva
Q92833	Protein Jumonji	82	°Unstimulated saliva
Q8N3A8	Protein mono-ADP-ribosyltransferase PARP8	512	°Unstimulated saliva
Q86WI3	Protein NLRC5	127	°Unstimulated saliva
Q5JSZ9	Protein PRRC2B (Fragment)	179	°Unstimulated saliva
Q9BVV6	Protein TALPID3	182	°Unstimulated saliva
Q9NQW1	Protein transport protein Sec31B	418	°Unstimulated saliva
Q93096	Protein tyrosine phosphatase type IVA 1	167	°Unstimulated saliva
Q14517	Protocadherin Fat 1	183	°Unstimulated saliva
Q9Y5F7	Protocadherin gamma-C4	225	°Unstimulated saliva
Q58FF6	Putative heat shock protein HSP 90-beta 4	170	°Unstimulated saliva
Q5VSP4	Putative lipocalin 1-like protein 1	221	°Unstimulated saliva
Q8N9H6	Putative uncharacterized protein C8orf31	195	°Unstimulated saliva
Q15929	Putative zinc finger protein 56	599	°Unstimulated saliva
Q2TAK8	PWWP domain-containing DNA repair factor 3A	199	°Unstimulated saliva
Q9Y3Y4	Pygopus homolog 1	294	°Unstimulated saliva
Q2PPJ7	Ral GTPase-activating protein subunit alpha-2	321	°Unstimulated saliva
J3QLV2	Receptor tyrosine-protein kinase erbB-2 (Fragment)	711	°Unstimulated saliva
P10586	Receptor-type tyrosine-protein phosphatase F	173	°Unstimulated saliva
P28827	Receptor-type tyrosine-protein phosphatase mu	247	°Unstimulated saliva
Q15256	Receptor-type tyrosine-protein phosphatase R	358	°Unstimulated saliva
Q13332	Receptor-type tyrosine-protein phosphatase S	63	°Unstimulated saliva
Q96P16	Regulation of nuclear pre-mRNA domain-containing protein 1A	634	°Unstimulated saliva
Q9P2N2	Rho GTPase-activating protein 28	848	°Unstimulated saliva
O94989	Rho guanine nucleotide exchange factor 15	304	°Unstimulated saliva
Q15434	RNA-binding motif_ single-stranded-interacting protein 2	167	°Unstimulated saliva
P49756	RNA-binding protein 25	93	°Unstimulated saliva
Q9UKM9	RNA-binding protein Raly	242	°Unstimulated saliva
H7C357	Run domain Beclin-1-interacting and cysteine-rich domain-containing protein (Fragment)	147	°Unstimulated saliva
Q9BY12	S phase cyclin A-associated protein in the endoplasmic reticulum	237	°Unstimulated saliva

A0A096LPE2	SAA2-SAA4 readthrough	187	°Unstimulated saliva
Q9UL12	Sarcosine dehydrogenase_ mitochondrial	323	°Unstimulated saliva
Q15424	Scaffold attachment factor B1	183	°Unstimulated saliva
Q7Z7L1	Schlafen family member 11	258	°Unstimulated saliva
P13521	Secretogranin-2	342	°Unstimulated saliva
Q5T5U6	Selenide_ water dikinase 1 (Fragment)	421	°Unstimulated saliva
Q96I15	Selenocysteine lyase	525	°Unstimulated saliva
Q92854	Semaphorin-4D	197	°Unstimulated saliva
Q9P0U3	Sentrin-specific protease 1	147	°Unstimulated saliva
Q14674	Separin	255	°Unstimulated saliva
E7EPG2	Septin-5 (Fragment)	159	°Unstimulated saliva
Q8IYP2	Serine protease 58	150	°Unstimulated saliva
E5RHP4	Serine/threonine-protein phosphatase (Fragment)	268	°Unstimulated saliva
P67775	Serine/threonine-protein phosphatase 2A catalytic subunit alpha isoform	268	°Unstimulated saliva
P62714	Serine/threonine-protein phosphatase 2A catalytic subunit beta isoform	268	°Unstimulated saliva
Q8N8A2	Serine/threonine-protein phosphatase 6 regulatory ankyrin repeat subunit B	130	°Unstimulated saliva
H7C0U8	Serrate RNA effector molecule homolog (Fragment)	219	°Unstimulated saliva
E9PQD6	Serum amyloid A protein	331	°Unstimulated saliva
P0DJI8	Serum amyloid A-1 protein	331	°Unstimulated saliva
P0DJI9	Serum amyloid A-2 protein	368	°Unstimulated saliva
Q9UHB9	Signal recognition particle subunit SRP68	253	°Unstimulated saliva
Q5JXA9	Signal-regulatory protein beta-2	171	°Unstimulated saliva
A0A2R8YCJ5	Small integral membrane protein 41	222	°Unstimulated saliva
H9KVA1	Solute carrier family 22 member 17	203	°Unstimulated saliva
A0A1B0GVP8	Solute carrier family 26 member 10 (Fragment)	273	°Unstimulated saliva
Q9UMY4	Sorting nexin-12	165	°Unstimulated saliva
Q96JI7	Spatacsin	153	°Unstimulated saliva
I3L228	Sphingomyelin phosphodiesterase 3 (Fragment)	234	°Unstimulated saliva
G5EA09	Syndecan binding protein (Syntenin)_ isoform CRA_a	229	°Unstimulated saliva
O15061	Synemin	107	°Unstimulated saliva
A0A0B4J271	T cell receptor alpha variable 12-3	223	°Unstimulated saliva
A0A0J9YWI7	Taste receptor type 2	154	°Unstimulated saliva
P59541	Taste receptor type 2 member 30	154	°Unstimulated saliva
A0A087WXG5	TBC1 domain family member 17	200	°Unstimulated saliva
Q9NUY8	TBC1 domain family member 23	266	°Unstimulated saliva
Q9P273	Teneurin-3	232	°Unstimulated saliva
Q5TAX3	Terminal uridylyltransferase 4	158	°Unstimulated saliva
Q9BZW7	Testis-specific gene 10 protein	113	°Unstimulated saliva
D6RDX8	Tetraspanin	179	°Unstimulated saliva
Q96FV3	Tetraspanin-17	179	°Unstimulated saliva
P37173	TGF-beta receptor type-2	146	°Unstimulated saliva
Q86W42	THO complex subunit 6 homolog	181	°Unstimulated saliva

Q9P031	Thyroid transcription factor 1-associated protein 26	170	°Unstimulated saliva
E9PMZ8	T-lymphoma invasion and metastasis-inducing protein 2 (Fragment)	108	°Unstimulated saliva
F6SA91	TNF receptor-associated factor	207	°Unstimulated saliva
Q9BUZ4	TNF receptor-associated factor 4	207	°Unstimulated saliva
M0R142	TP53-binding protein 1 (Fragment)	135	°Unstimulated saliva
Q8WXI9	Transcriptional repressor p66-beta	318	°Unstimulated saliva
O94759	Transient receptor potential cation channel subfamily M member 2	236	°Unstimulated saliva
Q9HBA0	Transient receptor potential cation channel subfamily V member 4	112	°Unstimulated saliva
P07437	Tubulin beta chain	201	°Unstimulated saliva
Q13885	Tubulin beta-2A chain	201	°Unstimulated saliva
Q9BVA1	Tubulin beta-2B chain	201	°Unstimulated saliva
Q13509	Tubulin beta-3 chain	201	°Unstimulated saliva
Q12923	Tyrosine-protein phosphatase non-receptor type 13	196	°Unstimulated saliva
Q70CQ3	Ubiquitin carboxyl-terminal hydrolase 30	210	°Unstimulated saliva
Q9H9J4	Ubiquitin carboxyl-terminal hydrolase 42	172	°Unstimulated saliva
Q9H0E7	Ubiquitin carboxyl-terminal hydrolase 44	311	°Unstimulated saliva
O14562	Ubiquitin domain-containing protein UBFD1	194	°Unstimulated saliva
D6RJB3	Ubiquitin-conjugating enzyme E2 D3	717	°Unstimulated saliva
Q9BZL1	Ubiquitin-like protein 5	732	°Unstimulated saliva
F8VRI7	Ubiquitinyl hydrolase 1	279	°Unstimulated saliva
P78381	UDP-galactose translocator	285	°Unstimulated saliva
H7C4K7	Uncharacterized protein (Fragment)	274	°Unstimulated saliva
Q9H972	Uncharacterized protein C14orf93	327	°Unstimulated saliva
A8MV24	Uncharacterized protein C17orf98	179	°Unstimulated saliva
O15063	Uncharacterized protein KIAA0355	262	°Unstimulated saliva
A0A2R8Y6P1	Uncharacterized protein KIAA1211 (Fragment)	751	°Unstimulated saliva
K7EP79	Uncharacterized serine/threonine-protein kinase SBK3 (Fragment)	124	°Unstimulated saliva
Q8WVF2	Unique cartilage matrix-associated protein	204	°Unstimulated saliva
Q14CZ0	UPF0472 protein C16orf72	201	°Unstimulated saliva
H0YD59	Upstream stimulatory factor 1 (Fragment)	200	°Unstimulated saliva
A0A0A0MSM3	Utrophin (Fragment)	184	°Unstimulated saliva
Q96RL7	Vacuolar protein sorting-associated protein 13A	196	°Unstimulated saliva
M0R3C3	Very-long-chain enoyl-CoA reductase	180	°Unstimulated saliva
Q00341	Vigilin	343	°Unstimulated saliva
P08670	Vimentin	210	°Unstimulated saliva
P01282	VIP peptides	449	°Unstimulated saliva
Q14508	WAP four-disulfide core domain protein 2	390	°Unstimulated saliva
Q8IZU2	WD repeat-containing protein 17	123	°Unstimulated saliva
O95388	WNT1-inducible-signaling pathway protein 1	282	°Unstimulated saliva
M0R1Y0	Zinc finger and SCAN domain-containing protein 30	277	°Unstimulated saliva
A0A0D9SF71	Zinc finger E-box-binding homeobox 2	577	°Unstimulated saliva

Q9UJU3	Zinc finger protein 112	478	°Unstimulated saliva
Q15928	Zinc finger protein 141	872	°Unstimulated saliva
D6RIY0	Zinc finger protein 141 (Clone pHZ-44)_ isoform CRA_c	872	°Unstimulated saliva
P17023	Zinc finger protein 19	155	°Unstimulated saliva
K7EL19	Zinc finger protein 235 (Fragment)	122	°Unstimulated saliva
Q9HBT8	Zinc finger protein 286A	256	°Unstimulated saliva
Q06732	Zinc finger protein 33B	224	°Unstimulated saliva
M0R0R1	Zinc finger protein 415 (Fragment)	226	°Unstimulated saliva
Q8N7K0	Zinc finger protein 433	302	°Unstimulated saliva
Q9BX82	Zinc finger protein 471	176	°Unstimulated saliva
Q8TB69	Zinc finger protein 519	906	°Unstimulated saliva
Q3MIS6	Zinc finger protein 528	181	°Unstimulated saliva
Q96ND8	Zinc finger protein 583	183	°Unstimulated saliva
Q8IYB9	Zinc finger protein 595	887	°Unstimulated saliva
Q6ZNG1	Zinc finger protein 600	184	°Unstimulated saliva
Q2M218	Zinc finger protein 630	532	°Unstimulated saliva
Q3SXZ3	Zinc finger protein 718	872	°Unstimulated saliva
B4E159	Zinc finger protein 721	872	°Unstimulated saliva
B4DXR9	Zinc finger protein 732	872	°Unstimulated saliva
Q6ZN06	Zinc finger protein 813	163	°Unstimulated saliva

[+]Identification is based on protein ID from UniProt protein database, reviewed only (http://www.uniprot.org/).
[*]Proteins with expression significantly altered are organized according to the ratio.
°Indicates unique protein in alphabetical order.
Proteins highlighted in bold are increased or decreased more than 2-fold.

Supplementary Table 3. Proteins with significantly altered expression in the stimulated saliva in comparison with Unstimulated saliva after radiotherapy (ART) in patients with head and neck cancer.

[+]Access number	**Protein name**	***PLGS* Score**	***Ratio ART Stimulated:Unstimulated**
O00763	**Acetyl-CoA carboxylase 2**	**183**	**32.46**
P12821	**Angiotensin-converting enzyme**	**148**	**4.48**
A0A087WZY1	**Uncharacterized protein**	**5219**	**3.19**
Q9Y4G6	**Talin-2**	**148**	**3.13**
P09228	**Cystatin-SA**	**3186**	**3.00**
Q9Y2G1	**Myelin regulatory factor**	**131**	**2.83**
Q12955	**Ankyrin-3**	**116**	**2.59**
Q6P2Q9	**Pre-mRNA-processing-splicing factor 8**	**340**	**2.23**
P02812	Basic salivary proline-rich protein 2	590	1.84
E5RJR3	Methionine adenosyltransferase 2 subunit beta	1414	1.75
P01834	Immunoglobulin kappa constant	765	1.55
P04745	Alpha-amylase 1	11385	1.17
P61626	Lysozyme C	2277	0.73
Q562R1	Beta-actin-like protein 2	651	0.70
F8VV32	Lysozyme	2084	0.70

P63261	Actin_ cytoplasmic 2	3468	0.70
P68133	Actin_ alpha skeletal muscle	3248	0.69
P60709	Actin_ cytoplasmic 1	3468	0.68
P68032	Actin_ alpha cardiac muscle 1	3248	0.68
P63267	Actin_ gamma-enteric smooth muscle	3248	0.68
P62736	Actin_ aortic smooth muscle	3248	0.67
Q6S8J3	POTE ankyrin domain family member E	861	0.67
A5A3E0	POTE ankyrin domain family member F	861	0.64
P13929	Beta-enolase	612	0.63
Q8N4F0	BPI fold-containing family B member 2	1695	0.63
P02810	Salivary acidic proline-rich phosphoprotein 1/2	5219	0.61
P0CG38	POTE ankyrin domain family member I	441	0.61
A0A0A0MT31	Proline-rich protein 4	5219	0.59
Q03112	Histone-lysine N-methyltransferase MECOM	184	0.58
H3BU78	Fructose-bisphosphate aldolase (Fragment)	251	0.54
P29401	Transketolase	185	0.54
P06733	Alpha-enolase	1527	0.51
Q96DA0	**Zymogen granule protein 16 homolog B**	**1704**	**0.50**
P06744	**Glucose-6-phosphate isomerase**	**602**	**0.50**
P69905	**Hemoglobin subunit alpha**	**1536**	**0.49**
P01037	**Cystatin-SN**	**799**	**0.49**
P04075	**Fructose-bisphosphate aldolase A**	**382**	**0.48**
P04406	**Glyceraldehyde-3-phosphate dehydrogenase**	**2661**	**0.48**
P04080	**Cystatin-B**	**891**	**0.45**
P01877	**Immunoglobulin heavy constant alpha 2**	**3330**	**0.45**
B9A064	**Immunoglobulin lambda-like polypeptide 5**	**3447**	**0.45**
P01036	**Cystatin-S**	**637**	**0.44**
P0CF74	**Immunoglobulin lambda constant 6**	**4054**	**0.42**
P0DOY2	**Immunoglobulin lambda constant 2**	**4054**	**0.42**
P01591	**Immunoglobulin J chain**	**510**	**0.42**
P0CG04	**Immunoglobulin lambda constant 1**	**3447**	**0.41**
P0DOY3	**Immunoglobulin lambda constant 3**	**4054**	**0.41**
P02814	**Submaxillary gland androgen-regulated protein 3B**	**5689**	**0.41**
P01876	**Immunoglobulin heavy constant alpha 1**	**4467**	**0.39**
P01833	**Polymeric immunoglobulin receptor**	**354**	**0.39**
P07737	**Profilin-1**	**1252**	**0.39**
P13646	**Keratin_ type I cytoskeletal 13**	**3271**	**0.39**
Q13439	**Golgin subfamily A member 4**	**146**	**0.36**
P52209	**6-phosphogluconate dehydrogenase_ decarboxylating**	**318**	**0.35**
Q15154	**Pericentriolar material 1 protein**	**90**	**0.32**
P31025	**Lipocalin-1**	**885**	**0.31**
P02788	**Lactotransferrin**	**637**	**0.31**
Q5VSP4	**Putative lipocalin 1-like protein 1**	**287**	**0.28**

P27482	**Calmodulin-like protein 3**	**915**	**0.27**
P12273	**Prolactin-inducible protein**	**1990**	**0.25**
P02768	**Serum albumin**	**6568**	**0.25**
C9JKR2	**Albumin_ isoform CRA_k**	**3810**	**0.24**
P31947	**14-3-3 protein sigma**	**731**	**0.14**
O00533	**Neural cell adhesion molecule L1-like protein**	**213**	**0.08**
Q15751	**Probable E3 ubiquitin-protein ligase HERC1**	**168**	**0.02**
K7EQ26	116 kDa U5 small nuclear ribonucleoprotein component (Fragment)	343	°Stimulated saliva
Q13200	26S proteasome non-ATPase regulatory subunit 2	158	°Stimulated saliva
Q9H9J2	39S ribosomal protein L44_ mitochondrial	116	°Stimulated saliva
P22557	5-aminolevulinate synthase_ erythroid-specific_ mitochondrial	138	°Stimulated saliva
Q9NUB1	Acetyl-coenzyme A synthetase 2-like_ mitochondrial	211	°Stimulated saliva
O95996	Adenomatous polyposis coli protein 2	64	°Stimulated saliva
P55263	Adenosine kinase	178	°Stimulated saliva
Q9BRR6	ADP-dependent glucokinase	205	°Stimulated saliva
O43572	A-kinase anchor protein 10_ mitochondrial	190	°Stimulated saliva
Q99996	A-kinase anchor protein 9	155	°Stimulated saliva
P47895	Aldehyde dehydrogenase family 1 member A3	199	°Stimulated saliva
P30533	Alpha-2-macroglobulin receptor-associated protein	122	°Stimulated saliva
Q9UQQ1	Aminopeptidase NAALADL1	174	°Stimulated saliva
A0A0G2JMD7	Amyloid-beta A4 precursor protein-binding family A member 1 (Fragment)	150	°Stimulated saliva
Q96NW4	Ankyrin repeat domain-containing protein 27	120	°Stimulated saliva
Q01484	Ankyrin-2	103	°Stimulated saliva
O75843	AP-1 complex subunit gamma-like 2	506	°Stimulated saliva
O43299	AP-5 complex subunit zeta-1	179	°Stimulated saliva
Q5VUY0	Arylacetamide deacetylase-like 3	118	°Stimulated saliva
Q6PL18	ATPase family AAA domain-containing protein 2	259	°Stimulated saliva
E9PK50	ATP-binding cassette sub-family C member 8	589	°Stimulated saliva
Q9Y3E2	BolA-like protein 1	177	°Stimulated saliva
Q13410	Butyrophilin subfamily 1 member A1	157	°Stimulated saliva
Q8N6L6	C2 protein	248	°Stimulated saliva
A4D0V7	Cadherin-like and PC-esterase domain-containing protein 1	120	°Stimulated saliva
F8VXS2	Calcium-binding and coiled-coil domain-containing protein 1 (Fragment)	413	°Stimulated saliva
P78358	Cancer/testis antigen 1	356	°Stimulated saliva
G3XAM7	Catenin (Cadherin-associated protein)_ alpha 1_ 102kDa_ isoform CRA_a	113	°Stimulated saliva
P35221	Catenin alpha-1	132	°Stimulated saliva
B4E258	cDNA FLJ52650_ moderately similar to Synaptopodin-2	327	°Stimulated saliva

B4DRP8	cDNA FLJ54872_ highly similar to Zinc finger protein 461	544	°Stimulated saliva
B4E1Z4	cDNA FLJ55673_ highly similar to Complement factor B	135	°Stimulated saliva
B7Z9X4	cDNA_ FLJ78988_ highly similar to Protein NDRG4	129	°Stimulated saliva
Q13352	Centromere protein R	168	°Stimulated saliva
Q8WUX9	Charged multivesicular body protein 7	89	°Stimulated saliva
B7Z3I4	Chromodomain-helicase-DNA-binding protein 2	141	°Stimulated saliva
Q6ZTR5	Cilia- and flagella-associated protein 47	176	°Stimulated saliva
A0A087WVQ6	Clathrin heavy chain	131	°Stimulated saliva
Q00610	Clathrin heavy chain 1	134	°Stimulated saliva
Q96JN2	Coiled-coil domain-containing protein 136	350	°Stimulated saliva
Q5TID7	Coiled-coil domain-containing protein 181	229	°Stimulated saliva
P12110	Collagen alpha-2(VI) chain	220	°Stimulated saliva
Q9BXJ2	Complement C1q tumor necrosis factor-related protein 7	222	°Stimulated saliva
P06681	Complement C2	254	°Stimulated saliva
P00751	Complement factor B	135	°Stimulated saliva
Q9BPX3	Condensin complex subunit 3	236	°Stimulated saliva
Q86XI2	Condensin-2 complex subunit G2	179	°Stimulated saliva
Q969H4	Connector enhancer of kinase suppressor of ras 1	220	°Stimulated saliva
G3V160	Connector enhancer of kinase suppressor of Ras 1_ isoform CRA_a	125	°Stimulated saliva
Q9H9E3	Conserved oligomeric Golgi complex subunit 4	210	°Stimulated saliva
D6RE78	Cyclin G associated kinase_ isoform CRA_c	442	°Stimulated saliva
Q14004	Cyclin-dependent kinase 13	153	°Stimulated saliva
O14976	Cyclin-G-associated kinase	470	°Stimulated saliva
Q69YQ0	Cytospin-A	286	°Stimulated saliva
E7EUC9	DNA mismatch repair protein Mlh1 (Fragment)	212	°Stimulated saliva
P36954	DNA-directed RNA polymerase II subunit RPB9	232	°Stimulated saliva
O75953	DnaJ homolog subfamily B member 5	328	°Stimulated saliva
Q96J02	E3 ubiquitin-protein ligase Itchy homolog	356	°Stimulated saliva
O43567	E3 ubiquitin-protein ligase RNF13	577	°Stimulated saliva
O95071	E3 ubiquitin-protein ligase UBR5	311	°Stimulated saliva
P98170	E3 ubiquitin-protein ligase XIAP	241	°Stimulated saliva
A0A0A0MRX1	ELAV-like protein	140	°Stimulated saliva
Q12926	ELAV-like protein 2	140	°Stimulated saliva
Q9Y6R1	Electrogenic sodium bicarbonate cotransporter 1	261	°Stimulated saliva
Q8TE02	Elongator complex protein 5	517	°Stimulated saliva
Q4L180	Filamin A-interacting protein 1-like	202	°Stimulated saliva
E9PPM4	Galectin-8	627	°Stimulated saliva
Q9UHL9	General transcription factor II-I repeat domain-containing protein 1	95	°Stimulated saliva
Q86W71	GOLGA4 protein	235	°Stimulated saliva

P47775	G-protein coupled receptor 12	187	°Stimulated saliva
A0A2R8YGI6	HCG2045904_ isoform CRA_b	199	°Stimulated saliva
Q4VXL4	HCG41426_ isoform CRA_c	180	°Stimulated saliva
Q12931	Heat shock protein 75 kDa_ mitochondrial	223	°Stimulated saliva
Q15477	Helicase SKI2W	171	°Stimulated saliva
I3L383	Homeobox protein Hox-B8 (Fragment)	159	°Stimulated saliva
Q537H9	HSD-43	167	°Stimulated saliva
P01871	Immunoglobulin heavy constant mu	133	°Stimulated saliva
Q70EL1	Inactive ubiquitin carboxyl-terminal hydrolase 54	151	°Stimulated saliva
Q8WYH8	Inhibitor of growth protein 5	271	°Stimulated saliva
F8SNU6	Integrin-linked kinase associated phosphatase	402	°Stimulated saliva
Q9H0C8	Integrin-linked kinase-associated serine/threonine phosphatase 2C	402	°Stimulated saliva
Q8NAC3	Interleukin-17 receptor C	278	°Stimulated saliva
Q5TF58	Intermediate filament family orphan 2	150	°Stimulated saliva
Q9NQN3	Jouberin	263	°Stimulated saliva
Q9NS87	Kinesin-like protein KIF15	204	°Stimulated saliva
P50748	Kinetochore-associated protein 1	149	°Stimulated saliva
Q71QC5	KRAB zinc finger protein (Fragment)	352	°Stimulated saliva
H7C5A4	Latexin (Fragment)	209	°Stimulated saliva
Q0VAA2	Leucine-rich repeat-containing protein 74A	140	°Stimulated saliva
O43679	LIM domain-binding protein 2	225	°Stimulated saliva
Q13136	Liprin-alpha-1	115	°Stimulated saliva
O75334	Liprin-alpha-2	110	°Stimulated saliva
O75335	Liprin-alpha-4	127	°Stimulated saliva
A0A3B3IS95	L-lactate dehydrogenase	137	°Stimulated saliva
P00338	L-lactate dehydrogenase A chain	213	°Stimulated saliva
P07195	L-lactate dehydrogenase B chain	137	°Stimulated saliva
Q14168	MAGUK p55 subfamily member 2	333	°Stimulated saliva
Q9NZW5	MAGUK p55 subfamily member 6	331	°Stimulated saliva
P27448	MAP/microtubule affinity-regulating kinase 3	169	°Stimulated saliva
Q96L34	MAP/microtubule affinity-regulating kinase 4	175	°Stimulated saliva
H0YF21	MAP7 domain-containing protein 1 (Fragment)	186	°Stimulated saliva
P43243	Matrin-3	396	°Stimulated saliva
Q14676	Mediator of DNA damage checkpoint protein 1	158	°Stimulated saliva
Q9Y2X0	Mediator of RNA polymerase II transcription subunit 16	152	°Stimulated saliva
B8ZZG1	Membrane protein_ palmitoylated 6 (MAGUK p55 subfamily member 6)_ isoform CRA_a	306	°Stimulated saliva
Q14832	Metabotropic glutamate receptor 3	140	°Stimulated saliva
P01033	Metalloproteinase inhibitor 1	180	°Stimulated saliva
Q9P267	Methyl-CpG-binding domain protein 5	91	°Stimulated saliva
Q8N6Q8	Methyltransferase-like protein 25	338	°Stimulated saliva

Q9H1A3	Methyltransferase-like protein 9	480	°Stimulated saliva
O75121	Microfibrillar-associated protein 3-like	310	°Stimulated saliva
C9JAF1	Mitochondrial fission factor (Fragment)	168	°Stimulated saliva
O60830	Mitochondrial import inner membrane translocase subunit Tim17-B	181	°Stimulated saliva
O43318	Mitogen-activated protein kinase kinase kinase 7	120	°Stimulated saliva
F6WRY4	Msx2-interacting protein (Fragment)	170	°Stimulated saliva
Q8N307	Mucin-20	336	°Stimulated saliva
Q6P1R3	Myb/SANT-like DNA-binding domain-containing protein 2	254	°Stimulated saliva
O14745	Na(+)/H(+) exchange regulatory cofactor NHE-RF1	189	°Stimulated saliva
C9JFW8	N-acetylated-alpha-linked acidic dipeptidase-like protein	154	°Stimulated saliva
H0YD04	NADH dehydrogenase [ubiquinone] flavoprotein 1_ mitochondrial (Fragment)	172	°Stimulated saliva
Q14CX7	N-alpha-acetyltransferase 25_ NatB auxiliary subunit	292	°Stimulated saliva
B4DIB3	Non-specific serine/threonine protein kinase	166	°Stimulated saliva
J3KNR0	Non-specific serine/threonine protein kinase	169	°Stimulated saliva
J3KT44	Nuclear receptor corepressor 1	285	°Stimulated saliva
Q8TE49	OTU domain-containing protein 7A	373	°Stimulated saliva
Q9Y236	Oxidative stress-induced growth inhibitor 2	155	°Stimulated saliva
Q8WX93	Palladin	184	°Stimulated saliva
Q8TEW0	Partitioning defective 3 homolog	125	°Stimulated saliva
Q53GG5	PDZ and LIM domain protein 3	63	°Stimulated saliva
P62937	Peptidyl-prolyl cis-trans isomerase A	97	°Stimulated saliva
Q9NYI0	PH and SEC7 domain-containing protein 3	101	°Stimulated saliva
P48426	Phosphatidylinositol 5-phosphate 4-kinase type-2 alpha	64	°Stimulated saliva
P78356	Phosphatidylinositol 5-phosphate 4-kinase type-2 beta	91	°Stimulated saliva
O95394	Phosphoacetylglucosamine mutase	221	°Stimulated saliva
P18669	Phosphoglycerate mutase 1	135	°Stimulated saliva
Q15102	Platelet-activating factor acetylhydrolase IB subunit gamma	354	°Stimulated saliva
Q9ULL4	Plexin-B3	251	°Stimulated saliva
Q9P0L9	Polycystic kidney disease 2-like 1 protein	179	°Stimulated saliva
Q92562	Polyphosphoinositide phosphatase	129	°Stimulated saliva
K7EJ44	Profilin	287	°Stimulated saliva
Q9BRP4	Proteasomal ATPase-associated factor 1	168	°Stimulated saliva
P84996	Protein ALEX	119	°Stimulated saliva
Q96LP2	Protein FAM81B	82	°Stimulated saliva
A2RTY3	Protein HEATR9	309	°Stimulated saliva
Q765P7	Protein MTSS 2	164	°Stimulated saliva
Q9ULP0	Protein NDRG4	129	°Stimulated saliva
Q8WZA1	Protein O-linked-mannose beta-1_2-N-acetylglucosaminyltransferase 1	121	°Stimulated saliva

H0YIL7	Protein phosphatase 1 regulatory subunit 12A (Fragment)	400	°Stimulated saliva
Q92540	Protein SMG7	155	°Stimulated saliva
Q92734	Protein TFG	198	°Stimulated saliva
Q14289	Protein-tyrosine kinase 2-beta	201	°Stimulated saliva
Q8N0V3	Putative ribosome-binding factor A_ mitochondrial	137	°Stimulated saliva
Q8N814	Putative uncharacterized protein FLJ40140	397	°Stimulated saliva
Q9H1K0	Rabenosyn-5	364	°Stimulated saliva
Q12967	Ral guanine nucleotide dissociation stimulator	429	°Stimulated saliva
D6REY8	Rap guanine nucleotide exchange factor 2 (Fragment)	162	°Stimulated saliva
P46940	Ras GTPase-activating-like protein IQGAP1	369	°Stimulated saliva
Q7LDG7	RAS guanyl-releasing protein 2	167	°Stimulated saliva
P61018	Ras-related protein Rab-4B	218	°Stimulated saliva
Q9H6L5	Reticulophagy regulator 1	139	°Stimulated saliva
G3V510	Retinol dehydrogenase 11	483	°Stimulated saliva
E9PGT3	Ribosomal protein S6 kinase	226	°Stimulated saliva
Q15418	Ribosomal protein S6 kinase alpha-1	234	°Stimulated saliva
Q8N1G1	RNA exonuclease 1 homolog	320	°Stimulated saliva
Q96IZ5	RNA-binding protein 41	544	°Stimulated saliva
P35913	Rod cGMP-specific 3'_5'-cyclic phosphodiesterase subunit beta	243	°Stimulated saliva
Q01196	Runt-related transcription factor 1	100	°Stimulated saliva
Q9NWH9	SAFB-like transcription modulator	391	°Stimulated saliva
O14983	Sarcoplasmic/endoplasmic reticulum calcium ATPase 1	152	°Stimulated saliva
P16615	Sarcoplasmic/endoplasmic reticulum calcium ATPase 2	157	°Stimulated saliva
Q68D06	Schlafen family member 13	403	°Stimulated saliva
Q8N1F8	Serine/threonine-protein kinase 11-interacting protein	139	°Stimulated saliva
Q9BZL6	Serine/threonine-protein kinase D2	276	°Stimulated saliva
Q9P0L2	Serine/threonine-protein kinase MARK1	166	°Stimulated saliva
E9PCD1	Serine/threonine-protein kinase WNK2	102	°Stimulated saliva
Q9C0I3	Serine-rich coiled-coil domain-containing protein 1	455	°Stimulated saliva
Q9UQR0	Sex comb on midleg-like protein 2	182	°Stimulated saliva
Q5VZ18	SH2 domain-containing adapter protein E	136	°Stimulated saliva
Q9H299	SH3 domain-binding glutamic acid-rich-like protein 3	212	°Stimulated saliva
A2RU48	Single-pass membrane and coiled-coil domain-containing protein 3	158	°Stimulated saliva
O15245	Solute carrier family 22 member 1	457	°Stimulated saliva
C9JK45	Solute carrier family 35 member E1 (Fragment)	444	°Stimulated saliva
Q14515	SPARC-like protein 1	208	°Stimulated saliva
F8WAN1	SPECC1L-ADORA2A readthrough (NMD candidate)	276	°Stimulated saliva
W5XKT8	Sperm acrosome membrane-associated protein 6	178	°Stimulated saliva

Q8IVG5	Sterile alpha motif domain-containing protein 9-like	170	°Stimulated saliva
Q9UMS6	Synaptopodin-2	394	°Stimulated saliva
Q8IYJ3	Synaptotagmin-like protein 1	440	°Stimulated saliva
A0A0B4J268	T cell receptor alpha variable 4	391	°Stimulated saliva
A0A075B6T8	T cell receptor alpha variable 9-1	259	°Stimulated saliva
Q9BX59	Tapasin-related protein	121	°Stimulated saliva
Q0IIM8	TBC1 domain family member 8B	143	°Stimulated saliva
B4DZS4	T-complex protein 11 X-linked protein 1	293	°Stimulated saliva
Q99973	Telomerase protein component 1	214	°Stimulated saliva
P10074	Telomere zinc finger-associated protein	111	°Stimulated saliva
A0A087WZG0	Testis-specific protein 10-interacting protein	175	°Stimulated saliva
Q6PJ65	Tetraspanin	264	°Stimulated saliva
H0YN95	THAP domain-containing protein 10 (Fragment)	204	°Stimulated saliva
H7BZY0	TP53-binding protein 1 (Fragment)	112	°Stimulated saliva
H0Y550	Trafficking protein particle complex subunit 12 (Fragment)	252	°Stimulated saliva
Q14135	Transcription cofactor vestigial-like protein 4	182	°Stimulated saliva
F8WEV4	Transcriptional activator GLI3	310	°Stimulated saliva
O95359	Transforming acidic coiled-coil-containing protein 2	193	°Stimulated saliva
Q9Y6A5	Transforming acidic coiled-coil-containing protein 3	256	°Stimulated saliva
Q2T9K0	Transmembrane protein 44	245	°Stimulated saliva
H0YB65	Transmembrane protein 71 (Fragment)	537	°Stimulated saliva
Q86UV5	Ubiquitin carboxyl-terminal hydrolase 48	306	°Stimulated saliva
Q9H8M7	Ubiquitin carboxyl-terminal hydrolase MINDY-3	152	°Stimulated saliva
O95155	Ubiquitin conjugation factor E4 B	220	°Stimulated saliva
F2Z2N1	Uncharacterized protein	199	°Stimulated saliva
A0A2R8Y471	Uncharacterized protein	429	°Stimulated saliva
Q8IYS4	Uncharacterized protein C16orf71	224	°Stimulated saliva
Q8IXQ3	Uncharacterized protein C9orf40	481	°Stimulated saliva
Q9HAI6	Uncharacterized protein CXorf21	146	°Stimulated saliva
B2RTY4	Unconventional myosin-IXa	125	°Stimulated saliva
P49754	Vacuolar protein sorting-associated protein 41 homolog	203	°Stimulated saliva
Q8NEY4	V-type proton ATPase subunit C 2	87	°Stimulated saliva
Q9Y4E6	WD repeat-containing protein 7	162	°Stimulated saliva
Q9GZV5	WW domain-containing transcription regulator protein 1	317	°Stimulated saliva
Q5T200	Zinc finger CCCH domain-containing protein 13	98	°Stimulated saliva
Q9HCG1	Zinc finger protein 160	140	°Stimulated saliva
Q9NQX6	Zinc finger protein 331	352	°Stimulated saliva
Q06732	Zinc finger protein 33B	22	°Stimulated saliva
Q8NA42	Zinc finger protein 383	351	°Stimulated saliva
Q8TAF7	Zinc finger protein 461	544	°Stimulated saliva

Q8WV37	Zinc finger protein 480	140	°Stimulated saliva
E5RGH0	Zinc finger protein 721	267	°Stimulated saliva
I3L119	Zinc finger protein 785 (Fragment)	1006	°Stimulated saliva
Q6PDB4	Zinc finger protein 880	149	°Stimulated saliva
P31946	14-3-3 protein beta/alpha	310	°Unstimulated saliva
P62258	14-3-3 protein epsilon	357	°Unstimulated saliva
Q04917	14-3-3 protein eta	310	°Unstimulated saliva
P61981	14-3-3 protein gamma	310	°Unstimulated saliva
P27348	14-3-3 protein theta	335	°Unstimulated saliva
P63104	14-3-3 protein zeta/delta	687	°Unstimulated saliva
Q15147	1-phosphatidylinositol 4_5-bisphosphate phosphodiesterase beta-4	533	°Unstimulated saliva
P82664	28S ribosomal protein S10_ mitochondrial	340	°Unstimulated saliva
Q9P2N4	A disintegrin and metalloproteinase with thrombospondin motifs 9	266	°Unstimulated saliva
Q13085	Acetyl-CoA carboxylase 1	144	°Unstimulated saliva
Q16515	Acid-sensing ion channel 2	114	°Unstimulated saliva
Q08AH3	Acyl-coenzyme A synthetase ACSM2A_ mitochondrial	412	°Unstimulated saliva
Q68CK6	Acyl-coenzyme A synthetase ACSM2B_ mitochondrial	311	°Unstimulated saliva
Q76L82	Additional sex combs like 1 (Drosophila)_ isoform CRA_d	243	°Unstimulated saliva
Q5TCS8	Adenylate kinase 9	746	°Unstimulated saliva
Q9Y3D8	Adenylate kinase isoenzyme 6	597	°Unstimulated saliva
O94910	Adhesion G protein-coupled receptor L1	141	°Unstimulated saliva
Q02952	A-kinase anchor protein 12	111	°Unstimulated saliva
H0YMW2	A-kinase anchor protein 13 (Fragment)	263	°Unstimulated saliva
Q9BTE6	Alanyl-tRNA editing protein Aarsd1	229	°Unstimulated saliva
O60218	Aldo-keto reductase family 1 member B10	252	°Unstimulated saliva
P02763	Alpha-1-acid glycoprotein 1	412	°Unstimulated saliva
P01011	Alpha-1-antichymotrypsin	254	°Unstimulated saliva
P01009	Alpha-1-antitrypsin	186	°Unstimulated saliva
P01023	Alpha-2-macroglobulin	158	°Unstimulated saliva
G3V5M4	Alpha-actinin-1 (Fragment)	345	°Unstimulated saliva
H0Y9H2	Alpha-adducin (Fragment)	333	°Unstimulated saliva
H7C5V0	Alpha-sarcoglycan (Fragment)	271	°Unstimulated saliva
Q8IWZ3	Ankyrin repeat and KH domain-containing protein 1	129	°Unstimulated saliva
Q5JPF3	Ankyrin repeat domain-containing protein 36C	110	°Unstimulated saliva
E5RK69	Annexin	123	°Unstimulated saliva
Q5T3N1	Annexin (Fragment)	925	°Unstimulated saliva
P04083	Annexin A1	925	°Unstimulated saliva
P08133	Annexin A6	137	°Unstimulated saliva
P02647	Apolipoprotein A-I	862	°Unstimulated saliva
P06727	Apolipoprotein A-IV	108	°Unstimulated saliva
G3V3T3	Apoptotic chromatin condensation inducer in the nucleus (Fragment)	110	°Unstimulated saliva
P16050	Arachidonate 15-lipoxygenase	250	°Unstimulated saliva

H7C264	Arf-GAP with dual PH domain-containing protein 1 (Fragment)	128	°Unstimulated saliva
Q9P2R6	Arginine-glutamic acid dipeptide repeats protein	161	°Unstimulated saliva
Q8NEN0	Armadillo repeat-containing protein 2	120	°Unstimulated saliva
O00327	Aryl hydrocarbon receptor nuclear translocator-like protein 1	205	°Unstimulated saliva
Q498B9	ASXL1 protein	214	°Unstimulated saliva
O94762	ATP-dependent DNA helicase Q5	141	°Unstimulated saliva
Q9BQ39	ATP-dependent RNA helicase DDX50	294	°Unstimulated saliva
Q8NHQ9	ATP-dependent RNA helicase DDX55	117	°Unstimulated saliva
Q8WXE1	ATR-interacting protein	140	°Unstimulated saliva
Q9Y2J2	Band 4.1-like protein 3	184	°Unstimulated saliva
P41182	B-cell lymphoma 6 protein	179	°Unstimulated saliva
O00587	Beta-1_3-N-acetylglucosaminyltransferase manic fringe	185	°Unstimulated saliva
P61769	Beta-2-microglobulin	655	°Unstimulated saliva
P35612	Beta-adducin	225	°Unstimulated saliva
P07686	Beta-hexosaminidase subunit beta	81	°Unstimulated saliva
Q8TDL5	BPI fold-containing family B member 1	1032	°Unstimulated saliva
A0A0A0MR97	Bromodomain adjacent to zinc finger domain protein 2B	62	°Unstimulated saliva
B7ZM11	C2orf73 protein	286	°Unstimulated saliva
P20807	Calpain-3	155	°Unstimulated saliva
Q6ZU35	Cancer-related regulator of actin dynamics	220	°Unstimulated saliva
Q9Y4C5	Carbohydrate sulfotransferase 2	155	°Unstimulated saliva
P00915	Carbonic anhydrase 1	1501	°Unstimulated saliva
P23280	Carbonic anhydrase 6	691	°Unstimulated saliva
H3BMH0	CCR4-NOT transcription complex subunit 1 (Fragment)	158	°Unstimulated saliva
B4DYW9	cDNA FLJ61485_ highly similar to Zinc finger protein 215	212	°Unstimulated saliva
G5EA36	Cell division cycle 27_ isoform CRA_c	434	°Unstimulated saliva
P30260	Cell division cycle protein 27 homolog	434	°Unstimulated saliva
P49454	Centromere protein F	124	°Unstimulated saliva
A0A0U1RRI6	Centromere protein V-like protein 3	154	°Unstimulated saliva
Q02224	Centromere-associated protein E	52	°Unstimulated saliva
Q5SW79	Centrosomal protein of 170 kDa	218	°Unstimulated saliva
Q9BV73	Centrosome-associated protein CEP250	43	°Unstimulated saliva
O00408	cGMP-dependent 3'_5'-cyclic phosphodiesterase	197	°Unstimulated saliva
A0A3B3IRY0	Chloride transport protein 6	158	°Unstimulated saliva
P51797	Chloride transport protein 6	159	°Unstimulated saliva
E9PM92	Chromosome 11 open reading frame 58	220	°Unstimulated saliva
F8VXK5	Chromosome 12 open reading frame 75	777	°Unstimulated saliva
O60271	C-Jun-amino-terminal kinase-interacting protein 4	79	°Unstimulated saliva
Q16630	Cleavage and polyadenylation specificity factor subunit 6	161	°Unstimulated saliva
P10909	Clusterin	154	°Unstimulated saliva
Q9UJ98	Cohesin subunit SA-3	219	°Unstimulated saliva

Q5VVM6	Coiled-coil domain-containing protein 30	84	°Unstimulated saliva
Q96ER9	Coiled-coil domain-containing protein 51	229	°Unstimulated saliva
H7BY33	Coiled-coil domain-containing protein 88B	84	°Unstimulated saliva
Q6ZUT6	Coiled-coil domain-containing protein 9B	123	°Unstimulated saliva
Q99715	Collagen alpha-1(XII) chain	76	°Unstimulated saliva
P12111	Collagen alpha-3(VI) chain	241	°Unstimulated saliva
P01024	Complement C3	497	°Unstimulated saliva
P17927	Complement receptor type 1	84	°Unstimulated saliva
Q14028	Cyclic nucleotide-gated cation channel beta-1	112	°Unstimulated saliva
Q00536	Cyclin-dependent kinase 16	219	°Unstimulated saliva
Q00537	Cyclin-dependent kinase 17	108	°Unstimulated saliva
Q07002	Cyclin-dependent kinase 18	153	°Unstimulated saliva
P01034	Cystatin-C	2691	°Unstimulated saliva
Q14204	Cytoplasmic dynein 1 heavy chain 1	113	°Unstimulated saliva
Q8NCM8	Cytoplasmic dynein 2 heavy chain 1	50	°Unstimulated saliva
O75891	Cytosolic 10-formyltetrahydrofolate dehydrogenase	420	°Unstimulated saliva
Q9UGM3	Deleted in malignant brain tumors 1 protein	294	°Unstimulated saliva
Q8NG44	Delta 3+6/2 progesterone receptor	104	°Unstimulated saliva
Q8NG42	Delta 6/2 progesterone receptor	104	°Unstimulated saliva
Q6IQ26	DENN domain-containing protein 5A	187	°Unstimulated saliva
E5RGY0	Derlin	143	°Unstimulated saliva
Q9BUN8	Derlin-1	205	°Unstimulated saliva
Q02487	Desmocollin-2	206	°Unstimulated saliva
P32926	Desmoglein-3	215	°Unstimulated saliva
A0A0B4J2C2	Discs_ large (Drosophila) homolog-associated protein 4_ isoform CRA_b	277	°Unstimulated saliva
Q9Y2H0	Disks large-associated protein 4	277	°Unstimulated saliva
P54098	DNA polymerase subunit gamma-1	266	°Unstimulated saliva
O75771	DNA repair protein RAD51 homolog 4	918	°Unstimulated saliva
Q9UBZ9	DNA repair protein REV1	121	°Unstimulated saliva
P49736	DNA replication licensing factor MCM2	704	°Unstimulated saliva
K7EMH3	DNA-directed RNA polymerase_ mitochondrial (Fragment)	109	°Unstimulated saliva
O75190	DnaJ homolog subfamily B member 6	314	°Unstimulated saliva
O75165	DnaJ homolog subfamily C member 13	146	°Unstimulated saliva
E9PEI6	DPCR1	105	°Unstimulated saliva
Q6P0N6	DST protein	64	°Unstimulated saliva
Q96M86	Dynein heavy chain domain-containing protein 1	192	°Unstimulated saliva
P11532	Dystrophin	180	°Unstimulated saliva
E9PJB5	E3 ubiquitin-protein ligase COP1 (Fragment)	205	°Unstimulated saliva
Q7Z6Z7	E3 ubiquitin-protein ligase HUWE1	150	°Unstimulated saliva
Q8IUD6	E3 ubiquitin-protein ligase RNF135	227	°Unstimulated saliva
Q53HC9	EARP and GARP complex-interacting protein 1	234	°Unstimulated saliva
Q8NDI1	EH domain-binding protein 1	242	°Unstimulated saliva

Q5T6L9	Endoplasmic reticulum membrane-associated RNA degradation protein	417	°Unstimulated saliva
Q9H6T0	Epithelial splicing regulatory protein 2	185	°Unstimulated saliva
I6L9I8	EPN3 protein	147	°Unstimulated saliva
Q9H201	Epsin-3	179	°Unstimulated saliva
Q14152	Eukaryotic translation initiation factor 3 subunit A	100	°Unstimulated saliva
Q0VAP4	FANCA protein	152	°Unstimulated saliva
O15360	Fanconi anemia group A protein	158	°Unstimulated saliva
P23142	Fibulin-1	320	°Unstimulated saliva
G5E965	Forkhead box P1_ isoform CRA_f	342	°Unstimulated saliva
A0A3B3IRS5	Forkhead box P1_ isoform CRA_g	342	°Unstimulated saliva
Q9H334	Forkhead box protein P1	351	°Unstimulated saliva
P09972	Fructose-bisphosphate aldolase C	64	°Unstimulated saliva
M0R108	Galectin-16	409	°Unstimulated saliva
P47929	Galectin-7	156	°Unstimulated saliva
Q86XP6	Gastrokine-2	302	°Unstimulated saliva
A0A2R8YG73	Girdin	80	°Unstimulated saliva
A0A2R8Y7X9	GLOBIN domain-containing protein	2599	°Unstimulated saliva
Q6IA69	Glutamine-dependent NAD(+) synthetase	477	°Unstimulated saliva
P09211	Glutathione S-transferase P	279	°Unstimulated saliva
P48637	Glutathione synthetase	207	°Unstimulated saliva
Q08378	Golgin subfamily A member 3	186	°Unstimulated saliva
Q86VD9	GPI mannosyltransferase 4	440	°Unstimulated saliva
P49685	G-protein coupled receptor 15	171	°Unstimulated saliva
P00738	Haptoglobin	966	°Unstimulated saliva
G5E9S6	HCG1994835	473	°Unstimulated saliva
Q7Z2R1	HCG19985_ isoform CRA_b	462	°Unstimulated saliva
K7EN88	HCG2039718_ isoform CRA_g	873	°Unstimulated saliva
G3XAL8	HCG21296_ isoform CRA_a	233	°Unstimulated saliva
O00165	HCLS1-associated protein X-1	166	°Unstimulated saliva
Q53T59	HCLS1-binding protein 3	169	°Unstimulated saliva
K7ENF6	Heat shock 70 kDa protein 12A (Fragment)	190	°Unstimulated saliva
P11142	Heat shock cognate 71 kDa protein	241	°Unstimulated saliva
P04792	Heat shock protein beta-1	1496	°Unstimulated saliva
Q03014	Hematopoietically-expressed homeobox protein HHEX	171	°Unstimulated saliva
P68871	Hemoglobin subunit beta	3014	°Unstimulated saliva
P02042	Hemoglobin subunit delta	2599	°Unstimulated saliva
P02100	Hemoglobin subunit epsilon	2599	°Unstimulated saliva
P69891	Hemoglobin subunit gamma-1	2599	°Unstimulated saliva
P69892	Hemoglobin subunit gamma-2	2599	°Unstimulated saliva
P35680	Hepatocyte nuclear factor 1-beta	166	°Unstimulated saliva
A0A3B3IRI4	Histone acetyltransferase	463	°Unstimulated saliva
C9JJY6	Histone acetyltransferase KAT6A	252	°Unstimulated saliva
Q8WYB5	Histone acetyltransferase KAT6B	463	°Unstimulated saliva
Q9UBN7	Histone deacetylase 6	264	°Unstimulated saliva

U3KQK0	Histone H2B	593	°Unstimulated saliva
Q96A08	Histone H2B type 1-A	489	°Unstimulated saliva
P33778	Histone H2B type 1-B	593	°Unstimulated saliva
P62807	Histone H2B type 1-C/E/F/G/I	593	°Unstimulated saliva
P58876	Histone H2B type 1-D	593	°Unstimulated saliva
Q93079	Histone H2B type 1-H	593	°Unstimulated saliva
P06899	Histone H2B type 1-J	593	°Unstimulated saliva
O60814	Histone H2B type 1-K	593	°Unstimulated saliva
Q99880	Histone H2B type 1-L	593	°Unstimulated saliva
Q99879	Histone H2B type 1-M	593	°Unstimulated saliva
Q99877	Histone H2B type 1-N	593	°Unstimulated saliva
P23527	Histone H2B type 1-O	593	°Unstimulated saliva
Q16778	Histone H2B type 2-E	593	°Unstimulated saliva
Q5QNW6	Histone H2B type 2-F	593	°Unstimulated saliva
Q8N257	Histone H2B type 3-B	593	°Unstimulated saliva
P57053	Histone H2B type F-S	593	°Unstimulated saliva
E9PR05	Histone-lysine N-methyltransferase 2A (Fragment)	167	°Unstimulated saliva
Q9H9B1	Histone-lysine N-methyltransferase EHMT1	134	°Unstimulated saliva
Q92800	Histone-lysine N-methyltransferase EZH1	159	°Unstimulated saliva
O96028	Histone-lysine N-methyltransferase NSD2	176	°Unstimulated saliva
E0YMJ8	HNF1 beta A splice variant 3	166	°Unstimulated saliva
P57058	Hormonally up-regulated neu tumor-associated kinase	91	°Unstimulated saliva
Q4G0P3	Hydrocephalus-inducing protein homolog	325	°Unstimulated saliva
P01857	Immunoglobulin heavy constant gamma 1	155	°Unstimulated saliva
P01859	Immunoglobulin heavy constant gamma 2	971	°Unstimulated saliva
P01860	Immunoglobulin heavy constant gamma 3	791	°Unstimulated saliva
P01861	Immunoglobulin heavy constant gamma 4	707	°Unstimulated saliva
A0M8Q6	Immunoglobulin lambda constant 7	3136	°Unstimulated saliva
Q8TDY8	Immunoglobulin superfamily DCC subclass member 4	122	°Unstimulated saliva
Q8NBJ7	Inactive C-alpha-formylglycine-generating enzyme 2	272	°Unstimulated saliva
Q14571	Inositol 1_4_5-trisphosphate receptor type 2	342	°Unstimulated saliva
Q9UKX5	Integrin alpha-11	122	°Unstimulated saliva
A0A087X131	Integrin alpha-X	323	°Unstimulated saliva
J3QQL2	Integrin beta (Fragment)	112	°Unstimulated saliva
P16144	Integrin beta-4	124	°Unstimulated saliva
P18510	Interleukin-1 receptor antagonist protein	118	°Unstimulated saliva
Q96CU4	Intraflagellar transport protein 56	214	°Unstimulated saliva
P06870	Kallikrein-1	226	°Unstimulated saliva
O95198	Kelch-like protein 2	146	°Unstimulated saliva
P13645	Keratin_ type I cytoskeletal 10	411	°Unstimulated saliva
P02533	Keratin_ type I cytoskeletal 14	171	°Unstimulated saliva
P19012	Keratin_ type I cytoskeletal 15	146	°Unstimulated saliva
P08779	Keratin_ type I cytoskeletal 16	200	°Unstimulated saliva

Q04695	Keratin_ type I cytoskeletal 17	84	°Unstimulated saliva
P08727	Keratin_ type I cytoskeletal 19	254	°Unstimulated saliva
Q2M2I5	Keratin_ type I cytoskeletal 24	190	°Unstimulated saliva
P04264	Keratin_ type II cytoskeletal 1	81	°Unstimulated saliva
P35908	Keratin_ type II cytoskeletal 2 epidermal	285	°Unstimulated saliva
Q01546	Keratin_ type II cytoskeletal 2 oral	122	°Unstimulated saliva
P19013	Keratin_ type II cytoskeletal 4	316	°Unstimulated saliva
P13647	Keratin_ type II cytoskeletal 5	338	°Unstimulated saliva
P02538	Keratin_ type II cytoskeletal 6A	497	°Unstimulated saliva
P04259	Keratin_ type II cytoskeletal 6B	497	°Unstimulated saliva
P48668	Keratin_ type II cytoskeletal 6C	497	°Unstimulated saliva
Q86Y46	Keratin_ type II cytoskeletal 73	85	°Unstimulated saliva
O95678	Keratin_ type II cytoskeletal 75	213	°Unstimulated saliva
Q5XKE5	Keratin_ type II cytoskeletal 79	213	°Unstimulated saliva
Q8IUB9	Keratin-associated protein 19-1	358	°Unstimulated saliva
Q5T011	KICSTOR complex protein SZT2	128	°Unstimulated saliva
Q6UWL6	Kin of IRRE-like protein 2	98	°Unstimulated saliva
Q4R9M9	Kinesin family member 1Bbeta isoform II	233	°Unstimulated saliva
E7EVH7	Kinesin light chain	143	°Unstimulated saliva
Q07866	Kinesin light chain 1	143	°Unstimulated saliva
O60333	Kinesin-like protein KIF1B	233	°Unstimulated saliva
Q96Q89	Kinesin-like protein KIF20B	490	°Unstimulated saliva
Q8NBT2	Kinetochore protein Spc24	169	°Unstimulated saliva
K7ERI5	KRAB domain-containing protein	989	°Unstimulated saliva
Q6PIL6	Kv channel-interacting protein 4	263	°Unstimulated saliva
Q8NBH2	Kyphoscoliosis peptidase	538	°Unstimulated saliva
P22079	Lactoperoxidase	575	°Unstimulated saliva
Q9UNP4	Lactosylceramide alpha-2_3-sialyltransferase	338	°Unstimulated saliva
O00515	Ladinin-1	168	°Unstimulated saliva
Q96JM4	Leucine-rich repeat and IQ domain-containing protein 1	177	°Unstimulated saliva
Q8TE12	LIM homeobox transcription factor 1-alpha	64	°Unstimulated saliva
Q8IVV2	Lipoxygenase homology domain-containing protein 1	231	°Unstimulated saliva
O95274	Ly6/PLAUR domain-containing protein 3	207	°Unstimulated saliva
Q9UJU2	Lymphoid enhancer-binding factor 1	178	°Unstimulated saliva
Q8N5G2	Macoilin	141	°Unstimulated saliva
Q8NFP4	MAM domain-containing glycosylphosphatidylinositol anchor protein 1	108	°Unstimulated saliva
C9JQX2	Mannosyltransferase	440	°Unstimulated saliva
Q86YW9	Mediator of RNA polymerase II transcription subunit 12-like protein	287	°Unstimulated saliva
Q8N4V1	Membrane magnesium transporter 1	204	°Unstimulated saliva
H7C4S7	Membrane-associated guanylate kinase_ WW and PDZ domain-containing protein 1 (Fragment)	359	°Unstimulated saliva
Q14831	Metabotropic glutamate receptor 7	232	°Unstimulated saliva

O75030	Microphthalmia-associated transcription factor	466	°Unstimulated saliva
Q9Y584	Mitochondrial import inner membrane translocase subunit Tim22	590	°Unstimulated saliva
O43615	Mitochondrial import inner membrane translocase subunit TIM44	283	°Unstimulated saliva
O43683	Mitotic checkpoint serine/threonine-protein kinase BUB1	88	°Unstimulated saliva
O15427	Monocarboxylate transporter 4	137	°Unstimulated saliva
Q8TAX7	Mucin-7	2050	°Unstimulated saliva
A0A1B0GV46	Mucin-like protein 3	108	°Unstimulated saliva
Q9H8L6	Multimerin-2	367	°Unstimulated saliva
O75970	Multiple PDZ domain protein	505	°Unstimulated saliva
A0A3B3ITT2	Myelin transcription factor 1-like protein	421	°Unstimulated saliva
P05164	Myeloperoxidase	181	°Unstimulated saliva
Q9NZM1	Myoferlin	57	°Unstimulated saliva
Q5VU43	Myomegalin	292	°Unstimulated saliva
P10916	Myosin regulatory light chain 2_ ventricular/cardiac muscle isoform	172	°Unstimulated saliva
A0A2R8Y4C3	Myosin-14	186	°Unstimulated saliva
M0R0W4	NACHT_ LRR and PYD domains-containing protein 5 (Fragment)	284	°Unstimulated saliva
Q6IQ20	N-acyl-phosphatidylethanolamine-hydrolyzing phospholipase D	220	°Unstimulated saliva
F8W029	Nascent polypeptide-associated complex subunit alpha	510	°Unstimulated saliva
O14513	Nck-associated protein 5	197	°Unstimulated saliva
O75161	Nephrocystin-4	167	°Unstimulated saliva
E9PNX2	Neuronal acetylcholine receptor subunit alpha-10	114	°Unstimulated saliva
P59665	Neutrophil defensin 1	950	°Unstimulated saliva
P59666	Neutrophil defensin 3	950	°Unstimulated saliva
H0YCT7	Non-receptor tyrosine-protein kinase TYK2 (Fragment)	218	°Unstimulated saliva
Q7Z6G3	N-terminal EF-hand calcium-binding protein 2	299	°Unstimulated saliva
D6RH30	Nuclear factor NF-kappa-B p105 subunit (Fragment)	99	°Unstimulated saliva
J3QL49	Nuclear pore complex protein Nup85 (Fragment)	735	°Unstimulated saliva
P52948	Nuclear pore complex protein Nup98-Nup96	334	°Unstimulated saliva
H7C0P3	Nuclear receptor corepressor 2 (Fragment)	76	°Unstimulated saliva
C9J0I9	Nuclear-interacting partner of ALK	397	°Unstimulated saliva
Q86WB0	Nuclear-interacting partner of ALK	397	°Unstimulated saliva
C9JTN7	Nucleolysin TIA-1 isoform p40	372	°Unstimulated saliva
Q01085	Nucleolysin TIAR	372	°Unstimulated saliva
Q9NWT1	p21-activated protein kinase-interacting protein 1	158	°Unstimulated saliva
H0Y2Y4	Palmitoyltransferase (Fragment)	341	°Unstimulated saliva
P49023	Paxillin	91	°Unstimulated saliva
Q96A99	Pentraxin-4	115	°Unstimulated saliva
Q9UIL8	PHD finger protein 11	132	°Unstimulated saliva

P00439	Phenylalanine-4-hydroxylase	297	°Unstimulated saliva
A0A0J9YVR0	Phosphatase and actin regulator (Fragment)	112	°Unstimulated saliva
Q8IZ21	Phosphatase and actin regulator 4	132	°Unstimulated saliva
Q9NTJ5	Phosphatidylinositide phosphatase SAC1	135	°Unstimulated saliva
P42338	Phosphatidylinositol 4_5-bisphosphate 3-kinase catalytic subunit beta isoform	197	°Unstimulated saliva
E9PEF1	Phosphodiesterase	191	°Unstimulated saliva
P00558	Phosphoglycerate kinase 1	195	°Unstimulated saliva
P07205	Phosphoglycerate kinase 2	249	°Unstimulated saliva
O14939	Phospholipase D2	259	°Unstimulated saliva
Q6IQ23	Pleckstrin homology domain-containing family A member 7	123	°Unstimulated saliva
D6RH25	Plexin-D1	234	°Unstimulated saliva
Q3YAB7	Potassium channel interacting protein 4	263	°Unstimulated saliva
Q6UN15	Pre-mRNA 3'-end-processing factor FIP1	108	°Unstimulated saliva
Q9UMS4	Pre-mRNA-processing factor 19	148	°Unstimulated saliva
Q9Y4D8	Probable E3 ubiquitin-protein ligase HECTD4	142	°Unstimulated saliva
P06401	Progesterone receptor	104	°Unstimulated saliva
P56975	Pro-neuregulin-3_ membrane-bound isoform	102	°Unstimulated saliva
H3BSI4	Protein CBFA2T3 (Fragment)	1058	°Unstimulated saliva
Q5W0V4	Protein FAM160B1	304	°Unstimulated saliva
A8MVW0	Protein FAM171A2	125	°Unstimulated saliva
Q658Y4	Protein FAM91A1	167	°Unstimulated saliva
D6RGZ9	Protein mono-ADP-ribosyltransferase PARP8 (Fragment)	462	°Unstimulated saliva
I3L2A7	Protein moonraker (Fragment)	370	°Unstimulated saliva
Q9Y520	Protein PRRC2C	307	°Unstimulated saliva
Q9Y2M2	Protein SSUH2 homolog	183	°Unstimulated saliva
E5RHH4	Protein YIPF (Fragment)	719	°Unstimulated saliva
E5RGR9	Protein YIPF5 (Fragment)	719	°Unstimulated saliva
Q7Z7L7	Protein zer-1 homolog	236	°Unstimulated saliva
Q86YA3	Protein ZGRF1	253	°Unstimulated saliva
Q08188	Protein-glutamine gamma-glutamyltransferase E	161	°Unstimulated saliva
Q9Y5I1	Protocadherin alpha-11	201	°Unstimulated saliva
Q9Y5F1	Protocadherin beta-12	933	°Unstimulated saliva
Q14517	Protocadherin Fat 1	202	°Unstimulated saliva
Q8NHS7	PTPRS protein	305	°Unstimulated saliva
P35247	Pulmonary surfactant-associated protein D	174	°Unstimulated saliva
Q58FF6	Putative heat shock protein HSP 90-beta 4	101	°Unstimulated saliva
Q5JWS8	Putative Polycomb group protein ASXL1	214	°Unstimulated saliva
P0CL83	Putative STAG3-like protein 1	217	°Unstimulated saliva
P0CL84	Putative STAG3-like protein 2	217	°Unstimulated saliva
Q5JXB2	Putative ubiquitin-conjugating enzyme E2 N-like	721	°Unstimulated saliva
Q9NSJ1	Putative zinc finger protein 355P	268	°Unstimulated saliva
Q15276	Rab GTPase-binding effector protein 1	192	°Unstimulated saliva

Q5T1S4	Rab9 effector protein with kelch motifs	127	°Unstimulated saliva
Q8TEU7	Rap guanine nucleotide exchange factor 6	217	°Unstimulated saliva
K7EIL6	RECA_2 domain-containing protein	867	°Unstimulated saliva
Q13332	Receptor-type tyrosine-protein phosphatase S	310	°Unstimulated saliva
Q504U0	Renal cancer differentiation gene 1 protein	539	°Unstimulated saliva
Q9BQY4	Rhox homeobox family member 2	357	°Unstimulated saliva
J3QRF4	RNA binding protein fox-1 homolog	203	°Unstimulated saliva
F5H5U2	RNA helicase	117	°Unstimulated saliva
P49756	RNA-binding protein 25	283	°Unstimulated saliva
K7EJX6	RNA-binding protein fox-1 homolog 3 (Fragment)	203	°Unstimulated saliva
Q96LT9	RNA-binding region-containing protein 3	260	°Unstimulated saliva
H7C4J7	Roundabout homolog 2 (Fragment)	726	°Unstimulated saliva
Q15413	Ryanodine receptor 3	182	°Unstimulated saliva
H3BT27	S phase cyclin A-associated protein in the endoplasmic reticulum (Fragment)	281	°Unstimulated saliva
A0A096LPE2	SAA2-SAA4 readthrough	319	°Unstimulated saliva
Q15424	Scaffold attachment factor B1	358	°Unstimulated saliva
P0DP57	Secreted Ly-6/uPAR domain-containing protein 2	836	°Unstimulated saliva
O14640	Segment polarity protein dishevelled homolog DVL-1	108	°Unstimulated saliva
Q9NQ38	Serine protease inhibitor Kazal-type 5	207	°Unstimulated saliva
Q13243	Serine/arginine-rich splicing factor 5	309	°Unstimulated saliva
Q9Y2H1	Serine/threonine-protein kinase 38-like	313	°Unstimulated saliva
Q13535	Serine/threonine-protein kinase ATR	306	°Unstimulated saliva
Q9Y3F4	Serine-threonine kinase receptor-associated protein	157	°Unstimulated saliva
P02787	Serotransferrin	144	°Unstimulated saliva
P29508	Serpin B3	293	°Unstimulated saliva
E9PQD6	Serum amyloid A protein	457	°Unstimulated saliva
P0DJI8	Serum amyloid A-1 protein	457	°Unstimulated saliva
P0DJI9	Serum amyloid A-2 protein	319	°Unstimulated saliva
H0YDR5	Single Ig IL-1-related receptor (Fragment)	339	°Unstimulated saliva
Q8ND83	SLAIN motif-containing protein 1	184	°Unstimulated saliva
O00193	Small acidic protein	220	°Unstimulated saliva
Q8NBW4	Sodium-coupled neutral amino acid transporter 9	504	°Unstimulated saliva
Q6ICL7	Solute carrier family 35 member E4	113	°Unstimulated saliva
O94875	Sorbin and SH3 domain-containing protein 2	638	°Unstimulated saliva
G5E9Y6	Spermatogenesis associated 4_ isoform CRA_a	161	°Unstimulated saliva
Q8NEY3	Spermatogenesis-associated protein 4	222	°Unstimulated saliva
Q9Y657	Spindlin-1	213	°Unstimulated saliva
Q5JUX0	Spindlin-3	213	°Unstimulated saliva
G3V0H1	SRY (Sex determining region Y)-box 5_ isoform CRA_f	133	°Unstimulated saliva
P0CL85	STAG3-like protein 3	217	°Unstimulated saliva
Q99470	Stromal cell-derived factor 2	451	°Unstimulated saliva

A6NHR9	Structural maintenance of chromosomes flexible hinge domain-containing protein 1	223	°Unstimulated saliva
E9PD53	Structural maintenance of chromosomes protein	161	°Unstimulated saliva
Q9NTJ3	Structural maintenance of chromosomes protein 4	163	°Unstimulated saliva
Q6ZRP7	Sulfhydryl oxidase 2	268	°Unstimulated saliva
O94901	SUN domain-containing protein 1	217	°Unstimulated saliva
P00441	Superoxide dismutase [Cu-Zn]	900	°Unstimulated saliva
J3KQV8	Synaptojanin-1	156	°Unstimulated saliva
Q86SS6	Synaptotagmin-9	303	°Unstimulated saliva
Q9NX95	Syntabulin	303	°Unstimulated saliva
A0A075B6T7	T cell receptor alpha variable 6	153	°Unstimulated saliva
E2GH26	T-cell factor-4 variant L	144	°Unstimulated saliva
C6ZRJ7	TCF7L2 isoform pFC8A_TCF7L2_A3_ex1-12_13_13a	144	°Unstimulated saliva
C6ZRJ6	TCF7L2 isoform pFC8A_TCF7L2_D5_ex3_4a-11_12_13a_14	144	°Unstimulated saliva
C6ZRK5	TCF7L2 isoform pFC8A_TCF7L2_ex1-11-13-14	144	°Unstimulated saliva
Q5VVR7	TCF7L2 isoform pFC8A_TCF7L2_H7_ex1-11-13-13b	144	°Unstimulated saliva
Q9UIF3	Tektin-2	157	°Unstimulated saliva
Q86US8	Telomerase-binding protein EST1A	386	°Unstimulated saliva
Q9BXU2	Testis-expressed protein 13B	220	°Unstimulated saliva
Q9BZW7	Testis-specific gene 10 protein	129	°Unstimulated saliva
Q96N46	Tetratricopeptide repeat protein 14	133	°Unstimulated saliva
Q8NDW8	Tetratricopeptide repeat protein 21A	104	°Unstimulated saliva
A0A0C4DG98	THO complex subunit 2	102	°Unstimulated saliva
Q6ZMP0	Thrombospondin type-1 domain-containing protein 4	515	°Unstimulated saliva
H0YLT6	Tight junction protein ZO-1 (Fragment)	194	°Unstimulated saliva
Q13009	T-lymphoma invasion and metastasis-inducing protein 1	96	°Unstimulated saliva
Q92844	TRAF family member-associated NF-kappa-B activator	189	°Unstimulated saliva
Q15560	Transcription elongation factor A protein 2	159	°Unstimulated saliva
P36402	Transcription factor 7	144	°Unstimulated saliva
B7WNT5	Transcription factor 7 (T-cell specific_ HMG-box)_ isoform CRA_c	144	°Unstimulated saliva
Q9HCS4	Transcription factor 7-like 1	245	°Unstimulated saliva
Q9NQB0	Transcription factor 7-like 2	144	°Unstimulated saliva
P35711	Transcription factor SOX-5	133	°Unstimulated saliva
A6H8Y1	Transcription factor TFIIIB component B" homolog	97	°Unstimulated saliva
Q7Z410	Transmembrane protease serine 9	68	°Unstimulated saliva
Q7Z2Z1	Treslin	120	°Unstimulated saliva
Q9H2D6	TRIO and F-actin-binding protein	105	°Unstimulated saliva
P60174	Triosephosphate isomerase	306	°Unstimulated saliva
Q9C040	Tripartite motif-containing protein 2	152	°Unstimulated saliva
E7EWD5	TSC22 domain family protein 3	146	°Unstimulated saliva

Q02223	Tumor necrosis factor receptor superfamily member 17	142	°Unstimulated saliva
Q8IYU4	Ubiquilin-like protein	140	°Unstimulated saliva
Q9Y4E8	Ubiquitin carboxyl-terminal hydrolase 15	211	°Unstimulated saliva
Q9NVE5	Ubiquitin carboxyl-terminal hydrolase 40	294	°Unstimulated saliva
A0JNW5	UHRF1-binding protein 1-like	304	°Unstimulated saliva
Q9H972	Uncharacterized protein C14orf93	959	°Unstimulated saliva
Q8N5S3	Uncharacterized protein C2orf73	299	°Unstimulated saliva
A0A2R8Y6P1	Uncharacterized protein KIAA1211 (Fragment)	214	°Unstimulated saliva
Q86XI8	Uncharacterized protein ZSWIM9	95	°Unstimulated saliva
Q9UBC5	Unconventional myosin-Ia	186	°Unstimulated saliva
Q9ULV0	Unconventional myosin-Vb	149	°Unstimulated saliva
Q9NQX4	Unconventional myosin-Vc	171	°Unstimulated saliva
P22415	Upstream stimulatory factor 1	272	°Unstimulated saliva
P11684	Uteroglobin	714	°Unstimulated saliva
A0A0A0MSM3	Utrophin (Fragment)	516	°Unstimulated saliva
P19320	Vascular cell adhesion protein 1	90	°Unstimulated saliva
M0R3C3	Very-long-chain enoyl-CoA reductase	183	°Unstimulated saliva
O60504	Vinexin	255	°Unstimulated saliva
Q6UXI7	Vitrin	327	°Unstimulated saliva
Q7Z3J2	VPS35 endosomal protein sorting factor-like	109	°Unstimulated saliva
Q14508	WAP four-disulfide core domain protein 2	309	°Unstimulated saliva
O43516	WAS/WASL-interacting protein family member 1	334	°Unstimulated saliva
Q8IWG1	WD repeat-containing protein 63	203	°Unstimulated saliva
Q5VTH9	WD repeat-containing protein 78	272	°Unstimulated saliva
Q96KN7	X-linked retinitis pigmentosa GTPase regulator-interacting protein 1	181	°Unstimulated saliva
C9J6P4	Zinc finger CCCH-type antiviral protein 1	277	°Unstimulated saliva
E5RHS1	Zinc finger homeobox protein 4 (Fragment)	269	°Unstimulated saliva
Q9UBW7	Zinc finger MYM-type protein 2	195	°Unstimulated saliva
Q9UJU3	Zinc finger protein 112	993	°Unstimulated saliva
Q15928	Zinc finger protein 141	168	°Unstimulated saliva
D6RIY0	Zinc finger protein 141 (Clone pHZ-44)_ isoform CRA_c	168	°Unstimulated saliva
E9PSE6	Zinc finger protein 195 (Fragment)	219	°Unstimulated saliva
Q9UL58	Zinc finger protein 215	228	°Unstimulated saliva
O75437	Zinc finger protein 254	471	°Unstimulated saliva
Q96JL9	Zinc finger protein 333	735	°Unstimulated saliva
M0R230	Zinc finger protein 417	412	°Unstimulated saliva
Q8N7K0	Zinc finger protein 433	886	°Unstimulated saliva
Q96JC4	Zinc finger protein 479	210	°Unstimulated saliva
Q8TB69	Zinc finger protein 519	128	°Unstimulated saliva
Q8NB42	Zinc finger protein 527	188	°Unstimulated saliva
O15090	Zinc finger protein 536	120	°Unstimulated saliva
C9J2D3	Zinc finger protein 566 (Fragment)	206	°Unstimulated saliva

Q8IYB9	Zinc finger protein 595	265	°Unstimulated saliva
Q14966	Zinc finger protein 638	414	°Unstimulated saliva
M0QYA4	Zinc finger protein 677	653	°Unstimulated saliva
P25311	Zinc-alpha-2-glycoprotein	544	°Unstimulated saliva
Q0P6G1	ZNF527 protein	188	°Unstimulated saliva

[+]Identification is based on protein ID from UniProt protein database, reviewed only (http://www.uniprot.org/).
[*]Proteins with expression significantly altered are organized according to the ratio.
°Indicates unique protein in alphabetical order.
Proteins highlighted in bold are increased or decreased more than 2-fold.

Supplementary Table 4. Proteins with significantly altered expression in the stimulated saliva in comparison with Unstimulated saliva in healthy patients (control group).

[+]Access number	**Protein name**	***PLGS* Score**	***Ratio Control Stimulated: Unstimulated**
P15515	**Histatin-1**	**1163**	**2.72**
P02768	Serum albumin	6056	1.62
C9JKR2	Albumin_ isoform CRA_k	3204	1.60
P09228	Cystatin-SA	2577	1.43
P04745	Alpha-amylase 1	40491	1.38
P04746	Pancreatic alpha-amylase	26183	1.38
P19961	Alpha-amylase 2B	32796	1.26
P02812	Basic salivary proline-rich protein 2	4204	0.63
P04280	Basic salivary proline-rich protein 1	2904	0.62
P02814	Submaxillary gland androgen-regulated protein 3B	8894	0.58
P01876	Immunoglobulin heavy constant alpha 1	5728	0.55
P01833	Polymeric immunoglobulin receptor	1562	0.55
P01877	**Immunoglobulin heavy constant alpha 2**	**4989**	**0.48**
Q96DA0	**Zymogen granule protein 16 homolog B**	**4692**	**0.28**
P02808	**Statherin**	**24107**	**0.26**
Q9H9V9	2-oxoglutarate and iron-dependent oxygenase JMJD4	153	°Stimulated saliva
Q66S35	6-phosphofructo-2-kinase/fructose-2_ 6-biphosphatase 4 isoform 1	155	°Stimulated saliva
Q16877	6-phosphofructo-2-kinase/fructose-2_6-bisphosphatase 4	155	°Stimulated saliva
P52209	6-phosphogluconate dehydrogenase_ decarboxylating	258	°Stimulated saliva
P01009	Alpha-1-antitrypsin	216	°Stimulated saliva
P06733	Alpha-enolase	559	°Stimulated saliva
A0A087WUP0	Annexin	345	°Stimulated saliva
Q5VT79	Annexin A8-like protein 1	345	°Stimulated saliva
P02647	Apolipoprotein A-I	656	°Stimulated saliva
B1AKN3	Arginine-glutamic acid dipeptide (RE) repeats_ isoform CRA_b	264	°Stimulated saliva
Q9P2R6	Arginine-glutamic acid dipeptide repeats protein	839	°Stimulated saliva
P13929	Beta-enolase	472	°Stimulated saliva

Q9NQY0	Bridging integrator 3	260	°Stimulated saliva
P55286	Cadherin-8	628	°Stimulated saliva
Q9NP86	Calcium-binding protein 5	502	°Stimulated saliva
C9JT99	Calcium-responsive transcription factor (Fragment)	721	°Stimulated saliva
P27482	Calmodulin-like protein 3	302	°Stimulated saliva
Q6ZRH7	Cation channel sperm-associated protein subunit gamma	292	°Stimulated saliva
Q8N8E3	Centrosomal protein of 112 kDa	232	°Stimulated saliva
O00408	cGMP-dependent 3'_5'-cyclic phosphodiesterase	385	°Stimulated saliva
Q9HC52	Chromobox protein homolog 8	285	°Stimulated saliva
F5GZK7	Condensin complex subunit 1 (Fragment)	350	°Stimulated saliva
A0A1W2PS52	Cystatin-B	473	°Stimulated saliva
E5RI01	Double-strand-break repair protein rad21 homolog	225	°Stimulated saliva
P49792	E3 SUMO-protein ligase RanBP2	305	°Stimulated saliva
E9PJB5	E3 ubiquitin-protein ligase COP1 (Fragment)	266	°Stimulated saliva
C9J6V3	Echinoderm microtubule-associated protein-like 3 (Fragment)	507	°Stimulated saliva
Q9BW60	Elongation of very long chain fatty acids protein 1	291	°Stimulated saliva
P14138	Endothelin-3	182	°Stimulated saliva
Q9BVV2	Fibronectin type III domain-containing protein 11	283	°Stimulated saliva
P09104	Gamma-enolase	438	°Stimulated saliva
Q8WUA4	General transcription factor 3C polypeptide 2	387	°Stimulated saliva
H0YIY4	Gephyrin (Fragment)	453	°Stimulated saliva
A0A2R8Y7X9	GLOBIN domain-containing protein	297	°Stimulated saliva
Q99062	Granulocyte colony-stimulating factor receptor	231	°Stimulated saliva
J3KTB1	Growth arrest-specific protein 7 (Fragment)	292	°Stimulated saliva
P36915	Guanine nucleotide-binding protein-like 1	321	°Stimulated saliva
G3V1N2	HCG1745306_ isoform CRA_a	242	°Stimulated saliva
P69905	Hemoglobin subunit alpha	290	°Stimulated saliva
P68871	Hemoglobin subunit beta	297	°Stimulated saliva
P02042	Hemoglobin subunit delta	297	°Stimulated saliva
P02100	Hemoglobin subunit epsilon	297	°Stimulated saliva
P69891	Hemoglobin subunit gamma-1	297	°Stimulated saliva
P69892	Hemoglobin subunit gamma-2	297	°Stimulated saliva
P09105	Hemoglobin subunit theta-1	377	°Stimulated saliva
Q9H0E3	Histone deacetylase complex subunit SAP130	145	°Stimulated saliva
Q09028	Histone-binding protein RBBP4	182	°Stimulated saliva
Q8TEK3	Histone-lysine N-methyltransferase_ H3 lysine-79 specific	254	°Stimulated saliva
P14902	Indoleamine 2_3-dioxygenase 1	312	°Stimulated saliva
Q15811	Intersectin-1	133	°Stimulated saliva
P50213	Isocitrate dehydrogenase [NAD] subunit alpha_ mitochondrial	317	°Stimulated saliva
Q07866	Kinesin light chain 1	85	°Stimulated saliva
H0YIM7	Kinesin-like protein (Fragment)	255	°Stimulated saliva

Q7Z4S6	Kinesin-like protein KIF21A	273	°Stimulated saliva
O75037	Kinesin-like protein KIF21B	267	°Stimulated saliva
Q9BRS8	La-related protein 6	102	°Stimulated saliva
E9PQN3	Lysosomal Pro-X carboxypeptidase (Fragment)	421	°Stimulated saliva
Q9NZW5	MAGUK p55 subfamily member 6	261	°Stimulated saliva
Q5T911	Mediator of RNA polymerase II transcription subunit 4 (Fragment)	231	°Stimulated saliva
B8ZZG1	Membrane protein_ palmitoylated 6 (MAGUK p55 subfamily member 6)_ isoform CRA_a	239	°Stimulated saliva
E5RJR3	Methionine adenosyltransferase 2 subunit beta	1216	°Stimulated saliva
Q9Y584	Mitochondrial import inner membrane translocase subunit Tim22	300	°Stimulated saliva
Q9Y2G1	Myelin regulatory factor	424	°Stimulated saliva
M0QXJ9	Myotonin-protein kinase (Fragment)	195	°Stimulated saliva
Q9NX02	NACHT_ LRR and PYD domains-containing protein 2	181	°Stimulated saliva
A0A0G2JI50	Negative elongation factor E (Fragment)	268	°Stimulated saliva
H7C1V7	N-glycosylase/DNA lyase (Fragment)	1024	°Stimulated saliva
Q9UMX2	Ornithine decarboxylase antizyme 3	269	°Stimulated saliva
P50542	Peroxisomal targeting signal 1 receptor	558	°Stimulated saliva
Q9Y446	Plakophilin-3	97	°Stimulated saliva
Q15102	Platelet-activating factor acetylhydrolase IB subunit gamma	247	°Stimulated saliva
Q5GLZ8	Probable E3 ubiquitin-protein ligase HERC4	575	°Stimulated saliva
O75081	Protein CBFA2T3	562	°Stimulated saliva
P18583	Protein SON	328	°Stimulated saliva
Q9NQW1	Protein transport protein Sec31B	352	°Stimulated saliva
Q8NHS7	PTPRS protein	521	°Stimulated saliva
Q9H853	Putative tubulin-like protein alpha-4B	261	°Stimulated saliva
H3BR70	Pyruvate kinase	624	°Stimulated saliva
P14618	Pyruvate kinase PKM	624	°Stimulated saliva
Q99666	RANBP2-like and GRIP domain-containing protein 5/6	307	°Stimulated saliva
O14715	RANBP2-like and GRIP domain-containing protein 8	315	°Stimulated saliva
Q13332	Receptor-type tyrosine-protein phosphatase S	528	°Stimulated saliva
Q7Z5H3	Rho GTPase-activating protein 22	127	°Stimulated saliva
Q9P2N2	Rho GTPase-activating protein 28	313	°Stimulated saliva
Q9UKM9	RNA-binding protein Raly	178	°Stimulated saliva
Q96LT9	RNA-binding region-containing protein 3	306	°Stimulated saliva
S6FRS6	SAM domain_ SH3 domain and nuclear localization signals 1	533	°Stimulated saliva
Q9NSI8	SAM domain-containing protein SAMSN-1	545	°Stimulated saliva
O14640	Segment polarity protein dishevelled homolog DVL-1	119	°Stimulated saliva
Q9C0C4	Semaphorin-4C	503	°Stimulated saliva
Q92854	Semaphorin-4D	227	°Stimulated saliva
Q8IYP2	Serine protease 58	192	°Stimulated saliva
O43464	Serine protease HTRA2_ mitochondrial	207	°Stimulated saliva

D6RB57	Serine/threonine-protein phosphatase 2A 55 kDa regulatory subunit B beta isoform	353	°Stimulated saliva
Q86WA9	Sodium-independent sulfate anion transporter	636	°Stimulated saliva
D6RDY9	Solute carrier family 35 member B1	186	°Stimulated saliva
Q96JI7	Spatacsin	105	°Stimulated saliva
Q86VE3	Spermidine/spermine N(1)-acetyltransferase-like protein 1	106	°Stimulated saliva
Q9BUD6	Spondin-2	246	°Stimulated saliva
Q9UJZ1	Stomatin-like protein 2_ mitochondrial	331	°Stimulated saliva
P31040	Succinate dehydrogenase [ubiquinone] flavoprotein subunit_ mitochondrial	288	°Stimulated saliva
Q9Y4G6	Talin-2	151	°Stimulated saliva
H0YDZ6	Terminal uridylyltransferase 4 (Fragment)	432	°Stimulated saliva
Q9BZW7	Testis-specific gene 10 protein	100	°Stimulated saliva
O43396	Thioredoxin-like protein 1	290	°Stimulated saliva
H7BZ10	TRAF3-interacting protein 1	233	°Stimulated saliva
A0A0D9SGJ4	Transcription factor 4	330	°Stimulated saliva
Q03167	Transforming growth factor beta receptor type 3	356	°Stimulated saliva
Q9C035	Tripartite motif-containing protein 5	318	°Stimulated saliva
F5H5D3	Tubulin alpha chain	318	°Stimulated saliva
Q71U36	Tubulin alpha-1A chain	318	°Stimulated saliva
P68363	Tubulin alpha-1B chain	318	°Stimulated saliva
Q9BQE3	Tubulin alpha-1C chain	318	°Stimulated saliva
P68366	Tubulin alpha-4A chain	318	°Stimulated saliva
Q05209	Tyrosine-protein phosphatase non-receptor type 12	160	°Stimulated saliva
E7EVH7	Uncharacterized protein	85	°Stimulated saliva
A0A2U3TZJ3	Uncharacterized protein (Fragment)	202	°Stimulated saliva
J3KSC3	Uncharacterized protein (Fragment)	230	°Stimulated saliva
H3BPC8	Uncharacterized protein (Fragment)	299	°Stimulated saliva
Q9H972	Uncharacterized protein C14orf93	569	°Stimulated saliva
Q8IYS4	Uncharacterized protein C16orf71	454	°Stimulated saliva
Q6ZUG5	Uncharacterized protein FLJ43738	166	°Stimulated saliva
A0A2R8YFM9	Uncharacterized protein KIAA1257	166	°Stimulated saliva
Q9BUW7	UPF0184 protein C9orf16	794	°Stimulated saliva
J3KNI2	UPF0598 protein C8orf82	193	°Stimulated saliva
Q7L1V2	Vacuolar fusion protein MON1 homolog B	437	°Stimulated saliva
Q12901	Zinc finger protein 155	212	°Stimulated saliva
Q9UK13	Zinc finger protein 221	187	°Stimulated saliva
Q06730	Zinc finger protein 33A	500	°Stimulated saliva
Q9H5I4	Zinc finger protein 33A_ isoform CRA_c	495	°Stimulated saliva
Q06732	Zinc finger protein 33B	495	°Stimulated saliva
Q8TE99	2-phosphoxylose phosphatase 1	364	°Unstimulated saliva
P42765	3-ketoacyl-CoA thiolase_ mitochondrial	363	°Unstimulated saliva
Q9H2P0	Activity-dependent neuroprotector homeobox protein	112	°Unstimulated saliva
O00116	Alkyldihydroxyacetonephosphate synthase_ peroxisomal	141	°Unstimulated saliva

E9PKC5	AMP deaminase	381	°Unstimulated saliva
Q01432	AMP deaminase 3	385	°Unstimulated saliva
H7C3N6	Anoctamin (Fragment)	278	°Unstimulated saliva
A0A087WW05	Aspartyl/asparaginyl beta-hydroxylase (Fragment)	1009	°Unstimulated saliva
Q5TC12	ATP synthase mitochondrial F1 complex assembly factor 1	416	°Unstimulated saliva
Q01813	ATP-dependent 6-phosphofructokinase_ platelet type	295	°Unstimulated saliva
O94762	ATP-dependent DNA helicase Q5	447	°Unstimulated saliva
P61769	Beta-2-microglobulin	286	°Unstimulated saliva
Q8TDL5	BPI fold-containing family B member 1	310	°Unstimulated saliva
Q9NRL2	Bromodomain adjacent to zinc finger domain protein 1A	453	°Unstimulated saliva
O00478	Butyrophilin subfamily 3 member A3	647	°Unstimulated saliva
P19022	Cadherin-2	660	°Unstimulated saliva
H7C555	Cadherin-related family member 3 (Fragment)	138	°Unstimulated saliva
P43235	Cathepsin K	153	°Unstimulated saliva
P16070	CD44 antigen	337	°Unstimulated saliva
B4DRP8	cDNA FLJ54872_ highly similar to Zinc finger protein 461	759	°Unstimulated saliva
P56749	Claudin-12	643	°Unstimulated saliva
C9J4L5	Cyclic AMP-responsive element-binding protein 1 (Fragment)	792	°Unstimulated saliva
P28325	Cystatin-D	5841	°Unstimulated saliva
H0YEA8	DENN domain-containing protein 5A (Fragment)	707	°Unstimulated saliva
Q9NRD9	Dual oxidase 1	308	°Unstimulated saliva
H0YAC4	Exosome RNA helicase MTR4 (Fragment)	799	°Unstimulated saliva
Q9BRP7	Ferredoxin-fold anticodon-binding domain-containing protein 1	227	°Unstimulated saliva
P98177	Forkhead box protein O4	274	°Unstimulated saliva
Q6ZNW5	GDP-D-glucose phosphorylase 1	719	°Unstimulated saliva
Q14687	Genetic suppressor element 1	162	°Unstimulated saliva
P06744	Glucose-6-phosphate isomerase	167	°Unstimulated saliva
Q9NZD1	G-protein coupled receptor family C group 5 member D	490	°Unstimulated saliva
C9JVX5	HCG1651889_ isoform CRA_d (Fragment)	519	°Unstimulated saliva
G3V201	HCG1985539_ isoform CRA_e	346	°Unstimulated saliva
C9JU02	Histone-lysine N-methyltransferase MECOM (Fragment)	201	°Unstimulated saliva
K7ERT9	Hsp70-binding protein 1 (Fragment)	335	°Unstimulated saliva
P0CG04	Immunoglobulin lambda constant 1	7427	°Unstimulated saliva
P0DOY2	Immunoglobulin lambda constant 2	7642	°Unstimulated saliva
P0DOY3	Immunoglobulin lambda constant 3	7642	°Unstimulated saliva
P0CF74	Immunoglobulin lambda constant 6 1	1034	°Unstimulated saliva
A0M8Q6	Immunoglobulin lambda constant 7	902	°Unstimulated saliva
P01714	Immunoglobulin lambda variable 3-19	331	°Unstimulated saliva
B9A064	Immunoglobulin lambda-like polypeptide 5	7427	°Unstimulated saliva
O95050	Indolethylamine N-methyltransferase	360	°Unstimulated saliva

H3BSR8	INMT-MINDY4 readthrough (NMD candidate) (Fragment)	330	°Unstimulated saliva
A0A3B3IS70	Inositol 1_4_5-trisphosphate receptor type 1 (Fragment)	190	°Unstimulated saliva
Q8N201	Integrator complex subunit 1	588	°Unstimulated saliva
P22079	Lactoperoxidase	437	°Unstimulated saliva
P42702	Leukemia inhibitory factor receptor	292	°Unstimulated saliva
P18428	Lipopolysaccharide-binding protein	329	°Unstimulated saliva
P61626	Lysozyme C	857	°Unstimulated saliva
Q13296	Mammaglobin-A	430	°Unstimulated saliva
A0A087WZ62	Mannosyltransferase	227	°Unstimulated saliva
Q8TCB7	Methyltransferase-like protein 6	298	°Unstimulated saliva
Q9H1A3	Methyltransferase-like protein 9	188	°Unstimulated saliva
P27816	Microtubule-associated protein 4	487	°Unstimulated saliva
O43684	Mitotic checkpoint protein BUB3	438	°Unstimulated saliva
Q9P1T7	MyoD family inhibitor domain-containing protein	420	°Unstimulated saliva
Q9BYH8	NF-kappa-B inhibitor zeta	263	°Unstimulated saliva
B3KNX7	Non-specific serine/threonine protein kinase	406	°Unstimulated saliva
E9PNR1	Oxysterol-binding protein-related protein 9 (Fragment)	289	°Unstimulated saliva
D6RC77	Phosphoacetylglucosamine mutase (Fragment)	350	°Unstimulated saliva
Q7Z3K3	Pogo transposable element with ZNF domain	357	°Unstimulated saliva
Q9P0L9	Polycystic kidney disease 2-like 1 protein	138	°Unstimulated saliva
H0YAT0	Probable C-mannosyltransferase DPY19L4 (Fragment)	361	°Unstimulated saliva
C9JH25	Proline-rich transmembrane protein 4	534	°Unstimulated saliva
Q8IVL5	Prolyl 3-hydroxylase 2	185	°Unstimulated saliva
O15460	Prolyl 4-hydroxylase subunit alpha-2	755	°Unstimulated saliva
Q92824	Proprotein convertase subtilisin/kexin type 5	443	°Unstimulated saliva
P49354	Protein farnesyltransferase/geranylgeranyltransferase type-1 subunit alpha	582	°Unstimulated saliva
Q96QU1	Protocadherin-15	305	°Unstimulated saliva
Q6ZTU2	Putative EP400-like protein	371	°Unstimulated saliva
Q7Z2F6	Putative protein ZNF720	355	°Unstimulated saliva
A6NKP2	Putative short-chain dehydrogenase/reductase family 42E member 2	97	°Unstimulated saliva
P49756	RNA-binding protein 25	185	°Unstimulated saliva
Q13153	Serine/threonine-protein kinase PAK 1	406	°Unstimulated saliva
Q9NY27	Serine/threonine-protein phosphatase 4 regulatory subunit 2	517	°Unstimulated saliva
H0YDR5	Single Ig IL-1-related receptor (Fragment)	354	°Unstimulated saliva
Q9Y345	Sodium- and chloride-dependent glycine transporter 2	198	°Unstimulated saliva
Q9NY46	Sodium channel protein type 3 subunit alpha	85	°Unstimulated saliva
P32418	Sodium/calcium exchanger 1	476	°Unstimulated saliva
X6R3N0	Solute carrier family 27 (Fatty acid transporter)_ member 3_ isoform CRA_d	364	°Unstimulated saliva
Q5K4L6	Solute carrier family 27 member 3	364	°Unstimulated saliva
Q96R06	Sperm-associated antigen 5	418	°Unstimulated saliva

I3L228	Sphingomyelin phosphodiesterase 3 (Fragment)	501	°Unstimulated saliva
Q8WXA9	Splicing regulatory glutamine/lysine-rich protein 1	329	°Unstimulated saliva
Q9H4L7	SWI/SNF-related matrix-associated actin-dependent regulator of chromatin subfamily A containing DEAD/H box 1	704	°Unstimulated saliva
F8WCE4	Synaptogyrin-1	319	°Unstimulated saliva
C9JA29	Syndetin (Fragment)	308	°Unstimulated saliva
Q9Y2K9	Syntaxin-binding protein 5-like	367	°Unstimulated saliva
Q99973	Telomerase protein component 1	860	°Unstimulated saliva
A6NNI4	Tetraspanin	863	°Unstimulated saliva
E7EWG2	TNFAIP3-interacting protein 1 (Fragment)	537	°Unstimulated saliva
Q9Y296	Trafficking protein particle complex subunit 4	404	°Unstimulated saliva
F8VRN7	Transmembrane protein 116	898	°Unstimulated saliva
Q70CQ2	Ubiquitin carboxyl-terminal hydrolase 34	351	°Unstimulated saliva
M0QZD8	Uncharacterized protein	410	°Unstimulated saliva
H3BUV5	Uncharacterized protein (Fragment)	435	°Unstimulated saliva
M0R1J3	Uncharacterized protein (Fragment)	403	°Unstimulated saliva
H0Y8H3	Uncharacterized protein C3orf67 (Fragment)	516	°Unstimulated saliva
Q8N3P4	Vacuolar protein sorting-associated protein 8 homolog	372	°Unstimulated saliva
Q8IZS8	Voltage-dependent calcium channel subunit alpha-2/delta-3	391	°Unstimulated saliva
A0A0A0MRV3	WD repeat domain 8_ isoform CRA_c	120	°Unstimulated saliva
Q96KV7	WD repeat-containing protein 90	353	°Unstimulated saliva
Q9P2S5	WD repeat-containing protein WRAP73	130	°Unstimulated saliva
G3V577	X-linked retinitis pigmentosa GTPase regulator-interacting protein 1 (Fragment)	366	°Unstimulated saliva
Q8TBC5	Zinc finger and SCAN domain-containing protein 18	124	°Unstimulated saliva
Q5T200	Zinc finger CCCH domain-containing protein 13	221	°Unstimulated saliva
Q8TAF7	Zinc finger protein 461	759	°Unstimulated saliva

[+]Identification is based on protein ID from UniProt protein database. reviewed only (http://www.uniprot.org/).
[*]Proteins with expression significantly altered are organized according to the ratio.
Proteins highlighted in bold are increased or decreased more than 2-fold.

2.5 ARTICLE 5

Article formatted and published according to Journal of Dentistry

DOI: 10.1016/j.jdent.2021.103642

Title: Radiotherapy changes acquired enamel pellicle proteome in head and neck cancer patients

Short title: Radiotherapy changes acquired pellicle proteins

Talita Mendes Oliveira Ventura[a]

Nathalia Regina Ribeiro[a]

Even Akemi Taira[a]

Cintia Maria de Souza-e-Silva[a]

Cássia Maria Fischer Rubira[b]

Paulo Sérgio da Silva Santos[b]

*Marília Afonso Rabelo Buzalaf [a]

[a] Department of Biological Sciences, Stomatology and Oral Biology – Discipline of Biochemistry, Bauru School of Dentistry, University of São Paulo, Bauru, SP, Brazil. Al. Octávio Pinheiro Brisolla, 9-75, Bauru, SP, 17012-90, Brazil.

[b] Department of Surgery, Stomatology, Pathology and Radiology – Discipline of Radiology and Stomatology, Bauru School of Dentistry, University of São Paulo, SP, Brazil. Al. Octávio Pinheiro Brisolla, 9-75, Bauru, SP, 17012-90, Brazil.

* Address correspondence to:

Marília Afonso Rabelo Buzalaf, PhD. Department of Biological Sciences, Bauru School of Dentistry, University of São Paulo, Al. Octávio Pinheiro Brisolla, 9-75, 17012-901, Bauru, São Paulo, Brazil Phone: 55-14-35358346. E-mail: mbuzalaf@fob.usp.br

Keywords: Acquired pellicle; enamel; saliva; proteomics; head and neck cancer; radiotherapy.

Received 18 November 2020; Revised 8 March 2021; Accepted 18 March 2021; Available online 20 March 2021.

Graphical Abstract

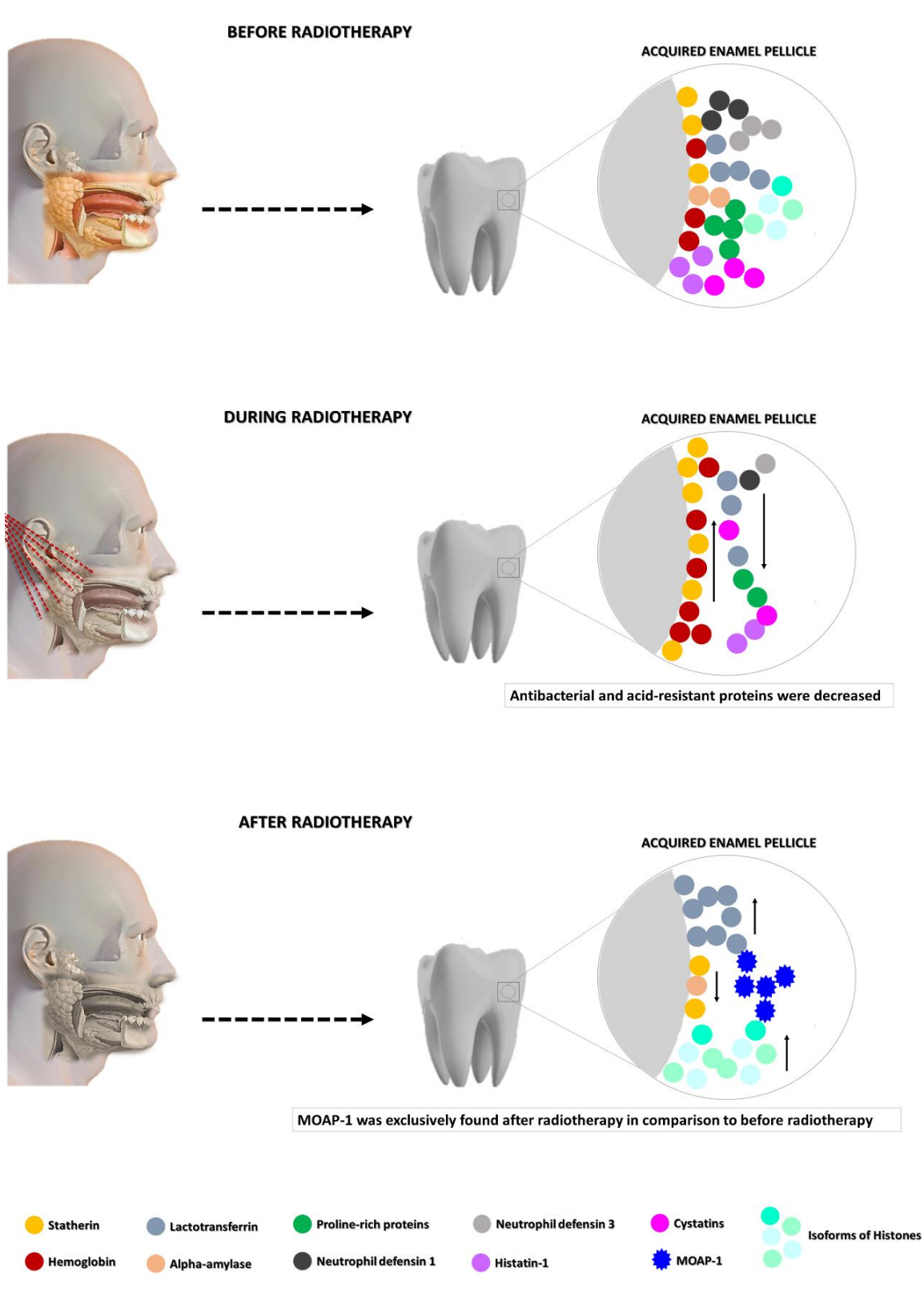

Radiotherapy changes acquired enamel pellicle proteome in head and neck cancer patients

Abstract

Objectives: To evaluate *in vivo* the proteomic profile of the acquired enamel pellicle (AEP) in patients with head and neck cancer (HNC) before, during and after radiotherapy.

Methods: Nine patients, after prophylaxis, had their AEPs collected before (BRT), during (DRT; 2-5 weeks) and after (ART; 3-4 months) radiotherapy. AEP was also collected from nine healthy patients (Control). The proteins were extracted in biological triplicate and processed by label-free proteomics.

Results: Statherin was increased more than 9-fold and several hemoglobin subunits were increased more than 5-fold DRT compared to BRT, while lactotransferrin, proline-rich proteins, cystatins, neutrophil defensins 1 and 3 and histatin-1 were decreased. ART, there was an increase in lactotransferrin and several isoforms of histones, while statherin and alpha-amylase proteins were decreased. MOAP-1 was exclusively found ART in comparison to BRT. When compared to Control, AEP of patients BRT showed an increase in proteins related to the perception of bitter taste, mucin-7 and alpha-amylases, while cystatin-S was decreased.

Conclusions: HNC and radiotherapy remarkably altered the proteome of the AEP. Antibacterial and acid-resistant proteins were decreased during radiotherapy.

Clinical Significance: Our results provide important information for designing more effective dental products for these patients, in addition to contributing to a better understanding of the differential protective roles of the AEP proteins during radiotherapy. Moreover, some proteins identified in the AEP after radiotherapy may serve as prognostic markers for survival of HNC patients.

Keywords: Acquired pellicle; enamel; saliva; proteomics; head and neck cancer; radiotherapy.

1. Introduction

Head and neck cancer represents 2.7% of cancer-related deaths worldwide [1], including several anatomic regions such as the oropharynx, hypopharynx, nasopharynx, larynx and oral cavity, in addition to the thyroid, trachea and salivary gland. Generally the risk factors for its development include exposure to tobacco and alcohol, associated with infection by oncogenic viruses such as human papillomavirus [2].

Radiotherapy is the most important non-surgical treatment for the HNC [3]. However, when applied in the head and neck region, it causes a negative impact on the quality of life of these patients, such as hyposalivation, xerostomia, oral mucositis, radiodermatitis, taste alteration and dental caries [4, 5]. These effects generally occur mainly because the salivary glands are often present in the irradiation field and, once affected, may suffer dysfunction and generate severe reduction in salivary flow.

Saliva also undergoes qualitative alterations due to radiotherapy, such as a decrease in amylase activity, buffer capacity and pH, with consequent acidification. There are also alterations in various electrolytes such as calcium, potassium, sodium and phosphate [6, 7]. In addition, irradiated patients are more susceptible to periodontal disease, rampant caries, fungal and bacterial oral infections [8] and erosive tooth wear [9].

Moreover, saliva plays a major role in the formation of the acquired enamel pellicle (AEP), a film constituted mainly of proteins that selectively adsorb onto the dental surface [10]. This proteinaceous layer acts as a semipermeable barrier, protecting the enamel against carious and erosive demineralization [11, 12].

Therefore, since the salivary glands are the main contributors to the protein composition of AEP, profound changes in the proteome of this integument are expected in patients undergoing head and neck radiotherapy. These results can help to add information about the best preventive strategies to be adopted in order to increase the quality of life of these patients. Thus, the objective of this study was to evaluate the proteomic profile in the AEP *in vivo* in HNC patients treated with radiotherapy. This evaluation was done before, during and after treatment. Healthy control patients were also evaluated for comparison. The null hypothesis evaluated was: there is no difference in the protein profile of the acquired pellicle formed on enamel *in vivo* in head and neck cancer patients submitted to radiotherapy treatment before, during or after radiotherapy or when compared to healthy patients.

2. Material and Methods

2.1 Patients and Ethical aspects

The AEP collection was done after approval by the Ethics Committee (No. 61484116.0.0000.5417) and after the signature of informed consent. This study was performed in accordance with the Declaration of Helsinki.

The number of patients (n=18; 9 HNC patients and 9 healthy controls) was chosen based on previous studies in which proteomic analysis of AEP was performed *in vivo* [13-18]. The sample size was calculated with MSstats [19] using data from our previous experiment [17], considering $\alpha = 0.05$ and $1-\beta = 0.8$. The effect size (difference in protein abundance) was considered as 1.5. The estimated number of samples was 3/group. Considering the low amounts of proteins typically recovered from the AEP *in vivo*, we decided to include 9 volunteers, in order to constitute 3 pools, so analysis were done in biological triplicates. HNC patients were recruited from the Clinical Research Center at Bauru School of Dentistry. HNC patients were aged between 34 and 72 years and were from both genders (7 male and 2 female). Healthy controls attended the same clinical facility and were paired by age (±5 years) and gender with the HNC patients.

The HNC patients were submitted to Linear Accelerator Radiotherapy, with irradiation doses of 187cGy during 33-36 sessions [20]. Among the affected sites in these patients were: Oropharynx Carcinoma and Tongue Base; Occult grade III Squamous Cell Carcinoma with cervical metastasis; Tongue Squamous Cell Carcinoma; Esophagus Squamous Cell Carcinoma and Amygdala; Retromolar Trigone (Jaw) Squamous Cell Carcinoma and Hypopharyngeal Squamous Cell Carcinoma. All patients were ex-smokers and ex-drinkers. Patients who had problems with oral hygiene (dental restorations, dental caries, periodontitis and tooth extraction) were treated before starting radiotherapy. The inclusion criteria were: patients older than 18 years of age, diagnosed with HNC, patients needed to be treated for oral conditions before collecting the acquired pellicle, patients that had not suffered surgery for removal of the tumor, patients who signed the informed consent. Exclusion criteria: patients who continued to smoke or to drink even after receiving the diagnosis of HNC. In addition, all patients presented mucositis during radiotherapy (4 patients with grade II, 3 patients with grades II and III, 1 patient with grade III and 1 patient with grade I and II). Therefore, all patients had to undergo laser therapy and analgesic/anti-inflammatory therapy during treatment.

The AEP was collected from the HNC patients in three different periods: before radiotherapy (BRT); during radiotherapy (DRT; between 2 and 5 weeks after start of radiotherapy); after radiotherapy (ART; 3 to 4 months after treatment). The control AEP was collected also from nine participants with good oral and general health, non-smokers, without caries, gingivitis, periodontitis or other oral conditions that could affect the composition of oral fluids, as well as those who were not using drugs, or tobacco. Patients who presented risk factors for erosive tooth wear, such as excessive consumption of carbonated beverages, fruits or acidic fruit juice, swimming or gastric disorders such as bulimia and gastroesophageal reflux were excluded (Control group). The mean (±SD) unstimulated salivary flow was 0.49±0.29, 0.17±0.24, 0.06±0.1 and 0.89±0.40 mL/min for BRT, DRT, ART and control, respectively.

2.2 AEP collection

The collections began in the morning, so that circadian cycle influences did not occur [20, 21]. The patients received meticulous dental prophylaxis with prophylactic paste. Then, they waited for 120 min for the AEP to naturally form on the tooth.

AEP collections were made from all teeth and all dental arches and were based strictly as described in a previous study [18]. The pellicle was collected after 120 min of formation to avoid possible bacterial aggregation, which could interfere with the results [22]. During this period, the patients were deprived of food and drink. The quadrants of the dental arches were rinsed with deionized water and air-dried twice and relative isolation with cotton rolls. The obtained pellicle was then collected with an electrode wick filter paper (Bio-Rad, Hercules, CA) of 5X10 mm pre-dipped in 3% citric acid. The filter paper was rubbed (without pressure) on the two thirds coronal (to avoid contamination of the gingival margin) of the surfaces of the teeth, in the vestibular, lingual and palatal regions [22]. The wick filters were placed in 2 mL cryotubes and stored at -80 ° C until proteomic analysis.

2.3 Proteomics analysis

The protocol was standardized by our research group [18]. However, samples from every 3 volunteers were pooled, so that 3 pools were obtained for each group in order the analyses were performed in biological triplicates. Papers were cut and stored in individual tubes for each volunteer. An extraction solution containing 6 M urea, 2 M thiourea in 50 mM NH4HCO3 pH 7.8 was added until the papers were covered. Samples were vortexed for 10 min

at 4 °C, sonicated for 5 min and centrifuged at 20,817 x g for 10 min at 4 °C. The supernatants were collected and pooled for each 3 volunteers, to obtain biological triplicates for each group.

After the supernatants were collected, the steps of the extraction procedures were repeated two more times, for good recovery of the sample. The papers were then placed in filter tubes (Corning® Costar® Spin-X® Plastic Centrifuge Tube Filters) and centrifuged at 20,817 x g for 10 min at 4 °C. The volume coming down from the filter tube was recovered and added to the previously collected supernatant. Soon after, the samples were centrifuged at 20,817 x g for 10 min at 4° C, the supernatant was collected and one and a half parts of 50 mM NH4HCO3 was added to the samples. This value was based on the total volume of the samples, so that the concentration of urea and thiourea decreased, as these could interfere with the action of trypsin. The samples were then transferred to Amicon tubes (Amicon Ultra-15 Centrifugal Filter Units - Merck Millipore®, Tullagreen, County Cork, Ireland) and centrifuged at 4,500 x g at 4 °C, to a volume of approximately 100 µL. After sample recovery, the total protein quantification was performed by the Bradford method (Bio-Rad Bradford Assays, Hercules, California, USA). The samples were then reduced with 5 mM dithiothreitol (DTT) (Bio Rad Laboratories) and incubated at 37 °C for 40 min. After this time, 10 mM Iodoacetamide (GE Healthcare, Little Chalfont, Buckinghamshire UK) was added and the samples were incubated for 30 min in the dark. After incubations, 100 µL of 50 mM NH4HCO3 pH 7.8 was added in the samples and then the tryptic digestion was carried out for 14 h at 37 °C by the addition of trypsin enzyme (Thermo Scientific Pierce Trypsin Protease, Rockford, lL, USA). After this time, 5% formic acid solution was added to stop the action of the trypsin and perform the procedure with the C18 spin column (Thermo Scientific, Rockford, Illinois, USA), for the desalting and purification of the samples. An aliquot of each sample (1 µL) was removed for protein quantification by the Bradford method (Bio-Rad Bradford Assays), after calculations for quantitative analysis, samples were resuspended in 3% acetonitrile and 0.1% formic acid, and used for application in nanoLC-ESI-MS/MS.

2.4 Acquisition nanoLC-ESI-MS/MS

The Xevo G2 (Waters) mass spectrometer coupled to the nanoACQUITY (Waters) system was used for the peptide analysis. All samples were analyzed in technical triplicate. The detailed parameters of the mass spectrometer have been detailed in a previous study [18].

ProteinLynx Global Server (PLGS) version 3.0 software was used to process and search for continuous LC-MSE data. The proteins were identified using the software's ion counting

algorithm, and a search was performed on the Homo sapiens database (only revised, UniProtKB/Swiss-Prot) downloaded in October 2019 from UniProtKB (http: //www.uniprot .org).

2.5 Shotgun Label-free quantitative proteomic analysis

The PLGS software (PLGs, v 3.0, Waters, Manchester, UK) was used for the label-free quantitative proteome and three raw MS files from each group were analyzed. In the quantitative analysis, all proteins identified with a confidence score greater than 95% were included. The identical peptides from each triplicate by sample were pooled according to mass accuracy (<10 ppm) and the retention time tolerance <0.25 min, using the clustering software included in the PLGS. The Monte-Carlo algorithm was used to calculated the difference in expression between the groups, expressed as $p < 0.05$ for the down-regulated proteins and $1\text{-}p > 0.95$ for the up-regulated proteins. The following relevant comparisons were performed: DRT x BRT; ART x BRT; ART x DRT; BRT x Control; DRT x Control; ART x Control.

2.6 Bioinformatics analysis

For protein analysis and data tabulation, unreviewed and reviewed proteins were analyzed by UNIPROT database (http: //www.uniprot .org). The reverse proteins, repeated proteins and repeated fragments were excluded. The analyses of the biological processes most affected based in the gene ontology were performed by Cytoscape® 3.7.2 Software with the ClueGo® plugins. The functional distribution of the proteins identified with differential expression in the period DRT vs BRT was selected. Protein categories were based on Gene Ontology (GO) annotation of the broad Biological Process, Molecular Function, Immune System Process and Cell Component. Terms of significance (Kappa = 0.04) and distribution were according to the percentage of the number of associated genes. The number of access to the proteins was provided by UNIPROT.

For the interaction networks, the database STRING® (https://string-db.org/cgi/network.pl) was used to establish the interaction between proteins identified with differential expression and unique proteins of each group for the comparison ART vs BRT.

3. Results

The total mean amount of protein recovered from BRT, DRT ART and control was 47.2, 52.3, 41.9 and 44.7 µg, respectively. A total of 204 proteins were identified, considering all groups.

In the comparison DRT vs BRT, the total number of proteins identified were 60 and 149, respectively, among which 53 proteins were common to both groups (Fig 1A). Seven proteins were identified exclusively DRT, while 96 proteins were uniquely identified BRT, such as Cystatin-C and -B, Histatin-3, 16 isoforms of Histones proteins, 3 isoforms of the Immunoglobulins proteins, Matrix metalloproteinase-9, Mucin-7, Protein S100-A11 and Serotransferrin. In the differentially expressed proteins, 24 and 15 proteins were increased and decreased, respectively, DRT. Among the down-regulated proteins DRT are: Lactotransferrin, Immunoglobulin heavy constant alpha 1 and 2, Neutrophil defensin 1 and 3, Proline-rich protein 4, Salivary acidic proline phosphoprotein ½, Histatin-1, Cystatin-S and AS, Submaxillary gland androgen-regulates protein 3B, Profilin-1. On the other hand, Serum albumin, Apolipoprotein AI, Haptoglobin, 6 isoforms of Hemoglobin (hemoglobin subunit alpha, gamma-1, beta, gamma-2, delta, epsilon) and Statherin (nearly 10-fold increase) were up-regulated DRT (Table S1).

Fig. 2 shows the functional analysis according to the biological process by Gene Ontologies (GO) with the most significant term, for the comparison between DRT *vs* BRT. Among them, the categories with the percentages of genes were antimicrobial humoral response (37%), oxygen carrier activity (18%), mesenchyme migration (12%), detection of chemical stimulus involves in sensory perception of bitter taste (9%), lipase inhibitor activity (9%), structural constituent of postsynaptic actin cytoskeleton (9%) and high-density lipoprotein particle remodeling (6%). In the functional analysis according to the molecular function process by Gene Ontologies (GO) with the most significant term, for the comparison between DRT *vs* BRT. Among them, the categories with the percentages of genes were peroxidase activity (44%), hemoglobin binding (25%), lipase inhibitor activity (19%) and signaling pattern recognition receptor (12%) (Fig. 2). In relation the functional analysis according to the cell component process by Gene Ontologies (GO) with the most significant term also done in this comparison. Among them, the categories with the percentages of genes were Golgi cis cisterna (37%), endocytic vesicle lumen (32%), postsynaptic actin cytoskeleton (11%), phagocytic vesicle lumen (10%) and secretory dimeric IgA immunoglobulin complex (10%) (Fig. 2). In

the functional analysis according to the immune system process by Gene Ontology (GO) with the most significant term, for the comparison between DRT *vs* BRT. Among them, the categories with the percentages of genes were antimicrobial humoral response (55%), antibacterial humoral response (27%) and mucosal immune response (18%) (Fig. 2).

When we compared ART vs BRT, the total number of proteins identified were 52 and 151, respectively, with 48 proteins common to both groups (Fig 1B). Among them, 4 proteins were identified exclusively ART, such as Modulator of apoptosis 1, Histone H2B type 1-A and Histone-lysine N-methyltransferase_ H3 lysine-79 specific, while 103 proteins were uniquely identified BRT, such as Alpha-amylase 2B, Cystatin-C, -S, -SA and -SN, Haptoglobin, 6 isoforms of Hemoglobin (hemoglobin subunit alpha, gamma-1, beta, gamma-2, delta, epsilon), Histatin-1 and -3, 15 isoforms of Immunoglobulin, 17 isoforms of Keratin, Lysozyme C, Matrix metalloproteinase-9, Mucin-7, Protein S100-A11, Salivary acidic proline-rich phosphoprotein ½, PRP-4 and Serotransferrin. In the differentially expressed proteins, 20 were increased ART, such as Apolipoprotein A-I, 17 isoforms of Histone, Protein S100-A8, Albumin_isofrom CRA_K and Lactotransferrin and only Alpha-amylase 1 was down-regulated ART in comparison to BRT (Table S2).

Fig. 3 shows the functional analysis according to the biological process by Gene Ontology (GO) with the most significant term, for the comparison between ART *vs* BRT. Among them, the categories with the percentages of genes were nucleosome assembly (50%), antimicrobial humoral response (21%), innate immune response in mucosa (17%), negative regulation of tumor necrosis factor-mediated signaling pathway (8%) and protein localization to bicellular tight junction (4%). In relation the function analysis according to the molecular function process by Gene Ontology (GO) with the most significant term, for the comparison between ART *vs* BRT. Among them, the categories with percentages of genes were involved with alpha-amylase activity (25%), structural constituent of postsynaptic actin cytoskeleton (25%), Toll-like receptor 4 binding (25%) and apolipoprotein A-I receptor binding (25%) (Fig. 4). Thus, functional classification according to the immune system process by Gene Ontology (GO) with the most significant term, for the comparison between ART *vs* BRT. Among them, the categories with the percentages of genes were innate immune response in mucosa (36%), antimicrobial humoral response (46%), negative regulation of macrophage chemotaxis (9%) and antifungal humoral response (9%) (Fig. 5).

For the comparison ART vs DRT, the total number of proteins identified were 50 and 59, respectively, with 29 proteins common to both groups (Fig 1C). Among them, 21 proteins were identified exclusively ART, such as Cystatin-B and 17 isoforms of Histones, while 30

proteins were uniquely identified DRT, such as Alpha-amylase 2B, Cystatin-S, -SA and -SN, Haptoglobin, 7 isoforms of Hemoglobin proteins, Histatin-1, Immunoglobulin heavy constant alpha 1 and 2, Lysozyme C, Proline-rich protein 4, Salivary acidic proline-rich phosphoprotein 1/2 and Submaxillary gland androgen-regulated protein 3B. In the differentially expressed proteins, 4 proteins were differentially expressed, among which Lactotransferrin and Serum albumin were increased, while Statherin and Alpha-amylase 1 were decreased ART (Table S3).

As for the comparison BRT vs Control, the total number of the proteins identified were 150 and 146, respectively, with 102 proteins common to both groups (Fig 1D). Among them, 48 proteins were identified exclusively BRT, such as 7 isoforms of Hemoglobin, Histatin-3, Matrix metalloproteinase-9, Protein S100-A11 and Serotransferrin, while 44 proteins were identified exclusively in the Control group. In the quantitative analysis, 20 and 16 proteins were increased and decreased, respectively, in the BRT group. Among the down-regulated proteins is Cystatin-S, while Zinc-alpha-glycoprotein, Prolactin-inducible protein, Alpha-amylase 1 and 2B, Mucin-7, Protein S100-A9, 6 isoforms of Immunoglobulin, Neutrophil defensin 1 and 3, Salivary acidic proline-rich phosphoprotein ½, Lysozyme C and Proline-rich protein 4 were up-regulated BRT in patients with HNC when compared to healthy patients (Table S4).

4. Discussion

It is important to emphasize that this is the first study to evaluate the AEP protein profile in HNC patients over the course of radiotherapy. Furthermore, regarding the methodology for proteomic analysis of the AEP, this is the first study in which the analyses were done in biological triplicate. In the previous studies by our group, AEP samples from 8-10 volunteers were combined into one single pool, which is not ideal since it does not contemplate the biological variation [16-18]. The total amount of recovered AEP proteins ranged from 30 to 62 µg for each pool, considering the distinct groups under study. For the quantitative analyses, all samples were adjusted to 30 µg. A total of 204 proteins were identified, showing that the methodology was satisfactory. In addition, it is also important to consider the quality of the proteins identified, since the proteins classically described in the acquired pellicle were all identified. This analysis in biological triplicates represents a major advance for the research involving proteomic analysis of the AEP *in vivo*, since there is much questioning regarding the limitation of the data when the biological variability is not taken into account. Another differential of this study was that the collections of the AEP were performed from the same

patients, thus making them their own controls when the treatment periods were compared to each other.

Radiotherapy is a therapeutic modality that uses ionizing radiations with the objective of destroying the neoplastic cells, aiming at a reduction or disappearance of the malignant neoplasia [24]. However, in the case of patients with HNC, the salivary glands are the most affected mainly because they are present in the irradiated field [25]. In the literature it is shown that due to radiotherapy, there is a great reduction of the salivary flow due to the radiation suffered in this region [26], which was confirmed when we measured the unstimulated salivary flow of our patients. It should be highlighted that even BRT, HNC patients had lower salivary flow compared with healthy controls. This is in-line with a previous study where the unstimulated flow was evaluated before and after treatment in HNC patients [27], showing a reduction in the flow before the treatment. However, it must be highlighted that despite the mean unstimulated salivary flow of HNC patients BRT (0.49 mL/min) was lower than that found for healthy controls, it still falls within the normal ranges [28]. Considering that saliva is the major contributor for the proteins found in the AEP [29], profound changes in the AEP proteome could be expected due to the reduction of the salivary flow, what was confirmed in our study (Tables S1-S4). Thus, the null hypothesis was rejected.

When patients with HNC were compared to healthy patients (BRT vs Control), Cystatin-S was decreased in the BRT group. The reduced expression of this protein in saliva is related to decreased salivary flow as well as dysfunctions in the salivary glands, especially the submandibular gland, in which the protein is secreted [27]. It should be highlighted that the mean salivary flow of BRT patients was 0.49 mL/min versus 0.89 mL/min in healthy controls. Still in relation to this comparison, 20 proteins were increased BRT in comparison with the control group. Among them are Zinc-alpha-glycoprotein protein, which is involved with immune response, wound healing and protection of the mucosa [28], as well as Prolactin-inducible protein, related to immune system responses and involved with the perception of bitter taste, besides being present in pathological conditions of the salivary gland (UNIPROT) [29]. Also increased BRT were Alpha-amylase 1 and 2B, which come from the parotid gland and are considered a biochemical indicator for salivary gland injury [30], in addition to being increased in psychological stress conditions [28, 31-33]. They also interact with several proteins in whole saliva, most of them presenting host protection properties [28]. Another increased protein in the BRT group was Mucin-7 that participates in essential processes for mucosa protection, wound healing and immune response (UNIPROT) [28]. Moreover, the increase in mucins is related to the characterization of the saliva of these patients as sticky and thick. With the decrease in

water, due to the reduction in the salivary flow, this protein becomes more concentrated in saliva and is adsorbed to a greater degree in the AEP of these patients.

An important comparison was made to verify whether the protein profile of the AEP of the HNC patients could be restored after radiotherapy treatment. We observed that when the ART group was compared with the BRT group, 20 proteins were increased, while Alpha-amylase 1, related to episodes of great psychological stress, as mentioned above, was decreased in the first group compared to the second. Therefore, considering that these patients had already undergone the process of treatment with radiotherapy, we believe that its decrease is also related to the decrease in stress in function of the completion of the treatment. It has been reported that radiotherapy not only causes physical injury, but also psychological and social damage [4, 34]. Among the increased proteins, we would like to highlight those that were increased more than 2-fold, such as S100-A8, related to immune system responses and regulation of inflammation (UNIPROT) [28], Lactotransferrin and 17 isoforms of Histone, which caught our attention. Therefore, interaction networks were carried out from the STRING database in order to verify the possible interactions of these proteins considered in this differential expression (ART vs BRT) (Table S2; Figure 1B). We found that these Histones proteins bind together, in addition to making secondary bindings with other proteins identified in these groups, such as Lactrotransferrin, involved with innate immune response to the mucosa (STRING) (Fig. 6). During radiotherapy treatment, patients have episodes of mucositis due to damage to the oral mucosa generated by radiation, so we believe that the increase in these proteins is an attempt to reestablish the injured mucosa of these patients after treatment.

The increased histones ART (Histone H2B type F-S; Histone H2B type 2-E; Histone H2B type 1-B; Histone H2B type 1-D; Histone H2B type 1-H; Histone H2B type 1-J; Histone H2B type 1-K; Histone H2B type 1-L; Histone H2B type 1-M; Histone H2B type 1-N; Histone H2B type 1-O) are involved with DNA methylation and interact with histone acetyltransferases (HATS), implicated with histone modifications (STRING) (Fig 6). DNA methylation is involved with the main epigenetic mechanisms, which are related to memory and cellular identity, influencing the cellular microenvironment. The epigenetic regulation of gene expression is mainly controlled by DNA methylation, action of non-coding RNAs and modification of histones [35]. Among the various types of modifications in histones, acetylation is characterized by playing an important role in the modulation of gene expression acting in the control of the cell cycle, in addition to participating in the development and progression of neoplasms [36, 37]. Histone acetylation is performed from enzymes called acetyltransferases

that add acetyl radicals to the lysine residues of histone proteins, leading to chromatin decompression and transcriptional activity [37].

H2B and H2A histones play important roles in chromatin processes that allow DNA transcription, replication and repair. In general, histones H2A and H2B form octamers with histones H3 and H4 and are involved in packaging DNA into nucleosomes [38-43]. In a study by Li et al, 2017 [39] based on gene expression profile data, they demonstrate that increased expression of histone variants is a strong prognostic biomarker in patients with cervical cancer. These measurements of histone expression can help select cervical cancer patients who can benefit from radiotherapy. Besides, they suggest that two sets of histone-variant genes (Histone H2B type 1-D, -J and -H; Histone H2A type 1-M and Histone H4-K) may be independent prognostic factors for better survival in patients with cervical cancer [39]. All these isoforms of histones, except histone H4-K were increased ART in comparison with BRT in the present study, indicating that the AEP can be used as a prognostic marker for HNC.

In addition, the Modulator of apoptosis 1 protein (MOAP-1) was identified exclusively ART when compared to BRT. This protein plays important role in cell death or apoptosis. Overexpression of MOAP-1 in several cancer cell lines resulted in the reduction of tumorigenesis and in the positive regulation of genes involved in the control of DNA damage and in cancer regulatory pathways that include apoptosis [44]. Besides, MOAP-1 expression levels appear to be regulated by mRNA control and ubiquitination [45]. Therefore, MOAP-1 can exert its tumor-suppressing function through involvement in apoptosis [46, 47]. This finding is of great importance and reinforces the analysis of the AEP as a prognostic marker to evaluate efficacy of the radiotherapy treatment. These findings should be evaluated in future studies.

The analysis of the differential expression also reveals that DRT there is a pronounced (more than twice) increase in the AEP of serum proteins originating mainly from the gingival crevicular fluid, such as various isoforms of Hemoglobin, Haptoglobin and Apolipoprotein 1. This can be explained by the reduction of salivary flow. Under conditions of normal salivary flow, the main source of proteins for the pellicle is saliva, since it contains several proteins with high capacity of adsorption to hydroxyapatite [51]. With the reduction of the salivary flow due to radiotherapy, the serum proteins from the gingival fluid [51] are favored, and they are then adsorbed to a greater extent. However, the protein with the greatest increase in expression DRT, compared to BRT, was Statherin (nearly 10-fold increase). This protein is derived from the secretions of parotid and submandibular glands [52], but it has already been identified in samples of the gingival fluid [53]. However, the authors themselves question whether its origin

would be even the serum or whether its presence in samples collected from the gingival fluid would be due to its presence in the acquired pellicle located near the gingival margin. The increase in Statherin DRT might be due to the decrease in the water content in saliva. As a consequence of the reduction in the salivary flow, this protein becomes more concentrated in saliva and due to its high binding force to hydroxyapatite, adsorbs to a greater degree on enamel.

Among the 15 decreased proteins DRT, we highlight proteins that have important functions such as Lactotrasnferrin, two immunoglobulins isoforms, Cystatin-S and SA, Neutrophil defensins 1 and 3, Histatin-1 and three isoforms of proline-rich proteins (Proline-rich protein 4, Salivary acidic proline-rich phosphoprotein ½ and Submaxillary gland androgen-regulated protein 3B) (Table S3). These proteins have antibacterial, antifungal, as well as acid-resistant functions (UNIPROT). Their decrease in the AEP of these patients DRT explains the damage to the teeth, not only due to the decrease in the salivary flow, but also due to the decrease in these protective proteins in the AEP, leaving these patients more susceptible to the development of caries and erosive tooth wear.

Considering the DRT vs BRT comparison of great biological interest, analyzes of the most affected processes were carried out based on the proteins identified in these comparisons. In Fig. 2, we can see that in relation to the biological process, 9% of these proteins are involved with the sensory perception of bitter taste, which is commonly reported by these patients, in addition to 37% of these proteins being involved with the humoral antimicrobial response. In relation to the processes of molecular function, we highlight that 25% of these proteins are involved with binding to hemoglobin protein, which was seen previously since during DRT there was a more than 5-fold increase in these proteins. We believe that this is due to damage to the mucosa, with consequent mucositis generated due to treatment.

It is important to mention that all patients presented mucositis during the treatment and all underwent laser therapy. We believe that this may be a limitation of our study, however due to the debility profile of these patients, it would not be ethical to deprive them of this important therapy for the recovery of the mucosa. This information becomes extremely important since when the processes involved with the cellular component were analyzed in the comparison DRT *vs* BRT, we observed that 10% of these proteins were involved with an immunoglobulin A complex (Fig. 2). This antibody is secreted in the saliva and is present when dysfunctions occur in the mucous membranes of some organs, such as the mouth. IgA plays a key role in defending mucosal surfaces against attack by infectious microorganisms [54], so we believe that the laser therapy increased the proteins involved with immunoglobulin A, in order to restore and protect the mucosa of these patients.

Finally, we also performed the functional analysis of the immune system process in the comparison DRT vs BRT and we found that 18% of these proteins are involved in the mucosal immune response, 55% in the antimicrobial humoral response and 27% involved in the antibacterial humoral response (Fig. 2) and in the comparison ART vs BRT 3% of these proteins are involved with innate immune response in mucosa, 46% with antimicrobial humoral response and 9% involved with antifungal humoral response (Fig. 5) . Moreover, in the functional analysis of the biological processes of the ART vs BRT groups, it was observed that 4% of these proteins are involved with protein localization to bicellular tight junction (Fig. 3). Bicellular tight junctions are functional intercellular structures that are present mainly in the epithelial and endothelial cells of all tissues and organs. In addition to their well-recognized roles in maintaining cell polarity and barrier functions, these structures are important regulators of signal transduction, which modulate cell proliferation, migration and differentiation, as well as some components of the immune response, homeostasis, besides developing a role for effective wound healing [55]. Therefore, a more complete understanding of these structures can provide better strategies to increase the regeneration of the oral mucosa and improve mucosal repair resulting from radiotherapy, but also to understand the cancer healing processes resulting from treatment.

5. Conclusion

HNC and radiotherapy remarkably altered the protein profile of the AEP. Antibacterial and acid-resistant proteins were decreased during radiotherapy, which impacts systemic and oral health homeostasis. These results provide important information for designing more effective dental products to improve the quality of life of these patients, in addition to contributing to a better understanding of the differential protective roles of the AEP proteins during radiotherapy. Moreover, some proteins identified in the AEP after radiotherapy, such as isoforms of histones and MOAP-1, may serve as prognostic markers for survival of HNC patients, which should be evaluated in further studies.

Declaration of Competing Interest

The authors have declared no conflict of interest.

Acknowledgements

The authors thank FAPESP for financial support and for the concession of a scholarship to the first (Proc. FAPESP 2017/05031-2) and second (Proc. FAPESP 2018/17860-6) authors. This study was financed in part by the Coordenação de Aperfeiçoamento de Pessoal de Nível Superior - Brazil (CAPES) - Finance Code 001. The funders had no role in study design, data collection and analysis, decision to publish or preparation of the manuscript. All authors gave their final approval and agree to be accountable for all aspects of the work. The authors are grateful especially the trial participants, their families and the staff of the Clinical Research Center at Bauru School of Dentistry. The authors are grateful to Mrs. Larissa Tercilia Grizzo for technical support with proteomic analysis.

CRediT authorship contribution statement

Talita Mendes Oliveira Ventura: Conceptualization, Methodology, Validation, Vizualization, Formal analysis, Investigation, Writing - Orginal Draft. **Nathalia Regina Ribeiro:** Methodology, Formal analysis, Investigation, Writing - Review & Editing. **Even Akemi Taira:** Methodology, Investigation, Writing - Review & Editing. **Cintia Maria de Souza-e-Silva**: Methodology, Investigation, Writing - Review & Editing. **Cássia Maria Fisher Rubira:** Conceptualization, Investigation, Writing - Review & Editing, Supervision. **Paulo Sérgio da Silva Santos:** Conceptualization, Investigation, Writing - Review & Editing, Supervision. **Marília Afonso Rabelo Buzalaf:** Conceptualization, Validation, Formal analysis, Investigation, Writing - Original Draft, Supervision.

All authors have revised and agreed with the final version of the manuscript.

REFERENCES

[1] F. Bray, J. Ferlay, I. Soerjomataram, R.L. Siegel, L.A. Torre, A. Jemal, Global cancer statistics 2018: GLOBOCAN estimates of incidence and mortality worldwide for 36 cancers in 185 countries, CA Cancer J Clin 68(6) (2018) 394-424.

[2] S. Marur, A.A. Forastiere, Head and Neck Squamous Cell Carcinoma: Update on Epidemiology, Diagnosis, and Treatment, Mayo Clin Proc 91(3) (2016) 386-96.

[3] R. Semrau, The Role of Radiotherapy in the Definitive and Postoperative Treatment of Advanced Head and Neck Cancer, Oncol Res Treat 40(6) (2017) 347-352.

[4] F.O. Cruz, E.B. Ferreira, C.I. Vasques, L.R. Mata, P.E. Reis, Validation of an educative manual for patients with head and neck cancer submitted to radiation therapy, Rev Lat Am Enfermagem 24 (2016).

[5] V.T. Stuani, P.S.S. Santos, C.A. Damante, M.S.R. Zangrando, S.L.A. Greghi, M.L.R. Rezende, A.C.P. Sant'Ana, Oral health impact profile of head and neck cancer patients after or

before oncologic treatment: an observational analytic case-control study, Support Care Cancer 26(7) (2018) 2185-2189.
[6] E.H. Pow, A.S. McMillan, W.K. Leung, M.C. Wong, D.L. Kwong, Salivary gland function and xerostomia in southern Chinese following radiotherapy for nasopharyngeal carcinoma, Clinical oral investigations 7(4) (2003) 230-4.
[7] S. Silverman, Jr., Oral cancer: complications of therapy, Oral Surg Oral Med Oral Pathol Oral Radiol Endod 88(2) (1999) 122-6.
[8] P.J. Hancock, J.B. Epstein, G.R. Sadler, Oral and dental management related to radiation therapy for head and neck cancer, J Can Dent Assoc 69(9) (2003) 585-90.
[9] C. Lajer, C. Buchwald, B. Nauntofte, L. Specht, A. Bardow, T. Jensdottir, Erosive potential of saliva stimulating tablets with and without fluoride in irradiated head and neck cancer patients, Radiother Oncol 93(3) (2009) 534-8.
[10] C.J. DAWES, G. N.; TONGE, C. H, The nomenclature of the integuments of the enamel surface of the teeth, Brit Dent J 115 (1963) 65-68.
[11] M.A.R. Buzalaf, A.R. Hannas, M.T. Kato, Saliva and dental erosion, J Appl Oral Sci 20(5) (2012) 493-502.
[12] D. Vukosavljevic, W. Custodio, M.A.R. Buzalaf, A.T. Hara, W.L. Siqueira, Acquired pellicle as a modulator for dental erosion, Archives of oral biology 59(6) (2014) 631-638.
[13] L.P.S. Cassiano, T.M.S. Ventura, C.M.S. Silva, A.L. Leite, A.C. Magalhaes, J.P. Pessan, M.A.R. Buzalaf, Protein Profile of the Acquired Enamel Pellicle after Rinsing with Whole Milk, Fat-Free Milk, and Water: An in vivo Study, Caries Res 52(4) (2018) 288-296.
[14] E.S.C.M. de Souza, T.M. da Silva Ventura, L. de Pau, C. la Silva, A. de Lima Leite, M.A.R. Buzalaf, Effect of gels containing chlorhexidine or epigallocatechin-3-gallate on the protein composition of the acquired enamel pellicle, Arch Oral Biol 82 (2017) 92-98.
[15] T.R. Delecrode, W.L. Siqueira, F.C. Zaidan, M.R. Bellini, E.B. Moffa, M.C. Mussi, Y. Xiao, M.A. Buzalaf, Identification of acid-resistant proteins in acquired enamel pellicle, J Dent 43(12) (2015) 1470-5.
[16] T. Martini, D. Rios, L.P.S. Cassiano, C.M.S. Silva, E.A. Taira, T.M.S. Ventura, H. Pereira, A.C. Magalhaes, T.S. Carvalho, T. Baumann, A. Lussi, R.B. Oliveira, R.G. Palma-Dibb, M.A.R. Buzalaf, Proteomics of acquired pellicle in gastroesophageal reflux disease patients with or without erosive tooth wear, J Dent 81 (2019) 64-69.
[17] E.A. Taira, T.M.S. Ventura, L.P.S. Cassiano, C.M.S. Silva, T. Martini, A.L. Leite, D. Rios, A.C. Magalhaes, M.A.R. Buzalaf, Changes in the Proteomic Profile of Acquired Enamel Pellicles as a Function of Their Time of Formation and Hydrochloric Acid Exposure, Caries Res 52(5) (2018) 367-377.
[18] T. Ventura, L.P.S. Cassiano, E.S.C.M. Souza, E.A. Taira, A.L. Leite, D. Rios, M.A.R. Buzalaf, The proteomic profile of the acquired enamel pellicle according to its location in the dental arches, Arch Oral Biol 79 (2017) 20-29.
[19] M.D. Shyh-An Yeh, Radiotherapy for Head and Neck Cancer, Seminars in Plastic Surgery 24(2) (2010) 127-136.
[20] J.N. Zimmerman, W. Custodio, S. Hatibovic-Kofman, Y.H. Lee, Y. Xiao, W.L. Siqueira, Proteome and peptidome of human acquired enamel pellicle on deciduous teeth, International journal of molecular sciences 14(1) (2013) 920-34.
[21] C. Dawes, Circadian rhythms in human salivary flow rate and composition, J Physiol 220(3) (1972) 529-45.
[22] W.L. Siqueira, W. Zhang, E.J. Helmerhorst, S.P. Gygi, F.G. Oppenheim, Identification of protein components in in vivo human acquired enamel pellicle using LC-ESI-MS/MS, Journal of proteome research 6(6) (2007) 2152-60.
[23] C. Van De Wiele, A. Signore, F. Scopinaro, R. Waterhouse, R.A. Dierckx, Imitt, Imaging tumour hypoxia: where are we?, Nucl Med Commun 22(9) (2001) 945-7.

[24] S.D. Zago, The radiotherapy effect on the quality of life of patients with head and neck cancer, Revista Brasileira de Cancerologia 52(4) (2006) 323-329.
[25] A.C. O'Connell, Natural history and prevention of radiation injury, Advances in dental research 14 (2000) 57-61.
[26] W.L. Siqueira, W. Custodio, E.E. McDonald, New Insights into the Composition and Functions of the Acquired Enamel Pellicle, Journal of dental research 91(12) (2012) 1110-1118.
[27] D. Martini, A. Gallo, S. Vella, F. Sernissi, A. Cecchettini, N. Luciano, E. Polizzi, P.G. Conaldi, M. Mosca, C. Baldini, Cystatin S-a candidate biomarker for severity of submandibular gland involvement in Sjogren's syndrome, Rheumatology (Oxford) 56(6) (2017) 1031-1038.
[28] K.T.B. Crosara, D. Zuanazzi, E.B. Moffa, Y. Xiao, M. Machado, W.L. Siqueira, Revealing the Amylase Interactome in Whole Saliva Using Proteomic Approaches, Biomed Res Int 2018 (2018) 6346954.
[29] M.I. Hassan, A. Waheed, S. Yadav, T.P. Singh, F. Ahmad, Prolactin inducible protein in cancer, fertility and immunoregulation: structure, function and its clinical implications, Cell Mol Life Sci 66(3) (2009) 447-59.
[30] A. Becciolini, S. Porciani, A. Lanini, A. Benucci, A. Castagnoli, A. Pupi, Serum amylase and tissue polypeptide antigen as biochemical indicators of salivary gland injury during iodine-131 therapy, Eur J Nucl Med 21(10) (1994) 1121-5.
[31] K. Obayashi, Salivary mental stress proteins, Clin Chim Acta 425 (2013) 196-201.
[32] V. Engert, S. Vogel, S.I. Efanov, A. Duchesne, V. Corbo, N. Ali, J.C. Pruessner, Investigation into the cross-correlation of salivary cortisol and alpha-amylase responses to psychological stress, Psychoneuroendocrinology 36(9) (2011) 1294-302.
[33] L. Ma, J. Wan, X. Shen, Salivary Alpha-Amylase and Behavior Reaction in Acute Stress and the Impact of Tridimensional Personality, Adv Exp Med Biol 1072 (2018) 431-436.
[34] J.M. Paula, H.M. Sonobe, A.C. Nicolussi, M.M. Zago, N.O. Sawada, Symptoms of depression in patients with cancer of the head and neck undergoing radiotherapy treatment: a prospective study, Rev Lat Am Enfermagem 20(2) (2012) 362-8.
[35] P. Blancafort, J. Jin, S. Frye, Writing and rewriting the epigenetic code of cancer cells: from engineered proteins to small molecules, Mol Pharmacol 83(3) (2013) 563-76.
[36] G. Zupkovitz, J. Tischler, M. Posch, I. Sadzak, K. Ramsauer, G. Egger, R. Grausenburger, N. Schweifer, S. Chiocca, T. Decker, C. Seiser, Negative and positive regulation of gene expression by mouse histone deacetylase 1, Mol Cell Biol 26(21) (2006) 7913-28.
[37] L.D. Moore, T. Le, G. Fan, DNA methylation and its basic function, Neuropsychopharmacology 38(1) (2013) 23-38.
[38] V. Kari, A. Shchebet, H. Neumann, S.A. Johnsen, The H2B ubiquitin ligase RNF40 cooperates with SUPT16H to induce dynamic changes in chromatin structure during DNA double-strand break repair, Cell Cycle 10(20) (2011) 3495-504.
[39] X. Li, R. Tian, H. Gao, Y. Yang, B.R.G. Williams, M.P. Gantier, N.A.J. McMillan, D. Xu, Y. Hu, Y. Gao, Identification of a histone family gene signature for predicting the prognosis of cervical cancer patients, Sci Rep 7(1) (2017) 16495.
[40] L. Sadeghi, L. Siggens, J.P. Svensson, K. Ekwall, Centromeric histone H2B monoubiquitination promotes noncoding transcription and chromatin integrity, Nat Struct Mol Biol 21(3) (2014) 236-43.
[41] P. Mao, M.N. Kyriss, A.J. Hodges, M. Duan, R.T. Morris, M.D. Lavine, T.B. Topping, L.M. Gloss, J.J. Wyrick, A basic domain in the histone H2B N-terminal tail is important for nucleosome assembly by FACT, Nucleic Acids Res 44(19) (2016) 9142-9152.
[42] M. Ransom, B.K. Dennehey, J.K. Tyler, Chaperoning histones during DNA replication and repair, Cell 140(2) (2010) 183-95.

[43] R. Nag, M. Kyriss, J.W. Smerdon, J.J. Wyrick, M.J. Smerdon, A cassette of N-terminal amino acids of histone H2B are required for efficient cell survival, DNA repair and Swi/Snf binding in UV irradiated yeast, Nucleic Acids Res 38(5) (2010) 1450-60.
[44] J. Law, M. Salla, A. Zare, Y. Wong, L. Luong, N. Volodko, O. Svystun, K. Flood, J. Lim, M. Sung, J.R. Dyck, C.T. Tan, Y.C. Su, V.C. Yu, J. Mackey, S. Baksh, Modulator of apoptosis 1 (MOAP-1) is a tumor suppressor protein linked to the RASSF1A protein, J Biol Chem 290(40) (2015) 24100-18.
[45] K.O. Tan, N.Y. Fu, S.K. Sukumaran, S.L. Chan, J.H. Kang, K.L. Poon, B.S. Chen, V.C. Yu, MAP-1 is a mitochondrial effector of Bax, Proc Natl Acad Sci U S A 102(41) (2005) 14623-8.
[46] S. Baksh, S. Tommasi, S. Fenton, V.C. Yu, L.M. Martins, G.P. Pfeifer, F. Latif, J. Downward, B.G. Neel, The tumor suppressor RASSF1A and MAP-1 link death receptor signaling to Bax conformational change and cell death, Mol Cell 18(6) (2005) 637-50.
[47] C.J. Foley, H. Freedman, S.L. Choo, C. Onyskiw, N.Y. Fu, V.C. Yu, J. Tuszynski, J.C. Pratt, S. Baksh, Dynamics of RASSF1A/MOAP-1 association with death receptors, Mol Cell Biol 28(14) (2008) 4520-35.
[48] D. Heller, E.J. Helmerhorst, F.G. Oppenheim, Saliva and Serum Protein Exchange at the Tooth Enamel Surface, Journal of dental research 96(4) (2017) 437-443.
[49] F.G. Oppenheim, D.I. Hay, D.J. Smith, G.D. Offner, R.F. Troxler, Molecular basis of salivary proline-rich protein and peptide synthesis: cell-free translations and processing of human and macaque statherin mRNAs and partial amino acid sequence of their signal peptides, Journal of dental research 66(2) (1987) 462-6.
[50] E. Pisano, T. Cabras, C. Montaldo, V. Piras, R. Inzitari, C. Olmi, M. Castagnola, I. Messana, Peptides of human gingival crevicular fluid determined by HPLC-ESI-MS, European journal of oral sciences 113(6) (2005) 462-8.
[51] P. de Sousa-Pereira, J.M. Woof, IgA: Structure, Function, and Developability, Antibodies (Basel) 8(4) (2019).

FIGURE LEGENDS

Fig. 1. Venn diagram showing the relation of the proteins identified in common between the groups, as well as the number of proteins identified exclusively in each of the groups, for each comparison. (A) Comparison DRT vs BRT, 60 unique proteins DRT, 149 unique proteins BRT and 53 proteins in common between the groups in this comparison. (B) Comparison ART vs BRT, 52 unique proteins ART, 151 unique proteins BRT and 48 proteins in common between the groups in this comparison. (C) Comparison ART vs DRT, 50 unique proteins ART, 59 unique proteins DRT and 29 proteins in common between the groups in this comparison. (D) Comparison BRT vs Control, 150 unique proteins BRT, 146 unique proteins and 102 proteins in common between the groups in this comparison.

Fig. 2. Functional analysis of the distribution of proteins identified with differential expression in the period DRT vs BRT. Protein categories based on Gene Ontology (GO) annotation of the broad Biological Process, Molecular Function, Immune System Process and Cell Component.

Terms of significance (Kappa = 0.04) and distribution according to the percentage of the number of associated genes. The number of access to proteins was provided by UNIPROT. The gene ontology was evaluated according to the ClueGo® pluggins of the software Cytoscape® 3.7.2.

Fig. 3. Functional analysis of the distribution of proteins identified with differential expression in the period ART vs BRT. Protein categories based on Gene Ontology (GO) annotation of the broad Biological Process. Terms of significance (Kappa = 0.04) and distribution according to the percentage of the number of associated genes. The number of access to proteins was provided by UNIPROT. The gene ontology was evaluated according to the ClueGo® pluggins of the software Cytoscape® 3.8.2.

Fig. 4. Functional analysis of the distribution of proteins identified with differential expression in the period ART vs BRT. Protein categories based on Gene Ontology (GO) annotation of the broad Molecular Function. Terms of significance (Kappa = 0.04) and distribution according to the percentage of the number of associated genes. The number of access to proteins was provided by UNIPROT. The gene ontology was evaluated according to the ClueGo® pluggins of the software Cytoscape® 3.8.2.

Fig. 5. Functional analysis of the distribution of proteins identified with differential expression in the period ART vs BRT. Protein categories based on Gene Ontology (GO) annotation of the broad Immune System Process. Terms of significance (Kappa = 0.04) and distribution according to the percentage of the number of associated genes. The number of access to proteins was provided by UNIPROT. The gene ontology was evaluated according to the ClueGo® pluggins of the software Cytoscape® 3.8.2.

Fig. 6. Interaction networks to establish the interaction between proteins identified with differential expression ART in relation to the BRT. Interaction networks created by STRING® (https://string-db.org/cgi/network.pl) to establish the interaction between proteins identified with differential expression ART vs BRT. The red color of the nodes indicates the Histone proteins that are involved with innate immune response in mucosa (Histone H2B type F-S; Histone cluster 1 H2B family member c; Histone H2B type 1-J; Histone H2B type 1-K; Histone H2B type 2-E; Lactotransferrin) and the blue color of the nodes represents Histones involved with DNA methylation (Histone H2B type F-S; Histone H2B type 2-E; Histone H2B type 1-B;

Histone H2B type 1-D; Histone H2B type 1-H; Histone H2B type 1-J; Histone H2B type 1-K; Histone H2B type 1-L; Histone H2B type 1-M; Histone H2B type 1-N; Histone H2B type 1-O).

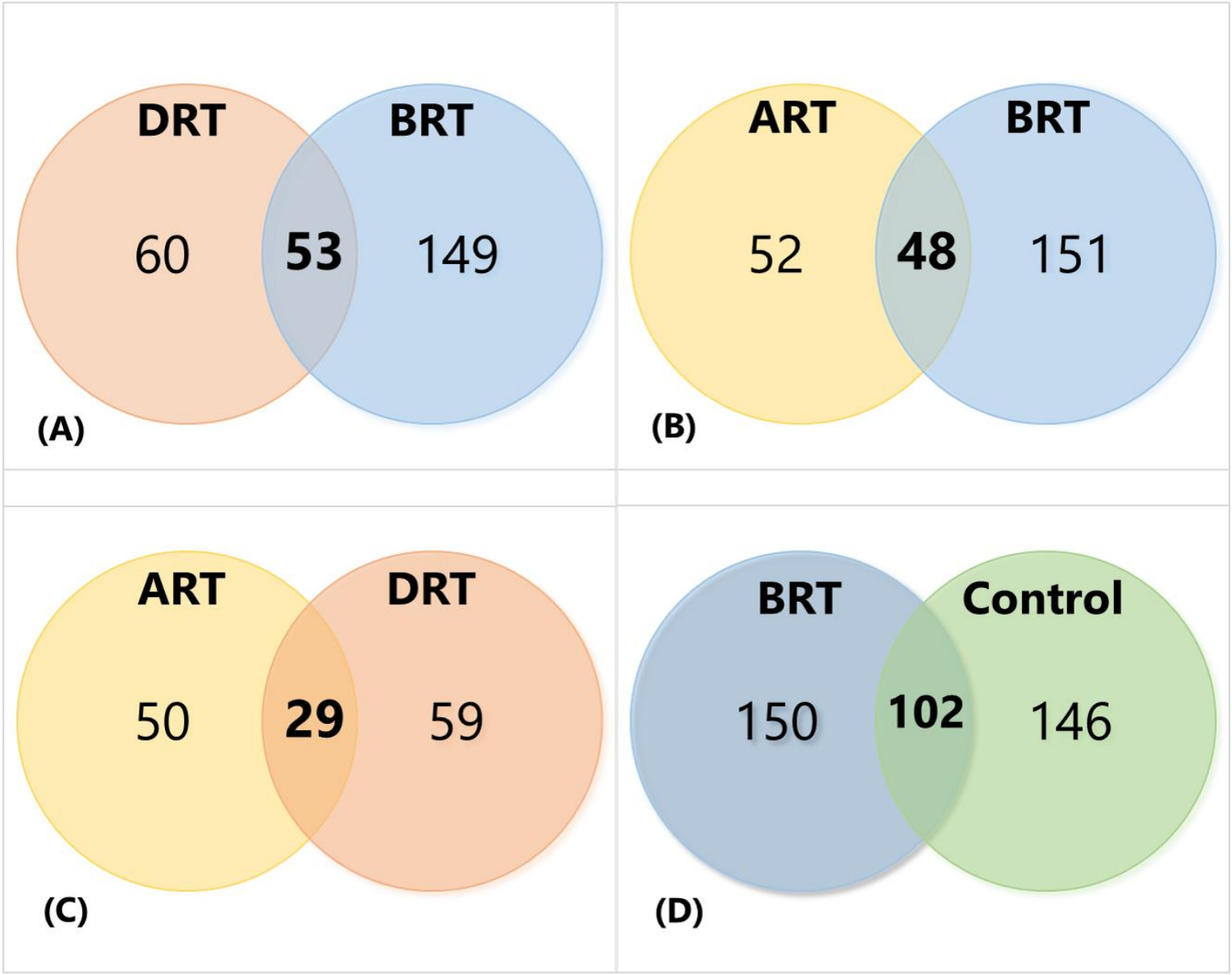
DRT
BRT
60
53
149
(A)
ART
BRT
52
48
151
(B)
ART
DRT
50
29
59
(C)
BRT
Control
150
102
146
(D)

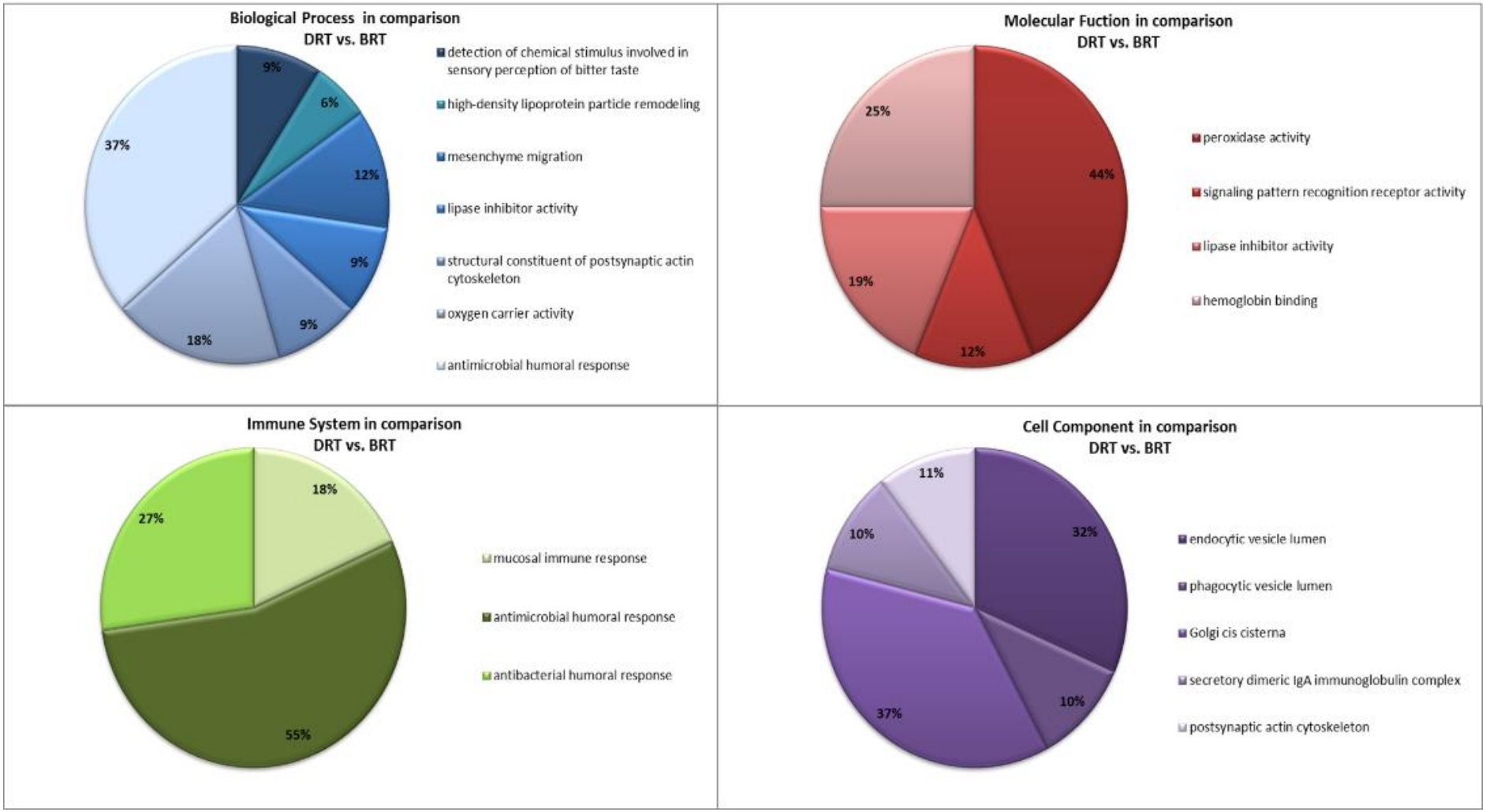
Biological Process in comparison
DRT vs. BRT
9%
6%
12%
9%
9%
18%
37%
detection of chemical stimulus involved in sensory perception of bitter taste
high-density lipoprotein particle remodeling
mesenchyme migration
lipase inhibitor activity
structural constituent of postsynaptic actin cytoskeleton
oxygen carrier activity
antimicrobial humoral response
Molecular Fuction in comparison
DRT vs. BRT
44%
12%
19%
25%
peroxidase activity
signaling pattern recognition receptor activity
lipase inhibitor activity
hemoglobin binding
Immune System in comparison
DRT vs. BRT
18%
55%
27%
mucosal immune response
antimicrobial humoral response
antibacterial humoral response
Cell Component in comparison
DRT vs. BRT
32%
10%
37%
10%
11%
endocytic vesicle lumen
phagocytic vesicle lumen
Golgi cis cisterna
secretory dimeric IgA immunoglobulin complex
postsynaptic actin cytoskeleton

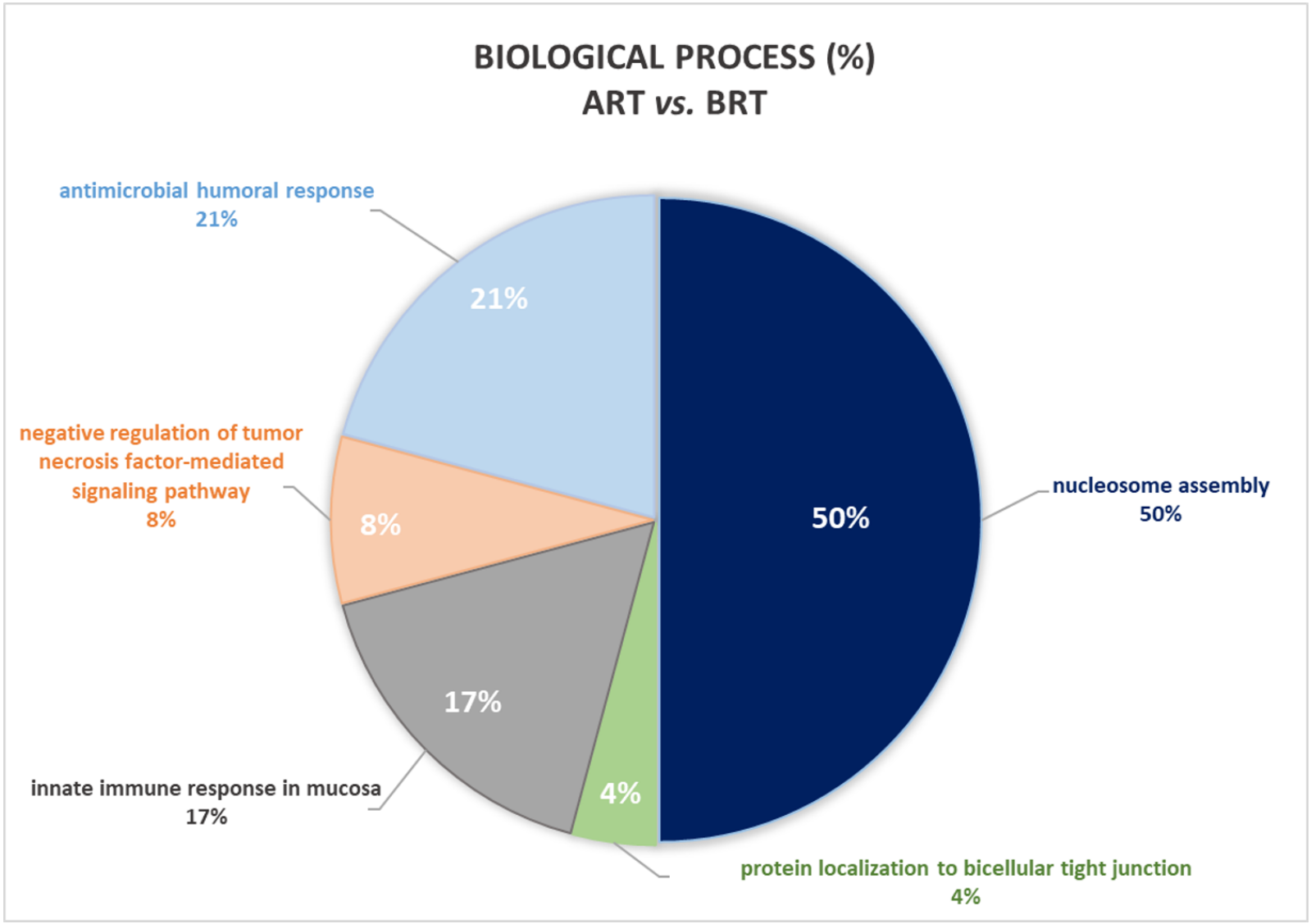
BIOLOGICAL PROCESS (%)
ART vs. BRT
antimicrobial humoral response
21%
21%
negative regulation of tumor
necrosis factor-mediated
signaling pathway
8%
8%
50%
nucleosome assembly
50%
17%
innate immune response in mucosa
17%
4%
protein localization to bicellular tight junction
4%

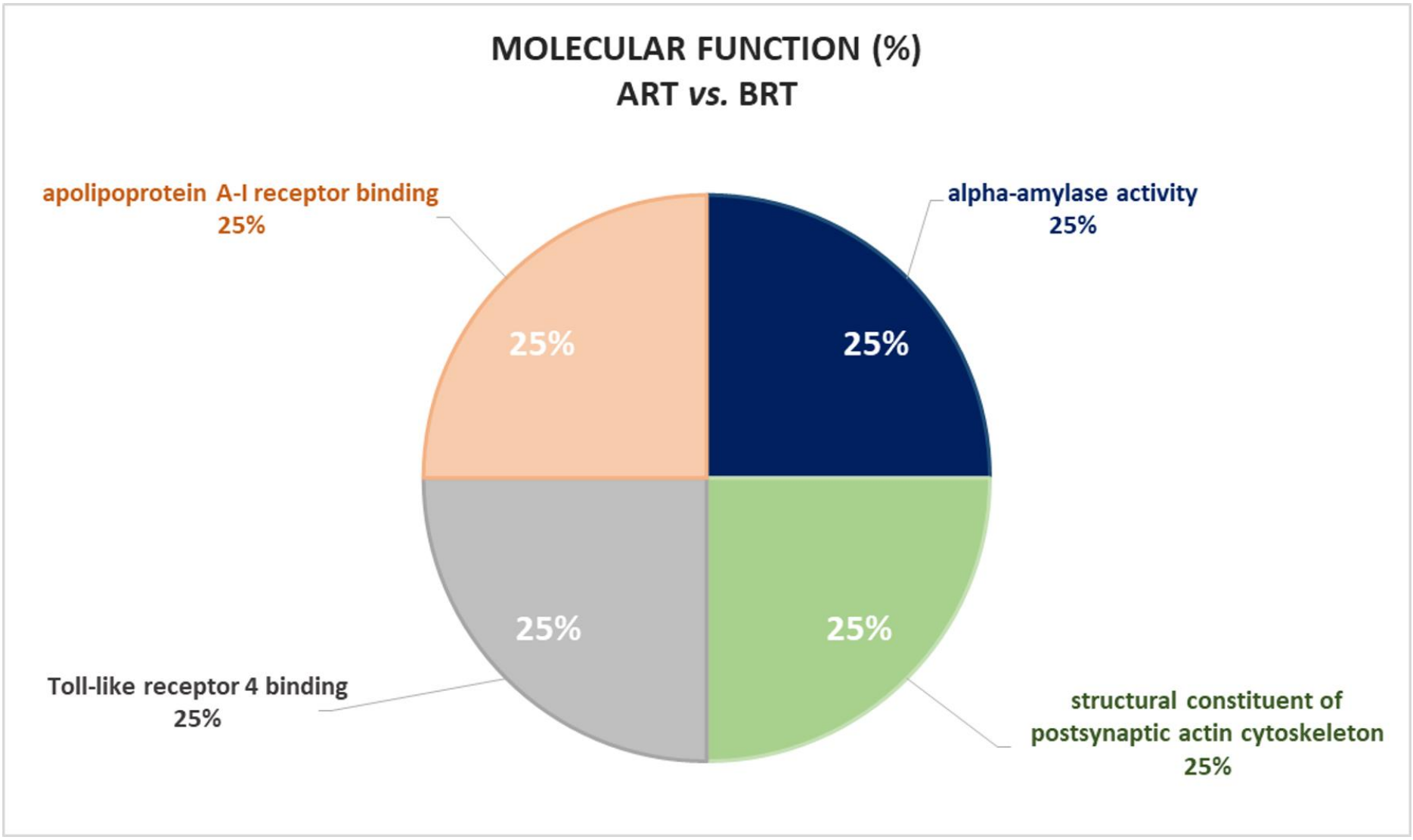
MOLECULAR FUNCTION (%)
ART vs. BRT
apolipoprotein A-I receptor binding
25%
alpha-amylase activity
25%
25%
25%
25%
25%
Toll-like receptor 4 binding
25%
structural constituent of
postsynaptic actin cytoskeleton
25%

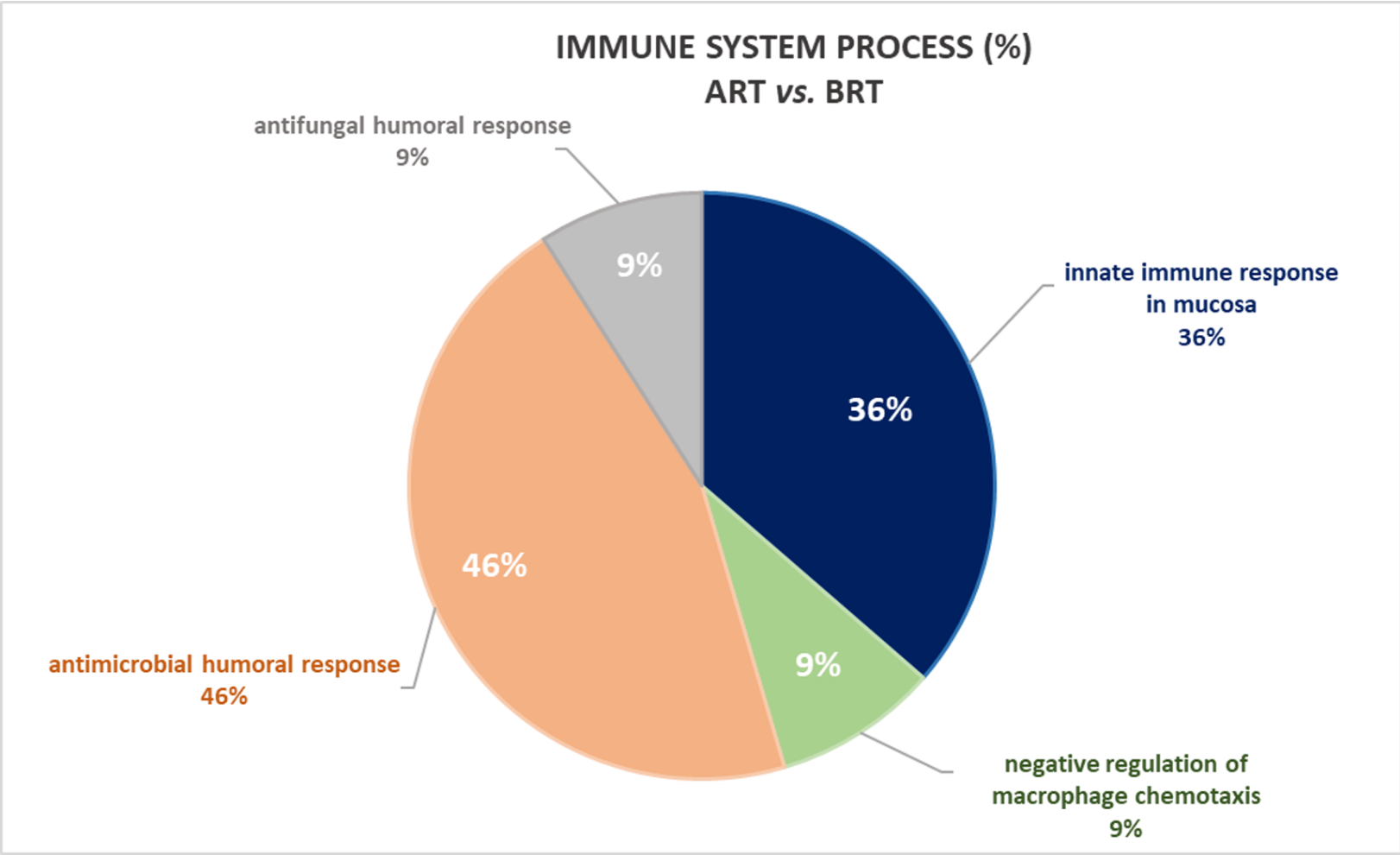
IMMUNE SYSTEM PROCESS (%)
ART vs. BRT
antifungal humoral response
9%
innate immune response
in mucosa
36%
antimicrobial humoral response
46%
negative regulation of
macrophage chemotaxis
9%
9%
36%
46%
9%

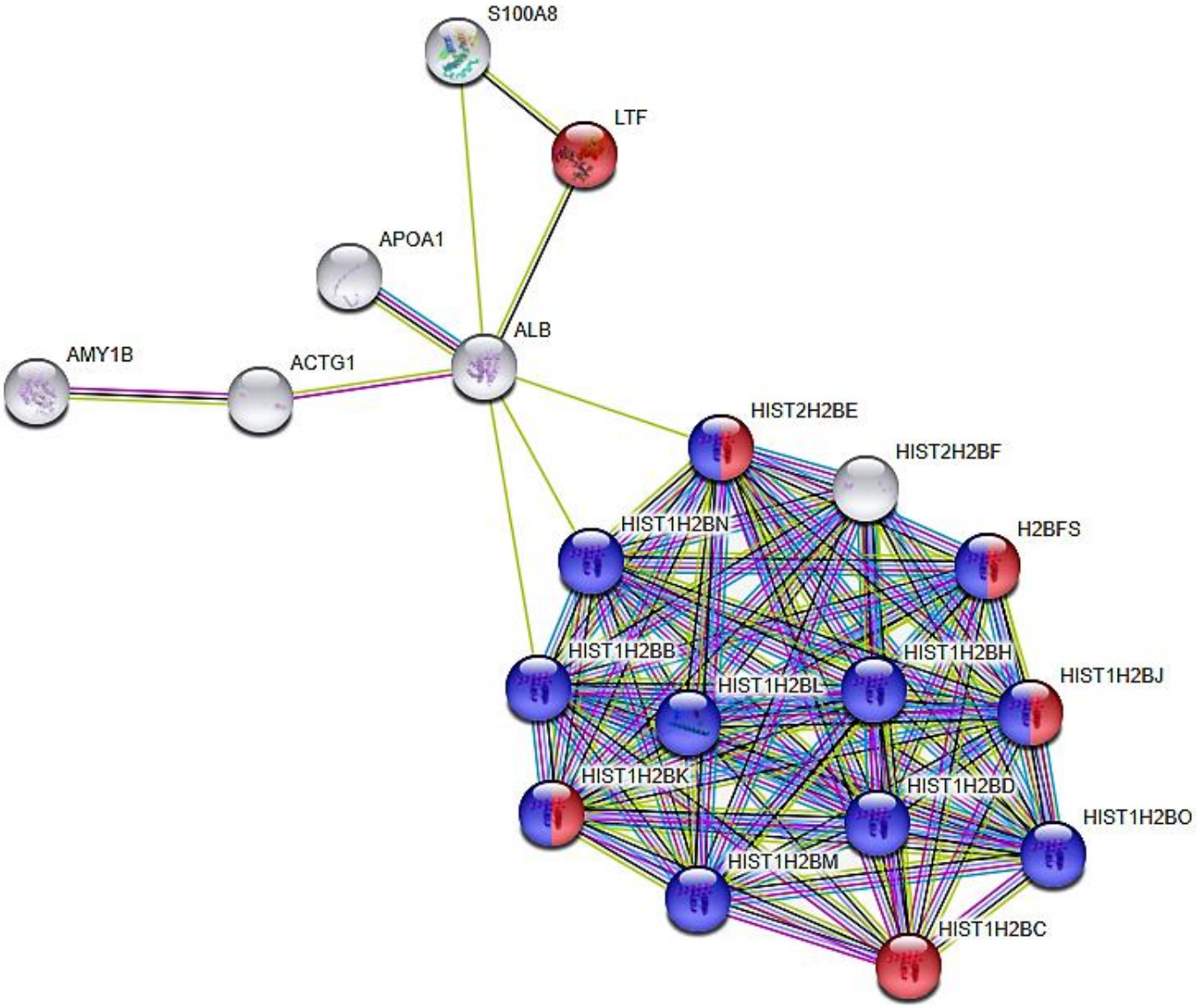
S100A8
LTF
APOA1
ALB
AMY1B
ACTG1
HIST2H2BE
HIST2H2BF
HIST1H2BN
H2BFS
HIST1H2BB
HIST1H2BH
HIST1H2BL
HIST1H2BJ
HIST1H2BK
HIST1H2BD
HIST1H2BO
HIST1H2BM
HIST1H2BC

Supplementary Tables

Supplementary Table 1. Proteins with significantly altered expression in the acquired enamel pellicle during radiotherapy (DRT) in comparison with before radiotherapy (BRT) in patients with head and neck cancer.

°Accession number	Protein name	PLGS Score	+Ratio DRT:BRT
P02808	**Statherin**	**2945**	**9.78**
P02100	**Hemoglobin subunit epsilon**	**404**	**5.26**
P02042	**Hemoglobin subunit delta**	**404**	**5.16**
P69892	**Hemoglobin subunit gamma-2**	**404**	**5.05**
A0A2R8Y7X9	**Uncharacterized protein**	**404**	**5.05**
P68871	**Hemoglobin subunit beta**	**582**	**5.00**
P69891	**Hemoglobin subunit gamma-1**	**404**	**4.85**
P69905	**Hemoglobin subunit alpha**	**280**	**3.46**
G3V1N2	**HCG1745306_ isoform CRA_a**	**161**	**2.97**
P00738	**Haptoglobin**	**328**	**2.44**
P02647	**Apolipoprotein A-I**	**2470**	**2.41**
Q5T3N1	**Annexin (Fragment)**	**4614**	**2.20**
P04083	**Annexin A1**	**4629**	**2.16**
Q562R1	Beta-actin-like protein 2	3165	1.68
P68032	Actin_ alpha cardiac muscle 1	14858	1.63
P68133	Actin_ alpha skeletal muscle	14858	1.63
P63267	Actin_ gamma-enteric smooth muscle	14848	1.58
P62736	Actin_ aortic smooth muscle	14848	1.57
P02768	Serum albumin	25904	1.49
A5A3E0	POTE ankyrin domain family member F	9933	1.46
Q6S8J3	POTE ankyrin domain family member E	10145	1.39
P63261	Actin_ cytoplasmic 2	18824	1.27
P60709	Actin_ cytoplasmic 1	18824	1.26

C9JKR2	Albumin_ isoform CRA_k	10501	1.23
P02788	Lactotransferrin	3884	0.58
P01877	Immunoglobulin heavy constant alpha 2	10164	0.54
Q9UGM3	Deleted in malignant brain tumors 1 protein	231	0.53
P59666	Neutrophil defensin 3	12855	0.53
P01876	**Immunoglobulin heavy constant alpha 1**	**18706**	**0.48**
P59665	**Neutrophil defensin 1**	**12855**	**0.48**
A0A087WZY1	**Uncharacterized protein**	**4410**	**0.45**
A0A0A0MT31	**Proline-rich protein 4**	**4410**	**0.44**
P02810	**Salivary acidic proline-rich phosphoprotein 1/2**	**4410**	**0.44**
P15515	**Histatin-1**	**14325**	**0.42**
P01036	**Cystatin-S**	**12377**	**0.30**
P02814	**Submaxillary gland androgen-regulated protein 3B**	**21895**	**0.27**
P07737	**Profilin-1**	**3506**	**0.23**
I3L3D5	**Profilin (Fragment)**	**3516**	**0.21**
P09228	**Cystatin-SA**	**3015**	**0.07**
E9PGV9	ATP-binding cassette sub-family G member 1	30	DRT*
Q8IU65	Axonemal dynein heavy chain 8 isoform 2 (Fragment)	40	DRT*
H0Y7V4	Dynein heavy chain 8_ axonemal	41	DRT*
Q6ZNJ1	Neurobeachin-like protein 2	144	DRT*
E9PGT3	Ribosomal protein S6 kinase	104	DRT*
Q15418	Ribosomal protein S6 kinase alpha-1	104	DRT*
Q86YL5	Testis development-related protein	43	DRT*
P31947	14-3-3 protein sigma	108	BRT*
P30566	Adenylosuccinate lyase	212	BRT*
P01009	Alpha-1-antitrypsin	125	BRT*
P12429	Annexin A3	176	BRT*
Q96DR5	BPI fold-containing family A member 2	78	BRT*
Q96KE9	BTB/POZ domain-containing protein 6	70	BRT*
P23280	Carbonic anhydrase 6	2723	BRT*

P04080	Cystatin-B	1293	BRT*
P01034	Cystatin-C	860	BRT*
P43351	DNA repair protein RAD52 homolog	166	BRT*
E9PDA6	DNA-binding protein RFX8	287	BRT*
Q01469	Fatty acid-binding protein 5	729	BRT*
P04075	Fructose-bisphosphate aldolase A	329	BRT*
P47929	Galectin-7	1923	BRT*
P09211	Glutathione S-transferase P	608	BRT*
P04406	Glyceraldehyde-3-phosphate dehydrogenase	747	BRT*
P0CJ92	Golgin subfamily A member 8H	100	BRT*
A6NMD2	Golgin subfamily A member 8J	100	BRT*
H3BSY2	Golgin subfamily A member 8M	100	BRT*
F8WBI6	Golgin subfamily A member 8N	100	BRT*
A6NCC3	Golgin subfamily A member 8O	100	BRT*
H3BV12	Golgin subfamily A member 8Q	100	BRT*
I6L899	Golgin subfamily A member 8R	100	BRT*
P04792	Heat shock protein beta-1	9797	BRT*
P15516	Histatin-3	4038	BRT*
U3KQK0	Histone H2B	1879	BRT*
P33778	Histone H2B type 1-B	1879	BRT*
P62807	Histone H2B type 1-C/E/F/G/I	1879	BRT*
P58876	Histone H2B type 1-D	1879	BRT*
Q93079	Histone H2B type 1-H	1879	BRT*
P06899	Histone H2B type 1-J	1879	BRT*
O60814	Histone H2B type 1-K	1879	BRT*
Q99880	Histone H2B type 1-L	1879	BRT*
Q99879	Histone H2B type 1-M	1879	BRT*
Q99877	Histone H2B type 1-N	1879	BRT*
P23527	Histone H2B type 1-O	1879	BRT*
Q16778	Histone H2B type 2-E	1879	BRT*

Q5QNW6	Histone H2B type 2-F	1879	BRT*
Q8N257	Histone H2B type 3-B	1879	BRT*
P57053	Histone H2B type F-S	1879	BRT*
P62805	Histone H4	1542	BRT*
P01857	Immunoglobulin heavy constant gamma 1	2967	BRT*
P01859	Immunoglobulin heavy constant gamma 2	1824	BRT*
P01860	Immunoglobulin heavy constant gamma 3	1013	BRT*
P01861	Immunoglobulin heavy constant gamma 4	1516	BRT*
S4R460	Immunoglobulin heavy variable 3/OR16-9 (non-functional)	451	BRT*
P01591	Immunoglobulin J chain	8725	BRT*
P01834	Immunoglobulin kappa constant	3185	BRT*
P0CG04	Immunoglobulin lambda constant 1	946	BRT*
P0DOY2	Immunoglobulin lambda constant 2	946	BRT*
P0DOY3	Immunoglobulin lambda constant 3	946	BRT*
P0CF74	Immunoglobulin lambda constant 6	946	BRT*
A0M8Q6	Immunoglobulin lambda constant 7	655	BRT*
B9A064	Immunoglobulin lambda-like polypeptide 5	946	BRT*
P06870	Kallikrein-1	152	BRT*
P13645	Keratin_ type I cytoskeletal 10	65	BRT*
P13646	Keratin_ type I cytoskeletal 13	2049	BRT*
P02533	Keratin_ type I cytoskeletal 14	664	BRT*
P19012	Keratin_ type I cytoskeletal 15	669	BRT*
P08779	Keratin_ type I cytoskeletal 16	753	BRT*
Q04695	Keratin_ type I cytoskeletal 17	221	BRT*
P05783	Keratin_ type I cytoskeletal 18	52	BRT*
P08727	Keratin_ type I cytoskeletal 19	288	BRT*
P35908	Keratin_ type II cytoskeletal 2 epidermal	167	BRT*
Q01546	Keratin_ type II cytoskeletal 2 oral	153	BRT*
P19013	Keratin_ type II cytoskeletal 4	108	BRT*
P13647	Keratin_ type II cytoskeletal 5	491	BRT*

P02538	Keratin_ type II cytoskeletal 6A	1262	BRT*
P04259	Keratin_ type II cytoskeletal 6B	981	BRT*
P48668	Keratin_ type II cytoskeletal 6C	1255	BRT*
O95678	Keratin_ type II cytoskeletal 75	59	BRT*
Q5XKE5	Keratin_ type II cytoskeletal 79	59	BRT*
P08493	Matrix Gla protein	2723	BRT*
P14780	Matrix metalloproteinase-9	102	BRT*
Q8TAX7	Mucin-7	6918	BRT*
P24158	Myeloblastin	75	BRT*
P05164	Myeloperoxidase	980	BRT*
P19105	Myosin regulatory light chain 12A	280	BRT*
O14950	Myosin regulatory light chain 12B	280	BRT*
P80188	Neutrophil gelatinase-associated lipocalin	288	BRT*
O75594	Peptidoglycan recognition protein 1	105	BRT*
Q16822	Phosphoenolpyruvate carboxykinase [GTP]_ mitochondrial	129	BRT*
P01833	Polymeric immunoglobulin receptor	625	BRT*
P12273	Prolactin-inducible protein	15557	BRT*
Q6P5S2	Protein LEG1 homolog	558	BRT*
P31949	Protein S100-A11	230	BRT*
A8MUU1	Putative fatty acid-binding protein 5-like protein 3	141	BRT*
P02787	Serotransferrin	1752	BRT*
Q9H299	SH3 domain-binding glutamic acid-rich-like protein 3	395	BRT*
Q9NYJ8	TGF-beta-activated kinase 1 and MAP3K7-binding protein 2	59	BRT*
P02766	Transthyretin	140	BRT*
P08670	Vimentin	373	BRT*
B0YJC4	Vimentin variant 3	393	BRT*
B0YJC5	Vimentin variant 4	67	BRT*
P25311	Zinc-alpha-2-glycoprotein	18663	BRT*
Q96DA0	Zymogen granule protein 16 homolog B	3690	BRT*

°Identification is based on protein ID from UniProt protein database, reviewed only (http://wwwwww.uniprot.org/).

[+]Proteins with expression significantly altered are organized according to the ratio.
*Indicates unique protein in alphabetical order.
Proteins highlighted in bold are increased or decreased more than 2-fold.

Supplementary Table 2. Proteins with significantly altered expression in the acquired enamel pellicle after radiotherapy (ART) in comparison with before radiotherapy (BRT) in patients with head and neck cancer.

[°]Accession number	Protein name	PLGS Score	[+]Ratio ART:BRT
Q93079	**Histone H2B type 1-H**	**1879**	**4.31**
Q16778	**Histone H2B type 2-E**	**1879**	**4.14**
Q5QNW6	**Histone H2B type 2-F**	**1879**	**4.06**
Q8N257	**Histone H2B type 3-B**	**1879**	**4.01**
P57053	**Histone H2B type F-S**	**1879**	**4.01**
P62807	**Histone H2B type 1-C/E/F/G/I**	**1879**	**3.97**
O60814	**Histone H2B type 1-K**	**1879**	**3.90**
P02647	**Apolipoprotein A-I**	**2470**	**3.86**
Q99879	**Histone H2B type 1-M**	**1879**	**3.82**
P23527	**Histone H2B type 1-O**	**1879**	**3.82**
P06899	**Histone H2B type 1-J**	**1879**	**3.74**
Q99877	**Histone H2B type 1-N**	**1879**	**3.60**
Q99880	**Histone H2B type 1-L**	**1879**	**3.56**
P58876	**Histone H2B type 1-D**	**1879**	**3.53**
U3KQK0	**Histone H2B**	**1879**	**3.46**
P33778	**Histone H2B type 1-B**	**1879**	**3.46**
P05109	Protein S100-A8	9010	1.86
C9JKR2	Albumin_ isoform CRA_k	10501	1.60
P02788	Lactotransferrin	3884	1.60
P63261	Actin_ cytoplasmic 2	18824	1.55
P04745	**Alpha-amylase 1**	**30419**	**0.32**
Q96A08	Histone H2B type 1-A	87	ART*

Q8TEK3	Histone-lysine N-methyltransferase_ H3 lysine-79 specific	36	ART*
Q96BY2	Modulator of apoptosis 1	30	ART*
Q14147	Probable ATP-dependent RNA helicase DHX34	25	ART*
P31947	14-3-3 protein sigma	108	BRT*
P30566	Adenylosuccinate lyase	212	BRT*
P01009	Alpha-1-antitrypsin	125	BRT*
P19961	Alpha-amylase 2B	23224	BRT*
P12429	Annexin A3	176	BRT*
P03973	Antileukoproteinase	1540	BRT*
Q96DR5	BPI fold-containing family A member 2	78	BRT*
Q96KE9	BTB/POZ domain-containing protein 6	70	BRT*
P23280	Carbonic anhydrase 6	2723	BRT*
P01034	Cystatin-C	860	BRT*
P01036	Cystatin-S	12377	BRT*
P09228	Cystatin-SA	3015	BRT*
P01037	Cystatin-SN	12113	BRT*
P43351	DNA repair protein RAD52 homolog	166	BRT*
D6RAX4	DNA-binding protein RFX8	287	BRT*
Q01469	Fatty acid-binding protein 5	729	BRT*
J3KPS3	Fructose-bisphosphate aldolase	340	BRT*
P04075	Fructose-bisphosphate aldolase A	329	BRT*
P47929	Galectin-7	1923	BRT*
A0A2R8Y7X9	GLOBIN domain-containing protein	404	BRT*
P09211	Glutathione S-transferase P	608	BRT*
P04406	Glyceraldehyde-3-phosphate dehydrogenase	747	BRT*
P0CJ92	Golgin subfamily A member 8H	100	BRT*
A6NMD2	Golgin subfamily A member 8J	100	BRT*
H3BSY2	Golgin subfamily A member 8M	100	BRT*
F8WBI6	Golgin subfamily A member 8N	100	BRT*
A6NCC3	Golgin subfamily A member 8O	100	BRT*

H3BV12	Golgin subfamily A member 8Q	100	BRT*
I6L899	Golgin subfamily A member 8R	100	BRT*
P00738	Haptoglobin	328	BRT*
G3V1N2	HCG1745306_ isoform CRA_a	161	BRT*
P04792	Heat shock protein beta-1	9797	BRT*
P69905	Hemoglobin subunit alpha	280	BRT*
P68871	Hemoglobin subunit beta	582	BRT*
P02042	Hemoglobin subunit delta	404	BRT*
P02100	Hemoglobin subunit epsilon	404	BRT*
P69891	Hemoglobin subunit gamma-1	404	BRT*
P69892	Hemoglobin subunit gamma-2	404	BRT*
P15515	Histatin-1	14325	BRT*
P15516	Histatin-3	4038	BRT*
P62805	Histone H4	1542	BRT*
P01876	Immunoglobulin heavy constant alpha 1	18706	BRT*
P01877	Immunoglobulin heavy constant alpha 2	10164	BRT*
P01857	Immunoglobulin heavy constant gamma 1	2967	BRT*
P01859	Immunoglobulin heavy constant gamma 2	1824	BRT*
P01860	Immunoglobulin heavy constant gamma 3	1013	BRT*
P01861	Immunoglobulin heavy constant gamma 4	1516	BRT*
S4R460	Immunoglobulin heavy variable 3/OR16-9 (non-functional)	451	BRT*
P01591	Immunoglobulin J chain	8725	BRT*
P01834	Immunoglobulin kappa constant	3185	BRT*
P0CG04	Immunoglobulin lambda constant 1	946	BRT*
P0DOY2	Immunoglobulin lambda constant 2	946	BRT*
P0DOY3	Immunoglobulin lambda constant 3	946	BRT*
P0CF74	Immunoglobulin lambda constant 6	946	BRT*
A0M8Q6	Immunoglobulin lambda constant 7	655	BRT*
B9A064	Immunoglobulin lambda-like polypeptide 5	946	BRT*
P06870	Kallikrein-1	152	BRT*

P13645	Keratin_ type I cytoskeletal 10	65	BRT*
P13646	Keratin_ type I cytoskeletal 13	2049	BRT*
P02533	Keratin_ type I cytoskeletal 14	664	BRT*
P19012	Keratin_ type I cytoskeletal 15	669	BRT*
P08779	Keratin_ type I cytoskeletal 16	753	BRT*
Q04695	Keratin_ type I cytoskeletal 17	221	BRT*
P05783	Keratin_ type I cytoskeletal 18	52	BRT*
P08727	Keratin_ type I cytoskeletal 19	288	BRT*
P35908	Keratin_ type II cytoskeletal 2 epidermal	167	BRT*
Q01546	Keratin_ type II cytoskeletal 2 oral	153	BRT*
P19013	Keratin_ type II cytoskeletal 4	108	BRT*
P13647	Keratin_ type II cytoskeletal 5	491	BRT*
P02538	Keratin_ type II cytoskeletal 6A	1262	BRT*
P04259	Keratin_ type II cytoskeletal 6B	981	BRT*
P48668	Keratin_ type II cytoskeletal 6C	1255	BRT*
O95678	Keratin_ type II cytoskeletal 75	59	BRT*
Q5XKE5	Keratin_ type II cytoskeletal 79	59	BRT*
P61626	Lysozyme C	20088	BRT*
P08493	Matrix Gla protein	2723	BRT*
P14780	Matrix metalloproteinase-9	102	BRT*
Q8TAX7	Mucin-7	6918	BRT*
P24158	Myeloblastin	75	BRT*
P19105	Myosin regulatory light chain 12A	280	BRT*
O14950	Myosin regulatory light chain 12B	280	BRT*
P80188	Neutrophil gelatinase-associated lipocalin	288	BRT*
P04746	Pancreatic alpha-amylase	12962	BRT*
O75594	Peptidoglycan recognition protein 1	105	BRT*
Q16822	Phosphoenolpyruvate carboxykinase [GTP]_ mitochondrial	129	BRT*
P01833	Polymeric immunoglobulin receptor	625	BRT*
P12273	Prolactin-inducible protein	15557	BRT*

A0A0A0MT31	Proline-rich protein 4	4410	BRT*
Q6P5S2	Protein LEG1 homolog	558	BRT*
P31949	Protein S100-A11	230	BRT*
A8MUU1	Putative fatty acid-binding protein 5-like protein 3	141	BRT*
P02810	Salivary acidic proline-rich phosphoprotein 1/2	4410	BRT*
P02787	Serotransferrin	1752	BRT*
Q9H299	SH3 domain-binding glutamic acid-rich-like protein 3	395	BRT*
P02814	Submaxillary gland androgen-regulated protein 3B	21895	BRT*
Q9NYJ8	TGF-beta-activated kinase 1 and MAP3K7-binding protein 2	59	BRT*
P02766	Transthyretin	140	BRT*
A0A087WZY1	Uncharacterized protein	4410	BRT*
P08670	Vimentin	373	BRT*
B0YJC4	Vimentin variant 3	393	BRT*
B0YJC5	Vimentin variant 4	67	BRT*
P25311	Zinc-alpha-2-glycoprotein	18663	BRT*
Q96DA0	Zymogen granule protein 16 homolog B	3690	BRT*

°Identification is based on protein ID from UniProt protein database, reviewed only (http://wwwwww.uniprot.org/).
+Proteins with expression significantly altered are organized according to the ratio.
*Indicates unique protein in alphabetical order.
Proteins highlighted in bold are increased or decreased more than 2-fold.

Supplementary Table 3. Proteins with significantly altered expression in the acquired enamel pellicle after radiotherapy (ART) in comparison with during radiotherapy (DRT) in patients with head and neck cancer.

°Accession number	**Protein name**	**PLGS Score**	**+Ratio ART:DRT**
P02788	**Lactotransferrin**	**129**	**2.56**
P02768	Serum albumin	2014	1.58
P02808	**Statherin**	**4092**	**0.23**
P04745	**Alpha-amylase 1**	**721**	**0.21**
P04080	Cystatin-B	236	ART*

U3KQK0	Histone H2B	142	ART*
Q96A08	Histone H2B type 1-A	87	ART*
P33778	Histone H2B type 1-B	142	ART*
P62807	Histone H2B type 1-C/E/F/G/I	142	ART*
P58876	Histone H2B type 1-D	142	ART*
Q93079	Histone H2B type 1-H	142	ART*
P06899	Histone H2B type 1-J	142	ART*
O60814	Histone H2B type 1-K	142	ART*
Q99880	Histone H2B type 1-L	142	ART*
Q99879	Histone H2B type 1-M	142	ART*
Q99877	Histone H2B type 1-N	142	ART*
P23527	Histone H2B type 1-O	142	ART*
Q16778	Histone H2B type 2-E	142	ART*
Q5QNW6	Histone H2B type 2-F	142	ART*
Q8N257	Histone H2B type 3-B	142	ART*
P57053	Histone H2B type F-S	142	ART*
Q8TEK3	Histone-lysine N-methyltransferase_ H3 lysine-79 specific	36	ART*
Q96BY2	Modulator of apoptosis 1	30	ART*
P05164	Myeloperoxidase	72	ART*
Q14147	Probable ATP-dependent RNA helicase DHX34	25	ART*
P19961	Alpha-amylase 2B	485	DRT*
P03973	Antileukoproteinase	194	DRT*
E9PGV9	ATP-binding cassette sub-family G member 1	30	DRT*
Q8IU65	Axonemal dynein heavy chain 8 isoform 2 (Fragment)	40	DRT*
P01036	Cystatin-S	469	DRT*
P09228	Cystatin-SA	451	DRT*
P01037	Cystatin-SN	604	DRT*
H0Y7V4	Dynein heavy chain 8_ axonemal	41	DRT*
A0A2R8Y7X9	GLOBIN domain-containing protein	350	DRT*
P00738	Haptoglobin	143	DRT*

G3V1N2	HCG1745306_ isoform CRA_a	119	DRT*
P69905	Hemoglobin subunit alpha	252	DRT*
P68871	Hemoglobin subunit beta	401	DRT*
P02042	Hemoglobin subunit delta	350	DRT*
P02100	Hemoglobin subunit epsilon	350	DRT*
P69891	Hemoglobin subunit gamma-1	350	DRT*
P69892	Hemoglobin subunit gamma-2	350	DRT*
P15515	Histatin-1	335	DRT*
P01876	Immunoglobulin heavy constant alpha 1	298	DRT*
P01877	Immunoglobulin heavy constant alpha 2	154	DRT*
P61626	Lysozyme C	144	DRT*
Q6ZNJ1	Neurobeachin-like protein 2	144	DRT*
P04746	Pancreatic alpha-amylase	273	DRT*
A0A0A0MT31	Proline-rich protein 4	807	DRT*
E9PGT3	Ribosomal protein S6 kinase	104	DRT*
Q15418	Ribosomal protein S6 kinase alpha-1	104	DRT*
P02810	Salivary acidic proline-rich phosphoprotein 1/2	807	DRT*
P02814	Submaxillary gland androgen-regulated protein 3B	469	DRT*
Q86YL5	Testis development-related protein	43	DRT*
A0A087WZY1	Uncharacterized protein	807	DRT*

°Identification is based on protein ID from UniProt protein database, reviewed only (http://wwwwww.uniprot.org/).
+Proteins with expression significantly altered are organized according to the ratio.
*Indicates unique protein in alphabetical order.
Proteins highlighted in bold are increased or decreased more than 2-fold.

Supplementary Table 4. Proteins with significantly altered expression in the acquired enamel pellicle before radiotherapy (BRT) in patients with head and neck cancer in comparison healthy patients (Control).

°Accession number	Protein name	PLGS Score	+Ratio BRT:Control
P25311	**Zinc-alpha-2-glycoprotein**	**1032**	**2.80**
P12273	**Prolactin-inducible protein**	**1936**	**2.41**
P19961	**Alpha-amylase 2B**	**2404**	**2.25**
Q8TAX7	**Mucin-7**	**1088**	**2.20**
Q9UGM3	**Deleted in malignant brain tumors 1 protein**	**102**	**2.14**
P04745	**Alpha-amylase 1**	**3334**	**2.10**
P04746	**Pancreatic alpha-amylase**	**1335**	**2.03**
P01834	Immunoglobulin kappa constant	562	1.93
P0CF74	Immunoglobulin lambda constant 6	315	1.86
P01859	Immunoglobulin heavy constant gamma 2	133	1.82
P01876	Immunoglobulin heavy constant alpha 1	1275	1.80
A0A0A0MT31	Proline-rich protein 4	1026	1.73
P61626	Lysozyme C	3188	1.70
A0A087WZY1	Uncharacterized protein	1026	1.70
P02810	Salivary acidic proline-rich phosphoprotein 1/2	1026	1.68
P59665	Neutrophil defensin 1	2023	1.63
P59666	Neutrophil defensin 3	2023	1.60
P01877	Immunoglobulin heavy constant alpha 2	545	1.57
P01857	Immunoglobulin heavy constant gamma 1	332	1.52
P06702	Protein S100-A9	8668	1.08
P01036	Cystatin-S	4390	0.84
P68032	Actin_ alpha cardiac muscle 1	5742	0.76
P63261	Actin_ cytoplasmic 2	9506	0.75

P60709	Actin_ cytoplasmic 1	9506	0.74
P63267	Actin_ gamma-enteric smooth muscle	5671	0.73
P68133	Actin_ alpha skeletal muscle	5742	0.72
P04792	Heat shock protein beta-1	369	0.60
Q9BYX7	Putative beta-actin-like protein 3	437	0.58
P48668	Keratin_ type II cytoskeletal 6C	419	0.54
Q562R1	Beta-actin-like protein 2	1360	0.53
P02538	Keratin_ type II cytoskeletal 6A	419	0.52
P04259	**Keratin_ type II cytoskeletal 6B**	**275**	**0.47**
Q5T3N1	**Annexin (Fragment)**	**835**	**0.46**
P04083	**Annexin A1**	**854**	**0.44**
P35908	**Keratin_ type II cytoskeletal 2 epidermal**	**54**	**0.27**
P19013	**Keratin_ type II cytoskeletal 4**	**54**	**0.24**
P31947	14-3-3 protein sigma	108	BRT*
P30566	Adenylosuccinate lyase	212	BRT*
P01009	Alpha-1-antitrypsin	125	BRT*
P12429	Annexin A3	176	BRT*
P03973	Antileukoproteinase	1540	BRT*
Q96DR5	BPI fold-containing family A member 2	78	BRT*
Q96KE9	BTB/POZ domain-containing protein 6	70	BRT*
P43351	DNA repair protein RAD52 homolog	166	BRT*
D6RAX4	DNA-binding protein RFX8	287	BRT*
Q01469	Fatty acid-binding protein 5	729	BRT*
A0A2R8Y7X9	GLOBIN domain-containing protein	404	BRT*
P09211	Glutathione S-transferase P	608	BRT*
P0CJ92	Golgin subfamily A member 8H	100	BRT*
A6NMD2	Golgin subfamily A member 8J	100	BRT*
H3BSY2	Golgin subfamily A member 8M	100	BRT*
F8WBI6	Golgin subfamily A member 8N	100	BRT*
A6NCC3	Golgin subfamily A member 8O	100	BRT*

H3BV12	Golgin subfamily A member 8Q	100	BRT*
I6L899	Golgin subfamily A member 8R	100	BRT*
G3V1N2	HCG1745306_ isoform CRA_a	161	BRT*
P69905	Hemoglobin subunit alpha	280	BRT*
P68871	Hemoglobin subunit beta	582	BRT*
P02042	Hemoglobin subunit delta	404	BRT*
P02100	Hemoglobin subunit epsilon	404	BRT*
P69891	Hemoglobin subunit gamma-1	404	BRT*
P69892	Hemoglobin subunit gamma-2	404	BRT*
P15516	Histatin-3	4038	BRT*
P62805	Histone H4	1542	BRT*
P06870	Kallikrein-1	152	BRT*
O95678	Keratin_ type II cytoskeletal 75	59	BRT*
Q5XKE5	Keratin_ type II cytoskeletal 79	59	BRT*
P14780	Matrix metalloproteinase-9	102	BRT*
P24158	Myeloblastin	75	BRT*
P19105	Myosin regulatory light chain 12A	280	BRT*
O14950	Myosin regulatory light chain 12B	280	BRT*
P80188	Neutrophil gelatinase-associated lipocalin	288	BRT*
O75594	Peptidoglycan recognition protein 1	105	BRT*
Q16822	Phosphoenolpyruvate carboxykinase [GTP]_ mitochondrial	129	BRT*
P01833	Polymeric immunoglobulin receptor	625	BRT*
Q6P5S2	Protein LEG1 homolog	558	BRT*
P31949	Protein S100-A11	230	BRT*
A8MUU1	Putative fatty acid-binding protein 5-like protein 3	141	BRT*
P02787	Serotransferrin	1752	BRT*
Q9H299	SH3 domain-binding glutamic acid-rich-like protein 3	395	BRT*
Q9NYJ8	TGF-beta-activated kinase 1 and MAP3K7-binding protein 2	59	BRT*
P02766	Transthyretin	140	BRT*
P25054	Adenomatous polyposis coli protein	58	Control*

Q86YJ7	Ankyrin repeat domain-containing protein 13B	50	Control*
Q06520	Bile salt sulfotransferase	42	Control*
Q86WJ1	Chromodomain-helicase-DNA-binding protein 1-like	37	Control*
Q68D86	Coiled-coil domain-containing protein 102B	51	Control*
P21399	Cytoplasmic aconitate hydratase	29	Control*
P17661	Desmin	80	Control*
A0A075B7B1	Desmuslin_ isoform CRA_a	47	Control*
E5RGY1	Disintegrin and metalloproteinase domain-containing protein 28	39	Control*
E9PEI6	DPCR1	27	Control*
Q8TES7	Fas-binding factor 1	60	Control*
P09972	Fructose-bisphosphate aldolase C	99	Control*
Q13439	Golgin subfamily A member 4	35	Control*
Q4VXL4	HCG41426_ isoform CRA_c	40	Control*
Q86XA9	HEAT repeat-containing protein 5A	29	Control*
Q96A08	Histone H2B type 1-A	368	Control*
K7ENM4	INO80 complex subunit C (Fragment)	90	Control*
Q15323	Keratin_ type I cuticular Ha1	173	Control*
Q14532	Keratin_ type I cuticular Ha2	173	Control*
Q14525	Keratin_ type I cuticular Ha3-II	173	Control*
Q92764	Keratin_ type I cuticular Ha5	173	Control*
O76013	Keratin_ type I cuticular Ha6	173	Control*
O76014	Keratin_ type I cuticular Ha7	173	Control*
O76015	Keratin_ type I cuticular Ha8	173	Control*
Q2M2I5	Keratin_ type I cytoskeletal 24	173	Control*
Q7Z3Y7	Keratin_ type I cytoskeletal 28	180	Control*
O95235	Kinesin-like protein KIF20A	44	Control*
Q86VH2	Kinesin-like protein KIF27	45	Control*
Q9BYG0	Lactosylceramide 1_3-N-acetyl-beta-D-glucosaminyltransferase	43	Control*
Q53EV4	Leucine-rich repeat-containing protein 23	74	Control*

Q96LZ2	Melanoma-associated antigen B10	109	Control*
Q5JRG1	Nucleoporin p58/p45 (Fragment)	42	Control*
P00558	Phosphoglycerate kinase 1	65	Control*
K7EJ44	Profilin	580	Control*
H3BQ34	Pyruvate kinase	179	Control*
P14618	Pyruvate kinase PKM	198	Control*
Q9BZZ2	Sialoadhesin	74	Control*
Q8WXA9	Splicing regulatory glutamine/lysine-rich protein 1	39	Control*
O15061	Synemin	47	Control*
Q16650	T-box brain protein 1	50	Control*
O95359	Transforming acidic coiled-coil-containing protein 2	44	Control*
H3BVG6	Tyrosine-protein kinase receptor	39	Control*
O14562	Ubiquitin domain-containing protein UBFD1	80	Control*
Q5T200	Zinc finger CCCH domain-containing protein 13	29	Control*

°Identification is based on protein ID from UniProt protein database. reviewed only (http://wwwwww.uniprot.org/).
+Proteins with expression significantly altered are organized according to the ratio.
*Indicates unique protein in alphabetical order.
Proteins highlighted in bold are increased or decreased more than 2-fold.

2.6 ARTICLE 6

Article formatted according to Heliyon

Acquired pellicle and its engineering with Statherin peptide instantly protects native enamel surfaces against dental erosion

Short title: Pellicle engineering with Statherin peptide

Talita Mendes Oliveira Ventura[ab] - talitaventura@usp.br
Marília Afonso Rabelo Buzalaf[a*] - mbuzalaf@fob.usp.br
Tommy Baumann[b] - tommy.baumann@zmk.unibe.ch
Vinícius Taioqui Pelá[bc] - vinicus_asb@hotmail.com
Samira Helena Niemeyer[b] - samira.niemeyer@zmk.unibe.ch
Edson Crusca[d] - ecrusca@gmail.com
Reinaldo Marchetto[d] - reinaldo.marchetto@unesp.br
Adrian Lussi[b] - adrian.lussi@zmk.unibe.ch
Thiago Saads Carvalho[b] - thiago.saads@zmk.unibe.ch

[a] Department of Biological Sciences, Stomatology and Oral Biology - Discipline of Biochemistry, Bauru School of Dentistry, University of São Paulo, Bauru, SP, Brazil.
[b] Department of Restorative, Preventive and Pediatric Dentistry, University of Bern, Bern, Switzerland.
[c] Department of Genetics and Evolution, Federal University of São Carlos, São Carlos, SP, Brazil.
[d] Department of Biochemistry and Technological Chemistry, Institute of Chemistry, School of Dentistry, São Paulo State University, Araraquara, SP, Brazil.

***Corresponding Author:** Marília Afonso Rabelo Buzalaf (ORCID ID: 0000-0002-5985-3951). Department of Biological Sciences, Bauru Dental School, University of São Paulo. Al. Octávio Pinheiro Brisolla, 9-75 Bauru-SP, 17012-901 Brazil. Tel. + 55 14 32358346; Fax + 55 14 32271486; E-mail: mbuzalaf@fob.usp.br.

(to whom reprint requests must be sent)

Graphical Abstract

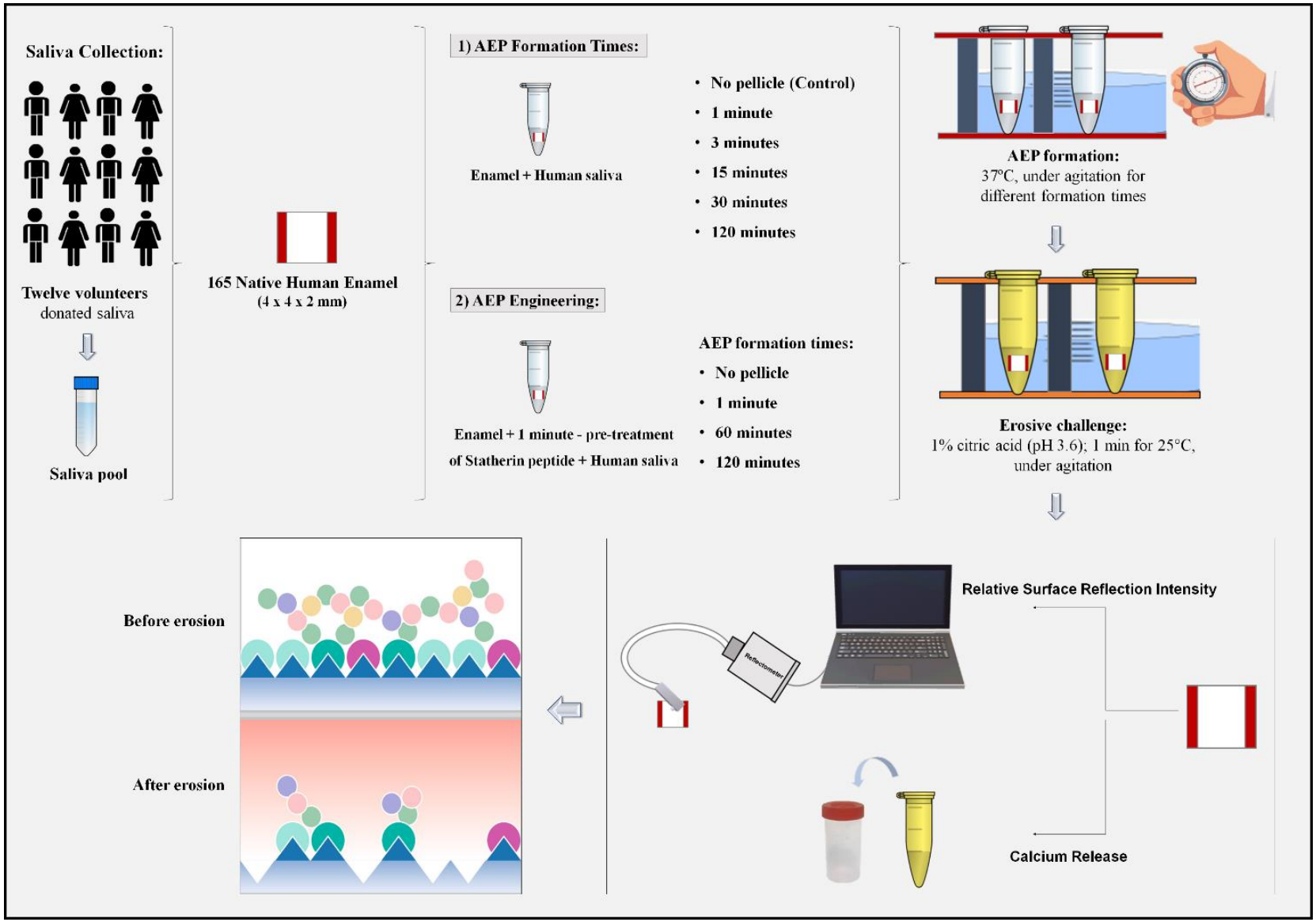

Abstract

Objectives: This study evaluated the protective effect of the acquired enamel pellicle (AEP) formed *in vitro* for different times, as well as its engineering with Statherin peptide, against initial dental erosion. **Methods:** Human native enamel specimens (n=165) were divided according to 1) AEP formation times (No pellicle, 1, 3, 15, 30, 60 and 120 minutes) and 2) AEP engineering (pre-treatment with 1 minute of Statherin peptide (StatpSpS) followed by 1, 60 and 120 minutes AEP formation). One group with only the StatpSpS was also included. The specimens were subjected to erosive challenge for 5 cycles. Relative surface reflection intensity (rSRI) and the calcium release were measured. **Results:** AEP formation caused less rSRI loss in comparison to No pellicle ($p<0.0001$), but there was no difference between AEP formation times. Pellicle engineering with StatpSpS caused no significant difference in rSRI between the different AEP formation times, however pellicle engineering presented less rSRI loss when compared to the No pellicle ($p<0.0001$). There was no significant difference in the calcium released when StatpSpS was used for pellicle engineering, but there was a significant difference regarding the time of AEP formation ($F=11.92$, $p<0.0001$). **Conclusion:** AEP provides almost instant protection, with formation times as short as 1 min protecting the native enamel against erosion *in vitro*, and longer formation times do not improve the protection. StatpSpS by itself provides similar protection as the AEP.

Clinical Significance: Acquired pellicle engineering with StatpSpS instantly protects against erosion. Thus, treatment with the StatpSpS may be an alternative for patients who suffer from diseases or treatment that reduced salivary flow. Our results open a new avenue for preventive approaches against dental erosion and for future *in vitro* studies.

Keywords: dental erosion; acquired enamel pellicle; statherin; surface reflection intensity; pellicle modification.

Introduction

Dental erosion is the loss of dental hard tissue due to the action of non-bacterial acids. Initially there is a loss of mineral ions from the surface of the enamel, leading to increased roughness and loss of surface reflectivity. The process progresses with the continuous dissolution, layer by layer, of the crystals of the enamel, leading to an irreversible loss of tissue (1, 2). Any structure forming on the dental surface can hinder the direct contact with the acids, protecting the tooth against erosion. This is the case of the acquired enamel pellicle (AEP), which acts as a diffusion barrier or semipermeable membrane, protecting against demineralization (3, 4).

In this context, AEP plays a fundamental role in protecting the dental surface against erosion (3). Its formation is dynamic, being influenced by several factors, such as circadian cycle, composition of buccal microbiota, proteolytic capacity of the buccal environment, physical-chemical properties of dental surfaces (5) as well as the location in the oral cavity (6). AEP formation begins only a few seconds after exposure of the enamel to the saliva, reaching a stable 10-20 nm thickness within the first few minutes of formation, and the thickness increases at longer formation times, reaching values of 20-80 nm after 120 minutes formation (7, 8). In this regard, many studies in the dental literature have been using 120 minutes of AEP formation time, though it has already been shown that shorter formation times, as short as 3 minutes, can already protect against erosion (9).

More recently with the advances in proteomic analyses, some acid-resistant proteins, such as Statherin, have been identified in the acquired pellicle (10-12). Statherin is present in saliva and acts in the initial phase of AEP formation, being considered a precursor protein of the pellicle (4, 13). It is a 43-residue phosphorylated salivary protein secreted by the parotid and submandibular glands (14, 15). The protein is formed by a neutral C-terminus and a negatively charged N-terminus, the latter being important in the interaction with hydroxyapatite (16, 17). Since the N-terminus is of interest, a peptide containing the 15 amino acid residues of the N-terminus was synthesized. This Statherin peptide, named StatpSpS has a strong adsorption capability to hydroxyapatite (18), and has great potential to be incorporated into dental products in order to increase protection against dental erosion (19).

The present study, therefore, aims to evaluate the effect of different formation times of the AEP, and to test the effect of pre-treatment with Statherin peptide on the prevention of initial dental erosion *in vitro*.

Material and methods

Ethical aspects

This study used human saliva and teeth from pooled biobanks. Because both teeth and saliva are from pooled biobanks, these specimens are categorized by the local ethics committee (Kantonale Ethikkommission: KEK) as "irreversibly anonymized" and no previous ethical approval was necessary for this study. Still, the volunteers provided their informed oral consent to use the saliva for this study. The experiment was performed in accordance with approved guidelines and regulations of the KEK.

Saliva Collection

Twelve young adults in good general (exclusion: smoker, pregnant women, patients with systemic diseases and with medication) and oral health (exclusion: low non-stimulated salivary flow, low buffer capacity, active caries and periodontal disease) donated saliva. Whole-mouth stimulated saliva was collected between 9:00 and 10:00 a.m. under masticatory stimulation (10 min) using Paraffin (20). The saliva was collected in chilled vials, which were then pooled and centrifuged at 3.000 g for 15 min at 4°C. The supernatant was collected, aliquoted, and stored at -80°C until the day of the experiment.

Preparation of human enamel specimens and experimental groups

Human native enamel specimens (n=165) were prepared from human molars. The teeth were cut using two diamond discs and a 4 mm spacer attached to a precision cutting machine (Buehler, Illinois, USA) to obtain standard specimens (4 x 4 x 2 mm). All specimens were protected with nail polish on the sides as well as at the lower part, in order to avoid undesirable demineralization. Only the native enamel surface was left exposed to the experiment. The specimens were randomized into one of the following groups (11 groups; n = 15), according to: 1) time of AEP formation or 2) treatment with Statherin peptide (StatpSpS). For part 1), the groups were: 1 min; 3 min; 15 min; 30 min; 60 min; 120 min of AEP formation times; one no pellicle group was used as control; for part 2), we modified the pellicle by pre-treating the enamel for 1 min with StatpSpS (peptide lyophilized and then diluted in deionized water to a final concentration of 1.88 x 10-5 M Statherin/peptide (DpSpSEEKFLRRIGRFG)), exactly as

described in a previous study (19). For that, we applied StatpSpS for 1 min, and then used AEP formation times of 0 min (No pellicle), 1 min; 60 min; 120 min.

Experimental Design

Surface reflection intensity (SRI) was measured at baseline. For AEP formation, the specimens were individually immersed in the human saliva (200 µL; 37ºC, under agitation) for the different formation times, depending on the group. For the groups with pellicle engineering, the enamel specimens were individually immersed in StatpSpS (200 µL; 1 min, 37ºC, under agitation) before AEP formation.

The specimens were then washed in deionized water and air-dried for 5 seconds, and individually immersed in 1% citric acid (pH 3.6, 1 mL; 1 min; 25ºC; under agitation). They were then rinsed with deionized water and air-dried for 5 seconds, and the acid was reserved for later calcium analyses. This procedure of AEP formation or modification and erosion was performed for a total of 5 cycles. Between cycles, the specimens were stored in a humid chamber at 4ºC. After the 5 days, the specimens were incubated in sodium hypochlorite (5 min; 1 mL, under agitation) to remove traces of the pellicle, and they had their final SRI measured.

Surface reflection intensity (SRI)

SRI measurement was done at baseline and after the last erosive challenge, using a hand-held reflectometer (21, 22). For that, the tip of the reflectometer was placed on the enamel surface, and inclined in different angles until the point of highest reflection intensity was registered (23). The point of highest reflection intensity was expressed as an SRI value. Lower SRI values represent lower reflection intensity of the enamel surface, which, in turn, corresponds to rougher enamel surfaces (in our case, this represents more erosion) (22).

For statistical analyses, we calculated the relative SRI (rSRI), as follows: rSRI = (SRIf/SRIi) x 100, where SRIi is the baseline values, and SRIf the final SRI values.

Calcium Analysis

For the calcium analysis, an atomic absorption spectrometer with acetylene-air flame (AAnalyst 400, Perkin Elmer Analytical Instruments, EUA) was used. A working curve was performed with standard calcium concentrations to obtain a calibration of the equipment. To

eliminate the interference of phosphate ions, lanthanum nitrate was added to citric acid and to the standards (final concentration of 0.5% w/v). The amount of calcium in the citric acid was measured and the values were normalized to the surface area of the enamel specimens. The enamel surface area was measured with a light microscope (Leica, M420) connected to a fixed camera (Leica, DFC495). Images of the enamel specimens were taken and the contour of the exposed enamel area was traced. The software program IM500 automatically calcualted the enamel surface area in mm2 (24). For statistical analyses, calcium results were presented in μmol Calcium/mm2 of enamel.

Statistical analysis

The data were analyzed using the software GraphPad Prism version 5.0 for Windows (GraphPad Software Inc., La Jolla, CA, USA). Initially, the data were checked for normality (Kolmogorov-Smirnov test) and homogeneity (Bartlett's test). The analyzes were performed in two parts. The first analyses considered the data referring to the different AEP formation times (Groups: No pellicle; and AEP formation for 1 min; 3 min; 15 min; 30 min; 60 min; 120 min). The second analyses considered the effect of the pre-treatment with StatpSpS (Groups: No pellicle, 1 min; 60 min; 120 min) comparing them with the groups without pellicle engineering.

The SRI data did not pass the normality test for all groups and were analyzed with Kruskal-Wallis test, followed by the post-hoc Dunn’s test ($p < 0.05$). The data referring to calcium release passed the normality test, and were analyzed with parametric tests: for the first analyses (AEP formation time) we used ANOVA and post-hoc Tukey's test ($p < 0.05$), and for the second analyses (effect of StatpSpS) we used Two-way ANOVA and Bonferroni post-hoc test ($p < 0.05$), with Statherin pretreatment (with or without) and AEP formation time (No pellicle, 1 min; 60 min; 120 min) as factors.

For the analysis between the No pellicle and StatpSpS No pellicle groups, the SRI and calcium results of both groups passed the normality test and we analyzed the differences with parametric t-tests ($p < 0.05$).

Results

Considering the effect of AEP formation times, a significant difference in SRI was observed between the groups ($p<0.0001$), where all formation times protected against erosion, presenting higher rSRI values when compared to the control group (No pellicle). However, no

significant difference was observed between AEP formation times from 1 min to 120 min (Table 1). Regarding calcium release, the groups No pellicle, 1 min, 3 min, 30 min and 60 min presented significantly lower values than the 120 min AEP formation group ($p<0.0001$). The 15 min AEP formation group showed no difference to 120 min (Table 1).

Regarding the effect of StatpSpS, no differences were observed between the groups with different AEP formation times. In general, there was no effect of pellicle engineering with StatpSpS, with no significant differences between the No Statherin and StatpSpS groups with same AEP formation times, but the group treated with StatpSpS / No pellicle presented higher SRI values ($p<0.0001$) than the No Statherin / No pellicle group (Table 1). Considering calcium release, no significant differences were observed when StatpSpS was added ($F=0.54$, p value=0.4643), but longer AEP formation times tended to result in more calcium release ($F=11.92$, $p<0.0001$) (Table 1).

Specifically analyzing the effect of StatpSpS, comparing to the No Statherin / No pellicle group, a better protection against erosion was observed for StatpSpS with a significantly higher SRI value ($p <0.0001$) (Table 1), which was not the case for calcium release, that showed no significant differences ($p = 0.0699$) between the two groups (Table 1).

Discussion

The present study aimed at evaluating the protective effect of different times of AEP formation *in vitro*, as well as to verify the effect of pre-treatment with Statherin peptide for a possible beneficial effect of the AEP's protective effect against initial dental erosion. It is important to emphasize that this is the first study to use native (human) enamel with this goal.

AEP formation begins with a basal layer made up of acid-resistant precursor proteins, such as acidic proline-rich proteins (PRPs), histatins and statherin (25). The thickness of the AEP can change according to the time of its formation, where, after the formation of the basal layer, other proteins can interact with the precursor proteins (4) maturing and modulating the AEP. Though some studies have shown that AEPs formed over 60 min can already offer a maximum protection against demineralization (26-28), other study (9) have found that pellicles formed for shorter periods of time (e.g. 3 min), can already protect the teeth, and no difference was found to a pellicle formed after 120 min. In addition, the initial layer with 3 min can be physiologically functional even without further maturation (29). This protection, with such short-term AEP formation, can be attributed to the electron-dense basal layer (9, 29). Since this

layer is formed within seconds of exposure to saliva, even shorter AEP formation times might protect the native enamel surface against demineralization, which is confirmed by our study.

We observed that the *in vitro* AEP was able to protect enamel against erosion, even at very short formation times, from 1 min onwards. The presence of the AEP was able to reduce demineralization, presenting less rSRI loss. Interestingly, no differences were observed between the different AEP formation times, even after 120 min formation, which is considered to be the time necessary for the AEP to reach a mature state (5, 13). Our data is along the same lines as another *in situ* study, which also showed that a short pellicle formation time (3 min) was also protective, and there was no significant differences between longer (60 min and 120 min) formation times (9). This suggests that the basal layer of the AEP is the one responsible for providing protection against erosive attacks. Perhaps, future studies with the pellicle can greatly reduce the AEP formation times based on our results.

Though the SRI data suggest that longer AEP formation did not increase the protection against erosion, the calcium data seem show greater release for where the time of 120 min presented higher calcium release compared to the other formation times. Actually, the calcium results must be viewed bearing in mind that saliva (and the AEP) also contains calcium (30) and the pellicle was formed on the whole enamel specimen (even on the surfaces covered with the nail varnish), so the calcium results from our study include that released from the pellicle, and not that only from the enamel. It is also known that longer AEP formation times allow for the maturation of the pellicle, increasing its thickness (31, 32) and, thus, its calcium content (25, 33). So, the higher amounts of calcium present in the 120 min pellicle group could simply be calcium from the pellicle itself, and not from enamel. This, in turn, confirms the SRI results, where, despite the more mature pellicle after 120 min formation, the protection against demineralization was not improved.

Since statherin plays an important role on the formation of the basal layer (4, 16, 17, 25) and it has already been identified as an acid-resistant protein (12, 18), we used the synthesized Statherin peptide for pellicle engineering. This peptide, named StatpSpS, consists of the N-terminal 15 amino acids of Statherin. Furthermore, the Serines are phosphorylated, as this has been shown to be important for the function of the peptide (34), resulting in a sequence of DpSpSEEKFLRRIGRFG, where “p” means phosphorylation in serine residues at positions 2 and 3. StatpSpS has previously been shown to protect from erosion (19), which was confirmed in the present study, as by itself, it caused a significantly protect enamel against erosion. Interestingly, when it was used to modify the AEP, there was no significant difference to unmodified AEP. We believe that this may be related to a competition between the StatpSpS

and the salivary proteins when binding to the enamel specimen *in vitro*. Because the treatment with the StatpSpS was performed immediately prior to incubation in the saliva, the peptide can already bind to the enamel, over the entire enamel surface, leaving very few binding sites available for other saliva proteins to bind. So, when AEP is formed, no further protection will be observed from the basal layer. However, if AEP is formed alone, without pellicle engineering with the peptide, the actual Statherin protein from saliva itself will also bind to the enamel surface, providing a protection against erosion. Our hypothesis of this mode of action is represented in Figure 1.

Remarkably, only the treatment with the StatpSpS was already sufficient to provide protection against acid attacks, which corroborates the fact that Statherin is an acid resistant protein (4, 12, 18) and is able to strongly bind to the tooth surface. Again, the lack of significant differences between the groups with and without StatpSpS when AEP was present is suggestive of the fact that the protection from the AEP is mostly from its basal layer, probably from the Statherin protein coming from the saliva. This hypothesis is also confirmed when the No pellicle group was compared only with the StatpSpS No pellcile group, where even without the presence of AEP, the peptide acting alone was able to produce greater protection and higher SRI values (Table 1). This, however, was not observed in the calcium results. But although we did not observe a significant difference between these groups in the calcium analysis, we must consider that the addition of the peptide may have influenced the release of calcium (Table 1). A previous study suggests that peptide StatpSpS in this concentration (1.88 x 10-5) may provide the best balance between the amount of adsorbed peptide and available free Ca^{2+} surrounding the hydroxyapatite surface (19). In this sense, some of the available Ca^{2+} may form complexes with proteins, and only the free Ca^{2+} is able to influence the demineralization process (35). On the other hand, salivary proteins such as statherin maintain high concentrations of Ca^{2+} by binding to Ca^{2+} and forming structures similar to salivary micelles (36) or salivary layers enriched with Ca^{2+} (37).

These data are of great value, since when thinking about a clinical application, treatment with the StatpSpS may be an alternative for patients who have a reduced salivary flow or patients who suffer from diseases that affect the salivary glands, such as autoimmune diseases, Sjögren's syndrome, or patients treated with radiotherapy in the region of head and neck. Perhaps, the StatpSpS could improve the reduced erosion protection these patients suffer from because of their reduced salivary flow rate.

It is important to recognize that these *in vitro* results do not necessarily represent the true nature of the *in vivo* AEP, as there are other important factors for its formation in addition

to saliva. However, our study provides strong evidence of how the pellicle can behave on native enamel surfaces and provide new perceptions for future *in vitro* studies, where pellicle formation times might be decreased. In addition, we cannot fail to mention that the grade of variation of the reflection intensity is due to the use of a native enamel surface. This surface is not polished, as customarily used in other studies, and it remains curved, thus influencing the reflectivity (24). However, it is worth mentioning that the initial and final analyzes were carried out in the same place, so despite the variations, the changes occurring on that surface are still measured. Moreover, this higher variation of SRI values has already been observed in previous studies (23) and, notwithstanding the variation, the reflectometer has been validated for erosive tooth wear studies in native enamel (22).

In conclusion, 1 min of AEP formed *in vitro* on native enamel can already provide erosion protection, and longer formation times do not improve its protective effect. In addition, the StatpSpS applied for 1 min provided similar enamel protection against erosion as the AEP, regardless of the time of formation.

Acknowledgments

The authors thank FAPESP for financial support and for the concession of Research Internships Abroad (BEPE) to the first author (Proc. FAPESP 2019/16815-0). The funders had no role in study design, data collection and analysis, decision to publish or preparation of the manuscript. All authors gave their final approval and agree to be accountable for all aspects of the work. The authors are grateful to Mrs. Barbara Beyeler and Mr. Samuel Furrer, University of Bern, for their technical support in this study and Bernadette Rawyler, University of Bern, for her support with the graphical design of the figure 1.

Conflicts of interest

The authors have declared no conflict of interest.

Author Contributions

Talita Mendes Oliveira Ventura: Conceptualization, Methodology, Validation, Visualization, Formal analysis, Data curation, Investigation, Writing - Original Draft. **Marília Afonso Rabelo Buzalaf:** Conceptualization, Methodology, Validation, Investigation, Resources, Writing - Review & Editing, Supervision, Project administration. **Tommy**

Baumann: Conceptualization, Investigation, Writing - Review & Editing. **Vinícius Taioqui Pelá:** Methodology, Investigation. **Samira Helena Niemeyer:** Methodology, Investigation, Writing - Review & Editing. **Edson Crusca** and **Reinaldo Marchetto:** Methodology, Investigation. **Adrian Lussi:** Conceptualization, Investigation, Writing - Review & Editing. **Thiago Saads Carvalho:** Conceptualization, Methodology, Validation, Formal analysis, Data curation, Investigation, Writing - Original Draft, Supervision, Project administration.

All authors have revised and agreed with the final version of the manuscript.

References

1. LUSSI A, SCHLUETER N, RAKHMATULLINA E, GANSS C. Dental erosion--an overview with emphasis on chemical and histopathological aspects. Caries Res 2011; 45 Suppl 1: 2-12.
2. LUSSI A, CARVALHO TS. Erosive tooth wear: a multifactorial condition of growing concern and increasing knowledge. Monogr Oral Sci 2014; 25: 1-15.
3. BUZALAF MA, HANNAS AR, KATO MT. Saliva and dental erosion. J Appl Oral Sci 2012; 20: 493-502.
4. VUKOSAVLJEVIC D, CUSTODIO W, BUZALAF MA, HARA AT, SIQUEIRA WL. Acquired pellicle as a modulator for dental erosion. Arch Oral Biol 2014; 59: 631-638.
5. LENDENMANN U, GROGAN J, OPPENHEIM FG. Saliva and dental pellicle--a review. Adv Dent Res 2000; 14: 22-28.
6. VENTURA T, CASSIANO LPS, SOUZA ESCM, TAIRA EA, LEITE AL, RIOS D, BUZALAF MAR. The proteomic profile of the acquired enamel pellicle according to its location in the dental arches. Arch Oral Biol 2017; 79: 20-29.
7. HANNIG M. Ultrastructural investigation of pellicle morphogenesis at two different intraoral sites during a 24-h period. Clin Oral Investig 1999; 3: 88-95.
8. ZHANG Y, ZHENG J, YU J, HE H. Mechanical characterization of in vitro-formed short-term salivary pellicle. J Biomech 2018; 66: 194-197.
9. HANNIG M, FIEBIGER M, GUNTZER M, DOBERT A, ZIMEHL R, NEKRASHEVYCH Y. Protective effect of the in situ formed short-term salivary pellicle. Arch Oral Biol 2004; 49: 903-910.
10. DELECRODE TR, SIQUEIRA WL, ZAIDAN FC, BELLINI MR, MOFFA EB, MUSSI MC, XIAO Y, BUZALAF MA. Identification of acid-resistant proteins in acquired enamel pellicle. J Dent 2015; 43: 1470-1475.
11. MARTINI T, RIOS D, CASSIANO LPS, SILVA CMS, TAIRA EA, VENTURA TMS, PEREIRA H, MAGALHAES AC, CARVALHO TS, BAUMANN T, LUSSI A, OLIVEIRA RB, PALMA-DIBB RG, BUZALAF MAR. Proteomics of acquired pellicle in gastroesophageal reflux disease patients with or without erosive tooth wear. J Dent 2019; 81: 64-69.
12. TAIRA EA, VENTURA TMS, CASSIANO LPS, SILVA CMS, MARTINI T, LEITE AL, RIOS D, MAGALHAES AC, BUZALAF MAR. Changes in the Proteomic Profile of Acquired Enamel Pellicles as a Function of Their Time of Formation and Hydrochloric Acid Exposure. Caries Res 2018; 52: 367-377.
13. HANNIG M, JOINER A. The structure, function and properties of the acquired pellicle. Monogr Oral Sci 2006; 19: 29-64.

14. OPPENHEIM FG, HAY DI, SMITH DJ, OFFNER GD, TROXLER RF. Molecular basis of salivary proline-rich protein and peptide synthesis: cell-free translations and processing of human and macaque statherin mRNAs and partial amino acid sequence of their signal peptides. J Dent Res 1987; 66: 462-466.
15. MUTAHAR M, O'TOOLE S, CARPENTER G, BARTLETT D, ANDIAPPAN M, MOAZZEZ R. Reduced statherin in acquired enamel pellicle on eroded teeth compared to healthy teeth in the same subjects: An in-vivo study. PLoS One 2017; 12: e0183660.
16. RAJ PA, JOHNSSON M, LEVINE MJ, NANCOLLAS GH. Salivary statherin. Dependence on sequence, charge, hydrogen bonding potency, and helical conformation for adsorption to hydroxyapatite and inhibition of mineralization. J Biol Chem 1992; 267: 5968-5976.
17. SANTOS O, KOSORIC J, HECTOR MP, ANDERSON P, LINDH L. Adsorption behavior of statherin and a statherin peptide onto hydroxyapatite and silica surfaces by in situ ellipsometry. J Colloid Interface Sci 2008; 318: 175-182.
18. YANG Y, YANG B, LI M, WANG Y, YANG X, LI J. Salivary acquired pellicle-inspired DpSpSEEKC peptide for the restoration of demineralized tooth enamel. Biomed Mater 2017; 12: 025007.
19. TAIRA EA, CARVALHO G, FERRARI CR, MARTINI T, PELA VT, VENTURA TMO, DIONIZIO AS, CRUSCA E, MARCHETTO R, BUZALAF MAR. Statherin-derived peptide protects against intrinsic erosion. Arch Oral Biol 2020; 119: 104890.
20. SIQUEIRA WL, DE OLIVEIRA E, MUSTACCHI Z, NICOLAU J. Electrolyte concentrations in saliva of children aged 6-10 years with Down syndrome. Oral Surg Oral Med Oral Pathol Oral Radiol Endod 2004; 98: 76-79.
21. CARVALHO TS, BAUMANN T, LUSSI A. A new hand-held optical reflectometer to measure enamel erosion: correlation with surface hardness and calcium release. Sci Rep 2016; 6: 25259.
22. CARVALHO TS, ASSUNCAO CM, JOST F, BURGIN WB, RODRIGUES JA, LUSSI A. In vitro validation of a hand-held optical reflectometer to measure clinically observed erosive tooth wear. Lasers Med Sci 2016; 31: 1105-1112.
23. RAKHMATULLINA E, BOSSEN A, BACHOFNER KK, MEIER C, LUSSI A. Optical pen-size reflectometer for monitoring of early dental erosion in native and polished enamels. J Biomed Opt 2013; 18: 117009.
24. CARVALHO TS, BAUMANN T, LUSSI A. Does erosion progress differently on teeth already presenting clinical signs of erosive tooth wear than on sound teeth? An in vitro pilot trial. BMC Oral Health 2016; 17: 14.
25. ASH A, RIDOUT MJ, PARKER R, MACKIE AR, BURNETT GR, WILDE PJ. Effect of calcium ions on in vitro pellicle formation from parotid and whole saliva. Colloids Surf B Biointerfaces 2013; 102: 546-553.
26. AMAECHI BT, HIGHAM SM, EDGAR WM, MILOSEVIC A. Thickness of acquired salivary pellicle as a determinant of the sites of dental erosion. Journal of Dental Research 1999; 78: 1821-1828.
27. HANNIG M, HESS NJ, HOTH-HANNIG W, DE VRESE M. Influence of salivary pellicle formation time on enamel demineralization--an *in situ* pilot study. Clin Oral Investig 2003; 7: 158-161.
28. WETTON S, HUGHES J, WEST N, ADDY M. Exposure time of enamel and dentine to saliva for protection against erosion: a study in vitro. Caries Res 2006; 40: 213-217.
29. TRAUTMANN S, KUNZEL N, FECHER-TROST C, BARGHASH A, SCHALKOWSKY P, DUDEK J, DELIUS J, HELMS V, HANNIG M. Deep Proteomic Insights into the Individual Short-Term Pellicle Formation on Enamel-An *In Situ* Pilot Study. Proteomics Clin Appl 2020; 14: e1900090.

30. ZHANG CZ, CHENG XQ, LI JY, ZHANG P, YI P, XU X, ZHOU XD. Saliva in the diagnosis of diseases. Int J Oral Sci 2016; 8: 133-137.
31. HANNIG M, BALZ M. Protective properties of salivary pellicles from two different intraoral sites on enamel erosion. Caries Res 2001; 35: 142-148.
32. AMAECHI BT, HIGHAM SM, EDGAR WM, MILOSEVIC A. Thickness of acquired salivary pellicle as a determinant of the sites of dental erosion. Journal of dental research 1999; 78: 1821-1828.
33. ZENG Q, ZHENG J, YANG D, TANG Y, ZHOU Z. Effect of calcium ions on the adsorption and lubrication behavior of salivary proteins on human tooth enamel surface. J Mech Behav Biomed Mater 2019; 98: 172-178.
34. XIAO Y, KARTTUNEN M, JALKANEN J, MUSSI MC, LIAO Y, GROHE B, LAGUGNE-LABARTHET F, SIQUEIRA WL. Hydroxyapatite Growth Inhibition Effect of Pellicle Statherin Peptides. J Dent Res 2015; 94: 1106-1112.
35. ANDERSON P, HECTOR MP, RAMPERSAD MA. Critical pH in resting and stimulated whole saliva in groups of children and adults. Int J Paediatr Dent 2001; 11: 266-273.
36. KOSORIC J, WILLIAMS RAD, HECTOR MP, ANDERSON P. A synthetic peptide based on a natural salivary protein reduces demineralisation in model systems for dental caries and erosion. Int J Pept Res Ther 2007; 13: 497-503.
37. PROCTOR GB, HAMDAN S, CARPENTER GH, WILDE P. A statherin and calcium enriched layer at the air interface of human parotid saliva. Biochem J 2005; 389: 111-116.

FIGURE LEGEND

Fig. 1. Mode of action of synthesized Statherin peptide on enamel or on the pellicle engineering, before and after initial erosion.

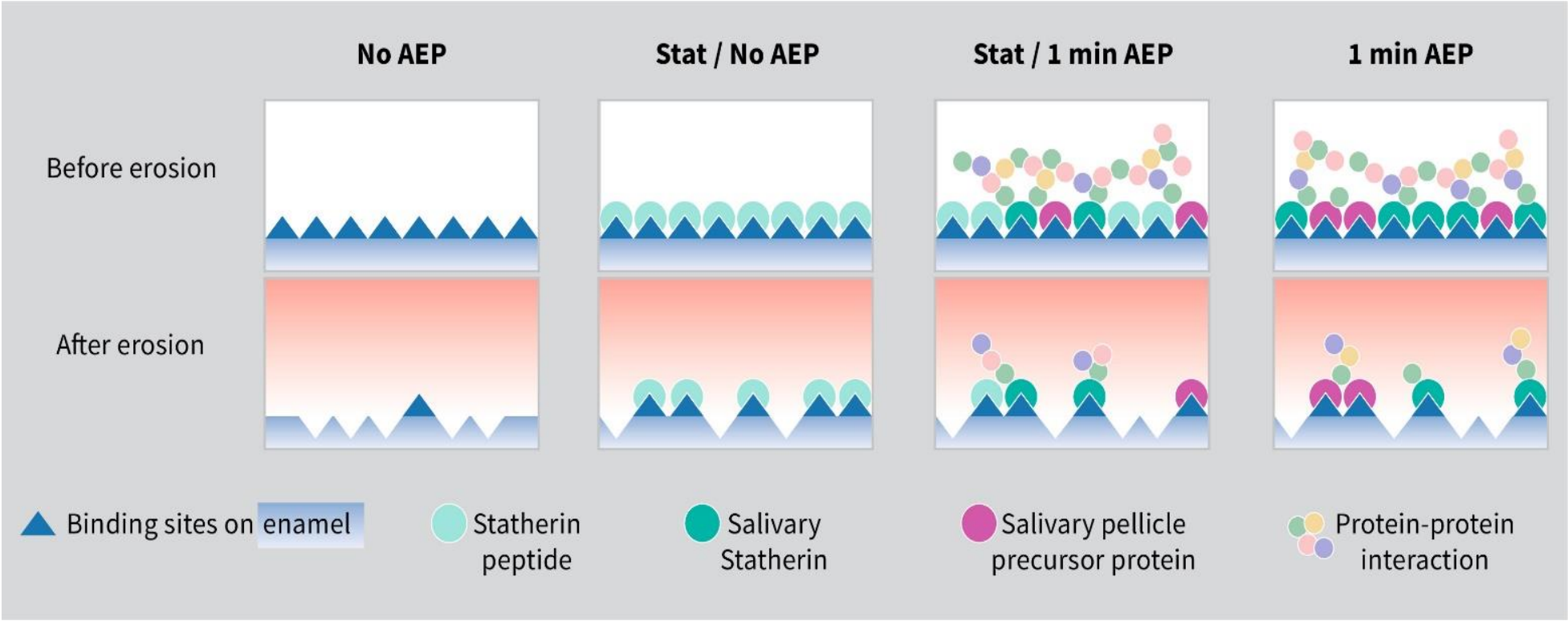
No AEP
Stat / No AEP
Stat / 1 min AEP
1 min AEP
Before erosion
After erosion
Binding sites on enamel
Statherin peptide
Salivary Statherin
Salivary pellicle precursor protein
Protein-protein interaction

Table 1. Median and interquartile range (IQR) for relative surface reflection intensity (rSRI) and mean ±standard deviation (SD) for calcium release for the different AEP formation times and for the pellicle engineering with StatpSpS.

Groups	AEP Formation Times	rSRI	Calcium release (nmolCa/nm²enamel)
		Median (IQR)	Mean ± SD
No Statherin	No pellicle	67.05 (59.65-74.92) ^{aA}	5.72 ± 1.11^{aA}
	1 min	93.71 (75.27-106.45) ^{bA}	6.74 ± 1.33^{aA}
	3 min	83.56 (80.81-87.54) ^{b}	6.21 ± 1.09^{a}
	15 min	92.21 (77.78-98.48) ^{b}	7.52 ± 1.52^{ab}
	30 min	85.71 (80.68-88.60) ^{b}	6.04 ± 1.30^{a}
	60 min	87.40 (77.86-102.40) ^{bA}	7.04 ± 1.10^{aA}
	120 min	92.86 (84.60-120.14) ^{bA}	9.00 ± 2.32^{bA}
StatpSpS	No pellicle	92.37 (85.92-98.04) ^{aB}	6.79 ± 1.24^{aA}
	1 min	97.62 (90.61-112.96) ^{aA}	6.88 ± 1.03^{aA}
	60 min	92.81 (78.49-99.91) ^{aA}	7.51 ± 1.03^{aA}
	120 min	95.35 (82.09-107.94) ^{aA}	8.17 ± 1.18^{aA}

Analyzing the rSRI and Calcium release columns individually, different small letters denote significant differences ($p<0.05$) between the different AEP formation times within the same (No Statherin or StatpSpS) group; capital letters denote pairwise comparisons between the same AEP formation time in the No Statherin and StatpSpS groups.

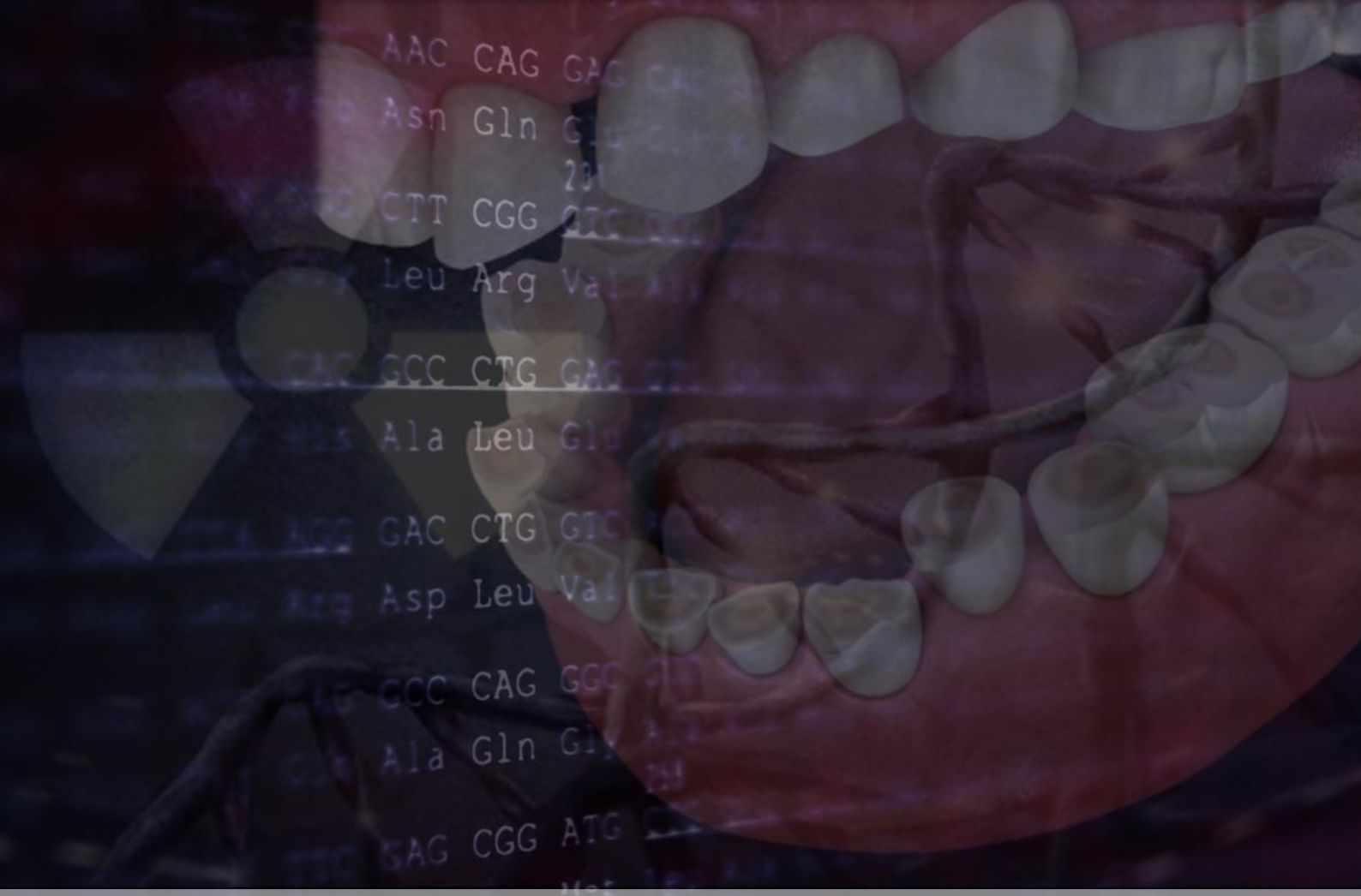

3- Discussion

“Comprimidos aliviam a dor, mas só o amor alivia o sofrimento.”

Patch Adamns - O amor é contagioso

3 DISCUSSION

The main objective of this thesis was to evaluate the proteomic profile in acquired pellicle formed on enamel and saliva in cancer patients, diagnosed with HNC and submitted to radiotherapy treatment in order to search for possible therapies and prognostic biomarkers for these patients. However, for the proposed objective to be achieved, a protocol for shotgun proteomic analysis of saliva was standardized so that we could identify proteins in the saliva. Thus, in this first analysis, two tests were performed with the aimed to standardize a protocol for proteomic analysis of saliva that is sensitive, easy to perform and of low cost, to be used in future experiments involving quantitative *shotgun* proteomics. The first issue to be solved was related to the necessity of depletion of highly abundant proteins in saliva, such as Albumin and IgG (Krief, Deutsch et al. 2012, Sivadasan, Gupta et al. 2015) that could mask and make difficult the identification of low abundance biomarkers. Krief and collaborators, evaluated whether depletion of salivary amylase, albumin and IgGs could improve the ability to visualize proteins in two-dimensional gel electrophoresis (2-DE) in oral fluids. They observed a total of 36 new spots after depletion and 58 spots showed more than two-fold increase intensity after depletion (Krief, Deutsch et al. 2011). Therefore, we hypothesized that this better identification profile could occur not only in two-dimensional electrophoresis gel (2-DE), but also in *shotgun* proteomics, when albumin and IgG were depleted. Thus, in the first test we performed, we compared the use or not of the albumin and IgG depletion column after the extraction process of the salivary proteins. For this, a *pool* of ten saliva samples was used.

Only 35 proteins were identified when the column was used. On the other hand, when the column was not employed, the number of proteins increased to 248. We believe that this occurred because when using the albumin and IgG depletion column, there was also the depletion of other proteins, since using the column increases one more process in the methodology and also, that many proteins could bind to albumin and IgGs, thus being depleted together. It is also noteworthy that among the identified proteins, in both situations, are proteins typically found in saliva. However, when the depletion column was employed, classical salivary proteins were not identified. Thus, contrarily to which was observed in gel-based proteomics (Krief, Deutsch et al. 2011),

in *shotgun* proteomics the use of albumin and IgG depletion column impaired protein identification according to our workflow. Some studies, however, report advantages in using depletion columns when more than one workflow is employed (Sivadasan, Gupta et al. 2015). However, the time and cost of the analysis are increases.

After the first test, in the subsequent one, we compared analysis of pooled samples (from ten individuals) *versus* individual analysis, without using the depletion column. In the individual analysis, 239 proteins were identified, while 212 proteins were identified in the pooled sample. One-hundred and twenty-three proteins were common to both groups and among them are most of the proteins typically found in saliva. The proteins exclusively found in the individual sample or in the pooled sample are proteins not typically reported in saliva, which might be related to individual variation. It should be noted that especially in quantitative *shotgun* proteomics the analysis of individual samples is important, to allow confident comparison among the groups under study. Therefore, the use of depletion columns is not necessary.

Regarding the identification of proteins in the AEP, one of the biggest issues is the analysis of pooled samples. In this sense, an *in vitro* protocol was carried out to identify the best method of collection of AEP and to standardize a new *in vitro* protocol for future studies. The proteomic analysis of AEP formed *in vitro* is an important tool in pre-clinical studies, since it allows preliminary evaluation of preventive agents for dental caries and dental erosion. In addition, in *in vitro* studies it is possible to recover the enamel specimens over which the AEP is formed to be submitted to distinct tests, which is not feasible *in vivo*. However, when our study was conducted, there was only one study in which the proteomic profile of the AEP formed *in vitro* had been evaluated (Siqueira, Custodio et al. 2012). In this sense, our main aim was to develop *an in vitro* protocol of AEP formation using different solutions previously described in the literature to collect AEP proteins for *shotgun* proteomic analysis.

The main reason for this scarcity of studies is the small amount of proteins that can be recovered from the *in vitro* formed AEP. In the *in vivo* condition, the AEP is formed under continuous salivary flow, which does not happen *in vitro*. In order to overcome this, in the present study we replaced the saliva in which the specimens were immersed every 30 min during the 2-h period of AEP formation. This procedure was successful for an *in vitro* study, since it allowed recovery of ~ 30 µg of proteins that is enough for proper proteomic analysis. Despite refreshing saliva every 30 min

increased the total amount of recovered proteins, it is possible that the solution used to collect the AEP proteins can also influence this amount.

To date, most of the studies available in the literature employ 3% citric acid (CA) for collecting the acquired pellicle (Vitorino, Calheiros-Lobo et al. 2007, Siqueira, Bakkal et al. 2012, Siqueira, Custodio et al. 2012, Delecrode, Siqueira et al. 2015, de Souza, da Silva Ventura et al. 2017, Ventura, Cassiano et al. 2017, Cassiano, Ventura et al. 2018, Taira, Ventura et al. 2018, Martini, Rios et al. 2019). However, in these studies, the proteins collected from 8-10 volunteers are pooled in order to obtain enough amount of proteins to be analyzed by mass spectrometry, i.e., it is not possible to perform individual analysis. More recently, the pellicle proteins formed on ceramic specimens *in situ* were eluted by incubation in TRIS-HCl buffer containing SDS, followed by ultrasonication in RIPA-buffer. This procedure allowed analysis of individual samples with high inter-individual and inter-day consistency (Delius, Trautmann et al. 2017). However, it cannot be done *in vivo*, due to the necessity of sonication and also to the toxicity of the detergents employed. SDS has been employed to collection AEP proteins *in vivo* in order to perform immunoblotting analysis (Mutahar, O'Toole et al. 2017). Since SDS is biocompatible and can be used to collected AEP proteins *in vivo*, we evaluated both 3% citric acid and 0.5% SDS, alone or in combination, in order to develop a method of collection of AEP proteins that results in large amount of proteins and can be employed in different protocols (*in vitro, in situ* and *in vivo*).

The obtained results indicate that the amount of proteins (ranging between 26 and 33 µg) recovered when these solutions were used was satisfactory, especially considering an *in vitro* study. Moreover, among the 55 proteins identified in all groups, 15 are common to all of them, most of which are classical players of the AEP. It could be expected that the combinations CA + SDS or SDS + CA could increase the total number of identified proteins, in comparison to CA or SDS only, since the acid and the detergent could be expected to remove different proteins of the AEP. However, this was not the case. It is also important to consider the quality of the identified proteins. Mucin, included among the pellicle precursors (Siqueira, Custodio et al. 2012) and associated with lubrication (Hannig and Joiner 2006) and protection against erosive challenges (Jordao, Ionta et al. 2017) was only identified in the CA and CA + SDS groups. This means that the use of SDS first might not remove this protein. Moreover, Enamelin, a typical enamel protein (UNIPROT), was identified only in the CA + SDS

group, indicating that this combination might remove a layer of enamel. Thus, 3% citric acid is, among the tested solutions, the best one to remove AEP proteins for *shotgun* proteomic analysis.

In this sense, with the standardized protocols, *shotgun* proteomic analyses of unstimulated saliva, stimulated saliva and AEP were performed from different periods of patients with HNC treated with radiotherapy and in healthy patients.

Radiotherapy is a therapeutic modality that uses ionizing radiations with the objective of destroying the neoplastic cells, aiming at a reduction or disappearance of the malignant neoplasia (Van De Wiele, Signore et al. 2001). However, in the case of patients with HNC, the salivary glands are the most affected mainly because they are present in the irradiated field (Zago 2006).

The reduction in the salivary flow during radiotherapy treatment in patients with HNC is well known. Due to the radiation received in the head and neck region, organs such as the salivary glands can be affected, causing irreversible tissue damage in some situations (Jasmer, Gilman et al. 2020). Due to the reduction in the salivary flow, the quality of life of these patients is reduced, since saliva is an important fluid for the homeostasis of the oral cavity (Buzalaf, Hannas et al. 2012), besides being considered an important source of biomarkers (Wang, Kaczor-Urbanowicz et al. 2017, Buzalaf, Ortiz et al. 2020) and being the main source of proteins for the formation of the AEP (Buzalaf, Hannas et al. 2012). Because its collection is noninvasive, its processing is considered simpler (but accurate) and does not cause discomfort to the patient, as in blood collection, for example. Thus, this fluid has great biological and clinical interest.

Among the cancer patients that have possibilities of cure (45-50%), nearly 70% receive radiotherapy, which is the most employed non-surgical treatment for cancer patients (Van De Wiele, Signore et al. 2001). Saliva has several functions that are essential to the homeostasis of the oral cavity and most of these functions are played by proteins (Buzalaf, Hannas et al. 2012). Therefore, profound alterations in the proteomic profile of saliva are expected during and after radiotherapy, which could impact in the quality of life of HNC patients. This is the first study to report the protein changes in the unstimulated saliva, in the stimulated saliva (and its comparisons) and in the AEP of HNC patients along radiotherapy. For this purpose, unstimulated saliva, stimulated saliva and AEP were collected from the same HNC patients before, during and after radiotherapy, as well as from healthy donors.

There was a remarkable reduction in the salivary flow DRT (2-5 weeks of treatment), of around 65% compared with BRT, which was reduced to around 10% of BRT values ART (3-4 months after radiotherapy). This is consistent with the literature (Shannon, Starcke et al. 1977, Dirix, Nuyts et al. 2006). The mechanism underlying salivary hypofunction after radiotherapy is not precisely known so far, despite the loss of acinar cells and disturbance in water secretion mediated by muscarinic receptors have been proposed (Vissink, Mitchell et al. 2010). In the unstimulated saliva, we found remarkably higher numbers of unique proteins in the DRT and ART groups (286 and 395 proteins, respectively) that presented the lower salivary flows (means of 0.17 and 0.06 mL/min, respectively). One possible explanation for these expressive numbers of unique proteins could be the dramatic decrease in salivary flow induced by radiotherapy, thus increasing the protein concentration in saliva. However, the total amounts of proteins found in the conditions BRT, DRT and ART were very similar in our study. In fact, the literature is contradictory regarding the protein concentration in saliva in function of irradiation. Some studies report an increase in total protein concentration (Cowman, Baron et al. 1983, Makkonen, Tenovuo et al. 1986, Funegard, Franzen et al. 1994), while another one did not find changes in this parameter during radiotherapy (Anderson, Izutsu et al. 1981). It should be noted that in all the above-mentioned studies stimulated saliva was collected, mostly from the parotid gland, while in the present study we collected whole unstimulated saliva, which makes it difficult the direct comparison of the results. All unique proteins found DRT and ART are intracellular proteins that most likely originate from the oral mucosa and are not secreted by the salivary glands. This might happen because of mucosal ulceration since the oral mucosa becomes dry and atrophic due to the poor lubrication in the function of the reduced salivary flow (Vissink, Jansma et al. 2003).

We could see an increase in several proteins such as cystatins, lysozyme, alpha-amylases and isoforms of PRPs that are typically described in saliva in the HNC patients BRT when compared with healthy patients. These expressive increases could be attributed to alterations provoked by the cancer itself.

Remarkable changes in the differential protein expression were found upon radiotherapy. Proteins with well-known functions in saliva, such as *Alpha-amylase 1* and *2B, Cystatins SN, S* and *SA*, as well as several isoforms of PRPs (both basic and acidic), were reduced BRT in comparison with DRT. The decrease in acidic PRPs is consistent with previous findings (Hannig, Dounis et al. 2006). The balance among

the different acidic PRPs in the saliva is closely related to microbial adhesion to the tooth structure (Stenudd, Nordlund et al. 2001). Thus, a reduction in acidic PRPs might impair the maintenance of oral health in irradiated patients.

On the other hand, DRT, *Lactotransferrin* was increased more than 7-fold in comparison with BRT. These findings are consistent with previous studies of increased *Lactotransferrin* levels in saliva not only during (Makkonen, Tenovuo et al. 1986), but also 3 to 6 months after radiotherapy (Richards, Hurley et al. 2017). *Lactotransferrin*, an important multifunctional iron-binding protein, is well-known for its antimicrobial activity, which includes both bacteriostasis due to its ability to sequester free iron, inhibiting the microbial growth, as well as direct bactericidal properties that lead to lipopolysaccharide release from the bacterial outer membrane (UNIPROT). The increase is beneficial to irradiated patients since *Lactotransferrin* has a radioprotective effect on salivary glands (Nishimura, Homma-Takeda et al. 2014). This is related to its action on cell proliferation and cell-cycle progression, affecting acinar cell structure and function after irradiation, suggesting that supplementation with this protein is as a good alternative to prevent irradiation effects in salivary glands (Sakai, Matsushita et al. 2017).

Cystatin-B, another protein with important functions in saliva and cancer progression was more than 3-fold increased DRT compared with BRT. Cystatins are reversible inhibitors of cysteine peptidases (Bobek and Levine 1992), which during carcinogenesis were found in the tumor microenvironment and they are related to proliferation, metastasis and invasion of tumor cells through the degradation of the extracellular matrix, cell suppression, extracellular interactions, in addition to the promotion of angiogenesis (Petushkova, Savvateeva et al. 2019). In addition, *Cystatin-B* has antibacterial function (Xiao, Hu et al. 2010) and is increased in the AEP under erosive and cariogenic challenges (Delecrode, Siqueira et al. 2015). Thus, the increase of *Cystatin-B* in saliva may not only be an indicator of the success of radiotherapy to fight the tumor, but also may have a protective effect against dental caries and erosion.

On the other hand*, Cystatin-B* is present in squamous mucous epithelia and has also been identified in extracellular fluids, such as urine in patients with bladder cancer (Feldman, Banyard et al. 2009). It is important to mention also that *Cystatin-B* and proline-rich proteins have been reported to be components of the cornified cell envelope of epidermal keratinocytes, a layer of isodipeptide-crosslinked proteins and disulfide bonds. In addition, the identification of *Cystatin-B* and -*S* proteins, which are

mainly of intracellular origin and represent the main constituents of the envelope of cornified cells may be an indication of inflammation of the mucosal epithelia (Manconi, Liori et al. 2017).

Among the proteins that were increased DRT compared with BRT was *D (2) dopamine receptor (D2R; 6-fold increase)*. This receptor is coupled to protein G and its activation inhibits adenylate cyclase-mediated cAMP production (Missale, Nash et al. 1998). D2R signaling contributes to the proliferation and maintenance of some cancer cells (Sachlos, Risueno et al. 2012). Its increase DRT might be related to cell lysis (both of acinar cells and mucosal cells) DRT, which is in-line with the increase in 7 isoforms of actin, as well as with damage to the cytoskeleton, which was the most affected process DRT. The same rationale could be applied for *Alpha-enolase* (ENO-1) that presented the highest increase in the present study DRT compared with BRT (36-fold). Besides its well-known classical action in the glycolytic pathway, this enzyme is now included among the “moonlighting” proteins, i.e., it has important functions in several cellular processes not related to its classical function in glycolysis (Kim and Dang 2005, Jung, Kim et al. 2014). It is reported that cell-surface enolase acts as a receptor for plasminogen that is activated upon binding to alpha-enolase (Miles, Dahlberg et al. 1991), increasing cancer cell invasion and metastasis (Dano, Behrendt et al. 2005).

For the comparison between the salivary flows, stimulated saliva and unstimulated saliva were compare quantitatively. Although the objective was not to compare the flows of the different groups, but to compare the stimulated and unstimulated salivary within the same group at this moment, it was possible to verify that BRT, the mean salivary flow falls within the normal range (> 1 mL/min and > 0.4 mL/min for stimulated and unstimulated flows, respectively) (Dawes 1987, Dawes 2004, Paim, Berbert et al. 2019), despite having a tendency of reduction when compared to the salivary flow values of healthy patients. However, when the patients undergo radiotherapy (DRT), the difference between stimulated and unstimulated salivary flows is not significant, which also occurs after radiotherapy treatment (ART). Thus, our data show that the reduction in salivary flow during and after radiotherapy occurs both in stimulated and unstimulated salivary flows. For this reason, therapeutic alternatives to increase salivary flow are prescribed to these patients, to stimulate salivary flow (Paim, Berbert et al. 2019).

Although we did not see any differences regarding the comparison in mL/min of salivary flows during and after treatment, in the proteomic analysis important proteins were differently expressed when we performed comparative and quantitative analyses of stimulated and unstimulated salivary flows in the different periods.

Firstly, in relation to the control group, acid-resistant proteins such as PRPs and *Statherin* (almost 4-fold decrease) (UNIPROT) were decreased in stimulated salivary flow in comparison to unstimulated salivary flow. Moreover, *Lysozyme C* and isoforms of immunoglobulin were identified exclusively in unstimulated salivary flow. On the other hand, proteins such as amylases, *Cystatin-SA*, albumin and *Histatin-1* were increased in the stimulated salivary flow in healthy patients. Histatins have several functions such as buffering, modulation of mineral formation, as well as potent antifungal and antibacterial activities (Siqueira, Lee et al. 2012). In addition, isoforms of hemoglobin and *Cystatin-B*, which are considered acid-resistant proteins, were identified exclusively in the stimulated salivavy flow in the control group. Hemoglobin is increased in the AEP and in saliva of patients suffering from gastroesophageal reflux who have a lower degree of erosive tooth wear (Martini, Rios et al. 2019, Martini, Rios et al. 2020).

Matrin-3 suppresses tumorigenicity, induces cell death by apoptosis and inhibits the migration and invasion of basal-type in breast cancer cells. Thus, analysis of this protein offers the possibility to predict the aggressiveness and metastatic potential of breast cancer and patient's survival (Yang, Lee et al. 2020). *Matrin-3* was identified exclusively BRT in the unstimulated salivary flow. Therefore, perhaps this protein can play an important role as a prognostic biomarker for HNC as well, which should be evaluated in future studies. In addition, proteins involved with oral health homeostasis such as amylases, hemoglobins, immunoglobulins, albumin, PRPs (basic and acidic), *Histatin-1*, *Statherin* and several isoforms of cystatins (B, C, S, A and SN) were decreased in the stimulated saliva BRT. Moreover, *Lactotransferrin*, *Mucin-7* and several immunoglobulins were also identified exclusively in the unstimulated saliva BRT.

In the comparison between stimulated saliva and unstilumated saliva DRT, *Lactotransferrin, Prolactin-inducible protein, Submaxillary gland androgen-regulated protein 3B, Protein S100-A9, Cystatin-B, -S, -SA, -SN*, as well as isoforms of amylases, keratins, albumins and immunoglobulins were decreased in stimulated salivary flow compared to unstimulated one. Regarding the unique proteins identified, *A disintegrin*

and metalloproteinase with thrombospondin motifs 12, A disintegrin and metalloproteinase with thrombospondin motifs 1, Apoptosis-resistant E3 ubiquitin protein ligase, 2 isoforms of 14-3-3 proteins and histones that are involved in processes of apoptosis (UNIPROT) and hemoglobins, immunoglobulins, *Lyzosyme C* and *Mucin-7*, were identified exclusively in the unstimulated salivary flow DRT. Among the exclusive proteins, *Mucin-7* works as a protection in the humoral antimicrobial immune response, promoting the elimination of bacteria in the oral cavity and assisting in chewing, speech and swallowing (UNIPROT) (Crosara, Zuanazzi et al. 2018).

Important proteins involved with apoptotic processes (UNIPROT) such as *Clusterin, Calpain-3, Lymphoid enhancer-binding factor 1 and Complement C3* and also, isoforms of hemoglobins, *Cystatin-C, Mucin-7*, isoforms of 14-3-3 protein (that is involved with deacetylation of histones) (Jain, Janning et al. 2020) and *A disintegrin and metalloproteinase with thrombospondin motifs 9* (involved with angiogenesis) (Tokuhara, Santesso et al. 2019) were identified exclusively in the unstimulated salivary flow in comparison to stimulated salivary flow ART.

On the other hand, ART, *Mucin-20* was identified exclusively in the stimulated salivary flow. *Mucin-20* is a transmembrane glycoprotein secreted by the epithelium and is largely overexpressed in epithelial tumor cells. It is a molecular biomarker for the prognosis of some epithelial tumors and squamous cell carcinoma of the esophagus in patients who received neoadjuvant chemotherapy followed by surgery (Wang, Shen et al. 2015). However, important proteins involved in the formation of the AEP and that are directly linked with the homeostasis of oral health (*Lysozyme C, Lactotrasnferrin*, PRPs, hemoglobin, cistatins (B, SN and S), several immunoglobulins and albumins) (Vukosavljevic, Custodio et al. 2014) were decreased in stimulated saliva in comparison with unstimulated saliva ART.

It is worth mentioning that in the different periods (BRT, DRT and ART), isoforms of amylases, albumins, immunoglobulins, PRPs, cystatins, which have important functions in the oral cavity, were decreased in the stimulated salivary flow when compared to the unstimulated salivary one.

Among the proteins identified, isoforms of keratin caught our attention. In the different comparisons of salivary flows for the healthy patients and before radiotherapy (BRT), this protein was not identified. However, when the stimulated and unstimulated salivas of the group DRT were quantitatively compared, two isoforms of the keratin protein were increased in the stimulated salivary flow, but 11 isoforms were decreased.

In addition, 4 keratin isoforms were identified exclusively in unstimulated saliva DRT. Also, 19 isoforms of keratin were identified exclusively in the unstimulated saliva and none isoform was identified in the stimulated saliva ART. Thus, the isoforms identified only in these groups can be related to the radiotherapy treatment. Due to this, we constructed interaction networks for these proteins using the String tool. In the network, it was possible to observe that these proteins have protein-protein interactions and are related to cornification processes. This process was also observed in the functional analysis of the most affected processes in the DRT group with 25.5% (Fig. 4, article 4). The cornification process is involved with programmed cell death that occurs in the epidermis, morphologically and biochemically unlike apoptosis processes. This leads to the formation of corneocytes, that is, dead keratinocytes that are necessary for the function of the cornified skin layer, such as mechanical resistance, elasticity, water repellency and structural stability (Eckhart, Lippens et al. 2013).

Thus, we raise the hypothesis that the unstimulated salivary flow might be the most appropriate fluid when it is intended to identify possible prognostic biomarkers in saliva. We cannot forget to mention that, although the two isoforms of the keratin protein are increased in the stimulated salivary flow DRT, the *Keratin_ type II cytoskeletal 6A* is also involved with wound healing and repair processes (UNIPROT). Thus, we believe that the increase in this protein may be related to the laser therapy treatments to which these patients were submitted, since episodes of mucositis are frequent due to radiation.

Considering that unstimulated saliva might have a better potential as a source for biomarkers, isoforms of histones that are involved with processes of DNA methylation, the main epigenetic mechanisms to memory and cellular identity, influencing the cellular microenvironment (Blancafort, Jin et al. 2013), were identified exclusively in unstimulated saliva DRT (19 isoforms) and ART (24 isoforms) (Tables S1 and S2; article 4). In the AEP of patients with HNC, the identification and increase of histones ART have already been reported (Ventura, Ribeiro et al. 2021). *Histone-lysine N-methyltransferase MECOM* that is involved with the regulation of the cell cycle and apoptotic process (UNIPROT) was identified in both groups. However, this protein was reduced in the stimulated saliva when compared to the unstimulated saliva. This provides additional support to our hypothesis that unstimulated salivary flow might be a better source of tumor and apoptotic biomarkers.

Taken together, our data suggest that future studies involving the search for biomarkers, should employ unstimulated saliva. In addition, stimulating salivary flow in cancer patients undergoing radiotherapy seems to reduce proteins involved with antibacterial and acid-resistant protection. On the other hand, however, we cannot forget to mention the importance of saliva in lubricating and increasing the quality of life of these patients.

For the proteomics analysis of AEP, this is the first study in which the analyses were done in biological triplicate. In the previous studies by our group, AEP samples from 8-10 volunteers were combined into one single *pool,* as mentioned above, which is not ideal since it does not contemplate the biological variation (Ventura, Cassiano et al. 2017, Taira, Ventura et al. 2018, Martini, Rios et al. 2019). The total amount of recovered AEP proteins ranged from 30 to 62 µg for each pool, considering the distinct groups under study. For the quantitative analyses, all samples were adjusted to 30 µg. A total of 204 proteins were identified, showing that the methodology was satisfactory. In addition, it is also important to consider the quality of the proteins identified, since the proteins classically described in the acquired pellicle were all identified. This analysis in biological triplicates represents a major advance for the research involving proteomic analysis of the AEP *in vivo*, since there is much questioning regarding the limitation of the data when the biological variability is not taken into account. Another differential of this study was that the collections of the AEP were performed from the same patients, thus making them their own controls when the treatment periods were compared to each other.

In the literature it is shown that due to radiotherapy, there is a great reduction of the salivary flow due to the radiation suffered in this region (O'Connell 2000), which was confirmed when we measured the unstimulated salivary flow of our patients. It should be highlighted that even BRT, HNC patients had lower salivary flow compared with healthy controls. This is in-line with a previous study where the unstimulated flow was evaluated before and after treatment in HNC patients (Lal, Bajpai et al. 2010), showing a reduction in the flow before the treatment. However, it must be highlighted that despite the mean unstimulated salivary flow of HNC patients BRT (0.49 mL/min) was lower than that found for healthy controls, it still falls within the normal ranges (Dawes 2004). Considering that saliva is the major contributor for the proteins found in the AEP (Siqueira, Custodio et al. 2012), profound changes in the AEP proteome could be expected due to the reduction of the salivary flow, what was confirmed in our study.

Cystatin-S was decresead BRT when patients with HNC were compared to healthy patients (BRT vs Control). The reduced expression of this protein in saliva is related to decreased salivary flow as well as dysfunctions in the salivary glands, especially the submandibular gland, in which the protein is secreted (Martini, Gallo et al. 2017). It should be highlighted that the mean salivary flow of BRT patients was 0.49 mL/min *versus* 0.89 mL/min in healthy controls. Still in relation to this comparison, 20 proteins were increased BRT in comparison with the healthy patients. Among them are *Zinc-alpha-glycoprotein* protein, which is involved with immune response, wound healing and protection of the mucosa (Crosara, Zuanazzi et al. 2018), as well as *Prolactin-inducible protein*, related to immune system responses and involved with the perception of bitter taste, besides being present in pathological conditions of the salivary gland (UNIPROT) (Hassan, Waheed et al. 2009). Also increased BRT were *Alpha-amylase 1* and *2B*, which come from the parotid gland and are considered a biochemical indicator for salivary gland injury (Becciolini, Porciani et al. 1994), in addition to being increased in psychological stress conditions (Engert, Vogel et al. 2011, Obayashi 2013, Crosara, Zuanazzi et al. 2018, Ma, Wan et al. 2018). They also interact with several proteins in whole saliva, most of them presenting host protection properties (Crosara, Zuanazzi et al. 2018). Another increased protein in the BRT group was *Mucin-7* that participates in essential processes for mucosa protection, wound healing and immune response (UNIPROT) (Crosara, Zuanazzi et al. 2018). Moreover, the increase in mucins is related to the characterization of the saliva of these patients as sticky and thick. With the decrease in water, due to the reduction in the salivary flow, this protein becomes more concentrated in saliva and is adsorbed to a greater degree in the AEP of these patients.

To verify whether the protein profile of the AEP of the HNC patients could be restored after radiotherapy treatment, the important comparison (BRT *vs* ART) was undertaken. We observed that 20 proteins were increased and *Alpha-amylase 1*, related to episodes of great psychological stress, as mentioned above, was decreased BRT compared to ART. Therefore, considering that these patients had already undergone the process of treatment with radiotherapy, we believe that its decrease is also related to the decrease in stress in function of the completion of the treatment. It has been reported that radiotherapy not only causes physical injury, but also psychological and social damage (Paula, Sonobe et al. 2012, Cruz, Ferreira et al. 2016). Among the increased proteins, we would like to highlight those that were

increased more than 2-fold, such as *S100-A8,* related to immune system responses and regulation of inflammation (UNIPROT) (Crosara, Zuanazzi et al. 2018), *Lactotransferrin* and 17 isoforms of Histone, which caught our attention. Therefore, interaction networks were carried out from the STRING database in order to verify the possible interactions of these proteins considered in this differential expression (ART *vs* BRT). We found that these Histones proteins bind together, in addition to making secondary bindings with other proteins identified in these groups, such as *Lactrotransferrin*, involved with innate immune response to the mucosa (STRING) (Fig. 6, article 5). DRT, patients have episodes of mucositis due to damage to the oral mucosa, so we believe that the increase in these proteins is an attempt to reestablish the injured mucosa of these patients after treatment.

ART, the increase in histones is involved with DNA methylation. Histones interact with histone acetyltransferases (HATS), implicated with histone modifications (STRING). DNA methylation is involved with the main epigenetic mechanisms, which are related to memory and cellular identity, influencing the cellular microenvironment. The epigenetic regulation of gene expression is mainly controlled by DNA methylation, action of non-coding RNAs and modification of histones (Blancafort, Jin et al. 2013). Among the various types of modifications in histones, acetylation is characterized by playing an important role in the modulation of gene expression acting in the control of the cell cycle, in addition to participating in the development and progression of neoplasms (Zupkovitz, Tischler et al. 2006, Moore, Le et al. 2013). Histone acetylation is performed from enzymes called acetyltransferases that add acetyl radicals to the lysine residues of histone proteins, leading to chromatin decompression and transcriptional activity (Moore, Le et al. 2013).

Histones that play important roles in chromatin processes that allow DNA transcription, replication and repair are H2B and H2A. In general, histones H2A and H2B form octamers with histones H3 and H4 and are involved in packaging DNA into nucleosomes (Nag, Kyriss et al. 2010, Ransom, Dennehey et al. 2010, Kari, Shchebet et al. 2011, Sadeghi, Siggens et al. 2014, Mao, Kyriss et al. 2016, Li, Tian et al. 2017). Based on gene expression profile data, the increased expression of histone variants is a strong prognostic biomarker in patients with cervical cancer (Li, Tian et al. 2017). These measurements of histone expression can help select cervical cancer patients who can benefit from radiotherapy. Besides, they suggest that two sets of histone-variant genes (Histone H2B type 1-D, -J and -H; Histone H2A type 1-M and

Histone H4-K) may be independent prognostic factors for better survival in patients with cervical cancer (Li, Tian et al. 2017). In the comparison ART *vs* BRT, all these isoforms of histones, except histone H4-K, were increased ART in the present study, indicating that the AEP can be used as a prognostic marker for HNC.

In addition, the *Modulator of apoptosis 1 protein* (MOAP-1) plays important role in cell death or apoptosis and it was identified exclusively ART when compared to BRT. Overexpression of MOAP-1 in several cancer cell lines resulted in the reduction of tumorigenesis and in the positive regulation of genes involved in the control of DNA damage and in cancer regulatory pathways that include apoptosis (Law, Salla et al. 2015). Besides, MOAP-1 expression levels appear to be regulated by mRNA control and ubiquitination (Tan, Fu et al. 2005). Therefore, MOAP-1 can exert its tumor-suppressing function through involvement in apoptosis (Baksh, Tommasi et al. 2005, Foley, Freedman et al. 2008). This finding is of great importance and reinforces the analysis of the AEP as a prognostic marker to evaluate efficacy of the radiotherapy treatment. These findings should be evaluated in future studies.

On the other hand, DRT, various isoforms of hemoglobins, *Haptoglobin* and *Apolipoprotein 1* that are serum proteins originating mainly from the gingival crevicular fluid had a pronounced (more than twice) increase in the AEP*.* This can be explained by the reduction of salivary flow. Under conditions of normal salivary flow, the main source of proteins for the pellicle is saliva, since it contains several proteins with high capacity of adsorption to hydroxyapatite (Heller, Helmerhorst et al. 2017). Radiotherapy causes a reduction of the salivary flow, thus favoring the serum proteins from the gingival fluid (Heller, Helmerhorst et al. 2017), leading to their adsorption to a greater extent. However, Statherin showed the greatest increase (nearly 10-fold) in expression DRT, compared to BRT. This protein is derived from the secretions of parotid and submandibular glands (Oppenheim, Hay et al. 1987), but it has already been identified in samples of the gingival fluid (Pisano, Cabras et al. 2005). Nevertheless, the authors themselves question whether its origin would be even the serum or whether its presence in samples collected from the gingival fluid would be due to its presence in the acquired pellicle located near the gingival margin. As a consequence of the reduction in the salivary flow DRT, Statherin becomes more concentrated in saliva (due to the decrease in the water content in saliva) and due to its high binding force to hydroxyapatite, adsorbs to a greater degree onto enamel.

We highlight proteins that have important functions have such as antibacterial, antifungal, as well as acid-resistant functions (UNIPROT). Among them are immunoglobulins, cystatins, *Lactotransferrin, Neutrophil defensins 1* and *3*, *Histatin-1* isoforms of proline-rich proteins (*Proline-rich protein 4, Salivary acidic proline-rich phosphoprotein ½ and Submaxillary gland androgen-regulated protein 3B*) that were among the decreased proteins DRT. Their decrease in the AEP of these patients DRT explains the damage to the teeth, not only due to the decrease in the salivary flow, but also due to the decrease in these protective proteins in the AEP, leaving these patients more susceptible to the development of caries and erosive tooth wear.

Due to the great biological interest in the DRT *vs* BRT comparison, analyzes of the most affected processes were carried out based on the proteins identified in this comparison. Regarding the biological process, 37% of the proteins with dfferential expression in this comparison are involved with the humoral antimicrobial response and 9% are involved with the sensory perception of bitter taste, which is commonly reported by these patients. In relation to the processes of molecular function, we highlight that 25% of these proteins are involved with binding to hemoglobin protein, which was seen previously since during DRT there was a more than 5-fold increase in these proteins. We believe that this is due to damage to the mucosa, with consequent mucositis generated due to treatment.

It is important to mention that all patients presented mucositis during the treatment and all underwent laser therapy. We believe that this may be a limitation of our study, however due to the debility profile of these patients, it would not be ethical to deprive them of this important therapy for the recovery of the mucosa. This information becomes extremely important since when the processes involved with the cellular component were analyzed in the comparison BRT *vs* DRT, we observed that 10% of these proteins were involved with an immunoglobulin A complex. This antibody is secreted in the saliva and is present when dysfunctions occur in the mucous membranes of some organs, such as the mouth. IgA plays a key role in defending mucosal surfaces against attack by infectious microorganisms (de Sousa-Pereira and Woof 2019), so we believe that the laser therapy increased the proteins involved with immunoglobulin A, in order to restore and protect the mucosa of these patients.

Finally, we also performed the functional analysis of the immune system process in the comparison DRT *vs* BRT (Fig. 2, article 5) and of the biological processes of the ART *vs* BRT groups (Fig. 3, article 5). We observed that 4% of these

proteins are involved with protein localization to bicellular tight junction. This process is involved with functional intercellular structures that are present mainly in the epithelial and endothelial cells of all tissues and organs. Moreover, due to their well-recognized roles in maintaining cell polarity and barrier functions, these structures are important regulators of signal transduction, which modulate cell proliferation, migration and differentiation, as well as some components of the immune response, homeostasis, besides developing a role for effective wound healing (Shi, Barakat et al. 2018). Therefore, a more complete understanding of these structures can provide better strategies to increase the regeneration of the oral mucosa and improve mucosal repair resulting from radiotherapy, but also to understand the cancer healing processes resulting from treatment. Altogether, based on our results, both null hypotheses were rejected.

As described above, from the analysis of the protein profile of the AEP, we observed that DRT there was a pronounced increase in the statherin (nearly 10-fold increase) in these patients. Thus, we decided evaluated the protective effect of different times of AEP formation *in vitro*, as well as to verify the effect of pre-treatment with Statherin peptide for a possible beneficial effect of the AEP's protective effect against initial dental erosion, since it can happen in cancer patients (Lajer, Buchwald et al. 2009, Jensdottir, Buchwald et al. 2013, Lieshout and Bots 2014), and also thinking about a possible future dental product more targeted at patients with HNC treated with radiotherapy. It is important to emphasize that this is the first study to use native (human) enamel with this goal. For this analysis, the Reflectometer Optipen (Rakhmatullina, Bossen et al. 2013) was used. The device has a fiber-optic design with a measurement head of 15 mm to ensure access to all positions. The pen-like shape provides an easy and light handling. Moreover, a software was created to provide fast and easy signal read-out, contributing to a reduction in analysis time. This pen-like device has been successfully employed to evaluate erosion *in vitro* (Carvalho, Baumann et al. 2016, Carvalho, Baumann et al. 2016). The results obtained with the hand-held reflectometer correlate well with surface hardness and calcium release measurements when erosion is evaluated (Carvalho, Baumann et al. 2016) and have potential clinical application. In addition, calcium analysis was also done by atomic absorption spectrometer.

Regarding the AEP formation, it begins with a basal layer made up of acid-resistant precursor proteins, such as acidic proline-rich proteins (PRPs), histatins and

statherin (Ash, Ridout et al. 2013). The thickness of the AEP can change according to the time of its formation, where, after the formation of the basal layer, other proteins can interact with the precursor proteins (Vukosavljevic, Custodio et al. 2014) maturing and modulating the AEP. Though some studies have shown that AEPs formed over 60 min can already offer a maximum protection against demineralization (Amaechi, Higham et al. 1999, Hannig, Hess et al. 2003, Wetton, Hughes et al. 2006), another study (Hannig, Fiebiger et al. 2004) have found that pellicles formed for shorter periods of time (e.g. 3 min), can already protect the teeth without difference from a pellicle formed for 120 min. In addition, the initial pellicle layer formed for 3 min can be physiologically functional even without further maturation (Trautmann, Kunzel et al. 2020). This protection, with such short-term AEP formation, can be attributed to the electron-dense basal layer (Hannig, Fiebiger et al. 2004, Trautmann, Kunzel et al. 2020). Since this layer is formed within seconds of exposure to saliva, even shorter AEP formation times might protect the native enamel surface against demineralization, which was confirmed by our study.

We observed that the *in vitro* AEP was able to protect enamel against erosion, even at very short formation times, from 1 min onwards. The presence of the AEP was able to reduce demineralization, presenting less rSRI loss. Interestingly, no differences were observed between the different AEP formation times, even after 120 min formation, which is considered to be the time necessary for the AEP to reach a mature state (Lendenmann, Grogan et al. 2000, Hannig and Joiner 2006). Our data is along the same lines as another *in situ* study, which also showed that a short pellicle formation time (3 min) was also protective, and there was no significant differences between longer (60 min and 120 min) formation times (Hannig, Fiebiger et al. 2004). This suggests that the basal layer of the AEP is the one responsible for providing protection against erosive attacks. Perhaps, future studies with the pellicle can greatly reduce the AEP formation times based on our results.

Though the SRI data suggest that longer AEP formation did not increase the protection against erosion, the calcium data seem show greater release for where the time of 120 min presented higher calcium release compared to the other formation times. Actually, the calcium results must be viewed bearing in mind that saliva (and the AEP) also contains calcium (Zhang, Cheng et al. 2016) and the pellicle was formed on the whole enamel specimen (even on the surfaces covered with the nail varnish), so the calcium results from our study include that released from the pellicle, and not that

only from the enamel. It is also known that longer AEP formation times allow for the maturation of the pellicle, increasing its thickness (Amaechi, Higham et al. 1999, Hannig and Balz 2001) and, thus, its calcium content (Ash, Ridout et al. 2013, Zeng, Zheng et al. 2019). So, the higher amounts of calcium present in the 120 min pellicle group could simply be calcium from the pellicle itself, and not from enamel. This, in turn, confirms the SRI results, where, despite the more mature pellicle after 120 min formation, the protection against demineralization was not improved.

Since statherin plays an important role on the formation of the basal layer (Raj, Johnsson et al. 1992, Santos, Kosoric et al. 2008, Ash, Ridout et al. 2013, Vukosavljevic, Custodio et al. 2014), it has already been identified as an acid-resistant protein (Yang, Yang et al. 2017, Taira, Ventura et al. 2018), and it was increased nearly 10-fold DRT, we decided to use the synthesized Statherin peptide for pellicle engineering. This peptide, named StatpSpS, consists of the 15 N-terminal amino acids of Statherin. Furthermore, serines are phosphorylated, as this has been shown to be important for the function of the peptide (Xiao, Karttunen et al. 2015), resulting in a sequence of DpSpSEEKFLRRIGRFG, where “p” means phosphorylation in serine residues at positions 2 and 3. StatpSpS has previously been shown to protect from erosion (Taira, Carvalho et al. 2020), which was confirmed in the present study, since by itself, it significantly protected enamel against erosion. Interestingly, when it was used to modify the AEP, there was no significant difference compared to unmodified AEP. We believe that this may be related to a competition between the StatpSpS and the salivary proteins when binding to the enamel specimen *in vitro*. Because the treatment with the StatpSpS was performed immediately prior to incubation in the saliva, the peptide can already bind to the enamel, over the entire enamel surface, leaving very few binding sites available for other salivary proteins to bind. So, when the AEP is formed, no further protection will be observed from the basal layer. However, if the AEP is formed alone, without pellicle engineering with the peptide, the Statherin protein from saliva itself will also bind to the enamel surface, providing a protection against erosion.

Remarkably, only the treatment with the StatpSpS was already sufficient to provide protection against acid attacks, which corroborates the fact that Statherin is an acid resistant protein (Vukosavljevic, Custodio et al. 2014, Yang, Yang et al. 2017, Taira, Ventura et al. 2018) and is able to strongly bind to the tooth surface. Again, the lack of significant differences between the groups with and without StatpSpS when the

AEP was present is suggestive of the fact that the protection from the AEP is mostly from its basal layer, probably from the Statherin protein coming from the saliva. This hypothesis is also confirmed when the No pellicle group was compared only with the StatpSpS No pellcile group, where even without the presence of AEP, the peptide acting alone was able to produce greater protection and higher SRI values. This, however, was not observed in the calcium results. But although we did not observe a significant difference between these groups in the calcium analysis, we must consider that the addition of the peptide may have influenced the release of calcium. A previous study suggests that peptide StatpSpS in this concentration (1.88×10^{-5}) may provide the best balance between the amount of adsorbed peptide and available free Ca^{2+} surrounding the hydroxyapatite surface (Taira, Carvalho et al. 2020). In this sense, some of the available Ca^{2+} may form complexes with proteins, and only the free Ca^{2+} is able to influence the demineralization process (Anderson, Hector et al. 2001). On the other hand, salivary proteins such as statherin maintain high concentrations of Ca^{2+} by binding to Ca^{2+} and forming structures similar to salivary micelles (Kosoric, Williams et al. 2007) or salivary layers enriched with Ca^{2+} (Proctor, Hamdan et al. 2005).

These data are of great value, since when thinking about a clinical application, treatment with the StatpSpS may be an alternative for patients who have a reduced salivary flow or patients who suffer from diseases that affect the salivary glands, such as patients treated with radiotherapy in the region of head and neck. Perhaps, the StatpSpS could improve the reduced erosion protection these patients suffer from because of their reduced salivary flow rate.

It is important to recognize that these *in vitro* results do not necessarily represent the true nature of the *in vivo* AEP, as there are other important factors for its formation in addition to saliva. However, our study provides strong evidence of how the pellicle can behave on native enamel surfaces and provide new perceptions for future *in vitro* studies, where pellicle formation times might be decreased. In addition, we cannot fail to mention that the grade of variation of the reflection intensity is due to the use of a native enamel surface. This surface is not polished, as customarily used in other studies, and it remains curved, thus influencing the reflectivity (Carvalho, Baumann et al. 2016). However, it is worth mentioning that the initial and final analyzes were carried out in the same place, so despite the variations, the changes occurring on that surface are still measured. Moreover, this higher variation of SRI values has already been observed in previous studies (Rakhmatullina, Bossen et al. 2013) and, notwithstanding

the variation, the reflectometer has been validated for erosive tooth wear studies in native enamel (Carvalho, Assuncao et al. 2016).

In summary, the protocol for salivary *shotgun* proteomic analysis was satisfactory, since it allowed the identification of a good number of proteins, including those typically found in saliva. Moreover, it is easy to perform and cheaper than methods previously described, since it does not require the use of depletion columns. The new technique developed by replaced of the saliva for the AEP formation *in vitro* was essential for a higher number of the proteins identified by proteomics analysis. In addition, 3% citric acid is, among the tested solutions, the best one to remove AEP proteins for *shotgun* proteomic analysis.

During and after radiotherapy there is a substantial increase in cellular proteins in saliva, not commonly reported in healthy patients. This is a consequence of cell lysis induced by radiotherapy in HNC patients. The high increase in alpha-enolase DRT compared with before in the unstimulated saliva reflects cell lysis induced by radiotherapy. In addition, DRT, *Scaffold attachment factor B1*, a protein related to the reduction in cell proliferation was increased more than 16-fold in comparison with DRT, indicating the beneficial effects of the therapy. These results suggest that monitoring alpha-enolase levels DRT in the unstimulated saliva might be a good indicative of the efficacy of the treatment, since high levels of this enzyme might indicate efficient cell lysis and this could be a possible strategy to predict the efficacy of the treatment, which should be evaluated in further studies.

There is a marked difference in the protein profile of stimulated and unstimulated salivary flows of patients with HNC treated by radiotherapy. This difference was observed before, during and after treatment, as well as in healthy patients. The unstimulated salivary flow seems to be the best alternative to search for biomarkers. In addition, saliva stimulation in patients with HNC decreases important proteins that participate in the oral health homeostasis, with antibacterial and acid-resistant properties. Moreover, we suggest the use of unstimulated saliva for future studies that search for salivary biomarkers.

HNC and radiotherapy remarkably altered the protein profile of the AEP. Antibacterial proteins were decreased during radiotherapy, which impacts systemic and oral health homeostasis. Moreover, some proteins identified in the AEP after radiotherapy, such as isoforms of histones and MOAP-1, may serve as prognostic markers for survival of HNC patients, which should be evaluated in further studies.

Regarding the AEP formation times and its engineering with StatpSpS, 1 min of AEP formed *in vitro* on native enamel can already provide erosion protection, and longer formation times do not improve its protective effect. In addition, the StatpSpS applied for 1 min provided similar enamel protection against erosion as the AEP, regardless of the time of formation.

Finally, our data contribute in an unprecedented way to a better understanding of the progressive changes in the salivary proteome and of the differential protective roles of the AEP proteins in HNC patients during radiotherapy. The present study provides important information for designing more effective dental products targeted to this group of patients, in order to improve their quality of life.

References

“Quando se ensina com amor, com amor também se aprende, e por amor se compartilha.”

Abilio Brunini

REFERENCES

Amaechi, B. T., S. M. Higham, W. M. Edgar and A. Milosevic (1999). "Thickness of acquired salivary pellicle as a determinant of the sites of dental erosion." Journal of Dental Research **78**(12): 1821-1828.

Amaechi, B. T., S. M. Higham, W. M. Edgar and A. Milosevic (1999). "Thickness of acquired salivary pellicle as a determinant of the sites of dental erosion." J Dent Res **78**(12): 1821-1828.

Anderson, M. W., K. T. Izutsu and J. C. Rice (1981). "Parotid-Gland Patho-Physiology after Mixed Gamma and Neutron-Irradiation of Cancer-Patients." Oral Surgery Oral Medicine Oral Pathology Oral Radiology and Endodontics **52**(5): 495-500.

Anderson, P., M. P. Hector and M. A. Rampersad (2001). "Critical pH in resting and stimulated whole saliva in groups of children and adults." Int J Paediatr Dent **11**(4): 266-273.

Antonadou, D., M. Pepelassi, M. Synodinou, M. Puglisi and N. Throuvalas (2002). "Prophylactic use of amifostine to prevent radiochemotherapy-induced mucositis and xerostomia in head-and-neck cancer." Int J Radiat Oncol Biol Phys **52**(3): 739-747.

Ash, A., M. J. Ridout, R. Parker, A. R. Mackie, G. R. Burnett and P. J. Wilde (2013). "Effect of calcium ions on in vitro pellicle formation from parotid and whole saliva." Colloids Surf B Biointerfaces **102**: 546-553.

Baksh, S., S. Tommasi, S. Fenton, V. C. Yu, L. M. Martins, G. P. Pfeifer, F. Latif, J. Downward and B. G. Neel (2005). "The tumor suppressor RASSF1A and MAP-1 link death receptor signaling to Bax conformational change and cell death." Mol Cell **18**(6): 637-650.

Becciolini, A., S. Porciani, A. Lanini, A. Benucci, A. Castagnoli and A. Pupi (1994). "Serum amylase and tissue polypeptide antigen as biochemical indicators of salivary gland injury during iodine-131 therapy." Eur J Nucl Med **21**(10): 1121-1125.

Blancafort, P., J. Jin and S. Frye (2013). "Writing and rewriting the epigenetic code of cancer cells: from engineered proteins to small molecules." Mol Pharmacol **83**(3): 563-576.

Bobek, L. A. and M. J. Levine (1992). "Cystatins - Inhibitors of Cysteine Proteinases." Critical Reviews in Oral Biology & Medicine **3**(4): 307-332.

Bray, F., J. Ferlay, I. Soerjomataram, R. L. Siegel, L. A. Torre and A. Jemal (2018). "Global cancer statistics 2018: GLOBOCAN estimates of incidence and mortality worldwide for 36 cancers in 185 countries." CA Cancer J Clin **68**(6): 394-424.

Buzalaf, M. A., A. R. Hannas and M. T. Kato (2012). "Saliva and dental erosion." J Appl Oral Sci **20**(5): 493-502.

Buzalaf, M. A. R., A. C. Ortiz, T. S. Carvalho, S. O. M. Fideles, T. T. Araujo, S. M. Moraes, N. R. Buzalaf and F. N. Reis (2020). "Saliva as a diagnostic tool for dental caries, periodontal disease and cancer: is there a need for more biomarkers?" Expert Rev Mol Diagn **20**(5): 543-555.

Carvalho, T. S., T. T. Araujo, T. M. O. Ventura, A. Dionizio, J. V. F. Camara, S. M. Moraes, V. T. Pela, T. Martini, J. C. Leme, A. L. B. Derbotolli, L. T. Grizzo, E. Crusca, P. Y. T. Shibao, R. Marchetto, F. Henrique-Silva, J. P. Pessan and M. A. R. Buzalaf (2020). "Acquired pellicle protein-based engineering protects against erosive demineralization." J Dent **102**: 103478.

Carvalho, T. S., C. M. Assuncao, F. Jost, W. B. Burgin, J. A. Rodrigues and A. Lussi (2016). "In vitro validation of a hand-held optical reflectometer to measure clinically observed erosive tooth wear." Lasers Med Sci **31**(6): 1105-1112.

Carvalho, T. S., T. Baumann and A. Lussi (2016). "Does erosion progress differently on teeth already presenting clinical signs of erosive tooth wear than on sound teeth? An in vitro pilot trial." BMC Oral Health **17**(1): 14.

Carvalho, T. S., T. Baumann and A. Lussi (2016). "A new hand-held optical reflectometer to measure enamel erosion: correlation with surface hardness and calcium release." Sci Rep **6**: 25259.

Cassiano, L. P. S., T. M. S. Ventura, C. M. S. Silva, A. L. Leite, A. C. Magalhaes, J. P. Pessan and M. A. R. Buzalaf (2018). "Protein Profile of the Acquired Enamel Pellicle after Rinsing with Whole Milk, Fat-Free Milk, and Water: An in vivo Study." Caries Res **52**(4): 288-296.

Chencharick, J. D. and K. L. Mossman (1983). "Nutritional consequences of the radiotherapy of head and neck cancer." Cancer **51**(5): 811-815.

Chow, L. Q. M. (2020). "Head and Neck Cancer." N Engl J Med **382**(1): 60-72.

Cowman, R. A., S. S. Baron, A. H. Glassman, M. E. Davis and A. M. Strosberg (1983). "Changes in Protein-Composition of Saliva from Radiation-Induced Xerostomia

Patients and Its Effect on Growth of Oral Streptococci." Journal of Dental Research **62**(3): 336-340.

Crosara, K. T. B., D. Zuanazzi, E. B. Moffa, Y. Xiao, M. Machado and W. L. Siqueira (2018). "Revealing the Amylase Interactome in Whole Saliva Using Proteomic Approaches." Biomed Res Int **2018**: 6346954.

Cruz, F. O., E. B. Ferreira, C. I. Vasques, L. R. Mata and P. E. Reis (2016). "Validation of an educative manual for patients with head and neck cancer submitted to radiation therapy." Rev Lat Am Enfermagem **24**.

Dandekar, M., V. Tuljapurkar, H. Dhar, A. Panwar and D. C. AK (2017). "Head and neck cancers in India." J Surg Oncol.

Dano, K., N. Behrendt, G. Hoyer-Hansen, M. Johnsen, L. R. Lund, M. Ploug and J. Romer (2005). "Plasminogen activation and cancer." Thrombosis and Haemostasis **93**(4): 676-681.

Davies, A. N., K. Broadley and D. Beighton (2002). "Salivary gland hypofunction in patients with advanced cancer." Oral Oncol **38**(7): 680-685.

Dawes, C. (1987). "Physiological factors affecting salivary flow rate, oral sugar clearance, and the sensation of dry mouth in man." J Dent Res **66 Spec No**: 648-653.

Dawes, C. (2004). "How much saliva is enough for avoidance of xerostomia?" Caries Research **38**(3): 236-240.

Dawes, C., G. N. Jenkins and C. H. Tongue (1963). "The nomenclature of the integuments of the enamel surface of the teeth." Brit Dent J **115**: 65-68.

de Oliveira, R. L., R. F. Dos Santos, S. H. de Carvalho, G. G. Agripino, M. M. Canto, M. de Vasconcelos Carvalho, S. A. Marinho, M. Gallottini and D. J. de Santana Sarmento (2017). "Prospective evaluation of quality of life in patients with head and neck cancer." Oral Surg Oral Med Oral Pathol Oral Radiol **123**(3): 350-357.

de Sousa-Pereira, P. and J. M. Woof (2019). "IgA: Structure, Function, and Developability." Antibodies (Basel) **8**(4).

de Souza, E. S. C. M., T. M. da Silva Ventura, L. de Pau, C. la Silva, A. de Lima Leite and M. A. R. Buzalaf (2017). "Effect of gels containing chlorhexidine or epigallocatechin-3-gallate on the protein composition of the acquired enamel pellicle." Arch Oral Biol **82**: 92-98.

Delecrode, T. R., W. L. Siqueira, F. C. Zaidan, M. R. Bellini, A. L. Leite, Y. Xiao, D. Rios, A. C. Magalhaes and M. A. Buzalaf (2015). "Exposure to acids changes the proteomic of acquired dentine pellicle." J Dent **43**(5): 583-588.

Delecrode, T. R., W. L. Siqueira, F. C. Zaidan, M. R. Bellini, E. B. Moffa, M. C. Mussi, Y. Xiao and M. A. Buzalaf (2015). "Identification of acid-resistant proteins in acquired enamel pellicle." J Dent **43**(12): 1470-1475.

Delius, J., S. Trautmann, G. Medard, B. Kuster, M. Hannig and T. Hofmann (2017). "Label-free quantitative proteome analysis of the surface-bound salivary pellicle." Colloids Surf B Biointerfaces **152**: 68-76.

Dirix, P., S. Nuyts and W. Van den Bogaert (2006). "Radiation-induced xerostomia in patients with head and neck cancer: a literature review." Cancer **107**(11): 2525-2534.

Dorr, W. and J. H. Hendry (2001). "Consequential late effects in normal tissues." Radiother Oncol **61**(3): 223-231.

Eckhart, L., S. Lippens, E. Tschachler and W. Declercq (2013). "Cell death by cornification." Biochim Biophys Acta **1833**(12): 3471-3480.

Engert, V., S. Vogel, S. I. Efanov, A. Duchesne, V. Corbo, N. Ali and J. C. Pruessner (2011). "Investigation into the cross-correlation of salivary cortisol and alpha-amylase responses to psychological stress." Psychoneuroendocrinology **36**(9): 1294-1302.

Epstein, J. B., E. A. Chin, J. J. Jacobson, B. Rishiraj and N. Le (1998). "The relationships among fluoride, cariogenic oral flora, and salivary flow rate during radiation therapy." Oral Surg Oral Med Oral Pathol Oral Radiol Endod **86**(3): 286-292.

Feldman, A. S., J. Banyard, C. L. Wu, W. S. McDougal and B. R. Zetter (2009). "Cystatin B as a tissue and urinary biomarker of bladder cancer recurrence and disease progression." Clin Cancer Res **15**(3): 1024-1031.

Ferlay, J., M. Colombet, I. Soerjomataram, C. Mathers, D. M. Parkin, M. Pineros, A. Znaor and F. Bray (2019). "Estimating the global cancer incidence and mortality in 2018: GLOBOCAN sources and methods." Int J Cancer **144**(8): 1941-1953.

Foley, C. J., H. Freedman, S. L. Choo, C. Onyskiw, N. Y. Fu, V. C. Yu, J. Tuszynski, J. C. Pratt and S. Baksh (2008). "Dynamics of RASSF1A/MOAP-1 association with death receptors." Mol Cell Biol **28**(14): 4520-4535.

Funegard, U., L. Franzen, T. Ericson and R. Henriksson (1994). "Parotid-Saliva Composition during and after Irradiation of Head and Neck-Cancer." Oral Oncology **30b**(4): 230-233.

Guchelaar, H. J., A. Vermes and J. H. Meerwaldt (1997). "Radiation-induced xerostomia: pathophysiology, clinical course and supportive treatment." Support Care Cancer **5**(4): 281-288.

Guebur., M. I., R. A., S. L. M., O. B. V., P. J. C. G. and R. G. H. A. (2004). "Alterations of total non stimulated salivary flow in patients with squamous cell carcinoma of the mouth and oropharynx submitted to hyperfractionated radiation therapy." Revista Brasileira de Cancerologia **50(2)**: 103-108.

Hancock, P. J., J. B. Epstein and G. R. Sadler (2003). "Oral and dental management related to radiation therapy for head and neck cancer." J Can Dent Assoc **69**(9): 585-590.

Hannig, M. (1999). "Ultrastructural investigation of pellicle morphogenesis at two different intraoral sites during a 24-h period." Clin Oral Investig **3**(2): 88-95.

Hannig, M. and M. Balz (2001). "Protective properties of salivary pellicles from two different intraoral sites on enamel erosion." Caries Res **35**(2): 142-148.

Hannig, M., E. Dounis, T. Henning, N. Apitz and L. Stosser (2006). "Does irradiation affect the protein composition of saliva?" Clin Oral Investig **10**(1): 61-65.

Hannig, M., M. Fiebiger, M. Guntzer, A. Dobert, R. Zimehl and Y. Nekrashevych (2004). "Protective effect of the in situ formed short-term salivary pellicle." Arch Oral Biol **49**(11): 903-910.

Hannig, M., N. J. Hess, W. Hoth-Hannig and M. De Vrese (2003). "Influence of salivary pellicle formation time on enamel demineralization--an in situ pilot study." Clin Oral Investig **7**(3): 158-161.

Hannig, M. and A. Joiner (2006). "The structure, function and properties of the acquired pellicle." Monogr Oral Sci **19**: 29-64.

Hara, A. T. and D. T. Zero (2010). "The caries environment: saliva, pellicle, diet, and hard tissue ultrastructure." Dent Clin North Am **54**(3): 455-467.

Hassan, M. I., A. Waheed, S. Yadav, T. P. Singh and F. Ahmad (2009). "Prolactin inducible protein in cancer, fertility and immunoregulation: structure, function and its clinical implications." Cell Mol Life Sci **66**(3): 447-459.

Hay, D. I. (1973). "The interaction of human parotid salivary proteins with hydroxyapatite." Arch Oral Biol **18**(12): 1517-1529.

Heller, D., E. J. Helmerhorst and F. G. Oppenheim (2017). "Saliva and Serum Protein Exchange at the Tooth Enamel Surface." J Dent Res **96**(4): 437-443.

Jain, N., P. Janning and H. Neumann (2020). "14-3-3 protein Bmh1 triggers short-range compaction of mitotic chromosomes by recruiting sirtuin deacetylase Hst2." J Biol Chem.

Jasmer, K. J., K. E. Gilman, K. Munoz Forti, G. A. Weisman and K. H. Limesand (2020). "Radiation-Induced Salivary Gland Dysfunction: Mechanisms, Therapeutics and Future Directions." J Clin Med **9**(12).

Jensdottir, T., C. Buchwald, B. Nauntofte, H. S. Hansen and A. Bardow (2013). "Saliva in relation to dental erosion before and after radiotherapy." Acta Odontol Scand **71**(3-4): 1008-1013.

Jordao, M. C., F. Q. Ionta, B. T. Bergantin, G. C. Oliveira, M. J. Moretto, H. M. Honorio, T. C. Silva and D. Rios (2017). "The Effect of Mucin in Artificial Saliva on Erosive Rehardening and Demineralization." Caries Res **51**(2): 136-140.

Jung, D. W., W. H. Kim and D. R. Williams (2014). "Chemical genetics and its application to moonlighting in glycolytic enzymes." Biochemical Society Transactions **42**: 1756-1761.

Kari, V., A. Shchebet, H. Neumann and S. A. Johnsen (2011). "The H2B ubiquitin ligase RNF40 cooperates with SUPT16H to induce dynamic changes in chromatin structure during DNA double-strand break repair." Cell Cycle **10**(20): 3495-3504.

Kawakita, D. and K. Matsuo (2017). "Alcohol and head and neck cancer." Cancer Metastasis Rev **36**(3): 425-434.

Kim, J. W. and C. V. Dang (2005). "Multifaceted roles of glycolytic enzymes." Trends in Biochemical Sciences **30**(3): 142-150.

Kosoric, J., R. A. D. Williams, M. P. Hector and P. Anderson (2007). "A synthetic peptide based on a natural salivary protein reduces demineralisation in model systems

for dental caries and erosion." International Journal of Peptide Research and Therapeutics **13**(4): 497-503.

Krief, G., O. Deutsch, S. Gariba, B. Zaks, D. J. Aframian and A. Palmon (2011). "Improved visualization of low abundance oral fluid proteins after triple depletion of alpha amylase, albumin and IgG." Oral Dis **17**(1): 45-52.

Krief, G., O. Deutsch, B. Zaks, D. T. Wong, D. J. Aframian and A. Palmon (2012). "Comparison of diverse affinity based high-abundance protein depletion strategies for improved bio-marker discovery in oral fluids." J Proteomics **75**(13): 4165-4175.

Lajer, C., C. Buchwald, B. Nauntofte, L. Specht, A. Bardow and T. Jensdottir (2009). "Erosive potential of saliva stimulating tablets with and without fluoride in irradiated head and neck cancer patients." Radiother Oncol **93**(3): 534-538.

Lal, P., R. Bajpai, R. Khurana, K. J. Das, P. Kumar, A. Tiwari, N. Gupta and S. Kumar (2010). "Changes in salivary flow rates in head and neck cancer after chemoradiotherapy." J Cancer Res Ther **6**(4): 458-462.

Law, J., M. Salla, A. Zare, Y. Wong, L. Luong, N. Volodko, O. Svystun, K. Flood, J. Lim, M. Sung, J. R. Dyck, C. T. Tan, Y. C. Su, V. C. Yu, J. Mackey and S. Baksh (2015). "Modulator of apoptosis 1 (MOAP-1) is a tumor suppressor protein linked to the RASSF1A protein." J Biol Chem **290**(40): 24100-24118.

Lee, Y. H., J. N. Zimmerman, W. Custodio, Y. Xiao, T. Basiri, S. Hatibovic-Kofman and W. L. Siqueira (2013). "Proteomic evaluation of acquired enamel pellicle during in vivo formation." PLoS One **8**(7): e67919.

Leemans, C. R., B. J. Braakhuis and R. H. Brakenhoff (2011). "The molecular biology of head and neck cancer." Nat Rev Cancer **11**(1): 9-22.

Lendenmann, U., J. Grogan and F. G. Oppenheim (2000). "Saliva and dental pellicle--a review." Adv Dent Res **14**: 22-28.

Li, X., R. Tian, H. Gao, Y. Yang, B. R. G. Williams, M. P. Gantier, N. A. J. McMillan, D. Xu, Y. Hu and Y. Gao (2017). "Identification of a histone family gene signature for predicting the prognosis of cervical cancer patients." Sci Rep **7**(1): 16495.

Lieshout, H. F. and C. P. Bots (2014). "The effect of radiotherapy on dental hard tissue--a systematic review." Clin Oral Investig **18**(1): 17-24.

Logemann, J. A., C. H. Smith, B. R. Pauloski, A. W. Rademaker, C. L. Lazarus, L. A. Colangelo, B. Mittal, E. MacCracken, J. Gaziano, L. Stachowiak and L. A. Newman (2001). "Effects of xerostomia on perception and performance of swallow function." Head Neck **23**(4): 317-321.

Ma, L., J. Wan and X. Shen (2018). "Salivary Alpha-Amylase and Behavior Reaction in Acute Stress and the Impact of Tridimensional Personality." Adv Exp Med Biol **1072**: 431-436.

Makkonen, T. (1988). "Studies on oral complications of head and neck cancer radiotherapy." Proc Finn Dent Soc **84 Suppl 4-5**: 1-111.

Makkonen, T. A., J. Tenovuo, P. Vilja and A. Heimdahl (1986). "Changes in the Protein-Composition of Whole Saliva during Radiotherapy in Patients with Oral or Pharyngeal Cancer." Oral Surgery Oral Medicine Oral Pathology Oral Radiology and Endodontics **62**(3): 270-275.

Manconi, B., B. Liori, T. Cabras, F. Iavarone, A. Manni, I. Messana, M. Castagnola and A. Olianas (2017). "Top-down HPLC-ESI-MS proteomic analysis of saliva of edentulous subjects evidenced high levels of cystatin A, cystatin B and SPRR3." Archives of Oral Biology **77**: 68-74.

Mandel, I. D. (1987). "The functions of saliva." J Dent Res **66 Spec No**: 623-627.

Mao, P., M. N. Kyriss, A. J. Hodges, M. Duan, R. T. Morris, M. D. Lavine, T. B. Topping, L. M. Gloss and J. J. Wyrick (2016). "A basic domain in the histone H2B N-terminal tail is important for nucleosome assembly by FACT." Nucleic Acids Res **44**(19): 9142-9152.

Martini, D., A. Gallo, S. Vella, F. Sernissi, A. Cecchettini, N. Luciano, E. Polizzi, P. G. Conaldi, M. Mosca and C. Baldini (2017). "Cystatin S-a candidate biomarker for severity of submandibular gland involvement in Sjogren's syndrome." Rheumatology (Oxford) **56**(6): 1031-1038.

Martini, T., D. Rios, L. P. S. Cassiano, C. M. S. Silva, E. A. Taira, T. M. S. Ventura, H. Pereira, A. C. Magalhaes, T. S. Carvalho, T. Baumann, A. Lussi, R. B. Oliveira, R. G. Palma-Dibb and M. A. R. Buzalaf (2019). "Proteomics of acquired pellicle in gastroesophageal reflux disease patients with or without erosive tooth wear." J Dent **81**: 64-69.

Martini, T., D. Rios, A. Dionizio, L. P. Cassiano, V. T. Pela, C. M. S. Silva, E. A. Taira, T. M. Ventura, A. C. Magalhães, T. S. Carvalho, T. Baumann, A. Lussi, R. B. Oliveira, R. G. Palma-Dibb and M. A. R. Buzalaf (2020). "Salivary hemoglobin protects against erosive tooth wear in gastric reflux patients." Caries Res **54**(5-6): 466-474.

Mateos, J. J., X. Setoain, J. Ferre, A. Rovirosa, B. Navalpotro, F. Martin, M. Ortega, F. Lomena, D. Fuster, J. Pavia and F. Pons (2001). "Salivary scintigraphy for assessing the protective effect of pilocarpine in head and neck irradiated tumours." Nucl Med Commun **22**(6): 651-656.

Miles, L. A., C. M. Dahlberg, J. Plescia, J. Felez, K. Kato and E. F. Plow (1991). "Role of Cell-Surface Lysines in Plasminogen Binding to Cells - Identification of Alpha-Enolase as a Candidate Plasminogen Receptor." Biochemistry **30**(6): 1682-1691.

Mira, J. G., G. D. Fullerton and W. B. Wescott (1982). "Correlation between initial salivary flow rate and radiation dose in the production of xerostomia." Acta Radiol Oncol **21**(3): 151-154.

Missale, C., S. R. Nash, S. W. Robinson, M. Jaber and M. G. Caron (1998). "Dopamine receptors: From structure to function." Physiological Reviews **78**(1): 189-225.

Moore, L. D., T. Le and G. Fan (2013). "DNA methylation and its basic function." Neuropsychopharmacology **38**(1): 23-38.

Murad AM, K. A. (1996). "Oncologia: bases clínicas do tratamento." Rio de Janeiro: Guanabara Koogan; **1.ed**.

Mutahar, M., S. O'Toole, G. Carpenter, D. Bartlett, M. Andiappan and R. Moazzez (2017). "Reduced statherin in acquired enamel pellicle on eroded teeth compared to healthy teeth in the same subjects: An in-vivo study." PLoS One **12**(8): e0183660.

Nag, R., M. Kyriss, J. W. Smerdon, J. J. Wyrick and M. J. Smerdon (2010). "A cassette of N-terminal amino acids of histone H2B are required for efficient cell survival, DNA repair and Swi/Snf binding in UV irradiated yeast." Nucleic Acids Res **38**(5): 1450-1460.

Nagler, R. M., B. J. Baum, G. Miller and P. C. Fox (1998). "Long-term salivary effects of single-dose head and neck irradiation in the rat." Arch Oral Biol **43**(4): 297-303.

Nishimura, Y., S. Homma-Takeda, H. S. Kim and I. Kakuta (2014). "Radioprotection of mice by lactoferrin against irradiation with sublethal X-rays." Journal of Radiation Research **55**(2): 277-282.

O'Connell, A. C. (2000). "Natural history and prevention of radiation injury." Adv Dent Res **14**: 57-61.

Obayashi, K. (2013). "Salivary mental stress proteins." Clin Chim Acta **425**: 196-201.

Oppenheim, F. G., D. I. Hay, D. J. Smith, G. D. Offner and R. F. Troxler (1987). "Molecular basis of salivary proline-rich protein and peptide synthesis: cell-free translations and processing of human and macaque statherin mRNAs and partial amino acid sequence of their signal peptides." J Dent Res **66**(2): 462-466.

Paim, E. D., M. C. B. Berbert, V. G. Zanella, V. B. Martins and F. E. Macagnan (2019). "Effects of transcutaneous electrical nerve stimulation on the salivary flow of patients with hyposalivation induced by radiotherapy in the head and neck region-A randomised clinical trial." Journal of Oral Rehabilitation **46**(12): 1142-1150.

Paula, J. M., H. M. Sonobe, A. C. Nicolussi, M. M. Zago and N. O. Sawada (2012). "Symptoms of depression in patients with cancer of the head and neck undergoing radiotherapy treatment: a prospective study." Rev Lat Am Enfermagem **20**(2): 362-368.

Peterson, D. E. and J. A. D'Ambrosio (1992). "Diagnosis and management of acute and chronic oral complications of nonsurgical cancer therapies." Dent Clin North Am **36**(4): 945-966.

Petushkova, A. I., L. V. Savvateeva, D. O. Korolev and A. A. Zamyatnin (2019). "Cysteine Cathepsins: Potential Applications in Diagnostics and Therapy of Malignant Tumors." Biochemistry-Moscow **84**(7): 746-761.

Pisano, E., T. Cabras, C. Montaldo, V. Piras, R. Inzitari, C. Olmi, M. Castagnola and I. Messana (2005). "Peptides of human gingival crevicular fluid determined by HPLC-ESI-MS." Eur J Oral Sci **113**(6): 462-468.

Pow, E. H., A. S. McMillan, W. K. Leung, M. C. Wong and D. L. Kwong (2003). "Salivary gland function and xerostomia in southern Chinese following radiotherapy for nasopharyngeal carcinoma." Clin Oral Investig **7**(4): 230-234.

Proctor, G. B., S. Hamdan, G. H. Carpenter and P. Wilde (2005). "A statherin and calcium enriched layer at the air interface of human parotid saliva." Biochem J **389**(Pt 1): 111-116.

Raj, P. A., M. Johnsson, M. J. Levine and G. H. Nancollas (1992). "Salivary statherin. Dependence on sequence, charge, hydrogen bonding potency, and helical conformation for adsorption to hydroxyapatite and inhibition of mineralization." J Biol Chem **267**(9): 5968-5976.

Rakhmatullina, E., A. Bossen, K. K. Bachofner, C. Meier and A. Lussi (2013). "Optical pen-size reflectometer for monitoring of early dental erosion in native and polished enamels." J Biomed Opt **18**(11): 117009.

Ransom, M., B. K. Dennehey and J. K. Tyler (2010). "Chaperoning histones during DNA replication and repair." Cell **140**(2): 183-195.

Rettig, E. M. and G. D'Souza (2015). "Epidemiology of head and neck cancer." Surg Oncol Clin N Am **24**(3): 379-396.

Richards, T. M., T. Hurley, L. Grove, K. J. Harrington, G. H. Carpenter, G. B. Proctor and C. M. Nutting (2017). "The effect of parotid gland-sparing intensity-modulated radiotherapy on salivary composition, flow rate and xerostomia measures." Oral Dis **23**(7): 990-1000.

Rudat, V., J. Meyer, F. Momm, M. Bendel, M. Henke, V. Strnad, K. Grotz and A. Schulte (2000). "Protective effect of amifostine on dental health after radiotherapy of the head and neck." Int J Radiat Oncol Biol Phys **48**(5): 1339-1343.

Sachlos, E., R. M. Risueno, S. Laronde, Z. Shapovalova, J. H. Lee, J. Russell, M. Malig, J. D. McNicol, A. Fiebig-Comyn, M. Graham, M. Levadoux-Martin, J. B. Lee, A. O. Giacomelli, J. A. Hassell, D. Fischer-Russell, M. R. Trus, R. Foley, B. Leber, A. Xenocostas, E. D. Brown, T. J. Collins and M. Bhatia (2012). "Identification of Drugs Including a Dopamine Receptor Antagonist that Selectively Target Cancer Stem Cells." Cell **149**(6): 1284-1297.

Sadeghi, L., L. Siggens, J. P. Svensson and K. Ekwall (2014). "Centromeric histone H2B monoubiquitination promotes noncoding transcription and chromatin integrity." Nat Struct Mol Biol **21**(3): 236-243.

Safdari, Y., M. Khalili, S. Farajnia, M. Asgharzadeh, Y. Yazdani and M. Sadeghi (2014). "Recent advances in head and neck squamous cell carcinoma--a review." Clin Biochem **47**(13-14): 1195-1202.

Sakai, M., T. Matsushita, R. Hoshino, H. Ono, K. Ikai and T. Sakai (2017). "Identification of the protective mechanisms of Lactoferrin in the irradiated salivary gland." Sci Rep **7**(1): 9753.

Santos, O., J. Kosoric, M. P. Hector, P. Anderson and L. Lindh (2008). "Adsorption behavior of statherin and a statherin peptide onto hydroxyapatite and silica surfaces by in situ ellipsometry." J Colloid Interface Sci **318**(2): 175-182.

Shannon, I. L., E. N. Starcke and W. B. Wescott (1977). "Effect of Radiotherapy on Whole Saliva Flow." Journal of Dental Research **56**(6): 693-693.

Shi, J., M. Barakat, D. Chen and L. Chen (2018). "Bicellular Tight Junctions and Wound Healing." Int J Mol Sci **19**(12).

Silverman, S., Jr. (1999). "Oral cancer: complications of therapy." Oral Surg Oral Med Oral Pathol Oral Radiol Endod **88**(2): 122-126.

Siqueira, W. L., M. Bakkal, Y. Xiao, J. N. Sutton and F. M. Mendes (2012). "Quantitative proteomic analysis of the effect of fluoride on the acquired enamel pellicle." PLoS One **7**(8): e42204.

Siqueira, W. L., W. Custodio and E. E. McDonald (2012). "New insights into the composition and functions of the acquired enamel pellicle." J Dent Res **91**(12): 1110-1118.

Siqueira, W. L., W. Custodio and E. E. McDonald (2012). "New Insights into the Composition and Functions of the Acquired Enamel Pellicle." Journal of Dental Research **91**(12): 1110-1118.

Siqueira, W. L., Y. H. Lee, Y. Z. Xiao, K. Held and W. Wong (2012). "Identification and characterization of histatin 1 salivary complexes by using mass spectrometry." Proteomics **12**(22): 3426-3435.

Siqueira, W. L. and F. G. Oppenheim (2009). "Small molecular weight proteins/peptides present in the in vivo formed human acquired enamel pellicle." Arch Oral Biol **54**(5): 437-444.

Siqueira, W. L., W. Zhang, E. J. Helmerhorst, S. P. Gygi and F. G. Oppenheim (2007). "Identification of protein components in in vivo human acquired enamel pellicle using LC-ESI-MS/MS." J Proteome Res **6**(6): 2152-2160.

Sivadasan, P., M. K. Gupta, G. J. Sathe, L. Balakrishnan, P. Palit, H. Gowda, A. Suresh, M. A. Kuriakose and R. Sirdeshmukh (2015). "Human salivary proteome--a resource of potential biomarkers for oral cancer." J Proteomics **127**(Pt A): 89-95.

Soulieres, D., S. Faivre, R. Mesia, E. Remenar, S. H. Li, A. Karpenko, A. Dechaphunkul, S. Ochsenreither, L. A. Kiss, J. C. Lin, R. Nagarkar, L. Tamas, S. B. Kim, J. Erfan, A. Alyasova, S. Kasper, C. Barone, S. Turri, A. Chakravartty, M. Chol, P. Aimone, S. Hirawat and L. Licitra (2017). "Buparlisib and paclitaxel in patients with platinum-pretreated recurrent or metastatic squamous cell carcinoma of the head and neck (BERIL-1): a randomised, double-blind, placebo-controlled phase 2 trial." Lancet Oncol.

Specht, L. (2002). "Oral complications in the head and neck radiation patient. Introduction and scope of the problem." Support Care Cancer **10**(1): 36-39.

Stenudd, C., A. Nordlund, M. Ryberg, I. Johansson, C. Kallestal and N. Stromberg (2001). "The association of bacterial adhesion with dental caries." J Dent Res **80**(11): 2005-2010.

Taira, E. A., G. Carvalho, C. R. Ferrari, T. Martini, V. T. Pela, T. M. O. Ventura, A. S. Dionizio, E. Crusca, R. Marchetto and M. A. R. Buzalaf (2020). "Statherin-derived peptide protects against intrinsic erosion." Arch Oral Biol **119**: 104890.

Taira, E. A., T. M. S. Ventura, L. P. S. Cassiano, C. M. S. Silva, T. Martini, A. L. Leite, D. Rios, A. C. Magalhaes and M. A. R. Buzalaf (2018). "Changes in the Proteomic Profile of Acquired Enamel Pellicles as a Function of Their Time of Formation and Hydrochloric Acid Exposure." Caries Res **52**(5): 367-377.

Tan, K. O., N. Y. Fu, S. K. Sukumaran, S. L. Chan, J. H. Kang, K. L. Poon, B. S. Chen and V. C. Yu (2005). "MAP-1 is a mitochondrial effector of Bax." Proc Natl Acad Sci U S A **102**(41): 14623-14628.

Tokuhara, C. K., M. R. Santesso, G. S. N. Oliveira, T. Ventura, J. T. Doyama, W. F. Zambuzzi and R. C. Oliveira (2019). "Updating the role of matrix metalloproteinases in mineralized tissue and related diseases." J Appl Oral Sci **27**: e20180596.

Trautmann, S., N. Kunzel, C. Fecher-Trost, A. Barghash, P. Schalkowsky, J. Dudek, J. Delius, V. Helms and M. Hannig (2020). "Deep Proteomic Insights into the Individual Short-Term Pellicle Formation on Enamel-An In Situ Pilot Study." Proteomics Clin Appl **14**(3): e1900090.

Van De Wiele, C., A. Signore, F. Scopinaro, R. Waterhouse, R. A. Dierckx and Imitt (2001). "Imaging tumour hypoxia: where are we?" Nucl Med Commun **22**(9): 945-947.

Ventura, T., L. P. S. Cassiano, E. S. C. M. Souza, E. A. Taira, A. L. Leite, D. Rios and M. A. R. Buzalaf (2017). "The proteomic profile of the acquired enamel pellicle according to its location in the dental arches." Arch Oral Biol **79**: 20-29.

Ventura, T. M. O., N. R. Ribeiro, E. A. Taira, E. S. C. M. de Souza, C. M. F. Rubira, P. S. da Silva Santos and M. A. R. Buzalaf (2021). "Radiotherapy changes acquired enamel pellicle proteome in head and neck cancer patients." J Dent: 103642.

Vissink, A., J. Jansma, F. K. L. Spijkervet, F. R. Burlage and R. P. Coppes (2003). "Oral sequelae of head and neck radiotherapy." Critical Reviews in Oral Biology & Medicine **14**(3): 199-212.

Vissink, A., J. B. Mitchell, B. J. Baum, K. H. Limesand, S. B. Jensen, P. C. Fox, L. S. Elting, J. A. Langendijk, R. P. Coppes and M. E. Reyland (2010). "Clinical management

of salivary gland hypofunction and xerostomia in head-and-neck cancer patients: successes and barriers." Int J Radiat Oncol Biol Phys **78**(4): 983-991.

Vissink, A., A. K. Panders, E. J. Gravenmade and A. Vermey (1988). "The causes and consequences of hyposalivation." Ear Nose Throat J **67**(3): 166-168, 173-166.

Vitorino, R., M. J. Calheiros-Lobo, J. Williams, A. J. Ferrer-Correia, K. B. Tomer, J. A. Duarte, P. M. Domingues and F. M. Amado (2007). "Peptidomic analysis of human acquired enamel pellicle." Biomed Chromatogr **21**(11): 1107-1117.

Vukosavljevic, D., W. Custodio, M. A. Buzalaf, A. T. Hara and W. L. Siqueira (2014). "Acquired pellicle as a modulator for dental erosion." Arch Oral Biol **59**(6): 631-638.

Vukosavljevic, D., J. L. Hutter, E. J. Helmerhorst, Y. Xiao, W. Custodio, F. C. Zaidan, F. G. Oppenheim and W. L. Siqueira (2014). "Nanoscale adhesion forces between enamel pellicle proteins and hydroxyapatite." J Dent Res **93**(5): 514-519.

Wang, H., L. Y. Shen, Y. Lin, Q. Shi, Y. B. Yang and K. N. Chen (2015). "The expression and prognostic significance of Mucin 13 and Mucin 20 in esophageal squamous cell carcinoma." Journal of Cancer Research and Therapeutics **11**(5): C74-C79.

Wang, X., K. E. Kaczor-Urbanowicz and D. T. Wong (2017). "Salivary biomarkers in cancer detection." Med Oncol **34**(1): 7.

Warde, P., B. O'Sullivan, J. Aslanidis, B. Kroll, G. Lockwood, J. Waldron, D. Payne, A. Bayley, J. Ringash, J. Kim, F. F. Liu, W. Maxymiw, S. Sprague and B. J. Cummings (2002). "A Phase III placebo-controlled trial of oral pilocarpine in patients undergoing radiotherapy for head-and-neck cancer." Int J Radiat Oncol Biol Phys **54**(1): 9-13.

Wetton, S., J. Hughes, N. West and M. Addy (2006). "Exposure time of enamel and dentine to saliva for protection against erosion: a study in vitro." Caries Res **40**(3): 213-217.

Winck, F. V., A. C. Prado Ribeiro, R. Ramos Domingues, L. Y. Ling, D. M. Riano-Pachon, C. Rivera, T. B. Brandao, A. F. Gouvea, A. R. Santos-Silva, R. D. Coletta and A. F. Paes Leme (2015). "Insights into immune responses in oral cancer through proteomic analysis of saliva and salivary extracellular vesicles." Sci Rep **5**: 16305.

Xiao, P. P., Y. H. Hu and L. Sun (2010). "Scophthalmus maximus cystatin B enhances head kidney macrophage-mediated bacterial killing." Developmental and Comparative Immunology **34**(12): 1237-1241.

Xiao, Y., M. Karttunen, J. Jalkanen, M. C. Mussi, Y. Liao, B. Grohe, F. Lagugne-Labarthet and W. L. Siqueira (2015). "Hydroxyapatite Growth Inhibition Effect of Pellicle Statherin Peptides." J Dent Res **94**(8): 1106-1112.

Yang, J., S. J. Lee, Y. Kwon, L. Ma and J. Kim (2020). "Tumor suppressive function of Matrin 3 in the basal-like breast cancer." Biol Res **53**(1): 42.

Yang, Y., B. Yang, M. Li, Y. Wang, X. Yang and J. Li (2017). "Salivary acquired pellicle-inspired DpSpSEEKC peptide for the restoration of demineralized tooth enamel." Biomed Mater **12**(2): 025007.

Zago, S. D. (2006). "The radiotherapy effect on the quality of life of patients with head and neck cancer." Revista Brasileira de Cancerologia **52(4)**: 323-329.

Zeng, Q., J. Zheng, D. Yang, Y. Tang and Z. Zhou (2019). "Effect of calcium ions on the adsorption and lubrication behavior of salivary proteins on human tooth enamel surface." J Mech Behav Biomed Mater **98**: 172-178.

Zhang, C. Z., X. Q. Cheng, J. Y. Li, P. Zhang, P. Yi, X. Xu and X. D. Zhou (2016). "Saliva in the diagnosis of diseases." Int J Oral Sci **8**(3): 133-137.

Zimmerman, J. N., W. Custodio, S. Hatibovic-Kofman, Y. H. Lee, Y. Xiao and W. L. Siqueira (2013). "Proteome and peptidome of human acquired enamel pellicle on deciduous teeth." Int J Mol Sci **14**(1): 920-934.

Zupkovitz, G., J. Tischler, M. Posch, I. Sadzak, K. Ramsauer, G. Egger, R. Grausenburger, N. Schweifer, S. Chiocca, T. Decker and C. Seiser (2006). "Negative and positive regulation of gene expression by mouse histone deacetylase 1." Mol Cell Biol **26**(21): 7913-7928.

Annex

“Conheça todas as teorias, domine todas as técnicas, mas ao tocar uma alma humana seja apenas outra alma humana.”

Carl Jung

ANNEX 1

USP - FACULDADE DE ODONTOLOGIA DE BAURU DA USP

PARECER CONSUBSTANCIADO DO CEP

DADOS DO PROJETO DE PESQUISA

Título da Pesquisa: Análise proteômica da película adquirida do esmalte e saliva em pacientes com câncer de cabeça e pescoço submetidos à radioterapia

Pesquisador: Talita Mendes da Silva Ventura

Área Temática:

Versão: 2

CAAE: 61484116.0.0000.5417

Instituição Proponente: Universidade de Sao Paulo

Patrocinador Principal: Financiamento Próprio

DADOS DO PARECER

Número do Parecer: 1.929.035

Continuação do Parecer: 1.929.035

Considerações sobre os Termos de apresentação obrigatória:

Foram apresentados todos os documentos necessários para que para que a pesquisa pudesse ser avaliada. Ou seja: O projeto, carta de encaminhamento em conjunto com o termo de aquiescência do departamento, orçamento, cronograma, folha de rosto e o TCLE.

Recomendações:

Não se aplica.

Conclusões ou Pendências e Lista de Inadequações:

O projeto foi avaliado neste CEP em reunião realizada na data de 16/11/2016. Naquela reunião o projeto foi considerado com pendencias para sua aprovação. Faltava esclarecer aonde se faria o recrutamento do GC, esclarecer melhor o orçamento, esclarecer qual a participação de dois colaboradores na pesquisa e adequar o cronograma. A pesquisadora retorna o projeto para uma nova análise e observa-se que todas as pendências foram esclarecidas, razão pela qual podemos aprovar a realização da pesquisa.

Considerações Finais a critério do CEP:

Esse projeto foi considerado APROVADO na reunião ordinária do CEP de 08.02.2017, com base nas normas éticas da Resolução CNS 466/12. Ao término da pesquisa o CEP-FOB/USP exige a apresentação de relatório final. Os relatórios parciais deverão estar de acordo com o cronograma e/ou parecer emitido pelo CEP. Alterações na metodologia, título, inclusão ou exclusão de autores, cronograma e quaisquer outras mudanças que sejam significativas deverão ser previamente comunicadas a este CEP sob risco de não aprovação do relatório final. Quando da apresentação deste, deverão ser incluídos todos os TCLEs e/ou termos de doação assinados e rubricados, se pertinentes.

ANNEX 2

Universidade de São Paulo
Faculdade de Odontologia de Bauru

Departamento de Ciências Biológicas

TERMO DE CONSENTIMENTO LIVRE E ESCLARECIDO

Caro participante da Clínica Multidisciplinar da Faculdade de Odontologia de Bauru, gostaria de convidá-lo a participar de uma pesquisa, onde serão analisadas as proteínas sobre os dentes e saliva. Caso você faça tratamento por radioterapia, a película adquirida e a saliva serão analisadas em diferentes períodos do tratamento, caso você não faça tratamento por radioterapia, a película adquirida e a saliva serão coletadas apenas em dois dias consecutivos, o trabalho experimental é intitulado "Análise proteômica da película adquirida do esmalte e da saliva em pacientes com câncer de cabeça e pescoço submetidos à radioterapia" e tem como objetivo avaliar as proteínas encontradas em películas adquiridas formadas sobre os dentes e na saliva em pacientes com câncer de cabeça e pescoço, submetidos a tratamento por radioterapia. Estas proteínas serão avaliadas antes, durante e após a radioterapia, a fim de se verificar alterações nas proteínas em comparações aos participantes sem o diagnóstico e que não realizam o tratamento. Você deverá comparecer a Clínica Multidisciplinar da Faculdade de Odontologia de Bauru, no dia e horário que normalmente você já frequenta, e nos dias que serão realizadas as coletas o pesquisador entrará em contato com você para avisar sobre as coletas da película adquirida e saliva, totalizando dois dias que serão necessários a sua presença para cada fase do tratamento por radioterapia, ou seja, dois dias antes, dois dias durante e dois dias após o tratamento.

A película adquirida é uma fina camada transparente formada sobre os dentes, que começa aparecer assim que os dentes entram em contato com a saliva.

O experimento consiste na coleta da película adquirida formada naturalmente sobre os seus dentes e para isso, realizaremos a coleta da saliva não estimulada (cuspindo) e estimulada (mastigando um plástico e cuspindo) durante 10 minutos em recipientes plásticos para primeiramente fazer o cálculo da sua quantidade de saliva em mL/minuto e pH. Uma parte da saliva não estimulada será utilizada também para a análise das proteínas, portanto a outra parte da saliva não estimulada e a saliva estimulada serão descartadas em local apropriado, segundo as normas de descarte de material biológico. Você receberá uma profilaxia dentária (limpeza nos dentes) com pedra pomes (não contendo aditivos), e em seguida aguardará por 120 minutos para que a película adquirida se forme naturalmente sobre os dentes, durante este período, você não poderá realizar o consumo de alimentos e bebidas. Assim, logo após 120 minutos a coleta da película formada em todos os seus dentes, pelo lado de fora e pelo lado de dentro, será feita. O período de coleta será realizado em dois dias consecutivos (para obter amostras em duplicata, ou seja, 2 amostras iguais), tendo início às 8 horas da manhã. Todos os procedimentos para cada coleta serão idênticos para ambos os dias e para cada fase de tratamento por radioterapia. Toda amostra de película adquirida coletada será utilizada para a realização da pesquisa, portanto não haverá descarte das mesmas.

Este projeto traz como benefícios á importância do conhecimento sobre quais proteínas da película adquirida são formadas em diferentes períodos da radioterapia, irá acrescentar informações de como seria a melhor maneira para o tratamento dentário durante este período e quais seriam as melhores estratégias preventivas a serem adotadas, de forma a aumentar a qualidade de vida.

Em relação aos benefícios oferecidos a você, no início do estudo será realizado um exame clínico em relação às suas condições bucais e o resultado deste exame será prontamente avisado a você. Caso algum problema seja detectado, faremos o encaminhamento para a triagem, segundo agendamento na clínica responsável da FOB. Além disto, você receberá a profilaxia dentária e serão fornecidas instruções sobre higiene bucal, por escrito e verbalmente.

Em relação aos riscos referentes à pesquisa, destacamos que pode ocorrer um possível constrangimento e desconforto pela espera de 120 minutos sem o consumo de alimentos e bebidas, esse período é necessário para que a película adquirida se forme naturalmente sobre os seus dentes, vale ressaltar que não há risco a sua saúde com a participação nesta pesquisa, já que a coleta da película adquirida e saliva não é um método invasivo e você receberá a profilaxia dentária com pedra pomes sem o uso de aditivos, similar ao procedimento utilizado na rotina de uma clínica odontológica.

Concordando em participar, você entende que este estudo será realizado em benefício das ciências médicas e odontológicas, e desta forma concorda com a divulgação dos dados obtidos por meio de

Rubrica do Pesquisador Responsável:

Rubrica do Participante da Pesquisa :

Al. Dr. Octávio Pinheiro Brisolla, 9-75 – Bauru-SP – CEP 17012-901 – C.P. 73
e-mail: drolivei@fob.usp.br – Fone/FAX (0xx14) 3235-8271
http://www.fob.usp.br

Universidade de São Paulo
Faculdade de Odontologia de Bauru

Departamento de Ciências Biológicas

publicações científicas. A participação será voluntária, e entenda-se que você poderá fazer qualquer pergunta sobre cada etapa dos procedimentos, sendo que será livre para desistir de participar a qualquer momento mesmo após assinar este termo, caso você mude de idéia e queira sair da pesquisa, poderá fazê-lo, sem nenhum prejuízo de sua parte. Contudo, você terá também a garantia do sigilo que assegura a sua privacidade, adicionalmente, este termo de consentimento livre e esclarecido constará de duas vias, uma permanecerá com o pesquisador e outra será entregue a você. Importante ressaltar que não está sendo considerado nenhum pagamento ou recompensa material pela sua participação neste estudo. O participante não terá despesas pela participação da pesquisa, os gastos que forem gerados por este trabalho ficarão a cargo da responsável pelo projeto, caso você necessite de ajuda financeira de transporte para participar desta pesquisa ela poderá ser ressarcida pelo pesquisador. Você terá garantido o direito de indenização compensatória caso fique comprovado que a sua participação na pesquisa acarretou algum problema a você.
Para esclarecimentos de dúvidas sobre sua participação na pesquisa poderá entrar em contato com pesquisador por meio do endereço institucional da Alameda Dr. Octávio Pinheiro Brisolla, 9-75, Departamento de Ciências Biológicos no Laboratório de Bioquímica, telefone (14) 3235-8246/ (14) 99769-5390 ou por e-mail: talitaventura@usp.br e, para denúncias e/ou reclamações entrar em contato com Comitê de Ética em Pesquisa-FOB/USP, à Alameda Dr. Octávio Pinheiro Brisolla, 9-75, Vila Universitária, ou pelo telefone (14)3235-8356, e-mail: cep@fob.usp.br, e a forma de contato com CONEP, pelo endereço SEPN 510 NORTE, BLOCO A, 3°Andar, Edifício Ex-INAN – Unidade II – Ministério da Saúde – Brasília-DF, telefone (61) 3315-5878 ou por e-mail: cns@saude.gov.br, quando pertinente.
Pelo presente instrumento que atende às exigências legais, o Sr. (a) _____, portador da cédula de identidade _____, após leitura minuciosa das informações constantes neste TERMO DE CONSENTIMENTO LIVRE E ESCLARECIDO, devidamente explicada pelos profissionais em seus mínimos detalhes, ciente dos serviços e procedimentos aos quais será submetido, não restando quaisquer dúvidas a respeito do lido e explicado, DECLARA e FIRMA seu CONSENTIMENTO LIVRE E ESCLARECIDO concordando em participar da pesquisa proposta. Fica claro que o participante da pesquisa, pode a qualquer momento retirar seu CONSENTIMENTO LIVRE E ESCLARECIDO e deixar de participar desta pesquisa e ciente de que todas as informações prestadas tornar-se-ão confidenciais e guardadas por força de sigilo profissional (Art. 9º do Código de Ética Odontológica). Por fim, como pesquisadora responsável pela pesquisa, DECLARO o cumprimento do disposto na Resolução CNS nº 466 de 2012, contidos nos itens IV.3 e IV.4, este último se pertinente, item IV.5.a e na íntegra com a resolução CNS nº 466 de dezembro de 2012.

Por estarmos de acordo com o presente termo o firmamos em duas vias igualmente válidas (uma via para o participante da pesquisa e outra para o pesquisador) que serão rubricadas em todas as suas páginas e assinadas ao seu término, conforme o disposto pela Resolução CNS nº 466 de 2012, itens IV.3.f e IV.5.d.

Bauru, SP, _____ de _____ de _____.

_____
Assinatura do Participante da Pesquisa

_____
Talita Mendes da Silva Ventura
Assinatura da Pesquisadora Responsável

Universidade de São Paulo
Faculdade de Odontologia de Bauru

Departamento de Ciências Biológicas

O **Comitê de Ética em Pesquisa – CEP**, organizado e criado pela **FOB-USP**, em 29/06/98 (**Portaria GD/0698/FOB**), previsto no item VII da Resolução CNS nº 466/12 do Conselho Nacional de Saúde do Ministério da Saúde (publicada no DOU de 13/06/2013), é um Colegiado interdisciplinar e independente, de relevância pública, de caráter consultivo, deliberativo e educativo, criado para defender os interesses dos participantes da pesquisa em sua integridade e dignidade e para contribuir no desenvolvimento da pesquisa dentro de padrões éticos.

Qualquer denúncia e/ou reclamação sobre sua participação na pesquisa poderá ser reportada a este CEP:

Horário e local de funcionamento:
Comitê de Ética em Pesquisa
Faculdade de Odontologia de Bauru-USP - Prédio da Pós-Graduação (bloco E - pavimento superior), de segunda à sexta-feira, no horário das **14hs às 17 horas**, em dias úteis.
Alameda Dr. Octávio Pinheiro Brisolla, 9-75.
Vila Universitária – Bauru – SP – CEP 17012-901
Telefone/FAX(14)3235-8356. E-mail: cep@fob.usp.br

Rubrica do Pesquisador Responsável:

Rubrica do Participante da Pesquisa :